Universiteit
Leiden
The Netherlands

Inherited retinal degenerations: clinical characterization on the road to therapy

Talib, M.

Citation
Talib, M. (2022, January 25). *Inherited retinal degenerations: clinical characterization on the road to therapy*. Retrieved from https://hdl.handle.net/1887/3250802

Version:	Publisher's Version
License:	Licence agreement concerning inclusion of doctoral thesis in the Institutional Repository of the University of Leiden
Downloaded from:	https://hdl.handle.net/1887/3250802

Note: To cite this publication please use the final published version (if applicable).

INHERITED RETINAL DEGENERATIONS: CLINICAL CHARACTERIZATION ON THE ROAD TO THERAPY

by

Mays Talib

ISBN | 978-94-6423-566-1

Design Cover | Véronique Baur – www.veerillustratie.nl

Lay-out | Bregje Jaspers – www.ProefschriftOntwerp.nl

Printing | ProefschriftMaken, Vianen, The Netherlands

The research described in this thesis was financially supported by
Curing Retinal Blindness Foundation, Janivo Stichting, Bayer, Stichting Blindenhulp

Financial support for the printing of this thesis was kindly provided by
Stichting Leids Oogheelkundig Ondersteuningsfonds, Rotterdamse Stichting Blindenbelangen, Stichting Blindenhulp, Landelijke Stichting voor Blinden en Slechtzienden, Universitaire Bibliotheken Leiden, Vitaminen op Recept, Oculenti Contactlenspraktijken, Revoir/Ergra Low Vision, Laservision Instruments B.V., Medical Workshop B.V., Bayer, Theapharma, Santen, Synga Medical, Tramedico B.V., Santen Pharmaceutical, D.O.R.C., ChipSoft, Low Vision Totaal.

All funding organizations provided unrestricted grants and had no role in the design or conduct of this research described.

© Mays Talib (maystal@gmail.com), 2022
No part of this thesis may be reproduced in any form without written permission from the author.

INHERITED RETINAL DEGENERATIONS: CLINICAL CHARACTERIZATION ON THE ROAD TO THERAPY

Proefschrift

ter verkrijging van
de graad van doctor aan de Universiteit Leiden
op gezag van rector magnificus prof. dr. ir. H. Bijl,
volgens besluit van het college voor promoties
te verdedigen op dinsdag 25 januari 2022
klokke 13:45
door

Mays Talib

Geboren te Al-Karg, Irak
In 1990

Promotoren:
Prof. dr. C.J.F. Boon
Prof. dr. N.E. Schalij-Delfos

Copromotor:
Dr. J. Wijnholds

Promotiecommissie:
Prof. dr. M.J. Jager (secretaris)
Prof. dr. A.M. Aartsma-Rus
Prof. dr. R.E. MacLaren (*University of Oxford, UCL Institute of Ophthalmology*)
Prof. dr. R.W.J. Collin (*Radboud universitair medisch centrum*)

Voor mijn ouders

LIST OF ABBREVIATIONS

ACD	anterior chamber depth
ADRP	autosomal dominant retinitis pigmentosa
AF	autofluorescence
ARRP	autosomal recessive retinitis pigmentosa
AZOOR	acute zonal occult outer retinopathy
BCVA	best-corrected visual acuity
BCEA	bivariate contour ellipse area
CF	counting fingers
CFC	cystoid fluid collections
CFT	central foveal thickness
CHM	choroideremia
CI	confidence interval
CME	cystoid macular edema
COD	cone dystrophy
CORD	cone-rod dystrophy
CRB1	Crumbs 1
CRISPR	clustered regularly interspaced short palindromic repeats
CRT	central retinal thickness
CSL	cone sensitivity loss
DA	dark-adapted
dB	decibel
DNA	deoxyribonucleic acid
ELM	external limiting membrane
EMA	European Medicines Association
ERG	electroretinography
ERM	epiretinal membrane
ETDRS	Early Treatment Diabetic Retinopathy Study
EZ	ellipsoid zone
FAF	fundus autofluorescence
FAZ	foveal avascular zone
FD	flow density
FDA	Food and Drug Administration
FfERG	full-field electroretinography
FST	full-field stimulus testing
FTMH	full-thickness macular hole
GCL	ganglion cell layer
GI	genetic isolate
GVF	Goldmann visual field
HM	hand motion

ILM	inner limiting membrane
INL	inner nuclear layer
IPL	inner plexiform layer
iPSC	induced pluripotent stem cells
IQR	interquartile range
IRD	inherited retinal dystrophy
ISCEV	International Society for Clinical Electrophysiology of Vision
IZ	interdigitation zone
LA	light-adapted
LCA	Leber congenital amaurosis
LogMAR	logarithm of the minimal angle of resolution
LP	light perception
LRAT	Lecithin:retinol acetyltransferase
MAIA	macular integrity assessment
MD	mean deviation
MP	microperimetry
NLP	no light perception
OCT	optical coherence tomography
OCTA	optical coherence tomography angiography
ONL	outer nuclear layer
OPL	outer plexiform layer
ORF15	open reading frame 15
P-AI	participation and activity inventory
PPRPE	para-arteriolar preservation of the retinal pigment epithelium
PSD	pattern standard deviation
RD	retinal dystrophy
REP-1	Rab escort protein 1
RHO	rhodopsin
RP	retinitis pigmentosa
RPA	retinitis punctate albescens
RPE	retinal pigment epithelium
RPE65	RPE specific protein 65 kDa
RPGR	retinitis pigmentosa GTPase regulator
SD	standard deviation
SD-OCT	spectral domain optical coherence tomography
SE	standard error
SER	spherical equivalent of the refractive error
SPC	subcapsular posterior cataract
VA	visual acuity
VF	visual field
XLRP	X-linked retinitis pigmentosa

CONTENTS

Chapter 1. General introduction **11**

Chapter 2. *CRB1*-associated retinal dystrophies **49**

2.1 Genotypic and phenotypic characteristics of *CRB1*-associated retinal dystrophies: A long term follow-up study 51
Ophthalmology 2017;124(6):884-895

2.2 *CRB1*-associated retinal dystrophies in a Belgian cohort: Genetic characteristics and long-term clinical follow-up 85
Br J Ophthalmol 2021; online ahead of print

2.3 Defining inclusion criteria and endpoints for clinical trials: A prospective cross-sectional study in *CRB1*-associated retinal dystrophies 115
Acta Ophthalmol 2021;99(3):e403-e414

Chapter 3. Choroideremia **147**

3.1 Long-term follow-up of patients with choroideremia with scleral pits and tunnels as a novel observation 149
Retina 2018;38(9):1713-1724

3.2 Outcome of full-thickness macular hole surgery in choroideremia 171
Genes 2017;8(7):187

Chapter 4. *RPGR*-associated retinal dystrophies **183**

4.1. Clinical and genetic characteristics of male patients with *RPGR*-associated retinal dystrophies: A long-term follow up study 185
Retina 2019;39(6):1186-1199

4.2 The spectrum of structural and functional abnormalities in female carriers of pathogenic variants in the *RPGR* gene 215
Invest Ophthalmol Vis Sci 2018;59(10):4123-4133

Chapter 5. ***LRAT*-associated retinal dystrophies** **245**

5.1. Long-term follow-up of retinal degenerations associated with *LRAT* mutations and their comparability to phenotypes associated with *RPE65* mutations 247
Transl Vis Sci Technol 2019;8(4):24

Chapter 6. ***RHO*-associated retinitis pigmentosa** **273**

6.1. Clinical characteristics and natural history of *RHO*-associated retinitis pigmentosa: A long-term follow-up study 275
Retina 2021;41(1):213-223

Chapter 7. **General Discussion** **299**

Chapter 8. English Summary 355
Dutch Summary (Nederlandse samenvatting) 363
Acknowledgments 371
About the author 377
List of publications 381

1.

GENERAL INTRODUCTION

Partly adapted from: Talib M[1], Van Cauwenbergh C[2,3], Boon CJF[1,4] (in preparation; expected release date December 23rd, 2021). Non-syndromic inherited retinal disease. In *Practical Genomics for Clinical Ophthalmology*. Elsevier.

1 Department of Ophthalmology, Leiden University Medical Center, The Netherlands;
2 Department of Ophthalmology, Ghent University & Ghent University Hospital, Belgium;
3 Center for Medical Genetics, Ghent University & Ghent University Hospital, Belgium;
4 Department of Ophthalmology, Amsterdam UMC, University of Amsterdam, Amsterdam, The Netherlands.

1. ANATOMY AND PHYSIOLOGY OF THE EYE

As light enters the eye, its waves are refracted by several structures. These waves cross a path through the cornea, the aqueous humor of the anterior chamber, the lens, the vitreous humor, eventually reaching the retina, where the focal point lies in the macula. In the retina, photons are converted to an electrical signal through a cascade of processes, and the collection of electrical signals is converted to an image in the visual cortex of the brain.

Two major components that determine the focal point at which the light waves converge, are the corneal radius of curvature, and the axial length of the eye. In emmetropic eyes, the focal point to which light waves converge lies on the retina. In eyes with a long axis (>26 mm), i.e. myopic eyes, the focal point lies in front of the retina. In eyes with a short axis (<20 mm), i.e. hyperopic eyes, this point lies behind the retina.

1.1 The vitreous

Occupying 80% of the eye volume, the healthy vitreous is a clear substance composed of water, hyaluronic acid, and collagen. Its anterior surface is firmly attached to the lens of the eye, and its posterior surface is attached to the retinal vessels, the macula of the retina, and the optic nerve. Other sites of attachment include the vitreous base, which is located posterior to the junction between the retina and the pars plana of the ciliary body (the ora serrata). Various pathological processes, such as inflammation, may affect the clarity of the vitreous.

1.2 The neurosensory retina

The neurosensory retina consists of 8 distinct layers (Figure 1), each consisting of synapses or nuclear bodies, along with supporting cells. Furthermore, the neuroretina contains two "membranes", the inner limiting membrane and external limiting membrane, which are not true membranes but junctional systems connecting retinal cells. The central 5.5 mm of the neurosensory retina is the macula, and the fovea is the central 1.5 mm of the macula. Light travels through all retinal layers in order to reach the light-sensitive cells of the retina, i.e. the photoreceptors, which may be rods (95% of photoreceptors; responsible for light-sensitivity in low-luminance environments and for peripheral vision), or cones (5% of photoreceptors; responsible for spatial acuity and color vision).[1] A third type of photoreceptor, the retinal ganglion cell, is not involved in the visual pathway but is involved in mechanisms such as pupillary responses, and circadian rhythm. Figure 2 shows the normal spatial distribution of rods and cones. The highest cone density is in the very center of the macula, the fovea, which contains no rods, allowing the fovea to enable high visual acuity, high contrast vision, and color vision. Although the cone density decreases rapidly outside the fovea, 90% of cones lie outside the fovea. The highest rod density is approximately 15° away from the fovea. As the peripheral retina contains predominantly rod cells, the peripheral retina provides night vision and the peripheral visual field.

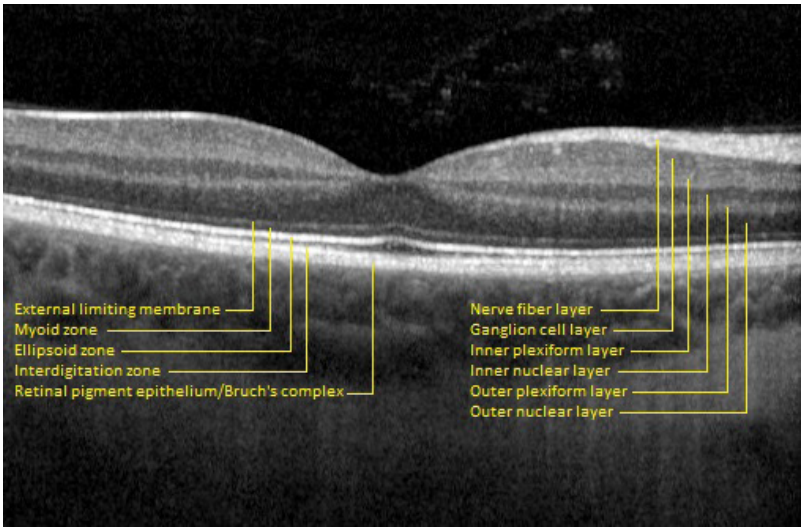

Figure 1. A cross section of the retina on spectral-domain optical coherence tomography, showing (from top-down) the inner limiting membrane, the retinal nerve fibre layer, the ganglion cell layer (containing the cell bodies of the ganglion cells), the inner plexiform layer (containing the synapses between ganglion cells and the bipolar cells), the inner nuclear layer (containing the cell bodies of the bipolar cells), the outer plexiform layer (containing the synapses between the bipolar cells and the photoreceptor cells), the outer nuclear layer (containing the cell bodies of photoreceptor cells), the external limiting membrane, the myoid zone (consisting of endoplasmic reticulum), the ellipsoid zone (i.e. the inner/outer segment junction, consisting of mitochondria, cilia, and inner discs), the outer segments, the interdigitation zone, and the retinal pigment epithelium/Bruch's complex.

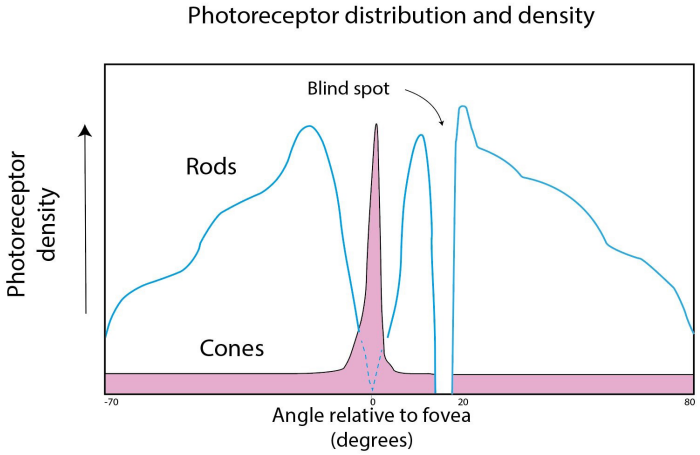

Figure 2. The spatial distribution of rod and cone photoreceptors in the normal human retina. Density curves show the highest cone density in the fovea centralis, where rods are absent. Away from the fovea centralis, cone density rapidly decreases, while rod density rapidly increases, reaching its maximum at approximately 15° eccentricity from the fovea. Rods further spread over a large area of the retina. (Adapted from © Brian Wandell, Foundations of Vision, Stanford University [http://foundationsofvision.stanford.edu/chapter-3-the-photoreceptor-mosaic])

Photoreceptors consist of four major compartments (Figure 3): the outer and inner segments, the cell body, and the synaptic terminal. The outer segment contains up to 1000 discs, stacked like pancakes, which contain the light-sensitive visual pigments. The outer and inner segments are separated by a ciliary transition zone, or the connecting cilium. The connecting cilium is the site of transport of lipids and proteins from the inner to the outer segment, and functions as a barrier between the differing plasma membrane compositions of the inner and outer segment. The photoreceptor inner segment contains mitochondria, which produce chemical energy (adenosine triphosphate).[2] These mitochondria, along with the outer segment discs, form the inner-outer segment junction. The photoreceptor inner segment further contains the Golgi apparatus, and endoplasmic reticulum, both responsible for protein synthesis. This area, visible on spectral domain optical coherence tomography as the "ellipsoid zone",[3] has been demonstrated to be of particular clinical relevance in predicting visual outcome.

Important support cells for retinal neurons are the Müller glial cells, which support homeostatic and metabolic cell functions, and maintain structural stability by regulating the tightness of the blood-retina barrier.[4] Their cell bodies are located in the inner nuclear layer, and their endfeet attach to the photoreceptors, forming adherens junctions at the external limiting membrane, at the level between the photoreceptor inner segment and the photoreceptor cell body.

1.3 The retinal pigment epithelium

The retinal pigment epithelium, or RPE, is a single layer of cells containing melanin pigment. It contributes to retinal function through a) visual pigment regeneration; b) light absorption; c) forming of the outer blood-retinal barrier through tight junctions; d) phagocytosis of rod and cone outer segments, regenerating the outer segments with a daily approximately 10% renewal rate; and e) molecular exchanges at the apical villi, such as water and ion transport ensuring the proper ionic environment. The maintenance of the ionic homeostasis occurs through various electrogenic pumps, such as the Na^+/K^+-ATPase pump.[5] The basal surface of the RPE lies on the Bruch's membrane, a thin elastin- and collagen-rich layer between the RPE and the fenestrated choroidal capillaries. Bruch's membrane acts as a molecular sieve, regulating the exchange of molecules and fluids, nutrients, oxygen, and metabolic waste.[6]

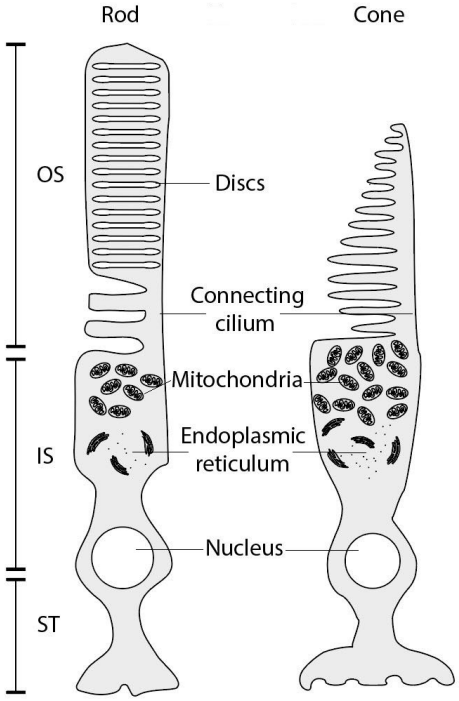

Figure 3. Schematic overview of the rod (left) and cone (right) photoreceptor anatomy. Light molecules, or photons, enter the photoreceptors through the inner segment first, and are then transmitted to the outer segment, which contains the visual pigments. OS = outer segment. IS = inner segment. ST = synaptic terminal. (Adapted from Cote RH, 2006[7])

1.3.1 The visual cycle

Visual pigment (chromophore: rhodopsin in rods; cone opsin in cones) is used in the process of photo-activation, and it must be regenerated in order to enable the next cycle of photo-activation. This regeneration occurs via the visual cycle, which takes place at the level of the photoreceptors and the RPE. As a photon enters the rod or cone photoreceptor, this stimulates a configurational change of 11-cis retinal opsin (the chromophore) into all-trans retinal.[8] In the RPE, this is converted to all-trans retinol, which is then modified to all-trans retinyl ester by lecithin retinol acyl transferase (protein LRAT). All-trans retinyl ester is in turn converted to 11-cis retinol by RPE-specific 65 kDa protein (protein RPE65). In the final step of the cycle, 11-cis retinol is converted back into 11-cis retinal by retinol dehydrogenase 5 (protein RDH5), which is then transported to the photoreceptor, where the next cycle starts upon activation by a photon.

This classical visual cycle is present in rods and cones, however in cones, an additional cone-specific, or non-canonical visual cycle, takes place. This alternative cycle is independent of the RPE, and instead relies on Müller glial cells in the retina.[9]

1.3.2 The choroid

Blood enters the choroid, the vascular layer of the eye, through the posterior ciliary arteries. The choroid supplies the retina, one of the most metabolically demanding tissues in the human body. The choroid has the highest blood flow rate of any tissue in the body. The outer layer of the choroid is known as the Haller layer, which contains large-caliber choroidal vessels. These vessels branch into smaller-caliber vessels and precapillary arterioles, forming the Sattler layer. These non-fenestrated vessels distribute blood over the breadth of the choroid, debouching into the capillary meshwork, or choriocapillaris, the most inner layer of the choroid. After passing the fenestrated choriocapillaris, blood drains into venules, which fuse to form the collecting channels of the four or five vortex veins, which eventually drain into the superior and inferior ophthalmic veins. The choroid is at its thickest (normally 0.22 mm) posteriorly, and thins as it moves anteriorly towards the ora serrata (normally 0.1 mm).

2. INHERITED RETINAL DEGENERATIONS

Inherited retinal degenerations (IRDs) comprise a collection of degenerative diseases, generally leading to visual dysfunction. IRDs are characterized by the usually progressive and sometimes stationary dysfunction of rods and/or cones. Patients may experience an array of symptoms, such as night blindness (nyctalopia), visual field deterioration, blurriness of vision, and a disturbance in color vision. These diagnoses generally have a profound impact on patient's lives, progressively affecting their social interactions, independence, professional functioning, and mobility.[10] Patients are often uncertain of their prognosis, questioning if and when they will go blind, and whether they will pass this disease onto their children.

More than 260 disease genes have been identified to date in association with IRD, each gene accounting for a portion of patients [RetNet, update of November 11, 2019, URL: sph.uth.edu/retnet/]. Moreover, IRDs can be categorized based on the phenotype and/or the type of photoreceptor which is primarily affected, the most common form being retinitis pigmentosa (RP), a rod-cone dystrophy. Other progressive forms include cone(-rod) dystrophy, isolated macular dystrophies, choroideremia, and Leber congenital amaurosis. Each IRD may be caused by different genes, and individual genes may be associated with several distinct forms of an IRD. Due to this clinical and genetic overlap, establishing a distinct diagnosis may be challenging in some cases, and can be subject to debate. While each IRD can be roughly distinguished clinically depending on the type of photoreceptor cells that are primarily affected, together they form a spectrum with variable presentation and severity, with an underlying broad range of different affected genes.

2.1 Retinitis pigmentosa

Retinitis pigmentosa (RP) is a group of progressive inherited retinal dystrophies (IRDs) in which rod photoreceptor degeneration precedes cone photoreceptor degeneration. Its worldwide incidence is estimated at 1:3500-1:4000,[11] but depending on the geographic location, incidence reports have varied between 1:9000 and 1:750.[12, 13] In addition to non-syndromic forms of RP, that encompass 65-70% of all RP cases, there are forms also displaying non-ocular signs, and more than 30 different RP-associated syndromes have been described.[11, 14] The most frequent syndromic form is Usher syndrome, which manifests with congenital hearing impairment followed by the development of RP in early adolescence.[15] Non-syndromic RP is a clinically and genetically heterogeneous disease entity, and its presentation may partially overlap with other IRDs, such as advanced cone-rod dystrophy. Furthermore, over 87 genes have been identified in association with RP, and individual genes may be associated with several distinct forms of an IRD, such as RP and Leber congenital amaurosis.

2.1.1 Presentation

The age at which symptoms present and the speed at which they evolve are variable and depend at least partially on the mode of inheritance and on the gene involved. The autosomal dominant forms of RP (ADRP) are usually the mildest, often with patients first experiencing symptoms in mid-adulthood, although symptom presentation in early childhood has also been described.[16, 17] Autosomal recessive (ARRP) and X-linked RP (XLRP) generally have a more severe disease course with an earlier onset, often within the first decade of life.[18] Typically, the initial symptom noticed by patients and/or their parents is decreased night vision (nyctalopia). In today's artificially lit environments, it may take years for patients to notice a disturbance in night vision. Moreover, these symptoms may be subtle, and patients may recognize these symptoms only when comparing their night vision to that of unaffected individuals. Often, patients report having first noticed nyctalopia during adolescence.[11] Loss of (mid-)peripheral visual field usually becomes apparent in adolescence or (young) adulthood, and patients may compensate for visual field loss by scanning their environment. In later stages, a central vision decrease, color vision disturbances, and light aversion may be present. Patients may also experience photopsia, which can manifest as static noise, background glow, flashes, or as static or moving phosphenes or shapes.[19] Depending on the location and frequency of these photopsia, they could disturb remaining vision. Photopsia may occur in early and in advanced disease stages,[19] and they have been postulated to be manifestations of spontaneous self-activation of impaired retinal cells or potentially as a result of retinal remodeling due to photoreceptor degeneration.[20]

2.1.2 Fundus features

Fundus examination in the early stage of disease can be normal, as changes may not yet be present or may be subtle. Typical features on fundoscopy in mid-stage RP include waxy optic disc pallor, which may be limited to the temporal optic disc in the early disease stage, vascular attenuation,

variable degrees of retinal atrophy, intraretinal bone-spicule-shaped pigment migrations, and retinal pigment epithelium (RPE) alterations or atrophy that typically start in the midperiphery and progress in a centripetal fashion (Figure 4). As the disease advances, RPE alterations appear in the posterior pole. The central macula is often spared until the late disease stages. In ADRP, the retinal degenerative changes may be sectorial, usually affecting the lower quadrants. Additional fundus features that may be present include cystoid macular edema (up to 50% of overall RP cases),[21, 22] cellophane maculopathy due to an epiretinal membrane (up to 35%),[23, 24] optic disc drusen (approximately 9% of RP cases) or hamartomas.[25] These features can be present in larger proportions depending on the gene-specific subtype of RP. Female carriers of XLRP may exhibit the pathognomonic tapetoretinal reflex, a golden-metallic sheen in the posterior pole. Some female carriers of XLRP develop symptoms and typical RP-associated fundus changes with advancing age.[26-30]

Non-retinal features that may be present include posterior subcapsular cataract (approximately 45% of RP patients),[31] and refractive error which, depending largely on the gene involved, could be myopia or hyperopia.[32] Vitreous abnormalities may be present, such as dust-like particles. Although nystagmus has been described, this is more closely associated with severe early-onset retinal dystrophies, such as Leber congenital amaurosis, rather than RP.[33]

2.2 Leber congenital amaurosis

Leber congenital amaurosis, or LCA, is the most severe form of IRD, with an onset that usually occurs congenitally or in infancy. Both rod and cone function are not detectable from infancy. The prevalence of LCA has been estimated at 1:100.000-1:30.000 births,[34-36] depending on the geographic location, and comprising approximately 5% of all IRDs. LCA is more prevalent in countries where consanguinity is more common.[37, 38]

To date, over 25 genes have been implicated in association with LCA. It is mostly inherited in the autosomal recessive form, but autosomal dominant (*IMPDH1* gene) and X-linked inheritance (*CRX* gene) have been described.

In literature, the terms LCA, early-onset IRD, and early-onset severe IRD, have been used interchangeably, to a certain extent. However, in the latter two phenotypes, more preservation of visual function into childhood is observed, along with some preservation of rod and/or cone responses on the electroretinogram. Establishing an LCA diagnosis is complicated by several factors, including difficulties associated with the ophthalmological examination of infants, and patient delay. This renders it nearly impossible in some cases to retrospectively distinguish between LCA and early-onset severe IRD, and a considerable clinical and genetic overlap between these entities should be taken into account.

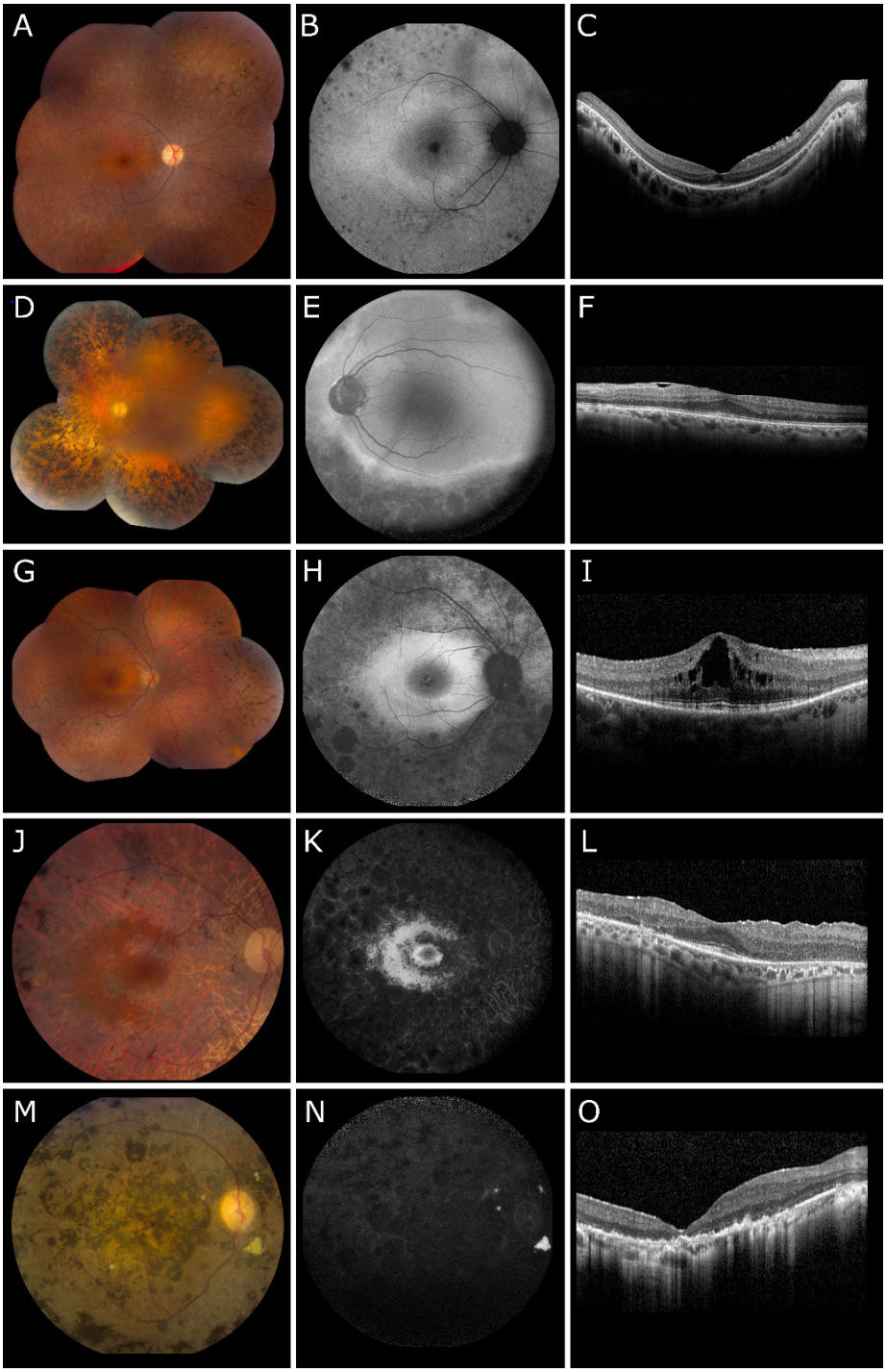

Figure 4. Multimodal imaging in non-syndromic retinitis pigmentosa (RP). A-C. A 20-year old North-African woman with autosomal recessive RP due to a homozygous mutation in the *IDH3A* gene (c.524C>T; p.(Ala175Val)).

Her nyctalopia and visual field symptoms started at the age of 14 years. Fundus photography (**A**) showed optic disc pallor, attenuated arteries, and bone-spicule-like pigmentation and mottled retinal pigment epithelium in the periphery. Fundus autofluorescence (FAF; **B**) shows round and mottled hypo-autofluorescence in the midperiphery, with sparing of the posterior pole. Spectral-domain optical coherence tomography (SD-OCT; **C**) showed an epiretinal membrane, and some relative foveal sparing of the outer nuclear layer (ONL), external limiting membrane (ELM), and ellipsoid zone (EZ), with thinning of these layers in the para- and perifovea. Corresponding best-corrected visual acuity (BCVA) was 20/22 in OD and 20/25 in OS. **D-F.** A 60-year old Caucasian man with RP. Next generation sequencing revealed no conclusive molecular result on the genetic basis for RP. Fundus photography (**D**) showed a pale optic disc with peripapillary atrophy, vascular attenuation, a relatively spared posterior pole, with atrophy and dense bone-spicule-like pigmentation in the periphery. FAF (**E**) revealed abnormalities in regions appearing relatively spared on fundoscopy, showing hypo-autofluorescent lesions with a hyperautofluorescent border, encroaching upon the posterior pole from the inferior retina. SD-OCT (**F**) showed an epiretinal membrane, relative preservation of the ONL, ELM, and EZ, with some disorganization of the interdigitation zone. He had visually significant posterior subcapsular cataract in both eyes, but considerably more in OS, and BCVA was 20/25 in OD and 20/29 in OS. After cataract surgery 2 years later, his BCVA improved to 20/20 in OD and 20/25 in OS. **G-I.** A 38-year old female patient with autosomal dominant RP due to a mutation in the *RHO* gene (c.541G>A; p.(Glu181Lys)). Fundus photography (**G**) revealed the typical RP-associated changes, which were more abundant in the inferior hemisphere. The posterior pole and the superior retina were relatively spared. FAF (**H**) showed mottled hypo-autofluorescent changes in the central macula and in the midperiphery extending into the posterior pole. In the inferior midperiphery, sharply circumscribed patches of absent autofluorescence are visible. A perimacular hyperautofluorescent ring is visible. The SD-OCT (**I**) shows relative preservation of the outer retina, with cystoid macular edema mostly in the inner nuclear layer, with a few cystoid spaces in the ONL and the ganglion cell layer. **J-L.** A 60-year old Middle-Eastern man with autosomal recessive RP due to a homozygous mutation in the *FAM161A* gene (c.1138T>C; p.(Arg380*)). He had been experiencing nyctalopia complaints since the age of 35-40 years. The fundus (J) showed optic disc pallor, vascular attenuation, bone-spicule-like pigmentation extending into the posterior pole, and generalized retinal atrophy with relative sparing in the central macula and the temporal posterior pole. The latter is also visualized on FAF (**K**). Due to the relative foveal sparing of the ONL, ELM, and EZ, as seen on SD-OCT (**L**), the corresponding best-corrected visual acuity was 20/20 OU. **M-O.** A 37-year old man with RP, and no other affected family members. Molecular analysis however revealed autosomal dominant RP due to a pathogenic mutation in the *NRL* gene (c.654del; p.(Cys219Valfs*4)). This incongruence with the pedigree raises suspicion that this is a de novo mutation. Fundus examination (**M**) revealed end-stage RP, with atrophy and dense intraretinal pigment migration in the posterior pole, and several hamartomas around the optic disc and in the posterior pole. FAF (**N**) showed barely any remaining autofluorescence, but hyperautofluorescence of the peripapillary hamartomas. SD-OCT (**O**) showed profound atrophy of the ONL and atrophy and disorganization of the hyperreflective outer retinal bands. The corresponding BCVA was 20/400 in OD and finger counting vision in OS.

2.2.1 Presentation

The typical presentation of LCA consists of severe and early loss of visual function, sensory nystagmus, amaurotic pupils, and non-detectable rod and cone function on the electroretinogram. Visual acuity usually ranges between 20/400 to light perception or even no light perception. A patient's parents usually notice the nystagmus or a lack of fixation. Patients may exhibit the oculodigital sign of Franceschetti, which is a repetitive and deep poking or pushing into the eye. This may lead to orbital fat atrophy, resulting in enophthalmos. Other signs include photoaversion and nyctalopia. Associated phenotypic features include a high refractive error, either hyperopia

or myopia, again depending on the gene involved, cataracts, and keratoconus. The latter may be resulting from the oculodigital sign.
Mental retardation has been described in a subset of patients with LCA.[39] The association between mental retardation and LCA has been arguable, as congenitally blind and mentally retarded patients may have a syndromic disease, such as Batten disease or peroxisomal diseases, which may initially only exhibit an LCA-like ocular phenotype, with other features occurring later in life.[40, 41]

Several forms of LCA, most notably *RPE65*-associated LCA, have been a focus of interest for gene-based therapeutic studies, as the relatively preserved retinal structure indicates the presence of viable photoreceptors, despite the severely affected visual function.[42] This dissociation of structure and function has also been described in *LRAT*-associated and *CEP290*-associated LCA.[43] The extensive studies in gene therapy for *RPE65*-associated LCA have resulted in the development of the first-ever FDA-approved clinical gene therapy, voretigene neparvovec (Luxturna®).

2.2.2 Fundus features

In infancy, patients may have a normal appearing fundus. Early abnormalities include macular atrophy, which may later progress to an appearance resembling retinitis pigmentosa, such as optic disc pallor and retina arteriolar narrowing. However, some patients maintain a relatively normal appearance of the retinal vessels and optic disc, into the third decade of life, despite an early maculopathy.[41] Other fundus features include a macular coloboma, choroidal sclerosis, optic disc drusen, and salt-and-pepper-like changes of the RPE.

2.3 Cone dystrophies and cone-rod dystrophies

Cone dystrophies are a heterogeneous group of disorders involving the cone photoreceptor system, while the rod system remains normal. In some patients, the disease progression involves secondary rod involvement in later life, developing into a cone-rod dystrophy. In cone-rod dystrophies, rods are affected relatively early in the disease process, albeit to a lesser degree than cones, but both rod and cone systems are abnormal. The prevalence of cone and cone-rod dystrophies is estimated at 1:30.00 to 1:40.000.[44, 45]

Over 42 genes have been implicated in cone and cone-rod dystrophies.[46] Inheritance may be autosomal recessive, autosomal dominant, and X-linked.[47-50] Cone and cone-rod dystrophies are mostly non-syndromic, but they may occur in syndromic form, as in Bardet-Biedl syndrome.[51]

Cone dystrophies differ from macular dystrophies, such as classic Stargardt disease or vitelliform degenerations, where the degeneration is confined to the macular cones, and where the degeneration is not usually detectable on full-field electroretinography.[52]

Although impaired color vision is a feature of cone dystrophies, cone dystrophies differ from congenital color blindness (protanopia, deuteranopia, and tritanopia), as patients with congenital color blindness maintain a normal visual acuity, do not have associated retinal degeneration, and do not show progression of their disease.[53]

2.3.1 Presentation

Cone dystrophies usually present in childhood, but may present in the teenage or adult years, and are characterized by the progressive loss of visual acuity and color discrimination in all three color axes. Patients' fixation may be eccentric, as they deviate their gaze to project images on the parafoveal regions that are less affected. Other signs are hemeralopia (day blindness) and photophobia. Peripheral vision remains normal in isolated cone dystrophies, but may be affected in cone-rod dystrophies. Patients with cone-rod dystrophies may also experience nyctalopia, and in later stages, their disease may be difficult to distinguish from RP. However, the clinical course of cone-rod dystrophies has been described as more severe and more rapid than many forms of RP.[44] Patients may be myopic, particularly in X-linked cone or cone-rod dystrophies.

2.3.2 Fundus features

Fundus appearance may be fully or near-normal in early disease stages. In cone dystrophies, abnormalities may range from mild RPE alterations, to a bull's eye pattern of macular atrophy, to more extensive and severe macular atrophy. Temporal pallor of the optic disc may be seen. In cone-rod dystrophies, these central abnormalities are accompanied by vascular attenuation, and various degrees of retinal atrophy and bone-spicule-like hyperpigmentation in the peripheral retina.

2.4 Choroideremia

Choroideremia is an X-linked chorioretinal dystrophy, with an estimated prevalence of 1:50.000-100.000, depending on the geographic location, and with a preponderance in the European population.[54] It is caused by mutations in *CHM*, a gene encoding Rab escort protein 1. This protein is an essential mediator of intracellular protein trafficking in photoreceptors and the RPE.[55]

2.4.1 Presentation

Symptoms usually present in childhood or adolescence. Male patients experience nyctalopia, followed by progressive visual field restriction. Visual acuity decline is slow, but rapidly ensues in the fifth to sixth decade of life.[56] Although more severe cases have been reported, patients usually reach legal blindness in mid-to-late adulthood.[56, 57]

Female carriers of *CHM* mutations typically remain asymptomatic and do not have abnormal electroretinographic signals.[58] However, some female carriers may experience nyctalopia.[56, 59, 60]

2.4.2 Fundus features

In affected male patients, the retina initially shows mottled areas of pigmentary changes in the equatorial region and in the macula. The degeneration gradually progresses and eventually manifests as widespread and sometimes serrated areas of atrophy of the retina, RPE, and choriocapillaris, in combination with scattered coarse intraretinal clumps of hyperpigmentation, which may even be observed in early childhood in severe cases.[61, 62] This results in a characteristic pale color of the fundus, due to the translucence of the sclera. Typically, larger choroidal vessels are preserved. The fovea is spared until later in the disease, and a residual island of foveal sparing is a frequent finding, although marked vision loss due to progression of foveal atrophy may ensue above the age of 50.[63] Female carriers of *CHM* mutations may show some retinal abnormalities, such as patchy or mottled pigmentary changes, or even RPE and choriocapillary atrophy,[58, 59] despite having no symptoms.

2.5 Macular dystrophies

The group of macular dystrophies encompasses a wide range of retinal dystrophies in which the degeneration is – at least initially – confined to the macular photoreceptors.[64] Therefore, this degeneration is usually not detectable on full-field electroretinography, but may be detectable on the multifocal electroretinogram. The most prevalent inherited macular dystrophy is Stargardt disease.[65,66] Best vitelliform macular dystrophy and adult-onset foveomacular vitelliform dystrophy are frequently encountered forms of autosomal-dominant macular dystrophy.[67]

2.5.1 Presentation

The presentation of symptoms may differ between each type of macular dystrophy. Stargardt macular dystrophy shows a highly variable age at symptom onset and variable severity.[65, 66, 68] Most cases present in childhood or early adulthood with central vision loss,[69] but onset in late-adulthood (age ≥ 45 years) has been described as well, usually accompanied by metamorphopsia rather than visual acuity loss.[65, 68, 70] In autosomal dominant Best vitelliform macular dystrophy, the age at onset is variable, and patients may present with reduced visual acuity, or with photophobia, metamorphopsia, and even night blindness.[67] In adult-onset foveomacular vitelliform dystrophy, the age at diagnosis is usually after the age of 40.[71] In central areolar choroidal dystrophy, early disease stages may be difficult to diagnose, due to the discrete and aspecific retinal changes, but later disease stages may be accompanied by profound central vision loss.[72] In North Carolina macular dystrophy, symptoms present in childhood, and are, along with the fundus features, typically stable throughout later years.

2.5.2 Fundus features

In Stargardt disease, characteristic irregular yellow-white fundus flecks are visible in the posterior pole, which later progress to chorioretinal atrophy.[65]

Best vitelliform macula dystrophy consists of several stages, in which the earliest is characterized by a normal fovea or subtle RPE alterations, followed by the "scrambled-egg" stage, a pseudohypopyon stage, ultimately progressing to chorioretinal atrophy. In 2-9% of patients with Best vitelliform macular dystrophy, choroidal neovascularization occurs.[67] The typical feature in adult-onset foveomacular vitelliform dystrophy is a solitary, slightly elevated, yellow-white, round to oval lesion. It may be complicated by choroidal neovascularization.

In some forms of macular dystrophy, drusen may be present, which may be small (≤63 μm), intermediate-sized (>63 μm and ≤125 μm), or large (>125 μm). Some forms of macular dystrophy may mimic age-related macular degeneration (AMD), as in Mallatia Leventinese, characterized by drusen, or Sorsby fundus dystrophy, characterized by choroidal neovascularization.[64] Central areolar choroidal dystrophy presents with aspecific RPE changes in its early stages, but progresses to a profound atrophy of the RPE and outer retina in the macula, that may easily be confused with geographic atrophy in AMD.[72]

3. CLINICAL EVALUATION OF RETINAL STRUCTURE IN INHERITED RETINAL DYSTROPHIES

The advent of novel therapeutic opportunities necessitates a thorough clinical insight in the natural history of inherited retinal dystrophies, further emphasizing the importance of longitudinal clinical examinations. The arrival of experimental therapeutic options has led to a paradigm shift: where, in the past, extensive examination at regular intervals in this patient population may have seemed unnecessarily burdensome to the patient, with no significant impact on the ophthalmologist's treatment policy, nowadays the regular and extensive examination of these patients can aid in natural history studies investigating the phenotypic disease spectrum, potential windows of opportunity, and the most sensitive parameter for documenting disease progression and treatment effect. The most common clinical parameters are described below.

3.1 Spectral-domain optical coherence tomography

Spectral-domain optical coherence tomography (SD-OCT) enables near-histological evaluation of the retinal architecture and the integrity of the photoreceptor structures in the macula. The photoreceptor nuclei are located in the outer nuclear layer. The external limiting membrane (ELM), which is the first hyperreflective outer retinal band, is thought to represent the adherens junctions between Müller cells and outer part of the photoreceptors.[73] The second hyperreflective outer retinal band, the so-called ellipsoid zone, represents the mitochondria-rich photoreceptor inner segments,[3, 74] but was previously thought to represent the inner segment/outer segment junction.[75] The photoreceptor outer segments co-localize with the interdigitation zone, the third hyperreflective outer retinal band, previously known as the cone outer segment tips line.

As photoreceptors degenerate, disorganization of the hyperreflective outer retinal bands occurs, corresponding with visual acuity loss,[76] accompanied by thinning of the outer nuclear layer. These changes are observed in the peripheral macula first, and encroach upon the fovea, showing a "transitional zone" between degenerated and relatively spared outer retina. Retinal sensitivity has been shown to decline faster in this transition zone than in other regions of the retina.[77] While the inner retinal layers may remain well-preserved, thinning of the ganglion cell layer has been described in advanced disease stages,[78] as well as thickening of the inner retina.[79, 80] The latter may be due to neuroglial remodeling reactive to photoreceptor loss, and may precede eventual inner retinal thinning in end-stage RP. With advanced retinal and RPE atrophy, and more so in cases with associated high myopia (such as in with XLRP), choroidal thinning and even posterior staphylomas may be observed.[81]

Optical coherence tomography angiography (OCTA) is a novel non-invasive imaging technique, that applies motion contrast between sequential OCT b-scans captured at the same cross-section. As a result, capillary blood flow can be visualized in the inner vascular plexus, the deep retinal vascular plexus, and the choriocapillaris.[82] Although it is prone to artifact, and may miss areas of slow blood flow (threshold artefacts), it is particularly useful in visualizing certain pathologies, such as choroidal neovascularization, or central serous chorioretinopathy.[83] Its utility in retinal dystrophies is undetermined.

3.2 Fundus autofluorescence

Short-wavelength fundus autofluorescence (FAF) provides information on the integrity and function of the RPE, through the visualization of lipofuscin (Figure 4). Lipofuscin is material derived from degraded photoreceptor outer segments that have been shed from photoreceptors and phagocytosed by the RPE, as part of a physiological outer segment turnover. Short excitation wavelengths (488 nm) of blue light will cause lipofuscin to autofluoresce, and light emitted at wavelengths between 500-800 nm is captured on the image. Areas of lipofuscin accumulation will appear hyperautofluorescent, while areas of atrophic RPE will appear hypo-autofluorescent. In RP, a perimacular concentric hyperautofluorescent ring or arc is seen in some patients, and is considered the transition zone between degenerated and relatively spared retina.[84] When overlaying a FAF image with a concurrent SD-OCT scan, the hyperreflective ring indeed colocalizes with an area of outer nuclear layer thinning and severe attenuation of the ellipsoid zone, with relative sparing of the photoreceptor structures internal to the ring. This ring often constricts progressively over time.[84] Double concentric hyperautofluorescent rings have also been described.[85] The origin of the hyperautofluorescence remains under debate. It has been postulated to stem from the increased rate of outer segment phagocytosis at the RPE level,[84, 86] or, more recently, from the accelerated lipofuscin synthesis pathway in compromised photoreceptors or photooxidation of liposfuscin.[87] Other RP-associated abnormalities are hypo-autofluorescent changes that can be granular, mottled, or bone-spicule-shaped.

An alternative mode of FAF is near-infrared-autofluorescence, which visualizes ocular melanin (as opposed to lipofuscin) through a longer excitation wavelength (787 nm). In turn, emitted light at wavelengths above 810 nm is captured on image.[88] Near-infrared-FAF may be particularly useful in patients with cataracts, severe photophobia, or a decreased capacity for attention (e.g. children), as image acquisition with this modality is faster, excites using less visible light, at wavelengths that better penetrate media opacities. The physiological autofluorescence pattern in near-infrared FAF differs from that in short-wavelength FAF, but in some patients with RP, a hyperautofluorescent ring can be observed with both imaging modalities.[89]

3.3 Adaptive optics

Adaptive optics high-resolution imaging is a method of in vivo histology, allowing the visualization of microscopic structures in the living human retina.[90] It has been used to visualize and quantify the human cone and rod photoreceptor mosaic, RPE cells and leukocytes. Techniques for imaging rods and cones differ, and this difference is thought to be based on the smaller size of rods and/or their reduced waveguide capabilities.[91] In severe retinal degeneration, adaptive optics may confirm the presence and integrity of target cells in the retina for gene therapy, thus estimating the therapeutic potential of gene therapy on a given retina. This estimate may be based on cell density and cell reflectivity. Adaptive optics may also be useful in monitoring the safety and efficacy of experimental therapeutic strategies. As gene therapy is not expected to add photoreceptors, but rather protect the remaining photoreceptors, cell reflectivity rather than cell density has been postulated as an indicator of treatment efficacy.[92]

3.4 Fluorescein angiography and indocyanine green angiography

Fluorescein angiography allows the study of the retinal and choroidal circulation. Retinal photographs are taken following the intravenous injection of fluorescein, an orange-red fluorescing molecule that diffuses through most body tissues. Its fluorescence is visualized on camera by blue light excitation (465-490 nm). The inner and outer blood-retinal barriers, formed by the tight junctions of the retinal capillary endothelial cells, and the RPE, respectively, normally prevent fluorescein from entering the retinal vessels or the subretinal space. However, when the capillary endothelium is damaged, fluorescein leaks into the retina. When RPE is damaged, fluorescein leaks into the subretinal space and the retinal interstitium.

Indocyanine green angiography allows the study of the choroidal circulation, through the use of indocyanine green dye. This dye is almost completely (95-98%) protein-bound after intravenous injection, and consists of relatively large molecules. As a result, diffusion through the small fenestration of the choriocapillaris is limited, and indocyanine green is mostly retained in the choroid, although diffusion through the choroidal stroma and accumulation within the RPE have also been demonstrated.[93] The fluorescence of indocyanine green occurs in the infrared range (790-805 nm).

In the diagnosis and follow-up of IRDs, fluorescein angiography may be useful in the visualization of cystoid macular edema, or the classic "dark choroid" in Stargardt disease, but is otherwise of limited added use.

4. CLINICAL EVALUATION OF RETINAL FUNCTION IN INHERITED RETINAL DYSTROPHIES

4.1 Central visual function

Measures of central visual function, such as best-corrected visual acuity (BCVA) and color vision, are usually normal in early disease stages. With the progression of central cone photoreceptor degeneration, BCVA will eventually decline. The age at which the visual acuity is expected to have declined to low vision or blindness, defined by the World Health Organization as BCVA<20/67 and BCVA<20/400, respectively, depends on the diagnosis. In RP, it depends partially on the mode of inheritance and the involved gene, but may differ even within the same family. ADRP generally has the best visual prognosis, with some patients maintaining good visual acuity well into the 6th and 7th decade of life.[17, 18] XLRP and ARRP have a worse visual prognosis. Some genetic subtypes of ARRP have been shown to lead to visual impairment within the first two decades of life in half the patient population.

While determining BCVA with a Snellen chart is the most conventional way of assessing central macular function, this method uses high-contrast charts that may not detect subtle changes in central visual function. Patients can experience difficulties with central vision in lower-luminance environments and may need visual aids or computer screen adjustments in their daily life, while still maintaining a well-preserved BCVA. A potentially more sensitive but less routinely examined parameter of central visual function is contrast sensitivity, which can be measured using e.g. the Pelli-Robson contrast sensitivity chart or sophisticated grating tests. Reports on contrast sensitivity in large populations of RP patients are limited, but RP patients with normal BCVA may still have significantly reduced contrast sensitivity.[94]

Color vision disturbances may be subtle and may be observed starting from the intermediate stages of RP. Different testing modalities have different sensitivities in detecting the presence, type, and severity of the color vision disturbance. Generally, tritanopia (blue-yellow deficiency) is the most frequently and first-observed color deficiency. In later stages, protanopia (red-green deficiency) may develop, and errors may become more chaotic with progressing central macular atrophy, advancing to total color blindness.

4.2 Visual field testing and microperimetry

Visual field impairment is a hallmark symptom of RP, typically beginning with patches of sensitivity loss in the midperiphery, which gradually form a ring scotoma. This ring scotoma then extends centripetally towards the far periphery and center. In advanced disease stages, a central island of vision and a peripheral wedge of vision are seen, which may or may not be connected to each other (Figure 5). In end-stage disease, some patients retain a central island of vision. Other visual field loss patterns have been described, such as progressive concentric visual field constriction without a preceding ring scotoma, or a predilection for visual field loss in the superior hemisphere.[95] These abnormalities and their progression with time should be examined periodically with kinetic perimetry and documented. In kinetic perimetry, visual stimuli of fixed size and intensity are moved by an operator from non-seeing areas into seeing areas of the visual field. Commonly, the Goldmann perimeter is used, and in recent years semi-automated perimeters such as the Octopus 900 (Haag-Streit International, Switzerland) are also used.

Central visual field measurements in the form of static perimetry or microperimetry map the sensitivity of the central macula, using stationary stimuli at different locations within the central 10° or 30° radius of the macula, adjusting the stimulus intensity based on the patient's response. This may be particularly useful in cone (-rod) dystrophies and macular dystrophies. However, in retinitis pigmentosa, central visual field measurements may remain within normal range in early disease stages. In microperimetry, this sensitivity is correlated to the exact location in the macula in real-time, and fixation stability is assessed. Microperimetry is particularly advantageous over conventional static perimetry in patients with fixation loss,[96] and it may detect macular sensitivity changes before BCVA changes occur.[97]

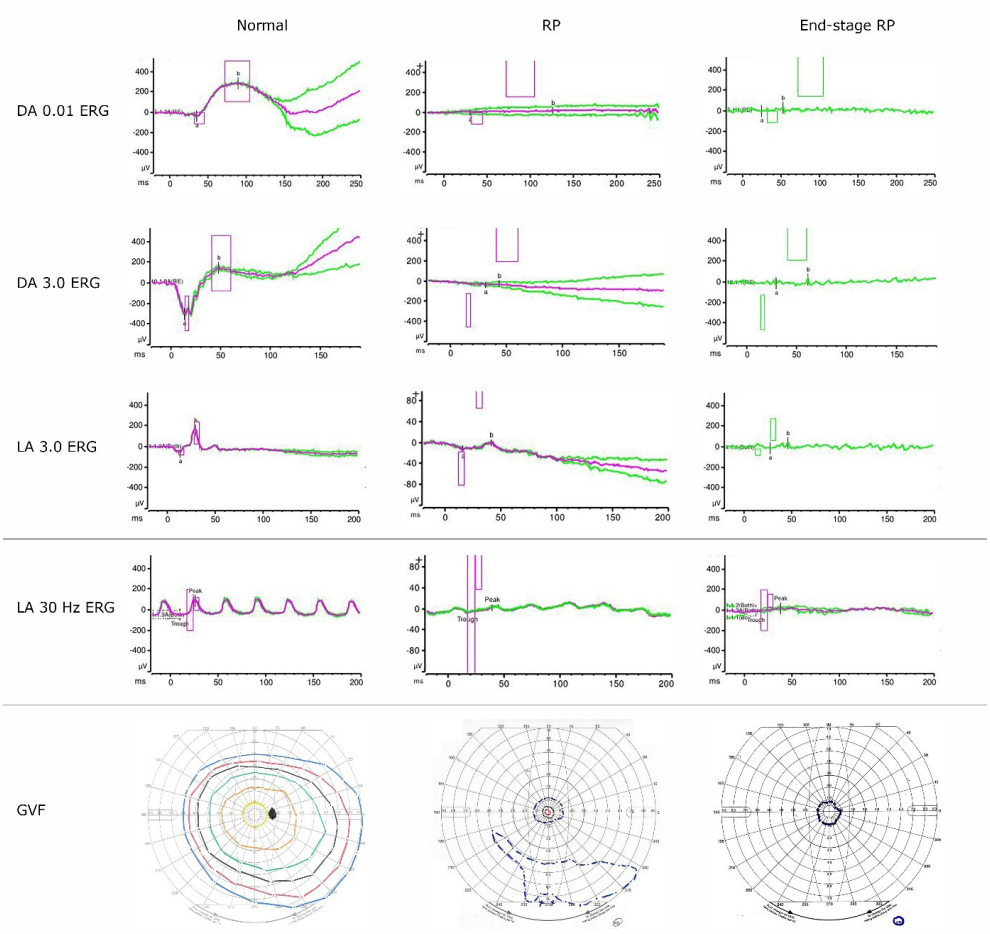

Figure 5. Overview of representative electrophysiological and visual field examination results in retinitis pigmentosa (RP). Each row represents the stimulus used in electroretinography (ERG) testing based on recommendations by the International Society for Clinical Electrophysiology of Vision (ISCEV). The dark-adapted (DA) 0.01 flash elicits a rod-driven response of ON-bipolar cells; the DA 3.0 flash elicits a mixed rod- and cone-driven yet rod-dominated response of both photoreceptors and bipolar cells; the light-adapted (LA) 3.0 flash elicits cone-driven responses from ON- and OFF-bipolar cells; and the 30 Hz flicker elicits a cone-driven response. Rod-driven responses are often non-detectable in early disease stages, while a 30 Hz flicker response progressively diminishes with advancing disease, i.e. a rod-cone pattern of dysfunction, as is seen in the 2nd and 3rd columns. The Goldmann visual fields (GVF) may show various patterns of (mid)peripheral visual field loss, eventually resulting in a small central remnant of vision.
Credit: the Department of Ophthalmology at the Leiden University Medical Center in Leiden, The Netherlands.

4.3 Electrophysiological testing

A full-field electroretinogram (ffERG) is an objective tool to measure the functional integrity of the inner and outer retina, and quantifies rod and cone dysfunction. This method measures dark- and

light-adapted responses to light flashes at different intensities, from which rod and cone electrical responses can be deduced, respectively. Isolated cone responses are measured after light-adaptation with a 30 Hz flicker stimulus (i.e. 30 stimuli per second), where rapidly repeating flashes stimulate the retina. Rods cannot respond to flickering light with a frequency above 20 Hz. The ffERG is usually performed for diagnostic purposes, and less commonly to clinically monitor disease progression. FfERGs should be evaluated on the amplitudes of the a-wave, a negative deflection that is generated by both rod and cone photoreceptor activation, and the b-wave, a positive deflection generated by activation from cells in the inner retina (i.e. bipolar cells, with some contribution from Müller cells), and on the implicit time, which is a time interval measured between stimulus onset and b-wave peak. The International Society for Clinical Electrophysiology of Vision (ISCEV) has established guidelines for a basic ffERG testing protocol, but also recommends extension of this protocol where relevant.[98]

FfERGs in RP show reduced dark-adapted (scotopic) responses from the early disease stages when light-adapted (mixed rod-cone) or cone-flicker responses can still be within normal limits. Wave amplitudes are reduced, and rod implicit times are often delayed. As the disease advances, rod and cone amplitudes further diminish and the implicit times are further delayed, but the attenuation is more marked for rod responses (a rod-cone pattern; Figure 5). In advanced stages of RP, the ffERG becomes extinguished, i.e. residual responses have become too small to be detectable. In sectorial RP, the ffERG can remain with the normal range, as a smaller retinal area is affected. Cone dystrophies are characterized by reduced light-adapted and/or cone-flicker responses. Dark-adapted responses remain normal, and may be reduced in end-stage cone dystrophy. In cone-rod dystrophy, both light-adapted and dark-adapted responses are reduced in the early disease stages, with a more profound reduction of the light-adapted and cone-flicker responses than the dark-adapted responses. As cone-rod dystrophy advances, it may be difficult to distinguish from RP. In macular dystrophies, typically no panretinal cone- and/or rod dysfunction is detectable on ffERG.

Multifocal electroretinography (mfERG) measures the retinal function across the central 40°-50° of the macula, mapping electrical responses to specific regions and requiring stable fixation, as opposed to the full-field approach. It is less commonly used as a diagnostic tool, as the cone function in the central macula is often spared in RP, but it can be used as a complementary tool in documenting disease progression and macular function.[99] It may be of particular use in cone-(rod) and macular dystrophies. The pattern electroretinogram (PERG) is another complementary tool in measuring the extent of macular function, as it measures responses from the macular retinal ganglion cells.

4.4 Full-field stimulus testing

In the most severe cases of IRD, where ffERG responses are non-detectable and where patients may have ultra-low vision or light perception vision, full-field stimulus threshold testing (FST) provides

a psychophysical outcome measure.[100] White light stimuli are used for testing the lowest luminance threshold a patient can detect. As the test measures the lowest luminance threshold, it detects the sensitivity of the most sensitive area of the retina, without further specification of the location of this area. Blue and red stimuli may be used to further specify whether the vision in this area of retina is cone- or rod-mediated.

This test is not part of the clinical workup routine in IRD patients, but is a useful tool in natural history studies and gene therapy trials, where the most severely affected IRD patients are usually the first patients to undergo safety testing in phase I. In such severely affected groups, FST may still be able to provide a measure of photoreceptor (rod and/or cone) function.

5. GENETICS

5.1 Inheritance patterns

All forms of Mendelian inheritance have been described in retinal dystrophies. For example, non-syndromic RP can be inherited in an autosomal dominant (15-25% of RP cases), autosomal recessive (5-20% of RP cases) or X-linked fashion (5-15% of RP cases).[14] The remaining 30-55% of RP cases cannot be classified as they have no reports of affected family members, and are denoted as isolated or simplex RP. Although the majority of simplex cases are predicted to be ARRP, approximately 15% of male patients with simplex RP have a mutation in the XLRP genes *RPGR* or *RP2*.[101] *De novo* ADRP mutations account for at least 1-2% of simplex RP cases.[102]

In XLRP, mild to severe phenotypic expression can occur in female carriers, probably due to non-random or skewed X-inactivation.[103] Consequently, some XLRP pedigrees may be misclassified as ADRP.[104] Approximately 8.5% of families initially considered to display ADRP are caused by mutations in XLRP genes.[105]

A very small proportion of cases have been reported to result from a non-Mendelian inheritance, such as digenic RP.[104]

5.2 Genetic heterogeneity

In the past two decades, mutations in at least 260 different genes have been identified in inherited retinal degenerations, with over 96 different genes in RP, 35 different genes in cone or cone-rod dystrophies, and 27 different genes in Leber congenital amaurosis [RetNet, update of June 21, 2021, URL: sph.uth.edu/retnet/]. Despite this high number of known disease-associated genes (locus heterogeneity), the mutation detection rate in e.g. RP is, depending on the RP type and the molecular technique used, 30-80%, leaving a considerable fraction of cases unexplained. Apart from this locus heterogeneity, allelic heterogeneity is also strikingly present, with over 3000

different mutations reported in non-syndromic RP. Within the same gene, different mutations can result in a different phenotypic outcome or variation in disease severity, illustrating a large clinical heterogeneity.[106, 107]

In some ADRP families, individual mutation carriers may not exhibit clinical signs of RP. Incomplete or reduced penetrance and variable expression has been reported for dominant mutations in a number of genes (e.g. *PRPH2*, *PRPF31, PRPF8, SNRNP200*).[108, 109]

5.3 Molecular analysis

Choosing the right molecular test for patients with a retinal dystrophy can be challenging, especially with the plethora of disease genes and the different tests that are provided by molecular laboratories. Several factors need to be taken into account, including the clinical findings, family history, presence or absence of consanguinity, previous molecular testing, the reimbursement options by the patients' insurance, and the expertise of the laboratory. An overview of the available genetic tests provided by accredited laboratories can be found on the orpha.net portal.

Since whole exome sequencing (WES) has become an affordable routine test, it competes with targeted gene-panel based next-generation sequencing (NGS) approaches. Despite screening of protein coding parts of a large part or all known inherited retinal dystrophy genes, many cases remain unsolved. In these cases, several considerations should be taken into account:

(1) Some panels only target a limited set of genes (e.g. the most prevalent RP genes). Furthermore, some regions of a specific gene might not be targeted using NGS. A molecular report should provide information about the targeted regions. It is expected that more RP-associated genes will be elucidated in the coming years, each accounting for a small percentage of cases.

(2) Some regions might not be well-covered using WES or targeted-NGS, especially GC-rich or highly repetitive sequences. The *RPGR* open reading frame (ORF) 15, a mutation hotspot for XLRP, is such an example. For XLRP it is recommended to start with a targeted approach that also provides coverage of the entire ORF15 sequence, especially since nearly 60-70% of the disease-causing *RPGR* mutations are located in this region.[81, 110]

(3) Inherent to the screening technique used, some specific genetic alterations might be missed, such as deep-intronic variants and structural variations (SVs).[111, 112] Whole genome sequencing (WGS) has proven to be a sensitive method for screening of both deep-intronic variants and SVs and will likely in the near future replace WES as a standard diagnostic test.[113, 114]

(4) Variants of unclassified significance (VUS), i.e. class 3 mutations, can be reported. The evidence of pathogenicity of these variants can evolve over time to benign or likely

pathogenic based on more biological evidence or the presence of the variant in multiple patients with an inherited retinal dystrophy. For partially solved cases, segregation analysis in affected and unaffected family members, may provide more insight in the pathogenicity of the VUS.[115]

6. PATIENT MANAGEMENT

For most forms of inherited retinal dystrophy, no effective and commercially approved treatment is available. Patient management should therefore consist mostly of elaborate counselling on the disease background and heredity, prognosis, low vision aids and advice on lighting where applicable, particularly at school or at the work place, and management of additional ocular conditions. Psychosocial counselling should also focus on a patient's coping strategy regarding the diagnosis and prognosis. However, as avenues for gene-specific and gene-independent treatments are investigated, establishing a reliable genetic diagnosis becomes increasingly important. Moreover, a molecular diagnosis provides the possibility to screen family members at risk, to perform carriership testing in partners, and to offer the option of prenatal testing or preimplantation genetic diagnosis. The visual function and retinal imaging should preferably be evaluated at regular intervals, such as every 1-3 years, also taking into account the patient's needs and preferences. Patients with associated ocular conditions such as cataract and glaucoma may require more frequent assessments. Careful documentation of the disease progression allows for a tailored estimate of the prognosis in any given patient. Moreover, with the relatively rapid advent of experimental therapeutic strategies, this documentation may prove invaluable in the setting of (retrospective) natural history studies. In prospective natural history studies and in gene therapy trials, retrospective documentation may prove a helpful aid, e.g. in determining the length of visit intervals.

Some patients may wish to be involved in patient groups or societies. Where possible, these patients should be referred to a tertiary expertise center, where the disease progression can be monitored, and where patients can be kept up to date on ongoing and future international clinical trials.

6.1 Family management and counselling

Determining the inheritance pattern is essential in family management and counselling. A detailed family history should be taken, including the number of potentially affected family members and their relation to the proband, as well as the presence of consanguinity in the family. Drawing a pedigree is advisable. Patients are usually referred to the genetic counsellor such as a clinical geneticist for queries regarding the reliability and implications of genetic test results. Usually, genetic testing is refrained from in presymptomatic children, as genetic testing should entail a well-considered decision process for which the child may be too young. Molecular testing can be

offered to family members at risk. If there is a higher risk of having affected children, the option of preconception counselling diagnosis and preimplantation genetic diagnosis should be discussed.

6.2 Treating associated ocular conditions

Ocular conditions associated with RP, such as refractive errors, macular edema or visually significant cataract, should be monitored and managed. Cystoid macular edema may be treated with systemic or topical carbonic anhydrase inhibitors, although this condition is often refractory in RP, and reports on potential visual benefit are inconsistent.[116] If the edema is unresponsive to carbonic anhydrase inhibitors, other treatments, including topical, oral or intravitreal steroids, intravitreal anti-vascular endothelial growth factors, laser photocoagulation, or pars plana vitrectomy, also appear of limited success.[115] Corrective glasses with specific color filters may be helpful in patients with light aversion or decreased contrast sensitivity. Visually significant cataracts should be surgically treated, as both visual outcome and patient satisfaction are generally favorable,[117, 118] but in the case of pre-operatively present macular atrophy, patients should be informed on the potentially limited visual benefit. In order to reduce potential light-induced toxicity to the retina, the intra-operative microscope light intensity can be reduced, and between different surgical steps the microscope light may be switched off in order to minimize light exposure.[118] Increased risks associated with cataract surgery in the RP population include zonular weakness, and the postoperative development of anterior capsular rhexisis phimosis, posterior capsule opacification and cystoid macular edema.[118, 119]

6.3 Retinal prostheses

Retinal prostheses can have a role in legally blind patients with end-stage RP, and require careful pre-operative screening and expectation management, counselling, and a comprehensive post-operative rehabilitation program at a specialized center.[120, 121] The two most studied epiretinal implants, the Argus II and alpha-IMS, have shown performance results that can overall be considered similar, despite large differences in implant design.[122] While most patients with a retinal prosthesis show an improvement in mobility and orientation tasks, approximately one third experiences measurable visual acuity improvement.[123] Reading speed can be improved in a subset of patients, although single-letter recognition may still take up to several minutes.[124] Pre-operative counselling should comprise the advice that the output from the prosthesis is an entirely new type of functional vision rather than the recovery of previous vision.[125] Due to the guarded benefit, and the frequent visits and intensive rehabilitation required to achieve it, patient selection and expectation management are key.

6.4 Oral nutritional supplements

The role of vitamin A supplementation remains debated.[126] At age-adjusted dosages, vitamin A supplementation has been shown to slow the decline of the cone amplitudes on ffERG in a recent study.[127] However, this result was described in a small, retrospective, observational study, where loss-

to-follow-up was higher among the group of RP patients who did not receive vitamin A, obscuring an already sparse finding. The randomized, controlled, double-blinded trial that prompted this recent study, was published in 1993 and found no significant beneficial effect of vitamin A supplementation.[128] As any effect has been shown in genetically undifferentiated RP populations, it remains unclear whether vitamin A supplementation works for all RP subtypes, or possibly be harmful to certain subgroups. Mouse studies have indicated that vitamin A supplementation might be avoided in *ABCA4*-associated retinal dystrophies, which do not entail RP, but nonetheless raise caution in prescribing vitamin A supplementation.[129] Moreover, hypervitaminosis A can lead to toxicity in several organ systems, and adverse reactions should be assessed at intervals. A synthetic vitamin A derivative, 9-cis-retinyl acetate, has shown efficacy in preserving visual field area and visual acuity in a clinical trial with patients with *RPE65*-associated and *LRAT*-associated retinal dystrophies, including RP, which comprise 5% of cases of childhood-onset RP.[130]

Care should be taken before prescribing oral supplements. Docohexaenoic acid (fish oils) has shown no clear efficacy in slowing disease progression, and oral valproic acid has been shown to lead to a worse visual outcome than placebo.[131,132] Vitamin E supplementation has been associated with a faster decline of light-adapted electroretinogram amplitude.[128]

6.5 Therapeutic advancements

As for treatments aimed at halting the degenerative process, the approval of subretinal injections of gene therapy (voretigene neparvovec, Luxturna®) for *RPE65*-associated retinal dystrophies in 2017 by the United States Federal Drug Administration offers promising perspectives for trials in retinal dystrophies associated with other genes.[133] With the advent of trials investigating therapeutic options, patients should be kept updated on ongoing or upcoming trials that may be relevant to them. All interventional efficacy trials in humans, including gene therapy studies, are registered (e.g. on the ClinicalTrials.gov platform). These trials will provide evidence on the safety and efficacy of a medical intervention. For several genes associated with ARRP or XLRP, clinical gene augmentation therapy trials are ongoing or being prepared for in the pre-clinical phase. For ADRP, gene augmentation alone is probably not enough, as the disease is based on a deleterious gain-of-function mechanism, and genome-editing approaches are under investigation, for example using the Clustered Regularly Interspaced Short Palindromic Repeats (CRISPR) and their associated genes (Cas) in a gene-replacement strategy. As these approaches usually need a viral vector, such as adeno-associated viral vectors, they are applicable in patients with remaining functional photoreceptor cells. Therefore, certain early-onset and rapidly progressive forms of RP would ideally require therapeutic intervention in childhood or adolescence.[134]

Another therapeutic strategy utilizes antisense oligonucleotides (AONs), which are short, synthetic, single-stranded oligodeoxynucleotides. They can be delivered as "naked" oligonucleotides or via a viral vector, and can interfere with splicing through several mechanisms.[135] AONs are useful

in blocking aberrant splice events and redirecting normal splicing. They are not applicable to all mutations, but preclinical efficacy studies have shown great potential for treating specific cases of e.g. Stargardt disease, and *CEP290*-associated LCA.[136, 137] In animal studies, AONs have shown promising results in the treatment of autosomal dominant IRD, such as *RHO*-associated RP.[138]

Expectations of the outcomes of such trials should be managed, as cell death is principally irreversible, and the highest aim is the stabilization of current vision, which may already be severely impaired. In rare cases, visual improvement has been reported with gene replacement therapy or antisense oligonucleotide therapy.[139, 140] Patients should be advised that these options are gene-specific or mutation-specific.

For more advanced disease stages, cell-based therapeutic options are investigated, which are not gene-specific. Examples include the intravitreal or subretinal administration of retinal progenitor cells or induced pluripotent stem cells.[141] As of yet, most studies investigating these methods have been performed in animal populations, and several drawbacks should be taken into consideration, including limited graft survival and limited in vivo graft function. Human cases of severe vision loss have been described after intravitreal injection of autologous adipose-tissue derived stem cells in the treatment of age-related macular degeneration at a "stem cell clinic" in the United States.[142] Intravitreal implants containing ciliary neurotrophic factor have shown short-term visual field sensitivity loss compared to sham treatment, and no long-term benefit.[143]

6.6 From bench to bedside: the gaps in clinical knowledge and the hurdles they present

The rapid evolution of therapeutic advancements is in stark contrast to the available clinical knowledge on the different disease phenotypes associated with each gene, and the rate of disease progression. This information is important in order to better understand the disease and to better inform patients on their prognosis, but it is also essential in the implementation of gene or cell-based therapy. Ideally, the preclinical development of a (gene) therapy should be paralleled by the available knowledge on the natural disease course, the identification of the patient subpopulation most likely to benefit from this therapy, and the identification of outcome parameters. However, the limited information available about the natural course of disease in many genetic subtypes of IRD is based predominantly on case reports or case series of single-visit patient data collected from single centers. Due to the relative rarity of some genetic subtypes, quantitative analysis often lacks from the available literature. Also, the available data from different reports may be inconsistent, as some studies may describe early blindness, while others report preservation of vision until relatively later years. Genotype-phenotype correlations are a particularly interesting point of focus in the potential explanation of these differences, and they remain to be elucidated.

Advances in retinal imaging, such as fundus autofluorescence and spectral-domain optical coherence tomography, and in functional testing, such as microperimetry, present new possibilities

for the definition of markers for disease progression. As most clinical trials last several years, the progression markers used as outcome parameters are ideally sensitive to change in a relatively short time-span. Thorough knowledge of the clinical aspects of a particular genetic IRD subtype is crucial in defining the window of therapeutic opportunity, patient candidacy criteria, and outcome parameters. These factors may be pivotal in the success of a gene therapy trial and the approval of a gene therapy by the FDA or EMA, further underlining the necessity of natural history studies.

AIMS AND OUTLINE OF THIS THESIS

As several studies investigating gene therapy trials and other cell-based therapeutic options have shown promising results, questions arise on the most appropriate implementation of these novel methods. The successful development and implementation of any new therapy requires an in-depth understanding of the disease, its phenotypic spectrum, and the speed at which it progresses. This theses aims to answer to these key issues, addressing the following questions for retinopathies associated with mutations in *CRB1*, *RPGR*, *RHO*, *LRAT*, and *CHM*:

- What is the window of opportunity for intervention through gene- or cell-based therapy?
- Which functional parameters are most time-sensitive to change? And which parameters will thus be the most appropriate clinical endpoints in a gene therapy trial?
- Which structural parameters correlate strongly to functional parameters, and may potentially serve as surrogate endpoints in a gene therapy trial?
- What are the genotype-phenotype associations, if any? I.e. can we identify characteristics that predict a specific phenotype, or that predict slower or faster disease progression?

Chapter 1 is the general introduction of this thesis, and provides the reader with information on the basic retinal anatomy and physiology. It introduces the reader to the general aspects of inherited retinal dystrophies.

Chapter 2.1. describes the largest longitudinal cohort of *CRB1*-associated autosomal recessive retinal dystrophies to date, combining patients from a large Dutch genetic isolate with patients from outside this genetic isolate. This study investigates the phenotypic spectrum and natural disease course in these patients. The size of this cohort allows for one of the first statistical analyses performed in this subgroup of patients. Yearly decline rates of the visual acuity and the visual field area are calculated, as well as time-to-event analyses for visual impairment. Some genotype-phenotype associations are described.

Chapter 2.2. contains a comprehensive description of several clinical parameters in the second largest longitudinal cohort of *CRB1*-associated retinal dystrophies, in a Belgian population. Some earlier findings from the Dutch population are corroborated in this Chapter, although the

phenotypes and, to a greater extent, the genotypes in the Belgian population were even more variable.

Chapter 2.3. is an extensive cross-sectional study of prospectively enrolled Dutch patients with *CRB1*-associated retinal dystrophies. This chapter focuses on the elucidation of structure-function correlations, in order to identify appropriate clinical endpoints and possible surrogate endpoints for future gene therapy trials for *CRB1*-associated retinal degenerations.

Chapter 3.1. describes the long-term clinical course and the visual outcome of (X-linked) choroideremia, with the longest follow-up time published to date, to our knowledge. Unique aspects of this Chapter include the focus on the effect of disease on the social participation of patients.

Chapter 3.2. describes the outcome of full-thickness macular hole surgery in a patient with choroideremia.

Chapter 4.1. describes a large study on the clinical characteristics and natural history of *RPGR*-associated X-linked retinitis pigmentosa and cone-/cone-rod dystrophy. Genotype-phenotype correlations are investigated, elucidating some differences between patients with mutations in the ORF15 mutational hotspot, and those with mutations in exons 1-14. The presence of high myopia and its effect on the disease course is featured in this chapter.

Chapter 4.2. studies female carriers of *RPGR* mutations, and uniquely highlights the phenotypic spectrum, and describes the effects of myopia and age on visual function. The complete expression of disease is demonstrated in a portion of subjects.

Chapter 5 describes the clinical spectrum and natural disease course in patients with *LRAT*-associated autosomal recessive retinal dystrophy, which is a particularly rare disease population. Inter- and intrafamilial differences are detailed.

Chapter 6 is a study of 100 patients with *RHO*-associated autosomal dominant RP. Detailed statistical analysis is performed, investigating the natural disease course as well as possible genotype-phenotype correlations in one of the largest studies on *RHO*-associated RP published to date.

REFERENCES

1. Jonas JB, Schneider U, Naumann GO. Count and density of human retinal photoreceptors. Graefes Arch Clin Exp Ophthalmol 1992;230(6):505-10.
2. Baker S, Kerov V. Photoreceptor Inner and Outer Segments. Curr Top Membr 2013;72C:231-65.
3. Spaide RF, Curcio CA. Anatomical correlates to the bands seen in the outer retina by optical coherence tomography: literature review and model. Retina 2011;31(8):1609-19.
4. Reichenbach A, Bringmann A. New functions of Müller cells. Glia 2013;61(5):651-78.
5. Sparrow JR, Hicks D, Hamel CP. The retinal pigment epithelium in health and disease. Curr Mol Med 2010;10(9):802-23.
6. Booij JC, Baas DC, Beisekeeva J, et al. The dynamic nature of Bruch's membrane. Prog Retin Eye Res 2010;29(1):1-18.
7. Cote R. Photoreceptor phosphodiesterase (PDE6): a G-protein-activated PDE regulating visual excitation in rod and cone photoreceptor cells. in Cyclic Nucleotide Phosphodiesterases in Health and Disease (Beavo JA, Francis SH, and Houslay MD eds.) 2006, CRC Press, Boca Raton, FL. p 165-193.
8. Tsin A, Betts B, Grigsby J. Visual cycle proteins: Structure, function, and roles in human retinal disease. J Biol Chem 2018;293(34):13016-13021.
9. Wang JS, Kefalov VJ. The cone-specific visual cycle. Prog Retin Eye Res 2011;30(2):115-28.
10. Prem Senthil M, Khadka J, Singh Gilhotra J, et al. Exploring the quality of life issues in people with retinal diseases: a qualitative study. J Patient Rep Outcomes 2017;1(1):15.
11. Hartong DT, Berson EL, Dryja TP. Retinitis pigmentosa. Lancet 2006;368(9549):1795-809.
12. Nangia V, Jonas JB, Khare A, Sinha A. Prevalence of retinitis pigmentosa in India: the Central India Eye and Medical Study. Acta Ophthalmol 2012;90(8):e649-50.
13. Na K-H, Kim HJ, Kim KH, et al. Prevalence, Age at Diagnosis, Mortality, and Cause of Death in Retinitis Pigmentosa in Korea—A Nationwide Population-based Study. Am J Ophthalmol 2017;176:157-65.
14. Daiger SP, Bowne SJ, Sullivan LS. Perspective on genes and mutations causing retinitis pigmentosa. Arch Ophthalmol 2007;125(2):151-8.
15. Mathur P, Yang J. Usher syndrome: Hearing loss, retinal degeneration and associated abnormalities. Biochim Biophys Acta 2015;1852(3):406-20.
16. Verbakel SK, van Huet RAC, Boon CJF, et al. Non-syndromic retinitis pigmentosa. Prog Retin Eye Res 2018;66:157-186.
17. Kemp CM, Jacobson SG, Faulkner DJ. Two types of visual dysfunction in autosomal dominant retinitis pigmentosa. Invest Ophthalmol Vis Sci 1988;29(8):1235-41.
18. Hamel C. Retinitis pigmentosa. Orphanet J Rare Dis 2006;1:40.
19. Bittner AK, Diener-West M, Dagnelie G. Characteristics and possible visual consequences of photopsias as vision measures are reduced in retinitis pigmentosa. Invest Ophthalmol Vis Sci 2011;52(9):6370-6.
20. Marc RE, Jones BW, Anderson JR, et al. Neural reprogramming in retinal degenerations. Invest Ophthalmol Vis Sci 2007;48(7):3364-71.

21. Adackapara CA, Sunness JS, Dibernardo CW, et al. Prevalence of cystoid macular edema and stability in oct retinal thickness in eyes with retinitis pigmentosa during a 48-week lutein trial. Retina 2008;28(1):103-10.
22. Hajali M, Fishman GA, Anderson RJ. The prevalence of cystoid macular oedema in retinitis pigmentosa patients determined by optical coherence tomography. Br J Ophthalmol 2008;92(8):1065-8.
23. Testa F, Rossi S, Colucci R, et al. Macular abnormalities in Italian patients with retinitis pigmentosa. Br J Ophthalmol 2014;98(7):946-50.
24. Fujiwara K, Ikeda Y, Murakami Y, et al. Association Between Aqueous Flare and Epiretinal Membrane in Retinitis Pigmentosa. Invest Ophthalmol Vis Sci 2016;57(10):4282-6.
25. Grover S, Fishman GA, Brown J, Jr. Frequency of optic disc or parapapillary nerve fiber layer drusen in retinitis pigmentosa. Ophthalmology 1997;104(2):295-8.
26. Pelletier V, Jambou M, Delphin N, et al. Comprehensive survey of mutations in RP2 and RPGR in patients affected with distinct retinal dystrophies: genotype-phenotype correlations and impact on genetic counseling. Hum Mutat 2007;28(1):81-91.
27. Bird AC. X-linked retinitis pigmentosa. Br J Ophthalmol 1975;59(4):177-99.
28. Acton JH, Greenberg JP, Greenstein VC, et al. Evaluation of Multimodal Imaging in Carriers of X-Linked Retinitis Pigmentosa. Exp Eye Res 2013;113:41-8.
29. Comander J, Weigel-DiFranco C, Sandberg MA, Berson EL. Visual Function in Carriers of X-Linked Retinitis Pigmentosa. Ophthalmology 2015;122(9):1899-906.
30. Talib M, van Schooneveld MJ, Van Cauwenbergh C, et al. The Spectrum of Structural and Functional Abnormalities in Female Carriers of Pathogenic Variants in the RPGR Gene. Invest Ophthalmol Vis Sci 2018;59(10):4123-33.
31. Fujiwara K, Ikeda Y, Murakami Y, et al. Risk Factors for Posterior Subcapsular Cataract in Retinitis Pigmentosa. Invest Ophthalmol Vis Sci 2017;58(5):2534-7.
32. Hendriks M, Verhoeven VJM, Buitendijk GHS, et al. Development of Refractive Errors-What Can We Learn From Inherited Retinal Dystrophies? Am J Ophthalmol 2017;182:81-9.
33. Booij JC, Florijn RJ, ten Brink JB, et al. Identification of mutations in the AIPL1, CRB1, GUCY2D, RPE65, and RPGRIP1 genes in patients with juvenile retinitis pigmentosa. J Med Genet 2005;42(11):e67.
34. Stone EM. Leber congenital amaurosis - a model for efficient genetic testing of heterogeneous disorders: LXIV Edward Jackson Memorial Lecture. Am J Ophthalmol 2007;144(6):791-811.
35. Koenekoop RK. An overview of Leber congenital amaurosis: a model to understand human retinal development. Surv Ophthalmol 2004;49(4):379-98.
36. Allikmets R. Leber congenital amaurosis: a genetic paradigm. Ophthalmic Genet 2004;25(2):67-79.
37. Saberi M, Golchehre Z, Karamzade A, et al. CRB1-Related Leber Congenital Amaurosis: Reporting Novel Pathogenic Variants and a Brief Review on Mutations Spectrum. Iran Biomed J 2019;23(5):362-8.
38. Srilekha S, Arokiasamy T, Srikrupa NN, et al. Homozygosity Mapping in Leber Congenital Amaurosis and Autosomal Recessive Retinitis Pigmentosa in South Indian Families. PLoS One 2015;10(7):e0131679.
39. Perrault I, Delphin N, Hanein S, et al. Spectrum of NPHP6/CEP290 mutations in Leber congenital amaurosis and delineation of the associated phenotype. Human Mutation 2007;28(4):416.

40. Steinfeld R, Reinhardt K, Schreiber K, et al. Cathepsin D deficiency is associated with a human neurodegenerative disorder. Am J Hum Genet 2006;78(6):988-98.
41. den Hollander AI, Roepman R, Koenekoop RK, Cremers FPM. Leber congenital amaurosis: Genes, proteins and disease mechanisms. Prog Retin Eye Res 2008;27(4):391-419.
42. Jacobson SG, Aleman TS, Cideciyan AV, et al. Human cone photoreceptor dependence on RPE65 isomerase. Proc Natl Acad Sci U S A 2007;104(38):15123-8.
43. Cideciyan AV, Aleman TS, Jacobson SG, et al. Centrosomal-ciliary gene CEP290/NPHP6 mutations result in blindness with unexpected sparing of photoreceptors and visual brain: implications for therapy of Leber congenital amaurosis. Hum Mutat 2007;28(11):1074-83.
44. Hamel CP. Cone rod dystrophies. Orphanet J Rare Dis 2007;2(1):7.
45. Michaelides M, Hunt DM, Moore AT. The cone dysfunction syndromes. Br J Ophthalmol 2004;88(2):291-7.
46. Thiadens AA, Phan TM, Zekveld-Vroon RC, et al. Clinical course, genetic etiology, and visual outcome in cone and cone-rod dystrophy. Ophthalmology 2012;119(4):819-26.
47. Thiadens AA, Soerjoesing GG, Florijn RJ, et al. Clinical course of cone dystrophy caused by mutations in the RPGR gene. Graefes Arch Clin Exp Ophthalmol 2011;249(10):1527-35.
48. Thiadens AA, Klaver CC. Genetic testing and clinical characterization of patients with cone-rod dystrophy. Invest Ophthalmol Vis Sci 2010;51(12):6904-5; author reply 5.
49. Riveiro-Alvarez R, Lopez-Martinez MA, Zernant J, et al. Outcome of ABCA4 disease-associated alleles in autosomal recessive retinal dystrophies: retrospective analysis in 420 Spanish families. Ophthalmology 2013;120(11):2332-7.
50. Ito S, Nakamura M, Nuno Y, et al. Novel complex GUCY2D mutation in Japanese family with cone-rod dystrophy. Invest Ophthalmol Vis Sci 2004;45(5):1480-5.
51. Beales PL, Elcioglu N, Woolf AS, et al. New criteria for improved diagnosis of Bardet-Biedl syndrome: results of a population survey. J Med Genet 1999;36(6):437-46.
52. Pierrache LHM, Messchaert M, Thiadens AAHJ, et al. Extending the Spectrum of EYS-Associated Retinal Disease to Macular DystrophyGenotype and Phenotype of EYS-Associated IRDs. Invest Ophthalmol Vis Sci 2019;60(6):2049-63.
53. Roosing S, Thiadens AA, Hoyng CB, et al. Causes and consequences of inherited cone disorders. Prog Retin Eye Res 2014;42:1-26.
54. MacDonald IM, Sereda C, McTaggart K, Mah D. Choroideremia gene testing. Expert Rev Mol Diagn 2004;4(4):478-84.
55. Preising M, Ayuso C. Rab escort protein 1 (REP1) in intracellular traffic: A functional and pathophysiological overview. Ophthalmic Genet 2004;25(2):101-10.
56. Coussa RG, Kim J, Traboulsi EI. Choroideremia: effect of age on visual acuity in patients and female carriers. Ophthalmic Genet 2012;33(2):66-73.
57. Kärnä J. Choroideremia. A clinical and genetic study of 84 Finnish patients and 126 female carriers. Acta ophthalmol Suppl 1986;176:1-68.
58. Moosajee M, C Ramsden S, Cm Black G, et al. Clinical utility gene card for: Choroideremia. Eur J Hum Genet : Eur J Hum Genet 2014;22(4):doi:10.1038/ejhg.2013.183.

59. Bonilha VL, Trzupek KM, Li Y, et al. Choroideremia: analysis of the retina from a female symptomatic carrier. Ophthalmic Genet 2008;29(3):99-110.
60. Edwards TL, Groppe M, Jolly JK, et al. Correlation of Retinal Structure and Function in Choroideremia Carriers. Ophthalmology 2015;122(6):1274-6.
61. Lee TK, McTaggart KE, Sieving PA, et al. Clinical diagnoses that overlap with choroideremia. Can J Ophthalmol 2003;38(5):364-72.
62. Mura M, Sereda C, Jablonski MM, et al. Clinical and functional findings in choroideremia due to complete deletion of the CHM gene. Arch Ophthalmol 2007;125(8):1107-13.
63. Zinkernagel MS, MacLaren RE. Recent advances and future prospects in choroideremia. Clin Ophthalmol 2015;9:2195-200.
64. Saksens NTM, Fleckenstein M, Schmitz-Valckenberg S, et al. Macular dystrophies mimicking age-related macular degeneration. Prog Retin Eye Res 2014;39:23-57.
65. Lambertus S, van Huet RAC, Bax NM, et al. Early-Onset Stargardt Disease: Phenotypic and Genotypic Characteristics. Ophthalmology 2015;122(2):335-44.
66. Valkenburg D, Runhart EH, Bax NM, et al. Highly Variable Disease Courses in Siblings with Stargardt Disease. Ophthalmology 2019;126(12):1712-21.
67. Boon CJ, Klevering BJ, Leroy BP, et al. The spectrum of ocular phenotypes caused by mutations in the BEST1 gene. Prog Retin Eye Res 2009;28(3):187-205.
68. Westeneng-van Haaften SC, Boon CJ, Cremers FP, et al. Clinical and genetic characteristics of late-onset Stargardt's disease. Ophthalmology 2012;119(6):1199-210.
69. Lambertus S, Bax NM, Fakin A, et al. Highly sensitive measurements of disease progression in rare disorders: Developing and validating a multimodal model of retinal degeneration in Stargardt disease. PLoS One 2017;12(3):e0174020.
70. Lambertus S, Lindner M, Bax NM, et al. Progression of Late-Onset Stargardt Disease. Invest Ophthalmol Vis Sci 2016;57(13):5186-91.
71. Chowers I, Tiosano L, Audo I, et al. Adult-onset foveomacular vitelliform dystrophy: A fresh perspective. Prog Retin Eye Res 2015;47:64-85.
72. Smailhodzic D, Fleckenstein M, Theelen T, et al. Central areolar choroidal dystrophy (CACD) and age-related macular degeneration (AMD): differentiating characteristics in multimodal imaging. Invest Ophthalmol Vis Sci 2011;52(12):8908-18.
73. Staurenghi G, Sadda S, Chakravarthy U, Spaide RF. Proposed lexicon for anatomic landmarks in normal posterior segment spectral-domain optical coherence tomography: the IN*OCT consensus. Ophthalmology 2014;121(8):1572-8.
74. Fernández EJ, Hermann B, Považay B, et al. Ultrahigh resolution optical coherence tomography and pancorrection for cellular imaging of the living human retina. Opt Express 2008;16(15):11083-94.
75. Miller D, P Kocaoglu O, Wang Q, Lee S. Adaptive optics and the eye (super resolution OCT). Eye (Lond) 2011;25:321-30.
76. Battaglia Parodi M, La Spina C, Triolo G, et al. Correlation of SD-OCT findings and visual function in patients with retinitis pigmentosa. Graefes Arch Clin Exp Ophthalmol 2016;254(7):1275-9.

77. Birch DG, Locke KG, Felius J, et al. Rates of Decline in fdOCT Defined Regions of the Visual Field in Patients with RPGR-mediated X-Linked Retinitis Pigmentosa (XLRP). Ophthalmology 2015;122(4):833-9.
78. Toto L, Borrelli E, Mastropasqua R, et al. Macular Features in Retinitis Pigmentosa: Correlations Among Ganglion Cell Complex Thickness, Capillary Density, and Macular Function. Invest Ophthalmol Vis Sci 2016;57(14):6360-6.
79. Aleman TS, Cideciyan AV, Sumaroka A, et al. Inner retinal abnormalities in X-linked retinitis pigmentosa with RPGR mutations. Invest Ophthalmol Vis Sci 2007;48(10):4759-65.
80. Aleman TS, Cideciyan AV, Sumaroka A, et al. Retinal laminar architecture in human retinitis pigmentosa caused by Rhodopsin gene mutations. Invest Ophthalmol Vis Sci 2008;49(4):1580-90.
81. Talib M, van Schooneveld MJ, Thiadens AA, et al. Clinical and genetic characteristics of male patients with RPGR-associated retinal dystrophies: A Long-Term Follow-up Study. Retina 2019;39(6):1186-99.
82. de Carlo TE, Romano A, Waheed NK, Duker JS. A review of optical coherence tomography angiography (OCTA). Int J Retina Vitreous 2015;1(1):5.
83. Teussink MM, Breukink MB, van Grinsven MJJP, et al. OCT Angiography Compared to Fluorescein and Indocyanine Green Angiography in Chronic Central Serous Chorioretinopathy. Invest Ophthalmol Vis Sci 2015;56(9):5229-37.
84. Lima LH, Burke T, Greenstein VC, et al. Progressive constriction of the hyperautofluorescent ring in retinitis pigmentosa. Am J Ophthalmol 2012;153(4):718-27, 27.e1-2.
85. Escher P, Tran HV, Vaclavik V, et al. Double concentric autofluorescence ring in NR2E3-p.G56R-linked autosomal dominant retinitis pigmentosa. Invest Ophthalmol Vis Sci 2012;53(8):4754-64.
86. Robson AG, Saihan Z, Jenkins SA, et al. Functional characterisation and serial imaging of abnormal fundus autofluorescence in patients with retinitis pigmentosa and normal visual acuity. Br J Ophthalmol 2006;90(4):472-9.
87. Sparrow JR, Yoon KD, Wu Y, Yamamoto K. Interpretations of fundus autofluorescence from studies of the bisretinoids of the retina. Invest Ophthalmol Vis Sci 2010;51(9):4351-7.
88. Duncker T, Tabacaru MR, Lee W, et al. Comparison of near-infrared and short-wavelength autofluorescence in retinitis pigmentosa. Invest Ophthalmol Vis Sci 2013;54(1):585-91.
89. Schuerch K, Marsiglia M, Lee W, et al. Multimodal imaging of disease-associated pigmentary changes in retinitis pigmentosa. Retina 2016;36 Suppl 1:S147-S158.
90. Liang J, Williams DR, Miller DT. Supernormal vision and high-resolution retinal imaging through adaptive optics. J Opt Soc Am A Opt Image Sci Vis 1997;14(11):2884-92.
91. Dubra A, Sulai Y, Norris JL, et al. Noninvasive imaging of the human rod photoreceptor mosaic using a confocal adaptive optics scanning ophthalmoscope. Biomed Opt Express 2011;2(7):1864-76.
92. Dubis AM, Cooper RF, Aboshiha J, et al. Genotype-dependent variability in residual cone structure in achromatopsia: toward developing metrics for assessing cone health. Invest Ophthalmol Vis Sci 2014;55(11):7303-11.
93. Chang AA, Morse LS, Handa JT, et al. Histologic localization of indocyanine green dye in aging primate and human ocular tissues with clinical angiographic correlation. Ophthalmology 1998;105(6):1060-8.

94. Lindberg CR, Fishman GA, Anderson RJ, Vasquez V. Contrast sensitivity in retinitis pigmentosa. Br J Ophthalmol 1981;65(12):855-8.
95. Jacobson SG, McGuigan DB, 3rd, Sumaroka A, et al. Complexity of the Class B Phenotype in Autosomal Dominant Retinitis Pigmentosa Due to Rhodopsin Mutations. Invest Ophthalmol Vis Sci 2016;57(11):4847-58.
96. Wu Z, Jung CJ, Ayton LN, et al. Test-Retest Repeatability of Microperimetry at the Border of Deep Scotomas. Invest Ophthalmol Vis Sci 2015;56(4):2606-11.
97. Liu H, Bittencourt MG, Wang J, et al. Retinal sensitivity is a valuable complementary measurement to visual acuity--a microperimetry study in patients with maculopathies. Graefes Arch Clin Exp Ophthalmol 2015;253(12):2137-42.
98. McCulloch DL, Marmor MF, Brigell MG, et al. ISCEV Standard for full-field clinical electroretinography (2015 update). Doc Ophthalmol 2015;130(1):1-12.
99. Nagy D, Schonfisch B, Zrenner E, Jagle H. Long-term follow-up of retinitis pigmentosa patients with multifocal electroretinography. Invest Ophthalmol Vis Sci 2008;49(10):4664-71.
100. Roman AJ, Cideciyan AV, Aleman TS, Jacobson SG. Full-field stimulus testing (FST) to quantify visual perception in severely blind candidates for treatment trials. Physiol Meas 2007;28(8):N51-6.
101. Branham K, Othman M, Brumm M, et al. Mutations in RPGR and RP2 account for 15% of males with simplex retinal degenerative disease. Invest Ophthalmol Vis Sci 2012;53(13):8232-7.
102. Neveling K, Collin RW, Gilissen C, et al. Next-generation genetic testing for retinitis pigmentosa. Hum Mutat 2012;33(6):963-72.
103. Ferrari S, Di Iorio E, Barbaro V, et al. Retinitis pigmentosa: genes and disease mechanisms. Curr Genomics 2011;12(4):238-49.
104. Sullivan LS, Bowne SJ, Birch DG, et al. Prevalence of disease-causing mutations in families with autosomal dominant retinitis pigmentosa: a screen of known genes in 200 families. Invest Ophthalmol Vis Sci 2006;47(7):3052-64.
105. Churchill JD, Bowne SJ, Sullivan LS, et al. Mutations in the X-linked retinitis pigmentosa genes RPGR and RP2 found in 8.5% of families with a provisional diagnosis of autosomal dominant retinitis pigmentosa. Invest Ophthalmol Vis Sci 2013;54(2):1411-6.
106. Daiger SP, Sullivan LS, Bowne SJ. Genes and mutations causing retinitis pigmentosa. Clin Genet 2013;84(2):132-41.
107. Inglehearn CF, McHale JC, Keen TJ, et al. A new family linked to the RP1 dominant retinitis pigmentosa locus on chromosome 8q. J Med Genet 1999;36(8):646-8.
108. Maubaret CG, Vaclavik V, Mukhopadhyay R, et al. Autosomal dominant retinitis pigmentosa with intrafamilial variability and incomplete penetrance in two families carrying mutations in PRPF8. Invest Ophthalmol Vis Sci 2011;52(13):9304-9.
109. Rose AM, Bhattacharya SS. Variant haploinsufficiency and phenotypic non-penetrance in PRPF31-associated retinitis pigmentosa. Clin Genet 2016;90(2):118-26.
110. Vervoort R, Lennon A, Bird AC, et al. Mutational hot spot within a new RPGR exon in X-linked retinitis pigmentosa. Nat Genet 2000;25(4):462-6.

111. Van Cauwenbergh C, Van Schil K, Cannoodt R, et al. arrEYE: a customized platform for high-resolution copy number analysis of coding and noncoding regions of known and candidate retinal dystrophy genes and retinal noncoding RNAs. Genet Med 2017;19(4):457-66.
112. Van Schil K, Naessens S, Van de Sompele S, et al. Mapping the genomic landscape of inherited retinal disease genes prioritizes genes prone to coding and noncoding copy-number variations. Genet Med 2018;20(2):202-13.
113. Ellingford JM, Barton S, Bhaskar S, et al. Whole Genome Sequencing Increases Molecular Diagnostic Yield Compared with Current Diagnostic Testing for Inherited Retinal Disease. Ophthalmology 2016;123(5):1143-50.
114. Carss KJ, Arno G, Erwood M, et al. Comprehensive Rare Variant Analysis via Whole-Genome Sequencing to Determine the Molecular Pathology of Inherited Retinal Disease. Am J Hum Genet 2017;100(1):75-90.
115. Richards S, Aziz N, Bale S, et al. Standards and guidelines for the interpretation of sequence variants: a joint consensus recommendation of the American College of Medical Genetics and Genomics and the Association for Molecular Pathology. Genet Med 2015;17(5):405-24.
116. Bakthavatchalam M, Lai FHP, Rong SS, et al. Treatment of cystoid macular edema secondary to retinitis pigmentosa: a systematic review. Surv Ophthalmol 2018;63(3):329-39.
117. De Rojas JO, Schuerch K, Mathews PM, et al. Evaluating Structural Progression of Retinitis Pigmentosa After Cataract Surgery. Am J Ophthalmol 2017;180:117-23.
118. Davies EC, Pineda R, 2nd. Cataract surgery outcomes and complications in retinal dystrophy patients. Can J Ophthalmol 2017;52(6):543-7.
119. Dikopf MS, Chow CC, Mieler WF, Tu EY. Cataract extraction outcomes and the prevalence of zonular insufficiency in retinitis pigmentosa. Am J Ophthalmol 2013;156(1):82-8.e2.
120. Ho AC, Humayun MS, Dorn JD, et al. Long-Term Results from an Epiretinal Prosthesis to Restore Sight to the Blind. Ophthalmology 2015;122(8):1547-54.
121. Edwards TL, Cottriall CL, Xue K, et al. Assessment of the Electronic Retinal Implant Alpha AMS in Restoring Vision to Blind Patients with End-Stage Retinitis Pigmentosa. Ophthalmology 2018;125(3):432-43.
122. Stronks HC, Dagnelie G. The functional performance of the Argus II retinal prosthesis. Expert Rev Med Devices 2014;11(1):23-30.
123. Ahuja AK, Behrend MR. The Argus II retinal prosthesis: factors affecting patient selection for implantation. Prog Retin Eye Res 2013;36:1-23.
124. da Cruz L, Coley BF, Dorn J, et al. The Argus II epiretinal prosthesis system allows letter and word reading and long-term function in patients with profound vision loss. Br J Ophthalmol 2013;97(5):632-6.
125. Farvardin M, Afarid M, Attarzadeh A, et al. The Argus-II Retinal Prosthesis Implantation; From the Global to Local Successful Experience. Front Neurosci 2018;12:584.
126. Rayapudi S, Schwartz SG, Wang X, Chavis P. Vitamin A and fish oils for retinitis pigmentosa. Cochrane Database Syst Rev 2013(12):Cd008428.
127. Berson EL, Weigel-DiFranco C, Rosner B, et al. Association of vitamin a supplementation with disease course in children with retinitis pigmentosa. JAMA Ophthalmol 2018;136(5):490-5.
128. Berson EL, Rosner B, Sandberg MA, et al. A randomized trial of vitamin A and vitamin E supplementation for retinitis pigmentosa. Arch Ophthalmol 1993;111(6):761-72.

129. Radu RA, Yuan Q, Hu J, et al. Accelerated accumulation of lipofuscin pigments in the RPE of a mouse model for ABCA4-mediated retinal dystrophies following Vitamin A supplementation. Invest Ophthalmol Vis Sci 2008;49(9):3821-9.
130. Koenekoop RK, Sui R, Sallum J, et al. Oral 9-cis retinoid for childhood blindness due to Leber congenital amaurosis caused by RPE65 or LRAT mutations: an open-label phase 1b trial. Lancet 2014;384(9953):1513-20.
131. Hoffman DR, Hughbanks-Wheaton DK, Pearson NS, et al. Four-year placebo-controlled trial of docosahexaenoic acid in X-linked retinitis pigmentosa (DHAX trial): a randomized clinical trial. JAMA Ophthalmol 2014;132(7):866-73.
132. Birch DG, Bernstein PS, Iannacone A, et al. Effect of Oral Valproic Acid vs Placebo for Vision Loss in Patients With Autosomal Dominant Retinitis Pigmentosa: A Randomized Phase 2 Multicenter Placebo-Controlled Clinical Trial. JAMA Ophthalmol 2018;136(8):849-56.
133. Voretigene neparvovec-rzyl (Luxturna) for inherited retinal dystrophy. Med Lett Drugs Ther 2018;60(1543):53-5.
134. Bennett J, Wellman J, Marshall KA, et al. Safety and durability of effect of contralateral-eye administration of AAV2 gene therapy in patients with childhood-onset blindness caused by RPE65 mutations: a follow-on phase 1 trial. Lancet 2016;388(10045):661-72.
135. Collin RW, den Hollander AI, van der Velde-Visser SD, et al. Antisense Oligonucleotide (AON)-based Therapy for Leber Congenital Amaurosis Caused by a Frequent Mutation in CEP290. Mol Ther Nucleic Acids 2012;1(3):e14.
136. Garanto A, Duijkers L, Tomkiewicz TZ, Collin RWJ. Antisense Oligonucleotide Screening to Optimize the Rescue of the Splicing Defect Caused by the Recurrent Deep-Intronic ABCA4 Variant c.4539+2001G>A in Stargardt Disease. Genes (Basel) 2019;10(6).
137. Garanto A, Chung DC, Duijkers L, et al. In vitro and in vivo rescue of aberrant splicing in CEP290-associated LCA by antisense oligonucleotide delivery. Hum Mol Genet 2016;25(12):2552-63.
138. Murray SF, Jazayeri A, Matthes MT, et al. Allele-Specific Inhibition of Rhodopsin With an Antisense Oligonucleotide Slows Photoreceptor Cell Degeneration. Invest Ophthalmol Vis Sci 2015;56(11):6362-75.
139. Cideciyan AV, Jacobson SG, Drack AV, et al. Effect of an intravitreal antisense oligonucleotide on vision in Leber congenital amaurosis due to a photoreceptor cilium defect. Nat Med 2019;25(2):225-8.
140. Russell S, Bennett J, Wellman JA, et al. Efficacy and safety of voretigene neparvovec (AAV2-hRPE65v2) in patients with RPE65-mediated inherited retinal dystrophy: a randomised, controlled, open-label, phase 3 trial. Lancet 2017;390(10097):849-60.
141. Tang Z, Zhang Y, Wang Y, et al. Progress of stem/progenitor cell-based therapy for retinal degeneration. J Transl Med 2017;15(1):99.
142. Kuriyan AE, Albini TA, Townsend JH, et al. Vision Loss after Intravitreal Injection of Autologous "Stem Cells" for AMD. N Engl J Med 2017;376(11):1047-53.
143. Birch DG, Bennett LD, Duncan JL, et al. Long-term Follow-up of Patients With Retinitis Pigmentosa Receiving Intraocular Ciliary Neurotrophic Factor Implants. Am J Ophthalmol 2016;170:10-4.

2.
CRB1-associated retinal dystrophies

2.1

Genotypic and phenotypic characteristics of *CRB1*-associated retinal dystrophies: a long-term follow-up study

Mays Talib, MD[1], Mary J. van Schooneveld, MD, PhD[2], Maria M. van Genderen, MD, PhD[3], Jan Wijnholds, PhD[1], Ralph J. Florijn, PhD[4], Jacoline B. ten Brink, BAS[4], Nicoline E. Schalij-Delfos, MD, PhD[1], Gislin Dagnelie[5], Frans P.M. Cremers, PhD[6], Ron Wolterbeek, PhD[7], Marta Fiocco, PhD[7,8], Alberta A. Thiadens, MD, PhD[9], Carel B. Hoyng, MD, PhD[10], Caroline C. Klaver, MD, PhD[9,10,11], Arthur A. Bergen, PhD[4,12], Camiel J.F. Boon, MD, PhD[1,2]

Ophthalmology 2017;124(6):884-895

1 Department of Ophthalmology, Leiden University Medical Center, Leiden, The Netherlands.
2 Department of Ophthalmology, Academic Medical Center, Amsterdam, The Netherlands.
3 Bartiméus, Diagnostic Centre for complex visual disorders, Zeist, The Netherlands.
4 Department of Clinical Genetics, Academic Medical Center, Amsterdam, The Netherlands.
5 Wilmer Eye Institute, Johns Hopkins University, Baltimore, Maryland.
6 Department of Human Genetics and Donders Institute for Brain, Cognition and Behaviour, Radboud University Medical Center, Nijmegen, The Netherlands.
7 Department of Medical Statistics, Leiden University Medical Center, Leiden, The Netherlands.
8 Mathematical Institute Leiden University, Leiden, The Netherlands.
9 Department of Ophthalmology, Erasmus Medical Center, Rotterdam, The Netherlands.
10 Department of Ophthalmology, Radboud University Medical Center, Nijmegen, The Netherlands.
11 Department of Epidemiology, Erasmus Medical Center, Rotterdam, The Netherlands.
12 The Netherlands Institute for Neuroscience (NIN-KNAW), Amsterdam, The Netherlands.

ABSTRACT

Objective: To describe the phenotype, long-term clinical course, clinical variability and genotype of patients with *CRB1*-associated retinal dystrophies.

Design: Retrospective cohort study.

Participants: Fifty-five patients with *CRB1*-associated retinal dystrophies from 16 families.

Methods: A medical record review of 55 patients for age at onset, medical history, initial symptoms, best-corrected visual acuity, ophthalmoscopy, fundus photography, full-field electroretinography (ffERG), Goldmann visual fields (VFs) and spectral-domain optical coherence tomography.

Main outcome measures: Age at onset, visual acuity survival time, visual acuity decline rate, and electroretinography and imaging findings.

Results: A retinitis pigmentosa (RP) phenotype was present in 50 patients, 34 of whom were from a Dutch genetic isolate (GI), and 5 patients had a Leber congenital amaurosis (LCA) phenotype. The mean follow-up time was 15.4 years (range, 0-55.5 years). For the RP patients, the median age at symptom onset was 4.0 years. In the RP group, median ages for reaching low vision, severe visual impairment, and blindness were 18, 32, and 44 years, respectively, with a visual acuity decline rate of 0.03 logarithm of the minimum angle of resolution per year. The presence of a truncating mutation did not alter the annual decline rate significantly ($p = 0.75$). Asymmetry in visual acuity was found in 31% of patients. The annual VF decline rate was 5% in patients from the genetic isolate, which was significantly faster than in non-GI patients ($p < 0.05$). Full-field electroretinography responses were extinguished in 50% of patients, were pathologically attenuated without a documented rod or cone predominance in 30% of patients, and showed a rod-cone dysfunction pattern in 20% of RP patients. Cystoid fluid collections in the macula were found in 50% of RP patients.

Conclusions: Mutations in the *CRB1* gene are associated with a spectrum of progressive retinal degeneration. Visual acuity survival analyses indicate that the optimal intervention window for subretinal gene therapy is within the first 2 to 3 decades of life.

INTRODUCTION

Mutations in the *CRB1* gene are associated with a wide variety of severe retinal dystrophies with variable phenotypes, including panretinal dystrophies such as retinitis pigmentosa (RP), Leber congenital amaurosis (LCA) and cone-rod dystrophy, as well as central phenotypes such as isolated macular dystrophy and foveal retinoschisis.[1-3]

RP is a clinically and genetically heterogeneous disorder. Mutations in the *CRB1* gene have been associated with RP12, a distinct form of RP characterized by preservation of para-arteriolar retinal pigment epithelium, progressive visual field loss starting from the first decade of life, and early macular involvement.[4] Other common features are hyperopia and optic disc drusen, previously described in a Dutch genetic isolate (GI).[5] Classic forms of early-onset RP, without preservation of para-arteriolar retinal pigment epithelium, also have been associated with mutations in the *CRB1* gene.[6, 7] The *CRB1* gene accounts for 3% to 9% of nonsyndromic cases of autosomal recessive RP.[8]

Leber congenital amaurosis (LCA) is considered the most severe and earliest occurring form of retinal dystrophy, often characterized by severe visual loss, roving eye movements or nystagmus, and nonrecordable or severely reduced cone and rod electroretinography (ERG) amplitudes within the first year of life. Mutations in the *CRB1* gene account for 7% to 17% of LCA cases.[8, 9]

A high phenotypic variability has been described in patients with *CRB1*-associated retinal dystrophies with respect to the age at onset, the general course of disease, macular involvement, and findings on imaging.[10, 11] *CRB1*-associated dystrophies, unlike other inherited retinal dystrophies, commonly are associated with retinal thickening on OCT.[12] However, normal or reduced retinal thickness also has been described.[13, 14] Specific features associated with *CRB1* gene mutations like Coats-like exudates, nanophthalmos, keratoconus, and macular dystrophy are not present consistently.

More than 200 different mutations in the *CRB1* gene have been described (http://www.LOVD.nl/CRB1; ref. 22065545), without a clear genotype-phenotype correlation. However, a previous study suggested that null mutations and complete loss of CRB1 protein are more likely to cause the earliest-onset *CRB1* phenotype of LCA.[10]

No treatment is available for *CRB1*-associated retinal dystrophies, but structural and functional rescue has been shown after gene therapy in a *CRB1* knockout mouse model.[15] This offers a promising perspective for therapeutic trials for human *CRB1*-associated disease. An optimal insight into the clinical characteristics, variability and natural disease course of *CRB1*-associated retinal dystrophies is important to optimally establish patient eligibility criteria for potential future treatment trials. The current knowledge on these aspects is limited because of the relatively small

population sizes in earlier studies. The purpose of this study was to provide a description of the initial and longitudinal clinical characteristics of a large cohort of patients with *CRB1*-associated retinal dystrophies.

MATERIALS AND METHODS

Study population

Patients were collected from the patient database for hereditary eye diseases (Delleman archive) at the Academic Medical Center in Amsterdam and from various other Dutch tertiary referral centers within the framework of the RD5000 consortium, a Dutch national consortium for the registry of patients with retinal dystrophies.[16] We included patients from a previously described Dutch GI,[5, 17] and patients from outside this GI. Inclusion criteria were a confirmed molecular diagnosis of two likely disease-causing variants in the *CRB1* gene or a clinical diagnosis of an inherited retinal dystrophy in a patient with a first-degree relative with 2 likely disease-causing variants in *CRB1*. Patients should have undergone at least 1 clinical ophthalmologic examination.

Diagnostic criteria for LCA were severe or moderately severe vision loss during the first year of life and non-detectable or severely reduced rod and cone amplitudes on full-field electroretinography (ffERG). Absence of nystagmus was not used as an exclusion criterion for LCA because LCA cases without nystagmus have been described previously.[13, 18]

The study was approved by the Medical Ethics Committee of Erasmus Medical Center and adhered to the tenets of the Declaration of Helsinki. Patients or their legal guardians signed informed consent forms for the use of their clinical data for research purposes.

Genetic analysis

Of the 55 patients, 50 had molecular genetic confirmation of 2 *CRB1* mutations through direct Sanger sequencing or whole exome sequencing. Five patients were first-degree relatives of patients who had received genetic confirmation of *CRB1* gene mutations on both alleles through Sanger sequencing or whole exome sequencing. Genetic analyses were performed at the Academic Medical Center in Amsterdam, The Netherlands, or at the Radboud University Medical Center in Nijmegen, The Netherlands.

The possible deleteriousness of *CRB1* missense variants was evaluated using the HumDiv program of Polymorphism Phenotyping-2 (available at http://genetics.bwh.harvard.edu/pph2/) and Sorting Intolerant from Tolerant (available at http://sift.jcvi.org/) at the public domains or using the Alamut® software (Interactive Biosoftware, Rouen, France).

Clinical data collection

Data were obtained through standardized review of medical records for demographic information, medical history, age at disease onset, initial symptoms, age at diagnosis, best-corrected visual acuity (BCVA), refractive error, biomicroscopy of the anterior segment, dilated fundus examination, fundus photography, ffERG, Goldmann VFs, and spectral-domain (SD) optical coherence tomography (OCT) where available. Age at onset of disease was defined as the age at which the first symptom was noted by the patient or by the patient's parents in case of onset in infancy or early childhood. When symptoms were reported to have been present always, the age at onset was considered to be the first year of life. Retinal cross-sections and retinal thickness measurements were obtained with OCT. Most OCT data were obtained with Topcon (3D OCT-1000, Topcon Medical Systems, Tokyo, Japan) or Heidelberg Spectralis (Heidelberg Engineering, Heidelberg, Germany). Goldmann VF areas of the V4e target were digitized and converted to seeing retinal areas in square millimeters using a method described by Dagnelie.[19]

Statistical analysis

Data were analyzed using SPSS version 23.0 (IBM Corp, Armonk, NY) and R version 3.3.1 (R Foundation for Statistical Computing, Vienna, Austria).[20] Results were considered statistically significant if p <0.05. Kaplan-Meier methodology was used to analyze the time-to-event for the following endpoints: low vision (decimal BCVA, <0.3), severe visual impairment (decimal BCVA, <0.1), and social blindness (decimal BCVA, <0.05). For further analyses, VA was divided into the following categories as defined by the World Health Organization criteria: mild or no visual impairment (≥0.3), moderate visual impairment (<0.3 and ≥0.1), severe visual impairment (<0.1 and ≥0.05) and blindness (<0.05). When BCVA differed between 2 eyes, the better eye was used for survival analyses. Because of the presence of left-, interval-, and right-censored data, the nonparametric maximum likelihood estimator was used to estimate the survival curve for time to reaching low vision, severe visual impairment, and blindness.[21] This statistical analysis was performed in the R software environment.[20]

Linear mixed-model analysis was used to evaluate the annual decline rate of BCVA, converting decimal visual acuities to logarithm of the minimum angle of resolution (logMAR) values and using the mean logMAR for both eyes, and of log retinal seeing areas, using the mean for both eyes. We used the values 2.7 for hand movements, 2.8 for light perception and 2.9 for no light perception. In the mixed model analysis, we controlled for gender, family (GI vs. non-GI), and the presence of a truncating mutation. Asymmetry in BCVA between 2 eyes was defined as a difference of 0.3 logMar or more (≥15 Early Treatment Diabetic Retinopathy Study letters), which is the threshold for clinical significance for changes in BCVA,[22] at 2 consecutive examinations.

RESULTS

Fifty-five patients from 16 families were investigated. Thirty-four patients were part of a large consanguineous pedigree from a genetically isolated town in The Netherlands.[23] Nine patients demonstrated simplex cases, and 12 non-GI patients were part of families with 2 to 3 affected siblings. The data that we were able to collect per patient group are represented in Table S1. All patients were white, and 54 were of European and 1 was of North African descent (patient 48; Table S2).

Five patients had an LCA phenotype and 50 patients had an RP phenotype. Two RP patients (1 GI, 1 non-GI), one of whom was reported previously,[24] initially showed bilateral intermediate uveitis. For the entire cohort, the mean follow-up time was 15.6 years (standard deviation, 13.8 years; range, 0-55.5 years), with a mean number of 6.6 visits per patient (standard deviation 5.3 visits; range, 1-31 visits). Tables S2 and S3 summarize the clinical characteristics of the patients.

Disease onset and visual acuity in *CRB1*-associated retinitis pigmentosa

Data on the age at onset of disease were available for 40 patients. When age at onset of the first symptom was not available, the age at diagnosis was used for analysis. The median age at onset of the first symptom was 4.0 years (standard deviation, 9.4 years; range, 0-47 years) for the entire group. The reported first symptoms are specified in Table S4 and were recognized by the patients' parents. For the GI population, the median age at onset was 2.0 years (standard deviation, 7.3 years; range, 0-36 years), whereas for patients from other families, this median age was 4.5 years (standard deviation, 12.2 years; range, 0-47 years), which was not significantly different ($p = 0.17$, Mann-Whitney *U* test).

The age at symptom onset was 10 years or older in 6 of 40 patients (15%), and the proportion of patients with this relatively late onset did not differ between GI patients (2/26 [8%]) and non-GI patients (4/14 [29%]; $p = 0.16$, Fisher exact test). One non-GI patient initially showed decreased visual acuity, cystoid fluid collections (CFC), and a large central scotoma bilaterally at the age of 47 years (patient 49; compound heterozygous p.(Tyr631Cys), c.2842+5G>A) (Tables S2 and S4).

Best-corrected visual acuity data were available for 49 of 50 patients. Figure 1A shows the proportion of patients in each visual category as defined by the World Health Organization against advancing age, based on BCVA, with Figure 1B showing these categories as defined according to central VF diameter. The median ages for reaching low vision category 1, severe visual impairment, and blindness were 18, 32, and 44 years, respectively (Figure 1C). The survival curves did not differ significantly between GI and non-GI patients. The mean BCVA decline rate was 0.03 logMAR per

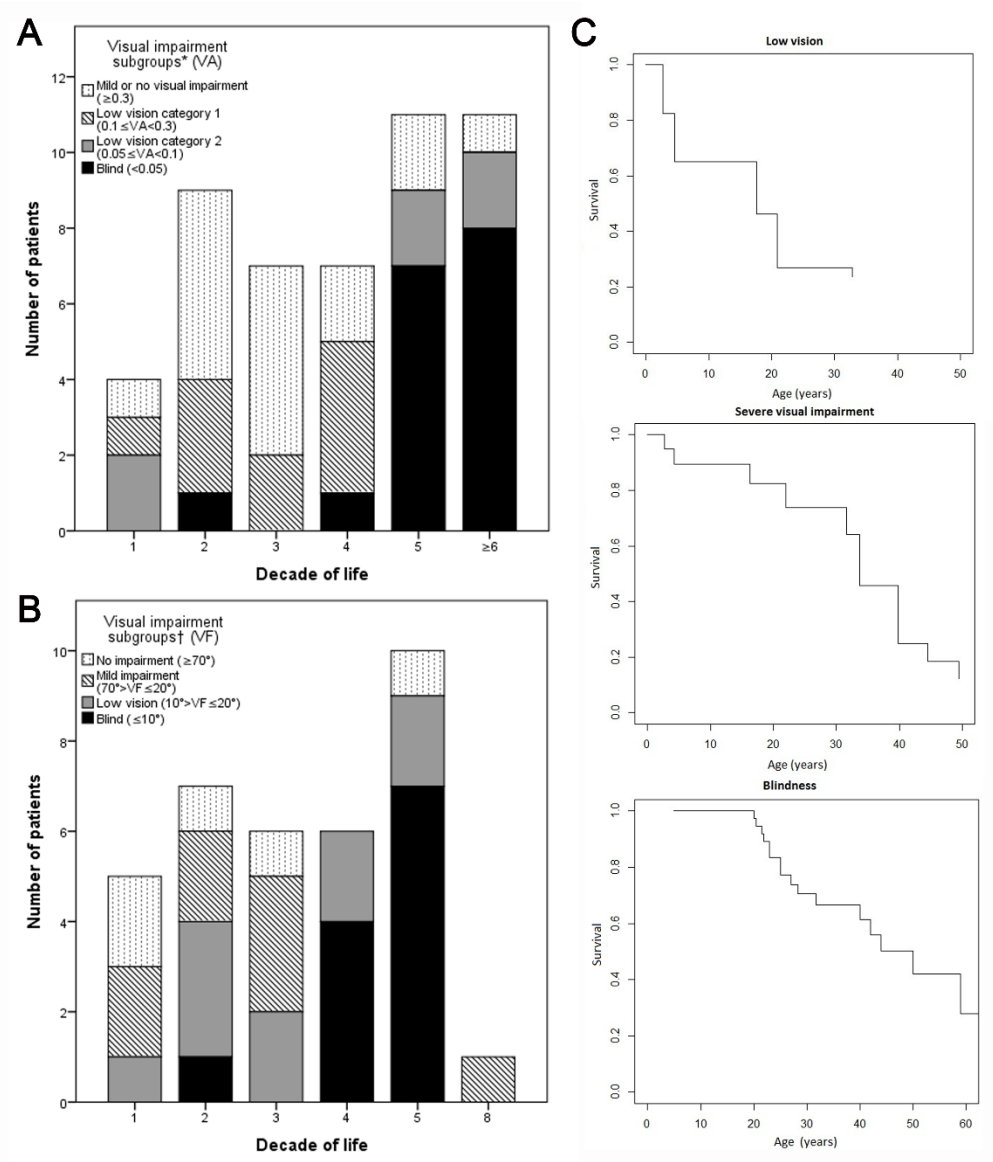

Figure 1. Graphs showing visual impairment with advancing age in patients with *CRB1*-associated retinitis pigmentosa. A. Bar graph showing the number (total = 49) and proportion of patients in each category of visual impairment, based on decimal best-corrected visual acuity (BCVA) with advancing age. The BCVA and age at last examination were used. A statistically significant trend toward worse visual subgroups was seen with advancing age ($P < 0.001$, exact chi-square test for trend). **B.** Bar graph showing the number (n = 35) and proportion of patients in each category of visual impairment, based on central visual field diameter, with advancing age. A statistically significant trend toward worse visual subgroups was seen with advancing age ($P < 0.01$, exact chi-square test for trend). **C.** Survival curves showing the time to reaching low vision (BCVA, <0.3), severe visual impairment (BCVA, <0.1), and blindness (BCVA, <0.05) in the better-seeing eye.

*As defined by the World Health Organization (WHO). †As defined by the WHO. Because the WHO considers visual field diameters of less than 20° to be low vision, we added a subgroup of mild impairment for patients with a central visual field diameter less than 70° but of at least 20° or more. VA = visual acuity; VF = visual field.

year ($p < 0.001$; 95% confidence interval, 0.02-0.03), showing no statistically significant differences between male and female patients and between GI and non-GI patients ($p = 0.61$). The presence of a truncating mutation did not alter the annual decline rate significantly ($p = 0.75$). Regression slopes of annual visual decline for individual patients ranged from 4.33×10^{-3} to 0.18. Repeating this analysis for the BCVA of the better-seeing eye and the worse-seeing eye separately to evaluate symmetry in decline rate yielded similar results: 0.02 logMAR per year ($p < 0.001$; 95% confidence interval, 0.02-0.03) and 0.03 logMAR per year ($p < 0.0001$; 95% confidence interval, 0.02-0.04), respectively.

Asymmetry in BCVA between eyes was found at the last 2 consecutive examinations in 15 of 49 patients (31%). The difference in the proportion of patients with BCVA asymmetry between the GI group (10/33 [30%]) and non-GI group (5/16 [31%]) was not significant ($p = 0.95$, chi-square test). In 9 of 15 patients (60%), the presumed cause of asymmetry could be determined (Table 5).

Ophthalmic and funduscopic findings in *CRB1*-associated retinitis pigmentosa

Forty of 41 patients (98%) were hyperopic (Table S6). Mean astigmatism in patients with known K values (n = 8 patients, 16 eyes) was 1.18 diopters (D; standard deviation, 0.73 D; range, 0.0-2.25 D), and none of the patients received a clinical diagnosis of keratoconus.

Glaucoma was diagnosed in 7 patients (14%) at a mean age of 36.6 years (standard deviation, 15.6 years; range, 14-57 years). In 5 of 7 patients (71%), this was acute angle-closure glaucoma, which was treated with laser peripheral iridotomy in 4 of 5 patients and with peripheral iridectomy in 1 patient. One 14-year-old glaucoma patient had secondary glaucoma after a long treatment for uveitis, for which he underwent a peripheral iridectomy.

Cataract was reported in 26 of 50 patients (52%). In these patients, the mean age at which cataracts first were reported was 31.9 years (standard deviation, 10.6 years; range, 11-47 years) for GI patients, which was significantly earlier than for non-GI patients, in whom cataracts were reported first at a mean age of 43.8 years (standard deviation, 17.0 years; range 21-75 years; $p = 0.038$; unpaired *t* test). In 4 patients, a history of uncomplicated cataract surgery in their second, fourth, fifth, and eighth decade of life resulting from visually significant cataract was documented.

Table 5 and Figure 2 show the fundoscopic findings in this cohort. Four patients had salt-and-pepper pigmentation of the peripheral retina (n = 2) or of the whole retina (n = 2) in the first decade of life, but by the second decade of life, the salt-and-pepper pigmentation had disappeared and bone spicules were found in the periphery.

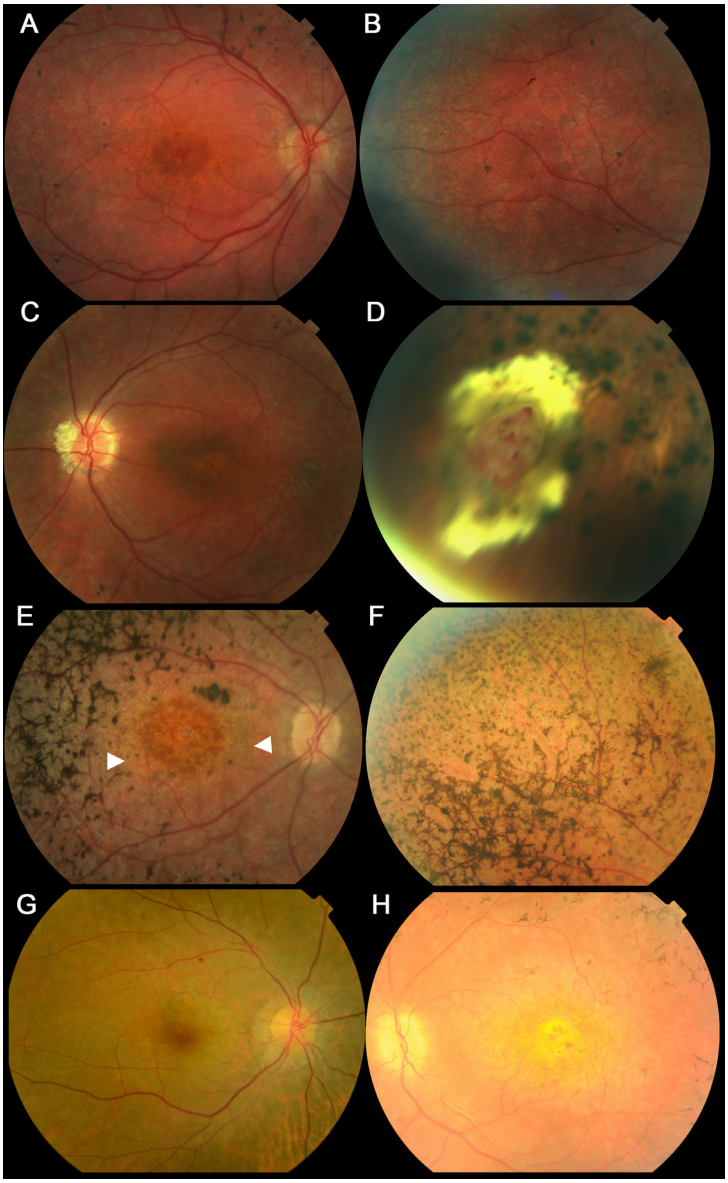

Figure 2. Fundus photographs showing the intrafamilial and interfamilial variability in retinal phenotype. **A-B.** Fundus photograph obtained at 8 years of age from patient 15, a girl from the genetic isolate (GI) group, showing extensive intraretinal hyperpigmentation and fine granular pigmentation in the periphery (best corrected visual acuity [BCVA] in the right eye, 0.16; BCVA in the left eye, 0.2). Electroretinography showed extinguished scotopic and photopic responses since the age of 4 years. **C-D.** Fundus photographs obtained at 23 years of age from patient 3, a man from the GI group who showed Coats-like vasculopathy, hard exudates, optic disc drusen, and a BCVA of 0.35 in both eyes. **E-F.** Fundus photographs obtained at 20 years of age from patient 40, a woman with extensive retinal atrophy, bone-spicule pigmentation, round pigmentation in the periphery, and low vision in both

eyes (BCVA in both eyes, 0.12). The posterior pole showed small yellow lesions with a reticular pseudodrusen-like aspect (arrowheads) that seemed to correspond with small hyperreflective outer retinal accumulations right above the retinal pigment epithelium on spectral-domain optical coherence tomography (Figure 4B). Her 2 sisters had a similar retinal phenotype and visual acuities in their third decade of life. **G.** Fundus photograph obtained at age 47 years from patient 49, a woman showing mild chorioretinal atrophy between the optic disc and macula (BCVA in the right eye, 0.9; in the left eye, 0.8). **H.** Fundus photograph obtained at age 18 years from patient 41, a man showing a pale waxy optic disc and profound atrophy of the posterior pole with bone spicule pigmentation in the midperiphery (BCVA in the right eye, 0.05; in the left eye 0.16).

The mean age at which any macular involvement initially was documented, based on fundoscopy, was 23.5 years (standard deviation, 17.4 years; range, 2-79 years), with no significant difference between the GI patients (mean, 22.2 years; standard deviation, 14.9 years) and the non-GI patients (mean, 25.8 years; standard deviation, 21.9 years). Two patients (6%) demonstrated a documented normal macular appearance at the time of their last examination at 4 and 3 years of age.

Bilateral optic disc drusen were reported in 10 GI patients (29%) and in none of the non-GI patients ($p = 0.025$, chi-square test). Coats-like exudative vasculopathy was reported in 5 patients (10%), with 1 patient showing bilateral peripheral hard exudates. Of these patients, 2 of 5 (40%) were in the non-GI group and 3 of 5 (60%) were in the GI group.

Full-field ERG and visual field findings

The median age at which extinguished electroretinography findings initially were found in this cohort was 13.2 years (mean, 20.7 years; range, 3.9-47.3 years), which did not differ significantly between the GI and non-GI patients or between patients with and without a truncating mutation ($p = 0.71$ and $p = 0.87$, respectively, Mann-Whitney *U* test).

Goldmann VFs were available for 21 RP patients (13 GI patients and 8 non-GI patients). There were various patterns of remaining VF (Figure S3). The mean seeing retinal areas ranged from 21.1 to 637.7 mm^2, corresponding to approximately 20° to 117° VF diameter (Table S7). Among individuals with follow-up Goldmann VFs (n = 6; 2 GI patients and 4 non-GI patients; median follow-up, 1.5 years; range, 1.0-22.1 years), VF areas decreased in size or remained relatively stable, with individual regression slopes varying from -0.3 to -171.9 mm^2/year.

Mixed model analysis of the logarithm of seeing retinal areas revealed a significantly faster VF decline in GI patients than in non-GI patients ($p < 0.05$), with a significant slope of decline in GI patients of -0.02 log seeing retinal area, corresponding to an annual decline of 5% on the original scale ($p < 0.05$). The slope of decline in non-GI patients of -0.04×10^{-2} log was not statistically significant ($p = 0.93$). The presence of a truncating mutation did not have a significant effect on the seeing retinal area decline rate.

Table 5. Clinical characteristics of patients with *CRB1*-associated retinitis pigmentosa or Leber congenital amaurosis

Characteristics	Retinitis pigmentosa (n = 50)	Leber congenital amaurosis (n = 5)
Age at last examination (yrs)		
Mean ± SD (range)	35.5±18.3	10.7±4.7
Range	2.0-78.9	3.9-15.9
Follow-up time (yrs)		
Mean ± SD (range)	16.2±14.3	9.0±4.4
Range	0-55.5	2.4-13.2
Median	13.6	8.7
No. of visits		
Mean ± SD	6.3±5.4	9.4±3.4
Range	1-31	4-13
European ethnicity, no. (%)	49 (98)	5 (100)
Nystagmus, no./total (%)	14/32 (44)	3 (60)
Photophobia, no./total (%)	19/25 (76)	3 (60)
Reported first symptom, no.	34	5
Nyctalopia, no. (%)	13 (38)	2 (40)
Subjective visual acuity loss, no. (%)	9 (26)	-
Subjective visual field loss, no. (%)	3 (9)	-
Subjective color vision loss, no. (%)	2 (6)	-
Nystagmus/eye poking, no. (%)	-	2 (40)
Multiple symptoms, no. (%)	7 (21)	1 (20)
Spherical equivalent refractive error, D		
Mean ± SD	4.2±2.4	5.75±2.5
Range	-0.6 to +8.5	2.0 -8.75
-1 D – 0, no. (%)	1 (2)	-
0 D - +2 D, no. (%)	8 (20)	1 (20)
+2 D - +4 D, no. (%)	12 (29)	-
+4 D - +6 D, no. (%)	10 (24)	2 (40)
>+6 D, no. (%)	10 (24)	2 (40)
Shallow anterior chamber, no. (%)	17/33 (52)	2 (40)
Glaucoma occurrence, no. (%)	7 (14)	-
Acute angle-closure	5 (71)	-
Type not specified	2 (29)	-
Vitreous abnormalities, no. (%)	27 (54)	2 (40)
Cells	8 (30)	1 (20)
Veils	5 (19)	-
Cells and veils	10 (37)	1 (20)
Asteroid hyalosis	4 (15)	-

Table 5. Continued

Fundoscopic examination, no./total (%)		
Optic disc pallor	32/38 (84)	4/5 (80)
Bone-spicule hyperpigmentation	34/37 (92)	-
Vascular attenuation	35/36 (97)	4/5 (80)
Nummular pigmentation	6/37 (16)	-
PPRPE	13/50 (26)	-
PPRPE not mentioned	33/50 (66)	5/5 (100)
Macular sheen	15/37 (41)	-
Macular RPE changes	34/37 (92)	5/5 (100)
Bull's eye maculopathy	8/34 (24)	-
Other form of RPE atrophy,	10/34 (29)	-
Alterations, no profound atrophy	16/34 (47)	5/5 (100)
Full-field electroretinography, no.	30	2
Scotopic and photopic extinguished, no./total (%)	15/30 (50)	2/2 (100)
Rod-cone pattern, no./total (%)	6/30 (20)	-
Cone-rod pattern, no./total (%)	-	-
Scotopic and photopic reduced, no clear cone or rod predominance documented, no./total (%)	9/30 (30)	-

- = no cases; D = diopters; PPRPE = para-arteriolar preservation of retinal pigment epithelium; RPE = retinal pigment epithelium; SD = standard deviation.

Findings on retinal imaging

Fundus autofluorescence (FAF) data were available for 9 patients. In 4 of 9 patients, little to no remaining FAF was found, and any remaining FAF was found in an indistinct pattern in the macula (at ages 17, 20, 27, and 35 years). Two patients showed some remaining FAF around the optic disc and in the fovea (at 29 and 31 years of age; Figure 4). Interestingly, 3 of 9 patients showed remarkably preserved FAF (patients 47, 49, and 50; Table S3) in the posterior pole, with a granular or patchy pattern of reduced FAF, and 1 patient showed a broad hypofluorescent crescent nasal to the macula (Figure 4).

Optical coherence tomography data were available for 22 patients with a mean age of 29.1 years (standard deviation, 16.7 years; range, 7.0-78.9 years). Spectral-domain OCT was available for 11 of 22 patients, whereas in 11 of 22 patients, a Topcon OCT device was used. A mild epiretinal membrane was found in 7 of 22 patients (32%). Central subfield retinal thickness measurements (CRT) were available for 17 patients (n = 9 GI patients, n = 8 non-GI patients) and did not differ significantly between GI and non-GI patients (p = 0.054 for Topcon measurements, p = 0.93 for Heidelberg measurements). Cystoid fluid collections were seen at any time point in the follow-

up period in 11 of 22 patients (50%) of the total population, with the same prevalence in the GI- and non-GI patients; the CFCs were treated in 8 of these patients with acetazolamide (n = 4), brinzolamide (n = 2), or a combination treatment of acetazolamide and methotrexate (n = 2) because of suspected uveitis. This led to CFC reduction in 2 patients and complete resolution in 1 patient. Compared with the Topcon normative database, CRT was normal in 3 of 11 patients (27%), reduced in 4 of 11 patients (36%), and thickened in 4 of 11 patients (36%; CFC in 3 of 4 patients [75%]), with increased or normal thickness in the outer Early Treatment Diabetic Retinopathy Study ring in 9 of 11 patients (82%) and 2 of 11 patients (18%), respectively. Mean CRT declined with advancing age in 7 of 10 patients (70%) with follow-up thickness data and because of CFC reduction in 5 of 7 patients (71%), whereas the mean CRT increased mildly in 3 of 10 patients (30%).

The foveal and peripheral macular ellipsoid zone (EZ) was visible but discontinuous or attenuated on SD-OCT in 8 of 11 patients (73%; ages 23-47 years) and almost absent in 2 non-GI patients (18%) in their second decade of life (Figure 4). Interestingly, the 2 patients with nearly absent EZ had relatively preserved Snellen VA in their better-seeing eye of 0.4 and 0.16 (but 0.05 in the other eye). One non-GI patient (9%; age 30 years) had a nearly continuous uninterrupted EZ in the fovea and peripheral macula. The external limiting membrane was identifiable on SD-OCT in 10 of 11 patients (91%), but was discontinuous in 7 of 10 such patients (70%) and unidentifiable in 1 of 11 patients (9%).

On OCT, the macula showed organisation in identifiable retinal tissue layers on OCT in 10 of 11 patients (91%) and in relatively coarsely laminated fashion in 1 of 11 patients (9%; Figure 4E). The separate retinal layers in the macula all were easily discernible in 7 of 11 patients (64%), and in 4 of 11 patients (36%), the borders between the inner nuclear layer, outer plexiform layer, and outer nuclear layer were more difficult to delineate (Figures 4E and H).

Small hyperreflective dots without shadowing, previously described by Aleman et al,[12] were found in the inner and outer retinal layers at different depths from the vitreoretinal surface in 11 of 11 patients (100%; Figures 4A-D). The origin of these hyperreflectivities was unclear. Larger hyperreflective intraretinal structures were found in 7 of 11 patients (64%) and corresponded with pigment migrations on fundoscopy (Figures 4B and E). Small hyperreflective accumulations at the level of the EZ corresponded with reticular pseudodrusen-like white spots on fundus photography in 4 of 11 patients (36%; Figures 2E and 4E).

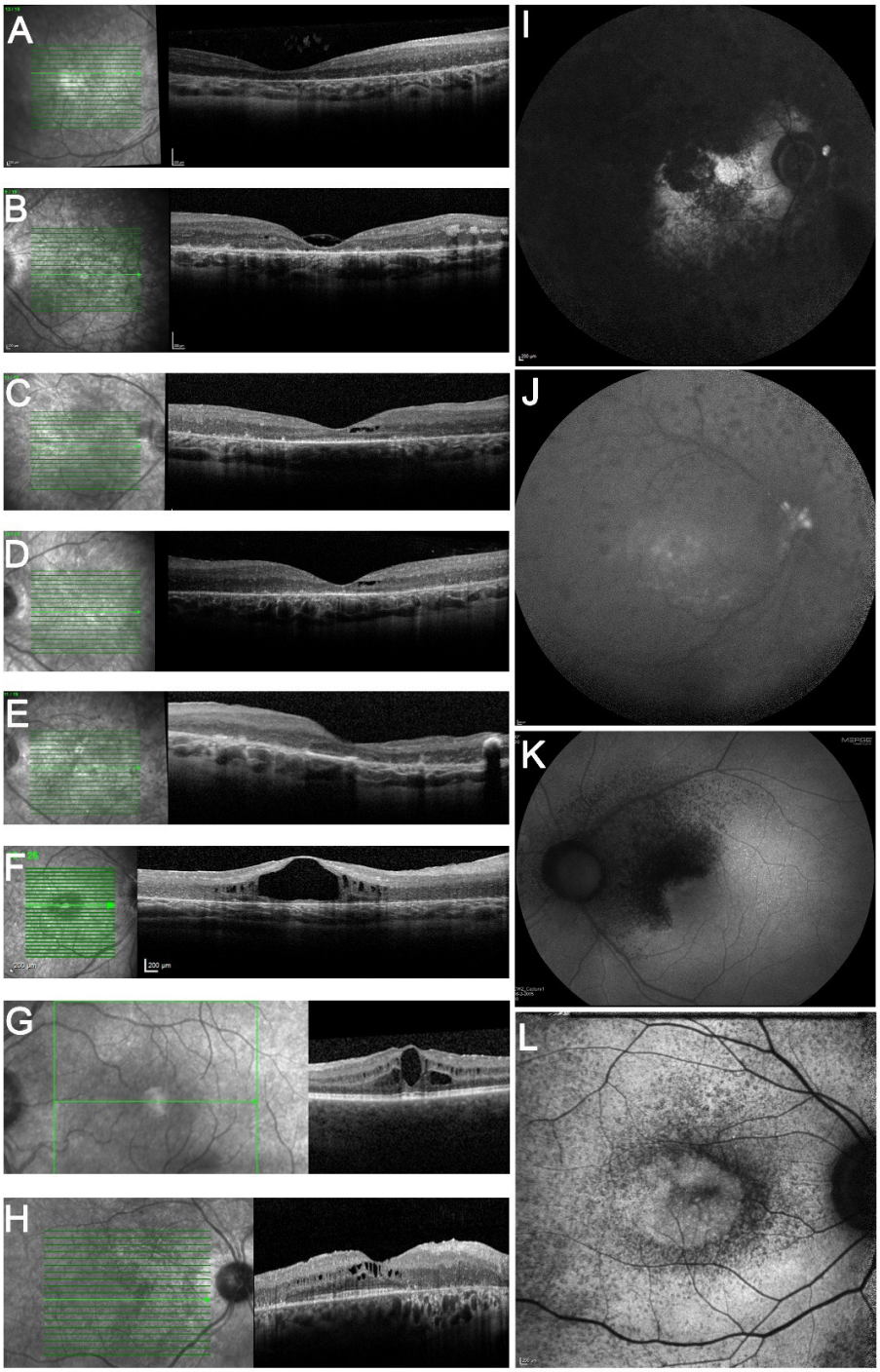

Figure 4. Imaging findings. A. Spectral-domain (SD) optical coherence tomography (OCT) image from patient 41, an 18-year-old man from the non-genetic isolate (GI) group, showing foveal atrophy and thickening of the peripheral

macula with preserved retinal lamination and an almost absent photoreceptor layer. Best-corrected visual acuity (BCVA) was 0.05 and 0.16 in the right and left eyes, respectively. **B.** Patient 40, a 27-year-old woman showing macular atrophy, intraretinal hyperreflectivities, and a discontinuous photoreceptor layer on SD-OCT. At the level of the ellipsoid zone (EZ), the scan shows small hyperreflective outer retinal accumulations right above the retinal pigment epithelium (RPE) that seem to correspond with a reticular pseudodrusenoid-like aspect on fundoscopy (Figure 2E). **C-D.** Patient 39, a 22-year-old woman with retinal asymmetric findings and visual acuity (VA) asymmetry (right eye, 0.4; left eye, 0.05), showing more atrophy of the EZ and the external limiting membrane (ELM) in the left eye and bilateral macular cysts on SD OCT. **E.** Patient 38, a 33-year-old woman showing relatively coarse lamination and an outer plexiform layer that seemed to merge with the inner nuclear and outer nuclear layer outside the fovea on SD-OCT. Clumping at the EZ level corresponded with a reticular pseudodrusenoid aspect on fundoscopy. **F.** Patient 15, a girl from the GI group at 13 years of ageshowing large cystoid fluid collections (CFC), a thickened retina, and an atrophic photoreceptor layer with some EZ signal in a remaining central island on SD-OCT (BCVA in both eyes, 0.16). **G.** Patient 46, a man from the non-GI group at 30 years of age showing CFC and an epiretinal membrane, but with preservation of the EZ and the ELM, corresponding with a relatively preserved BCVA (right eye, 0.72; left eye, 0.82) on SD-OCT. **H.** Patient 49, a 47-year-old woman showing intraretinal CFC in the inner and outer nuclear layer and a preserved EZ and ELM signal in a remaining central island on SD-OCT. Nasally, a confluent hyperreflective layer seemed to be a mixture of outer and inner nuclear layers because of attenuation of the outer plexiform layer. **I.** Fundus autofluorescence (FAF) image from patient 16, a man from the GI group at 29 years of age with relatively preserved vision (VA, 0.3 in the better eye) showing an absence of FAF in most of the retina because of RPE atrophy, except for residual central areas of FAF preservation. **J.** Fundus autofluorescence imagefrom patient 15 showing hyperautofluorescent optic disc drusen and a generally decreased retinal autofluorescence, with some residual autofluorescence in the macula. **K.** Fundus autofluorescence image from patient 49, a 47-year-old woman from the non-GI group with late disease onset and CFC (BCVA declined from 0.7 to 0.5 in both eyes in a few months) showing a broad hypo-autofluorescent crescent nasal to the macula. **L.** Fundus autofluorescence image from patient 47, a 20-year-old man from the non-GI group showing reduced FAF around the macula and in the fovea. This patient had a relatively preserved BCVA (right eye 0.6; left eye 0.3).

Clinical characteristics of *CRB1*-associated Leber congenital amaurosis patients

For the LCA patients (n = 5), the mean age at diagnosis was 2.0 years (standard deviation, 1.1 years; range, 1-3 years). The clinical findings at the last examination are shown in Table S3. Of the 5 patients, 2 patients (patients 3 and 4) were legally blind (first reported at ages 4 and 2 years) and the others were severely visually impaired (first reported at ages 3, 7, and 2 years).

Patients 2 and 4 had a shallow anterior chamber and patient 2 had undergone prophylactic peripheral iridectomy in both eyes at the age of 4 years. Patient 2 also had a history of central retinal vein occlusion in the left eye and panuveitis before the age of 5 in both eyes. The mean age of first reported macular involvement was 2.2 years (standard deviation, 0.8 years; range, 1.2-3.2 years). Patient 1 had a salt-and-pepper fundus at the age of 1 year; patient 2 had granular pigmentation at the age of 5 years, whereas a fundus examination in her first year showed no fundus abnormalities; and patient 4 was described to have a “powdered” pigmentary appearance of the peripheral retina at the age of 2 years. Retinal pigmentation was not described in the other patients. In patients 3 and 4, an ffERG showed extinguished cone and rod responses at the ages of

2 and 3 years, respectively. Confrontation perimetry in all LCA patients and kinetic perimetry in 1 patient showed peripheral VF restriction in all patients that progressed to a small central island of preserved VF in 1 patient at the age of 13 years.

Genetic characteristics and genotype-phenotype correlations

The presence of a truncating mutation and the in silico predictive categories (Table S8) of mutations did not alter significantly the extent of intraindividual visual acuity asymmetry, the age at disease onset, and the age at first macular involvement. The p.(Tyr631Cys) mutation was found in 2 patients with RP with well-preserved visual acuity at the ages of 30 and 48 years, despite the presence of CFC (patients 46 and 49, respectively; Table S2), suggesting that this may be a mild mutation. The p.(Cys948Tyr) mutation was found in compound heterozygous form in 3 of 5 LCA patients (60%) and 4 of 50 RP patients (8%). The RP phenotype was relatively severe in these patients, with Coats-like exudates and blindness in 1 patient (patient 42) and low vision in the other (patient 41) in the third decade of life, progressing to blindness in the fourth decade of life (patient 43). Only patient 47 had no visual impairment in the better eye at age 22 years, based on a relatively preserved BCVA and midperipheral VF loss with a relatively preserved central and peripheral VF. This was the only patient with a p.(Cys948Tyr) mutation combined with a presumably mild missense mutation, p.(Tyr631Cys). The p.(Thr745Met) mutation was found in 4 of 5 LCA patients (80%), consisting of 2 pairs of siblings, and in 1 RP patient (2%), suggesting this may be a severe mutation.

DISCUSSION

In this retrospective cohort study, we examined the natural disease history and phenotypic spectrum of *CRB1*-associated retinal dystrophies in 55 patients from 16 different families. To our knowledge, this is the largest study of patients with *CRB1*-associated retinal dystrophies described to date. The age at symptom onset for RP patients ranged from 0 to 47 years, with a median age at onset of 4.0 years. There was variability in initial presentation, with 15% of RP patients showing symptoms after the first decade.

Most patients in this study showed typical RP fundus features. Early childhood-onset maculopathy in *CRB1*-associated RP and LCA has been described previously in small cohorts and 1 larger cohort of 23 patients,[25-27] and some reports have described *CRB1*-associated isolated maculopathy or cone-rod dystrophy.[2, 3] The proportion of patients with some degree of macular involvement (92% of RP patients and 100% of LCA patients) in the current cohort is higher than in some earlier reports.[28, 29] Coats-like exudative vasculopathy was found in 10% of RP patients and in none of the LCA patients. Previous reports have found Coats-like exudates in 0% to 25%.[12, 17, 18, 29] Full-field electroretinography responses became unrecordable on average in the second decade of life in 50% of our RP cohort and in the first decade of life in our LCA cohort, with high intrafamilial

and interfamilial variability in the RP group. These electroretinography results indicate that most patients with *CRB1*-associated RP and LCA are affected by early panretinal rod and cone dysfunction.

The median ages for reaching low vision (VA, <0.3), severe visual impairment (VA, <0.1), and blindness (VA, <0.05) were 18, 32, and 44 years, respectively. These ages are comparable with those reported by Mathijssen et al,[17] who found median ages of 18 and 35 years for reaching a VA of 0.3 or less and 0.1 or less, respectively. When testing for statistical difference between the survival curves, we found no significant difference between the GI patients and the non-GI patients in this study. Several previous smaller studies have reported cases of *CRB1*-associated retinal dystrophy with low vision in the first and second decades of life and severe visual disability and blindness in the third decade of life.[6, 27, 30, 31] The current study suggests a variable VA spectrum in *CRB1*-associated RP, with a mean VA decline rate of 0.03 logMAR per year and with relatively prolonged preservation of BCVA in a subset of patients.

The peripheral macular area typically was thickened on OCT, with high interpatient variability, and macular CFCs were found in 50% of patients. The outer photoreceptor layers still were well identifiable in 82% of patients, although they showed a certain degree of attenuation, irregularity, or both in most of these patients. Interestingly, these layers included the external limiting membrane, which is assumed to include the Crumbs (CRB) complex that plays a role in the adhesion between photoreceptors and Müller cells.[32, 33] Two patients with a nearly absent EZ still had a relatively preserved VA in the better-seeing eye, suggesting that retinal function may still be relatively intact despite structural signs of photoreceptor degeneration on OCT. Retinal thickness declined with advancing age, mostly because of CFC reduction. Previous studies have reported retinal thinning with advancing age.[12, 17] A relatively disorganized retina with suboptimally visible retinal layers on OCT was present in 9% of patients, and outer retinal layers were more difficult to discern than inner retinal layers in 36% of the total population. The retinal laminar structure on SD-OCT in our patient cohort was relatively intact compared with that of earlier studies that described coarse lamination, defined as unclearly delineated retinal layers, in mice and patients with *CRB1*-associated retinal dystrophies, in both thickened and atrophic areas of retina.[3, 12, 13, 34] Although our findings suggest progressive over congenital changes, a limitation of this study is the lack of longitudinal OCT follow-up, which could clarify if such coarse OCT lamination is the result of a congenital or a degenerative process. The finding of peripheral loss of delineation with central islands of intact lamination in an RP phenotype with centripetal progression would support the notion of intact retinal lamination at birth followed by progressive retinal dystrophy with consequent loss of outer retinal lamination in the affected areas.

Hyperopia, a narrow anterior chamber angle predisposing to glaucoma, and vitreous abnormalities were common features, found in 97%, 52%, and 54% of patients, respectively. These nonretinal

ocular abnormalities in *CRB1*-associated retinal dystrophies point to a multifunctional role of the CRB1 protein in normal ocular development, as has been proposed for other retinal dystrophies such as the bestrophinopathies associated with mutations in the *BEST1* gene.[35] Angle-closure glaucoma occurred in 14% of *CRB1* patients with RP, which is a higher rate than the previously reported 5.9% to 8.7%.[28, 29] Periodic assessment of glaucoma risk and cataract development in these patients therefore may be advisable. Of the GI patients, 29% showed bilateral optic disc drusen. Optic disc drusen in this GI population carrying a homozygous p.(Met1041Thr) mutation in *CRB1* previously were reported in similar numbers.[5, 17] We found no optic disc drusen in the non-GI patients. Interestingly, optic disc drusen have been reported in patients with different *CRB1* genotypes.[6, 36-38] They occur typically in small optic discs and are hypothesized to be caused by abnormalities in axoplasmic transport, axonal degeneration and possibly a small scleral canal.[39] Calcium deposits within the optic nerve axonal mitochondria and the extracellular space lead to optic disc drusen.[40] Retinitis pigmentosa accompanied by optic disc drusen has also been reported in association with mutations in the *MFRP* gene, where it is accompanied by (posterior) microphthalmos, and high hyperopia,[41, 42] as well as in some reports of Usher syndrome.[43] An earlier study showed an incidence of optic disc drusen or parapapillary drusen of 9.2% in autosomal-dominant, autosomal-recessive, and X-linked recessive types of RP,[44] indicating that optic disc drusen are not a unique feature of *CRB1*-associated retinal dystrophies. It is unclear why some *CRB1* genotypes lead to a higher incidence of optic disc drusen than others, but these findings suggest that certain CRB1 domains may play a different role in ocular development.

In this study, we were able to compare clinical long-term follow-up data from a large consanguineous family (GI group) with a cohort of patients with various other *CRB1* mutations (non-GI group). Interestingly, we found genotype-phenotype correlations, including a significantly earlier onset of cataract and a significantly faster decline of the seeing retinal area in the GI population than in the non-GI population. However, these rates of seeing retinal area loss were obtained from mostly cross-sectional data, with longitudinal data available only in 6 patients, and thus may be different in a larger longitudinal study.[45, 46] Also, optic disc drusen were found only in GI patients ($P < 0.05$). Genetic isolate patients had an earlier onset of disease symptoms than non-GI patients and a shorter time span of measurable electroretinography amplitudes, but these differences were not statistically significant, potentially because of underpowered subgroup analyses. The high interindividual variability in disease onset, retinal thickness on OCT, and VF sizes supports the earlier suggestion of the involvement of genetic and possibly environmental modifiers in *CRB1*-associated disease.[47] In mice, *Crb2* is a modifier of *Crb1*,[48] and human *CRB2* can rescue the phenotype in mice lacking *Crb1*.[15] Sequence variants in human *CRB2* cause a renal and cerebral syndrome with possible loss of BCVA and EZ loss on OCT in some patients.[49]

With regard to future therapeutic options such as gene therapy, the visual acuity survival results in this retrospective study show a potential intervention window for gene therapy in the first 3 decades

of life, because we found the median age for reaching severe visual impairment and blindness to be in the fourth and fifth decades of life, respectively, indicating relative preservation of foveal photoreceptors in these first 3 decades. Best-corrected visual acuity is only 1 aspect of determining a therapeutic intervention window, but it is unknown if retinal structure and function are still rescuable at less than certain levels of BCVA. However, MacLaren et al.[50] showed a potentially even greater BCVA improvement in patients with a lower baseline BCVA and limited function, but with intact anatomic features, although the goal of gene therapy in RP phenotypes generally is considered to be a slowing or stopping of progressive worsening rather than BCVA improvement. If the entire retina can be targeted, for instance with intravitreal instead of subretinal gene therapy, parameters such as peripheral VF and ffERG amplitudes also may be important in determining the therapeutic window of opportunity. This intervention window could be expanded in a subset of patients with relatively later disease onset and slower disease progression. Further studies including multimodal imaging are needed to increase our insight in the preservation of retinal structures, because our current retrospective study included a limited number of SD-OCT scans.

Intraindividual asymmetry in visual acuity between 2 eyes was found in 31% of patients. In 60% of these patients, the asymmetry in BCVA between 2 eyes likely was explained by glaucoma or by structural asymmetry in corneal, vitreous, or retinal appearance. In the other patients with asymmetry in BCVA, no structural asymmetry was found. These results suggest that *CRB1*-associated retinal dystrophies are symmetrical between eyes in most patients and use of the contralateral eye as an untreated control in future (gene) therapeutic studies may be appropriate. Our study indicates that intraindividual visual and structural asymmetry should be taken into account when assessing patient eligibility for (gene) therapy inclusion. Prospective natural history studies with standardized visits are needed to understand further the phenotypical spectrum and prognosis of *CRB1*-associated disease to establish candidacy criteria for gene therapy trial inclusion and to determine appropriate outcome measures to evaluate emerging therapeutic options.

REFERENCES

1. Vincent A, Ng J, Gerth-Kahlert C, et al. Biallelic Mutations in CRB1 Underlie Autosomal Recessive Familial Foveal Retinoschisis. Invest Ophthalmol Vis Sci. 2016;57(6):2637-46.
2. Tsang SH, Burke T, Oll M, et al. Whole exome sequencing identifies CRB1 defect in an unusual maculopathy phenotype. Ophthalmology. 2014;121(9):1773-82.
3. Khan AO, Aldahmesh MA, Abu-Safieh L, Alkuraya FS. Childhood cone-rod dystrophy with macular cystic degeneration from recessive CRB1 mutation. Ophthalmic Genet 2014;35(3):130-7.
4. Heckenlively JR. Preserved para-arteriole retinal pigment epithelium (PPRPE) in retinitis pigmentosa. Br J Ophthalmol. 1982;66(1):26-30.
5. van den Born LI, van Soest S, van Schooneveld MJ, et al. Autosomal recessive retinitis pigmentosa with preserved para-arteriolar retinal pigment epithelium. Am J Ophthalmol. 1994;118(4):430-9.
6. Lotery AJ, Malik A, Shami SA, et al. CRB1 mutations may result in retinitis pigmentosa without para-arteriolar RPE preservation. Ophthalmic Genet. 2001;22(3):163-9.
7. den Hollander AI, Davis J, van der Velde-Visser SD, et al. CRB1 mutation spectrum in inherited retinal dystrophies. Hum Mutat. 2004;24(5):355-69.
8. Corton M, Tatu SD, Avila-Fernandez A, et al. High frequency of CRB1 mutations as cause of Early-Onset Retinal Dystrophies in the Spanish population. Orphanet J Rare Dis. 2013;8:20.
9. Vallespin E, Cantalapiedra D, Riveiro-Alvarez R, et al. Mutation screening of 299 Spanish families with retinal dystrophies by Leber congenital amaurosis genotyping microarray. Invest Ophthalmol Vis Sci. 2007;48(12):5653-61.
10. den Hollander AI, Heckenlively JR, van den Born LI, et al. Leber congenital amaurosis and retinitis pigmentosa with Coats-like exudative vasculopathy are associated with mutations in the crumbs homologue 1 (CRB1) gene. Am J Hum Genet. 2001;69(1):198-203.
11. McKibbin M, Ali M, Mohamed MD, et al. Genotype-phenotype correlation for leber congenital amaurosis in Northern Pakistan. Arch Ophthalmol. 2010;128(1):107-13.
12. Aleman TS, Cideciyan AV, Aguirre GK, et al. Human CRB1-associated retinal degeneration: comparison with the rd8 Crb1-mutant mouse model. Invest Ophthalmol Vis Sci. 2011;52(9):6898-910.
13. Simonelli F, Ziviello C, Testa F, et al. Clinical and molecular genetics of Leber's congenital amaurosis: a multicenter study of Italian patients. Invest Ophthalmol Vis Sci. 2007;48(9):4284-90.
14. McKay GJ, Clarke S, Davis JA, et al. Pigmented paravenous chorioretinal atrophy is associated with a mutation within the crumbs homolog 1 (CRB1) gene. Invest Ophthalmol Vis Sci. 2005;46(1):322-8.
15. Pellissier LP, Quinn PM, Alves CH, et al. Gene therapy into photoreceptors and Muller glial cells restores retinal structure and function in CRB1 retinitis pigmentosa mouse models. Hum Mol Genet. 2015;24(11):3104-18.
16. van Huet RA, Oomen CJ, Plomp AS, et al. The RD5000 database: facilitating clinical, genetic, and therapeutic studies on inherited retinal diseases. Invest Ophthalmol Vis Sci. 2014;55(11):7355-60.
17. Mathijssen IB, Florijn RJ, van den Born LI, et al. Long-term follow-up of patients with retinitis pigmentosa type 12 caused by CRB1 mutations: a severe phenotype with considerable interindividual variability. Retina. 2017;37(1):161-172.

18. Galvin JA, Fishman GA, Stone EM, Koenekoop RK. Evaluation of genotype-phenotype associations in leber congenital amaurosis. Retina. 2005;25(7):919-29.
19. Dagnelie G. Conversion of planimetric visual field data into solid angles and retinal areas. Clinical Vision Science. 1990;5(1):95-100.
20. R Core Team (2013). R: A Language and Environment for Statistical Computing. R Foundation for Statistical Computing, Vienna, Austria. http://www.R-project.org; 2013; Accessed September 23, 2016.
21. Wellner JA, Zhan Y. A Hybrid Algorithm for Computation of the Nonparametric Maximum Likelihood Estimator From Censored Data. J Am Statistical Assoc. 1997;92(439):945-59.
22. Csaky KG, Richman EA, Ferris IIIFL. Report from the NEI/FDA Ophthalmic Clinical Trial Design and Endpoints Symposium. Invest Ophthalmol Vis Sci. 2008;49(2):479-89.
23. van Soest S, van den Born LI, Gal A, et al. Assignment of a gene for autosomal recessive retinitis pigmentosa (RP12) to chromosome 1q31-q32.1 in an inbred and genetically heterogeneous disease population. Genomics. 1994;22(3):499-504.
24. Hettinga YM, van Genderen MM, Wieringa W, et al. Retinal Dystrophy in 6 Young Patients Who Presented with Intermediate Uveitis. Ophthalmology. 2016;123(9):2043-2046.
25. Jonsson F, Burstedt MS, Sandgren O, et al. Novel mutations in CRB1 and ABCA4 genes cause Leber congenital amaurosis and Stargardt disease in a Swedish family. Eur J Hum Genet. 2013;21(11):1266-71.
26. Vamos R, Kulm M, Szabo V, et al. Leber congenital amaurosis: first genotyped Hungarian patients and report of 2 novel mutations in the CRB1 and CEP290 genes. Eur J Ophthalmol. 2016;26(1):78-84.
27. Khaliq S, Abid A, Hameed A, et al. Mutation screening of Pakistani families with congenital eye disorders. Exp Eye Res. 2003;76(3):343-8.
28. Henderson RH, Mackay DS, Li Z, et al. Phenotypic variability in patients with retinal dystrophies due to mutations in CRB1. Br J Ophthalmol. 2011;95(6):811-7.
29. Coppieters F, Casteels I, Meire F, et al. Genetic screening of LCA in Belgium: predominance of CEP290 and identification of potential modifier alleles in AHI1 of CEP290-related phenotypes. Hum Mutat. 2010;31(10):E1709-66.
30. Riveiro-Alvarez R, Vallespin E, Wilke R, et al. Molecular analysis of ABCA4 and CRB1 genes in a Spanish family segregating both Stargardt disease and autosomal recessive retinitis pigmentosa. Mol Vis. 2008;14:262-7.
31. Tosi J, Tsui I, Lima LH, et al. Case report: autofluorescence imaging and phenotypic variance in a sibling pair with early-onset retinal dystrophy due to defective CRB1 function. Curr Eye Res. 2009;34(5):395-400.
32. Alves CH, Pellissier LP, Wijnholds J. The CRB1 and adherens junction complex proteins in retinal development and maintenance. Prog Retin Eye Res. 2014;40:35-52.
33. Spaide RF, Curcio CA. Anatomical correlates to the bands seen in the outer retina by optical coherence tomography: literature review and model. Retina. 2011;31(8):1609-19.
34. Pellissier LP, Alves CH, Quinn PM, et al. Targeted ablation of CRB1 and CRB2 in retinal progenitor cells mimics Leber congenital amaurosis. PLoS Genet. 2013;9(12):e1003976.
35. Boon CJ, Klevering BJ, Leroy BP, et al. The spectrum of ocular phenotypes caused by mutations in the BEST1 gene. Prog Retin Eye Res. 2009;28(3):187-205.

36. Zenteno JC, Buentello-Volante B, Ayala-Ramirez R, Villanueva-Mendoza C. Homozygosity mapping identifies the Crumbs homologue 1 (Crb1) gene as responsible for a recessive syndrome of retinitis pigmentosa and nanophthalmos. Am J Med Genet A. 2011;155a(5):1001-6.
37. Paun CC, Pijl BJ, Siemiatkowska AM, et al. A novel crumbs homolog 1 mutation in a family with retinitis pigmentosa, nanophthalmos, and optic disc drusen. Mol Vis. 2012;18:2447-53.
38. Cordovez JA, Traboulsi EI, Capasso JE, et al. Retinal Dystrophy with Intraretinal Cystoid Spaces Associated with Mutations in the Crumbs Homologue (CRB1) Gene. Ophthalmic Genet. 2015;36(3):257-64.
39. Lam BL, Morais CG, Jr., Pasol J. Drusen of the optic disc. Curr Neurol Neurosci Rep. 2008;8(5):404-8.
40. Tso MO. Pathology and pathogenesis of drusen of the optic nervehead. Ophthalmology. 1981;88(10):1066-80.
41. Ayala-Ramirez R, Graue-Wiechers F, Robredo V, et al. A new autosomal recessive syndrome consisting of posterior microphthalmos, retinitis pigmentosa, foveoschisis, and optic disc drusen is caused by a MFRP gene mutation. Mol Vis. 2006;12:1483-9.
42. Crespi J, Buil JA, Bassaganyas F, et al. A novel mutation confirms MFRP as the gene causing the syndrome of nanophthalmos-renititis pigmentosa-foveoschisis-optic disk drusen. Am J Ophthalmol. 2008;146(2):323-8.
43. Edwards A, Grover S, Fishman GA. Frequency of photographically apparent optic disc and parapapillary nerve fiber layer drusen in Usher syndrome. Retina. 1996;16(5):388-92.
44. Grover S, Fishman GA, Brown J, Jr. Frequency of optic disc or parapapillary nerve fiber layer drusen in retinitis pigmentosa. Ophthalmology. 1997;104(2):295-8.
45. Massof RW, Dagnelie G, Benzschawel T, et al. First order dynamics of visual field loss in retinitis pigmentosa. Clinical Vision Science. 1990;5(1):1-26.
46. Grover S, Fishman GA, Anderson RJ, et al. Rate of visual field loss in retinitis pigmentosa. Ophthalmology. 1997;104(3):460-5.
47. Yzer S, Fishman GA, Racine J, et al. CRB1 heterozygotes with regional retinal dysfunction: implications for genetic testing of leber congenital amaurosis. Invest Ophthalmol Vis Sci. 2006;47(9):3736-44.
48. Pellissier LP, Lundvig DM, Tanimoto N, et al. CRB2 acts as a modifying factor of CRB1-related retinal dystrophies in mice. Hum Mol Genet. 2014;23(14):3759-71.
49. Lamont RE, Tan WH, Innes AM, et al. Expansion of phenotype and genotypic data in CRB2-related syndrome. Eur J Hum Genet. 2016;24(10):1436-44.
50. MacLaren RE, Groppe M, Barnard AR, et al. Retinal gene therapy in patients with choroideremia: initial findings from a phase 1/2 clinical trial. Lancet. 2014;383(9923):1129-37.

SUPPLEMENTAL MATERIAL

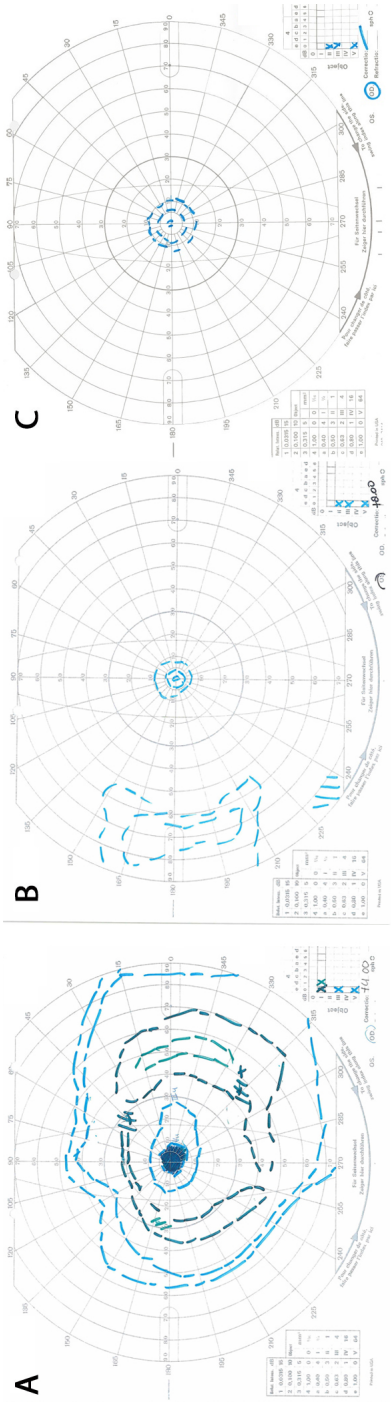

Figure S3. Goldmann visual fields (GVFs) illustrating the variability in residual visual fields. A. A 35-year old woman with concentric visual field constriction and a central scotoma for the V-4e target. At the last visit, this patient was 56 years old and had not yet experienced subjective visual field loss or nyctalopia. **B.** 48-year old woman, small central field with temporal island for the V-4e target. **C.** 17-year old female with a small residual central visual field. Visual fields were symmetrical between eyes.

Table S1. Data collected for patients with *CRB1*-associated RP and LCA

Retrieved data	RP patients, n (%)	LCA patients, n (%)
Age at onset	40 (80)	5 (100)
Visual acuity	49 (98)	5 (100)
Refractive error	41 (82)	5 (100)
K-values	8 (16)	0 (0)
Fundoscopy data	46 (92)	5 (100)
Optic disc color	38 (76)	5 (100)
Pigmentation aspect	37 (74)	5 (100)
Vascular caliber	36 (72)	5 (100)
Retinal pigment epithelium aspect	37 (74)	5 (100)
Electroretinogram pattern	30 (60)	2 (40)
Description of visual field	35 (70)	5 (100)
Goldmann visual field	21 (42)	1 (20)
Fundus autofluorescence	9 (18)	0 (0)
OCT	22 (44)	0 (0)
SD-OCT	11	-
Topcon OCT	11	-

Table S2. Clinical characteristics of *CRB1*-associated retinitis pigmentosa patients with clinical findings at last examination

ID/Sex	Age at diagnosis	Age at onset first symptom	Age at last exam	Nystagmus at last exam	BCVA at last exam (logMAR [Snellen])		SER (D)*	ERG scotopic/ photopic†
					OD	OS		
1/F	6	0	33	No	1.3 (20/400)	1.00 (20/200)	+1.5	ND/ND
2/M	18	3	56	No	1.77 (20/1176)	1.77 (20/1176)	+1.2	ND/ND
3/M	7	0	23	No	0.46 (20/58)	0.46 (20/58)	+6.75	ND/MR
4/F	5	NA	14	No	1.30 (20/400)	0.70 (20/100)	+5.2	ND/MR
5/F	NA	NA	37	NA	NA	NA	NA	NA
6/F	29	0	57	Yes	2.90 (NLP)	2.80 (LP)	+3.75	NA
7/F	NA	NA	49	NA	1.38 (20/476)	0.48 (20/60)	+1.43	NA
8/F	28	7	65	Yes	2.80 (LP)	2.80 (LP)	+3.75	ND/ND
9/F	4	4	6	Yes	0.7 (20/100)	1.00 (20/200)	+6.5	RR/RR
10/F	7	1	7	Yes	1.30 (20/400)	1.30 (20/400)	+7.75	NA
11/M	2	2	4	NA	1.30 (20/400)	1.30 (20/400)	+5.375	NA
12/F	4	0	17	Yes	1.48 (20/606)	2.70 (HM)	+4.6	ND/ND
13/M	3	2	11	NA	0.70 (20/100)	0.22 (20/33)	+2.25	RR/MR
14/M	4	0	16	No	0.23 (20/34)	0.22 (20/33)	+3.9	ND/MR
15/F	NA	1	13	NA	0.80 (20/125)	0.80 (20/125)	+3.3	ND/ND
16/M	6	5	29	No	1.00 (20/200)	0.48 (20/60)	+0.6	ND/ND
17/M	6	0	61	Yes	2.90 (NLP)	2.80 (LP)	+7.5	ND/ND
18/M	26	0	49	Yes	2.80 (LP)	2.90 (NLP)	+8	NA
19/F	NA	NA	50	Yes	1.20 (20/317)	2.10 (20/2500)	+8.5	NA
20/F‡	NA	NA	45	NA	2.80 (LP)	2.80 (LP)	>+4	NA
21/M	16	0	43	No	2.10 (20/2500)	1.60 (20/800)	+6.9	NA

Table S2. Continued

22/F	NA	6	47	Yes	2.80 (LP)	2.10 (20/2500)	+6	NA
23/F	10	6	48	Yes	1.08 (20/241)	1.24 (20/345)	+7	NA
24/F	9	0	56	No	1.30 (20/400)	1.77 (20/1250)	+7.3	RR/RR
25/M	4	0	36	No	1.77 (20/1250)	1.77 (20/1250)	+3.75	ND/ND
26/F	NA	NA	25	NA	0.7 (20/100)	1.48 (20/600)	+1.7	NA
27/M	NA	NA	38	NA	0.7 (20/100)	1.0 (20/200)	+4.0	NA
28/F	6	NA	40	NA	1.3 (20/400)	1.89 (2/160)	+2.7	NA
29/M	NA	NA	34	Yes	1.00 (20/200)	0.70 (20/100)	+2.1	ND/ND
30/F)	5	4	53	Yes	2.80 (LP)	2.80 (LP)	+1.5	ND/ND
31/F	7	7	7	No	0.52 (20/66)	0.40 (20/50)	+3.6	ND/MR
32/M	38	36	38	NA	0.1 (20/200)	0.01 (2/200)	+2.6	RR/RR
33/F	14	NA	23	NA	0.4 (20/50)	0.8 (20/125)	NA	NA
34/F	NA	NA	13	NA	1.00 (20/200)	0.5 (20/63)	NA	ND/RR
35/M	6	6	43	Yes	2.80 (LP)	2.80 (LP)	NA	NA
36/M	NA	10	58	No	2.90 NLP	2.80 (LP)	NA	ND/ND
37/M	6	5	41	No	2.80 (LP)	2.80 (LP)	+7.9	MR/MR
38/F	NA	4	33	NA	0.80 (20/127)	1.00 (20/200)	+5.75	MR/MR
39/F	2	2	22	NA	0.40 (20/50)	1.30 (20/400)	+7.6	ND/ND
40/F	3	0	29	NA	0.70 (20/100)	1.00 (20/200)	+5.9	ND/ND
41/M	4	4	19	No	1.30 (20/400)	0.8 (20/125)	+3.2	ND/MR
42/M	NA	NA	40	NA	2.70 (HM)	2.70 (HM)	NA	NA
43/F	16	NA	45	NA	2.70 (HM)	1.89 (20/155)	+2.8	ND/ND
44/M	33	0	59	No	2.80 (LP)	2.80 (LP)	NA	NA
45/F	NA	NA	78	NA	0.22 (20/33)	0.70 (20/100)	NA	NA
46/M	NA	0	30	NA	0.14 (20/28)	0.09 (20/24)	+0.5	RR/RR

47/M	18	13	21	No	0.40 (20/50)	0.80 (20/125)	+0	RR/RR
48/F	NA	9	19	No	0.30 (20/40)	0.30 (20/40)	+1.4	NA
49/F	47	47	48	No	0.30 (20/40)	0.30 (20/40)	NA	RR/RR
50/F	4	0	11	No	0.4 (20/50)	1.3 (20/400)	+5	RR/RR

NA = not available. SER = spherical equivalent of refractive error. ERG = electroretinogram. ND = not detectable (extinguished ERG). MR = minimal response. RR = reduced response.

* SER (D) is the mean of the last available refractive error of OD and OS.

† Last available ERG. The ERG was often performed once to confirm diagnosis.

‡ This patient has microphthalmia with opaque corneas.

Table S3. Clinical characteristics of *CRB1*-associated Leber congenital amaurosis patients with clinical findings at last examination

ID/Sex	Age at diagnosis	Age at onset first symptom	Age at last exam	Nystagmus at last exam	BCVA at last exam (logMAR [Snellen])		SER (D)*	ERG scotopic/ photopic†
					OD	OS		
1/F	1	0	3	Yes	1.25 (20/357)*		+2	NA
2/F†	NA	0	8	No	1.1 (20/250)	2.80 (LP)	+7	NA
3/F†	3	0	23	Yes	2.15 (20/2857)	1.52 (20/667)	+6	ND/ND
4/M‡	3	NA	15	Yes	1.59 (20/769)	1.85 (20/1429)	+8.75	ND/ND
5/M‡	1	0	14	No	1.1 (20/250)	1.3 (20/400)	+5	NA

* OU vision. This was measured due to the patient's age.

† Sibling pair I.

‡ Sibling pair II.

Table S4. Genetic characteristics of patients with *CRB1*-associated retinal dystrophies

	Allele 1		Allele 2			
Patient	**DNA change**	**Amino acid change**	**DNA change**	**Amino acid change**	**Diagnosis**	
1-34*	c.3122T>C	p.(Met1041Thr)	c.3122T>C	p.(Met1041Thr)	RP12/early onset RP (+ Coats in n = 3)	
35, 36	c.2290C>T	p.(Arg764Cys)	c.2290C>T	p.(Arg764Cys)	RP	
37	c.2290C>T	p.(Arg764Cys)	c.1208C>G	p.(Ser403*)	RP + Coats + PPRPE	
38-40	c.2290C>T	p.(Arg764Cys)	c.2983G>T	p.(Glu995*)	RP, PPRPE (patient 39)	
41	c.2843G>A	p.(Cys948Tyr)	c.3122T>C	p.(Met1041Thr)	RP	
42	c.2843G>A	p.(Cys948Tyr)	c.2978+5G>A	p.(?)	RP + Coats	
43	c.2843G>A	p.(Cys948Tyr)	c.2509G>C	p.(Asp837His)	RP	Mutation 3†: c.4060G>A; p.(Ala1354Thr)
44, 45	c.1892A>G	p.(Tyr631Cys)	c.2983G>T	p.(Glu995*)	RP	
46	c.2983G>T	p.(Glu995*)	c.1892A>G	p.(Tyr631Cys)	RP	
47	c.1892A>G	p.(Tyr631Cys)	c.2843G>A	p.(Cys948Tyr)	RP	
48*	c.2693A>C	p.(Asn898Thr)	c.2693A>C	p.(Asn898Thr)	RP	
49	c.1892A>G	p.(Tyr631Cys)	c.2842+5G>A	p.(?)	Late onset RP	
50	c.2234C>T	p.(Thr745Met)	c.2842+5G>A	p.(?)	RP	
51	c.2843G>A	p.(Cys948Tyr)	c.3152G>A	p.(Trp1051*)	LCA	
52, 53	c.2234C>T	p.(Thr745Met)	c.2234C>T	p.(Thr745Met)	LCA	
54, 55	c.2234C>T	p.(Thr745Met)	c.2843G>A	p.(Cys948Tyr)	LCA	

* consanguineous parents

† This variant is likely not pathogenic.

No patient in our cohort had *CRB1* null mutations on both alleles. Of the patients with one null mutation and one missense mutation (n = 8), one patient had LCA and the others had an RP phenotype with variable visual performances.

Table S6. Patients with asymmetry in visual acuity

Patient number	Presumed cause of asymmetry
4	Corneal opacity in worse eye
7	Unknown
9	Monocular rotatory nystagmus in worse eye
16	Unknown
26	Anisometropia, which may point to amblyopia (spherical OD +1.25D; OS +2.75D)
27	Unknown
28	Combination of CFC, thicker cataract, more prominent optic disc drusen, gliosis, and an epiretinal membrane in the worse eye
29	Unknown
33	Unknown
34	Unknown
39	More retinal atrophy and interruption of EZ and ELM in the worse eye
41	More EZ atrophy in worse eye
45	Asteroid hyalosis and macular RPE alterations in worse eye
47	Secondary glaucoma and more foveal atrophy in the worse eye. Patient had undergone ELM peeling in both eyes at the age of 14 after years of treatment for CFC. It is unknown if there is an iatrogenic contribution to the increased foveal atrophy in the worse eye.
50	Fundus autofluorescence showed a slightly larger area of absent autofluorescence in the worst eye, but SD-OCT and fundus findings showed no other structural asymmetries.

CFC = cystoid fluid collections in the macula. EZ = ellipsoid zone. ELM = external limiting membrane.

Table S7. Visual field sizes and patterns

Seeing retinal area by decade of life	**Mean (SD [range])**
2 (n = 5)	187.2 (239.8 [23.8-603.7])
3 (n = 4)	209.8 (186.4 [63.4-482.9])
4 (n = 7)	178.6 (180.7 [32.2-548.5])
5 (n = 5)	150.9 (272.9 [1.9-637.7])
Seeing retinal area size*	**n (%)**
Large	4 (19)
Medium	14 (67)
Small	3 (14)
Visual field pattern	**n (%)**
Concentric constriction	2 (10)
Central island only	2 (10)
Central island with peripheral islands	9 (43)
Para-central scotomas	3 (14)
Other†	5 (24)

* Seeing retinal area sizes were divided in 3 groups of large (>250 mm^2), medium (25-250 mm^2), and small (<25 mm^2).

Seeing retinal area = last available retinal seeing area in mm^2. The mean seeing retinal areas in mm^2 corresponded with 58°, 62°, 56°, and 52° in the second, third, fourth, and fifth decades of life, respectively.

† Other: In 1 patient, a paracentral rest remained. In 3/21 patients, only (mid-)peripheral islands remained, varying in size between patients. Only 1/21 patients had a central scotoma.

Table S8. *CRB1* mutations in this study; pathogenicity and deleteriousness of found mutations as defined by in silico prediction tools

Mutation	Effect	SIFT	Polyphen-2	Grantham	PhyloP	References*
c.3122T>C	p.(Met1041Thr)	Deleterious	Possibly damaging	81 (moderate)	4.73	1
c.2290C>T	p.(Arg764Cys)	Tolerated	Benign	180 (large)	-0.04	1
c.1208C>G	p.(Ser403*)					1
c.2983G>T	p.(Glu995*)					1
c.2843G>A	p.(Cys948Tyr)	Deleterious	Probably damaging	194 (large)	5.29	1
c.2978+5G>A	p.(?)					1
c.4060G>A	p.(Ala1354Thr)	Deleterious	Possibly damaging	58 (small)	2.38	2
c.1892A>G	p.(Tyr631Cys)	Tolerated	Benign	194 (large)	-0.76	3
c.2693A>C	p.(Asn898Thr)	Deleterious	Possibly damaging	65 (small)	4.64	This study
c.3152G>A	p.(Trp1051*)					4
c.2234C>T	p.(Thr745Met)	Deleterious	Probably damaging	81 (moderate)	4.16	2
c.2509G>C	p.(Asp837His)	Deleterious	Possibly damaging	81 (moderate)	3.68	2
c.2842+5G>A	p.(?)					

In silico predictions of SIFT and Polyphen-2 (using the HumDiv program), together with Grantham and PhyloP conservation scores.

*1 = Den Hollander et al., 1999

*2 = Den Hollander et al., 2004

*3 = van Huet et al., 2015

*4 = Corton et al., 2013

2.2

CRB1-associated retinal dystrophies in a Belgian cohort: genetic characteristics and long-term clinical follow-up

Mays Talib, MD[1], Caroline Van Cauwenbergh, PhD[2,3], Julie De Zaeytijd, MD[2], David Van Wynsberghe, MD[4], Elfride De Baere, MD, PhD[3], Camiel JF Boon, MD, PhD[1,5], Bart P Leroy, MD, PhD[2,3,62,7]

Br J Ophthalmol 2021; online ahead of print

1 Department of Ophthalmology, Leiden University Medical Centre, Leiden, The Netherlands.
2 Department of Ophthalmology, Ghent University and Ghent University Hospital, Ghent, Belgium.
3 Center for Medical Genetics, Ghent University and Ghent University Hospital, Ghent, Belgium.
4 Department of Ophthalmology, Maria Middelares General Hospital, Ghent, Belgium.
5 Department of Ophthalmology, Amsterdam UMC, Academic Medical Center, University of Amsterdam, Amsterdam, The Netherlands.
6 Division of Ophthalmology, The Children's Hospital of Philadelphia, Philadelphia, PA, USA.
7 Centre for Cellular & Molecular Therapeutics, The Children's Hospital of Philadelphia, Philadelphia, PA, USA.

ABSTRACT

Aim: To investigate the natural history in a Belgian cohort of *CRB1*-associated retinal dystrophies.

Methods: An in-depth retrospective study focusing on visual function and retinal structure.

Results: Forty patients from 35 families were included (ages: 2.5-80.1 years). In patients with a follow-up of >1 year (63%), the mean follow-up time was 12.0 years (range: 2.3-29.2). Based on patient history, symptoms and/or electroretinography, 22 patients (55%) were diagnosed with retinitis pigmentosa (RP), 15 (38%) with Leber congenital amaurosis (LCA) and 3 (8%) with macular dystrophy (MD), the latter being associated with the p.(Ile167_Gly169del) mutation (in compound heterozygosity). MD later developed into a rod-cone dystrophy in one patient. Blindness at initial presentation was seen in the first decade of life in LCA, and in the fifth decade of life in RP. Eventually, 28 patients (70%) reached visual acuity-based blindness (<0.05). Visual field-based blindness (<10°) was documented in 17/25 patients (68%). Five patients (13%) developed Coats-like exudative vasculopathy. Intermediate/posterior uveitis was found in three patients (8%). Cystoid maculopathy was common in RP (9/21; 43%) and MD (3/3; 100%). Macular involvement, varying from retinal pigment epithelium alterations to complete outer retinal atrophy, was observed in all patients.

Conclusion: Bi-allelic *CRB1* mutations result in a range of progressive retinal disorders, most of which are generalised, with characteristically early macular involvement. Visual function and retinal structure analysis indicates a window for potential intervention with gene therapy before the fourth decade of life in RP and the first decade in LCA.

INTRODUCTION

Inherited retinal dystrophies (IRDs) comprise a genetically and clinically heterogeneous group of disorders, characterised by progressive degeneration of photoreceptors. The most severe form of IRD is Leber congenital amaurosis (LCA), with an estimated prevalence of 1:33.000 - 1:81.000.[1, 2] LCA presents in infancy with nystagmus and aberrant or absent visual behaviour, and poor pupillary responses. The electrophysiological responses are non-detectable from birth. The most common form of IRD, however, is retinitis pigmentosa (RP), occurring in approximately 1:3.000 - 1:4.000 worldwide.[3] RP is characterised by a progressive rod-cone degeneration, leading to isolated night blindness initially, followed by progressive (mid)peripheral visual field loss, and eventually some degree of central visual loss.

Mutations in the *CRB1* gene account for 7%-17% of LCA cases, and 3%-9% of isolated, non-syndromic, autosomal recessive RP patients, depending on geographic location, making it one of the most common genetic causes of both LCA and RP.[4, 5] *CRB1* mutations are further associated with rare cases of cone-rod dystrophy or macular dystrophy (MD).[6, 7] To date, more than 230 pathogenic variants in *CRB1* have been reported,[8] and some genotype-phenotype correlations have emerged.[9, 10] Relatively few clinical cohorts have been described thus far.[9, 11] In the largest clinical long-term follow-up cohort published thus far, we have described 55 patients, who were found to have either *CRB1*-associated RP or LCA, and we found the window of therapeutic opportunity to be in the first three decades of life in RP, while LCA presented with much earlier blindness.[9]

Although for most IRDs no effective and approved treatment is currently available, the recent approval of subretinal gene therapy for *RPE65*-associated IRDs presents a promising perspective for other candidate genes.[12] One such candidate gene is *CRB1*, for which retinal gene therapy has shown efficacy in rescuing the retinal structure and function in mouse models.[13] As human subretinal gene therapy is being developed for *CRB1*-associated retinopathies, a full understanding of the natural disease course, clinical variability and potential genotype-phenotype correlations in diverse patient populations is essential to provide patients and their families with an accurate prognosis, to assess the best clinical endpoints for future trials, and to enable consequent efficient patient selection for treatment. The aim of the present study was to investigate the natural history and longitudinal characteristics in a large cohort of Belgian patients with *CRB1*-associated IRDs.

METHODS

Subjects and data collection

This study identified patients with *CRB1*-associated IRDs, who underwent ≥1 clinical examination. Inclusion criteria were molecular confirmation of two likely disease-causing variants in *CRB1*,

or a clinical diagnosis of IRD in a patient with a sibling with two molecularly confirmed likely disease-causing variants in *CRB1*. This study was approved by the ethics committee of the Ghent University Hospital, and adhered to the tenets of the Declaration of Helsinki. The local ethics committee waivered the need for informed consent on the condition of pseudonymisation.

All patients were seen in the ophthalmic genetics outpatient clinics at the department of ophthalmology of Ghent University Hospital in Belgium, the national referral centre for genetic eye diseases. A standardised retrospective analysis of existing medical records was performed for data collection of the ophthalmic history, including the age at symptom onset and/or age at diagnosis, best-corrected visual acuity (BCVA), slit-lamp biomicroscopy, fundoscopy with white light fundus pictures, manual Goldmann visual fields (GVF), colour vision testing, full-field dark-adapted and light-adapted single flash and 30 Hz ISCEV standard electroretinography (ERG),[14] spectral-domain optical coherence tomography (SD-OCT) and fundus autofluorescence (FAF) where available. SD-OCT and FAF images were obtained with the Heidelberg Spectralis (Heidelberg Engineering, Heidelberg, Germany). GVF areas of the V4e and I4e targets were digitised and converted to seeing retinal areas in mm^2, using a method described by Dagnelie.[15]

Diagnostic criteria for LCA were (1) aberrant or absent visual behaviour or severe visual impairment from infancy, with or without nystagmus, and (2) non-detectable dark-adapted and light-adapted amplitudes on ERG in the first year of life, if available.

Molecular diagnosis

Of the 40 subjects, 38 (95%) had received a molecular diagnosis through different approaches over the course of 10 years (2007-2017), which comprised arrayed primer extension microarray chip (APEX chip, Asper Bio, Tartu, Estonia) including; LCA chip (n = 5), autosomal recessive (ARRP) chip (n = 4), gene and LCA panel analysis using Sanger sequencing (n = 8 and n = 4, respectively), next-generation sequencing (n = 8, ERD4000, n = 3), a combination of Sanger sequencing with LCA chip (n = 4) or ARRP chip (n = 1), or a combination of LCA chip and LCA panel (n = 1). Mutational analyses were either performed at the Ghent University Hospital in Belgium, or at the Manchester Centre for Genomic Medicine. There were no subjects with mono-allelic *CRB1* mutations included in this study. Carrier status testing with Sanger sequencing confirmed mono-allelic *CRB1* variants in all available family members (n = 24) of confirmed patients. Clinical data was available for 3 out of 24 carrier family members, showing no ophthalmological abnormalities.

Statistical analysis

Data were analysed using SPSS V.23.0. For normally distributed data, means and SD were used. For non-normally distributed data, medians and IQR were used. Longitudinal analysis of Snellen BCVA and the seeing retinal area were performed using linear mixed models, using the logarithmic transformation of these parameters, that is, the logarithm of the minimum angle of resolution

(logMAR) and the logarithmic conversion of the seeing retinal area. Visual endpoints were low vision (BCVA <0.3 and ≥0.1, and/or visual field diameter <20°), severe visual impairment (BCVA <0.1 and ≥0.05) and blindness (BCVA <0.05, and/or visual field diameter <10°), based on WHO criteria. In our analysis of visual fields, we added a category of mild visual field-based impairment (20°≤ visual field diameter <70°). Intra-individual asymmetry in BCVA was defined as a between-eye difference of ≥15 Early Treatment Diabetic Retinopathy Study letters (logMAR scale). In cases where the patient was blind in both eyes, the last examinations prior to reaching blindness were used, in order to avoid a floor effect.

RESULTS

Of the 40 patients who were included from 35 families (online supplemental figure 1), 25 (63%) had follow-up of longer than 1 year (median follow-up time: 12.0 years; IQR: 16.3; range: 2.3-29.2 years). Six patients (15%) were from consanguineous families, and only 2 of these (ID-2 and ID-13) were compound heterozygous. Based on initial symptomatology and ERG results, 22 patients (55%) had RP and 15 patients (38%) had LCA. Three patients (8%) had an isolated MD, one of whom (ID-36) was initially misdiagnosed as a central areolar choroidal dystrophy. The mean age at last examination was 35.2 years (SD: 20.3; range: 2.5-80.1 years). The clinical characteristics are listed in table 1.

Thirty distinct mutations were found (online supplemental table 1), with most mutations clustering in exon 6 (20% of mutations) and exon 7 (23% of mutations). Three patients carried the c.498_506del p.(Ile167_Gly169del) mutation in compound heterozygous form, and they had isolated MD, which progressed to mild rod-cone dystrophy, based on full-field ERG findings in patient ID-33, while the peripheral retina maintained a normal appearance on fundoscopy. In the group of patients who had a truncating mutation on ≥1 allele, LCA was not significantly more prevalent than RP ($p = 0.10$).

Disease onset and visual function

Data on the age at symptom onset or at diagnosis were available for 31/40 patients (78%). The median age at symptom onset or diagnosis was during the first year of life for patients with LCA (IQR: 0.75; range: first year of life-3 years), 5 years for patients with RP (IQR 6.0; range: first year of life-26 years), and 18 years for patients with (initial) isolated MD(range 7-23 years). Of note, the early age at symptom onset seen in patients with RP is based on symptoms of nyctalopia, whereas the age at onset in patients with LCA is based on non-detectable ERG responses, nystagmus and/or reports of severe vision loss in the first years of life. In RP, 3/15 patients (20%) presented with symptoms or received their diagnosis after the first decade of life. Two patients with RP, ID-9 and ID-14, presented initially with an intermediate or panuveitis, at the ages of 26 and 5 years,

respectively. They were treated with intravitreal injections of anti-vascular endothelial growth factor and adalimumab (ID-9), which led to either no or only very limited improvement, and intravitreal triamcinolone injections (ID-14), which elicited secondary glaucoma.

Table 1. Clinical characteristics of patients with *CRB1*-associated IRDs

Characteristics*	**RP (n = 22)**	**LCA (n = 15)**	**MD (n = 3)**
Age at last examination (years; mean ± SD)	33.8 ± 21.5	38.7 ± 22.0	32.1 ± 4.9
Age at symptom onset or diagnosis (years; mean ± SD)	7.2 ± 6.4	0.2 ± 0.4	16.0 ± 8.2
Follow-up time (years; median (IQR))	2.8 (14.6)	2.8 (7.9)	13.9 (-)
Western European ethnicity†	19 (86)	12 (80)	3 (100)
Spherical equivalent refractive error available, n	12	7	3
Mean ± SD, D	+2.5 ± 1.9	+6.5 ± 1.5	+0.5 ±1.9
Range	-0.3 to +5.9	+4 to +9	-1.1 to +2.6
-1 D to 0 D, n (%)	1 (8)	-	2
0-2 D, n (%)	4 (33)	-	-
2-4 D, n (%)	4 (33)	-	1
4-6 D, n (%)	3 (25)	2 (29)	-
≥6 D, n (%)	-	5 (71)	-
Nystagmus present, n (%)	6 (27)	13 (87)	0 (0)
Shallow anterior chamber, n (%)	5/9 (56)	1/3 (33)	0/2
Cataract, n (%)	11 (52)	3 (20)	-
Keratoconus with stromal cicatrisation, n (%)	-	2 (13)	-
Enophthalmos‡, n (%)	-	6 (40)	-
Vitreous abnormalities, n (%)	4 (19)	1 (13)	1 (33)
Cells	1	-	1
Synchysis scintillans	3	1	-
Fundoscopic examination, n (%)			
Optic disc pallor	13 (62)	5 (33)	2 (67)
Optic disc hyperaemia	2 (9)	1 (13)	-
Pseudopapillary oedema	1 (5)	2 (25)	-
Macular RPE alterations/atrophy §	20/20 (100)	12/12 (100)	3 (100)
Spicular intraretinal pigmentation	10 (48)	1 (13)	-
Nummular intraretinal pigmentation	8 (36)	9 (60)	-
Vascular attenuation	12 (55)	4 (27)	1 (13)
PPRPE	8 (36)	7 (47)	1 (33)
Fine yellow drusenoid deposits	10 (45)	7 (47)	2 (67)

*Clinical characteristics at the last examination were used.

†In the LCA group, 2 patients were Eastern-European; 1 was Southern-European. In the RP group, 1 patient was Middle-Eastern, 1 patient was Black, and 1 was Southeast Asian.

‡This was due to atrophy of peri-orbital tissue, associated with frequent eye rubbing/poking.
§ Alteration or atrophy of the macular retinal pigment epithelium (RPE) was observed in 35 patients (88%). In the remaining 5 patients, who were blind (BCVA range no light perception – light perception), the macula could not be evaluated due to dense cataract (n = 2), synchysis scintillans (n = 1), miosis due to posterior synechiae, or phthysis bulbi (n = 1).
BCVA, best-corrected visual acuity; D, dioptres; LCA, Leber congenital amaurosis; MD, macular dystrophy; PPRPE, preservation of the para-arteriolar retinal pigment epithelium; IRDs, inherited retinal dystrophies; RPE, retinal pigment epithelium.

Figure 1 shows the proportion of patients in each category of visual impairment at the initial visit, based on BCVA and visual fields, against age. During follow-up, 28 patients (70%) reached BCVA-based blindness, 14 of whom had LCA, 13 of whom had RP and 1 had MD. Visual field-based blindness was documented in 17/25 patients (68%). Of these patients, 15 (38%) were blind based on both BCVA and visual field. Intra-individual asymmetry in BCVA was found in 13 patients (33%). The presumed cause of asymmetry was determined in 10 patients (online supplemental table 2).

The rate of BCVA decline in the better-seeing eye was 15.2%/year in patients with RP ($p < 0.0000001$) and 8.2%/year in patients with LCA ($p = 0.002$). In the worse-seeing eye, these rates were 16.9% ($p < 0.00000001$) and 5.7% ($p = 0.013$), respectively.

GVFs were available for 25 patients (55%), 14 of whom had follow-up GVFs with a mean follow-up time of 11.5 years (SD: 6.4; range: 4.0-24.4). The rates of visual field decline for the V4e and I4e isopter in the better-seeing eye was 16.0%/year ($p < 0.0001$) and 20.1%/year ($p = 0.002$) in patients with RP, respectively. In the worse-seeing eye, these rates were 20.4%/year ($p < 0.0001$) and 21.3%/year ($p = 0.0004$) in patients with RP. In patients with LCA, the visual field decline for the V4e isopter was 18.9%/year, while the other parameters were too affected at baseline to allow reliable calculation of the decline rate. The number of patients with MD was too low to calculate reliable decline rates for BCVA or visual fields.

Ophthalmic and funduscopic findings

The mean spherical equivalent of the refractive error at the last examination was +3.7 D (SD: 2.8; range: -1.1 D to +9.0 D), and hyperopia was present in 16/22 patients (73%) with available data on the refractive error. The only patient with myopia (spherical equivalent <-0.75 D) had an isolated MD phenotype. Angle-closure glaucoma was diagnosed in three patients (8%; one with LCA and two with RP), and was treated with a surgical peripheral iridectomy in two cases, one of whom also received cataract surgery and with laser peripheral iridotomy in one case. One additional patient received prophylactic peripheral iridotomy due to a shallow anterior chamber, and one patient had received a surgical peripheral iridectomy, the indication for which could not be retrieved from the available clinical history. Patient ID-32 was diagnosed with uveitis and angle closure due to

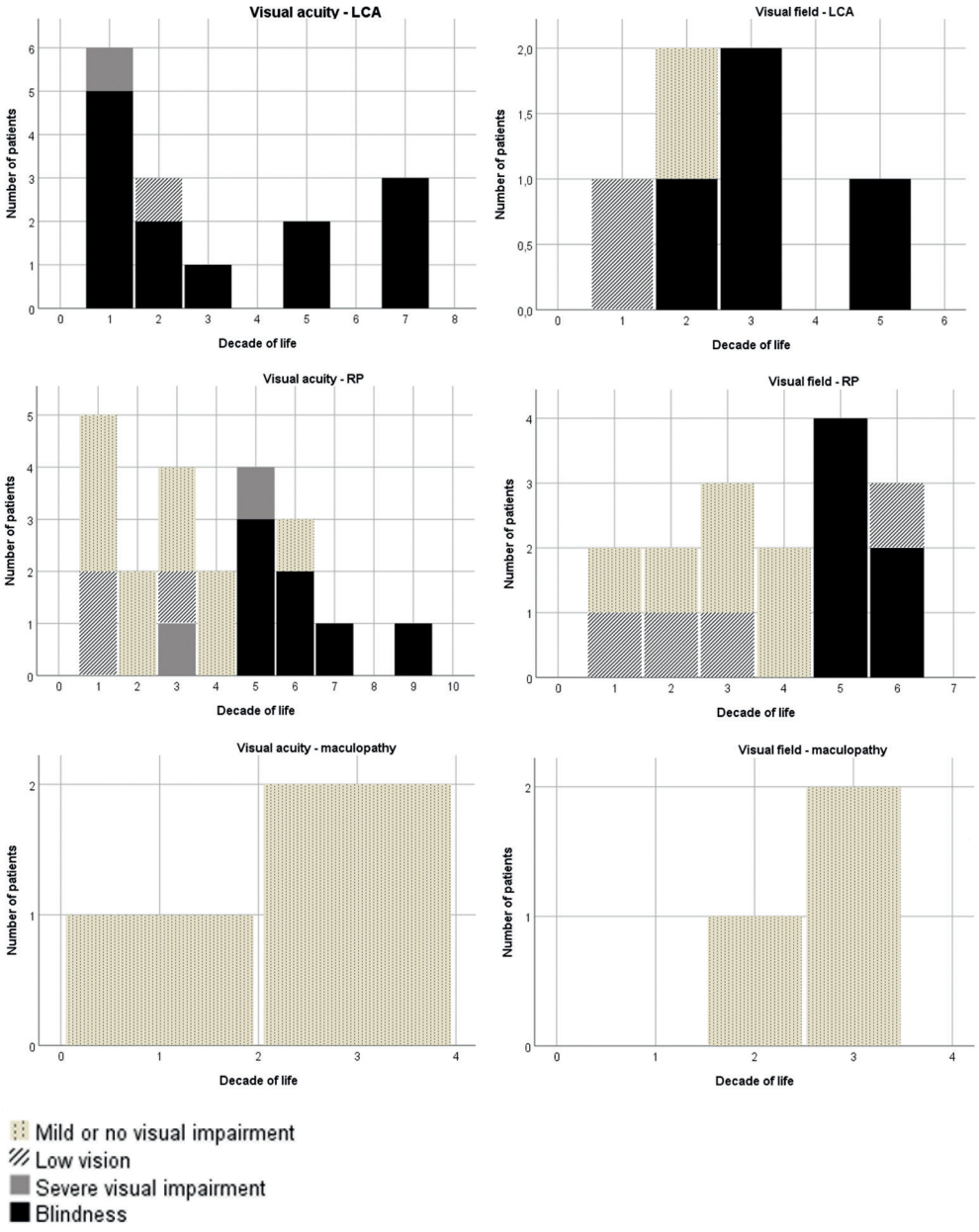

Figure 1. Visual function in *CRB1*-associated retinal degenerations, stratified by diagnosis. Data were collected from the initial visit, and the better-seeing eye was used for this analysis. Panels on the left indicate visual impairment based on best-corrected visual acuity (BCVA), showing mild or no visual impairment (BCVA ≥0.3), low vision (BCVA <0.3), severe visual impairment (BCVA <0.1), and blindness (BCVA <0.05), based on WHO criteria. Panels on the right indicate visual impairment based on visual field, showing no visual impairment (visual field diameter ≥70°), mild visual impairment (diameter <70°), low vision (diameter <20°), or blindness (diameter <10°). The graphs

show visual impairment with advancing age in patients with *CRB1*-associated Leber congenital amaurosis (LCA) in the top row, for *CRB1*-associated retinitis pigmentosa (RP) in the second row, and for *CRB1*-associated macular dystrophy (MD) in the third row. In LCA, BCVA-based blindness is common from the first decade of life, but some visual field may still be intact. In RP, BCVA-based as well as visual field-based blindness is common from the fifth decade of life onward. In MD, BCVA and visual field are well-preserved, although the few patients in this population were still young at the final visit.

seclusio pupillae at the age of 54 years, and was treated with diode laser cyclodestruction, followed by trabeculectomy. Optic disc drusen (5/40 patients; 13%) or hamartomas (1/40 patients; 3%) were found in patients with LCA (n = 1) and RP (n = 5), who had mutations in *CRB1* exons 5-9. Alterations or atrophy of the macular retinal pigment epithelium (RPE) were universal (table 1).

Intraretinal pigment migrations were present in 36/40 patients (90%). Nummular pigmentations were much more frequent than those of the spicular type in LCA patients (7/8 patients). Nummular pigmentations were present in 7/21 RP patients (33%). Of the patients without intraretinal pigment migrations, 3 had an isolated MD phenotype, and one patient had RP but was aged 6 years at the last examination. The earliest fundus changes were found in patient ID-13 (RP), at the age of 11 months, and consisted of mild macular RPE alterations only. Macular pseudocoloboma was observed in three patients with LCA. Preservation of the peri-arteriolar retina and RPE was present in 16/40 patients (40%), across all diagnostic groups (table 1). Fine yellow punctate deposits in the peripheral retina were present in 19/40 patients (48%). Patients ID-1 and ID-31 had a unilateral and bilateral retinal detachment, respectively. The underlying cause was Coats-like vasculopathy in ID-1, and not documented in ID-31.

Full-field ERG

Full-field ERGs, available for 16 patients (40%), were non-detectable in 3/3 patients with LCA. One patient with LCA (ID-24) had some remaining light-adapted responses in his first year of life, despite having only light perception vision. Dark-adapted and light-adapted responses were extinguished in 5/9 patients with RP at the first ERG examination (ages: 4-40 years), while others had a rod-cone pattern of dysfunction. Three patients with MD had normal dark-adapted and light-adapted ERG responses. One of these patients, patient ID-33, who had no generalised panretinal dysfunction on ERG between the ages of 23 years and 26 years, had developed a mild rod-cone dystrophy by the age of 28 years.

Table 2. Integrity of photoreceptor layers on SD-OCT in patients with *CRB1*-associated IRDs

Retinitis pigmentosa		**N**	**Age (years)**
EZ	Granular or attenuated in peripheral macula, with relative sparing in fovea	4/12*	14-54
	(Nearly) unidentifiable in peripheral macula, but sparing in the fovea	3/12	35-43
	(Nearly) unidentifiable in entire macula	5/12	5-80
ELM	(Nearly) unidentifiable or severely attenuated in peripheral macula, with foveal sparing	6/12	14-54
	(Nearly) unidentifiable in entire macula	6/12	5-80
ONL	Normal thickness or only mild attenuation in entire macula	1/12	54
	Normal thickness or mild attenuation in fovea, with more severe attenuation in peripheral macula	2/12	14-16
	Severe attenuation in entire macula	3/12	5-40
	(Nearly) unidentifiable in entire macula	5/12	35-80
	Severe attenuation in fovea, with sparing in peripheral macula	1/12	26
Leber congenital amaurosis		**N**	**Age (years)**
EZ	Fully unidentifiable in entire macula	1/6	11
	Unidentifiable in peripheral macula, nearly unidentifiable in fovea	2/6	4-7
	Unidentifiable in fovea, nearly unidentifiable in peripheral macula	3/6	3-20
ELM	Fully unidentifiable in entire macula	5/6	3-20
	Some foveal sparing (nearly unidentifiable)	1/6	7
ONL	Severely attenuated or (nearly) unidentifiable in entire macula	6/6	3-20
Macular dystrophy		**N**	**Age (years)**
EZ	Somewhat granulated in peripheral macula, with sparing in the fovea	1/3	26
	Sparing in the peripheral macula and fovea, with atrophy in the parafovea (bull's eye maculopathy) †	1/3	29
	Almost absent in fovea, sparing in peripheral macula	1/3	31
ELM	Good quality in fovea and peripheral macula	1/3	26
	Good quality in fovea, granulated in peripheral macula†	1/3	29
	Unidentifiable in fovea, good preservation in peripheral macula	1/3	31
ONL	Normal in entire macula	1/3	26
	Severe attenuation with some foveal sparing†	1/3	29
	Severe attenuation, more atrophy in fovea	1/3	31

*Six patients (one with LCA; five with RP) who had undergone SD-OCT imaging were not included in this table, as either only single scans or only descriptions of the images were available in the medical records, describing atrophy of the outer retina and photoreceptor layers.

†This was patient ID-33, who later developed rod-cone dystrophy. The pattern of atrophy on SD-OCT did not change, although the atrophy was progressive.

ELM, external limiting membrane; EZ, ellipsoid zone; IRDs, inherited retinal dystrophies; LCA, Leber congenital amaurosis; MD, macular dystrophy; ONL, outer nuclear layer; RP, retinitis pigmentosa; SD-OCT, spectral-domain optical coherence tomography.

Retinal imaging

SD-OCT data (see table 2), available for 27 patients (68%), showed inner retinal thickening (21/27; 78%), cystoid macular oedema (CMO; 14/27; 52%; unilateral in 3 cases), and disorganization of the lamellar retinal structure (14/27; 52%). The other patients maintained an intact lamellar retinal structure, where despite a mildly coarse aspect (8/27; 30%), each individual retinal layer was discernible throughout the macula. Online supplemental table 3 shows the treatment regimens for CMO, which in two cases disappeared spontaneously. Conversely, patient ID-13 had no CMO until the age of 11 years, and developed bilateral CMO at the age of 12 years. An epiretinal membrane was present in 13 patients (48%), and was mild in 9 patients, but formed a pucker in 4 patients. A unilateral lamellar hole was present in patient ID-9, which later developed into a full-thickness macular hole.

Blue-light (short wavelength) autofluorescence imaging (SWAF) was performed in 20 patients (50%). Six of those had either nystagmus (n = 5) and/or were blind in both eyes (n = 5), so that it was impossible to obtain interpretable SWAF images. In the others, SWAF showed variable patterns (Figures 2 and 3), with relative sparing of the foveal autofluorescence in eight patients.

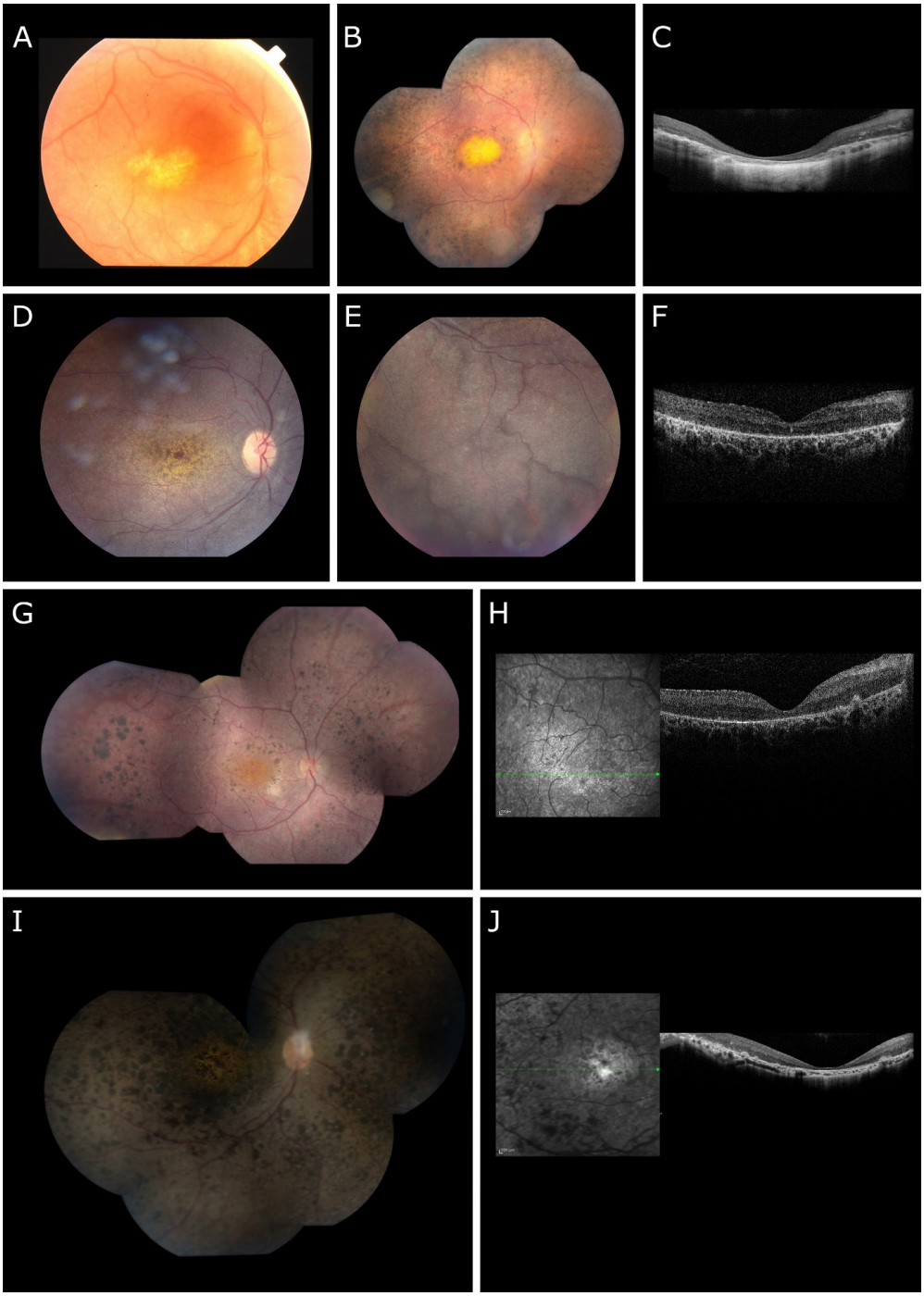

Figure 2. Imaging in *CRB1*-associated Leber congenital amaurosis (LCA) or retinitis pigmentosa (RP). A-C. Long-term disease progression in a patient with LCA. At the age of 6 years (**A**), an area of outer retinal atrophy

including the retinal pigment epithelium (RPE) was observed in the central macula (decimal best-corrected visual acuity (BCVA) of the right eye (OD): 0.03). The periphery (not shown here) had a salt-and-pepper aspect, but no obvious spicular hyperpigmentation. At the age of 25 years (**B**), the central atrophic area had grown into what was described as a macular pseudocoloboma (BCVA OD: hand motion vision), and mixed intraretinal nummular and spicular pigmentation migration extended from the periphery into the posterior pole. White-yellow drusenoid deposits are visible in the midperiphery, similar to the deposits seen in *CRB1*-associated retinitis pigmentosa (Figure 3). Spectral-domain optical coherence tomography (SD-OCT) (**C**) showed profound atrophy of outer retinal layers. The external limiting membrane (ELM) and ellipsoid zone (EZ) were undetectable. On short-wavelength fundus autofluorescence imaging (not shown here), no autofluorescence signal could be detected. Decimal BCVA was 0.03. **D-F.** A 7-year-old patient with RP, whose sibling had LCA. The fundus (**D**) showed a yellow profound macular atrophy, with some foveal preservation (BCVA OD: 0.4; left eye (OS): 0.06). Note the white-yellow drusenoid deposits in the macula, also abundant in the (mid)periphery. The periphery (**E**) showed pronounced para-arteriolar preservation of the RPE (PPRPE), a feature typical of *CRB1*-associated retinopathies. Nummular intraretinal hyperpigmentation (not shown here) was present, but sparse. SD-OCT (**F**) showed atrophy of the outer retinal layers. No identifiable ELM or EZ could be discerned, and only small hyperreflective tufts were scattered along the macula. **G-H.** An 11-year-old patient with LCA. Composite fundus photography (**G**) shows yellowish atrophy of the macula, nummular intraretinal pigmentation in the perimacular region and the periphery (BCVA OD: 0.03), and PPRPE in the periphery. In the papillomacular region, fibrous scar tissue formation is visible. This fibrous tissue was present to a greater extent in the other eye, in the same papillomacular region. The SD-OCT (**H**) shows inner retinal thickening, and severe outer retinal atrophy, with some remaining outer nuclear layer, but no identifiable ELM or EZ. **I-J.** A 12-year-old patient with LCA. The fundus (**I**) shows optic disc drusen (note irregular optic disc border), profound retinal atrophy (BCVA OU: finger counting vision) and panretinal nummular hyperpigmentation. Yellow drusenoid deposits are visible throughout the retina. A coincidental finding is the Bergmeister optic disc, seen as the small tuft of fibrous tissue on the optic disc. The SD-OCT (**J**) shows no evident inner retinal thickening, but profound atrophy of the outer retina, particularly in the fovea. No identifiable ELM or EZ is visible.

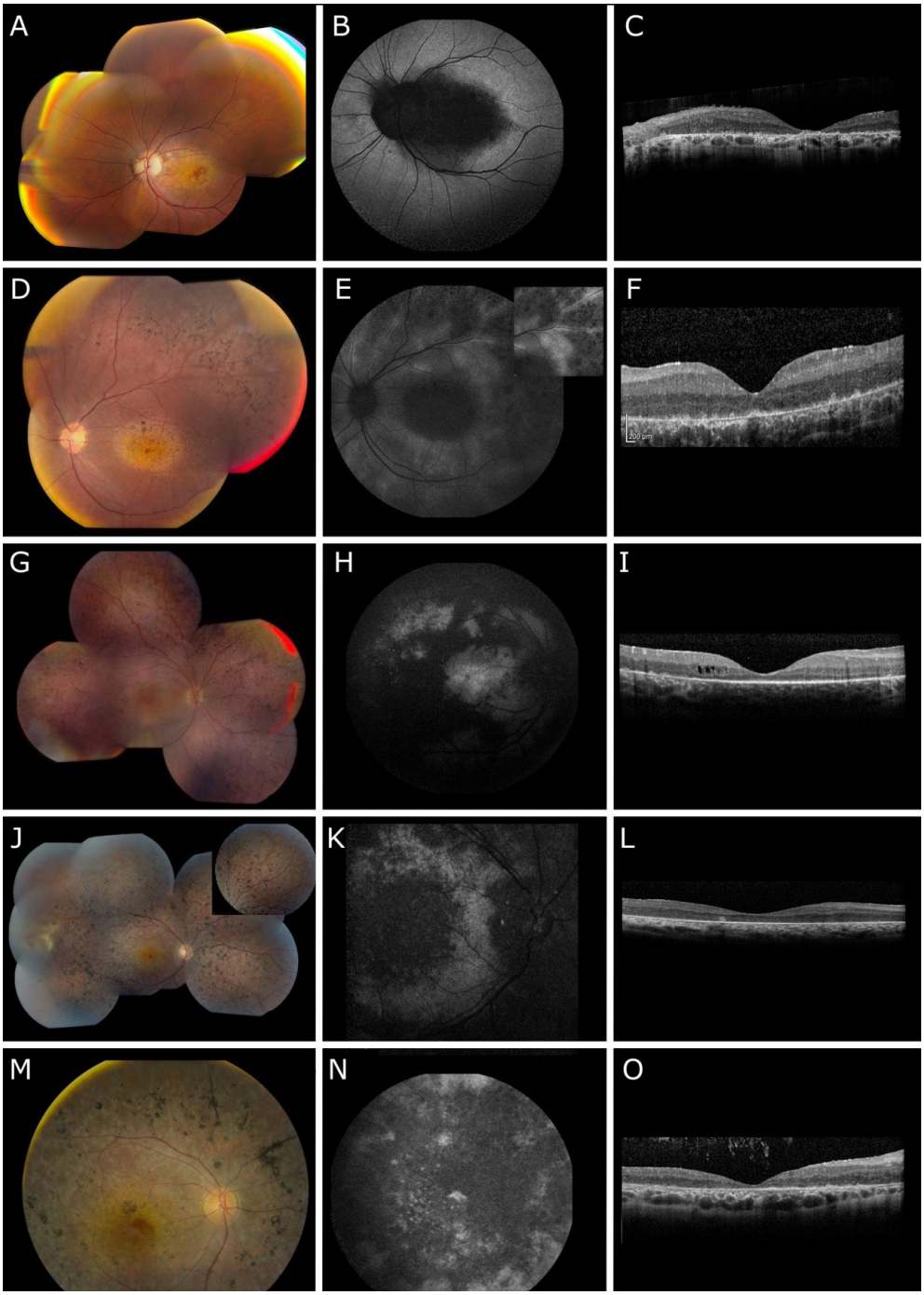

Figure 3. Multimodal imaging in patients with *CRB1*-associated macular dystrophy (MD) or retinitis pigmentosa (RP). A-C. A 36-year-old patient with an isolated MD, which was initially diagnosed as central areolar

choroidal dystrophy. Composition fundus photography (**A**) shows chorioretinal atrophy in the central macula, with relative sparing of the fovea. The peripheral macula and the retinal (mid)periphery, including the vasculature, appear entirely normal. The short-wavelength fundus autofluorescence (FAF) image (**B**) shows severely reduced to absent autofluorescence in the corresponding area of the macula. Spectral-domain optical coherence tomography (SD-OCT) scan (**C**) shows profound atrophy of the outer nuclear layer (ONL) and the hyperreflective outer retinal bands (external limiting membrane and ellipsoid zone), and a near absence thereof in the fovea. The decimal best-corrected visual acuity (BCVA) was 0.01 in this eye. **D-F.** A 14-year-old patient with RP. The fundus (**D**) shows a distinctive, yellow, relatively circumscribed area of macular atrophy, with small areas of foveal and parafoveal sparing, which explains a BCVA of 0.5 in this eye. In the superotemporal periphery, para-arteriolar preservation of the retinal pigment epithelium (PPRPE) is seen, a feature highly typical of *CRB1*-associated RP. Spicular intraretinal pigmentation in seen in the periphery, along with small, yellowish, drusenoid deposits. FAF (**E**) shows severe hypo-autofluorescence in the macula, and strokes of reduced FAF in the midperiphery. Autofluorescence is relatively preserved in the peripheral macula and around the arterioles (picture-in-picture). SD-OCT (**F**) shows inner retinal thickening, outer retinal atrophy, and relative preservation of the ONL and the hyperreflective outer retinal bands in the fovea. **G-I.** A 16-year-old patient with RP. The fundus (**G**) shows extensive bone-spicule hyperpigmentation in the periphery, extending into the temporal posterior pole, with a spared central macula. FAF (**H**) confirms this pattern, showing normal autofluorescence in the central macula and severely reduced FAF in the remaining posterior pole and midperiphery. Patches of relative preservation are scattered in the superior midperiphery. SD-OCT (**I**) shows relative foveal preservation of the ONL and the hyperreflective outer retinal bands. The ellipsoid zone seemed more preserved than the external limiting membrane. Mild cystoid macular oedema was visible in the temporal parafovea. BCVA was 0.5. **J-L.** A 26-year-old patient with RP and Coats-like exudative vasculopathy. The fundus (**J**) shows a pale optic disc, and the distinct yellow coloration of the atrophic macula, with relative foveal sparing. A greyish reticular pattern of outer retinal atrophy is seen in the posterior pole and the nasal (mid)periphery. Nummular intraretinal pigmentation is seen. PPRPE is particularly visible in the nasal and superior quadrants. White drusenoid deposits are scattered in atrophic as well as in relatively preserved areas (picture-in-picture). The Coats-like exudate is seen in the temporal periphery. FAF (**K**) shows profound hypo-autofluorescence in the central macula and midperiphery, with relative sparing in the peripheral posterior pole. The SD-OCT scan (**L**) shows atrophy of the ONL and the hyperreflective outer retinal bands. The BCVA in this eye was 0.05. **M-O.** A 45-year-old patient with RP. The fundus (**M**) shows yellowish areas of macular atrophy with foveal sparing. Extensive nummular pigmentation, along with a greyish reticular pattern of outer retinal atrophy, is seen in the midperiphery, extending into the posterior pole. FAF (**N**) shows generalised mottled hypo-autofluorescence with limited patchy regions of preserved autofluorescence. FAF in the fovea is attenuated. SD-OCT (**O**) shows atrophy of the ONL and the hyperreflective outer retinal bands, which are not evidently identifiable. The inner retina is mildly thickened. The BCVA in this eye was 0.2.

DISCUSSION

In this retrospective cohort study, we detail the natural disease course and clinical spectrum of *CRB1*-associated IRDs in a large Belgian cohort of 40 patients from 35 families. Patients were evaluated extensively with functional testing and multimodal imaging, with a follow-up time up to 29 years. We elucidate several genotype-phenotype correlations.

In this study, 55% of patients had an RP diagnosis, 8% had an MD, while the other patients presented with the more severe LCA (38%). In previous literature, the terms LCA and early-onset severe

retinal dystrophy (EOSRD) have been used interchangeably to some extent.[16] The phenotypes were more severe in this Belgian cohort than in the previously published Dutch cohort, where LCA comprised only 9% of the *CRB1*-RD population.[9] Within the RP groups, however, findings were relatively similar. The median age at symptom onset for patients with *CRB1*-RP in the current cohort was 5 years, versus 4 years in the Dutch cohort, and 20% of patients in the current cohort had a disease onset after the first decade of life, versus 15% of patients with *CRB1*-RP in the Dutch cohort.[9] A salient finding is the initial presentation with uveitis in two patients with RP (10%), which has been reported before in *CRB1*-associated retinopathy.[17] The prevalence of uveitis in any form (anterior, intermediate and posterior) in the genetically undifferentiated RP population has been estimated at 0.26%,[18] although some studies have shown a higher prevalence of inflammatory activity in patients with RP in the vitreous cavity (37%), indicating an association between RP and inflammation.[19]

Besides typical RP-associated fundus hallmarks, distinctive features included fine yellow punctate spots, found in 48%, and which have been noted in cases of patients with *CRB1*-RD,[20] as well as in *Crb1*$^{rd8/rd8}$ mutant mice, where immunostaining indicated that these spots represent subretinal microglia/microphages.[21] This suggests that these spots are indicative of a pro-inflammatory phenotype. Alternatively, they may represent degenerated or migrated Müller cells. The full significance and relevance of this feature remains elusive. Another distinctive characteristic was peri-arteriolar preservation of the RPE, which was present across all diagnoses, but was most prevalent in *CRB1*-LCA. Earlier smaller studies and case series have found early macular involvement a notable finding in *CRB1*-RP and *CRB1*-LCA.[22-24] In this study, macular RPE alterations or atrophy was universal in all patients where the macula could be visualised, confirming our findings in the Dutch cohort.[9] A particularly interesting finding is the macular pseudocoloboma in three patients with LCA. Case series have described macular (pseudo)coloboma in LCA associated mostly with mutations in *CRX* and *AIPL1*, but also with mutations in *NMNAT1*, *LCA5* (encoding Lebercilin) and *IDH3A*.[25-27] To the best of our knowledge, this is only the second report of macular pseudocoloboma in *CRB1*-LCA.[28] Coats-like exudative vasculopathy was found in 13% of patients in this cohort, similar to earlier reports.[9, 29] ERG responses were extinguished in 100% of LCA patients and 56% of patients with RP with available ERGs, compared to 50% of patients with RP in the Dutch cohort. This suggests that, in a future *CRB1* gene therapy trial, ERG examination may not be an appropriate outcome measure of efficacy.

The high proportion of left-censored data for low vision and blindness, that is, patients who had low vision or were blind at the initial presentation, was too high to calculate reliable survival curves in this cohort. In fact, 75% of patients in this cohort reached blindness: 70% reached BCVA-based blindness, and 68% reached visual field-based blindness, with considerable overlap. In RP, mild visual impairment was observed in the first decade of life, while both BCVA-based and visual

field-based blindness were mostly observed from the fifth decade of life and onward, corroborating observations from earlier large cohorts.[9, 11]

Meaningful findings on SD-OCT included inner retinal thickening (78%), and cystoid maculopathy (52%), similar to findings in the Dutch population, as well as findings in *Crb1*$^{-/-}$/*Crb2*$^{-/-}$ mice.[30] Disorganization of the retinal laminar structure, however, was more prevalent: 52% in the Belgian cohort versus 9% of Dutch patients. In these patients, the amenability of the retina to subretinal gene therapy may be less likely. The results are confounded by the higher proportion of patients with *CRB1*-LCA in the Belgian population, while the few patients with *CRB1*-LCA in the Dutch population had no SD-OCTs available for analysis. In the other 48% of Belgian patients, mostly patients with RP or MD, but also two with LCA, the laminar structure of the retina was essentially maintained, despite some degree of coarseness. Other crucial biomarkers indicating amenability to gene therapy include the ellipsoid zone (EZ), external limiting membrane (ELM) and outer nuclear layer (ONL). In ≥ 50% of patients with RP, EZ and ELM were spared in the fovea (table 2). However, the ONL was more severely attenuated. This suggests that in these patients, gene therapy has some anatomical basis for potential success, as CRB1 protein supports the adhesion between photoreceptors and Müller cells at the level of the ELM.[31] Again, the atrophy of the photoreceptor layers on SD-OCT was more profound in the Belgian *CRB1*-RP population compared with the Dutch *CRB1*-RP population. In Belgian patients with LCA, the EZ, ELM and ONL were (nearly) unidentifiable in almost all patients. These findings were based on multiple single scans, as nystagmus or the lack of fixation challenged image capture in LCA patients, but are in keeping with the more severe nature of congenital and early-onset *CRB1*-related disease.

Non-retinal features included hyperopia (73%), a narrow anterior chamber (63% of patients with RP; 43% of total, where information on anterior chamber depth was available) and optic disc drusen or hamartomas (16%). These data propose a role for CRB1, a large and complex protein, in normal ocular development, although its precise role in this context is not known. Acute angle-closure glaucoma occurred in 8% of patients, in line with previous findings,[32, 33] but with a lower incidence than found in the Dutch population.[9]

The genotypic distribution in this cohort was decidedly different from that in the Dutch cohort. The Belgian cohort was genotypically and ethnically more diverse, as 30 distinct mutations were found, and 15% of patients were of non-Western-European descent. Meanwhile, the Dutch cohort consists largely of a genetic isolate carrying a homozygous p.(Met1041Thr) mutation, which was not present in this Belgian cohort. This genotypic difference, and particularly the higher prevalence of nonsense mutations in this cohort may hold at least part of the explanation for the contrasting phenotypic severity between this and the previously published Dutch cohort. In the current cohort, six patients had bi-allelic truncating mutations, four of whom had LCA and two had RP. In the Dutch cohort, no patient had bi-allelic truncating mutations. This partially substantiates the earlier

suggestion of an association between truncating mutations and an LCA phenotype,[34] although this association was not significant in this cohort ($p = 0.10$).

The presence of genotype-phenotype correlations in many types of inherited IRDs, including *CRB1*-associated IRDs, has been contentious. An association between null mutations and a higher likelihood of an LCA phenotype has been suggested, due to the complete loss of CRB1 protein.[34] Although we observed the trend, we could not statistically corroborate this suggestion. This study also robustly confirms the association between the p.(Ile167_Gly169del) mutation and phenotypes predominantly affecting the macula, with or without measurable cone dysfunction on full-field ERG. A recent case series has shown this mutation in homozygous or heterozygous form in seven unrelated individuals with *CRB1*-MD.[10] In these patients, emmetropia or myopia is more prevalent than the typical hyperopia seen in *CRB1*-RDs.[35]

Although there are no therapeutic options available for patients with *CRB1*-associated RP and LCA, gene therapy is being developed, and has shown efficacy in preserving retinal structure and function in mouse models of the disease.[8, 13, 36, 37] Recently, an exclusive license agreement was signed between HORAMA, a French biotech company, and Leiden University Medical Centre, developer of the drug candidate (HORA-001) targeting *CRB1* mutations to treat *CRB1*-RDs.[38]

This study provides useful information for future (gene) therapeutic trials. Of particular interest remains the degree of intra-individual interocular symmetry, and thus comparability. This comparability is an important assumption when using the non-treated eye as a control in trials. This study found interocular asymmetry in 33% of patients, similar to the findings in the Dutch population (31%).[9] Yearly decline rates of BCVA and visual field area were relatively symmetric between the better- and worse-seeing eye, particularly for BCVA and the I4e isopter for the visual field. We find that the first three decades of life provide the more tenable window of opportunity for potential therapeutic intervention in patients with RP. In LCA, therapeutic intervention should be within the first years of life, if any efficacy were to be expected. In RP patients, SD-OCT imaging provides insight in the remaining structures to be targeted by gene therapy, and is thus useful in determining patient inclusion. Image acquisition is more challenging in severely visually impaired patients, such as those with LCA.

Strengths of this study include the population size and the comprehensive availability of functional and imaging studies, all of which were performed in a very standardized way at a single tertiary referral centre. This allowed for robust statistical analysis – a challenge in rare diseases. Limitations of this study include the retrospective design. The vast genotypic heterogeneity, although representative of the general population, impeded statistical genotype-phenotype analysis. Nonetheless, confirmation of many phenotypic features found in previous large cohorts, and

further substantiation of one genotype-phenotype correlation, indicate that retrospective studies, despite the limitations, provide robust information that is reproducible in different cohorts.

Funding

This study was in part funded by the Curing Retinal Blindness Foundation (CJFB), and the Research Foundation Flanders (Belgium) (FWO); Support: FWO Flanders Grant OZP 3G004306 (BPL).

REFERENCES

1. Koenekoop RK. An overview of Leber congenital amaurosis: a model to understand human retinal development. Surv Ophthalmol 2004;49(4):379-98.
2. Stone EM. Leber congenital amaurosis - a model for efficient genetic testing of heterogeneous disorders: LXIV Edward Jackson Memorial Lecture. Am J Ophthalmol 2007;144(6):791-811.
3. Hamel C. Retinitis pigmentosa. Orphanet J Rare Dis 2006;1:40.
4. Corton M, Tatu SD, Avila-Fernandez A, et al. High frequency of CRB1 mutations as cause of Early-Onset Retinal Dystrophies in the Spanish population. Orphanet J Rare Dis 2013;8:20.
5. Vallespin E, Cantalapiedra D, Riveiro-Alvarez R, et al. Mutation screening of 299 Spanish families with retinal dystrophies by Leber congenital amaurosis genotyping microarray. Invest Ophthalmol Vis Sci 2007;48(12):5653-61.
6. Tsang SH, Burke T, Oll M, et al. Whole exome sequencing identifies CRB1 defect in an unusual maculopathy phenotype. Ophthalmology 2014;121(9):1773-82.
7. Khan AO, Aldahmesh MA, Abu-Safieh L, Alkuraya FS. Childhood cone-rod dystrophy with macular cystic degeneration from recessive CRB1 mutation. Ophthalmic Genet 2014;35(3):130-7.
8. Quinn PM, Pellissier LP, Wijnholds J. The CRB1 Complex: Following the Trail of Crumbs to a Feasible Gene Therapy Strategy. Front Neurosci 2017;11:175.
9. Talib M, van Schooneveld MJ, van Genderen MM, et al. Genotypic and Phenotypic Characteristics of CRB1-Associated Retinal Dystrophies: A Long-Term Follow-up Study. Ophthalmology 2017;124(6):884-95.
10. Khan KN, Robson A, Mahroo OAR, et al. A clinical and molecular characterisation of CRB1-associated maculopathy. Eur J Hum Genet 2018;26(5):687-94.
11. Mathijssen IB, Florijn RJ, van den Born LI, et al. Long-term follow-up of patients with retinitis pigmentosa type 12 caused by CRB1 mutations: a severe phenotype with considerable interindividual variability. Retina 2017;37(1):161-72.
12. Maguire AM, Russell S, Wellman JA, et al. Efficacy, Safety, and Durability of Voretigene Neparvovec-rzyl in RPE65 Mutation-Associated Inherited Retinal Dystrophy: Results of Phase 1 and 3 Trials. Ophthalmology 2019;126(9):1273-85.
13. Pellissier LP, Quinn PM, Alves CH, et al. Gene therapy into photoreceptors and Muller glial cells restores retinal structure and function in CRB1 retinitis pigmentosa mouse models. Hum Mol Genet 2015;24(11):3104-18.
14. McCulloch DL, Marmor MF, Brigell MG, et al. ISCEV Standard for full-field clinical electroretinography (2015 update). Doc Ophthalmol 2015;130(1):1-12.
15. Dagnelie G. Conversion of planimetric visual field data into solid angles and retinal areas. Clinical Vision Science 1990;5(1):95-100.
16. Kumaran N, T Moore A, Weleber R, Michaelides M. Leber congenital amaurosis/early-onset severe retinal dystrophy: clinical features, molecular genetics and therapeutic interventions. Br J Ophthalmol 2017;101:1147-54.
17. Hettinga YM, van Genderen MM, Wieringa W, et al. Retinal Dystrophy in 6 Young Patients Who Presented with Intermediate Uveitis. Ophthalmology 2016;123(9):2043-6.

18. Dutta Majumder P, Menia N, Roy R, et al. Uveitis in Patients with Retinitis Pigmentosa: 30 Years' Consecutive Data. Ocul Immunol Inflamm 2018;26(8):1283-8.
19. Yoshida N, Ikeda Y, Notomi S, et al. Clinical Evidence of Sustained Chronic Inflammatory Reaction in Retinitis Pigmentosa. Ophthalmology 2013;120(1):100-5.
20. Li, Shen, Xiao, et al. Detection of CRB1 mutations in families with retinal dystrophy through phenotype-oriented mutational screening. Int J Mol Med 2014;33(4):913-8.
21. Aredo B, Zhang K, Chen X, et al. Differences in the distribution, phenotype and gene expression of subretinal microglia/macrophages in C57BL/6N (Crb1rd8/rd8) versus C57BL6/J (Crb1wt/wt) mice. J Neuroinflammation 2015;12(1):6.
22. McKibbin M, Ali M, Mohamed MD, et al. Genotype-phenotype correlation for leber congenital amaurosis in Northern Pakistan. Arch Ophthalmol 2010;128(1):107-13.
23. Hanein S, Perrault I, Gerber S, et al. Leber congenital amaurosis: comprehensive survey of the genetic heterogeneity, refinement of the clinical definition, and genotype-phenotype correlations as a strategy for molecular diagnosis. Hum Mutat 2004;23(4):306-17.
24. Jonsson F, Burstedt MS, Sandgren O, et al. Novel mutations in CRB1 and ABCA4 genes cause Leber congenital amaurosis and Stargardt disease in a Swedish family. Eur J Hum Genet 2013;21(11):1266-71.
25. Sun W, Zhang Q. A novel variant in IDH3A identified in a case with Leber congenital amaurosis accompanied by macular pseudocoloboma. Ophthalmic Genet 2018;39(5):662-3.
26. Testa F, Surace EM, Rossi S, et al. Evaluation of Italian Patients with Leber Congenital Amaurosis due to AIPL1 Mutations Highlights the Potential Applicability of Gene Therapy. Invest Ophthalmol Vis Sci 2011;52(8):5618-24.
27. Chacon-Camacho O, Zenteno J. Review and update on the molecular basis of Leber congenital amaurosis. World J Clin Cases 2015;3(2):112-24.
28. Lotery AJ, Jacobson SG, Fishman GA, et al. Mutations in the CRB1 gene cause Leber congenital amaurosis. Arch Ophthalmol 2001;119(3):415-20.
29. Jacobson SG, Cideciyan AV, Aleman TS, et al. Crumbs homolog 1 (CRB1) mutations result in a thick human retina with abnormal lamination. Hum Mol Genet 2003;12(9):1073-8.
30. Pellissier LP, Alves CH, Quinn PM, et al. Targeted ablation of CRB1 and CRB2 in retinal progenitor cells mimics Leber congenital amaurosis. PLoS Genet 2013;9(12):e1003976.
31. Mehalow AK, Kameya S, Smith RS, et al. CRB1 is essential for external limiting membrane integrity and photoreceptor morphogenesis in the mammalian retina. Hum Mol Genet 2003;12(17):2179-89.
32. Henderson RH, Mackay DS, Li Z, et al. Phenotypic variability in patients with retinal dystrophies due to mutations in CRB1. Br J Ophthalmol 2011;95(6):811-7.
33. Coppieters F, Casteels I, Meire F, et al. Genetic screening of LCA in Belgium: predominance of CEP290 and identification of potential modifier alleles in AHI1 of CEP290-related phenotypes. Hum Mutat 2010;31(10):E1709-66.
34. den Hollander AI, Heckenlively JR, van den Born LI, et al. Leber congenital amaurosis and retinitis pigmentosa with Coats-like exudative vasculopathy are associated with mutations in the crumbs homologue 1 (CRB1) gene. Am J Hum Genet 2001;69(1):198-203.

35. Shah N, Damani MR, Zhu XS, et al. Isolated maculopathy associated with biallelic CRB1 mutations. Ophthalmic Genet 2017;38(2):190-3.
36. Alves CH, Wijnholds J. AAV Gene Augmentation Therapy for CRB1-Associated Retinitis Pigmentosa. Methods Mol Biol 2018;1715:135-51.
37. Boon N, Wijnholds J, Pellissier LP. Research Models and Gene Augmentation Therapy for CRB1 Retinal Dystrophies. Front Neurosci 2020;14:860.
38. HORAMA. (n.d.). *HORA-001 is in early-stage development for eye diseases caused by defects in the CRB1 gene*. Horama.fr, 2020. Available: https://www.horama.fr/pipeline/hora-pde6b-2/ [Accessed September 6 2021].

SUPPLEMENTAL MATERIAL

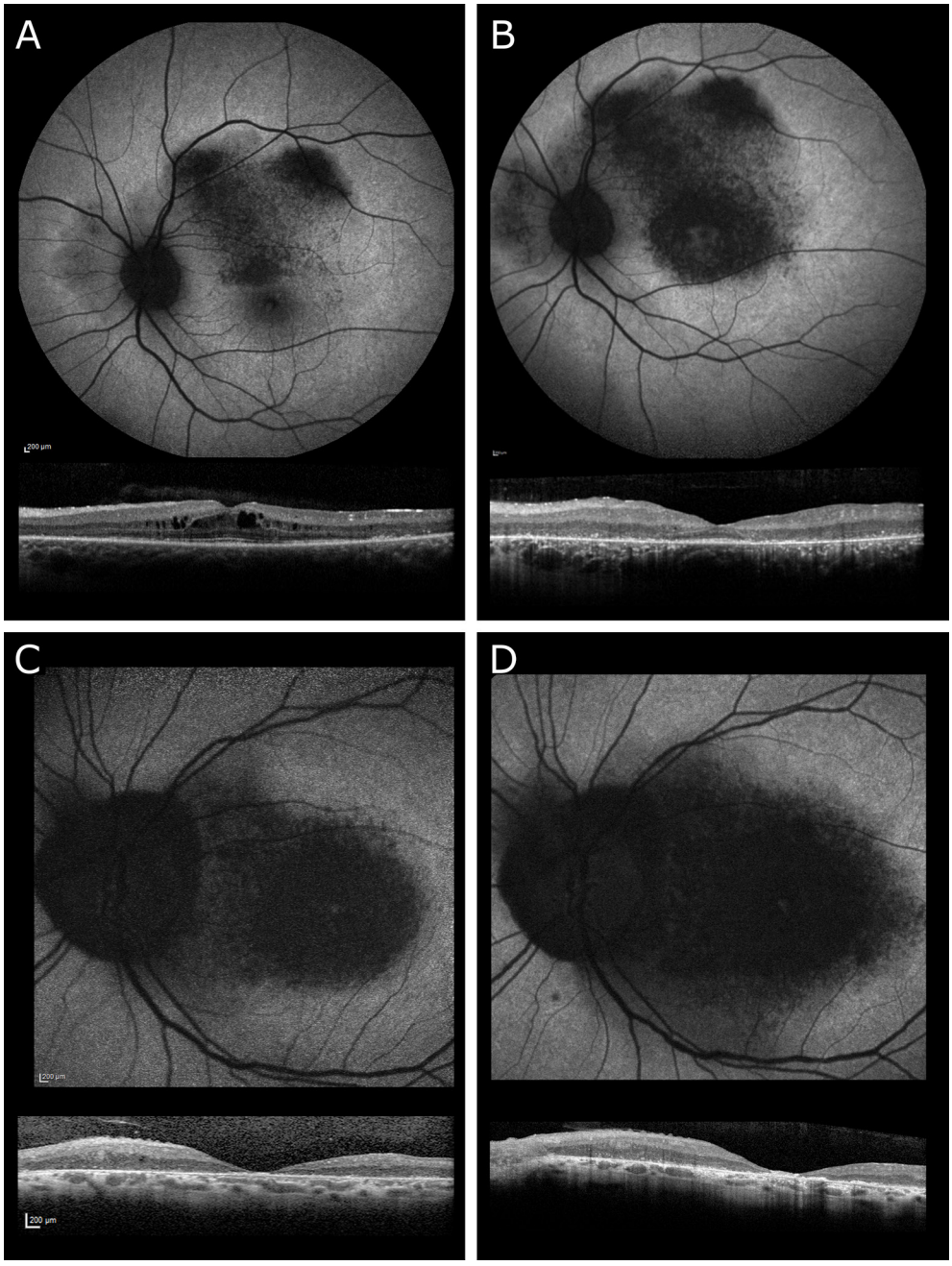

Supplementary Figure 1. Progression of degenerative changes in the macula on different imaging modalities in patients with *CRB1*-associated macular dystrophy associated with the p.Ile167_Gly169del mutation. A-B. A male patient between the ages of 24 to 28 years. At the age of 24, dense granular hypo-autofluorescence was seen around the central macula and in the superior part of the posterior pole on the fundus autofluorescence (FAF) image.

Some granular hypo-autofluorescence was seen in nasally from the optic disc. Otherwise, the midperipheral retina showed normal autofluorescence. Spectral-domain optical coherence tomography (SD-OCT) showed parafoveal cystoid macular oedema, and preservation of the central outer nuclear layer. The external limiting membrane and the ellipsoid zone were well-preserved in the fovea, but granular in the peripheral macula. At this time, the full-field electroretinogram showed scotopic and photopic responses within the normal range. The decimal best-corrected visual acuity (BCVA) was 0.6. Four years later, FAF (**B**) showed an increase in the granular hypo-autofluorescence, which had now fully encircled the relatively spared fovea. The SD-OCT showed that the cystoid macula oedema had disappeared, and that the outer nuclear layer and the hyperreflective outer retinal bands were now spared only at the fovea, but severely atrophic elsewhere in the macula. At this stage, the full-field electroretinogram showed a mild rod-cone dystrophy, showing a progression of the isolated macular dystrophy phenotype to a retinitis pigmentosa phenotype. Due to the foveal sparing, the BCVA had not decreased. **C-D.** A male patient between the ages of 28 and 37 years. FAF imaging between the ages of 28 (**C**) and 37 (**D**) years showed an increase of the profound central macula hypo-autofluorescence, with a very small area of relative foveal sparing (BCVA OU: 0.03). The SD-OCT scan showed severe atrophy of the outer retina at baseline, without much change in the peripheral macula through the years (BCVA remained 0.03). A small epiretinal membrane is visible in the nasal macula.

Supplementary Table 1. Genetic characteristics of patients with *CRB1*-associated retinopathies

	Allele 1		Allele 2		
ID	**DNA change**	**AA change**	**DNA change**	**AA change**	**Diagnosis**
1	c.2308G>A	p.Gly770Ser	c.2308G>A	p.Gly770Ser	RP + Coats
2	c.3879G>A	p.Trp1293*	c.3074G>A	p.Ser1025Asn	RP
3	c.1892A>G	p.Tyr631Cys	c.4005+1 G>A	Splice	RP
4	c.1256A>G	p.Tyr419Cys	c.2401A>T	p.Lys801*	RP
5	c.929G>A	p.Cys310Tyr	c.1268G>A	p.Cys423Tyr	RP + Coats
6, 7	c.2688T>A	p.Cys896*	c.4135T>C	p.Tyr1379His	RP
8	c.2401A>T	p.Lys801*	c.2401A>T	p.Lys801*	RP + Coats
9	c.929G>A	p.Cys310Tyr	c.1892A>G	p.Tyr631Cys	RP
10	c.2401A>T	p.Lys801*	c.3988del	p.Glu1330Serfs*11	LCA
11	c.2842+5G>A	Splice	c.2843G>A	p.Cys948Tyr	LCA
12	c.2401A>T	p.Lys801*	c.2688T>A	p.Cys896*	LCA
13†	c.3487T>C	p.Cys1163Arg	c.2401A>T	p.Lys801*	RP
14	c.2290C>T	p.Arg764Cys	c.2290C>T	p.Arg764Cys	RP + Coats
15	c.2533_2545del	p.Gly845_ Ile1406delinsSerSer	c.2843G>A	p.Cys948Tyr	LCA
16	c.601T>C	p.Cys201Arg	c.601T>C	p.Cys201Arg	RP
17-19†	c.3487T>C	p.Cys1163Arg	c.3487T>C	p.Cys1163Arg	RP, LCA
20	c.2843G>A	p.Cys948Tyr	c.1472A>T	p.Asp491Val	RP
21	c.2533_2539del	p.Gly845Serfs*9	c.2533_2539del	p.Gly845Serfs*9	RP
22†	c.3487T>C	p.Cys1163Arg	c.1349G>A	p.Cys450Tyr	LCA
23	c.2687G>T	p.Cys896Phe	c.2842+5G>A	Splice	RP
24	c.2688T>A	p.Cys896*	c.2688T>A	p.Cys896*	LCA
25	c.1892A>G	p.Tyr631Cys	c.2842+5G>A	Splice	RP
26	c.2842+5G>A	Splice	c.2842+5G>A	Splice	RP
27	c.3307G>A	p.Gly1103Arg	c.3988del	p.Glu1330Serfs*11	RP
28	c.1689C>A	p.Ser563Arg	c.1689C>A	p.Ser563Arg	LCA
29	c.2234C>T	p.Thr745Met	c.2752A>T	p.Ser918Cys	RP
30	c.2498G>A	p.Gly833Asp	c.3879G>A	p.Trp1293*	LCA
31	c.2842+5G>A	Splice	c.4005+1G>A	Splice	LCA
32	c.1084C>T	p.Gln362*	c.1084C>T	p.Gln362*	LCA
33-34	c.498_506del	p.Ile167_Gly169del	c.2401A>T	p.Lys801*	Macular dystrophy
35	c.1084C>T	p.Gln362*	c.2401A>T	p.Lys801*	RP
36	c.498_506del	p.Ile167_Gly169del	c.1084C>T	p.Gln362*	Macular dystrophy
37-38	c.613_619del	p.Ile205Aspfs*13	c.2290C>T	p.Arg764Cys	LCA
39	c.2843G>A	p.Cys848Tyr	c.2842+5G>A	Splice	LCA
40	c.2401A>T	p.Lys801*	c.2688T>A	p.Cys896*	LCA

Patient ID-1 also has a variant of unknown significance (VUS) in *RDH12*: c.635G>A; p.Arg212His. Patient ID-3 also has a VUS in *USH2A*: c.1663C>T; p.Leu555Val.

†These patients are related to each other. They were considered to be from 3 different families, based on the different mutations on the second allele.

Supplementary Table 2. Patients with asymmetry in visual acuity

Patient ID	Presumed cause of asymmetry	BCVA better-seeing vs. worse-seeing eye
1	Unilateral Coats-like vasculopathy and a subsequent exudative retinal detachment in the worse-seeing eye	0.05 – LP+ (progression to blindness OU)
3	More atrophy of the foveal ONL in the worse-seeing eye	0.2 – 0.02
5	Unilateral Coats-like vasculopathy in the worse-seeing eye	0.45 – 0.04
9	More CMO and optic disc oedema (initially diagnosed as uveitis) in the worse-seeing eye, with an earlier onset in the worse-seeing eye	0.4 – 0.9 (progression to blindness OU)
11	Unknown, both eyes either blind or severely visually impaired	LP+ – 0.06 (progression to no LP OU)
23	More RPE atrophy (FAF) in the worse-seeing eye, and a very narrow band of RPE sparing in the better-seeing eye. On SD-OCT, both eyes displayed extensive atrophy of the outer retina	0.15 – 0.04
25	An ocular trauma in the worse-seeing eye, which led to an orbital and a cranial fracture	0.8 – LP+
29	More atrophy of the ELM, EZ, and ONL in the worse-seeing eye, a small remnant of foveal sparing remained longer in the better-seeing eye	0.1 – CF (progression to blindness OU)
33	More atrophy of the ELM, EZ, and ONL in the worse-seeing eye (although the better-seeing eye had CMO including in the fovea)	0.05 – 0.6
35	Unknown. More posterior subcapsular cataract in the worse-seeing eye, although not convincingly explanatory for difference in BCVA	0.2 – LP+
36	Unknown (FAF and SD-OCT available only after patient reached blindness in both eyes)	0.25 – 0.08 (progression to blindness OU)
37	More foveal atrophy of ONL in worse-seeing eye	0.03 – 1.00
38	More foveal atrophy of ONL in worse-seeing eye (atrophy of ELM and EZ in both eyes)	0.4-0.63

BCVA, best-corrected visual acuity; CF, counting fingers; CMO, cystoid macular edema; ELM, external limiting membrane; EZ, ellipsoid zone; FAF, fundus autofluorescence; LP, light perception vision; ONL, outer nuclear layer; SD-OCT, spectral-domain optical coherence tomography.

Supplementary Table 3. Treatment histories for cystoid macular oedema in *CRB1*-associated retinal degenerations

ID	Age during follow-up	Phenotype	Treatment	Treatment duration	Treatment response
3	36-48 years	RP	Oral acetazolamide 250 mg 2dd (at age 36)	15 days	Due to interval censoring (patient visited again after 7 years, age 43), the direct effect on CMO could not be evaluated. CMO had disappeared.
4	11-16 years	RP	None (mild CMO)	-	-
5	54 years	RP + Coats-like exudates OS	- At age 49, a vitrectomy and ILM peeling was performed in OS, due to vitreomacular traction and CMO. - CMO in OD was mild to moderate and was not treated.	-	CMO disappeared after vitrectomy and ILM peeling.
6‡	47 years	RP	None documented (1st visit)	-	-
9	25-49 years	RP (initial differential diagnosis of uveitis)	- Initially (age 25): subconjunctival celestone and topical indometacine and NSAID - A history of mycophenolate mofetil (suspected uveitis), cyclosporine (until the age of 45), and intramuscular ledertrexate (until the age of 46) - Corticosteroids, initially methylprednisolone, then prednisolone 16 mg - Adalimumab injections were initiated at age 45 - Intravenous Infliximab - Intravitreal injections of bevacizumab, several at age 47, restart at age 49 - Oral acetazolamide - Intravitreal injection of triamcinolone at age 48	24 years and ongoing	All medication had an insufficient to no effect on CMO, and the patient still had severe CMO at the final visit. - Oral acetazolamide was discontinued due to side effects - Intravitreal triamcinolone led to elevated intra-ocular pressure, which was treated with intravenous mannitol and topical brinzolamide and latanoprost. A cataract extraction was performed. - Patient developed a renal insufficiency, which was linked to the long-term use of cyclosporine. The renal insufficiency responded well to corticosteroids.
13	0-14 years	RP	None, mild CMO occurred at the age of 12	-	CMO remains mild at the final visit
14	4-22 years	RP + Coats-like exudates OU	Intravitreal triamcinolone OS at age 17		Secondary glaucoma OS in response to steroid, with insufficient response to oral acetazolamide, topical bimatoprost and brimonidine/timolol. Glaucoma was then treated with a trabeculectomy with mitomycin C, followed by hypotony. Intra-ocular pressure normalised after intravitreal triamcinolone, followed maintenance with topical brinzolamide/timolol.
16	26 years	RP	Brinzolamide 3dd at age 26	Ongoing	To be evaluated

Supplementary Table 3. Continued

20	4-20 years	RP	None documented (expectative)	-	Persistent CMO during follow-up
23	4-6 years	RP	None (expectative)	-	Persistent CMO during follow-up (age 4-6 years)
33	23-29 years	Macular dystrophy (unilateral CMO, OS)	- Initially: intravitreal injection of triamcinolone - Then (ages 25-6) 5 intravitreal injections of bevacizumab - Spironolactone 1dd 50 mg due to a differential diagnosis of atypical CSC* - Age 26: start topical brinzolamide - Age 27: stop brinzolamide, restart intravitreal bevacizumab Age 27: continue with spironolactone only	4 years and ongoing	- No response to intravitreal triamcinolone - Initial reduction of CMO after the 1st bevacizumab injection, but increase of CMO after 2nd and 3rd injection - Initially no response to spironolactone. In later stages a mild reduction in CMO, so spironolactone was continued. At the final visit, no CMO was found, under usage of only spironolactone . - Mild reduction of CMO after brinzolamide, insufficient response - After restart of bevacizumab, a mild increase in CMO
34	7-29 years	Macular dystrophy	None (expectative)	-	Spontaneous resolution at age 26 (CMO confirmed on OCT between ages 10-18)
36	23-37 years	Macular dystrophy	Due to the concurrent symptomatic pucker: vitrectomy with ILM peeling, laser and air† at age 37	-	No remaining CMO after vitrectomy
38	4-7 years	RP	None (very mild CMO)	-	-

CMO, cystoid macular oedema; CSC, central serous chorioretinopathy; ILM, inner limiting membrane; NSAID, non-steroidal anti-inflammatory drugs; RP, retinitis pigmentosa.

*No subretinal fluid was found in this patient.

†In one eye. The other eye did not receive treatment.

‡This patient visited the Ghent University Hospital once for a second opinion, and limited information was available on any prior treatment of CMO.

2.3

Defining inclusion criteria and endpoints for clinical trials: a prospective cross-sectional study in *CRB1*-associated retinal dystrophies

Mays Talib, MD[1], Mary J. van Schooneveld, MD, PhD[2,3], Jan Wijnholds, PhD[1], Maria M. van Genderen, MD, PhD[3], Nicoline E. Schalij-Delfos, MD, PhD[1], Herman E. Talsma[1,3], Ralph J. Florijn, PhD[4], Jacoline B. ten Brink, BAS[4], Frans P.M. Cremers, PhD[5], Alberta A.H.J. Thiadens, MD, PhD[6], L. Ingeborgh van den Born, MD, PhD[7], Carel B. Hoyng, MD, PhD[8], Magda A. Meester-Smoor[6], Arthur A. Bergen, PhD[4,9], Camiel J.F. Boon, MD, PhD[1,2]

Acta Ophthalmol 2021;99(3):e403-e414

1 Department of Ophthalmology, Leiden University Medical Center, Leiden, The Netherlands.
2 Department of Ophthalmology, Amsterdam UMC, University of Amsterdam, Amsterdam, The Netherlands.
3 Bartiméus, Diagnostic Centre for complex visual disorders, Zeist, The Netherlands.
4 Department of Clinical Genetics, Amsterdam UMC, University of Amsterdam, Amsterdam, The Netherlands.
5 Department of Human Genetics and Donders Institute for Brain, Cognition and Behaviour, Radboud University Medical Center, Nijmegen, The Netherlands.
6 Department of Ophthalmology, Erasmus Medical Center, Rotterdam, The Netherlands.
7 Rotterdam Eye Hospital, Rotterdam, The Netherlands.
8 Department of Ophthalmology, Radboud University Medical Center, Nijmegen, The Netherlands.
9 The Netherlands Institute for Neuroscience (NIN-KNAW), Amsterdam, The Netherlands.

ABSTRACT

Purpose: To investigate the retinal structure and function in patients with *CRB1*-associated retinal dystrophies (RD) and to explore potential clinical endpoints.

Methods: In this prospective cross-sectional study, 22 patients with genetically confirmed *CRB1*-RD (aged 6-74 years), and who had a decimal best-corrected visual acuity (BCVA) ≥ 0.05 at the last visit, were studied clinically with ETDRS BCVA, corneal topography, spectral-domain optical coherence tomography (SD-OCT), fundus autofluorescence, Goldmann visual field (VF), microperimetry, full-field electroretinography (ERG) and full-field stimulus testing (FST). Ten patients were from a genetic isolate (GI).

Results: Patients had retinitis pigmentosa (n = 19; GI and non-GI), cone-rod dystrophy (n = 2; GI), or macular dystrophy (n = 1; non-GI). Median age at first symptom onset was 3 years (range 0.8-49). Median decimal BCVA in the better and worse-seeing eye was 0.18 (range 0.05-0.83) and 0.08 (range light perception-0.72), respectively. Spectral-domain optical coherence tomography (SD-OCT) showed cystoid maculopathy in 8 subjects; inner retinal thickening (n = 20), a well-preserved (para)foveal outer retina (n = 7) or severe para(foveal) outer retinal atrophy (n = 14). All retinal layers were discernible in 13/21 patients (62%), with mild to moderate laminar disorganization in the others. Nanophthalmos was observed in 8 patients (36%). Full-field stimulus testing (FST) provided a subjective outcome measure for retinal sensitivity in eyes with (nearly) extinguished ERG amplitudes.

Conclusions: Despite the generally severe course of *CRB1*-RDs, symptom onset and central visual function are variable, even at advanced ages. Phenotypes may vary within the same family. Imaging and functional studies in a prospective longitudinal setting should clarify which endpoints may be most appropriate in a clinical trial.

INTRODUCTION

Pathogenic variants in the *CRB1* gene are associated with a spectrum of retinal dystrophies (IRD). Each IRD can be distinguished clinically depending on the age at symptom onset, electrophysiological findings and other phenotypic features. *CRB1* mutations cause up to 17% of cases of Leber congenital amaurosis (LCA), and up to 9% of cases of autosomal recessive non-syndromic retinitis pigmentosa (RP), [1-3] as well as rare cases of isolated maculopathy.[4, 5] *CRB1*-associated LCA causes severe visual impairment or blindness from infancy, and *CRB1*-RP usually has an early onset of symptoms such as nyctalopia and visual field restriction, although cases of a later symptom onset and/or relative preservation of visual acuity in *CRB1*-RP have also been described.[6, 7] While most clinical studies of the human *CRB1*-associated phenotype have been case series or small cohorts,[4, 8-12] recent studies in larger populations have shown that half of *CRB1*-RP patients are expected to reach low vision or blindness by the ages of 18 and 44, respectively.[6, 7] Reports on associated features in *CRB1*-RP or LCA, such as keratoconus, have shown a variable prevalence.[9, 13-18] As protein CRB1 is crucial for the integrity of the retinal structure, *CRB1*-associated IRDs have shown an association with variable degrees of disorganization of the retinal laminar structure.[19] While no effective and approved treatment for *CRB1*-associated retinopathies is currently available, subretinal adeno-associated virus (AAV)-mediated *CRB1-CRB2* gene augmentation therapy has shown functional and structural rescue in murine models of *CRB1*-associated LCA and RP.[20] As human *CRB1* gene therapy is under development,[21] defining an optimal window of therapeutic opportunity and clinical endpoints for a *CRB1* gene therapy trial is essential. In such trials, measures that are time-dependent and can still remain stable in certain decades of life, such as visual acuity,[6] may need to be complemented with other, potentially more sensitive functional or structural outcome measures. These additional outcome measures have not yet been elucidated, as an inevitable limitation of retrospective studies is the limited availability of extensive imaging and functional examinations, as well as the unstandardized design. The aim of the present study was to extensively investigate the retinal structure and function in patients with *CRB1*-RDs in a clinical study of prospectively enrolled patients and to study the correlation between structural and functional parameters in order to assess potentially sensitive efficacy endpoints for a future gene therapy trial.

MATERIALS AND METHODS

Human subjects

This is a nationwide collaborative study, based on the Delleman archive for hereditary eye diseases at the Amsterdam UMC (University of Amsterdam) and the RD5000 consortium, the Dutch national consortium for the registry of patients with retinal dystrophies. Inclusion criteria for this prospective, cross-sectional study were (1) the presence of two confirmed pathogenic variants in

the *CRB1* gene (class 4 or 5), (2) a decimal BCVA of ≥0.05 in the better-seeing eye at the last available clinical examination, which (3) should not have been >20 years prior to enrolment in this study. Of the 63 identified *CRB1*-RD patients in the Netherlands, 22 could be included based on these inclusion criteria (Figure S1). In one patient (ID-9), the worse-seeing eye had light perception vision, and not all tests could be performed in the worse-seeing eye. The cohort included patients from a Dutch genetic isolate, that is a consanguineous pedigree described earlier.[22] Patients and/or their parents signed informed consent. This study was approved by the Medical Ethics Committee of the Erasmus Medical Center, as it was performed in the framework of the RD5000 consortium,[23] and by the local review board of the Leiden University Medical Center (LUMC), and complied with the tenets of the Declarations of Helsinki.

Ophthalmological assessment

A detailed medical and ophthalmological history was recorded in all subjects. Patients were surveyed on the history of their symptoms, the presence of photopsia, and in the case of photopsia, where in the visual field these were located (full field, periphery, or central areas). Participants underwent a complete ophthalmological examination, including best-corrected visual acuity (BCVA) measurements with the Early Treatment of Diabetic Retinopathy Study (ETDRS) ESV-3000 chart by Precision Vision,[24, 25] slit-lamp biomicroscopy, fundoscopy and Goldmann kinetic perimetry. Corneal topography was evaluated using the 4-map refractive report and the Belin/Ambrósio Enhanced Ectasia report (Oculus Optikgerate GmbH, Wetzlar, Germany). Biometry was performed (EyeSuite™ IOL, Haag-Streit Diagnostics) to measure eye axis length and anterior chamber depth. Macular threshold sensitivities were measured under mesopic conditions with Macular Integrity Assessment microperimetry (MAIA, Centervue, Padova, Italy) in 20 patients, as the youngest two patients (aged 6 and 9 years) could not complete the procedure. To minimize a learning effect, each eye was tested using the '4-levels-fixed' protocol, which familiarizes the patient to the test, followed by testing with the '4-2 staircase strategy', projected on a 10-2 Cartesian grid (37 points covering the central 10°). The latter was used to evaluate the macular sensitivity (average threshold) and fixation stability (bivariate contour ellipse area; BCEA). The 95% or 65% BCEA indicates the ellipse area that comprises 95% or 65%, respectively, of the fixation points used by the patients during the test. Thus, a smaller area indicates a more stable fixation. Seven-field colour fundus photographs were obtained (Topcon TRC-50DX, Topcon Medical Systems, Inc. Oakland, NJ, USA). Spectral-domain optical coherence tomography (SD-OCT; Spectralis, Heidelberg Engineering, Heidelberg, Germany) of the macula and optic disc was performed in 21 patients, but could not be reliably performed in the 6-year-old patient. Segmentation of SD-OCT images was performed with the integrated automatic segmentation Spectralis software, and errors in the segmentation were manually corrected. Thickness of the photoreceptor-retinal pigment epithelium complex (PR + RPE) was measured as the distance from the external limiting membrane (ELM) to the basal membrane, based on methods used earlier [26]. The horizontal width of detectable and uninterrupted (even if attenuated) ellipsoid zone (EZ) was measured drawing a

line parallel to the retinal pigment epithelium (RPE), starting at the fovea. In patients where the EZ signal became indistinguishable from other hyperreflective outer retinal signals and could no longer be differentiated from the ELM or interdigitation zone, the horizontal width of detectable hyperreflective outer retinal band was measured. The laminar organization of the retina, that is the retinal alignment into distinct layers, was assessed and categorized (Figure S2). In 20 patients, 488 nm wavelength fundus autofluorescence (FAF; Spectralis, Heidelberg Engineering, Heidelberg) was performed, which could not be reliably performed in the two youngest patients (aged 6 and 9 years). The fovea was defined as the central 5°, the parafovea as the following circumferential 3° around the fovea, and the perifovea or peripheral macula as the circumferential 10° around the parafovea.

Pupil dilation protocol

Initially, all pupils were dilated using phenylephrine 2.5% and tropicamide 1%. After the occurrence of acute angle-closure glaucoma in one patient during mydriatic dark-adaptation with tropicamide only (patient-ID 15, the 9th consecutive patient who participated), the pupil dilation protocol was revised: only patients with an anterior chamber depth ≥ grade 2, as graded with the pen torch method and Van Herick's technique, received phenylephrine 2.5% and tropicamide 1%. In patients with an anterior chamber depth of grade 2, pupils were dilated using only tropicamide 1%. The pupils of one patient (patient-ID 4, the 10th consecutive patient) with an anterior chamber depth of grade 1, and a family history of acute angle-closure glaucoma in relatives with *CRB1*-RP, were not dilated.

Electrophysiological testing

Full-field electroretinography (ERG) was performed according to an extended protocol, which incorporated the International Society for Clinical Electrophysiology Standards [27]. All ERG responses were recorded using Dawson Trick Litzkow (DTL) fibre electrodes with the Espion ColorDome™ and console (Diagnosys LLC, Cambridge, UK). The set-up and reference values of the Rotterdam Eye Hospital (Rotterdam, The Netherlands) and Bartiméus (Zeist, The Netherlands) were used. For an RP diagnosis, attenuation of the dark-adapted responses had to be more severe than attenuation of the light-adapted responses. The reverse was the case for a cone-rod dystrophy (CORD) diagnosis. In the case of non-detectable responses, the diagnosis was made based on the clinical evidence (e.g. fundoscopy). For an isolated macular dystrophy diagnosis, the full-field ERG should display no panretinal dysfunction of dark- or light-adapted responses. Full-field stimulus testing (FST) was successfully performed in 15 subjects (28 eyes) with the Espion ColorDome™ LED full-field stimulator (Diagnosys LLC, Lowell, MA, USA) using methods described previously,[28-30] after dark-adaptation of ≥30 minutes, and using white, red, and blue stimuli, each lasting 4 milliseconds. Each eye was tested separately, and the fellow eye was patched. The reference luminance (0 dB) was set at 0.1 cd.s/m^2. Sensitivity thresholds were determined three times for each colour, and the three trials were averaged to determine the final thresholds.

General sensitivity thresholds were determined using the white stimuli. Chromatic sensitivities were used to determine whether these responses were rod-mediated (blue-red difference of >22 dB), cone-mediated (blue-red difference of <3 dB) or mixed rod- and-cone-mediated (blue-red difference between 3 and 22 dB). Based on earlier studies,[28, 31] and correcting for differences in reference luminance, the normal FST threshold for white stimuli was determined at -53 dB and should be rod-mediated.

Statistical analysis

Data were analysed using SPSS version 23.0 (IBM Corp, Armonk, NY, USA). Normality was tested using the normal probability plot and quantile-quantile plot, and the Shapiro-Wilk test. Normally distributed data were presented with means and standard deviations (SD). Non-normally distributed data were presented with medians and interquartile ranges (IQR). Goldmann visual field areas of the V4e target were digitized and converted to seeing retinal areas in mm^2 using a method described by Dagnelie.[32] Visual field areas were classified as large (>250 mm^2), intermediate (25-250 mm^2) or small (<25 mm^2), based on an earlier study.[33] Medians were compared using the Mann-Whitney *U*-test. The correlation between visual function parameters (BCVA, macular sensitivity on microperimetry, V4e and I4e visual field extent) and biomarkers on retinal imaging was tested with Spearman's correlation testing. Visual impairment, based on the BCVA, was categorized as defined by the World Health Organization: mild or no visual impairment (BCVA ≥ 0.3), low vision (BCVA < 0.3 and ≥ 0.1), severe visual impairment (BCVA < 0.1 and ≥ 0.05) and blindness (BCVA < 0.05). For statistical analysis, ETDRS BCVA was converted to the logarithm of the minimal angle of resolution (logMAR).

RESULTS

Twenty-two patients with *CRB1*-RD were included, from 12 families. Table 1 shows the baseline clinical characteristics. Ten patients (45%) were from the genetic isolate. The median age at examination was 25 years (IQR 20; range 6-74) and did not differ significantly between patients from within and from outside the genetic isolate ($p = 0.57$). Nine patients (41%) were male (aged 6-74), and 13 (59%) were female (aged 9-38). Based on current and previous ERG examinations, 19 patients (86%) were diagnosed with RP, 2 patients (9%; 1 from the genetic isolate) had a cone-rod dystrophy, and 1 patient (5%) had a macular dystrophy. Table S1 shows the genetic characteristics, including the novel *CRB1* variant p.(Phe978Ser) in a patient with severe RP (ID-16), and the homozygous p.(Ile167_Gly169del) variant in the macular dystrophy patient (ID-22). Nineteen patients (86%) were of Dutch Caucasian descent, 2 were of North-African origin (9%), and 1 patient was of Caribbean descent (Dutch Antilles; 5%).

Table 1. Demographics and baseline findings in ophthalmological examination in patients with *CRB1*-associated retinal dystrophies

		Age (y) at onset 1st symptom	BCVA (ETDRS letters [decimal Snellen])				Central horizontal VF diameter (°)		Total seeing retinal area V4e (mm^2)	
ID/Sex/ Family	Age (y)		OD	OS	SER (D)**	ffERG	OD	OS	OD	OS
1/M/GI*	29	6	34 (0.10)	61 (0.33)	+0.56	ND	27	30	154.6	158.1
2/F/GI	13	1.5	39 (0.12)	40 (0.13)	+3.06	ND‡	24	24	33.9	36.9
3/F/GI	16	1	52 (0.20)	56 (0.25)	+0.56	RCD	22	28	119.7	160.7
4/F/GI	38	<1	23 (0.06)	40 (0.13)	+1.00	ND‡	25	24	34.1	38.8
5/M/GI	41	2	40 (0.13)	13 (0.04)	+3.88	ND	19	19	90.5	74.9
6/F/GI	11	3	56 (0.26)	64 (0.38)	+3.19	MR	29	105	260.9	296.2
7/F/GI	9	2	19 (0.05)	19 (0.05)	+6.31		30	21	240.0	183.9
8/F/GI	10	3	31 (0.08)	22 (0.05)	+7.06	MR	150	45	624.4	450.4
9/F/GI	28	8	5 (0.03)	35 (0.10)	+5.75	ND	25	21	164.3	185.6
10/M/GI	39	34-35	78 (0.72)	78 (0.72)	+2.5	CORD	150	150	746.9	711.8
11/M	31	7-8	70 (0.50)	81 (0.83)	+1.00	MR	62	125	278.9	370.3
12/F	26	9	53 (0.23)	61 (0.33)	+1.44	ND	51	110	279.1	345.8
13/M	21	2	12 (0.03)	30 (0.08)	+2.56	ND‡	70	53	215.0	189.9
14/F	24	2	52 (0.22)	20 (0.05)	+5.25	ND‡	36	26	79.1	85.5
15/F	31	1	41 (0.13)	42 (0.14)	+4.75	ND‡	22	24	175.2	146.24
16/M	6	1-2	11 (0.03)	25 (0.06)	+3.38	NP	72	62	231.9	123.19
17/M	23	12	63 (0.36)	27 (0.07)	***	RCD	101	20	553.6	348.1
18/F	12	3	40 (0.13)	19 (0.05)	+5.00	ND	15	16	135.0	116.8
19/M	53	17	52 (0.22)	0 (NLP) †	***	ND	18	0	33.4	0
20/M	74	49	75 (0.63)	58 (0.29)	***	ND	20	19	17.9	22.4
21/F	31	4	30 (0.08)	31 (0.08)	+0.88	CORD	65	25	703.0	717.3
22/F	24	11-12	66 (0.41)	42 (0.14)	-5.75	Normal	148	148	723.7	754.8

BCVA = best-corrected visual acuity, CORD = cone-rod dystrophy, ETDRS = Early Treatment of Diabetic Retinopathy Study, ERG = full-field electroretinography, GI = genetic isolate, MR = minimal response, ND = no detectable responses, NP = not performed (patient did not tolerate the electrodes), SER = spherical equivalent of the refractive error, VF = (Goldmann) visual field.

*These patients were also included in the previous retrospective cohort. One patient (ID-1) underwent electrophysiological testing with a different device (MetroVision) prior to the acquisition of the Diagnosys device.

**Averaged between eyes.

***These patients had undergone cataract surgery in one (patient 17) or both (patients 19-20) eyes, and these refractive error measurements are postoperative. Preoperatively, the SER was -0.5 D and -1.875 D in patients 19 and 20, respectively.

†Patient 19 reported no light perception in OS during BCVA measurement, but after dark-adaptation in mydriasis in preparation for electrophysiological examination, he could perceive white, red, and blue stimuli with OS.

‡Scotopic and photopic responses had been nondetectable in ERG examination performed prior to this study.

Onset and visual acuity

The median self-reported or parent-reported age at symptom onset was 3 years in the RP group (IQR 6.5 years; range 9 months-49 years) and 11 years in patients with a cone-rod or macular dystrophy (range 4-34 years). In the RP group, the first-experienced symptoms, as noticed either by the patient or by the parents, were visual field loss (8/19; 42%), nyctalopia (5/19; 26%), central vision loss (4/19; 21%) or nystagmus (2/19; 11%). In RP patients ID-6 and ID-17, the initial erroneous diagnosis was intermediate uveitis, based on central vision loss, CME and vitreous cells, all of which preceded pigmentary fundus changes. After 1 and 4 years, respectively, the correct diagnosis of RP was established based on full-field ERG responses, and the course toward the correct diagnosis has been described previously.[34] In the three patients with cone-rod or macular dystrophy, the first symptom was subjective central vision loss. There was no statistically significant difference in median age at symptom onset between patients from within and from outside the genetic isolate ($p = 0.22$). Photopsia were reported by 13 patients (59%) in areas of decreased/no vision (n = 3), areas of good vision (n = 2), or in both (n = 8).

The median decimal BCVA in the better-seeing eye was 0.18 (0.05-0.83), and 0.08 in the worse-seeing eye (range light perception vision-0.72), with a moderate symmetry between the right and left eye (Spearman's rho = 0.467; $p < 0.028$). Best-corrected visual acuity (BCVA) in the better-seeing eye did not significantly differ between patients from within or from outside the genetic isolate ($p = 0.53$), but was significantly better in older patients (Spearman's rho = 0.435; $p = 0.04$; Figure 1).

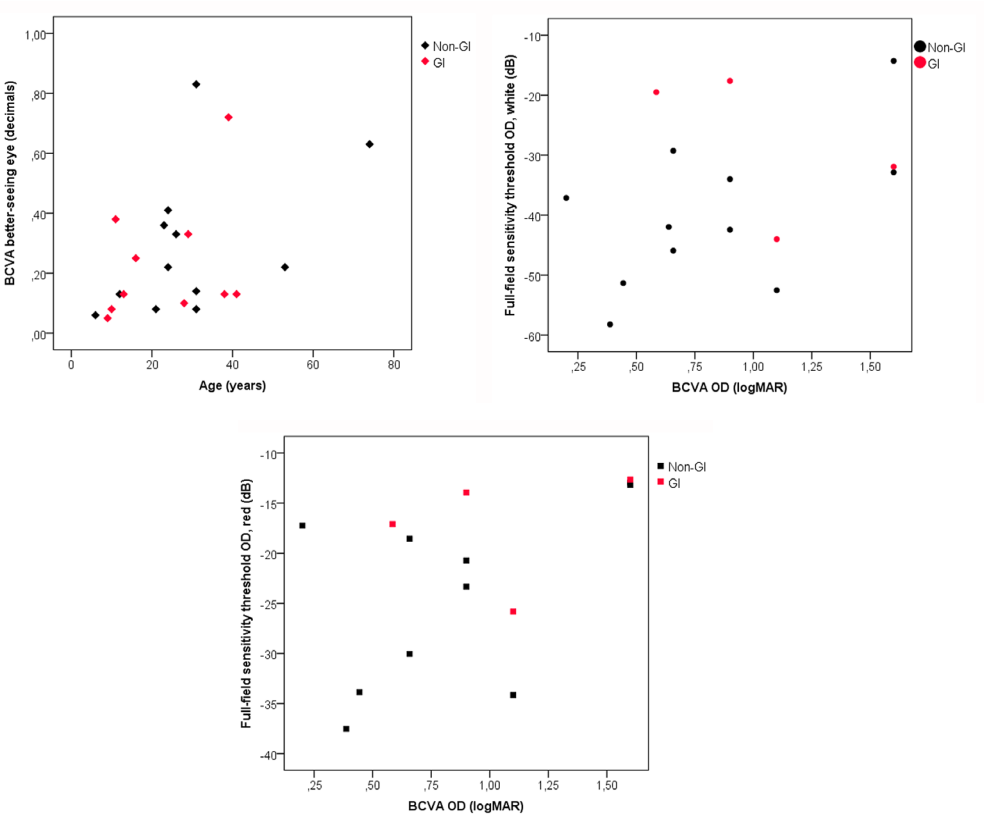

Figure 1. Visual function in patients with *CRB1*-associated retinal dystrophies. Patients from the genetic isolate (GI) are indicated in red, and the other patients are indicated in black. The top row, left panel shows the best-corrected visual acuity (BCVA) as plotted against age. A higher BCVA is seen in older patients (Spearman's rho = 0.435; $p = 0.043$), possibly because the inclusion criterion of a BCVA ≥ 0.05 allows only for the inclusion of either young patients with a severe phenotype, or patients with a mild phenotype, who have a wider window of opportunity for study inclusion. **The top row, right panel** shows the full-field sensitivity threshold to white light (in dB), plotted against BCVA. Although sensitivity thresholds to white stimuli appeared better (signified by lower dB) in patients with a better BCVA, this trend was not significant (Spearman's rho = 0.344; $p = 0.209$). **The second row** shows full-field sensitivity threshold to red light (dB), plotted against BCVA. Again, sensitivity thresholds to red stimuli appeared lower in those with a higher BCVA. This trend seemed more strongly apparent for the red stimuli than for the white stimuli, but was still not significant (Spearman's rho = 0.493; $p = 0.073$).

Ocular and fundus features

The median spherical equivalent of the refractive error, as averaged between both eyes, was +3.1D (IQR 4.0, range -5.75D - +7.06D). The median eye axis length was 20.7 mm, with a median anterior chamber depth of 2.8 mm. Nanophthalmos (axial length < 20.5 mm) was observed in eight patients (36%). Cataracts, defined as significant opacification of the lens, were observed in 11 eyes of six patients (27%), and 3 patients (14%) were pseudophakic in at least one eye. Corneal topography could be reliably performed in 20 patients and revealed a mild to moderate with-the-rule astigmatism in 15 patients (75%), a mild oblique astigmatism in 1 patient (5%), and a mild against-the-rule astigmatism in 1 patient (5%). One patient had a mild forme fruste keratoconus (patient ID-21), and 3 more had a corneal topography suspicious of a mild forme fruste keratoconus, which would need to be confirmed upon follow-up (patients ID-11; ID-15; ID-22). Vitreous abnormalities in 14 patients (63%) included cells (n = 12), veils (n = 3), and asteroid hyalosis (n = 1). Two patients had undergone a pars plana vitrectomy with inner limiting membrane peeling due to cystoid macular oedema (patients ID-17 and ID-19) or the presumably erroneous diagnosis of intermediate uveitis, which was unresponsive to lengthy immunosuppressive treatment. Fundus features were variable, even within the genetic isolate (Figures 2 and 3), but all patients had macular alterations of the retinal pigment epithelium, and 16/22 patients (73%), aged 10-53, had atrophic changes of the macula. Drusen within or hamartomas around the optic nerve head were seen in seven patients (32%), and were observed more frequently in patients from the genetic isolate (6/10 versus 1/12; $p = 0.02$). Fine yellow punctate spots in the peripheral retina were observed in eight patients (36%), all with RP, and were more prominent in the nasal periphery (Figure 2). Intraretinal pigment migrations were present in 21/22 patients with RP or CORD (95%; aged 6-74 years), and not in the patient with a macular dystrophy. These pigment migrations were bone-spicule-like (n = 5), nummular (n = 1) or a combination of both (n = 15). Preservation of the para-arteriolar retinal pigment epithelium (PPRPE) was observed in 3/22 patients (14%). Retinal vascular changes included a unilateral preretinal haemorrhage of unknown origin in patient ID-8, aged 10, and parapapillary hard exudates in patient ID-5 (Figure 2), whose affected younger sister (not included in the current study) had unilateral Coats-like exudates. Furthermore, vascular attenuation was featured in 18/22 patients (82%), but was absent in the macular dystrophy patient (age 24) and in the youngest RP patients (aged 6-10), considerably mild in the adolescent RP patients (aged 12-16), and was mild in the CORD patients (aged 31 and 39).

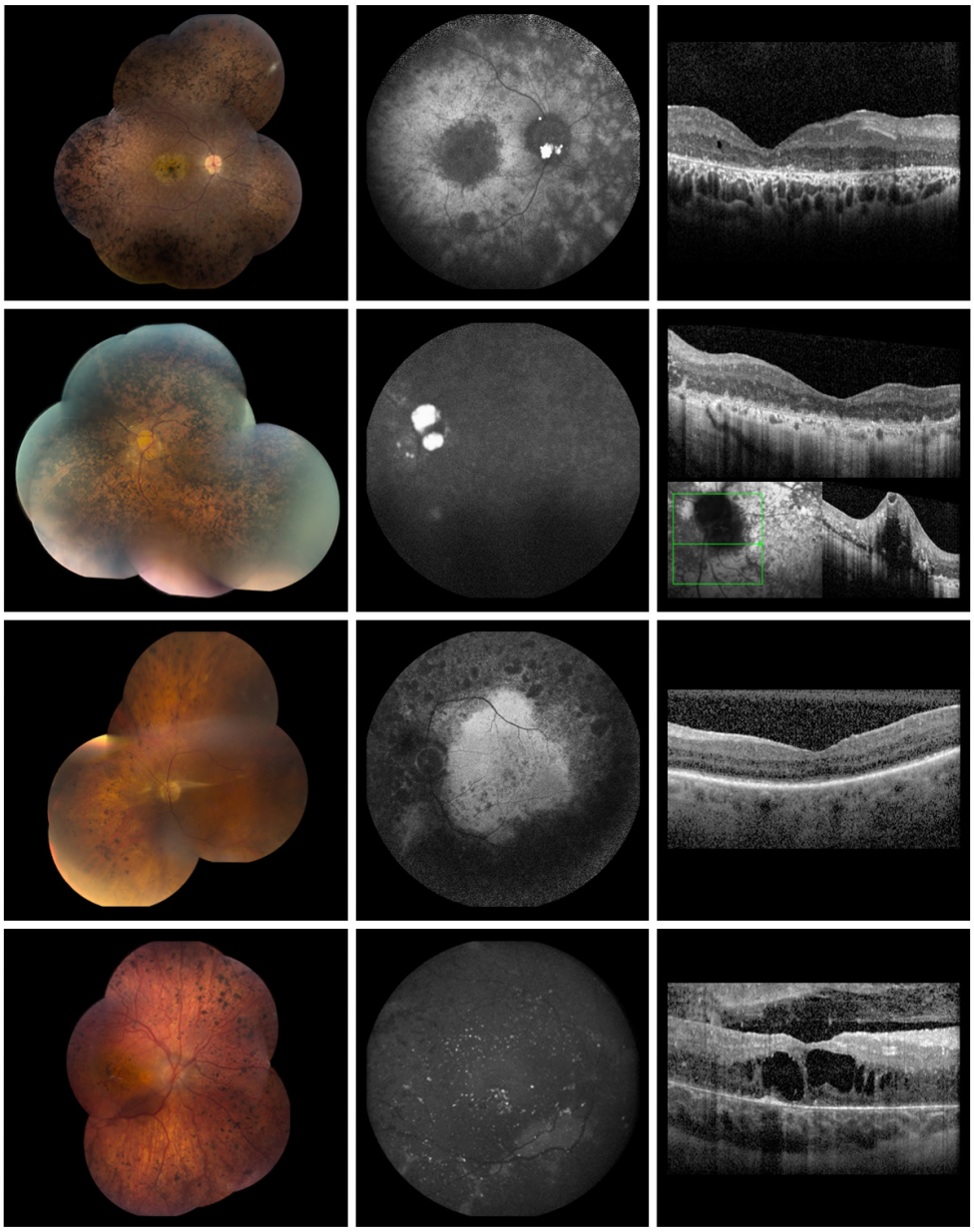

Figure 2. Multimodal imaging in patients with *CRB1*-associated retinitis pigmentosa (RP). The **top row** shows the right eye of patient ID-9, a 28-year-old female patient from the genetic isolate (GI) with a decimal best-corrected visual acuity (BCVA) of 0.03, whose fundus (left panel) showed the typical RP-associated changes of bone-spicule-like pigmentation in the (mid)periphery, vascular attenuation and optic disc palor, but also large parapapillary hamartomas, atrophy of the retina and retinal pigment epithelium (RPE) in the posterior pole, and white flecks resembling reticular pseudodrusen throughout the retina, associated with outer retinal atrophy. Fundus autofluorescence (FAF; middle panel) showed large meshwork-like areas of hypo-autofluorescence in the midperiphery and central macula,

with relatively spared perimacular autofluorescence. Spectral-domain optical coherence tomography (SD-OCT; right panel) showed inner retinal thickening, outer retinal atrophy, (para)foveal granular remnants of the hyperreflective outer retinal bands, but no laminar disorganization. The **second row** shows the left eye of patient ID-5, a 41-year-old male patient from the GI (BCVA 0.04). The fundus (left panel) was profoundly atrophic with dense intraretinal pigmentation, parapapillary hamartomas, fine drusenoid deposits in the nasal periphery, and parapapillary hard exudates that indicate a vascular disease component. FAF (middle panel) showed a near absence of autofluorescence. SD-OCT (right panel) showed mild laminar disorganization, a relatively thickened inner retina, outer retinal atrophy with a severely disrupted ellipsoid zone (EZ) and a barely identifiable external limiting membrane (ELM), and small hyperreflective foci mainly in the inner nuclear layer and ganglion cell layer. SD-OCT of the optic disc (right panel) showed the hamartoma, and dense hyperreflective foci colocalizing with the parapapillary exudates, but no source of the exudation. The **third row** shows the left eye of patient ID-20, a 74-year-old male patient from outside the GI (BCVA 0.29), which showed typical RP-associated changes (left panel), along with mild macular RPE alterations. FAF (middle panel) was relatively preserved in the posterior pole with scattered round hypo-autofluorescent lesions and severe hypo-autofluorescence outside the vascular arcades. SD-OCT (right panel) showed a relatively preserved outer nuclear layer, ELM, and EZ. The **fourth row** shows the right eye of patient ID-8, a 10-year-old female patient from the GI (BCVA 0.08), whose fundus (left panel) showed bone-spicule-like and round intraretinal pigmentation, atrophy in the posterior pole, a preretinal bleeding under the central macula, some preservation of the peri-arteriolar RPE in the inferior and superior periphery, and limited fine drusenoid deposits, mostly in the nasal midperiphery. FAF (middle panel) showed severely decreased autofluorescence, with some relative preservation along the inferior vascular arcade, and sharply circumscribed hyperautofluorescent speckles, which may be photoreceptor debris containing lipofuscin precursors. These speckles were also found in patient ID-18. SD-OCT (right panel) showed cystoid macular oedema, a thickened inner retina, and a severely atrophic ELM and EZ, with scattered para- and perifoveal remnants.

Perimetry

Visual field areas, averaged between right and left eyes, were large in 8/22 patients (36%), intermediate in 12/22 (55%) and small in 2/22 patients (9%). Visual field areas did not significantly correlate to age ($p = 0.25$ and $p = 0.61$ for the V4e and I4e isopter).

Microperimetry could not be reliably performed in the two youngest patients and was challenging to perform in patients with severe visual impairment: between the test run using the 4-levels-fixed strategy, and the examination using the 4-2 strategy, the preferred retinal locus had shifted in nine eyes of six patients (three eyes with low vision; five eyes with severe visual impairment; and one blind eye). The average threshold of the macular sensitivity on microperimetry was 8.0 dB (SD 6.9; range 0.2-25.3; normal range 26.0-36.0 dB; Table S2). Macular sensitivity was significantly lower in eyes with decreased fixation stability, as indicated by a higher BCEA 95%, averaged between right and left eyes (Spearman's rho = -0.478; $p = 0.045$). Inter-eye symmetry was very high for the average threshold of the macular sensitivity (Spearman's rho = 0.821; $p < 0.0001$) and V4e visual field area (Spearman's rho = 0.955; $p < 0.00001$; Figure S3). There was no significant difference between patients from within and from outside the genetic isolate in visual field areas for the V4e ($p = 0.74$) and I4e ($p = 0.60$), or macular sensitivity ($p = 0.66$).

Rod and cone function

Dark- and light-adapted full-field ERG responses were nondetectable in 12/20 patients (60%; aged 12-73; Table 1). Dark-adapted FST thresholds were obtained in 15 subjects (28 eyes for white stimulus; 27 eyes for red and blue stimuli), nine of whom had no detectable dark- or light-adapted responses on ERG, and two more with nearly non-detectable responses. General FST sensitivity for the white stimulus, averaged between eyes, ranged between -56.2 and -13.4 dB (mean -36.1; SD 12.7). Sensitivity thresholds were mediated by a mixed rod-cone response (17/27 eyes; 63%) or were rod-mediated (10/27 eyes; 37%, which included the four eyes of two patients with cone-rod or macular dystrophy). The FST thresholds for red stimuli, which are typically mostly cone-mediated, were not significantly associated with biomarkers on SD-OCT (Table 2). The median inter-eye difference in FST threshold was 4.0 dB (IQR 7.8; range 0.24-14.0). For each eye, each threshold was tested three times. The results of the three intra-ocular measurements were generally consistent (median largest within-visit difference between each pair of measurements of the white stimulus threshold was 2.07 dB; IQR 1.84; range 0.31-8.62).

Table 2. Structure and function correlations in *CRB1*-associated retinopathies

	Foveal EZ width		PR+RPE thickness		CRT**	
Visual function parameter	**Spearman's rho**	***p*-value**	**Spearman's rho**	***p*-value**	**Spearman's rho**	***p*-value**
BCVA (logMAR)	-0.581	0.007	0.656	**0.001**	0.424	0.070
Average threshold for MS (dB)	0.433	0.064	0.489	0.029	0.449	0.062
Central sensitivity* (dB)	0.506	0.027	0.502	0.024	0.424	0.080
BCEA 63%	-0.385	0.127	-0.453	0.059	-0.159	0.557
BCEA 95%	-0.385	0.127	-0.453	0.059	-0.159	0.557
Seeing retinal area V4e	-0.095	0.691	-0.226	0.324	-0.144	0.557
Seeing retinal area I4e	0.123	0.605	0.097	0.674	0.181	0.457
FST thresholds white light (dB)	0.319	0.289	0.319	0.267	0.140	0.665
FST thresholds red light (dB)	0.396	0.181	0.358	0.208	0.259	0.417

Values for all parameters were averaged between the right and left eye for each patient. When data were available for one eye only, the data for that eye were used. For measurement of the EZ width, values were measured from the central fovea. If the EZ band was interrupted and continued in the peripheral macula, this peripheral EZ was not included in the EZ width. Significance level was set at $p < 0.002$ following Bonferroni correction.

BCEA = bivariate contour ellipse area, BCVA = best-corrected visual acuity, CRT = central retinal thickness, EZ = ellipsoid zone, FST = full-field stimulus testing, MS = macular sensitivity on microperimetry, PR = photoreceptor layers, RPE = retinal pigment epithelium.

*Sensitivity at the central fixation point, as measured with microperimetry, which was the fovea in 17/39 eyes (44%), and an eccentric location in the other eyes.

**Patients with cystoid macular oedema, and therefore increased central retinal thickness, were not included in the analysis of correlations between central retinal thickness and visual function parameters.

Imaging

Spectral-domain optical coherence tomography (SD-OCT) showed bilateral cystoid macular oedema (CME) in the inner nuclear layer (INL) of 8/21 patients (38%), two of whom also had CME in the ONL. Patient ID-11 also had macular retinoschisis with splitting in the outer plexiform layer. Patients with CME seemed younger (mean age 21.1; SD 10.4; range 10-39) than those without CME (mean age 31.9; SD 17.1; range 9-74), although this difference was not statistically significant (p = 0.13). However, decimal BCVA was higher in patients with CME (median 0.25; IQR 0.43; range 0.07-0.72) than in those without CME (median 0.10; IQR 0.10; range 0.05-0.46; p = 0.03). CME was mostly refractory to treatment (Table S3). A mild epiretinal membrane was observed in nine patients (41%; bilateral in 6/9), and patient ID-11 had a lamellar pseudohole in one eye. The retinal laminar organization was relatively disorganized in 8/21 patients (38%), had a coarse aspect but no disorganization in 8/21 patients (38%) and was normal in 5/21 patients (24%; Figure S2). No outer retinal tubulations were observed.

The outer retinal layers at the (para) fovea, that is, outer nuclear layer and hyperreflective outer retinal bands (external limiting membrane and ellipsoid), showed moderate to severe disintegration in 14/21 patients (67%) aged 13-53, with a near absence of these layers in three of these patients, but only mild thinning in 7/21 patients (33%) aged 9-74. In the more peripheral macula, the outer retinal layers were nearly absent in 5/21 (24%), markedly attenuated in 10/21 patients (48%) and only mild thinning in 6/21 patients (29%). The general pattern consisted of more severe outer retinal attenuation in the peripheral macula with relative foveal remnants of the outer retina, with the exception of patients ID-10, ID-21 and ID-22, who had more intact outer retina in the peripheral macula. Figure S4 shows the horizontal width of detectable uninterrupted ellipsoid zone band for each patient. No significant correlations were found between foveal retinal thickness or the horizontal width of visible ellipsoid zone and visual function parameters after correction for multiple testing, but the PR + RPE thickness correlated significantly with BCVA (p = 0.001; Table 2). Mild to severe thickening of the inner retinal layers was observed in 20/21 patients (95%), which was not correlated to thinning of the outer retina and RPE (Figure S4). Fundus autofluorescence (FAF) images showed intra- and interfamilial variability in the degree of retinal pigment epithelium preservation (Figures 2 and 3), ranging from generalized severely decreased or (nearly) absent autofluorescence (n = 4; aged 13-41 years), to relative preservation of autofluorescence in the posterior pole or around the vascular arcade (n = 10; aged 11-74 years), to a generally normal or mildly hypo-autofluorescent retina with zones of granular or bone-spicule-like hypo-autofluorescence (n = 3; aged 16-31 years). Patients with CORD had different patterns of macular hypo-autofluorescence. A hyperautofluorescent ring was only observed in patient ID-22 with a macular dystrophy.

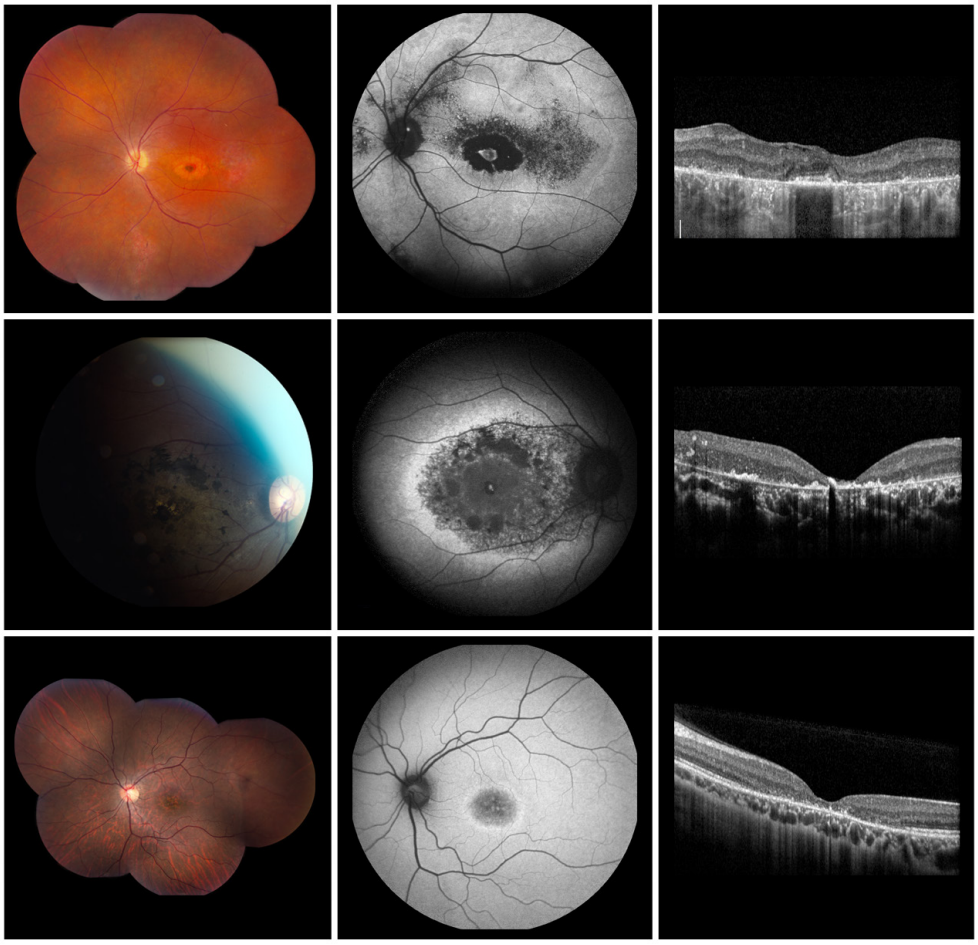

Figure 3. Multimodal imaging in patients with *CRB1*-associated cone-rod or macular dystrophy. The **top row** shows the left eye of patient ID-10, a 39-year-old male patient from the genetic isolate with cone-rod dystrophy (CORD) and a decimal best-corrected visual acuity (BCVA) of 0.72, whose fundus (left panel) showed mild parapapillary atrophy, mild vascular attenuation and stretching in the periphery, atrophy of the retina and retinal pigment epithelium (RPE) in a parafoveal ring around a hyperpigmented fovea, along with RPE alterations in the temporal posterior pole and regional chorioretinal atrophy with limited bone-spicule-like pigmentation in the inferior periphery. Fundus autofluorescence (FAF; middle panel) showed a small optic disc druse, a parafoveal ring of absent autofluorescence, surrounded by dense granular hypo-autofluorescence with scattered hyperautofluorescent lesions mainly in the superior and temporal posterior pole. These granular changes are also visible along the superior vascular arcade, and in the nasal and inferior midperiphery. Spectral-domain optical coherence tomography (SD-OCT) (right panel) showed a thickened inner retina, a severely attenuated outer nuclear layer (ONL) and relative sparing of the hyperreflective outer retinal bands in the fovea and to a lesser extent in the peripheral macula, with severe disruption in the parafoveal region. The **second row** shows the right eye of patient ID-21, a 31-year-old female patient of Caribbean origin (Dutch Antilles) with CORD (BCVA 0.08), which showed (left panel) relative preservation of the optic disc colour and vascular calibre, but atrophy of the retina and RPE in the posterior pole, with large round and bone-spicule-like pigmentations that partially fused, and some bright RPE alterations in the

central macula. The (mid)peripheral retina (not shown here) was well-preserved. FAF (middle panel) showed a large parafoveal area of even hypo-autofluorescence around a foveal hyperautofluorescent lesion, surrounded by patches of absent autofluorescence and granular hypo-autofluorescence. A broad and mildly hyperautofluorescent ring encircled this region of hypo-autofluorescent changes. SD-OCT (right panel) showed a mildly thickened inner retina and a profoundly atrophic outer retina, and a relatively preserved laminar structure. The **third row** shows the left eye of patient ID-22, a 24-year-old female patient of North-African origin with macular dystrophy (BCVA 0.14), whose fundus (left panel) showed a mild temporal pallor of the optic disc, atrophic macular RPE alterations with visible choroid, and an otherwise normal fundus. FAF (middle panel) showed hypo-autofluorescent changes in the central macula, encircled by a hyperautofluorescent ring, surrounded by normo-autofluorescent retina. The granular hypo-autofluorescent changes corresponded with severe ONL atrophy, and disruptions of the external limiting membrane and the ellipsoid zone on SD-OCT (right panel).

DISCUSSION

In this prospective cross-sectional study, we performed detailed clinical examinations in patients with *CRB1*-associated IRDs, demonstrating a wide clinical spectrum. We define parameters that are potentially the most appropriate clinical and surrogate endpoints for a future *CRB1*-gene therapy trial, as well as risk factors for potential adverse treatment reactions. Complementary to time-dependant endpoints, which may remain stable for years and which we investigated earlier in the largest retrospective longitudinal study to date, potential surrogate endpoints were evaluated in this cross-sectional study through careful structure-function correlation analysis. Diagnoses included RP (86%), CORD (9%) and macular dystrophy (5%). Interfamilial variability and a degree of intrafamilial variability were observed on ophthalmoscopy and retinal imaging, with both adulthood-onset CORD and infancy-onset RP present in the same genetic isolate, in patients carrying the same homozygous mutation. Generally, interfamilial variability was greater than intrafamilial variability. There was a wide range of age at initial symptom onset, although half of RP patients reported this onset to be either in infancy or first years of life. Patients with a cone-rod or macular dystrophy had a later symptom onset, which follows some reports of *CRB1*-associated macular dystrophies that have a decidedly milder phenotype than *CRB1*-RP.[35]

Contrasting the progressive nature of *CRB1*-associated disease in individual patients,[6, 7] in this cross-sectional study we found lower visual acuities in younger patients. This counterintuitive finding may be a result of the inclusion criterion of a BCVA ≥ 0.05, which could result in a narrow and particularly early-in-life window for study inclusion in patients with severe early-onset RP, while posing a broader window for inclusion in patients with mild RP or CORD, who maintain a better BCVA into mid-adulthood. Our results show that despite the previously demonstrated intra-individual progressive visual deterioration,[6, 7] at a cross-sectional population level no simple relationship is found between age and visual function parameters, such as BCVA and visual field area.

Spectral-domain optical coherence tomography (SD-OCT) revealed CME in 38% of patients in this cohort, which is a comparable number to earlier reports of CME in genetically diverse or undifferentiated RP cohorts.[36, 37] Patients with CME in this cohort were on average 10 years younger and had a significantly better BCVA than those without CME, despite the trend for a lower BCVA in younger patients at a cross-sectional level. This suggests that CME is an early disease feature in *CRB1* retinopathy. Follow-up SD-OCTs in the same patients should reveal whether the CME reduces after an extended period of time and whether the macula is more strongly degenerated in areas of previous cystoid maculopathy. The aetiology for CME in RP is not fully clear. Müller cell dysfunction and oedema has been posed as a potential cause of CME,[38] which is supported by the location of the CME in the INL. Müller cells have already been shown to play an important role in the etiology of *CRB1*-associated vascular abnormalities in mice and rats.[39, 40] Earlier fluorescein angiography in three cases of *CRB1*-retinopathy has shown no leakage in patients with CME,[10, 41] in contrast with extensive leakage starting from the early phases in Coats-like exudative vasculopathy,[42] which is a recurring finding in *CRB1*-retinopathies.[22, 43] Our current findings of parapapillary hard exudates in a 41-year old patient and a preretinal haemorrhage of unknown origin in a 10-year-old patient further point to a vascular component of *CRB1* retinopathies. The parapapillary hard exudates may be a precursor of Coats-like exudative vasculopathy, which the older and blind sibling of this patient had been diagnosed with, but SD-OCT of the optic disc revealed no source of the exudation. A preretinal haemorrhage as in the 10-year-old has been described in *CRB1* retinopathies once before in two affected sisters (aged 3 and 5) undergoing interventions in the alternative circuit involving the Valsalva manoeuvre and repeated intense pressure on the soft palate, where these haemorrhages were bilateral and self-limiting.[44] Other findings on SD-OCT included thickening of the inner retina (95%), and coarsening (38%) or disorganization (38%) of the retinal laminar structure. Inner retinal thickening has been observed in human patients with *CRB1* retinopathy,[45] and has also been demonstrated in mice lacking CRB1 and CRB2 in retinal progenitor cells, in which the thickening was caused by a proliferation of retinal progenitors which resulted in an increase in the number of rod photoreceptors, Müller cells and bipolar cells.[46] A recent mouse study showed a role for Crb2 in the thickening of the ganglion cell layer due to ectopic photoreceptors.[47] Some studies have shown a milder degree of inner retinal thickening in association with ONL thinning, for example in *RHO*- and *RPGR*-associated retinopathies.[48, 49] These studies have suggested that this inner retinal thickening may be due to a remodelling process, and may precede eventual inner retinal atrophy.[48, 49] Retinal remodelling could possibly interfere with a functional (gene) therapeutic effect. However, in this cohort, inner retinal thickness was not associated with thinning of the outer retina and RPE, indicating that the cause for the inner retinal thickening is more likely the presence of ectopic photoreceptors, or Müller cell or bipolar cell proliferation, rather than remodelling.

In some cases, the *CRB1*-associated phenotype appears associated with the genotype. For instance, optic nerve head drusen or hamartomas were more prevalent in patients from the genetic isolate

in our cohort (p = 0.02), confirming the findings in our previous retrospective study.[6] Patients from the genetic isolate did not have significant differences in visual function with patients from outside the genetic isolate. Another genotype-phenotype correlation in this study involved the p.(Ile167_Gly169del) mutation, found in homozygous form in patient ID-22, who had an isolated maculopathy, and which has been reported before in most cases of isolated maculopathy, even in compound heterozygosity.[1, 5, 35, 50] *CRB1*-associated maculopathy has also been reported in association with other mutations.[4, 51] It should be noted that in our study, the p.(Tyr631Cys) mutation, which to our knowledge has not been described outside of this cohort, was observed in two patients with an unusually mild phenotype, characterized by preserved BCVA, a normal retinal laminar organization and preservation of outer retinal structures into the 4th and 8th decade of life. The p.(Pro836Thr) mutation was found in association with CORD in this study (patient 21; originally from the Caribbean), but has been reported before in association with early-onset retinal dystrophy in a Malinese patient.[52] As genotype-phenotype correlations do not explain the contrasting phenotypic findings in this cohort or the intrafamilial phenotypic variability, there may be a role for genetic and/or environmental modifiers. Disruption of one allele or two alleles of *Crb2* has recently been shown to aggravate the *Crb1*-associated phenotype in mice,[47] and may be an avenue for further investigation.

Implications of this study for therapeutic interventions such as gene therapy include the assessment of the phenotype's amenability to treatment, identification of potential risk factors and the evaluation of structure function correlations. The amenability of the *CRB1*-associated phenotype to treatment is supported by the variable degrees of EZ preservation on SD-OCT, and the (near-) normal laminar structure in 24% of patients, and laminar coarsening without disorganization in another 38% of patients. However, the visual deterioration in young patients, and the universal presence of macular RPE alterations or atrophy appears to suggest that intervention is desirable before the 3rd or 4th decades of life. Some retinas may have been weakened by the presence of CME, as is illustrated by the presence of lamellar pseudohole in one patient, and this may be a contra-indication for intervention using subretinal injection due to the risk of for instance macular hole formation. Generally, intra-ocular surgery in nanophthalmic eyes has been associated with a higher intra-operative and postoperative complication rate,[53, 54] although no data have been published on the technical challenges in subretinal gene therapy surgery in nanophthalmic eyes. Appropriate preoperative assessment and careful intra-operative measures should be taken in these high-risk eyes. A risk factor for complications in a future gene therapy trial is the narrow anterior chamber angle, as the associated risk of acute angle-closure glaucoma may be increased by repeated mydriasis and dark adaptation during a trial, as happened with patient ID-15 in this study. In clinical practice, biometry and assessment of the anterior chamber angle and intra-ocular pressure are useful in patients with *CRB1* retinopathies, and at-risk patients should be instructed on alarm features. In the case of acute angle-closure glaucoma, prophylactic peripheral iridotomy in the contralateral eye may be indicated.

An important assumption in gene therapy trials where one eye is treated in each patient, and the nontreated eye is used as a control, is the symmetry and thus the comparability in visual function between eyes. We have found statistically significant intra-individual between-eye symmetry in all measures of visual function in our study, with a moderate degree of symmetry in BCVA, and very high degrees of symmetry in sensitivity thresholds on full-field stimulus testing and microperimetry, and in seeing retinal areas on Goldmann visual fields. Therefore, the nontreated contralateral eye is a suitable control in a future gene therapy trial for *CRB1*-associated IRDs.

The most robust structure-function correlation, and the only statistically significant one after stringent correction for multiple testing, was the foveal PR + RPE thickness, as measured from the ELM to the basal membrane, to BCVA. The granular aspect of the hyperreflective outer retinal bands, including the EZ, complicated the evaluation of the EZ diameter and may explain why EZ diameter proved a less robust correlation with function parameters, such as BCVA and macular sensitivity. In other forms of RP, EZ diameter has been sensitive in detecting disease progression,[55, 56] and further prospective follow-up measurements are necessary to test this sensitivity in *CRB1* retinopathies. On the other hand, substantial photoreceptor populations have been demonstrated with adaptive optics in areas of low or no EZ reflectivity, indicating that biomarkers on SD-OCT do not always accurately represent photoreceptor cytology.[57] Prospective longitudinal measurements of the biomarkers on SD-OCT need to be correlated to visual function decline in *CRB1* retinopathies, in order to assess their potential as a surrogate endpoint in a future clinical gene therapy trial. Performing microperimetry was challenging in patients with severe visual impairment and could not be reliably performed in the two youngest patients. Inconveniently, these patients groups are of particular interest for microperimetric evaluation, as severely visually impaired patients (over the age of 18) will be the most likely to be included in a phase I trial. The shifting of the preferred retinal locus between the test run and the examination, which occurred in six patients, might pose a challenge in the second measurement for these patients. Prospective longitudinal measurements will decide whether this is correct and whether microperimetry offers a reliable functional outcome parameter. In this study, FST was successful in determining retinal sensitivity thresholds in patients with a wide range of vision loss and loss of electrophysiological responses. FST response to red stimuli at a lower intensity is mostly cone-mediated and would thus provide a method for measuring changes in cone sensitivity. A limitation of FST is its inability to localize the retinal area mediating the sensitivity threshold. In future subretinal gene therapy trials, this area may not co-localize with the location of the retinal area that was treated with subretinal injection of the treatment vector. Nonetheless, it has been sensitive in detecting sensitivity changes in gene therapy trials, while BCVA proved less sensitive.[58] Based on our findings, changes in FST would have to exceed the variability threshold of 4 dB in order to be reliably attributed to a therapeutic effect.

In conclusion, this prospective cross-sectional study provides extensive phenotypic characterization of *CRB1*-associated retinopathies, which are a candidate for gene therapy. Longitudinal prospective measurements of the same parameters are necessary in order to assess which outcome measures are the most sensitive in detecting the rate of progression and potential treatment effect in a future gene therapy trial.

Acknowledgements

Funding/Support: This work was supported by the Curing Retinal Blindness Foundation (Ivyland, PA, USA), Stichting Blindenhulp (The Netherlands), Janivo Stichting (The Netherlands), and Bayer Ophthalmology Research Award (The Netherlands).

Financial Disclosures: The Leiden University Medical Center (LUMC) is the holder of patent application PCT/NL2014/050549, which describes the potential clinical use of CRB2; JW is listed as inventor on this patent, and JW is an employee of the LUMC.

Other Acknowledgements: The authors wish to acknowledge dr. Y.Y. Cheng (LUMC) for reviewing the corneal topography results.

All authors attest that they meet the current ICMJE criteria for authorship.

REFERENCES

1. Sánchez-Alcudia R, Cortón M, Ávila-Fernández A, et al. Contribution of Mutation Load to the Intrafamilial Genetic Heterogeneity in a Large Cohort of Spanish Retinal Dystrophies Families. Invest Ophthalmol Vis Sci 2014;55(11):7562-71.
2. Corton M, Tatu SD, Avila-Fernandez A, et al. High frequency of CRB1 mutations as cause of Early-Onset Retinal Dystrophies in the Spanish population. Orphanet J Rare Dis 2013;8:20.
3. Vallespin E, Cantalapiedra D, Riveiro-Alvarez R, et al. Mutation screening of 299 Spanish families with retinal dystrophies by Leber congenital amaurosis genotyping microarray. Invest Ophthalmol Vis Sci 2007;48(12):5653-61.
4. Tsang SH, Burke T, Oll M, et al. Whole exome sequencing identifies CRB1 defect in an unusual maculopathy phenotype. Ophthalmology 2014;121(9):1773-82.
5. Mucciolo DP, Murro V, Giorgio D, et al. Long-term follow-up of a CRB1-associated maculopathy. Ophthalmic Genet 2018;39(4):522-5.
6. Talib M, van Schooneveld MJ, van Genderen MM, et al. Genotypic and Phenotypic Characteristics of CRB1-Associated Retinal Dystrophies: A Long-Term Follow-up Study. Ophthalmology 2017;124(6):884-95.
7. Mathijssen IB, Florijn RJ, van den Born LI, et al. Long-term follow-up of patients with retinitis pigmentosa type 12 caused by CRB1 mutations: A Severe Phenotype With Considerable Interindividual Variability. Retina 2017;37(1):161-72.
8. Yang L, Wu L, Yin X, et al. Novel mutations of CRB1 in Chinese families presenting with retinal dystrophies. Mol Vis 2014;20:359-67.
9. Jalkh N, Guissart C, Chouery E, et al. Report of a novel mutation in CRB1 in a Lebanese family presenting retinal dystrophy. Ophthalmic Genet 2014;35(1):57-62.
10. Khan AO, Aldahmesh MA, Abu-Safieh L, Alkuraya FS. Childhood cone-rod dystrophy with macular cystic degeneration from recessive CRB1 mutation. Ophthalmic Genet 2014;35(3):130-7.
11. Vincent A, Ng J, Gerth-Kahlert C, et al. Biallelic Mutations in CRB1 Underlie Autosomal Recessive Familial Foveal Retinoschisis. Invest Ophthalmol Vis Sci 2016;57(6):2637-46.
12. Morarji J, Lenassi E, Black GC, Ashworth JL. Atypical presentation of CRB1 retinopathy. Acta Ophthalmol 2016;94(6):e513-4.
13. McKibbin M, Ali M, Mohamed MD, et al. Genotype-phenotype correlation for leber congenital amaurosis in Northern Pakistan. Arch Ophthalmol 2010;128(1):107-13.
14. Bernal S, Calaf M, Garcia-Hoyos M, et al. Study of the involvement of the RGR, CRPB1, and CRB1 genes in the pathogenesis of autosomal recessive retinitis pigmentosa. J Med Genet 2003;40(7):e89.
15. Lotery AJ, Jacobson SG, Fishman GA, et al. Mutations in the CRB1 gene cause Leber congenital amaurosis. Arch Ophthalmol 2001;119(3):415-20.
16. Lotery AJ, Malik A, Shami SA, et al. CRB1 mutations may result in retinitis pigmentosa without para-arteriolar RPE preservation. Ophthalmic Genet 2001;22(3):163-9.
17. Galvin JA, Fishman GA, Stone EM, Koenekoop RK. Evaluation of genotype-phenotype associations in leber congenital amaurosis. Retina 2005;25(7):919-29.

18. den Hollander AI, ten Brink JB, de Kok YJ, et al. Mutations in a human homologue of Drosophila crumbs cause retinitis pigmentosa (RP12). Nat Genet 1999;23(2):217-21.
19. van de Pavert SA, Kantardzhieva A, Malysheva A, et al. Crumbs homologue 1 is required for maintenance of photoreceptor cell polarization and adhesion during light exposure. J Cell Sci 2004;117(Pt 18):4169-77.
20. Pellissier LP, Quinn PM, Alves CH, et al. Gene therapy into photoreceptors and Muller glial cells restores retinal structure and function in CRB1 retinitis pigmentosa mouse models. Hum Mol Genet 2015;24(11):3104-18.
21. Quinn PM, Pellissier LP, Wijnholds J. The CRB1 Complex: Following the Trail of Crumbs to a Feasible Gene Therapy Strategy. Front Neurosci 2017;11:175.
22. van den Born LI, van Soest S, van Schooneveld MJ, et al. Autosomal recessive retinitis pigmentosa with preserved para-arteriolar retinal pigment epithelium. Am J Ophthalmol 1994;118(4):430-9.
23. van Huet RA, Oomen CJ, Plomp AS, et al. The RD5000 database: facilitating clinical, genetic, and therapeutic studies on inherited retinal diseases. Invest Ophthalmol Vis Sci 2014;55(11):7355-60.
24. Ferris FL, 3rd, Kassoff A, Bresnick GH, Bailey I. New visual acuity charts for clinical research. Am J Ophthalmol 1982;94(1):91-6.
25. Ferris FL, 3rd, Bailey I. Standardizing the measurement of visual acuity for clinical research studies: Guidelines from the Eye Care Technology Forum. Ophthalmology 1996;103(1):181-2.
26. van Huet RA, Siemiatkowska AM, Ozgul RK, et al. Retinitis pigmentosa caused by mutations in the ciliary MAK gene is relatively mild and is not associated with apparent extra-ocular features. Acta Ophthalmol 2015;93(1):83-94.
27. McCulloch DL, Marmor MF, Brigell MG, et al. ISCEV Standard for full-field clinical electroretinography (2015 update). Doc Ophthalmol 2015;130(1):1-12.
28. Roman AJ, Cideciyan AV, Aleman TS, Jacobson SG. Full-field stimulus testing (FST) to quantify visual perception in severely blind candidates for treatment trials. Physiol Meas 2007;28(8):N51-6.
29. Klein M, Birch DG. Psychophysical assessment of low visual function in patients with retinal degenerative diseases (RDDs) with the Diagnosys full-field stimulus threshold (D-FST). Doc Ophthalmol 2009;119(3):217-24.
30. Collison FT, Fishman GA, McAnany JJ, et al. Psychophysical measurement of rod and cone thresholds in stargardt disease with full-field stimuli. Retina 2014;34(9):1888-95.
31. Roman AJ, Schwartz SB, Aleman TS, et al. Quantifying rod photoreceptor-mediated vision in retinal degenerations: dark-adapted thresholds as outcome measures. Exp Eye Res 2005;80(2):259-72.
32. Dagnelie G. Conversion of planimetric visual field data into solid angles and retinal areas. Clin Vis Sci 1990;5(1):95-100.
33. Koenekoop RK, Sui R, Sallum J, et al. Oral 9-cis retinoid for childhood blindness due to Leber congenital amaurosis caused by RPE65 or LRAT mutations: an open-label phase 1b trial. Lancet 2014;384(9953):1513-20.
34. Hettinga YM, van Genderen MM, Wieringa W, et al. Retinal Dystrophy in 6 Young Patients Who Presented with Intermediate Uveitis. Ophthalmology 2016;123(9):2043-6.
35. Khan KN, Robson A, Mahroo OAR, et al. A clinical and molecular characterisation of CRB1-associated maculopathy. Eur J Hum Genet 2018;26(5):687-94.
36. Hajali M, Fishman GA, Anderson RJ. The prevalence of cystoid macular oedema in retinitis pigmentosa patients determined by optical coherence tomography. Br J Ophthalmol 2008;92(8):1065-8.

37. Testa F, Rossi S, Colucci R, et al. Macular abnormalities in Italian patients with retinitis pigmentosa. Br J Ophthalmol 2014;98(7):946-50.
38. Reichenbach A, Wurm A, Pannicke T, et al. Muller cells as players in retinal degeneration and edema. Graefes Arch Clin Exp Ophthalmol 2007;245(5):627-36.
39. Zhao M, Andrieu-Soler C, Kowalczuk L, et al. A New CRB1 Rat Mutation Links Müller Glial Cells to Retinal Telangiectasia. J Neurosci 2015;35(15):6093-106.
40. van de Pavert SA, Sanz AS, Aartsen WM, et al. Crb1 is a determinant of retinal apical Muller glia cell features. Glia 2007;55(14):1486-97.
41. Cordovez JA, Traboulsi EI, Capasso JE, et al. Retinal Dystrophy with Intraretinal Cystoid Spaces Associated with Mutations in the Crumbs Homologue (CRB1) Gene. Ophthalmic Genet 2015;36(3):257-64.
42. Hasan SM, Azmeh A, Mostafa O, Megarbane A. Coat's like vasculopathy in leber congenital amaurosis secondary to homozygous mutations in CRB1: a case report and discussion of the management options. BMC Res Notes 2016;9:91.
43. den Hollander AI, Heckenlively JR, van den Born LI, et al. Leber congenital amaurosis and retinitis pigmentosa with Coats-like exudative vasculopathy are associated with mutations in the crumbs homologue 1 (CRB1) gene. Am J Hum Genet 2001;69(1):198-203.
44. Bifari IN, Khan AO. Bilateral retinal hemorrhages following finger pressure against the soft palate in recessive CRB1-related retinopathy. Ophthalmic Genet 2016;37(4):441-4.
45. Aleman TS, Cideciyan AV, Aguirre GK, et al. Human CRB1-associated retinal degeneration: comparison with the rd8 Crb1-mutant mouse model. Invest Ophthalmol Vis Sci 2011;52(9):6898-910.
46. Pellissier LP, Alves CH, Quinn PM, et al. Targeted ablation of CRB1 and CRB2 in retinal progenitor cells mimics Leber congenital amaurosis. PLoS Genet 2013;9(12):e1003976.
47. Quinn PM, Alves CH, Klooster J, Wijnholds J. CRB2 in immature photoreceptors determines the superior-inferior symmetry of the developing retina to maintain retinal structure and function. Hum Mol Genet 2018;27(18):3137-53.
48. Aleman TS, Cideciyan AV, Sumaroka A, et al. Retinal laminar architecture in human retinitis pigmentosa caused by Rhodopsin gene mutations. Invest Ophthalmol Vis Sci 2008;49(4):1580-90.
49. Aleman TS, Cideciyan AV, Sumaroka A, et al. Inner retinal abnormalities in X-linked retinitis pigmentosa with RPGR mutations. Invest Ophthalmol Vis Sci 2007;48(10):4759-65.
50. Shah N, Damani MR, Zhu XS, et al. Isolated maculopathy associated with biallelic CRB1 mutations. Ophthalmic Genet 2017;38(2):190-3.
51. Wolfson Y, Applegate CD, Strauss RW, et al. CRB1-Related Maculopathy With Cystoid Macular Edema. JAMA Ophthalmol 2015;133(11):1357-60.
52. Bujakowska K. CRB1 mutations in inherited retinal dystrophies. 2012;33(2):306-15.
53. Jung KI, Yang JW, Lee YC, Kim SY. Cataract surgery in eyes with nanophthalmos and relative anterior microphthalmos. Am J Ophthalmol 2012;153(6):1161-8.e1.
54. Steijns D, Bijlsma WR, Van der Lelij A. Cataract surgery in patients with nanophthalmos. Ophthalmology 2013;120(2):266-70.

55. Cabral T, Sengillo JD, Duong JK, et al. Retrospective Analysis of Structural Disease Progression in Retinitis Pigmentosa Utilizing Multimodal Imaging. Sci Rep 2017;7(1):10347.
56. Cai CX, Locke KG, Ramachandran R, et al. A comparison of progressive loss of the ellipsoid zone (EZ) band in autosomal dominant and x-linked retinitis pigmentosa. Invest Ophthalmol Vis Sci 2014;55(11):7417-22.
57. Scoles D, Flatter JA, Cooper RF, et al. Assessing photoreceptor structure associated with ellipsoid zone disruptions visualized with optical coherence tomography. Retina 2016;36(1):91-103.
58. Bennett J, Wellman J, Marshall KA, et al. Safety and durability of effect of contralateral-eye administration of AAV2 gene therapy in patients with childhood-onset blindness caused by RPE65 mutations: a follow-on phase 1 trial. Lancet 2016;388(10045):661-72.

SUPPLEMENTAL MATERIAL

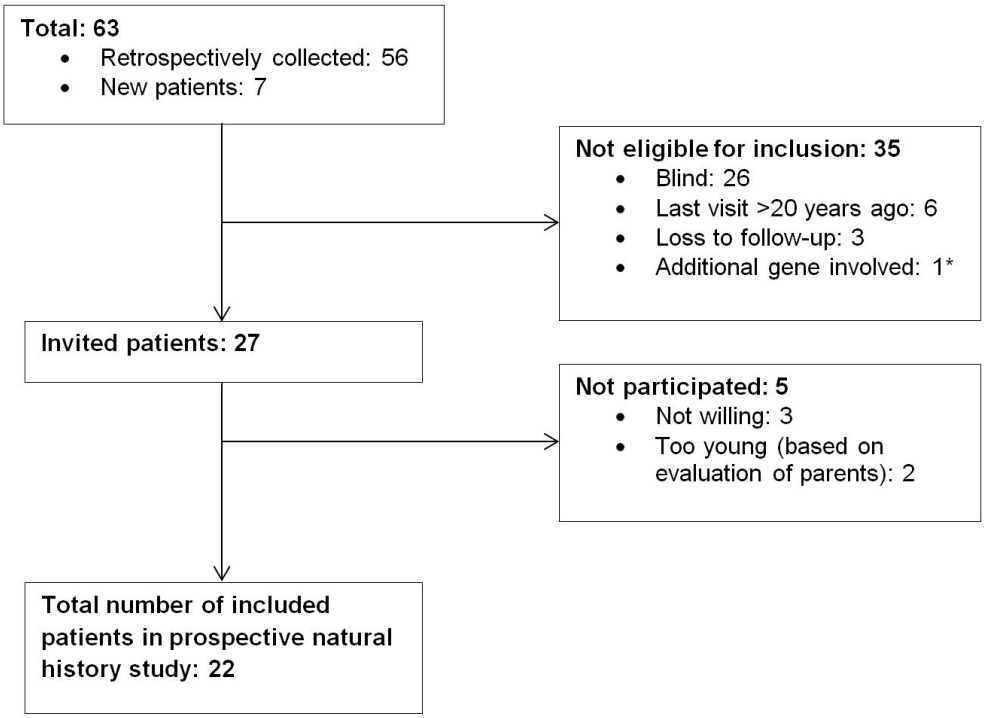

Supplemental Figure 1. Flowchart showing the patient outreach and inclusion process.

*One patient, the brother of patient 12, had a pathogenic variant in the *RS1* gene, as well as the same pathogenic *CRB1* variants as patient 12.

Laminar organization of retinal layers

Category	Examples	N (%); ages
1. Normal lamination. Outer retinal layers and the hyperreflective outer retinal bands may still be atrophic. Shown in the upper row: ID-20; second row: ID-21.	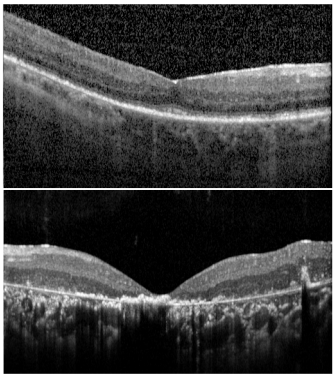	5 (24%); ages 24-74 years
2. No disorganization, all separate layers are identifiable. However, coarse aspect of layers. Attenuation of the OPL may locally obscure distinction between INL and ONL. Shown in the third row: ID-3.	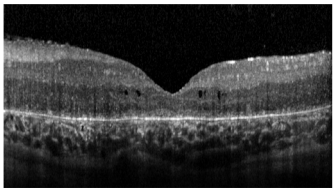	8 (38%); ages 12-53 years
3. Mild to moderate disorganization: not each layer is fully discernible throughout the macula,with the impression of coalescence of the inner retinal layers. Hypo-reflective layers have increased reflectivity. Shown in the fourth row: ID-2. Shown in the fifth row: ID-6.	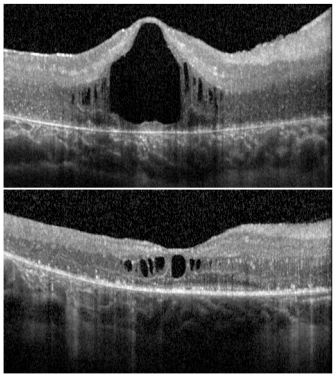	8 (38%); ages 9-41 years

Supplemental Figure 2. Evaluation of laminar organization and retinal architecture on spectral domain optical coherence tomography (SD-OCT) in patients with *CRB1*-associated retinal dystrophy. INL = inner nuclear layer. ONL = outer nuclear layer. OPL = outer plexiform layer. Patients with normal laminar architecture were not overall younger than those with relative disorganization, as disorganization was seen across age groups.

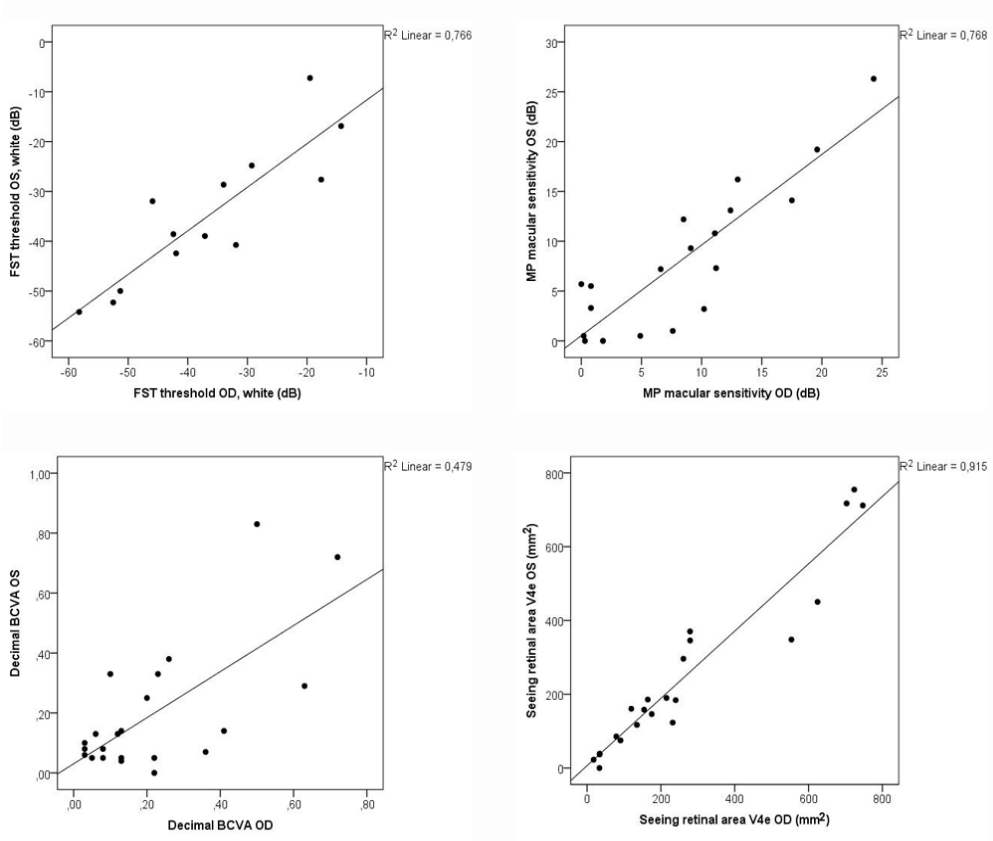

Supplemental Figure 3. Scatterplots of between-eye symmetry of visual function in patients with *CRB1*-associated retinal dystrophies. Top row, left panel. Sensitivity thresholds on full-field stimulus testing (FST) of white stimuli show a very high degree of between-eye symmetry (Spearman's rho = 0.857; p = 0.0002). **Top row, right panel.** Average thresholds for the macular sensitivity on microperimetry (MP) show very high between-eye symmetry. **Second row, left panel.** Best-corrected visual acuity (BCVA) show a moderate between-eye symmetry (Spearman's rho = 0.467; p 0.028). **Second row, right panel.** Seeing retinal areas in mm² for the V4e isopter on Goldmann visual fields show a very high degree of between-eye symmetry.

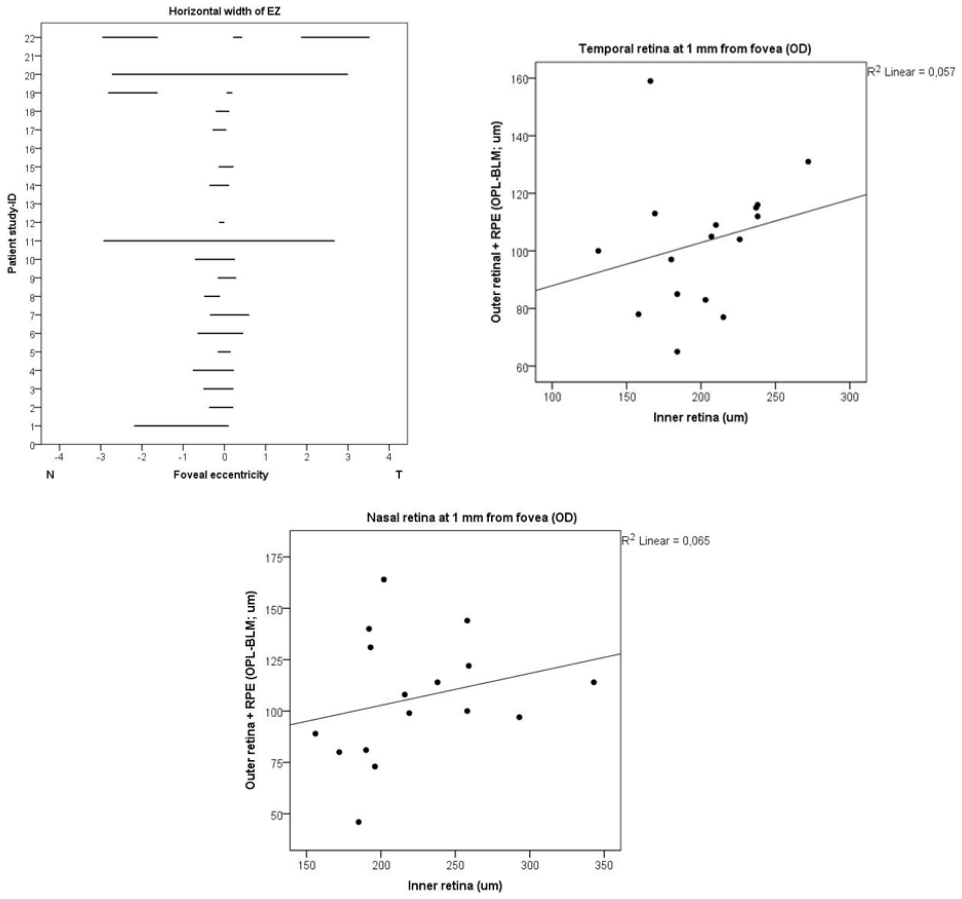

Supplemental Figure 4. Quantitative analysis of biomarkers on spectral-domain optical coherence tomography (SD-OCT) in *CRB1*-retinopathies. The left panel shows the horizontal extent of the ellipsoid zone (EZ) plotted as a function of foveal eccentricity in mm for each patient. The right eye was used for analysis. Negative values indicate the nasal (N) extent of EZ. In patient 13, no EZ-band was detected in the central scan of the macula. Patient 16 did not undergo SD-OCT analysis, and in patient 21 the hyperreflective outer retinal bands including the EZ were indistinguishable from other hyperreflective structures, such as retinal pigment epithelium and intraretinal pigment migrations (but the EZ was intact in the peripheral macula). Aside from the (para)foveal EZ, all patients had isolated regions of intact EZ, separated from the (para)foveal EZ by areas of absent hyperreflective outer retinal bands, except for patient 11, who had a fully intact EZ. The middle and right panel show the relation between the inner retina, as measured from the vitreoretinal interface to the inner border of the outer plexiform layer (OPL), and the outer retina and retinal pigment epithelium (RPE) complex, as measured from the OPL to the basal membrane (BM), as measured at 1 mm from the fovea in the temporal (middle panel) and nasal (right panel) retina. Thickness of the outer retina and RPE complex and the inner retinal thickness were not correlated at 1 mm temporally (Spearman's rho = 0.367; p = 0.162) or nasally (Spearman's rho = 0.424; p = 0.102) from the fovea. Patients who had cystoid macular edema lesions at 1 mm from the fovea were not included in this analysis.

Supplemental Table 1. *CRB1* mutations in this study

	Allele 1		Allele 2		
ID	**Mutation**	**Effect**	**Mutation**	**Effect**	**Phenotype**
1-10	c.3122T>C	p.(Met1041Thr)	c.3122T>C	p.(Met1041Thr)	RP, CORD
11*	c.2983G>T	p.(Glu995*)	c.1892A>G	p.(Tyr631Cys)	Mild RP
12	c.2693A>C	p.(Asn898Thr)	c.2693A>C	p.(Asn898Thr)	RP
13	c.2843G>A	p.(Cys948Tyr)	c.3122T>C	p.(Met1041Thr)	RP
14, 15	c.2290C>T	p.(Arg764Cys)	c.2983G>T	p.(Glu995*)	RP
16**	c.929G>A	p.(Cys310Tyr)	c.2933T>C	p.(Phe978Ser)	Severe RP
17	c.2843G>A	p.(Cys948Tyr)	c.1892A>G	p.(Tyr631Cys)	RP
18	c.2234C>T	p.(Thr745Met)	c.2842+5G>A	p.(?)	RP
19	c.2234C>T	p.(Thr745Met)	c.1602G>T	p.(Lys534Asn)	RP with severe early macular involvement
20	c.2945C>A	p.(Thr982Lys)	c.1892A>G	p.(Tyr631Cys)	Mild RP
21***	c.2506C>A	p.(Pro836Thr)	c.2842T>A	p.(Cys948Ser)	CORD
22	c.498_506del	p.(Ile167_Gly169del)	c.498_506del	p.(Ile167_Gly169del)	Macular dystrophy

The mutation notation is based on the NM_201253.2 nomenclature.

*This patient also had the variant c.1892A>G (p.(His631Arg)) in the *RPGRIP1* gene, which was classified as a variant of unknown significance.

**This patient also carried the heterozygous variant c.2991+1655A>G (p.(Cys988*)) in *CEP290*.

***This patient was originally from the Caribbean (Dutch Antilles).

Supplemental Table 2. Retinal sensitivity measurements in *CRB1*-associated retinal dystrophies

		Average macular sensitivity (dB)		Foveal sensitivity		Fixation		FST threshold for white stimulus (dB)	
ID/Sex	**Age**	**OD**	**OS**	**OD**	**OS**	**OD**	**OS**	**OD**	**OS**
1/M	29	1.8	0.0	5.0		Unstable	Unstable	NP	NP
2/F	13	9.1	9.3	14.0	14.0	Stable	Stable	NP	NP
3/F	16	12.4	13.1	17.0	21.0	Stable	Stable	NP	NP
4/F	38	0.0	5.7		16.0	Unstable	Unstable	NP	NP
5/M	41	4.9	0.5	14.0		Stable	Rel. unstable	-17.6 (MM)	-27.6 (RM)
6/F	11	17.5	14.1	20.0	24.0	Stable	Stable	-19.5 (MM)	-7.2 (MM)
7/F	9	NA	NA					*	
8/F	10	10.2	3.2	22.0		Stable	Unstable	-44.0 (RM)	NP
9/F	28	0.8	5.5	0.0	5.0	Unstable	Unstable	-31.9 (MM)	-40.8 (MM)
10/M	39	11.1	10.8	24.0	24.0	Stable	Stable		
11/M	31	24.3	26.3	22.0	26.0	Stable	Stable		
12/F	26	8.5	12.2	15.0	21.0	Stable	Rel. unstable	-42.0**	-42.4 (RM)
13/M	21	0.8	3.3		20.0	Unstable	Unstable	-14.3 (MM)	-16.9 (MM)
14/F	24	11.2	7.3	27.0	0.0	Stable	Stable	-29.3 (MM)	-24.8 (MM)
15/F	31	6.6	7.2	12.0	14.0	Unstable	Stable	-34.0 (MM)	-28.7 (MM)
16/M	6	NA	NA					-32.9 (MM)	NP
17/M	23	7.6	1.0	19.0	0.0	Stable	Unstable	-51.3 (MM)	-50.0 (MM)
18/F	12	0.2	0.5	8.0		Unstable	Rel. unstable	-42.4 (RM)	-38.6 (MM)
19/M	53	4.4	NA	13.0		Rel. unstable		-45.9 (RM)	-32.0 (MM)
20/M	74	13.0	16.2	18.0	14.0	Stable	Stable	-37.1 (MM)	-39.0 (MM)
21/F	31	0.3	0.0	6.0	0.0	Stable	Rel. unstable	-52.5 (RM)	-52.3 (RM)
22/F	24	19.6	19.2	19.0	17.0	Stable	Unstable	-58.2 (RM)	-54.2 (RM)

The range of normal values for the average threshold of the macular sensitivity (dB) on microperimetry is 26 to 36 dB. Sensitivity thresholds to red and blue FST stimuli were used to determine whether these responses were rod-mediated (blue-red difference of >22 dB), cone-mediated (blue-red difference of <3 dB), or mixed rod-and-cone-mediated (blue-red difference between 3 and 22 dB). The normal FST thresholds for white stimuli was considered -56 dB, and should be rod-mediated.

FST = full-field stimulus testing. MM = mixed rod-cone mediation. NP = not performed. RM = rod-mediated. General sensitivity was obtained with white stimuli.

*FST was attempted in this young patient, but could not be reliably performed due to exhaustion.

**The white, red, and blue FST stimuli were tested for the left eye (the better-seeing eye), but not for the right eye, as the patient was exhausted. Therefore, it cannot be determined for the right eye whether the responses were predominantly rod-mediated, cone-mediated, or mediated by a mix of rods and cones.

Supplemental Table 3. Treatment histories for cystoid macular edema in *CRB1*-associated retinopathies

ID	Treatment	Age at treatment initiation	Treatment duration	Treatment response
2	Initially topical brinzolamide. After several months, switch to oral acetazolamide, due to irritation to the eyes.	8 years	5 years and ongoing	Refractory; Patient still has severe CME.
3	None; CME is mild	-	-	-
6	Currently none. Previously methotrexate, due to an initial diagnosis of panuveitis.	7 years	3-4 months	Mild to moderate, but insufficient. Temporary serum aminotransferase elevations.
8	Initial CME discovery during current study. Referral to own ophthalmologist, with the advice to start with topical brinzolamide (due to age), followed by acetazolamide in the case of non-response.	10 years	Ongoing	To be evaluated.
10	None; CME is mild	-	-	-
11	Oral acetazolamide, after insufficient response to topical brinzolamide.	30 years (acetazolamide since age 31)	1 year and ongoing	Refractory; Patient still has severe CME.
12	None; CME is moderate	-	-	-
17	Combination treatment of methotrexate with prednisone and oral acetazolamide, due to an initial diagnosis of intermediate uveitis. Due to non-response, intravenous methylprednisolone was administered, later followed by bilateral intravitreal triamcinolone depot, which resulted in glaucoma in the left eye. Glaucoma was treated and triamcinolone depots were removed. Eventually, bilateral pars plana vitrectomy and inner limiting membrane peeling was performed, and CME persisted nonetheless. Combination treatment of timolol and dorzolamide did not have a sufficient effect. Oral acetazolamide and oral prednisolone did not have a sufficient effect. Treatment was tapered to acetazolamide only, which did not have a sufficient effect on the CME.	13 years	9 years (patient quit acetazolamide use on his own initiative due to perceived inefficacy, followed by a shared decision with his ophthalmologist)	Refractory, but the patient currently has very mild remaining CME, consisting mostly of degenerative cystoid spaces.
20	Bilateral pars plana vitrectomy and inner limiting membrane peeling following insufficient response to intravitreal triamcinolone injection.	37 years (right eye); 39 years (left eye)	Several months	No remaining CME; only degenerative cystoid spaces.

CME = cystoid macular edema.

3.
Choroideremia

3.1

Long-term follow-up of choroideremia patients with scleral pits and tunnels as a novel observation

Sanne M. van Schuppen, MD[1*], Mays Talib, MD[2*], Arthur A. Bergen, PhD[3,4], Jacoline B. ten Brink, BAS[4], Ralph J. Florijn, PhD[4], Camiel J.F. Boon, MD, PhD[1,2], Mary J. van Schooneveld, MD, PhD[1]

Retina 2018;38(9):1713-1724

* Joint first authors.

1 Department of Ophthalmology, Academic Medical Center, Amsterdam, The Netherlands.

2 Department of Ophthalmology, Leiden University Medical Center, Leiden, The Netherlands.

3 The Netherlands Institute for Neuroscience (NIN-KNAW), Amsterdam, The Netherlands.

4 Department of Clinical Genetics, Academic Medical Center, Amsterdam, The Netherlands.

ABSTRACT

Purpose: To evaluate the long-term clinical course and visual outcome of patients with choroideremia.

Methods: Clinical examination, a social questionnaire, and medical records review of 21 patients with choroideremia from 14 families.

Results: The mean follow-up time was 25.2 years (SD: 13.3; range 2-57 years). The mean age at symptom onset was 15.1 years (SD: 10.1; range 5-40 years). Best-corrected visual acuity was stable until the age of 35 ($p = 0.96$), but declined significantly faster after the age of 35 (11%/year, $p = 0.001$), with a high variability between individual patients. The mean age at which patients discontinued working was 48.1 years (SD: 11.7, range 25-65 years). The reason for work discontinuation was vision related in 60% of cases. Most patients (70%) reported visual field constriction as the most debilitating symptom. The authors report scleral pits and tunnels as a novel finding visible on spectral domain optical coherence tomography and ophthalmoscopy.

Conclusion: Choroideremia is a severely debilitating disease showing a rapid decline of visual acuity generally after the age of 35, but a more gradual decline for other abnormalities.

INTRODUCTION

Choroideremia (CHM, OMIM 303100) is an X-linked (Xq21) progressive degeneration of the retinal pigment epithelium (RPE), outer retina, and choroid, with an estimated prevalence of 1:50.000 individuals.[1] Choroideremia is caused by loss-of-function mutations in the *CHM* gene, which encodes the Rab escort protein 1 (REP-1).[2] Affected males often start experiencing night blindness in their adolescence, a progressive visual field restriction in early adulthood, and slow or no visual acuity loss, typically until the fourth to sixth decade of life, after which visual acuity starts to decline.

It is unclear whether the disease primarily affects the choroid and RPE or the photoreceptors. Some studies in patients have suggested a primary photoreceptor disease,[3, 4] whereas other studies provide evidence that the degeneration first affects the RPE, with subsequent photoreceptor and choroidal loss.[5, 6] A recent clinical study supports this argument, showing RPE loss in early stages of disease, with subsequent loss of photoreceptor outer segments and the formation of retinal tubulations in zones of transition between intact and degenerated retina.[7] In this study, choroidal thinning occurred only after complete degeneration of the ellipsoid zone. A mouse model study has suggested that *CHM* gene mutations affect the photoreceptors and RPE independently, but because of a mutually dependant component, the degeneration occurs at an accelerated pace once both photoreceptors and RPE become progressively more dysfunctional.[8, 9]
Chorioretinal degeneration in CHM is irreversible and no treatment is available for CHM to date, but ongoing phase I/II gene therapy trials show structural and functional rescue after gene therapy.[10, 11] These results offer a promising perspective for clinical application. As gene therapy trials advance, an optimal insight into the clinical characteristics, variability, and natural disease course of CHM is needed, to define outcome measures for ongoing and future treatment trials.
Knowledge on the quality of life and social participation in affected males with CHM is currently limited, but these outcomes may become an increasingly important consideration in potential therapeutic trials. The purpose of this study was to describe the initial and longitudinal clinical characteristics of a cohort of patients with CHM, with special consideration of social participation, to gain insight into the disease's natural history.

MATERIALS AND METHODS

Study population

We ascertained 56 male probands with a clinical diagnosis of CHM from the patient database for hereditary eye diseases at the Academic Medical Center in Amsterdam (Delleman archive). Of these, 21 patients from 14 families were identified for inclusion by their present general practitioner and were included in this study. The others had moved to an unknown destination,

died, or their current general practitioner was not traceable. All 21 patients conformed to the following inclusion criteria: aged 18 years and older at the moment of clinical examination at our center, a clinical diagnosis of CHM based on a history of nyctalopia, peripheral visual field loss, and a characteristic funduscopic appearance of extensive atrophy of the RPE and choroid, made by a senior clinician with expertise in inherited retinal disease (MJS), combined with an X-linked inheritance pattern of this disease, and/or a likely disease-causing variant in the *CHM* gene. In addition, longitudinal clinical data had to be available, containing at least two measurements of best-corrected visual acuity (BCVA).

The study was approved by the Medical Ethics Committee of the Academic Medical Center in Amsterdam (the Netherlands) and adhered to the tenets of the Declaration of Helsinki. All patients provided written informed consent.

Clinical examination

Longitudinal data were obtained through a standardized review of medical records. Before clinical examination, patients were asked for age at onset of disease and at diagnosis, initial symptoms, course of complaints, family history, and overall health, through a home-sent questionnaire. Special attention was paid to socioeconomic participation in the questionnaire, enquiring on hobbies, (paid) work, driver's license, and the use of visual support devices, with a questionnaire (see Table, Supplemental Digital Content 1, which shows the topics addressed in the questionnaire and interview).

Participants were interviewed and clinically examined at the Department of Ophthalmology of the Academic Medical Center in Amsterdam, the Netherlands. Ophthalmic examinations performed included best-corrected Snellen visual acuity (BCVA) using the Early Treatment Diabetic Retinopathy Study (ETDRS) chart, central visual field tests with the Humphrey Field Analyzer (central 20° with 10-2), slit-lamp examination, ophthalmoscopy, color fundus photography, and spectral domain optical coherence tomography (SD-OCT; Topcon 3D OCT-2000, Topcon, Tokyo, Japan).

Goldmann visual field (GVF) areas of the V4e target, where available, were digitized and converted to seeing retinal areas in square millimeter using a method described by Dagnelie.[12]

Statistical analysis

Data were analyzed using SPSS version 23.0 (Version 23.0; IBM Corp, Armonk, NY). Kaplan-Meier curves for BCVA survival were used to analyze the time-to-event for the following endpoints: subnormal visual acuity in Snellen (BCVA <20/40), low vision (BCVA <20/67 and ≥20/400), and blindness (BCVA <20/400). For further analyses, BCVA was divided into the following categories based on the World Health Organization criteria: mild or no visual impairment (BCVA ≥20/67),

low vision (BCVA <20/67 and ≥20/200), and blindness (BCVA <20/400). To these categories, we added a category of "subnormal visual acuity" (BCVA ≥20/40). When visual acuity differed between two eyes, the better seeing eye was used for survival analyses.

Linear spline mixed-model analysis, used to explore rate (β) changes after a certain age, was used to evaluate the annual decline rate of BCVA, stratifying in age groups of under 35 years and ≥35 years, and converting Snellen visual acuities to logarithm of the minimum angle of resolution (logMAR), using the better seeing eye. We used the logMAR values 2.3 for counting fingers, 2.7 for hand motion, 2.8 for light perception, and 2.9 for no light perception. Simple linear regression was used to examine the association between central retinal thickness and age, after testing for linear regression assumptions.

Assessing for intra-individual symmetry in BCVA between eyes, asymmetry was defined as a difference of ≥15 ETDRS letters, which is a greater difference than the test-retest variability for visual acuity, at the last two consecutive examinations.

RESULTS

Twenty-one patients from 14 families were investigated. All patients were white males. The mean age of the participants at the time of the clinical visit was 52.9 years (SD: 15.6; range 18-73 years), and the mean age at the time of first available retrospective clinical data was 28.4 years (SD: 12.0; range 7-45 years). The mean follow-up time was 25.2 years (SD: 13.3; range 2-57 years; median 22 years), with a mean number of 5.6 visits per patient (SD: 3.3; range 2-12 visits; median 5.0). Table 1 summarizes the clinical characteristics of the patients.

Disease onset and visual acuity

The mean age at onset of the first symptom was 15.1 years (SD: 10.1; range 5-40 years), and the mean age at which an ophthalmologist was first visited was 16.5 years (SD: 9.5; range 5-39 years). In 6/21 (29%) patients, the ophthalmologist was first consulted for problems other than CHM, namely strabismus in three patients and suboptimal BCVA due to a refractive error in the three other patients. The age at disease onset was ≥10 years in 13/21 (62%) patients. Only 8/21 (38%) patients experienced their first symptom in the first decade of life. The reported first symptoms are specified in Table 2.

Although color vision difficulties were not the first reported symptoms in any of the patients, reported disturbance of color vision was present in 13/21 (62%) patients at the last visit. The mean age of patients who reported color vision complaints was 56.6 years (SD: 11.7; range 37-73 years). Patients with photoaversion (n = 18, 86%) were older (mean age 30.7, SD: 12.0, range 9-51 years)

than patients without photoaversion (mean age 19.7, SD: 17.0, range 7-39 years), although this difference was not statistically significant ($p = 0.18$, unpaired t-test).

Figure 1A shows the proportion of patients in each visual category of visual impairment against advancing age. Patients started reaching subnormal BCVA, low vision, and blindness from the fifth decade onward, with a significant trend towards worse visual categories with increasing age ($p = 0.02$, linear-by-linear association). A visual acuity of light perception was present in 6/21 (29%) patients with a mean age of 66.3 years (SD: 5.2, range 58-73 years). No patients had absence of light perception.

Kaplan Meier curves of BCVA showed a stable plateau of good vision until the fifth decade of life (Figure 1B). Mean ages for reaching subnormal vision (BCVA <20/40), low vision (BCVA <20/67 and ≥20/200), and blindness (BCVA <20/400) were 56.4 (standard error: 3.1; 95% confidence interval: 50.3-62.4), 61.3 (standard error: 2.8; 95% confidence interval: 55.9-66.8), and 65.2 (standard error: 2.7; 95% confidence interval: 59.9-70.4) years, respectively.

Figure 2A shows the BCVA at the time of examination at our clinic, showing that 7 (33%) patients between the ages of 51 and 73 were blind. The other patients, aged between 18 and 70 years were not yet blind or severely visually impaired. Figure 2B displays the course of BCVA decline with time for individual patients, generally showing a rapid BCVA decline after the age of 35 years, but with inter-individual variability, with some patients maintaining a stable BCVA well into the sixth decade of life. BCVA decline before the age of 35 was rarely seen. This age was consequently used as a spline in a linear mixed model analysis, which revealed no significant effect of age on BCVA in patients younger than 35 years ($p = 0.96$), i.e. on average a stable BCVA under the age of 35, but a significantly faster ($p = 0.001$) BCVA decline rate in patients older than 35 years of 0.045 logMAR per year ($p < 0.0001$), which translates to a yearly decline of 11% on the original Snellen scale. Although patients within the same family generally had a similar BCVA decline course, a high intrafamilial variability was observed in one family, where a patient with CHM was severely visually impaired since the age of 22 and blind since the age of 40, whereas an affected brother and cousin maintained a BCVA of 20/50 in the better seeing eye at the ages of 62 and 68, respectively.

Intra-individual asymmetry in BCVA, defined as a difference of ≥15 ETDRS letters between eyes, was found at the last two consecutive examinations in 3/21 (14%) patients. The mean BCVA was not significantly different between patients with or without an asymmetrical BCVA ($p = 0.33$, unpaired t-test), and neither was age ($p = 0.76$, unpaired t-test). In 3/7 (43%) patients, the refractive error was more myopic in the worse seeing eye. Exotropia in the worse seeing eye was noted in 3/7 (43%) patients with asymmetrical BCVA, but this was probably a consequence and not a cause of the worse BCVA, as the asymmetry in BCVA occurred at a later age in two of these patients (fifth and seventh decade of life). The other patient had a long history of asymmetry in BCVA between

eyes, and he had a large central floater in the vitreous and more foveal atrophy on SD-OCT in the worse eye.

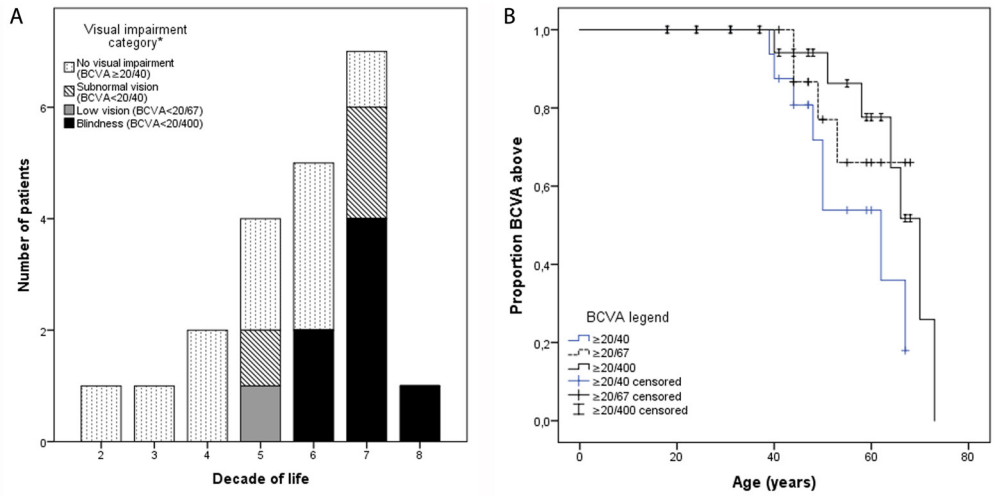

Figure 1. Age-related BCVA decline in CHM. A. Bar chart showing the number and proportion of patients in each category of visual impairment with advancing age. The BCVA and age at the last examination were used. Patients reached low vision and blindness from the fifth decade onward. **B.** Kaplan-Meier plots showing the proportion of patients with a BCVA above subnormal vision (≥20/40), above low vision (≥20/67), and above blindness (≥20/400). Censored observations, i.e. patients who had not reached the visual impairment category of interest at the last follow-up moment, are depicted as vertical bars. Median ages for reaching subnormal vision and blindness were 62.0 (standard error: 6.8; 95% confidence interval: 48.6-75.4) and 70.0 (standard error: 3.1; 95% confidence interval: 63.9-76.1) years, respectively. Although a median could not be calculated for low vision, because visual acuities rapidly declined to blindness, the curve shows that 25% of patients had low vision at the age of 50 years.

Table 1. Characteristics of individual patients with CHM at the last clinical examination

ID	Age	Eye	BCVA	Optic nerve pallor	Relative foveal sparing	Macular pigmentation	Visible vortex veins	Peripheral areas of relatively preserved retina
7	58	OD OS	LP* LP	No	Yes	Yes	Yes	Yes
9	60	OD OS	20/23 20/400	Yes	Yes	Pigment depositions along the arcades	No	No
13	24	OS OD	20/20 20/20	No	Yes	No	Yes	Yes
15	68	OS OD	20/46 20/253	Yes	Yes	No	No	Yes
18	67	OD OS	LP LP	No	No (only peripapillary remnant of retina)	No	Yes	Yes
19	62	OS OD	20/55 20/63	Yes	Yes	No	No	Yes
24	70	OD OS	LP LP	No	Yes	Yes (black granular pigment depositions)	Yes	Yes
59	51	OD OS	CF† CF	No	Yes	No	Yes	No
29	44	OD OS	20/62 20/83	No	Yes	Yes	Yes	Hyperpigmentations
30	41	OD OS	20/36 20/40	No	Yes	No	No	Yes
36	59	OD OS	20/32 20/91	Yes	Yes	No	No	Yes
38	73	OS OD	LP LP	Yes	No	No	No	Yes (only far periphery)
42	67	OS OD	20/42 20/400	No	Yes	Yes	Yes	Yes
43	47	OD OS	20/20 20/33	No	Yes	No	Yes	Yes
48	55	OD OS	20/31 20/46	No	Yes	No	Yes	Yes
51	31	OD OS	20/30 20/31	No	Yes	No	No	No
53	18	OD OS	20/20 20/400	No	Yes	No	No	Yes
54	48	OD OS	20/110 LP	No	Yes	No	Yes	Yes
57	64	OD OS	LP LP	No	Yes	No	Yes	Yes
60	37	OS OD	20/23 20/24	Yes	Yes	Yes	Yes	Yes
61	66	OS OD	LP LP	No	Yes	No	Yes	Yes

CF, counting fingers; LP, light perception vision.

Ophthalmic and funduscopic findings

A myopic refractive error was found in 20/21 (95%) patients (Table 2). Cataract was reported in 18/20 (90%) patients (mean age 54.2 years, SD: 14.1, range 18-70 years). These patients were significantly older than the two patients who had a clear lens in both eyes at the ages of 24 and 37 years, respectively (p = 0.034, unpaired t-test). Of the patients with cataract, six had undergone uncomplicated cataract surgery (mean age 57.8 years, SD: 8.1, range 44-68 years). In the remaining 12 patients with cataract, the predominant cataract type was posterior subcapsular in four (33%) patients, nuclear in one (8%) patient, both posterior subcapsular and nuclear in five (42%) patients, anterior subcapsular in one (8%) patient, and star shaped in one (8%) patient.

All patients showed the characteristic appearance of a whitish fundus with large areas of profound atrophy of the choroid and retina (Figure 3). The optic disc appearance was normal in 16/21 (76%) patients. Scattered coarse hyperpigmentations in the atrophic fundus were seen in 19/21 (90%) and not mentioned or documented in 2/21 (10%) patients. In 15/21 (71%) patients, a small island of RPE and retina (relative foveal sparing) persisted in the fovea and/or perifoveal area. In 4/21 (19%) patients, small islands of relatively preserved RPE persisted outside the vascular arcade. In 13/21 patients (62%), large choroidal vessels or vortex veins in the periphery were visible on fundoscopy. In 7/21 patients (33%), small excavations or "pits" in the sclera were visible on fundoscopy, either in the macula (2/21, 10%) or at the border of the posterior pole and in the midperiphery (5/21, 24%) (Figure 4). From some pits, a vessel emerged (Figure 4). Peripapillary atrophy was found in one (5%) patient.

Table 2. Cohort characteristics of patients with CHM

Characteristics	
Nystagmoid eye movements, n (%)	6/19 (32)
Photophobia, n (%)	18 (86)
Reported first symptom, n	
Nyctalopia, n (%)	17 (81)
Subjective visual acuity loss, n (%)	3 (14)
Photophobia, n (%)	1 (5)
Subjective visual field loss, n (%)	-
Subjective color vision loss, n (%)	-
Mean refractive error (SER) ±SD, D (range)	-3.17±2.6 (-9.63 – 0.5)
SER ≤-6D, n (%)	5 (24)
-2D ≥ SER > -6D, n (%)	8 (38)
0D ≥ SER > -2D, n (%)	7 (33)
2D ≥ SER > 0D, n (%)	1 (5)
Shallow anterior chamber, n (%)	9 (43)
Fundoscopic examination	
Optic disc pallor, n (%)	6 (29)
Vascular attenuation, n (%)	13 (62)

SER, spherical equivalent of the refractive error.

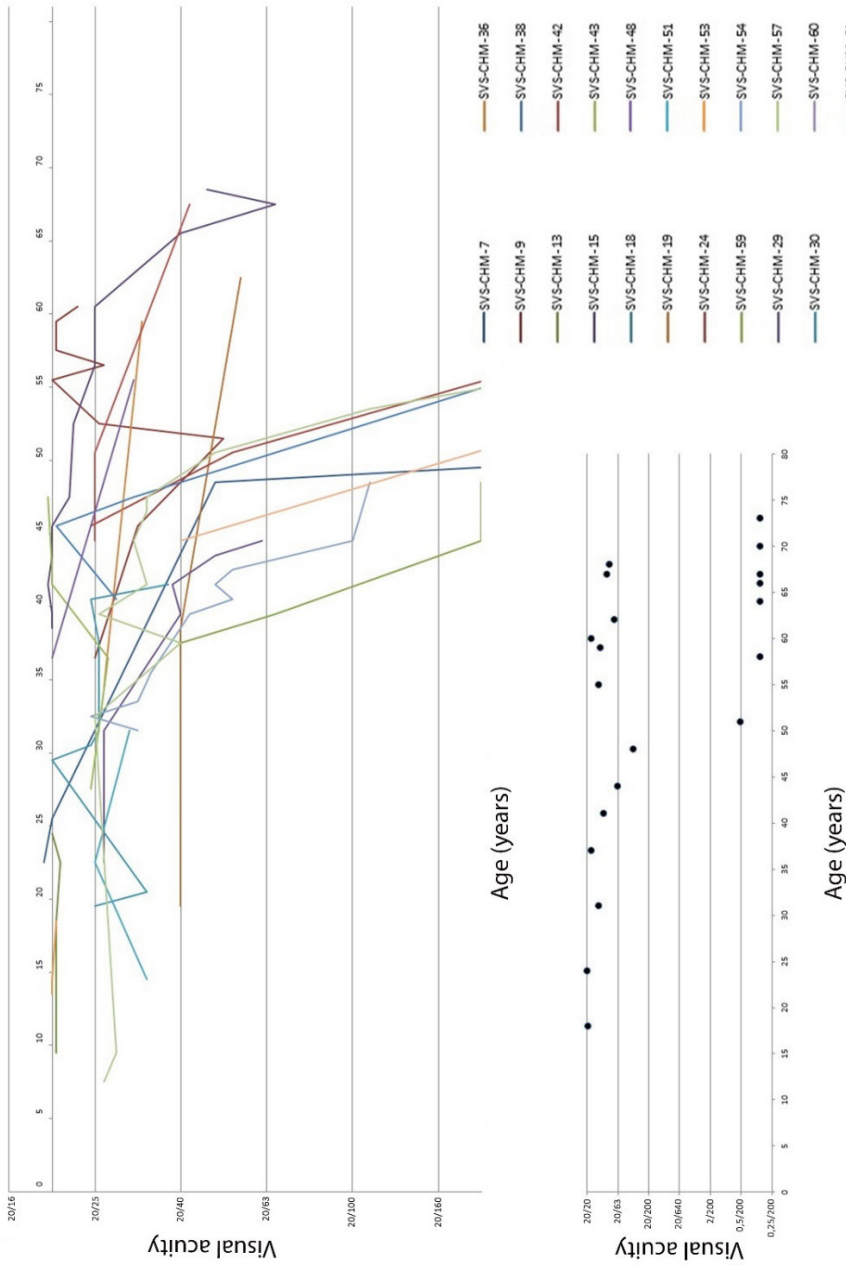

Figure 2. Visual acuities of individual participants. A. BCVA of individuals at the final clinical examination. **B.** The course of BCVA decline in individual participants. Although some individuals (n = 8) showed a rapid decline in BCVA within the age range of 35-50 years, others showed a slower decline in BCVA from this age onward. Some patients showed a (temporary) increase in BCVA after cataract surgery or a certain degree of BCVA measurement variability.

Findings on retinal imaging

The SD-OCT images were available for all patients, but because of eccentric or insufficient fixation and decentered images, measurements of the central retinal thickness could be performed in 17/21 (81%) cases (n of eyes = 29). OCT images of 13/21 (62%) patients showed retinal thinning of all layers with foveal atrophy. Four patients (19%) aged 18 to 37 years had a fully intact foveal ellipsoid zone (Figure 4), whereas the other patients, aged 41 to 70, had a fragmented or absent ellipsoid zone. The mean central retinal thickness was 140 μm (SD: 67, range 54-273 μm). Simple linear regression revealed a significant correlation between central retinal thickness and age at examination (p = 0.007), with 35% of the variance in central retinal thickness explained by age (adjusted R^2 = 0.35). When assessing the fundus and SD-OCT images of individual eyes (total n = 42), we found that all eyes with low vision (BCVA <20/67) or blindness (BCVA <20/400) based on the BCVA at the last examination (n = 22) showed atrophy of all retinal layers in the macula on SD-OCT and/or profound macular chorioretinal atrophy on fundus photography. In eyes with mild BCVA impairment (BCVA <20/40) at the last examination (n = 6), at least a small area of central relative preservation of the RPE and retinal layers was visible on SD-OCT and/or fundus photography. In patients who had no visual acuity impairment (BCVA ≥20/40) at the last examination (n = 14), preservation of the RPE and retinal layers in the macula was visible on SD-OCT and fundus photography in 13/14 (93%) patients, and in one patient, no SD-OCT or fundus photography of the better seeing eye was present.

Scleral tunnels were visible on OCT in 13/21 (62%) patients. On fundoscopy, these features seemed a pit, but OCT showed in nine patients (43%) an interruption of the sclera, RPE, and the remaining choroid at the location of the pit (Figure 4), whereas a scleral tunnel under an uninterrupted RPE was visible in eight patients (38%), with some patients having both scleral pits and tunnels. In one patient, a scleral tunnel emerged into an interruption of the choroid and RPE. Multiple outer retinal tubulations were found in the outer nuclear layer in 16/21 (76%) patients, aged between 18 and 70 years (Figure 4), who had visual acuities ranging between 20/20 and light perception (n = 4). In 10/21 (48%) patients, aged between 18 and 67 years, intraretinal cystoid fluid collections were present in the outer (10/10, 100%) and inner retina (3/10, 30%) (Figure 4). An epiretinal membrane was found in 13/21 (62%) patients. In two patients (10%) with an epiretinal membrane and cystoid fluid collections, aged 44 and 51 years, a full-thickness macular hole was seen on OCT (Figure 4). One other 41-year old patient with an epiretinal membrane had a lamellar macular hole.

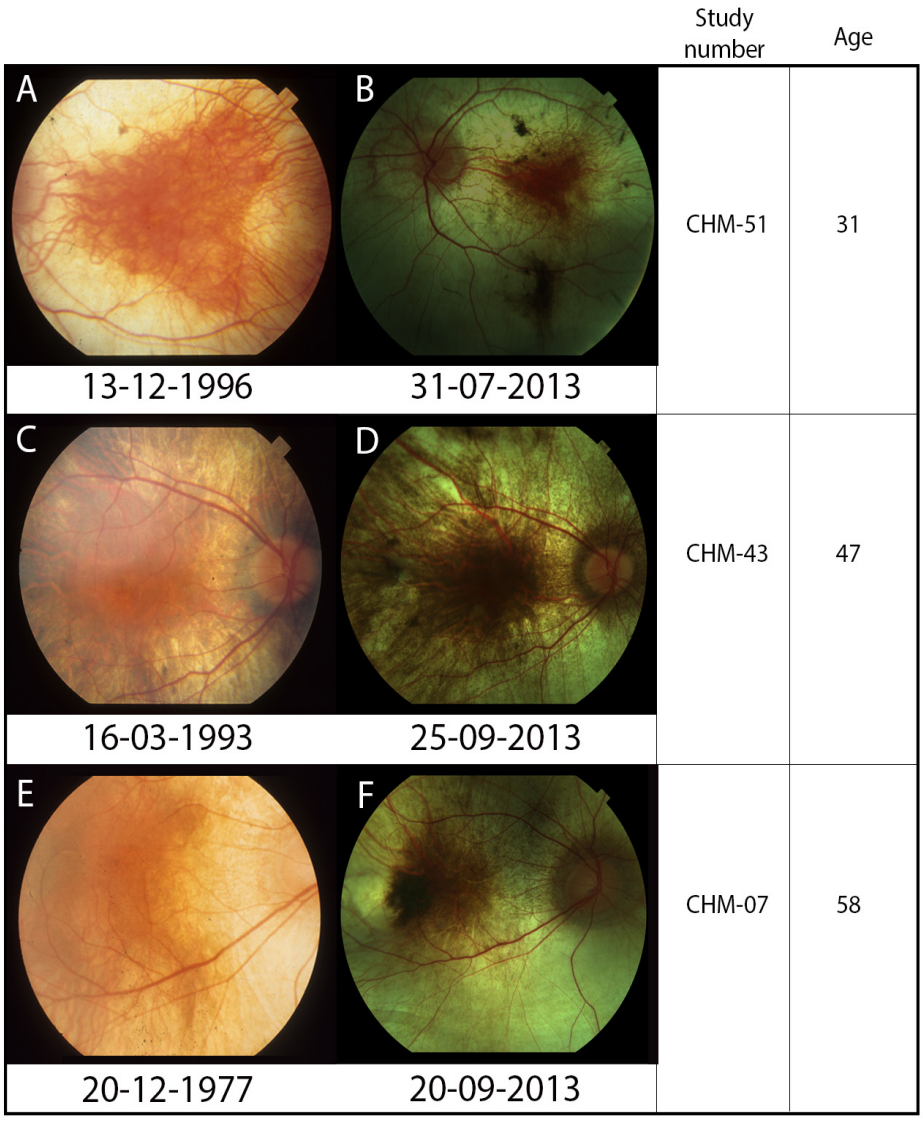

Figure 3. Fundoscopic images of patients with CHM. The first column (**A, C,** and **E**) shows fundus photographs of patients in the past and the date on which the image was taken. The second column (**C, D,** and **F**) shows a fundus photograph taken during the study examination and the date of this visit. The third and fourth columns display the study number and age at the last examination, respectively. Patients show mild vascular attenuation, progression of chorioretinal atrophy, and scattered coarse hyperpigmentations in the posterior pole. The optic disc maintains a relatively normal color and aspect.

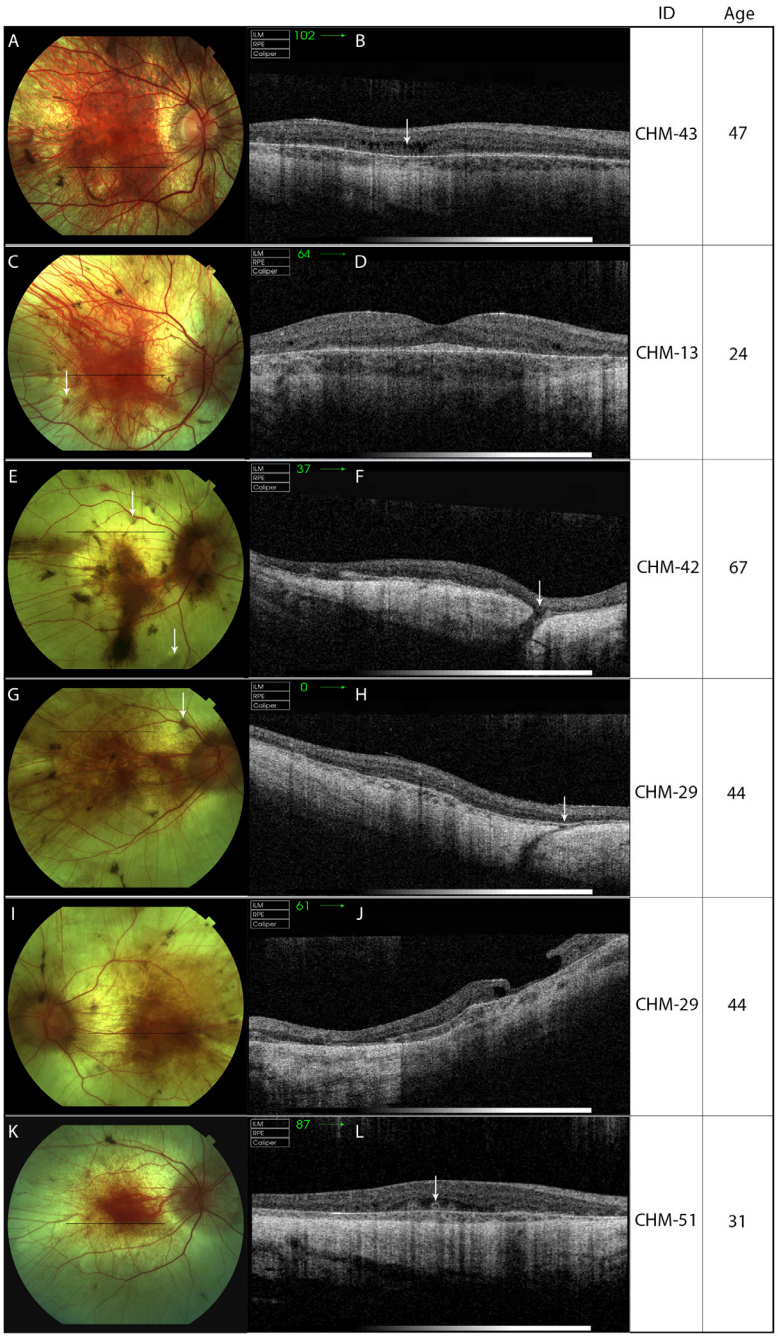

Figure 4. SD-OCT images of patients with choroideremia. The first column shows fundus photographs with typical findings in choroideremia. The black lines indicate the location of the corresponding SD-OCT image. The second column shows the corresponding SD-OCT scans, and the third and fourth column show the patient study number and age at examination, respectively. **A** and **B.** Fundus photograph and SD-OCT image of a patient with macular

cystoid fluid collections (arrow) in the outer retinal layers. **C** and **D.** Imaging of a patient with a scleral pit (**C**, white arrow) and relative foveal sparing on fundus photography, the latter corresponding with preservation of the ellipsoid zone, external limiting membrane and outer nuclear layer on SD-OCT. The peripheral macula showed attenuation of these layers, and cystoid fluid collections. **E** and **F.** Imaging of a patient with scleral pits on fundus photography (**E**, white arrows) and a scleral tunnel (**F**, white arrow) with interruption of the sclera, remaining choroid, and retinal pigment epithelium (RPE) on SD-OCT. **G** and **H.** A patient with a scleral pit on fundus photography (**G**, white arrow) and a scleral tunnel under an uninterrupted RPE layer on SD-OCT (**H**, white arrow). **I** and **J.** A patient with a full-thickness macular hole, visible on SD-OCT. **K** and **L.** Imaging of a patient with outer retinal tubulations in the outer nuclear layer on SD-OCT (**L**, white arrow).

Visual field findings

GVFs (n = 28) were available for seven patients. The median age at the first available GVF was 32.0 years (range 14.0-62.0 years). Within individuals with follow-up GVFs (n = 5; median follow-up time 7.0 years, range 2.0-17.0 years), seeing retinal areas, averaged between eyes, declined in size with a mean slope of decline of 22.0 mm^2/year, corresponding with approximately 20° visual field diameter per year (SD: 10.4 mm^2/year, range 4.8-30.3 mm^2/year, corresponding with 9°-23°/year). There were various patterns of remaining visual field: 4/7 patients, aged 36 to 62 years, had a central island with one or multiple mainly temporal remnants of variable sizes; one patient, aged 30, had a midperipheral scotoma; one patient, aged 47 only had a central island; and the youngest patient, aged 14, had a fully intact GVF for the V4e isopter. Reliable visual field testing of the central 20° (10-2) was only possible in five patients (24%; n of eyes = 9), because central BCVA and fixation were too impaired to allow for reliable central visual field testing in the other patients. Patients in whom reliable central visual field testing could be performed had relative foveal sparing and were younger (mean 44.2 years, SD: 16.3, range 24-60 years) than patients in whom it could not be reliably performed (mean age 55.7, SD: 14.8, range 18-73 years), although this age difference was not statistically significant ($p = 0.15$, unpaired *t*-test). With the exception of one 24-year-old patient with a virtually normal central visual field, static perimetry revealed sharply delineated absolute parafoveal scotomas with low foveal sensitivity (mean 26.6 dB, SD: 10.8, range 8.0-35.5 dB). No correlation between age and foveal sensitivity could be established in this cohort. The mean deviation was -26.9 dB (SD: 7.3, range -33.2 to -14.92 dB, $p < 1\%$ in all tested eyes). The mean pattern standard deviation was 8.3 dB (SD: 3.4, range 3.7-12.2, $p < 1\%$ in all tested eyes). The mean central visual field size in horizontal diameter was 8.7° (SD: 3.8, range 4.5°-14°).

Social participation

All patients completed a questionnaire which contained a section dedicated to social participation and were interviewed on this topic. Table 3 displays these questions and the patients' responses. The mean age at which patients discontinued working, was 48.1 years (SD: 11.7, range 25-65 years). Of the patients who had obtained a driver's license in the past, only one, aged 39, was still able to drive. Patients who used visual aid devices (17/21, 71%) were significantly older (mean 58.2 years, SD: 11.1, range 31-73 years) than patients who did not need visual aid devices (mean 30.5 years,

Table 3. Social topics addressed in the questionnaire

Topic adressed				
1.	Still working	6/21 (29%) yes	15/21 (71%) no	
2.	Reason to stop working	9/15 (60%) vision-related	6/15 (40%) other (reorganization, retirement)	Not applicable in 6/21 (29%), still working
3.	Reason not to work full-time	6/21 (29%) vision-related	15/21 (71%) work(-ed) fulltime	
4.	Most debilitating symptom in daily life	14/20 (70%) visual field constriction	3/20 (15%) blindness	2/20 (10%) visual acuity or 1/10 (5%) other symptom
5.	Reading ability	7/21 (33.3%) without visual aid	7/21 (33%) with visual aids	7/21 (33%) not able to read anymore
6.	Driver's license in the past	10/21 (47.6%) yes	11/21 (52.4%) never	
7.	Use of visual aid devices	17/21 (71%) yes	4/21 (19%) no	
	a. Speech output system for computer	8/21 (38%) yes	12/21 (57%) no	1/21 (5%) unknown
	b. Cane	9/21 (43%) yes	11/21 (53%) no	1/21 (5%) unknown
	c. Braille	4/21 (19%) yes	16/21 (76%) no	1/21 (5%) unknown
	d. Guide dog	2/21 (10%) yes	18/21 (86%) no	1/21 (5%) unknown
8.	Smoking	7/20 (35%) yes	2/20 (10%) smoked in past	11/20 (55%) never
9.	Alcohol consumption	18/20 (90%) yes	2/20 (10%) no	
10.	Other ophthalmologic diagnoses	7/21 (33%) yes (6/7 cataract, 1/7 Charles-Bonnet syndrome)	14/21 (67%) no	
11.	Chronic systemic diseases	6/20 (30%) yes	14/20 (70%) no	

SD: 11.3, range 18-41 years) ($p < 0.001$, unpaired *t*-test). Of the patients who reported subjective peripheral visual field loss as the most debilitating symptom (14/20, 70%), 11 /14 (79%) had normal or mildly subnormal BCVA, 1/14 (7%) had low vision, and 2/14 (14%) were legally blind. Of the eight patients with low vision or blindness, 3/8 (38%) found subjective peripheral visual field loss the most debilitating symptom despite the central visual impairment. The other patients with visual impairment reported visual acuity complaints or blindness as the most debilitating symptom. Interviews with patients generally revealed increased dependence on their spouse or partner due to their CHM-related debilitations, often leading to tension in the relationship due to increased responsibilities of the patient's partner. Four patients (19%) were currently living alone and had no children. All patients were still able to commute independently, using aid devices such as a cane.

DISCUSSION

This work provides a cross-sectional and retrospective analysis of the age-related BCVA changes and clinical characteristics in CHM. These results extend the previous observations about the natural disease course in patients with CHM, in the wake of gene therapeutic trials showing promising results and the surging demand for more careful phenotyping and longitudinal follow-up of patients with CHM.[10]

The long mean follow-up of 25.2 years and the standardized clinical work-up in this study allowed for comprehensive analysis of the natural course of the BCVA in this patient group. To the best of our knowledge, this is the longest reported follow-up of a CHM cohort. The rate of disease progression remains a key question in the context of therapeutic outcome measures and prognostic counselling. In this study a rapid loss of BCVA rarely occurred before the age of 35 years, which is consistent with previous findings of a correlation of BCVA decline with age only after 30 and 40 years of age.[13, 14] Our observed annual BCVA decline of 11% (0.045 logMAR units per year) was similar to a recent finding by Freund et al,[14] but faster than the previously documented 0.007 to 0.0206 logMAR units.[15, 16] The high degree of intra-individual symmetry in BCVA supports the use of the contralateral eye as a nontreated control in ongoing and future gene therapy trials.

The visual field loss was severe in this cohort, with a mean seeing retinal area decline rate of 22.0 mm^2/year, or 20° visual field diameter per year, and a mean remaining horizontal central visual field size of 8.7° at the mean age of 44 years, although this was measured in a small group of patients (n = 5) with ages ranging between 14 and 62 years. Previously, Freund et al found a biphasic model of visual field loss, with a critical age at 20 years, and high interindividual variability below that age. As ongoing gene therapy trials for retinal dystrophies have mainly focused on the central retina, static threshold perimetry and microperimetry results have been important in evaluating the therapeutic

outcome in gene therapy for *RPE65*-related retinal dystrophies.[10, 17] The small sample size and the relatively old age of our cohort were limitations to establishing an accurate relationship between age and visual field size, and a preferably prospective longitudinal analysis of visual field size in a larger group of patients is necessary, particularly as results of recent studies suggest that visual field may be at least as important as BCVA as a tool for evaluating treatment efficacy in trials.[14] Of note, current gene therapeutic strategies use subretinal injection in the macula of an adenoviral vector carrying the normal *CHM* gene,[10] and a gene therapy effect in this case could be only expected on parameters reflecting macular function such as BCVA and central retinal sensitivity.

Although we did not perform standardized color vision testing during the clinical work-up, subjective reports of color vision complaints in 62% of this cohort support the earlier suggestions that color vision should be part of the clinical workup of patients with CHM.[13, 18] However, as we did not perform color vision testing, we cannot conclude whether color vision defects are an early symptom in CHM and could be of prognostic value.

Scleral features in the form of interruptions or tunnels were visible in a large proportion (13/21; 62%) in our study. To our knowledge, such areas have not been previously described in patients with CHM, and we coin the term "scleral pits" when there was a clear interruption of the sclera, choroid and RPE, and used the term "scleral tunnel" in the case of an uninterrupted RPE. The significance of this finding is unclear, because in individuals without choroidal atrophy these scleral tunnels may also be present, but masked by the intact choroid and/or RPE. Possibly, these scleral areas may correspond to zones of sclera-perforating blood vessels and scleral emissaries in which these blood vessels have become progressively atrophic, leaving the scleral pits and tunnels that harbored this vasculature. The presence of outer retinal tubulations, previously described as round or ovoid hyporeflective spaces with hyperreflective margins and usually located in the outer nuclear layer on SD-OCT,[19, 20] in this cohort is an interesting finding, because previous studies using SD-OCT have reported the presence of outer retinal tubulations in CHM patients in varying numbers, ranging from no mention to 91% of eyes.[7, 13, 21] These structures are typically found in advanced age-related macular degeneration and other degenerative retinal conditions, and although the underlying pathogenesis remains unknown, they are postulated to result from a tubular rearrangement of degenerating photoreceptors.[19] Previous studies showed no relation of the presence of these structures with age,[13, 19] or with findings on fundus photography.[22] However, outer retinal tubulations have been found to be present around areas of surviving retina, and could therefore be clues of areas retaining some visual function.[7] In some patients in our cohort, these tubulations were found near areas of more intact photoreceptor layers on SD-OCT, although this finding was not consistently present and four patients had only light perception vision in both eyes, suggesting that in our study there is no clear relation between visual acuity and the presence of outer retinal tubulations. We also identified epiretinal membrane in the macula in 11/20 (55%) patients with CHM who underwent OCT imaging. Also, patients with CHM may

be at an increased risk of developing a macular hole. If clinically significant, macular hole and/or epiretinal membrane can be treated with vitrectomy, inner limiting membrane peeling, and gas tamponade.[23] Areas of outer retinal tubulations, macular holes, epiretinal membrane, and retinal thinning in or near the fovea may increase the risk of complications during and after subretinal gene therapy administration, and may influence the functional outcome of gene therapy. Even after anatomically and/or functionally successful surgical treatment of macular hole and/or epiretinal membrane, the macula may still be more vulnerably during gene therapy surgery, for instance in terms of an increased risk of re-opening a macular hole during submacular gene therapy vector delivery. These findings, including the finding of scleral pits and tunnels, warrant further investigation, using longitudinal SD-OCT images in larger patient populations.

A unique feature of our study was the focus on the disease influence on social participation in these patients. Patients generally remained professionally active well into the fifth decade of life and nearly half (48%) of patients obtained a driver's license, although only one patient still retained a driver's license at the time of the last examination. Current gene therapeutic trials focus on parameters reflecting central retinal function, but 70% of patients in our study indicated that they experienced peripheral visual field restriction as the most debilitating factor in their daily life. In patients with visual impairment, the proportion experiencing peripheral visual field restriction as the most debilitating symptom was 38%. Future therapeutic strategies for CHM may therefore be aimed at a timely intervention targeting not only the central retina, but also the peripheral retina in an attempt to prevent or stop a decline in peripheral visual function. As ongoing gene therapy trials in patients with CHM have shown clinically promising results, the effect on social participation may become an increasingly important outcome measure to evaluate.

The limitations of the current study include the relatively small sample size and the lack of peripheral visual field data. We did not find genotype-phenotype correlations in this CHM cohort, in part because subgroup analysis is impeded by the inadequate sample size, and as previous studies have shown no genotype-phenotype correlations, probably due the virtually complete lack of REP-1 protein expression in CHM, independent of the causative mutation.[14, 24, 25] Future studies investigating the social participation in patients with an inherited retinal dystrophy could use a comprehensive, standardized and validated questionnaire, adapted for a visually impaired population.[26, 27]

In conclusion, patients with CHM in this cohort had a sudden and rapid BCVA decline that first started between the ages of 35 and 60 years, with scleral pits or tunnels as a novel common finding. Longitudinal follow-up of other outcome measures, such as visual field decline, central sensitivity, and structural retinal changes, is necessary to evaluate efficacy of therapeutic options.

REFERENCES

1. MacDonald IM, Sereda C, McTaggart K, Mah D. Choroideremia gene testing. Expert Rev Mol Diagn 2004;4:478-484.
2. van den Hurk JA, Schwartz M, van Bokhoven H, et al. Molecular basis of choroideremia (CHM): mutations involving the Rab escort protein-1 (REP-1) gene. Hum Mutat 1997;9:110-117.
3. Jacobson SG, Cideciyan AV, Sumaroka A, et al. Remodeling of the human retina in choroideremia: rab escort protein 1 (REP-1) mutations. Invest Ophthalmol Vis Sci 2006;47:4113-4120.
4. Syed N, Smith JE, John SK, et al. Evaluation of retinal photoreceptors and pigment epithelium in a female carrier of choroideremia. Ophthalmology 2001;108:711-720.
5. Mura M, Sereda C, Jablonski MM, et al. Clinical and functional findings in choroideremia due to complete deletion of the CHM gene. Arch Ophthalmol 2007;125:1107-1113.
6. Flannery JG, Bird AC, Farber DB, et al. A histopathologic study of a choroideremia carrier. Invest Ophthalmol Vis Sci 1990;31:229-236.
7. Xue K, Oldani M, Jolly JK, et al. Correlation of Optical Coherence Tomography and Autofluorescence in the Outer Retina and Choroid of Patients With Choroideremia. Invest Ophthalmol Vis Sci 2016;57:3674-3684.
8. Tolmachova T, Anders R, Abrink M, et al. Independent degeneration of photoreceptors and retinal pigment epithelium in conditional knockout mouse models of choroideremia. J Clin Invest 2006;116:386-394.
9. Tolmachova T, Wavre-Shapton ST, Barnard AR, et al. Retinal pigment epithelium defects accelerate photoreceptor degeneration in cell type-specific knockout mouse models of choroideremia. Invest Ophthalmol Vis Sci 2010;51:4913-4920.
10. MacLaren RE, Groppe M, Barnard AR, et al. Retinal gene therapy in patients with choroideremia: initial findings from a phase 1/2 clinical trial. Lancet 2014;383:1129-1137.
11. Edwards TL, Jolly JK, Groppe M, et al. Visual Acuity after Retinal Gene Therapy for Choroideremia. N Engl J Med 2016;374:1996-1998.
12. Dagnelie G. Conversion of planimetric visual field data into solid angles and retinal areas. Clin Vis Sci 1990;5:95-100.
13. Heon E, Alabduljalil T, Iii DB, et al. Visual Function and Central Retinal Structure in Choroideremia. Invest Ophthalmol Vis Sci 2016;57:377-387.
14. Freund PR, Sergeev YV, MacDonald IM. Analysis of a large choroideremia dataset does not suggest a preference for inclusion of certain genotypes in future trials of gene therapy. Mol Genet Genomic Med 2016;4:344-358.
15. Roberts MF, Fishman GA, Roberts DK, et al. Retrospective, longitudinal, and cross sectional study of visual acuity impairment in choroideraemia. Br J Ophthalmol 2002;86:658-662.
16. Coussa RG, Kim J, Traboulsi EI. Choroideremia: effect of age on visual acuity in patients and female carriers. Ophthalmic Genet 2012;33:66-73.
17. Bainbridge JW, Mehat MS, Sundaram V, et al. Long-term effect of gene therapy on Leber's congenital amaurosis. N Engl J Med 2015;372:1887-1897.
18. Jolly JK, Groppe M, Birks J, et al. Functional Defects in Color Vision in Patients With Choroideremia. Am J of Ophthalmol 2015;160:822-831.e3.

19. Zweifel SA, Engelbert M, Laud K, et al. Outer retinal tubulation: a novel optical coherence tomography finding. Arch Ophthalmol 2009;127:1596-1602.
20. Goldberg NR, Greenberg JP, Laud K, et al. Outer retinal tubulation in degenerative retinal disorders. Retina 2013;33:1871-1876.
21. Khan KN, Islam F, Moore AT, Michaelides M. Clinical and Genetic Features of Choroideremia in Childhood. Ophthalmology 2016;123:2158-2165.
22. Iriyama A, Aihara Y, Yanagi Y. Outer retinal tubulation in inherited retinal degenerative disease. Retina 2013;33:1462-1465.
23. Zinkernagel MS, Groppe M, MacLaren RE. Macular hole surgery in patients with end-stage choroideremia. Ophthalmology 2013;120:1592-1596.
24. Esposito G, De Falco F, Tinto N, et al. Comprehensive mutation analysis (20 families) of the choroideremia gene reveals a missense variant that prevents the binding of REP1 with Rab geranylgeranyl transferase. Hum Mutat 2011;32:1460-1469.
25. Simunovic MP, Jolly JK, Xue K, et al. The Spectrum of CHM Gene Mutations in Choroideremia and Their Relationship to Clinical Phenotype. Invest Ophthalmol Vis Sci 2016;57:6033-6039.
26. Massof RW, Ahmadian L, Grover LL, et al. The Activity Inventory: an adaptive visual function questionnaire. Optom Vis Sci 2007;84:763-774.
27. Bruijning JE, van Rens G, Fick M, et al. Longitudinal observation, evaluation and interpretation of coping with mental (emotional) health in low vision rehabilitation using the Dutch ICF Activity Inventory. Health Qual Life Outcomes 2014;12:182.

SUPPLEMENTAL MATERIAL

Supplemental Digital Content 1. Topics addressed in the questionnaire and the interview

Topics addressed in questionnaire and interview
Ophthalmic history; other ophthalmological diagnoses
Age at onset symptoms
Subjective symptoms and debilitating effect on daily life; nyctalopia, complaints of visual field, visual acuity, color vision, or other complaints
Ethnicity
Reading abilities
Professional life
Educational levels obtained
Employment, reasons for unemployment if applicable
Driver's license
Use of visual aid devices
General health
Chronic/systemic diseases, allergies
Surgery ocular/non-ocular
Smoking/alcohol consumption/drug use
Medication history
Family history of choroideremia
Family situation
Civil status
Children
Effect of choroideremia on relationships; dependency on partner

3.2

Outcome of full-thickness macular hole surgery in choroideremia

Mays Talib[1], Leonoor S. Koetsier [1], Robert E. MacLaren[2] and Camiel J.F. Boon[1,3]

Genes 2017;8(7):187

1 Department of Ophthalmology, Leiden University Medical Center, Leiden, 2333 ZA Leiden, The Netherlands

2 Nuffield Laboratory of Ophthalmology, University of Oxford and Oxford Eye Hospital, Oxford University Hospitals NHS Foundation Trust, Oxford OX3 9DU, UK

3 Department of Ophthalmology, Academic Medical Center, Amsterdam 1000 AE, The Netherlands

ABSTRACT

The development of a macular hole is relatively common in retinal dystrophies eligible for gene therapy such as choroideremia. However, the subretinal delivery of gene therapy requires an uninterrupted retina to allow dispersion of the viral vector. A macular hole may thus hinder effective gene therapy. Little is known about the outcome of macular hole surgery and its possible beneficial and/or adverse effects on retinal function in patients with choroideremia. We describe a case of a unilateral full-thickness macular hole (FTMH) in a 45-year-old choroideremia patient (c.1349_1349+2dup mutation in *CHM* gene) and its management. Pars plana vitrectomy with internal limiting membrane (ILM) peeling and 20% SF_6 gas tamponade was performed, and subsequent FTMH closure was confirmed at 4 weeks, 3 months and 5 months postoperatively. No postoperative adverse events occurred, and fixation stability improved on microperimetry from respectively 11% and 44% of fixation points located within a 1° and 2° radius, preoperatively, to 94% and 100% postoperatively. This case underlines that pars plana vitrectomy with ILM peeling and gas tamponade can successfully close a FTMH in choroideremia patients, with subsequent structural and functional improvement. Macular hole closure may be important for patients to be eligible for future submacular gene therapy.

INTRODUCTION

Choroideremia (CHM) is an X-linked recessive, progressive degeneration of the retinal pigment epithelium (RPE), outer retina, and choroid. It is caused by mutations in the *CHM* gene, which encodes the Rab escort protein 1 (REP1). Affected males characteristically experience night blindness in the first decade of life, a progressive visual field restriction in early adulthood, and slow visual acuity (VA) loss until the fifth and sixth decade of life, after which visual acuity (VA) may decrease more rapidly.[1]

Few studies have reported cases of a macular hole in CHM patients, which may occur in up to 10% of patients with advanced CHM.[2,3] Little is known about the outcome of macular hole surgery and possible beneficial and/or adverse effects of vitrectomy surgery and inner limiting membrane (ILM) peeling on retinal function. Here, we describe the clinical findings and outcome of pars plana vitrectomy with ILM peeling and gas tamponade in a CHM patient with a full-thickness macular hole (FTMH).

MATERIALS AND METHODS

We describe a patient with a clinical diagnosis of CHM established at the Department of Ophthalmology of Leiden University Medical Center (LUMC), a tertiary referral center for inherited retinal diseases. Sanger sequencing of genomic DNA revealed a hemizygous pathogenic mutation in the *CHM* gene (NM_000390.2; c.1349_1349+2dup), genetically confirming CHM. The last full-field electroretinogram was performed at the age of 19, showing a rod-cone pattern, with remaining rod responses of 10–15% of the normal values, and remaining cone responses of 40–50% of the normal values.

The patient provided written informed consent for the publication of the genetic and clinical data. The informed consent was signed within the framework of the RD5000 consortium, a Dutch national consortium for the registry of patients with inherited retinal dystrophies,[4] as approved by the Medical Ethics Committee of the Erasmus Medical Center (MEC-2010-359), and as locally approved by the Institutional Review Board at the LUMC (ID P11.100). Patient examinations were performed following best-practice guidelines and equipment at the LUMC.

To close the full-thickness macular hole, 23-gauge pars plana vitrectomy was performed under general anaesthesia, by one of the authors (C.J.F.B.), with creation of a triamcinolone-assisted posterior vitreous detachment, subsequent epiretinal membrane (ERM) and ILM peeling using a 23-gauge end-gripping forceps (Bausch & Lomb Incorporated, Rochester, NY, USA) and a plano-concave silicone magnifying lens (FCI Ophthalmics, Paris, France), after staining the ERM

and ILM with Membrane Blue Dual™ dye (D.O.R.C. International, Zuidland, The Netherlands), consisting of 0.15% trypan blue, 0.025% brilliant blue G, and 4% PEG (polyethylene glycol), to stain the ERM and ILM. Postoperative face-down positioning was prescribed for 5 days.

RESULTS

Preoperative Presentation

A 45-year-old man with a history of CHM, clinically diagnosed at 11 years of age, was referred to our hospital by the general practitioner for referral to a visual rehabilitation centre. He had complaints of nyctalopia and visual field restriction, mainly in the periphery, but increasingly in the central visual field. The visual acuity of his left eye had always been worse than his right eye due to amblyopia, and had been fluctuating around 20/50–20/67 in the last decade. He had noticed a decline in subjective visual acuity for at least a few months, with no clear predominance in one eye. The best-corrected visual acuity (BCVA) was 20/20 in the right eye, and 20/100 in the left eye, with a spherical refractive error of −1.75 D and −2.75 D in the right and left eye, respectively, and an astigmatism of −0.75 D in both eyes. Fundoscopy showed extensive chorioretinal atrophy in the posterior pole and the retinal periphery in both eyes, with irregularly-shaped islands of residual relatively preserved retina in the macula, with a full-thickness macular hole in the left eye (Figure 1A). Goldmann visual fields showed bilateral nasal peripheral visual field constriction with a midperipheral scotoma (Supplementary Materials Figure S1).

Fundus autofluorescence images (Spectralis, HRA, Heidelberg Engineering) showed a marked decrease of autofluorescence, with a central area of relative RPE preservation. Inside this island of relative RPE preservation, a juxtafoveal hypo-autofluorescent lesion, indicative of RPE change, could be seen in both eyes (Figure 1B-D).

A spectral-domain optical coherence tomography (SD-OCT) scan (Heidelberg Engineering, Heidelberg, Germany) showed typical CHM features in both eyes (Figure 1E,F), including extrafoveal atrophy of the external limiting membrane, ellipsoid zone, RPE, and choroid, and confirmed the full-thickness macular hole in the left eye, with a mild epiretinal membrane, and mild secondary parafoveal retinal thickening (Figure 1F). The right eye showed relative sparing of the macular structures without evidence of (impending) macular hole. Outer retinal tubulations were visible on the transitional zone between atrophic and relatively preserved areas of ellipsoid zone in both eyes. This distance between the fovea and the transitional zone could not be reliably determined in the left eye, but was 770 μm temporally and 605 μm nasally in the right eye.

Preoperative microperimetry (MAIA, CenterVue, Padova, Italy) showed reduced central retinal sensitivity in both eyes (supra-threshold testing in the left eye: 0% ≥ 25 dB; 32% 15–25 dB range)

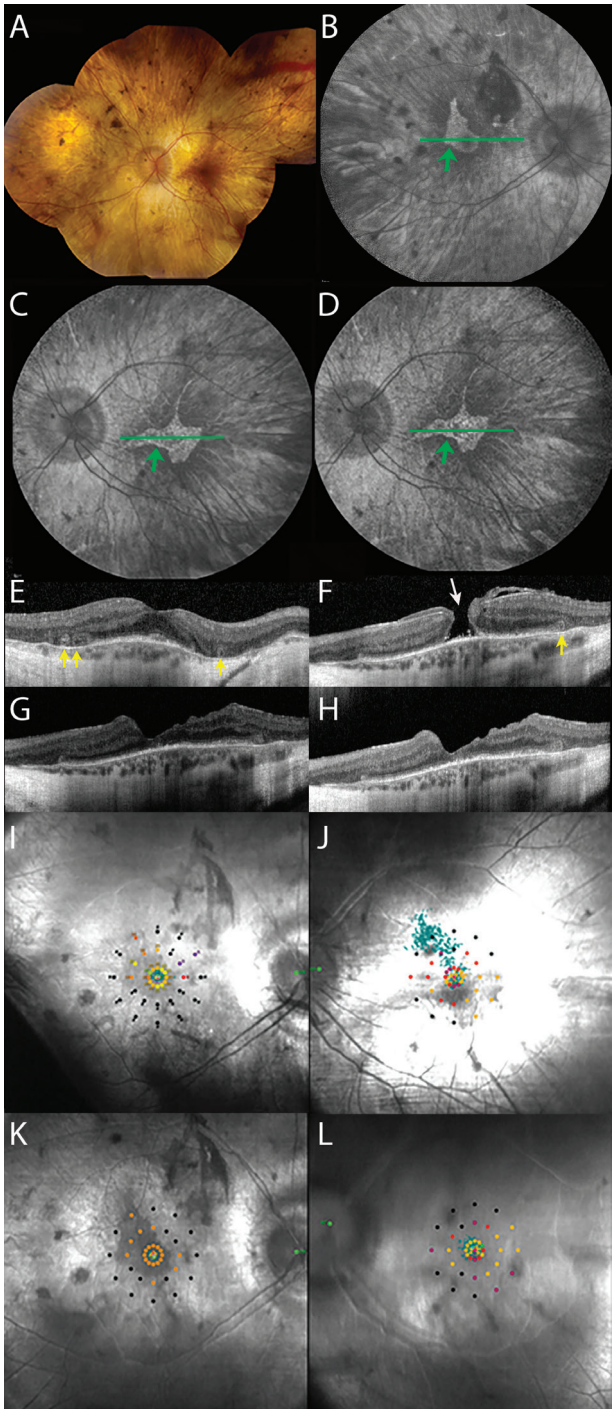

Figure 1. Imaging and functional findings before and after macular hole surgery in a choroideremia patient with a full-thickness macular hole. A. Preoperative fundus photography of the left eye, showing bilateral atrophy of the

retinal pigment epithelium (RPE), vascular attenuation, and waxy pallor of the optic discs. **B-C**. Pre-operative fundus autofluorescence image of the right (**B**) and left (**C**) eye, showing relatively preserved RPE, with a sharply demarcated central island of relative preservation (green arrows), encompassing a temporal juxtafoveal hypo-autofluorescent lesion. **D.** Postoperative fundus autofluorescence image of the left eye, showing no changes other than a mild deepening of the juxtafoveal hypo-autofluorescent lesion. The green horizontal lines in the fundus autofluorescence images (B-D) show the location of the complementary spectral-domain optical coherence tomography (SD-OCT) scans (E-H). **E.** SD-OCT scan of the right eye, showing relative foveal preservation of the retinal layers in an atrophic retina, and outer retinal tubulations (yellow arrows). **F.** Pre-operative SD-OCT of the left eye, showing a full-thickness macular hole (white arrow). Other central retinal abnormalities include an outer retinal tubulation (yellow arrow). **G-H.** SD-OCT scans of the left eye, confirming closure of the macular hole 3 (**G**) and 5 (**H**) months postoperatively, and showing an altered temporal foveal contour, which is a common post-operative occurrence. **I-J.** Preoperative microperimetry of the right (**I**) and left (**J**) eye, showing eccentric fixation in the left eye as compared to the right eye, as indicated by the cloud of green fixation points. **K-L.** Microperimetry of the right (**K**) and left (**L**) eye, 5 months postoperatively, showing markedly improved fixation stability and sensitivity in the left eye, as the cloud of green fixation points spans a smaller and more centrally located area. The scotoma inferior to the final fixation locus mildly deepened post-operatively.

and eccentric fixation in the left eye (unstable fixation; 11% and 44% of fixation points located within a distance of 1° and 2°, respectively) as compared to the right eye (stable fixation; 100% of fixation points located within a distance of 1°).

The patient underwent 23-gauge pars plana vitrectomy under general anaesthesia, followed by postoperative face-down positioning for 5 days. No preoperative or postoperative complications occurred.

Postoperative Clinical Course

According to the patient, the gas bubble had disappeared after 3.5 weeks. After gas reabsorption, SD-OCT confirmed full-thickness macular hole closure at 1, 3, and 5 months postoperatively, with some inner retinal dimpling and an altered temporal foveal contour at 3 and 5 months (Figure 1G,H). No objective visual acuity improvement was achieved, with a BCVA of 20/133 to 20/100 in the left eye, but both the patient and his partner reported a mild subjective visual acuity improvement and less distorted near vision 3 months after surgery. Autofluorescence images (Spectralis HRA, Heidelberg Engineering) did not show postoperative changes as compared to the preoperative situation (Figure 1C,D), other than a mild deepening of the juxtafoveal hypo-autofluorescent lesion within the central island of relative RPE preservation. The size of this central area of relative preservation of autofluorescence, as delineated with the Heidelberg Spectralis Region Finder tool, did not decline postoperatively (preoperative 4.53 mm^2; 5 months postoperative 4.8 mm^2).

Compared to preoperative microperimetry (Figure 1I,J), microperimetry 5 months postoperatively showed an improvement in the macular sensitivity (supra-threshold testing in the left eye: 3% ≥ 25 dB; 41% 15–25 dB range), and an improvement in fixation stability in the operated eye (stable

fixation; 94% and 100% of fixation points located within a distance of 1° and 2°, respectively; Figure 1K,L). Postoperative Goldmann visual fields did not show changes in the operated eye (Supplementary Materials Figure S1), and the seeing retinal area for all investigated isopters, as measured with the Field Digitizer,[5] did not decline (preoperative 354.97 mm^2 for the V4e; 5 months postoperative 369.9 mm^2 for the V4e).

DISCUSSION

Gene therapy for CHM patients has been described to be safe and potentially effective, using an adeno-associated viral vector to deliver *CHM* via a submacular injection using a pars plana vitrectomy approach.[6] However, as many as 10% of advanced CHM patients may develop a macular hole, possibly due to increased vulnerability of the fovea to anteroposterior vitreous traction, tangential tractional forces of the ILM/epiretinal membrane, and/or chronic low-grade inflammation resulting from outer retinal cell death. A macular hole will preclude successful submacular viral vector delivery in the context of gene therapy in these patients.[2]

We described a FTMH in a patient with genetically confirmed CHM, which was successfully managed with pars plana vitrectomy, and ERM and ILM peeling, leading to a mild subjective improvement as well as improvement of retinal structure and function on OCT and microperimetry, respectively. The postoperative abnormal temporal foveal contour is a common occurrence following macular hole surgery,[7] and may point to mechanical trauma, or to changes in the retinal microstructural stability due to ILM peeling. Central structural abnormalities on SD-OCT associated with CHM in this patient included outer retinal tubulations and a transition zone in relatively close proximity to the foveal centre, both of which have generally been noted to dictate caution when considering potential gene therapy trial inclusion,[8] as mechanical trauma may further damage the already fragile photoreceptors. Gas resorption in CHM patients may be slower than usual due to extensive atrophy of the choroid. The duration until complete 20% SF_6 gas tamponade resolution of 4 weeks in our case was longer than the previously reported median of 2 weeks in a macular hole patient population without CHM,[9] but shorter than the 6 weeks described in a previously described CHM patient with macular hole, who received gas tamponade with 30% SF_6.[2] In this earlier case series of 3 CHM patients, gas tamponade with either 16% C_3F_8 or 30% SF_6 generally lasted approximately twice as long as expected in standard FTMH surgery, which is consistent with our findings. We found no postoperative visual acuity decline or any adverse effects on autofluorescence, microperimetry, and Goldmann peripheral visual field testing during a 5-month follow-up period. One case report described a successful vitrectomy in a CHM patient with retinal detachment due to a macular hole, with postoperative macular hole closure, retinal reattachment, and improvement of subjective symptoms.[3] In the current case report, we show that an FTMH in CHM can be successfully closed with improvement in retinal function

and without adverse effects. Such surgical FTMH closure may enable future treatment with gene therapy. The incidence of macular hole reopening after initial closure has been shown to be less than ten percent,[10] and repeatedly less than one percent,[11,12] in large study populations of patients without known inherited retinal dystrophies. However, it is currently unclear if CHM patients with a history of an FTMH are still more vulnerable to macular damage and reopening of the macular hole after submacular injection of gene therapy vector, despite the previous surgical closure of the macular hole.

Acknowledgments
M.T. and C.J.F.B. are supported by grants from the Curing Retinal Blindness Foundation, Stichting Blindenhulp, and Janivo Stichting. The authors did not receive funds for covering the costs to publish in open access.

Author Contributions: C.J.F.B., R.E.M., L.S.K., and M.T. conceived and designed the case report. C.J.F.B. performed the surgical procedure.

Conflicts of Interest: The authors declare no financial conflicts of interest or proprietary interest. Robert E.MacLaren is an academic founder and director of Nightstar Ltd, a choroideremia gene therapy company established by the University of Oxford and the Wellcome Trust. The founding sponsors had no role in the design of the study; in the collection, analyses, or interpretation of data; in the writing of the manuscript, and in the decision to publish the results.

REFERENCES

1. Coussa, R.G.; Kim, J.; Traboulsi, E.I. Choroideremia: Effect of age on visual acuity in patients and female carriers. Ophthalmic Genet. 2012;33: 66–73.
2. Zinkernagel, M.S.; Groppe, M.; MacLaren, R.E. Macular hole surgery in patients with end-stage choroideremia. Ophthalmology. 2013;120: 1592–1596.
3. Shinoda, H.; Koto, T.; Fujiki, K.; Murakami, A.; Tsubota, K.; Ozawa, Y. Clinical findings in a choroideremia patient who underwent vitrectomy for retinal detachment associated with macular hole. Jpn J. Ophthalmol. 2011;55: 169–171.
4. Van Huet, R.A.; Oomen, C.J.; Plomp, A.S.; van Genderen, M.M.; Klevering, B.J.; Schlingemann, R.O.; Klaver, C.C.; van den Born, L.I.; Cremers, F.P.; RD5000 Study Group. The RD5000 database: Facilitating clinical, genetic, and therapeutic studies on inherited retinal diseases. Invest. Ophthalmol. Vis. Sci. 2014;55: 7355–7360.
5. Dagnelie, G. Conversion of planimetric visual field data into solid angles and retinal areas. Clin. Vis. Sci. 1990;5: 95–100.
6. MacLaren, R.E.; Groppe, M.; Barnard, A.R.; Cottriall, C.L.; Tolmachova, T.; Seymour, L.; Clark, K.R.; During, M.J.; Cremers, F.P.M.; Black, G.C.M.; et al. Retinal gene therapy in patients with choroideremia: Initial findings from a phase 1/2 clinical trial. Lancet 2014;383: 1129–1137.
7. Kim, J.H.; Kang, S.W.; Lee, E.J.; Kim, J.; Kim, S.J.; Ahn, J. Temporal changes in foveal contour after macular hole surgery. Eye (Lond) 2014;28: 1355–1363.
8. Aleman, T.S.; Han, G.; Serrano, L.W.; Fuerst, N.M.; Charlson, E.S.; Pearson, D.J.; Chung, D.C.; Traband, A.; Pan, W.; Ying, G.S.; et al. Natural History of the Central Structural Abnormalities in Choroideremia: A Prospective Cross-Sectional Study. Ophthalmology 2017;124: 359–373.
9. Kim, S.S.; Smiddy, W.E.; Feuer, W.J.; Shi, W. Outcomes of sulfur hexafluoride (SF_6) versus perfluoropropane (C_3F_8) gas tamponade for macular hole surgery. Retina 2008;28: 1408–1415.
10. Abbey, A.M.; Van Laere, L.; Shah, A.R.; Hassan, T.S. Recurrent Macular Holes in the Era of Small-Gauge Vitrectomy: A Review of Incidence, Risk Factors, and Outcomes. Retina 2017;37: 921–924.
11. Kumagai, K.; Furukawa, M.; Ogino, N.; Larson, E. Incidence and factors related to macular hole reopening. Am. J. Ophthalmol. 2010;149: 127–132.
12. Yoshida, M.; Kishi, S. Pathogenesis of macular hole recurrence and its prevention by internal limiting membrane peeling. Retina 2007;27: 169–173.

SUPPLEMENTAL MATERIAL

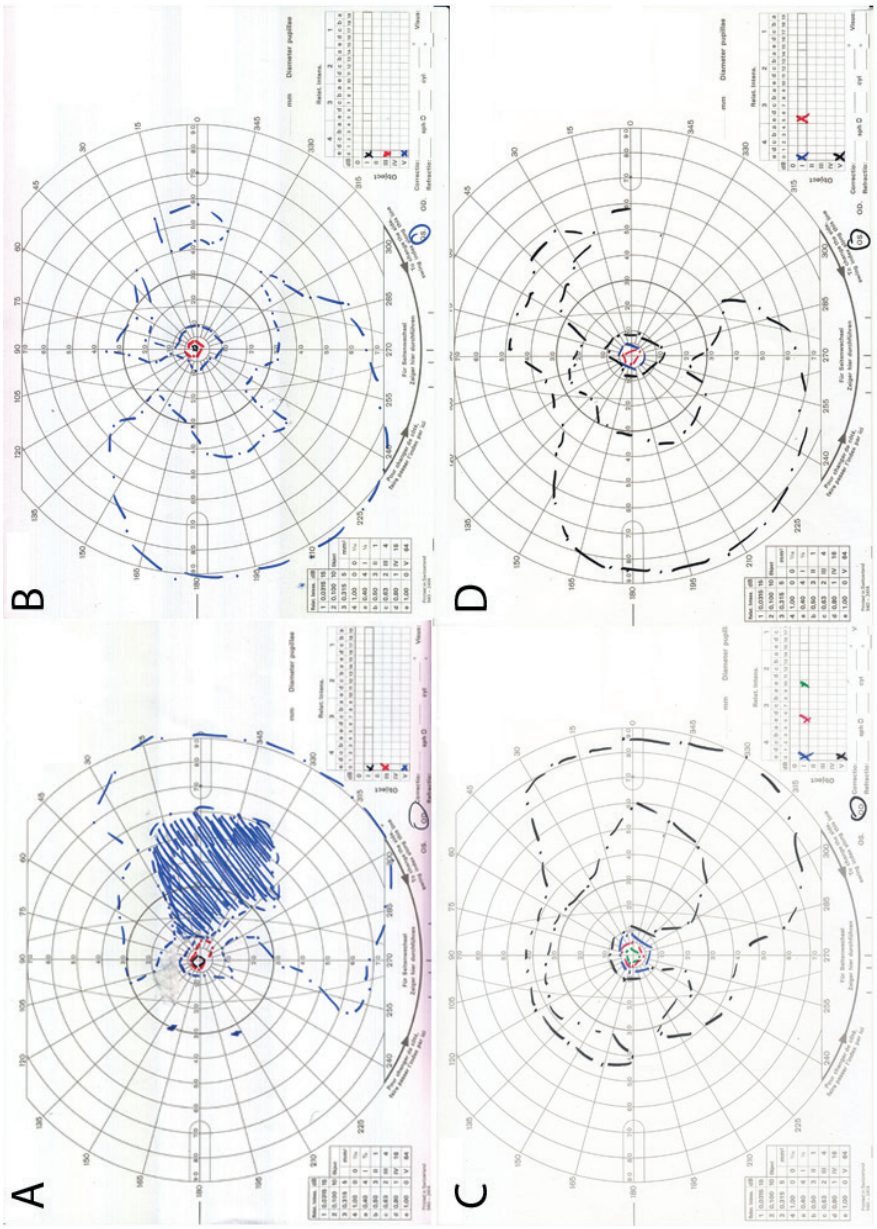

Figure S1. Goldmann visual fields before and after macular hole surgery in a choroideremia patient with a full-thickness macular hole. **A-B.** Preoperative Goldmann visual fields of the right (**A**) and left (**B**) eye, showing bilateral nasal peripheral visual field constriction with a midperipheral scotoma. **C-D.** Postoperative Goldmann visual fields showing no significant changes.

4.
RPGR-associated retinal dystrophies

4.1

Clinical and genetic characteristics of male patients with *RPGR*-associated retinal dystrophies: a long-term follow-up study

Mays Talib, MD[1], Mary J. van Schooneveld, MD, PhD[2], Alberta A. Thiadens, MD, PhD[3], Marta Fiocco, PhD[4,5], Jan Wijnholds, PhD[1], Ralph J. Florijn, PhD[6], Nicoline E. Schalij-Delfos, MD, PhD[1], Maria M. van Genderen, MD, PhD[7], H. Putter, PhD[4], Frans P.M. Cremers, PhD[8], Gislin Dagnelie, PhD[9], Jacoline B. ten Brink, BAS[6], Caroline C.W. Klaver, MD, PhD[3,10,11], L. Ingeborgh van den Born, MD, PhD[12], Carel B. Hoyng, MD, PhD[11], Arthur A. Bergen, PhD[6,13], Camiel J.F. Boon, MD, PhD[1,2]

Retina 2019;39(6):1186-1199

1 Department of Ophthalmology, Leiden University Medical Center, Leiden, The Netherlands.
2 Department of Ophthalmology, Academic Medical Center, Amsterdam, The Netherlands
3 Department of Ophthalmology, Erasmus Medical Center, Rotterdam, The Netherlands.
4 Department of Medical Statistics, Leiden University Medical Center, Leiden, The Netherlands.
5 Mathematical Institute Leiden University, Leiden, The Netherlands.
6 Department of Clinical Genetics, Academic Medical Center, Amsterdam, The Netherlands.
7 Bartiméus, Diagnostic Centre for Complex Visual Disorders, Zeist, The Netherlands.
8 Department of Human Genetics and Donders Institute for Brain, Cognition and Behaviour, Radboud University Medical Center, Nijmegen, The Netherlands.
9 Wilmer Eye Institute, Johns Hopkins University, Baltimore, Maryland, The United States of America.
10 Department of Epidemiology, Erasmus Medical Center, Rotterdam, The Netherlands.
11 Department of Ophthalmology, Radboud University Medical Center, Nijmegen, The Netherlands.
12 Rotterdam Eye Hospital, Rotterdam, The Netherlands.
13 The Netherlands Institute for Neuroscience (NIN-KNAW), Amsterdam, The Netherlands.

ABSTRACT

Purpose: To describe the phenotype and clinical course of patients with *RPGR*-associated retinal dystrophies, and to identify genotype-phenotype correlations.

Methods: A multicenter medical records review of 74 male patients with *RPGR*-associated retinal dystrophies.

Results: Patients had retinitis pigmentosa (RP; n = 52; 70%), cone dystrophy (COD; n = 5; 7%), or cone-rod dystrophy (CORD; n = 17; 23%). The median follow-up time was 11.6 years (range 0-57.1). The median age at symptom onset was 5.0 years (range 0-14 years) for patients with RP and 23.0 years (range 0-60 years) for patients with COD/CORD. The probability of being blind (best-corrected visual acuity <0.05) at the age of 40 was 20% and 55% in patients with RP and COD/CORD, respectively. *RPGR*-ORF15 mutations were associated with high myopia ($p = 0.01$), which led to a faster best-corrected visual acuity decline in patients with RP ($p < 0.001$) and COD/CORD ($p = 0.03$). Patients with RP with *RPGR*-ORF15 mutations had a faster visual field decline ($p = 0.01$) and thinner central retina ($p = 0.03$) than patients with mutations in exon 1 to 14.

Conclusion: Based on best-corrected visual acuity survival probabilities, the intervention window for gene therapy for *RPGR*-associated retinal dystrophies is relatively broad in patients with RP. *RPGR*-ORF15 mutations were associated with COD/CORD and with a more severe phenotype in RP. High myopia is a risk factor for faster best-corrected visual acuity decline.

INTRODUCTION

Pathogenic variants in the *RPGR* gene account for 70% to 80% of X-linked retinitis pigmentosa (RP) cases,[1, 2] and have also been described in rare cases of syndromic RP.[3] X-linked RP is one of the most severe forms of RP. Affected male patients typically start experiencing night blindness in childhood, with ensuing visual field restriction, and they have been described to reach blindness typically in the fourth or fifth decade of life.[4, 5] Mutations in the *RPGR* gene are also an important cause of cone dystrophy (COD) and cone-rod dystrophy (CORD).[2, 6]

X-linked COD and CORD are progressive diseases primarily affecting cones. The age at symptom onset of X-linked COD/CORD ranges between the second and fourth decade of life, and patients typically experience loss of visual acuity and color vision, photophobia, and central visual field defects,[7, 8] followed by rod dysfunction early in the disease course in X-linked CORD.[6] More than 300 different mutations in the *RPGR* gene have been identified,[9] with most mutations located in the guanine-cytosine-rich mutational hotspot ORF15.[10] Some studies have suggested genotype-phenotype correlations, showing a relatively more severe X-linked RP phenotype in patients with mutations in exon 1 to 14 than in patients with ORF15 mutations,[4, 11-13] whereas the opposite has also been observed, with a milder phenotype in patients with a mutation in exon 1 to 14 than in patients with ORF15 mutations.[14] So far, all the reported mutations in patients with X-linked COD/CORD have been found in the ORF15 region.[6, 15, 16] Mutations located toward the 3' end of ORF15 seem to be more often associated with predominant cone disease,[8, 16, 17] whereas mutations located toward the 5' end are more often found in RP.

Although no approved and effective treatment is clinically available for *RPGR*-related retinal dystrophies, functional and structural improvement has recently been shown after gene therapy in a canine *RPGR*-XLRP model,[18] and the first human gene therapy trial for *RPGR*-associated retinal dystrophies has started recently.[19] This promising progress in the development of human gene therapy for *RPGR*-associated retinal dystrophies necessitates an optimal insight in the natural disease course, which will help in the determination of the optimal therapeutic intervention window and in the identification of patients who are most likely to benefit from such treatments.

The aim of this study is to investigate the spectrum of phenotypes and the longitudinal clinical characteristics after long-term follow-up of a large cohort of patients with *RPGR*-related retinal dystrophies in the Netherlands.

MATERIALS AND METHODS

Study population

This study identified male patients with disease-causing variants in *RPGR* who underwent at least one clinical examination. Inclusion criteria were the following: a likely disease-causing variant in *RPGR* or a clinical diagnosis of an inherited retinal dystrophy, and a first- or second-degree relative with a likely disease-causing variant. We identified 96 male patients with *RPGR*-related retinal dystrophies. Of these patients, we excluded 22 male patients from further analyses, because they were from a large Dutch pedigree that was previously described,[7] and no additional follow-up data of these patients could be retrieved. Four male patients from that family had additional follow-up data and were included in our analyses.

Patients were collected from the patient database ("Delleman database") for genetic eye diseases at the Netherlands Institute for Neuroscience and Academic Medical Center (AMC) in Amsterdam,[20] and from various Dutch medical centers within the framework of the RD5000 consortium,[21] a Dutch registry of patients with retinal dystrophies. The study was approved by the Medical Ethics Committee of the Erasmus Medical Center and adhered to the tenets of the Declaration of Helsinki. Patients and/or their legal guardians signed informed consent forms for the use of their clinical data for research purposes.

Genetic analysis

Of the 74 male patients, 71 had received genetic mutational confirmation of their disease through direct Sanger sequencing (n = 52) or linkage analysis (n = 19) according to established protocols. DNA analysis was assisted by the CodonCode software (CodonCode Co). Three patients had not undergone genetic analysis but were affected first-degree relatives of a patient who had received genetic confirmation of an *RPGR* mutation. Mutational analyses were performed at the DNA diagnostics centers of Academic Medical Center (AMC) in Amsterdam, the Netherlands, or Radboud University Medical Center in Nijmegen, the Netherlands. Disease-causing variants in exon 16 to 19 were not detected in our set of 74 patients.

Clinical data collection

Data were obtained through standardized review of medical records for medical history, age at symptom onset and diagnosis, initial symptoms, visual acuity, refractive error, biomicroscopy of the anterior segment, dilated fundus examination, fundus photography, full-field electroretinography (ERG), Goldmann visual fields, spectral-domain optical coherence tomography (SD-OCT), and fundus autofluorescence (FAF) images (see Table, Supplemental Digital Content 1, which presents the data we were able to collect for this cohort).

Age at onset of disease was defined as the age at which the first symptom was noticed by the patient or the patients' parents in case of onset in infancy or early childhood. When symptoms were reported to have always been present, the age at onset was considered to be the first year of life.

Retinal cross sections and retinal thickness measurements were obtained with OCT. Most OCT data were obtained with Topcon (3D OCT-1000; Topcon Medical Systems, Tokyo, Japan) or Heidelberg Spectralis (Heidelberg Engineering, Heidelberg, Germany).
Goldmann visual field areas of the V4e target were digitized and converted to seeing retinal areas in mm^2, using a method described by Dagnelie.[22]

Statistical analysis
For statistical analysis, patients were stratified by predominant disease pattern: predominantly rod disease (RP), and predominant cone dystrophy (COD), defined as cone dysfunction without rod dysfunction on full-field ERG at the time of first evaluation, or cone-rod dystrophy (CORD), defined as both cone and rod dysfunction on full-field ERG, with relatively worse cone function. In most patients, full-field ERG was made only once, for diagnostic purposes, and therefore, ERG data could not be used for follow-up. In patients who were not examined by ERG, the diagnosis was made on clinical grounds. Categorical variables were expressed as proportions and continuous variables as mean values with SDs and medians with interquartile ranges (IQRs). To study the disease progression, a multistate model was estimated,[23] using the following states of visual impairment in the better-seeing eye: low vision (best-corrected visual acuity [BCVA] <20/67 and ≥20/200), severe visual impairment (BCVA <20/200 and ≥20/400), and blindness (BCVA <20/400), according to World Health Organisation criteria.[24] Linear mixed-model analysis was used to evaluate the annual decline rate of the seeing retinal area and of visual acuity, converting Snellen or decimal visual acuities to logMAR and using the better-seeing eye. We repeated this analysis for the worse-seeing eye to assess symmetry in BCVA decline rate. We used the values 2.7 for hand motion, 2.8 for light perception, and 2.9 for no light perception. We controlled for mutation location (ORF15 or exon 1 to 14), extent of myopia, defining high myopia as a spherical equivalent of the refractive error of more than -6 diopters (D),[25] moderate myopia as a spherical equivalent of the refractive error of more than -3D and ≤-6D, and mild myopia as a spherical equivalent of the refractive error of more than -0.75D and ≤-3D, and we stratified by diagnosis.

Asymmetry in visual acuity between two eyes was defined as a difference of ≥0.3 logMar (≥15 Early Treatment Diabetic Retinopathy Study letters), which is the threshold for clinical significance for changes in BCVA,[26] at two consecutive examinations or, in cases where only one BCVA measurement was available, the only examination. Data were analyzed using SPSS version 23.0 (IBM Corp). The multistate analysis was performed in the R software environment, version 3.3.1.[27]

RESULTS

Seventy-four patients from 39 families were investigated. Fifty-two patients (70%) had an RP phenotype, 17/74 (23%) had a CORD, 5/74 (7%) had a COD. Seventy patients (95%) were whites, three patients (4%) were blacks, and one patient (1%) was Asian.

Genetic analysis yielded 31 distinct pathogenic variants in the *RPGR* gene (see Table, Supplemental Digital Content 2, which further specifies these variants): 9 variants in exon 1 to 14 (20 patients, 27%) and 22 variants in exon ORF15 (54 patients, 73%). Of these variants, 24 (77% of all mutations) were frameshift mutations, one (3%) was a missense mutation, 4 (13%) were nonsense mutations, and 2 (6%) were splice-site mutations. The mutation type was not associated with the type of dystrophy (p = 0.8), but mutations in ORF15 were found in higher proportions (p = 0.005) in patients with COD/CORD (21/22, 95%) than in patients with RP (33/52, 63%). For the whole cohort, the median follow-up time was 11.6 years (IQR 18.4; range 0.0-57.1 years), with a median number of 5 visits per patient (IQR 7, range 1-55). The baseline characteristics of the patients in this study are shown in Table 1.

Disease onset and visual acuity

Data on the age at onset of symptoms were available for 25/51 (49%) patients with RP and 19/23 (83%) patients COD/CORD. When age at onset of the first symptom was not available, the age at diagnosis was used for analysis. The median age at symptom onset was 5.0 years (IQR 7.0; mean 5.2; range 0 [infancy]-14.0 years) in patients with RP and 23.0 years (IQR 39.0; mean 24.7; range 0-60.0 years) for patients with COD/CORD. Although the range in age at onset was high for patients with COD/CORD, patients within the same family reported an age at initial onset within the same decade of life, with the exception of 3 families. In one family, 2 brothers reported the same loss of subjective visual acuity, starting at the age of 35 in one brother, at the age of 60 in the other brother, and a grandson with visual acuity loss in the first decade of life, first noticed by the parents. In 2 other families, the large difference of 2 to 3 decades in age at first reported symptom was intergenerational, with an earlier recognition in the younger generation. The reported initial symptoms are specified in Table 1.

In 2/39 (5%) families, one harbouring a deletion after exon 10 and the other a truncating mutation relatively downstream in the ORF15 region of the *RPGR* gene, both RP and CORD phenotypes were reported in different patients within the same family. The prevalence of reported asthma and bronchitis was similar to the prevalence in the general Dutch population (Table 1).[28] BCVA data were available for 70/74 (95%) patients. Curves showing the probability of being in a state of low vision, severe visual impairment, or blindness, based on BCVA, are shown in Figure 1. For patients with RP, an ORF15 mutation signified a significantly higher yearly risk of reaching low vision than

a mutation in exon 1 to 14 (hazard ratio 2.2; 95% CI 0.8-6.1), and a higher yearly risk of becoming severely visually impaired after reaching low vision (hazard ratio 5.8; 95% CI 1.2-28.9).

For patients with RP, linear mixed models showed the age effect on BCVA decline to be 0.015 (3.5%) and 0.022 (5.3%) logMAR per year for patients with mutations in exon 1 to 14 ($p < 0.001$) and in ORF15 ($p < 0.0001$), respectively, which did not differ significantly from each other ($p = 0.11$). Considering the high proportion of patients with moderate or high myopia in this cohort, we assessed in patients with RP whether the extent of myopia significantly changed the BCVA decline rate compared to patients with emmetropia or hyperopia. In patients with RP, this was only the case for high myopia ($p = 0.003$) and not for mild ($p = 0.67$) or moderate myopia ($p = 0.58$). Patients with RP with high myopia had a BCVA decline rate of 0.032 logMAR (7.9%) per year ($p < 0.00001$), which was significantly faster ($p < 0.001$) than in patients with a refractive error less negative than -6D, where the BCVA decline was 0.013 logMAR (3.1%) per year. These rates were not significantly different between patients with mutations in exon 1 to 14 versus ORF15 ($p = 0.64$).

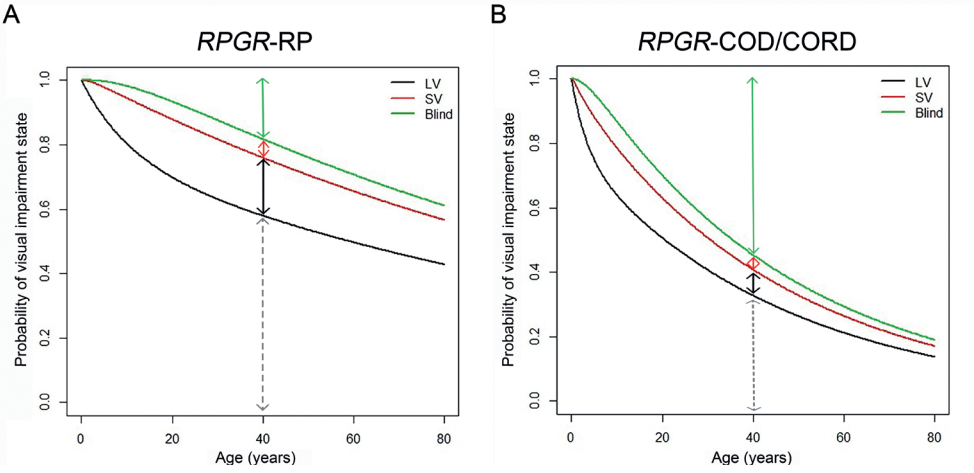

Figure 1. Multistate model-based disease progression curves showing the probability of being in a state of no visual impairment (BCVA ≥20/67), low vision (LV, BCVA <20/67 and ≥20/200), severe visual impairment (SV, BCVA <20/200 and ≥20/400), and blindness (BCVA <20/400) in the better-seeing eye in patients with RP (**A**) and patients with COD/CORD (**B**). The distances between the lines indicate the probability of being in a certain state at any age. The distance between 1) the 0% mark and the black line indicates the probability of not having low vision yet; 2) between the black and red line indicates the probability of having low vision; 3) between the red and green line indicates the probability of being severely visually impaired; 4) between the green line and the 100% mark indicates the probability of being blind. (Left panel) Patients with RP at the age of 40 had a 58% probability of not being visually impaired, a 17% probability of having low vision, a 7% probability of being severely visually impaired, and an 18% probability of being blind. They had a 50% probability of not being visually impaired at the age of 58. (Right panel) Patients with COD/CORD at the age of 40 had a 35% probability of not being visually impaired, a 10% probability of having low vision, a 5% probability of being severely visually impaired, and a 55% probability of being blind.

Performing this analysis for the BCVA decline of the worse-seeing eye yielded decline rates of 0.053 (12.9%) and 0.022 (5.3%) logMAR per year for patients with and without high myopia, respectively. Spline mixed models, used to explore rate (β) changes after a certain age, revealed faster BCVA decline rates at later decades of life in patients with RP, whereas before the age of 20, the BCVA in the overall RP group did not decline.

For patients with COD/CORD, like in RP, a significant overall age effect ($p < 0.0001$) on BCVA decline was seen, with a yearly decline of 0.023 logMAR or 5.5% in the better-seeing eye and 0.033 logMAR or 7.9% in the worse-seeing eye. The presence of high myopia was associated with a significantly faster BCVA decline ($p = 0.03$). A spline mixed model revealed a significantly faster BCVA decline of 0.038 (9.2%) logMAR per year in the better-seeing eye after 50 years of age, as compared to 0.019 (4.5%) logMAR per year before the age of 50 ($p < 0.001$). This same analysis did not reveal a significant change in slope of BCVA decline before and after the age of 20 ($p = 0.74$), 30 ($p = 0.89$), and 40 ($p = 0.72$) years in patients with COD/CORD. We found no significant differences in slope of decline before and after reaching low vision ($p = 0.32$ for COD/CORD; $p = 0.68$ for RP) and severe visual impairment ($p = 0.16$ for COD/CORD; $p = 0.24$ for RP).

Asymmetry in BCVA between eyes at the last 2 consecutive examinations was found in 11/48 (23%) patients with RP and 4/22 (18%) patients with COD/CORD. The presumed cause of asymmetry could be determined in 6/11 (55%) patients with RP and in 2/4 (60%) patients with COD/CORD (See Table, Supplemental Digital Content 3).

Ophthalmic and funduscopic findings

Myopia was present in 36/43 (84%) patients with RP and 17/20 (85%) patients with COD/CORD with available refractive error measurements. Patients became significantly more myopic with advancing age in the RP group (-0.07 D per year; $p < 0.001$) and the COD/CORD group (-0.09 D per year; $p = 0.014$). Based on the last available spherical equivalent, averaged between eyes, patients with an ORF15 mutation were significantly more myopic (mean -6.3 D; SD 3.9; range -14.1 D to +1.2 D) than patients with a mutation in exon 1 to 14 (mean -2.8 D; SD 3.5; range -7.9 D to +5.1 D; $p = 0.001$), and high myopia was found in a higher frequency than in patients with mutations in exon 1 to 14 ($p = 0.01$, chi-square test). The extent of myopia and other ophthalmic findings are shown in Table 1. Cataract or a history of cataract was reported in 26/43 (60%) patients with RP and 7/21 (33%) patients with COD/CORD with known lens status. In these patients, the median age at which cataracts were first reported was 33.3 years (n = 21; IQR 12.4; range 18.4-55.5 years) in patients with RP and was significantly earlier ($p < 0.001$, Mann-Whitney *U* test) than in patients with COD/CORD (n = 7; median 58; IQR 19; range 54-78 years).

Table 1. Cohort characteristics of *RPGR*-associated retinal dystrophies

Characteristics	Group total (n = 74)	RP (n = 52)	COD/CORD (n = 22)
Mean age at last exam ± SD (range), yrs	41.1 ± 20.2 (3.9-88.3)	39.3 ± 18.1 (9.2-77.5)	45.2 ± 24.3 (3.9-88.3)
Mean follow-up time ± SD, yrs	13.9 ± 13.2	13.8 ± 13.1	14.1 ± 13.7
Median follow-up time (range; IQR)	11.6 (0.0-57.1; 18.4)	10.9 (0.0-54.0; 19.8)	12.7 (0.0-57.1; 17.4)
Median number of visits (range; IQR)	5 (1-55; 7)	5 (1-22; 7)	5 (1-55; 5)
Mean number of visits ± SD	7.1 ± 7.7	6.6 ± 5.9	8.2 ± 11.0
Caucasian, n (%)	70 (95)	48 (92)	22 (100)
Asthma or bronchitis	7 (9)	5 (10)	2 (9)
Nystagmus or roving eye movements, n (%)	9 (12)	8 (16)*	1 (4)
Photophobia, n (%)	30 (41)	10/16 (63)	10/14 (71)
Reported first symptom, n (%)	45 (61)	25 (48)	20 (91)
Nyctalopia, n (%)	20 (44)	18 (72)	1 (5)
Visual field loss, n (%)	2 (4)	2 (8)	-
Photophobia, n (%)	1 (2)	-	1 (5)
Visual acuity loss, n (%)	18 (40)	3 (12)	17 (85)
Unknown, diagnosis used, n (%)	3 (7)	2 (8)	1 (5)
No symptom yet, n (%)	1 (2)	-	-
Mean refractive error ± SD (range)† (SER; n = 65), D	-5.3 ± 4.1 (-14.1 to +5.1)	-4.9 ± 3.9 (-13.0 to +5.1)	-6.3 ± 4.5 (-14.1 to +4.0)
High myopia (<-6D), n (%)	24 (38)	16/45 (36)	10/20 (50)
Moderate myopia (-3D > SER ≥ -6D), n (%)	21 (33)	16/45 (36)	7/20 (35)
Mild myopia (-0.75D > SER ≥ -3D), n (%)	8 (13)	7/45 (16)	1/20 (5)
≥-0.75D, n (%)	10 (16)	6/45 (13)	2/20 (10)
Fundoscopic examination			
Optic disc pallor, n (%)	50/60 (83)	39/40 (98)	11/20 (55)
Peripapillary atrophy, n (%)	15/60 (25)	9/40 (23)	6/20 (30)
Bone-spicule or coarse hyperpigmentation, n (%)	44/58 (76)	37/42 (88)	7/16 (44)
Vascular attenuation, n (%)	52/63 (81)	43/44 (98)	10/19 (53)
Macular phenotype described, n (%)	55 (74)	34 (65)	21 (95)

Table 1. Continued

No macular RPE changes	7/55 (13)	4/34 (12)	3/21 (14)
RPE atrophy with relative foveal sparing, resembling bull's eye maculopathy, n (%)	10/55 (18)	6/34 (18)	4/21 (19)
Other form of RPE atrophy, n (%)	24/55 (44)	13/34 (38)	10/21 (48)
Alterations, no profound atrophy, n (%)	14/55 (25)	11/34 (32)	4/21 (19)
Electroretinography pattern last seen, n (%)	48 (65)	30 (58)	18 (82)
Scotopic and photopic ND, n (%)	22/48 (46)	21/30 (70)	1/18 (6)
Rod-cone pattern, n (%)	6/48 (13)	6/30 (20)	-
Cone-rod pattern, n (%)	11/48 (23)	-	11/18 (61)
Cone isolated, n (%)	3/48 (6)	-	3/18 (17)
Scotopic and photopic reduced, pattern not further specified, n (%)	5/48 (10)	3/30 (10)	2/18 (11)
Normal, n (%)	1/48 (2)	-	1/18 (6)

* One of these patients had nystagmus after a head trauma.

† Mean spherical equivalent of the right eye and the left eye. If patients had undergone cataract surgery, the last SER before surgery was used.

ND, nondetectable amplitudes; SER, spherical equivalent of the refractive error.

Table 1 shows the funduscopic findings in this cohort. Retinal pigment epithelium changes in the macula were found in all but 3 patients with RP aged 17, 20, and 31 and in all but 4 patients with COD/CORD aged 3 to 10 at the time of the last funduscopic examination. Optic disc drusen were found in 5/52 (10%) patients with RP and not in patients with COD/CORD. A tapetal reflex was reported in one RP patient (2%) at the age of 20, and in 2/23 (9%) patients with COD/CORD, at the ages of 9 and 39. White drusen-like deposits were found in the (mid-) peripheral retina in 4/51 (8%) patients with RP (see Figure, Supplemental Digital Content 4, showing fundus photographs for *RPGR*-RP), in the peripheral macula in one patient with COD, and in the peripheral retina in one patient with CORD (see Figure, Supplemental Digital Content 5, showing fundus photographs for *RPGR*-COD/CORD).

In 10 patients, a history of uncomplicated cataract surgery at the median age of 46 in patients with RP (n = 7; IQR 40; range 29-69) and at the median age of 66 in patients with COD/CORD (n = 3; ages 64, 66, and 79 years), due to visually significant cataract, was documented.

Full-field ERG and visual field findings

Electroretinography was available for 30/52 (58%) patients with RP and 18/22 (82%) patients with COD/CORD. For patients with RP, the median age at which cone and rod ERG amplitudes were first found to be nondetectable, was 17.4 years (IQR 24.0; range 5.3-40.6 years; mean 22.4 years; SD 12.5). Of the 21 patients with RP with a nondetectable ERG, 6 had previously documented recordable cone (6/6) and rod (3/6) ERG responses. The median age at this last-documented ERG response before progressing to a nondetectable ERG was 12.6 years (IQR 24.5, range 4.7-30.5 years).

In patients with COD/CORD, only one patient had a nondetectable cone and rod ERG at the age of 35.1 years, with the last documented recordable but attenuated cone and rod ERG response at 9 years of age. One 4-year-old patient from a large CORD pedigree had a normal ERG, in the presence of suboptimal BCVA and a mild color vision deficiency as measured with Ishihara plates, and no clear fundus abnormalities. The ERG patterns are further specified in Table 1. Progression of ERG from an isolated COD pattern to a CORD pattern was not documented in this cohort, but all patients with COD/CORD only received one (56%) or 2 (44%) ERGs during the observational period.

Goldmann visual fields were available for 25/52 (48%) patients with RP and 6/22 (27%) patients with COD/CORD, and within individuals with follow-up Goldmann visual fields (n = 11; 9 patients with RP and 2 patients with COD/CORD), the median follow-up time was 11.0 years (IQR 11.9; range 2.0-35.9 years; see Figure, Supplemental Digital Content 6, which shows the individual visual field areas). Linear mixed-model analysis of the age effect on logarithm of the seeing retinal areas revealed a significantly faster Goldmann visual field decline in patients with RP than in patients COD/CORD patients ($p = 0.001$), with a yearly decline in seeing retinal area of 6.6% ($p < 0.0001$) in the overall RP population. Significant differences in baseline seeing retinal area were seen between individual patients with COD/CORD ($p = 0.001$), and no significant overall age effect in patients with COD/CORD ($p = 0.26$) was found. However, in patients with COD/CORD, there was a yearly decline rate of 2.1% in seeing retinal area after the age of 40 that was significantly faster ($p = 0.02$) than before the age of 40.

In patients with RP, the logarithm of the seeing retinal area size was significantly smaller at baseline in patients with mutations in exon 1 to 14 than in patients with mutations in ORF15 ($p = 0.05$) of *RPGR*, but declined significantly faster ($p = 0.014$) in patients with a mutation in the ORF15

region, with a yearly decline rate of 9.0% ($p < 0.00001$), as compared to 4.2% in patients with mutations in exon 1 to 14 ($p = 0.004$).

Findings on retinal imaging in *RPGR*-associated retinitis pigmentosa

Fundus autofluorescence images were available for 17/52 (33%) patients with RP, and general age-related changes are further specified in Table 2. A hyperautofluorescent ring was found in 8/17 (47%) patients with RP, all under the age of 22 and with a BCVA ≥0.5 in both eyes (Figure 2). In patients with a hyperautofluorescent ring and available concurrent SD-OCT scans (n = 5), this ring demarcated a relatively preserved macula on OCT (Figure 2), and the ring represented a transition from a relatively preserved outer retina to a more degenerated outer retina on SD-OCT. Larger ring diameters were found in younger patients, with the largest ring diameter spanning the posterior pole in a 9-year-old patient, and the smallest ring diameter in the oldest patient.

Optical coherence tomography data were available for 15/52 (29%) patients with RP with a mean age of 28.1 years (SD 14.8, range 13.2-67.2 years). No patients with RP had documented cystoid fluid collections in the macula at any time point in the follow-up period, and 6/15 (40%) had some degree of eccentric or parafoveal macular epiretinal membrane in at least one eye (Figure 2D).

Central retinal thickness (CRT) measurements with Heidelberg SD-OCT were available for 14/52 (27%) patients with RP. Mixed-model analysis of longitudinal and cross-sectional CRT data revealed a significant age effect on CRT (-3 μm/year; $p = 0.004$). *RPGR* mutations in exon 1 to 14 were associated with a significantly thicker CRT than mutations in the ORF15 region ($p = 0.03$). The median of the last-measured CRT was 244 μm (IQR 102; range 102-265 μm) in exon 1 to 14 and 147 μm (IQR 61; range 88-227 μm) in ORF15, with similar ages between both groups. Data on the structural integrity of the foveal and peripheral macular ellipsoid zone (EZ) and outer nuclear layer (ONL) are specified in Table 2.

Table 2. Imaging findings in patients with *RPGR*-associated retinal dystrophies

Retinitis pigmentosa			N (%)	Age (years)
FAF	No FAF abnormalities or only a hyper-AF ring around the macula		3/17 (18)	12-16
	Granular/mottled hypo-AF changes, more abundant outside the vascular arcade than in the posterior pole		9/17 (53)	9-30
	Marked FAF decrease in periphery, with some remnants of FAF in the posterior pole		3/17 (18)	36-45
	Near-complete absence of FAF in the whole retina		2/17 (12)	68-70
	Structural integrity on SD-OCT		N (%)	Age (years)
EZ	Central macula	Peripheral macula		
	Intact	Intact	3/12 (25)	14-19
	Intact	Granular/attenuated	4/12 (33)	16-31
	Attenuated, relatively spared	Almost absent	4/12 (33)	27-45
	Not visible	Not visible	1/12 (8)	67
ONL	Intact	Intact	3/12 (25)	16-19
	Intact/relatively spared	Attenuated	3/12 (25)	14-31
	Atrophic	Atrophic	5/12 (42)	27-45
	Nearly absent	Nearly absent	1/12 (8)	67
Cone/cone-rod dystrophy			N (%)	Age (years)
FAF	No FAF abnormalities*		1/11 (9)	3
	Only hyper-AF ring, no FAF abnormalities in- or outside ring		2/11 (18)	18-31
	Central FAF decrease with or without a hyper-AF ring, surrounded by (nearly) normal FAF		5/11 (45)	38-63
	Central FAF decrease and a hyper-AF ring, surrounded by mild patchy hypo-AF changes		1/11 (9)	11
	Central FAF absence, surrounded by a hyper-AF border; paravascular satellite lesions of absent autofluorescence		1/11 (9)	79
	Granular AZOOR-like changes		1/11 (9)	67
	Structural integrity on SD-OCT		N (%)	Age (years)
EZ	Central macula	Peripheral macula		
	Intact	Intact	4/10 (40)	3-19
	Interrupted	Intact	5/10 (50)	37-67
	Nearly absent	Granular/interrupted	1/10 (10)	79
ONL	Intact	Intact	3/10 (30)	3-19
	Atrophic	Intact	3/10 (30)	40-59
	Atrophic†	Atrophic	3/10 (30)	31-79
	Intact	Atrophic	1/10 (10)	18

* Because of the very young patient age, the picture quality was relatively low and did not allow for reliable visualization outside of the posterior pole.

† Atrophy of the foveal ONL in cone/cone-rod dystrophy patients was always more marked than the atrophy of the ONL outside of the central macula.

AZOOR, acute zonal occult outer retinopathy.

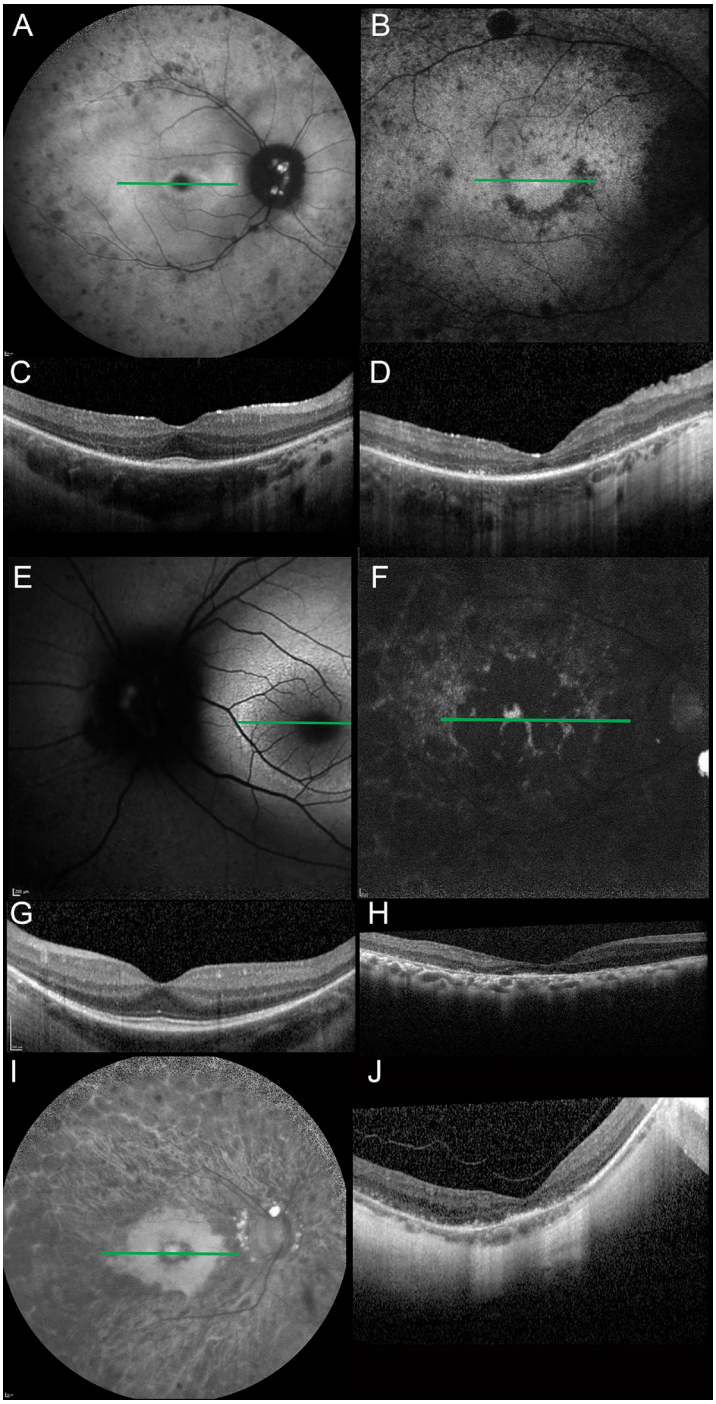

Figure 2. Findings on imaging in patients with *RPGR*-associated retinitis pigmentosa. The green lines in the FAF images show the location of the complementary SD-OCT scans. **A.** Fundus autofluorescence image of a 19-year-

old patient with a missense mutation in exon 5 (c.425T>G; p.(Ile142Ser); BCVA in the right eye 20/25; in the left eye 20/20), showing optic disc drusen, a small hyperautofluorescent ring around the central macula, surrounded by patchy regions of decreased autofluorescence (AF). **B.** Fundus autofluorescence image of a 28-year-old patient with a frameshift mutation (c.2362_2366del; p.(Glu788Argfs*45)) in *RPGR*-ORF15 (BCVA in the right eye 20/50; in the left eye 20/67), showing dense granular areas of decreased AF around the optic disc, vascular arcade, and in the posterior pole, with a hypo-AF border around the central macula. **C.** Spectral domain OCT of the same patient in (**A**), showing central sparing of the EZ, external limiting membrane (ELM), and ONL, whereas these layers are attenuated toward the peripheral macula. **D.** Spectral domain OCT of the same patient described in (**B**), showing an epiretinal membrane, and atrophic EZ, ELM, and ONL, with a granular aspect of the EZ, but with relative central sparing. **E.** Fundus autofluorescence image of a 16-year-old patient with a missense mutation in exon 5 (BCVA in both eyes 20/20), showing a hyper-AF ring. **F.** Fundus autofluorescence image of a 45-year-old patient with a pathogenic frameshift mutation (c.2405_2406del; p.(Glu802Glyfs*32)) in *RPGR*-ORF15 (BCVA in the right eye 20/125; in the left eye 20/400), showing markedly decreased patchy AF with scattered granular remnants of hyper-AF. **G.** Spectral domain OCT of the same patient described in (**E**), showing a wide sparing of the EZ, ELM and ONL, but with attenuation in the peripheral macula. **H.** Spectral domain OCT of the same patient in (**F**), showing markedly attenuated EZ, ELM, and ONL in the macula, more so in the peripheral macula. **I.** Fundus autofluorescence image of a 42-year-old patient with a pathogenic frameshift mutation (c.27del; p.(Asp10Ilefs*58)) in exon 1 (BCVA in both eyes 20/63), showing generally decreased AF, papillary drusen, and a hyper-AF fovea, encircled by a hypo-AF ring, surrounded by a region of hyper-AF. Foveal hyperautofluorescence, surrounded by hypo-autofluorescence in varying intensities, was found in 3/15 (20%) patients with RP, aged 28 years to 42 years and with a BCVA between 20/100 and 20/50. **J.** Spectral domain OCT of the same patient described in (**I**), showing atrophy of the ONL. The EZ has a granular aspect in the fovea, and is almost absent outside of the fovea.

Findings on retinal imaging in *RPGR*-associated cone dystrophy/cone-rod dystrophy

Fundus autofluorescence images were available for 11/22 (50%) patients with COD/CORD, and generally showed a hyperautofluorescent ring around a hypo-autofluorescent macula (7/11, 64%) (Figure 3). Further details are given in Table 2. In patients with COD/CORDwith a hyperautofluorescent ring and a concurrent SD-OCT scan (n = 4), this ring demarcated an area of a relatively atrophic macula in 3 patients aged 38 to 79, which was essentially the opposite pattern as compared to the RP group, with marked attenuation of the external limiting membrane, the ellipsoid zone (EZ), and the retinal pigment epithelium centrally within the hyperautofluorescent ring (Figure 3). Only in the youngest patient with CORD, aged 18, who had a double concentric hyperautofluorescent ring, the inner ring demarcated an area of relatively healthy EZ, external limiting membrane, and ONL (Figure 3, A and B). We did not observe a consistent relation between hyperautofluorescent ring diameter size and age.

Optical coherence tomography data were available for 12/22 (55%) patients with COD/CORD with a mean age of 41.8 years (SD 25.8, range 3.9-79.4 years). Cystoid fluid collections in both eyes were noted in 2/12 (17%), and 1/12 (8%) had a bilateral epiretinal membrane. Central retinal thickness measurements with Heidelberg SD-OCT were available for 10/22 (45%) patients. Mixed-model analysis of longitudinal and cross-sectional CRT data revealed a significant age effect on CRT (-2 μm/year; $p = 0.008$). Only 1/10 patients with CORD with SD-OCT had a mutation in

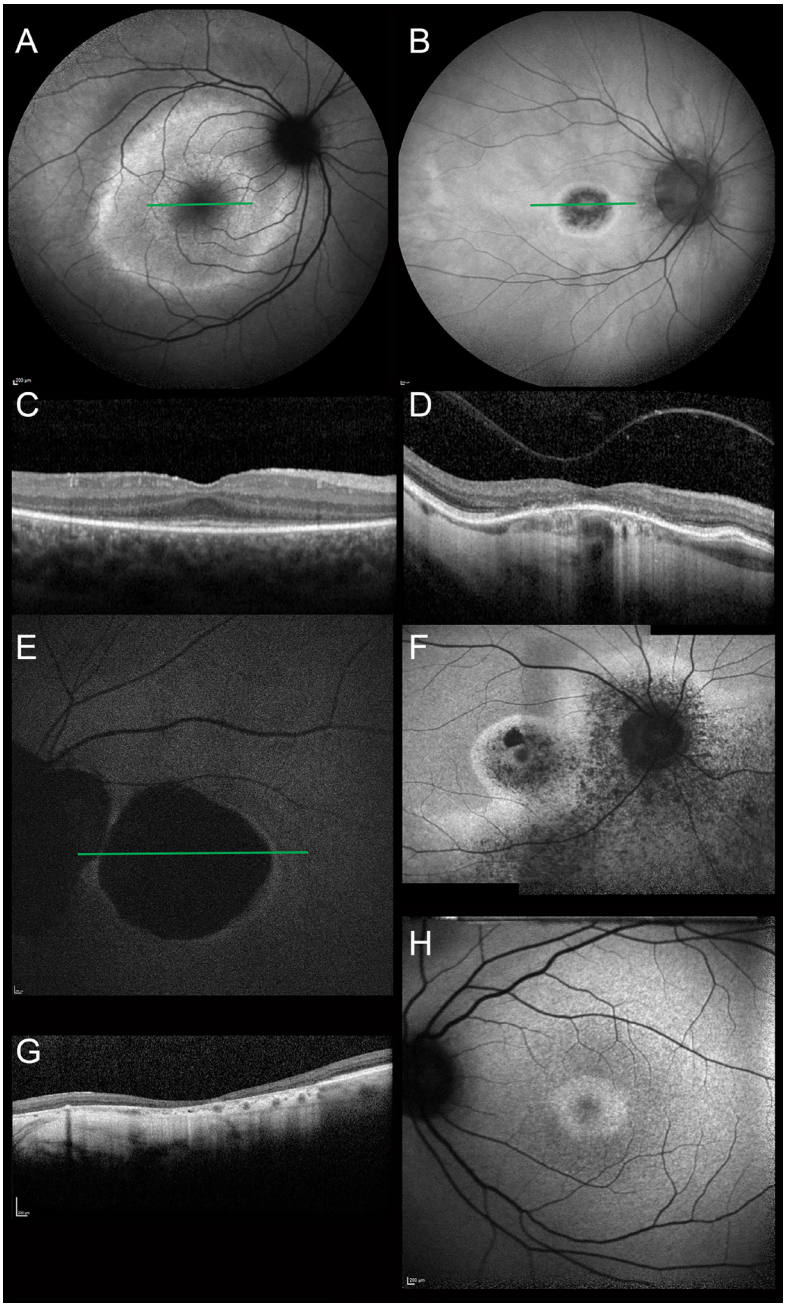

Figure 3. Findings on imaging in patients with *RPGR*-associated predominantly cone-involving dystrophies. The green lines in the FAF images show the location of the complementary SD-OCT scans. The retina around the hyperautofluorescent ring (in 8 patients) showed normal autofluorescence in 6/8 (75%) patients, whereas in the other 2 patients, this ring was surrounded by mild patchy hypo-autofluorescent changes in one patient, and by paravascular

satellite lesions of absent autofluorescence in another patient. **A.** Fundus autofluorescence image of an 18-year-old patient with a deletion after *RPGR* exon 10 (c.1246-?_*1091-?) and a CORD pattern on electroretinogram (BCVA in the right eye 20/67; in the left eye 20/40), showing a double concentric hyper-AF ring. **B.** Fundus autofluorescence image of a 54-year-old patient with a nonsense mutation (c.2959G>T; p.(Glu987*)) in *RPGR*-ORF15 (BCVA in the right eye 20/100; in the left eye 20/400), showing central hypo-AF with relatively preserved foveal AF, a hyper-AF ring, and normal surrounding retina. **C.** Spectral domain OCT scan of the same patient described in (**A**), showing relatively well-preserved EZ, ELM, and ONL in the central macula, with some attenuation toward the periphery. **D.** Spectral domain OCT of the same patient described in (**B**), showing a continuous EZ and ELM and a relatively healthy ONL in the peripheral retina, but attenuation of these layers in the central macula. The choroid is markedly thinned, mainly in the peripheral macula. **E.** Fundus autofluorescence image of a 79-year-old patient with a frameshift mutation in *RPGR*-ORF15 (c.3317dup; p.(Ser1107Valfs*4); BCVA in the right eye 20/400; in the left eye 2/100), showing peripapillary atrophy, a central absence of AF, surrounded by a thin border of slightly increased AF. **F.** Fundus autofluorescence image of a 67-year-old patient with a frameshift mutation (c.2993_2996del; p.(Glu998Glyfs*90)) in *RPGR*-ORF15 (BCVA in the right eye 20/40; in the left eye 20/50). This patient had bilateral granular hypo-AF and hyper-AF changes around the optic disc and in the central macula, encircled by an area of increased AF, and extending to the inferotemporal vessels and inferior retina, in an acute zonal occult outer retinopathy-like distribution, and a relatively preserved aspect of the fovea. No SD-OCT was available for this patient. **G.** Spectral domain OCT of the same patient described in (**E**), showing a markedly thinned neuroretina, retinal pigment epithelium, and choroid. **H.** Fundus autofluorescence image of a 31-year-old patient with a frameshift mutation (c.3039_3040del; p.(Glu1014fs)) in *RPGR*-ORF15 (BCVA in both eyes 20/33), showing a small but broad hyper-AF ring around the fovea. No SD-OCT scan was available for this patient.

the exon 1 to 14 region, and his CRT (247 μm, averaged between eyes) was higher than the CRT in patients with COD/CORD with ORF15 mutations (126 μm, range 93-173 μm). Data on the structural integrity of the foveal and peripheral macular EZ and ONL are depicted in Table 2.

DISCUSSION

is retrospective cohort study, we describe the natural disease history and phenotypic spectrum of *RPGR*-associated retinal dystrophies in 74 patients from 38 different families.

We found variability in the initial presentation. Phenotypic heterogeneity associated with a single mutation in the same family was seen in 2 families, each comprising 2 to 3 patients, pointing to a modest influence of genetic and/or environmental modifiers on the phenotype. Cases of RP and CORD within the same family carrying an identical *RPGR* mutation have been described previously,[11, 29, 30] and significant intrafamilial variability in the age at symptom onset and BCVA has been described within families with *RPGR*-associated RP.[31]

Most patients with RP in this cohort showed typical RP fundus features and macular involvement from the second decade of life onward. In patients with COD/CORD, a normal macula was only seen in the youngest patients up to 10 years of age.

The median age at symptom onset in patients with COD/CORD was 23 years in this cohort, with a wide range. This is more than 10 years earlier than reported previously in a single large *RPGR* family,[7] but 7 years to 11 years later than in a previously described genetically heterogeneous COD/CORD cohort.[32] However, the accuracy of self-reported age at symptom onset could not be ascertained in this retrospective study setting. Progression on full-field ERG from a COD pattern to a CORD pattern was not documented in this cohort, because ERG is used in the clinical setting for diagnostic rather than follow-up purposes. An earlier review described characteristic early secondary rod involvement in CORD, and no or possibly late rod involvement in COD, signifying considerable overlap between these two diagnoses and meaning that rod involvement in later life could still be concurrent with a COD diagnosis.[6]

In our study cohort, the rate of BCVA decline in patients with COD/CORD showed a significantly faster decline after the age of 50. A recent natural history study in patients with Stargardt disease found a significant association of baseline BCVA level with the yearly rate of BCVA change, as BCVA in eyes with moderate impairment declined faster than the BCVA in eyes with mild or no impairment, but slower than in eyes with severe impairment.[33] We did not observe this difference in this cohort of *RPGR*-associated COD/CORD and RP.

Imaging findings in this cohort included the presence of a hyperautofluorescent ring in 47% of patients with RP with available FAF imaging, with larger rings in younger patients, demarcating an area of relatively spared retina. In patients with COD/CORD with available FAF, a hyperautofluorescent ring was found in 73%, with larger rings in older patients, demarcating an area of relatively atrophic retina with EZ and ONL attenuation. In all patients, the hyperautofluorescent ring represented a transitional zone between relatively healthy and more severely affected retina. This further supports the earlier findings that larger rings in RP and smaller rings in COD/CORD indicate greater preservation of structure and function, with progressive ring size reduction indicating disease progression outside the ring in RP,[34-36] and progressive ring expansion indicating disease progression within the ring in COD/CORD.[8, 37] In this context, the implication of our finding of a double concentric ring in an 18-year-old patient with CORD with a relatively healthy fovea within the inner concentric ring is unclear. An earlier study of *NR2E3*-associated autosomal dominant RP found progressive centripetal and centrifugal degeneration in the area between both concentric rings, with the inner ring becoming progressively smaller, closing in on the healthy central macula, and the outer ring size expanding.[38] This pattern would explain the relatively healthy fovea in this patient with CORD, despite the cone-rod pattern on ERG. However, there was no SD-OCT available of the macular area colocalizing with the outer concentric ring that could support this hypothesis. Multifocal ERG would allow the measurement of localized retinal function, particularly the integrity of the central macular area. Longitudinal FAF imaging in a prospective setting is necessary to further assess whether the presence and size of a hyperautofluorescent ring can assist in identifying regions amenable to future gene therapy.

We found several genotype-phenotype correlations in this study. In summary, we found a potentially more deleterious effect of mutations in the ORF15 region of the *RPGR* gene than mutations in exon 1 to 14. First, patients with RP with a pathogenic *RPGR*-ORF15 variant had a significantly higher yearly hazard of reaching low vision and severe visual impairment. Next, patients with RP with ORF15 mutations had higher myopia, a significantly thinner central retina, and a significantly faster decline of the V4e seeing retinal area than patients with exon 1 to 14 mutations, with decline rates of 9.0% and 4.2%, respectively. By contrast, most studies in literature have reported a more severe phenotype in patients with exon 1 to 14 mutations, as defined by a faster loss of ERG amplitudes,[4, 12] or a smaller visual field.[13] Exceptions have been described, with a more severe phenotype in patients with mutations in ORF15,[14] and worse visual function even in female carriers of *RPGR*-ORF15.[39] To further complicate the picture, similar decline rates in BCVA and visual field have been described between patients with mutations in exon 1 to 14 and ORF15, despite a faster loss of ERG cone function in patients with mutations in exon 1 to 14.[4] Finally, a higher degree of phenotypic heterogeneity has been reported in patients with *RPGR*-ORF15 mutations than in patients with exon 1 to 14 mutations, which could in part explain the variable observations.[12, 29] In interpreting the novel associations in this study, it is judicious to consider the relatively small numbers of patients in subgroup analyses of the visual field data (n = 31) and SD-OCT data (n = 27), as compared to the BCVA (n = 70) and refractive error (n = 65) data. In addition, the interpretation of retrospective data is complicated by potential between-center and interexaminer variability, which may not always be statistically accounted for in the retrospective study setting. Although data gathered from clinical practice are useful, these findings warrant further investigation, in larger patient groups and in a controlled prospective setting.

So far, most of all previously reported cases of *RPGR*-associated COD/CORD have contained a mutation in the 3' end of the ORF15 region. By contrast, mutations toward the 5' end were associated with a higher RP frequency.[6, 8, 11, 15, 16] Patients with COD/CORD in our study generally had ORF15 mutations toward the 3' end, supporting these earlier findings, but we also report the first case of a predominantly cone-affecting dystrophy caused by a deletion after exon 10. This adds to the phenotypic heterogeneity in exon 1 to 14. This patient was member of a family with RP patients.

Regarding future (gene) therapeutic options, the visual acuity survival results in this retrospective study suggest a potentially broad intervention window for gene therapy in the first 6 decades of life in patients with RP, as we found a 50% probability of not being visually impaired (i.e., BCVA <20/67) at the age of 58, indicating relative preservation of foveal photoreceptors before this time. In patients with COD/CORD, the potential intervention window for gene therapy is narrower than in RP, although the wide range in symptom onset and high variability in clinical course warrants additional patient-by-patient eligibility assessment. The relatively fast BCVA decline rates in this cohort suggest that BCVA change may be a potentially sensitive outcome parameter of treatment in future therapeutic trials, particularly in patients with RP with increasing age and in patients

with COD/CORD after the age of 50. In patients with RP under the age of 20, BCVA may not be a sensitive measure to detect therapeutic effect. When assessing patient eligibility for a gene therapy trial, special attention to the presence of high myopia is warranted, as high myopia was prevalent in this RP and COD/CORD cohort, and was significantly associated with a faster annual BCVA decline, potentially due to additional myopic degeneration. Earlier studies have shown that, of all refractive errors, high myopia entails the highest risk of visual impairment.[40, 41] As retinal structure also needs to be assessed to determine the potential therapeutic intervention window, we found an intact foveal EZ on SD-OCT up until the fifth decade of life in patients with RP, although the EZ in the extrafoveal and more peripheral macula was attenuated from the second decade of life onward, indicating a progressive centripetal degeneration. Outer nuclear layer attenuation seemed to occur earlier, from the second decade of life onward, although detecting ONL thinning on SD-OCT may be easier than visualizing change in EZ intensity. This is an interesting observation nonetheless, as protein RPGR-ORF15 localizes to the connecting cilium of the photoreceptors and therefore probably the EZ on OCT. In a canine model with a naturally occurring *RPGR* mutation in the ORF15 region, severe photoreceptor outer segment disintegration preceded thickness reduction of the ONL, which only started to decline at older ages in the inferior retina, with preserved thickness in the visual streak.[42, 43] Another canine model with a naturally occurring *RPGR*-ORF15 mutation showed a more rapid ONL thickness decline, with the visual streak more severely affected than the periphery.[42]

In patients with COD/CORD in this cohort, the foveal EZ and ONL were only intact until the second decade of life and showed a granular appearance until the seventh decade of life in some patients, although in others the EZ was nearly absent from the sixth decade onward. *RPGR* gene therapy in a canine model has shown retinal functional and structural rescue in initial stage disease, that is, before ONL reduction, midstage disease, that is, 40% ONL loss, and late-stage disease, that is, 50% to 60% ONL loss, expanding the therapeutic window, although the time between subretinal injection and observed rescue increased with advancing disease stage. The relatively common occurrence of an epiretinal membrane may complicate the outcome of subretinal gene therapy surgery, possibly requiring removal of the epiretinal membrane before subretinal injection of the therapeutic vector.

This study suggests that the use of the contralateral eye as an untreated control in future therapeutic trials may be appropriate, as we found symmetry in BCVA between eyes in 77% of patients with RP and patients with COD/CORD, suggesting that *RPGR*-associated retinal dystrophies are commonly symmetrical between eyes in most patients. However, we did find a faster yearly BCVA decline rate in the worse eye than in the better eye. Asymmetry of structural progression on FAF and OCT in *RPGR*-associated RP has been described before.[35] So far, gene therapeutic trials have treated the worse-seeing eye and used the better-seeing eye as an untreated control.[44-47] In future clinical trials, it may be useful to include a retrospective comparison of the natural course of structural and functional decline between eyes of individual patients when assessing therapeutic effect.

REFERENCES

1. Shu X, Black GC, Rice JM, et al. RPGR mutation analysis and disease: an update. Hum Mutat 2007;28:322-328.
2. Pelletier V, Jambou M, Delphin N, et al. Comprehensive survey of mutations in RP2 and RPGR in patients affected with distinct retinal dystrophies: genotype-phenotype correlations and impact on genetic counseling. Hum Mutat 2007;28:81-91.
3. Zito I, Downes SM, Patel RJ, et al. RPGR mutation associated with retinitis pigmentosa, impaired hearing, and sinorespiratory infections. J Med Genet 2003;40:609-615.
4. Sandberg MA, Rosner B, Weigel-DiFranco C, et al. Disease course of patients with X-linked retinitis pigmentosa due to RPGR gene mutations. Invest Ophthalmol Vis Sci 2007;48:1298-1304.
5. Flaxel CJ, Jay M, Thiselton DL, et al. Difference between RP2 and RP3 phenotypes in X linked retinitis pigmentosa. Br J Ophthalmol 1999;83:1144-1148.
6. Michaelides M, Hardcastle AJ, Hunt DM, Moore AT. Progressive cone and cone-rod dystrophies: phenotypes and underlying molecular genetic basis. Surv Ophthalmol 2006;51:232-258.
7. Thiadens AA, Soerjoesing GG, Florijn RJ, et al. Clinical course of cone dystrophy caused by mutations in the RPGR gene. Graefes Arch Clin Exp Ophthalmol 2011;249:1527-1535.
8. Ebenezer ND, Michaelides M, Jenkins SA, et al. Identification of novel RPGR ORF15 mutations in X-linked progressive cone-rod dystrophy (XLCORD) families. Invest Ophthalmol Vis Sci 2005;46:1891-1898.
9. Shu X, McDowall E, Brown AF, Wright AF. The human retinitis pigmentosa GTPase regulator gene variant database. Hum Mutat 2008;29:605-608.
10. Vervoort R, Lennon A, Bird AC, et al. Mutational hot spot within a new RPGR exon in X-linked retinitis pigmentosa. Nat Genet 2000;25:462-466.
11. Yang L, Yin X, Feng L, et al. Novel mutations of RPGR in Chinese retinitis pigmentosa patients and the genotype-phenotype correlation. PLoS One 2014;9:e85752.
12. Fahim AT, Bowne SJ, Sullivan LS, et al. Allelic heterogeneity and genetic modifier loci contribute to clinical variation in males with X-linked retinitis pigmentosa due to RPGR mutations. PLoS One 2011;6:e23021.
13. Sharon D, Sandberg MA, Rabe VW, et al. RP2 and RPGR mutations and clinical correlations in patients with X-linked retinitis pigmentosa. Am J Hum Genet 2003;73:1131-1146.
14. Andreasson S, Breuer DK, Eksandh L, et al. Clinical studies of X-linked retinitis pigmentosa in three Swedish families with newly identified mutations in the RP2 and RPGR-ORF15 genes. Ophthalmic Genet 2003;24:215-223.
15. Branham K, Othman M, Brumm M, et al. Mutations in RPGR and RP2 account for 15% of males with simplex retinal degenerative disease. Invest Ophthalmol Vis Sci 2012;53:8232-8237.
16. Demirci FY, Rigatti BW, Wen G, et al. X-linked cone-rod dystrophy (locus COD1): identification of mutations in RPGR exon ORF15. Am J Hum Genet 2002;70:1049-1053.
17. Yang L, Wu L, Yin X, et al. Novel mutations of CRB1 in Chinese families presenting with retinal dystrophies. Mol Vis 2014;20:359-367.
18. Beltran WA, Cideciyan AV, Iwabe S, et al. Successful arrest of photoreceptor and vision loss expands the therapeutic window of retinal gene therapy to later stages of disease. Proc Natl Acad Sci U S A 2015;112:E5844-E5853.

19. New trial for Blindness Rewrites the Genetic Code. University of Oxford, 2017. Available at: http://www.ox.ac.uk/news/2017-03-17-new-trial-blindness-rewrites-genetic-code. Accessed May 2, 2017.
20. van den Born LI, Bergen AA, Bleeker-Wagemakers EM. A retrospective study of registered retinitis pigmentosa patients in The Netherlands. Ophthalmic Paediatr Genet 1992;13:227-236.
21. van Huet RA, Oomen CJ, Plomp AS, et al. The RD5000 database: facilitating clinical, genetic, and therapeutic studies on inherited retinal diseases. Invest Ophthalmol Vis Sci 2014;55:7355-7360.
22. Dagnelie G. Conversion of planimetric visual field data into solid angles and retinal areas. Clin Vis Sci 1990;5:95-100.
23. Putter H, Fiocco M, Geskus RB. Tutorial in biostatistics: competing risks and multi-state models. Stat Med 2007;26:2389-2430.
24. World Health Organization. International Statistical Classification of Diseases and Related Health Problems, 10th Revision (ICD-10). 2003. Available at: http://www.who.int/classifications/icd/en/. Accessed April 5, 2017.
25. Verhoeven VJ, Buitendijk GH, Rivadeneira F, et al. Education influences the role of genetics in myopia. Eur J Epidemiol 2013;28:973-980.
26. Csaky KG, Richman EA, Ferris IIIFL. Report from the NEI/FDA Ophthalmic Clinical Trial Design and Endpoints Symposium. Invest Ophthalmol Vis Sci 2008;49:479-489.
27. R Core Team. R: A Language and Environment for Statistical Computing. Vienna, Austria: R Foundation for Statistical Computing, 2013.
28. Cai Y, Zijlema WL, Doiron D, et al. Ambient air pollution, traffic noise and adult asthma prevalence: a BioSHaRE approach. Eur Respir J 2017;49.
29. Ruddle JB, Ebenezer ND, Kearns LS, et al. RPGR ORF15 genotype and clinical variability of retinal degeneration in an Australian population. Br J Ophthalmol 2009;93:1151-1154.
30. Walia S, Fishman GA, Swaroop A, et al. Discordant phenotypes in fraternal twins having an identical mutation in exon ORF15 of the RPGR gene. Arch Ophthalmol 2008;126:379-384.
31. Sheng X, Li Z, Zhang X, et al. A novel mutation in retinitis pigmentosa GTPase regulator gene with a distinctive retinitis pigmentosa phenotype in a Chinese family. Mol Vis 2010;16:1620-8.
32. Thiadens AA, Phan TM, Zekveld-Vroon RC, et al. Clinical course, genetic etiology, and visual outcome in cone and cone-rod dystrophy. Ophthalmology 2012;119:819-826.
33. Kong X, Strauss RW, Michaelides M, et al. Visual Acuity Loss and Associated Risk Factors in the Retrospective Progression of Stargardt Disease Study (ProgStar Report No. 2). Ophthalmology 2016;123:1887-1897.
34. Duncker T, Tabacaru MR, Lee W, et al. Comparison of near-infrared and short-wavelength autofluorescence in retinitis pigmentosa. Invest Ophthalmol Vis Sci 2013;54:585-591.
35. Sujirakul T, Lin MK, Duong J, et al. Multimodal Imaging of Central Retinal Disease Progression in a 2-Year Mean Follow-up of Retinitis Pigmentosa. Am J Ophthalmol 2015;160:786-798.e4.
36. Robson AG, Tufail A, Fitzke F, et al. Serial imaging and structure-function correlates of high-density rings of fundus autofluorescence in retinitis pigmentosa. Retina 2011;31:1670-1679.
37. Robson AG, Michaelides M, Luong VA, et al. Functional correlates of fundus autofluorescence abnormalities in patients with RPGR or RIMS1 mutations causing cone or cone rod dystrophy. Br J Ophthalmol 2008;92:95-102.

38. Escher P, Tran HV, Vaclavik V, et al. Double concentric autofluorescence ring in NR2E3-p.G56R-linked autosomal dominant retinitis pigmentosa. Invest Ophthalmol Vis Sci 2012;53:4754-4764.
39. Comander J, Weigel-DiFranco C, Sandberg MA, Berson EL. Visual Function in Carriers of X-Linked Retinitis Pigmentosa. Ophthalmology 2015;122:1899-1906.
40. Verhoeven VJ, Wong KT, Buitendijk GH, et al. Visual consequences of refractive errors in the general population. Ophthalmology 2015;122:101-109.
41. Tideman JW, Snabel MC, Tedja MS, et al. Association of Axial Length With Risk of Uncorrectable Visual Impairment for Europeans With Myopia. JAMA Ophthalmol 2016;134:1355-1363.
42. Beltran WA, Cideciyan AV, Lewin AS, et al. Gene therapy rescues photoreceptor blindness in dogs and paves the way for treating human X-linked retinitis pigmentosa. Proc Natl Acad Sci U S A 2012;109:2132-2137.
43. Beltran WA, Hammond P, Acland GM, Aguirre GD. A frameshift mutation in RPGR exon ORF15 causes photoreceptor degeneration and inner retina remodeling in a model of X-linked retinitis pigmentosa. Invest Ophthalmol Vis Sci 2006;47:1669-1681.
44. Maguire AM, Simonelli F, Pierce EA, et al. Safety and Efficacy of Gene Transfer for Leber's Congenital Amaurosis. N Engl J Med 2008;358:2240-2248.
45. Jacobson SG, Cideciyan AV, Ratnakaram R, et al. Gene Therapy for Leber Congenital Amaurosis caused by RPE65 mutations: Safety and Efficacy in Fifteen Children and Adults Followed up to Three Years. Arch Ophthalmol 2012;130:9-24.
46. Bainbridge J, Mehat M, Sundaram V, et al. Long-Term Effect of Gene Therapy on Leber's Congenital Amaurosis. N Engl J Med 2015;372:1887-1897.
47. Edwards TL, Jolly JK, Groppe M, et al. Visual Acuity after Retinal Gene Therapy for Choroideremia. N Engl J Med 2016;374:1996-1998.

SUPPLEMENTAL MATERIAL

Supplemental Digital Content 1. Data collected for patients with *RPGR*-associated retinal dystrophies

Retrieved data	RP patients, n (%)	COD/CORD patients, n (%)
Longitudinal data available	46 (88)	21 (95)
Only cross-sectional data available	6 (12)	1 (5)
Follow-up time ≥2 years	39 (75%)	18 (82)
Age at onset first symptom	25 (48)	20 (91)
Visual acuity	49 (94)	21 (95)
Refractive error	45 (87)	20 (91)
Electroretinogram pattern	30 (58)	18 (82)
Goldmann visual field	25 (48)	6 (27)
Fundus autofluorescence	15 (29)	11 (50)
OCT	15 (29)	12 (55)
Heidelberg SD-OCT	14 (27)	11 (45)
Zeiss	-	1 (5)
Topcon	4 (8)	-

RP, retinitis pigmentosa; COD, cone dystrophy; CORD, cone-rod dystrophy; OCT, Optical Coherence Tomography; SD-OCT, Spectral Domain Optical Coherence Tomography.

Supplemental Digital Content 2. Mutations in the *RPGR* gene found in this cohort

Diagnosis	Exon	Nucleotide	Protein	N patients (n families)	Reference
RP	1	c.27del	p.(Asp10Ilefs*58)	7 (1)	This study
RP	3	c.248-28_248-10del	p.(?)	1 (1)	This study
RP	5	c.423del	p.(Ile142Leufs*14)	1 (1)	This study
RP	5	c.425T>G	p.(Ile142Ser)	3 (1)	This study
RP	6	c.485_486del	p.(Phe162Tyrfs*4)	1 (1)	Sharon et al. 2000
RP	7	c.706C>T	p.(Gln236*)	1 (1)	Buraczynska et al. 1997
CORD/RP*	10	c.1246-?_*1091-?	Deletion after exon 10	3 (2)	This study
RP	11	c.1345C>T	p.(Arg449*)	2 (1)	Breuer et al. 2002; Demirci et al. 2003
RP	14	c.1573-?_1753+?del	p.(Lys525Argfs*17)	1 (1)	This study
RP	ORF15	c.1773_1776del	p.(Gly592Glnfs*9)	1 (1)	This study
RP	ORF15	c.2236_2237del	p.(Glu746Argfs*23)	5 (4)	Vervoort et al. 2000
RP	ORF15	c.2237_2241del	p.(Glu746Glyfs*22)	2 (1)	This study
RP	ORF15	c.2323_2324del	p.(Arg775Glufs*59)	2 (1)	Breuer et al. 2002
RP	ORF15	c.2362_2366del	p.(Glu788Argfs*45)	4 (2)	This study
RP	ORF15	c.2405_2406del	p.(Glu802Glyfs*32)	9 (4)	Vervoort et al. 2000; Breuer et a.l 2002; Andreasson et al. 2003
CORD	ORF15	c.2426_2427del	p.(Glu809Glyfs*25)	3 (1)	Vervoort et al. 2000, Breuer et al. 2002; Andreasson et al. 2003; Jin et al. 2006
RP	ORF15	c.2730_2731del	p.(Glu911Glyfs*167)	1 (1)	Vervoort et al. 2000
RP	ORF15	c.2838_2839del	p.(Glu947Glyfs*131)	1 (1)	Pelletier et al. 2007
RP	ORF15	c.2840dup	p.(Glu949Glyfs*130)	4 (1)	Neidhardt et al. 2008
COD	ORF15	c.2950G>T	p.(Glu984*)	1 (1)	This study
CORD/RP*	ORF15	c.2959G>T	p.(Glu987*)	3 (1)	This study
RP	ORF15	c.2964_2965del	p.(Glu989Glyfs*89)	1 (1)	Garica-Hoyos et al. 2006
RP	ORF15	c.2993_2996del	p.(Glu998Glyfs*90)	3 (1)	Vervoort et al. 2000
RP	ORF15	c.3011_3012del	p.(Glu1004Glyfs*74)	1 (1)	Sharon et al. 2003
COD	ORF15	c.3039_3040del	p.(Glu1014Glyfs*64)	1 (1)	Zahid et al. 2013

*Multiple diagnoses within one family.

Nucleotide changes in cDNA are noted with transcript NM_001034853.1 as reference.

COD, cone dystrophy; CORD = cone-rod dystrophy; RP, retinitis pigmentosa.

Supplemental Digital Content 3. Patients with asymmetry in visual acuity

Study ID	Diagnosis	Presumed cause of asymmetry
11	RP	Unknown
15	RP	Recurring anterior uveitis in the worse seeing eye after an exudative retinal detachment due to extensive neovascularization
20	RP	Unknown
28	RP	Unknown
51	RP	Amblyopia, potentially due to strabismus or anisometropia (SER OD -8.625D; OS -7.125D)
62	RP	Unknown
66	RP	More atrophy of the EZ and ELM in the worse seeing eye
72	RP	ERM and subtly more EZ atrophy in the worse seeing eye
76	RP	Unexplained episodes of transient stabbing pain in the worse seeing eye with variable effect on BCVA
95	RP	Unknown
104	RP	Anisometropia, which may point to amblyopia (SER OD -13.5; OS -12.0D)
89	CORD	Unknown, but the worse seeing eye has more extensive peripapillary atrophy
120	CORD	Unknown, subtly more EZ atrophy in the worse seeing eye
131	CORD	Anisometropia, which may point to amblyopia (SER OD -7.25; OS -4.75D)
190	COD	More ELM attenuation in the worse seeing eye

BCVA, best corrected visual acuity; ELM, external limiting membrane; ERM, epiretinal membrane; EZ, ellipsoid zone; ONL, outer nuclear layer; SER, spherical equivalent of the refractive error.

In 3 RP patients (6%), one eye was consistently the better seeing eye by 2-3 Snellen lines until the ages of 14, 18, and 32 respectively, followed by a 10-year period of symmetry in the 14-year old patient, after which the other eye became the better seeing eye by 1-3 lines in all 3 patients. In 1 CORD patient, the left eye was consistently the better seeing eye by 1-3 lines until the age of 76, after which a period of symmetry ensued, followed by the right eye becoming the better seeing eye by 1-3 lines.

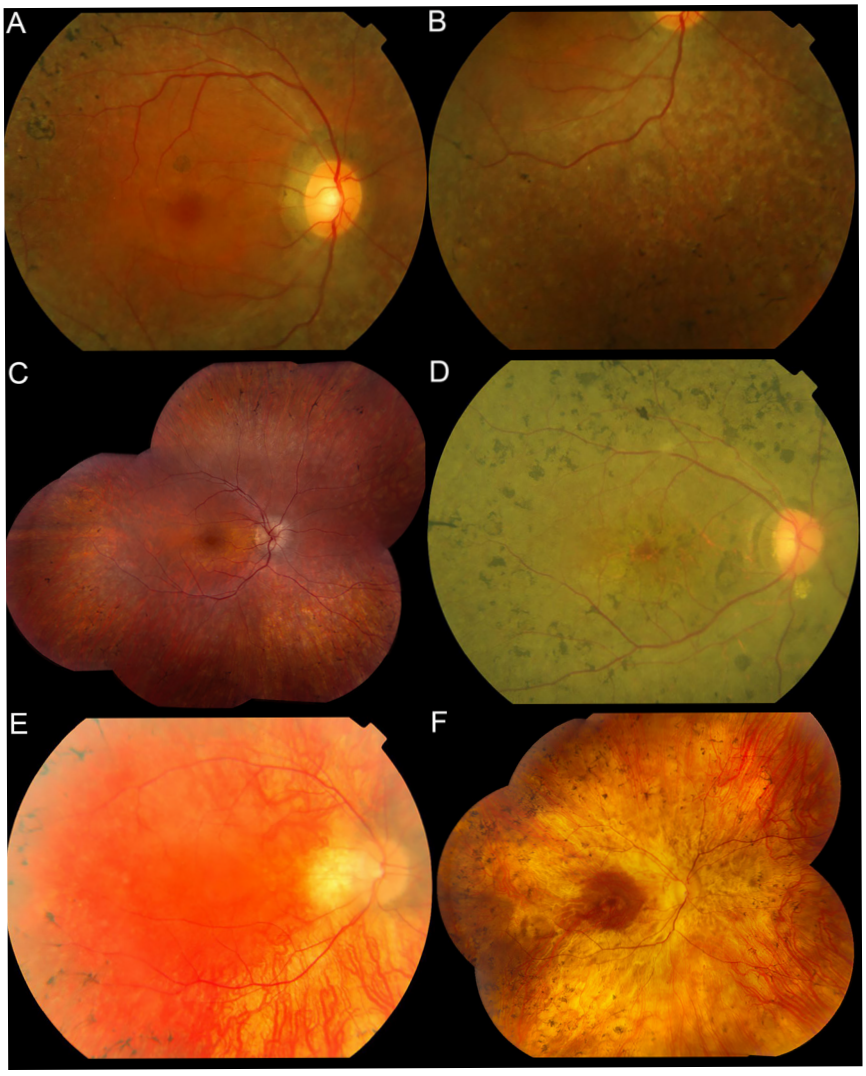

Supplemental Digital Content 4. Fundus photographs of patients with *RPGR*-associated retinitis pigmentosa. **A-B.** Fundus of a 30-year-old Asian patient with a pathogenic frameshift mutation (c.2405_2406del; p.(Glu802Glyfs*156)) in *RPGR*-ORF15 (BCVA in the right eye 20/100; in the left eye 20/67), showing peripapillary atrophy, retinal pigment epithelium atrophy, bone spicule pigmentation in the midperiphery, and yellow-white lesions resembling pseudoreticular-like drusen (arrowhead). **C.** Fundus of a 19-year-old Caucasian patient with a missense mutation (c.425T>G; p.(Ile142Ser)) in exon 5 of *RPGR* (BCVA in the right eye 20/25; in the left eye 20/20), showing a pale optic disc with pseudopapilledema due to optic disc drusen, relative sparing of the foveal retinal pigment epithelium, and scattered bone spicule pigmentation in the (mid-)periphery. **D.** Fundus of a 44-year-old patient with a pathogenic frameshift mutation (c.2405_2406del; p.(Glu802Glyfs*156)) in *RPGR*-ORF15 (BCVA in the right eye 20/100; in the left eye 20/1200) showing atrophic retinal pigment epithelium alterations and coarse hyperpigmentation outside and inside the posterior pole, with an astrocytic hamartoma near the optic disc, which was only found in his right eye. **E.** Fundus of a 28-year-old patient with a frameshift mutation (c.2359_2363del;

p.(Glu788Argfs*45)) in *RPGR*-ORF15 (BCVA in the right eye 20/50; in the left eye 20/67), showing a pale optic disc with temporal peripapillary atrophy, relatively intact retinal pigment epithelium in the posterior pole, and bone spicule pigmentation outside of the vascular arch. **F.** Fundus of a 42-year-old patient with a pathogenic frameshift mutation (c.27del; p.(Asp10Ilefs*58)) in exon 1 (BCVA in both eyes 20/63), showing a pale optic disc, relatively spared retinal pigment epithelium in the fovea surrounded by a ring of atrophy, coarse and bone spicule pigmentations, and visible choroidal vessels in the periphery due to extensive retinal pigment epithelium atrophy.

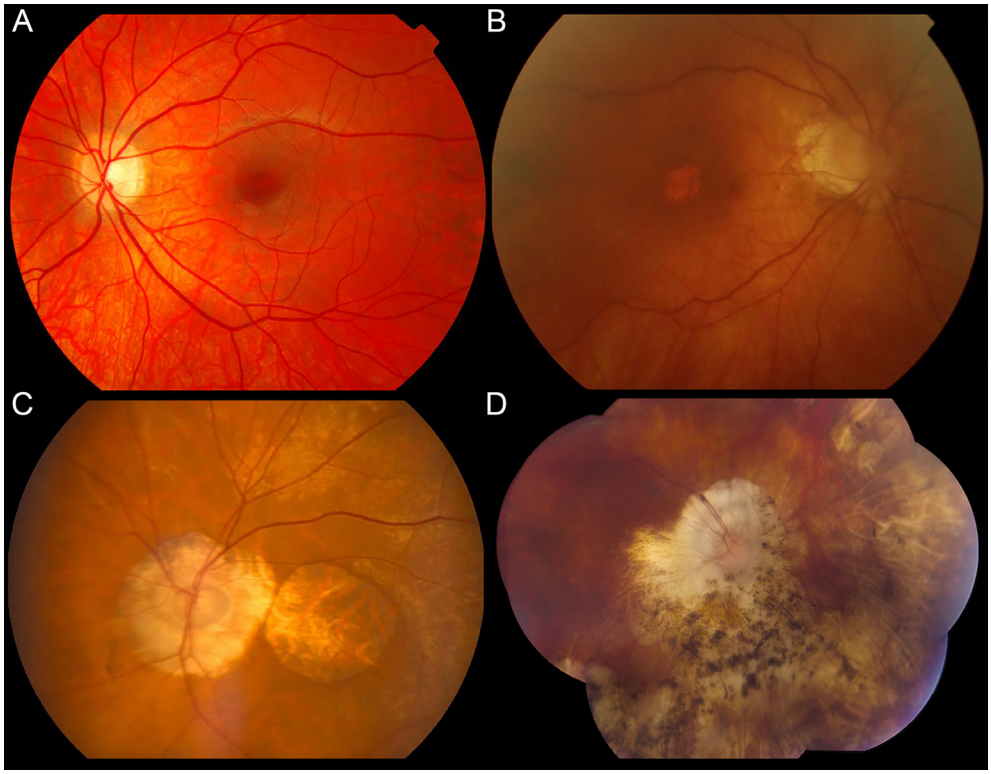

Supplemental Digital Content 5. Fundus photographs of patients with *RPGR*-associated predominantly cone-involving dystrophies. A. Fundus of a 19-year-old COD patient (BCVA in both eyes 20/50) carrying a c.3317dup (p.(Ser1107Valfs*4)) mutation in *RPGR*-ORF15, showing mild mottling alterations of the retinal pigment epithelium in macula, and mild optic disc pallor. **B.** Fundus of a 75-year-old CORD patient with a frameshift variant (c.3300_3301del; p.(His1100Glnfs*10)) in *RPGR*-ORF15 (BCVA in both eyes 20/125), showing peripapillary atrophy and a small region of atrophy in the central macula, surrounded by mild retinal pigment epithelium alterations. The periphery, not depicted here, showed fine salt-and-pepper pigmentation. **C.** Colour fundus photograph of a 79-year-old COD patient (BCVA in the right eye 20/400; in the left eye 2/100) carrying a c.3317dup (p.(Ser1107Valfs*4)) mutation in *RPGR*-ORF15, with sharply demarcated profound chorioretinal and retinal pigment epithelium atrophy in the macula and around the optic disc. In the posterior pole and around the retinal vessels, small and densely packed drusenoid deposits were also visible. **D.** Fundus of an 88-year-old CORD patient with a frameshift mutation (c.3092del; p.(Glu1031Glyfs*58)) in *RPGR*-ORF15 (BCVA in the right eye 20/320; in the left eye 2/100), showing profound atrophy of the retinal pigment epithelium and coarse hyperpigmentation nasally and inferiorly reaching into the macula and around the optic disc.

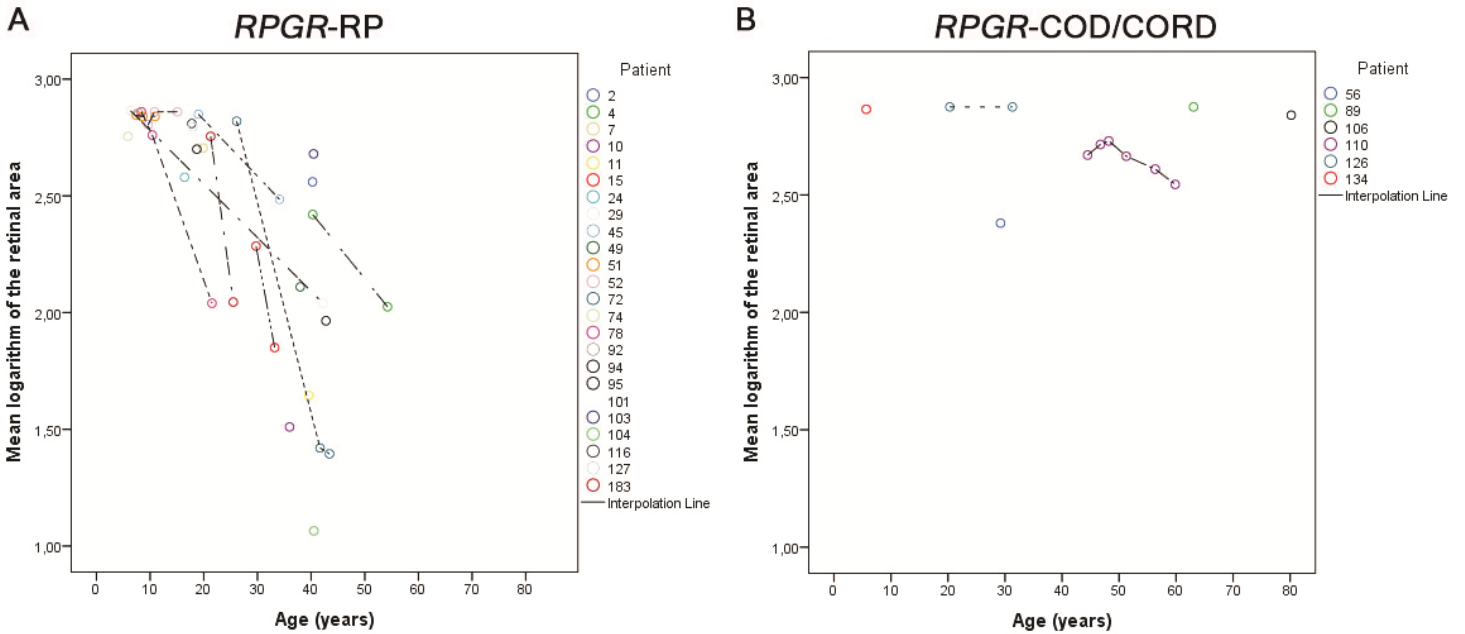

Supplemental Digital Content 6. Individual visual field areas of patients with *RPGR*-associated retinitis pigmentosa (A) and predominantly cone-involving dystrophies (B).

4.2

The spectrum of structural and functional abnormalities in female carriers of pathogenic variants in the *RPGR* gene

Mays Talib, MD[1], Mary J. van Schooneveld, MD, PhD[2], Caroline Van Cauwenbergh, PhD[3,4], Jan Wijnholds, PhD[1], Jacoline B. ten Brink, BAS[5], Ralph J. Florijn, PhD[5], Nicoline E. Schalij-Delfos, MD, PhD[1], Gislin Dagnelie, PhD[6], RD5000 Consortium, Maria M. van Genderen, MD, PhD[7], Elfride De Baere, MD, PhD[4], Julie de Zaeytijd[3], Frans P.M. Cremers, PhD[8], L. Ingeborgh van den Born, MD, PhD[9], Alberta A. Thiadens, MD, PhD[10], Carel B. Hoyng, MD, PhD[11], Caroline C. Klaver, MD, PhD[10,11,12], Bart P. Leroy, MD, PhD[3,4,13], Arthur A. Bergen, PhD[5,14], Camiel J.F. Boon, MD, PhD[1,2]

Invest Ophthalmol Vis Sci 2018;59(10):4123-4133

1 Department of Ophthalmology, Leiden University Medical Center, Leiden, The Netherlands.
2 Department of Ophthalmology, Academic Medical Center, Amsterdam, The Netherlands.
3 Department of Ophthalmology, Ghent University and Ghent University Hospital, Ghent, Belgium.
4 Center for Medical Genetics, Ghent University and Ghent University Hospital, Ghent, Belgium.
5 Department of Clinical Genetics, Academic Medical Center, Amsterdam, The Netherlands.
6 Wilmer Eye Institute, Johns Hopkins University, Baltimore, Maryland, USA.
7 Bartiméus, Diagnostic Centre for complex visual disorders, Zeist, The Netherlands.
8 Department of Human Genetics and Donders Institute for Brain, Cognition and Behaviour, Radboud University Medical Center, Nijmegen, The Netherlands.
9 Rotterdam Eye Hospital, Rotterdam, The Netherlands.
10 Department of Ophthalmology, Erasmus Medical Center, Rotterdam, The Netherlands.
11 Department of Ophthalmology, Radboud University Medical Center, Nijmegen, The Netherlands.
12 Department of Epidemiology, Erasmus Medical Center, Rotterdam, The Netherlands.
13 Ophthalmic Genetics & Visual Electrophysiology, Division of Ophthalmology, The Children's Hospital of Philadelphia, Philadelphia, Pennsylvania, USA.
14 The Netherlands Institute for Neuroscience (NIN-KNAW), Amsterdam, The Netherlands.

ABSTRACT

Purpose: The purpose of this study was to investigate the phenotype and long-term clinical course of female carriers of *RPGR* mutations.

Methods: This was a retrospective cohort study of 125 heterozygous *RPGR* mutation carriers from 49 families.

Results: Eighty-three heterozygotes were from retinitis pigmentosa (RP) pedigrees, 37 were from cone-/cone-rod dystrophy (COD/CORD) pedigrees, and 5 heterozygotes were from pedigrees with mixed RP/CORD or unknown diagnosis. Mutations were located in exon 1-14 and in ORF15 in 42 of 125 (34%) and 83 of 125 (66%) subjects, respectively. The mean age at the first examination was 34.4 years (range, 2.1 to 86.0). The median follow-up time in heterozygotes with longitudinal data (n = 62) was 12.2 years (range, 1.1 to 52.2). Retinal pigmentary changes were present in 73 (58%) individuals. Visual symptoms were reported in 51 (40%) cases. Subjects with both symptoms and pigmentary fundus changes were older than the other heterozygotes ($p = 0.01$) and had thinner foveal outer retinas ($p = 0.006$). Complete expression of the RP or CORD phenotype was observed in 29 (23%) heterozygotes, although usually in milder forms than in affected male relatives. Best-corrected visual acuity (BCVA) was <20/40 and <20/400 in at least one eye in 45 of 116 (39%) and 11 of 116 (9%) heterozygotes, respectively. Myopia was observed in 74 of 101 (73%) subjects and was associated with lower BCVA ($p = 0.006$). Increasing age was associated with lower BCVA ($p = 0.002$) and decreasing visual field size ($p = 0.012$; I4e isopter).

Conclusions: *RPGR* mutations lead to a phenotypic spectrum in female carriers, with myopia as a significantly aggravating factor. Complete disease expression is observed in some individuals, who may benefit from future (gene) therapeutic options.

INTRODUCTION

Pathogenic variants in the *RPGR* gene are associated with a wide variety of severe X-linked retinal degenerations in male patients, including retinitis pigmentosa (RP3), cone-rod dystrophy (CORD), and isolated cone dystrophy (COD).[1-4] Female carriers of X-linked RP usually experience no or mild symptoms and signs of ocular involvement.[5, 6] However, variable degrees of disease expression have been reported,[2, 7-10] and a few studies have shown a correlation between fundus features and retinal function measures.[10, 11] A pathognomic retinal feature in carriers of X-linked RP is the tapetal-like reflex,[5] a golden metallic-luster sheen of the perimacular retina, but this is often absent or only seen in a subset of female carriers of *RPGR* mutations.[8, 12, 13]

Although a wide spectrum of severity has been described in female carriers from RP pedigrees, female carriers from *RPGR*-associated COD/CORD pedigrees usually display no or mild fundus abnormalities.[14, 15] Genotype-phenotype correlations in female carriers of pathogenic variants in *RPGR*, linking the genotype to the degree of disease expression, have rarely been described, as large cohorts of female heterozygotes are scarce.[10]

The recent initiation of a human gene therapy trial for *RPGR*-associated retinal dystrophies in male patients offers a promising therapeutic perspective (ClinicalTrials.gov number: NCT03116113).[16] An optimal insight into the clinical characteristics and variability of disease expression in female carriers of pathogenic *RPGR* variants becomes increasingly important to further understand the phenotypic spectrum. The purpose of this study was to expand our knowledge of the initial and longitudinal clinical characteristics of a large cohort of female carriers of pathogenic *RPGR* variants, and to assess whether upcoming *RPGR* gene therapy trials may consider the inclusion of affected female carriers.

MATERIALS AND METHODS

Study population

This study identified female carriers of disease-causing *RPGR* variants who underwent at least one clinical examination. Inclusion criteria were a molecular confirmation of an *RPGR* mutation or an obligate carrier status. Additionally, two subjects had not undergone molecular genetic analysis, but an *RPGR* mutation was molecularly confirmed in a first-degree relative, along with the presence of a tapetal-like reflex in the female subject, which is considered a pathognomonic sign of XLRP carriership.[11, 17]

Obligate carriers were defined as daughters of an affected father, mothers of at least two affected sons, or mothers of one affected son along with at least one other affected male patient or confirmed carrier in the family, to exclude the possibility of a *de novo* mutation.

Heterozygotes were collected from the database (Delleman database) for genetic eye diseases at the Academic Medical Center (AMC) in Amsterdam, from various other Dutch medical centers within the framework of the RD5000 consortium,[18] and from the Ghent University Hospital in Belgium. Of the 125 included female carriers of pathogenic *RPGR* variants, 21 were from a large Dutch pedigree that has been previously described,[14] and additional follow-up data since the publication of that study was available in three subjects.

The study was approved by the Medical Ethics Committee of Erasmus Medical Center for the Dutch subjects and by the Ethics Committee of Ghent University Hospital for the Belgian subjects and adhered to the tenets of the Declaration of Helsinki. Dutch participants provided informed consent for the use of their clinical data for research purposes. In Dutch subjects who were no longer traceable, the subject-specific information was deleted after data collection and the subjects were pseudonymized. For Belgian subjects, the local Ethics Committee waivered the need for informed consent on the condition of pseudonymization.

Genetic analysis

Of the 125 heterozygotes, 108 had received molecular confirmation of their carrier status through Sanger direct sequencing (n = 71), linkage analyses (n = 35), or whole exome sequencing (n = 2), 15 were obligate carriers with no further molecular analysis, and two nonobligate carriers had a tapetal-like reflex and were first-degree relatives to patients who had received genetic confirmation of an *RPGR* mutation. Mutational analyses were performed at the AMC in Amsterdam, The Netherlands (n = 77), the Radboud University Medical Center in Nijmegen, The Netherlands (n = 2), Ghent University Hospital, Ghent, Belgium (n = 14), or at the Manchester Centre for Genomic Medicine, Manchester, United Kingdom (n = 15).

Clinical data collection

Medical records were reviewed for symptoms, best-corrected visual acuity (BCVA), biomicroscopy, fundus examination, full-field dark- and light-adapted single flash and 30 Hz electroretinography (ffERG) according to the International Society for Clinical Electrophysiology of Vision standards,[19] Goldmann visual field (GVF) examination, spectral-domain optical coherence tomography (SD-OCT), and fundus autofluorescence (FAF) where available. Color vision testing was performed in 45 subjects, using Hardy-Rand-Rittler plates (n = 24), Ishihara plates (n = 26), Farnsworth Panel D15 testing (n = 33), and Farnsworth Tritan plates (n = 23). GVF areas of the V4e and I4e target were digitized and converted to seeing retinal areas in mm^2, using a method described by Dagnelie.[20] Not all subjects underwent all clinical examinations. All FAF images and most SD-

OCT images (n = 41) were obtained with the Heidelberg Spectralis (Heidelberg Engineering, Heidelberg, Germany). For these patients, retinal thickness measurements and segmentation analyses were obtained using the Spectralis software, measuring the total central retinal thickness (from the inner limiting membrane to the basal membrane), outer nuclear layer thickness, and the outer retinal thickness + RPE complex (from the external limiting membrane to the basal membrane). In the other three subjects SD-OCT images were taken with the Topcon (n = 1; 3D OCT-1000; Topcon Medical Systems, Tokyo, Japan) or Zeiss CIRRUS version 6.0 (n = 2; Carl Zeiss Meditec Inc., Dublin, CA, USA).

We categorized fundus status based on previously used criteria,[10, 11] using clinical notes and fundus photographs: grade 0 (no fundus abnormalities); grade 1 (a tapetal-like reflex without pigmentary changes in the retina); grade 2 (regional pigmentary changes, e.g., bone-spicule-like pigmentation, involving at least two quadrants, and/or macular RPE alterations, with or without a tapetal-like reflex); grade 3 (at least three quadrants of pigmentary changes or RPE atrophy in the periphery).

Statistical analysis

Data were analyzed using SPSS version 23.0 (IBM Corp., Armonk, NY, USA). BCVA was divided into the following categories, based on the World Health Organization criteria, adding a category of "mild visual impairment" (BCVA <20/40 and ≥20/67): normal or subnormal visual acuity (BCVA ≥20/40), low vision (BCVA <20/67 and ≥20/200), severe visual impairment (BCVA <20/200 and ≥20/400), and blindness (BCVA <20/400). For statistical analysis, we converted visual acuities to logMAR. We used the unpaired *t*-test, Mann-Whitney test, and chi-square tests to compare means, medians, and proportions, respectively. Longitudinal changes in BCVA and seeing retinal area were analyzed using linear mixed models.

RESULTS

One hundred twenty-five female carriers from 49 families were investigated. Genetic analysis yielded 39 distinct pathogenic *RPGR* variants (Supplementary Table S1). Mutations were located in exon 1-14 and in ORF15 in 41 of 125 (33%) and 84 of 125 (67%) subjects, respectively. Longitudinal data were available for 62 of 125 subjects (50%). In these subjects, the median follow-up time was 12.2 years (interquartile range [IQR]: 12.8; range, 1.1 to 52.2 years), with a median of 4.5 visits per subject (IQR: 5; range, 2 to 31). The follow-up was significantly longer ($p = 0.001$) and more frequent ($p = 0.001$) in subjects with symptoms or pigmentary fundus changes, and in myopic heterozygotes ($p = 0.01$ and $p = 0.002$). The mean age at the first examination was 34.4 years (SD, 17.8; range, 2.1 to 86.0 years).

Symptoms and fundus features

Of the 49 families, 36 (73%) comprised at least one heterozygote with mild to severe symptoms and/or pigmentary fundus changes. At the most severe end of the spectrum of *RPGR* carrier phenotypes, we identified a subset of heterozygotes (n = 29; from 23 pedigrees; Supplementary Figure S1) who displayed extensive intraretinal pigmentary changes or retinal atrophy in at least two quadrants (n = 29), usually with macular RPE alterations or atrophy (26 of 29; 90%), as well as multiple visual symptoms beyond nyctalopia (n = 29), and objectified visual field restriction (27 of 28; 96%; unavailable in n = 1), and/or a BCVA-based visual impairment in at least one eye (23 of 29; 79%), and significantly attenuated scotopic and/or photopic responses on ERG in all cases where an ERG was available (n = 24). There was a significant difference ($p = 0.01$) in mean age between heterozygotes with both symptoms and pigmentary fundus changes (mean, 45.6 years; SD, 18.1; range, 11.7 to 80.2 years) and the other female carriers (mean, 37.7 years; SD, 15.7; range, 7.0 to 86.0 years).

Symptoms were reported by 51 heterozygotes (41%) and included variable degrees of nyctalopia (n = 40; 32%), subjective visual field restriction (n = 17; 14%), subjective central vision decline (n = 29, 23%), and/or photophobia (n = 20; 16%). The presence of symptoms was not associated with the location of the mutation ($p = 0.20$), and no significant genotype-phenotype correlations were found (Supplementary Table S2).

The presence or absence of a tapetal-like reflex was explicitly reported in 60 cases, and was found to be present in 24 of 60 heterozygotes (40%), with no significant age difference between those with and without a tapetal-like reflex ($p = 0.67$), and no significant association between the presence of the tapetal-like reflex and the development of symptoms ($p = 0.54$) or intra-retinal pigmentary changes ($p = 0.37$).

An adequate assessment of both symptomatology and fundus features could be made in 117 subjects. Heterozygotes were asymptomatic and had no pigmentary fundus changes in 35 of 117 cases (30%). Eighty-two heterozygotes (70%) had some degree of disease expression in the form of symptoms and/or pigmentary changes (Table 1): 9 of 117 heterozygotes (8%) had symptoms associated with a retinal dystrophy, without retinal pigmentary changes; 31 of 117 heterozygotes (26%) had retinal pigmentary changes without symptoms; and 42 of 117 heterozygotes (36%) had both symptoms and retinal pigmentary changes.

Of the heterozygotes with retinal pigmentary changes (n = 73), peripheral and midperipheral pigmentations were more marked in the inferior quadrants of the retina in 14 of 73 (19%).
Applying the fundus grading criteria to the last available fundus examination, we were able to distinguish the fundus grade for 117 of 125 heterozygotes (94%; Table 1). An evident change in fundus grade with time was observed in 8 of 117 heterozygotes (7%), and was based either on the new appearance of retinal pigmentary changes (n = 6) in the third to fifth decade of life or on an

increase of previously observed pigmentary changes (n = 2) from one quadrant or hemisphere to at least three quadrants in the fifth decade of life.
Intra-individual asymmetry in the presence or extent of retinal pigmentary changes was noted in 11 of 117 heterozygotes (9%).

Visual acuity
BCVA in the better seeing eye was generally associated with age (0.8% decline/y; $p = 0.002$) and BCVA was lower in individuals with myopia ($p = 0.006$) and with a mutation in exon 1-14 ($p = 0.0003$), but was not significantly associated with the presence of retinal pigmentary changes ($p = 0.17$). BCVA was impaired in at least one eye in 45 of 116 individuals (39%; Figure 1). Mildly impaired visual acuity and low vision in the better seeing eye were seen from the second decade of life onward, whereas blindness was observed from the sixth decade of life onward. BCVA decline in heterozygotes at the most severe end of the spectrum (i.e., full expression of the RP or CORD phenotype) was 1.9%/y ($p = 0.003$). The median BCVA in Dutch male *RPGR* hemizygotes who were related to these affected female carriers was relatively lower ($p = 0.03$) than in the other male patients, despite no significant age difference ($p = 0.39$). The decimal BCVA in female carriers at the last visit, averaged between eyes, was lower in those with exon 1-14 mutations (median BCVA, 0.55; IQR: 0.6; range, light perception to 1.125) than in those with ORF15 mutations (median BCVA, 0.9; IQR: 0.5; range, light perception to 1.6; $p = 0.002$). However, the median BCVA was also lower in heterozygotes from RP pedigrees ($p = 0.00001$) than in those from COD/CORD pedigrees, and mutations in exon 1-14 were almost exclusively found in RP pedigrees. We therefore investigated these genotype-phenotype correlations further by stratifying between heterozygotes from RP pedigrees and COD/CORD pedigrees and analyzing genotype-phenotype correlations within those groups. After this stratification, no difference between heterozygotes with exon 1-14 and those with ORF15 mutations was found ($p = 0.10$). Color vision testing identified a deuteranopic (n = 3), combination deuteranopic and tritanopic (n = 3), unspecified (n = 5), or total (n = 1) deficiency in 12 of 45 (27%) of subjects.

A strong intraindividual symmetry in BCVA was observed (Spearman's correlation coefficient = 0.65; $p < 0.00001$). An intraindividual difference in BCVA between eyes of ≥15 ETDRS letters (0.3 logMAR) at two consecutive examinations or only examination in the case of one BCVA measurement, was found in 31 of 116 (27%), and was most likely attributable to anisometropic amblyopia (interocular difference of ≥2 diopters [D]; n = 10), amblyopia associated with strabismus (n = 3), amblyopia with unclear cause (n = 4), asymmetry in cataract (n = 1), unilateral stronger disease expression (n = 5), or an unknown cause (n = 8). A myopic refractive error (below -0.75D) was found in 74 of 101 (73%) heterozygotes (Table 1), using the last phakic refractive error in the case of pseudophakia (n = 8) or laser-assisted in situ keratomileusis (n = 4). Myopia-associated posterior staphyloma (n = 4), lacquer cracks (n = 4), Fuchs spot (n = 1), and patchy chorioretinal atrophy (n = 8) were reported in 16 subjects. Anisometropia was present in 34 of 101 (34%) subjects.

Table 1. Clinical characteristics of *RPGR* heterozygotes

Characteristics	All (n = 125)	Origin RP pedigree (n = 83)*	Origin COD/CORD pedigree (n = 37)*	*P*-value
Exon 1-14, n (%)	42 (34)*	38 (46)	-	**<0.00001**
ORF15, n (%)	83 (66)	45 (54)	37 (100)	
Median refractive error (IQR; range), D†	-3.6 (8.6; -21.25D - +4.13D)	-5.5 (8.4; -21.25D +4.13D)	-1.0 (3.4; -17.25D - +2.38D)	**0.01**
High myopia (< -6D), n (%)	36/102* (35)	31/68 (46)	5/29 (17)	**0.007**
Moderate myopia (-3D > SER ≥ -6D), n (%)	22/102 (22)	17/68 (25)	4/29 (14)	
Mild myopia (-0.75D > SER ≥ -3D), n (%)	16/102 (16)	6/68 (9)	8/29 (28)	
≥-0.75D	28/102 (27)	14/68 (21)	12/29 (41)	
Cataract, n (%)	33/107 (31)	27/72 (38)	5/32 (16)	**0.02**
SPC, n	9	8	1	
Other or unspecified, n	24	19	4	
Fundoscopic examination				
Optic disc pallor, n (%)	32/94 (34)	26/58 (45)	6/33 (18)	**0.02**
Peripapillary atrophy, n (%)	36/94 (38)	29/58 (50)	7/33 (21)	**0.02**
Vascular attenuation, n (%)	40/93 (43)	35/62 (56)	5/28 (18)	**0.001**
Fundus grade assessable	117*	79	34	
Grade 0, n (%)	21 (17)	12	8	
Grade 1, n (%)	11 (9)	6	4	
Grade 0 or 1, n (%)‡	12 (10)	8	4	
Grade 2, n (%)	43 (34)	34	8	
Grade 3, n (%)	17 (14)	13	4	
Grade 2 or 3, n (%)‡	13* (10)	6	6	
Pigment changes, any type, n (%)	73/117* (62)	53/79 (67)	17/34 (50)	0.10
Bone spicule-like/round, n (%)	46* (37)	39	6	
Salt-and-pepper, *n* (%)	4 (4)	2	2	
Macular RPE alterations/atrophy, n (%)	40 (32)	31	8	0.08
Mean age at macular RPE involvement ± SD, y (range)	43.6±17.5 (12.2-77.7)	44.1±18.2 (12.2-77.7)	43.2±15.8 (21.4-59.3)	0.90
RPE alterations in periphery, n (%)	37 (29)	23	14	
Tigroid/tessellated fundus, *n* (%)	15 (12)	8	7	

ERG pattern§	59*	44	11	
No abnormalities, n (%)	11 (19)	7 (11)	4 (36)	0.06‖
Subnormal/low-to-normal amplitudes, n (%)	6 (10)*	4	1	
Electronegative, n (%)¶	2 (3)	2	-	
Rod-cone, n (%)	9 (15)	9	-	
Reduced rods and cones, no predominance specified, n (%)	19* (32)	17#	1	
Cone-rod, n (%)	8 (14)	2	4	
Isolated cone reduction, n (%)	2 (3)	1	1	
Nondetectable, n (%)	2 (3)	2	-	

Significant *p* values (<0.05) are indicated in bold. SER, spherical equivalent of the refractive error; SPC, subcapsularis posterior cataract.

* Five heterozygotes with mutations in exon 1-14 (n = 4) or ORF15 (n = 1) were not included in the columns distinguishing based on pedigree (RP or COD/CORD), as the diagnosis in the pedigrees could not be established or confirmed in four subjects, and one heterozygote with a mutation in exon 10 (deletion after exon 10) was from a mixed RP/CORD pedigree.

† Averaged between eyes.

‡ In 18 (20%) carriers, no distinction between fundus grades 0 and 1 (n = 9; 10%) or 2 and 3 (n = 9; 10%) could be made based on the notes in the medical record. In seven (8%) heterozygotes, no sufficient data on their fundus appearance were available to estimate the fundus grade.

§ One of the heterozygotes with nondetectable responses had previously documented rod-cone responses. One heterozygote with anisometropia had significantly reduced rod and cone amplitudes in her highly myopic eye, and normal amplitudes in her mildly myopic eye.

‖ Fisher's exact test.

¶ Markedly reduced b-wave with a response resembling an electronegative ERG.

One heterozygote had significantly reduced rod and cone amplitudes in one eye (OS), but normal amplitudes in OD. Other measures of visual function (GVF, BCVA) in this subject showed marked asymmetry in favor of OD.

Full-field ERG and visual field findings

ERGs, available for 59 heterozygotes, showed significantly reduced amplitudes in various patterns in 42 of 59 (71%) heterozygotes (Table 1), with no significant age difference between heterozygotes with normal and those with attenuated responses (p = 0.9). Pigmentary fundus changes were present in 37 of 42 (88%) heterozygotes with significantly reduced ERG amplitudes, and 32 of 42 (76%) had visual symptoms. Heterozygotes with reduced scotopic or photopic amplitudes were significantly (p = 0.005) more myopic (mean, -8.4 D; SD, 6.1) than those with normal amplitudes (mean, -3.3 D; SD, 3.6), although mild (4 of 13), moderate (2 of 13), and high myopia (3 of 13) were also found in those with normal ERG amplitudes.

Between heterozygotes, little intrafamilial variability was seen, as heterozygotes with abnormal ERGs tended to cluster within families. However, intrafamilial differences between heterozygotes and male hemizygotes were observed: five heterozygotes from different pedigrees had a cone- or cone-rod pattern on ERG whereas their affected male relatives had RP.

Goldmann visual fields, available for 53 heterozygotes (106 eyes), showed variable degrees of sensitivity reduction in 46 of 53 subjects (87%; Supplementary Figure S2; Supplementary Table S3), with a unilateral sensitivity reduction in two subjects and relatively more severely affected superior hemifields in 13 subjects. Age was associated with the I4e isopter size (decline rate 4.9%/y; p = 0.012), but not with the V4e isopter size (p = 0.06).

Of the 90 eyes with variable degrees of sensitivity reduction, 69 (77%) had peripheral retinal pigment changes or chorioretinal atrophy. Heterozygotes had a better preserved visual field than their age-matched affected male relatives, with three exceptions from one family (Supplementary Figure S2).

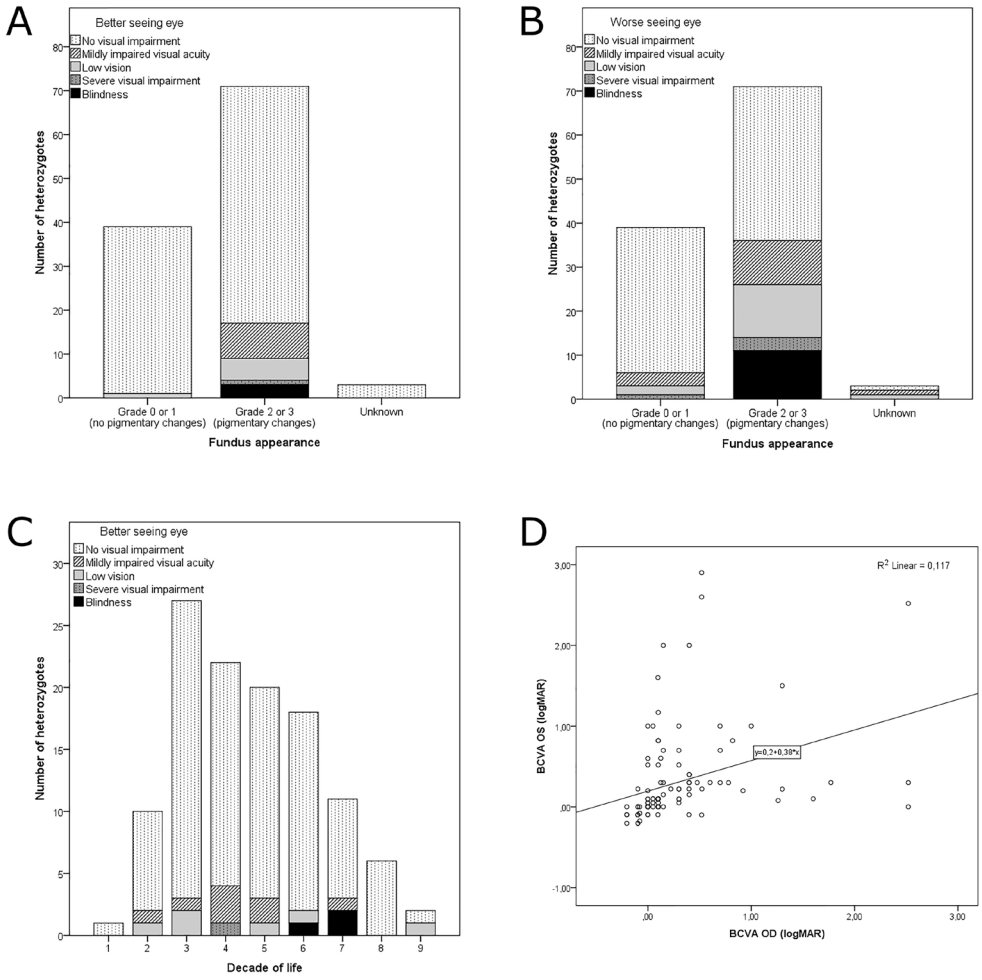

Figure 1. Bar chart of visual impairment category by fundus appearance and by decade of life. Visual impairment in the better (**A**) and worse (**B**) seeing eye, stratified by fundus appearance. **C.** Visual impairment in the better seeing eye, by decade of life, showing a general trend toward visual impairment with increasing age, although the visual acuity in the better seeing eye remains favorable. **D.** The relation of the BCVA in logMAR between the right and left eye, showing a not fully linear relationship. The Spearman's correlation coefficient, taking into account this nonlinear relationship, showed a fair symmetry in visual acuity between eyes (0.64).

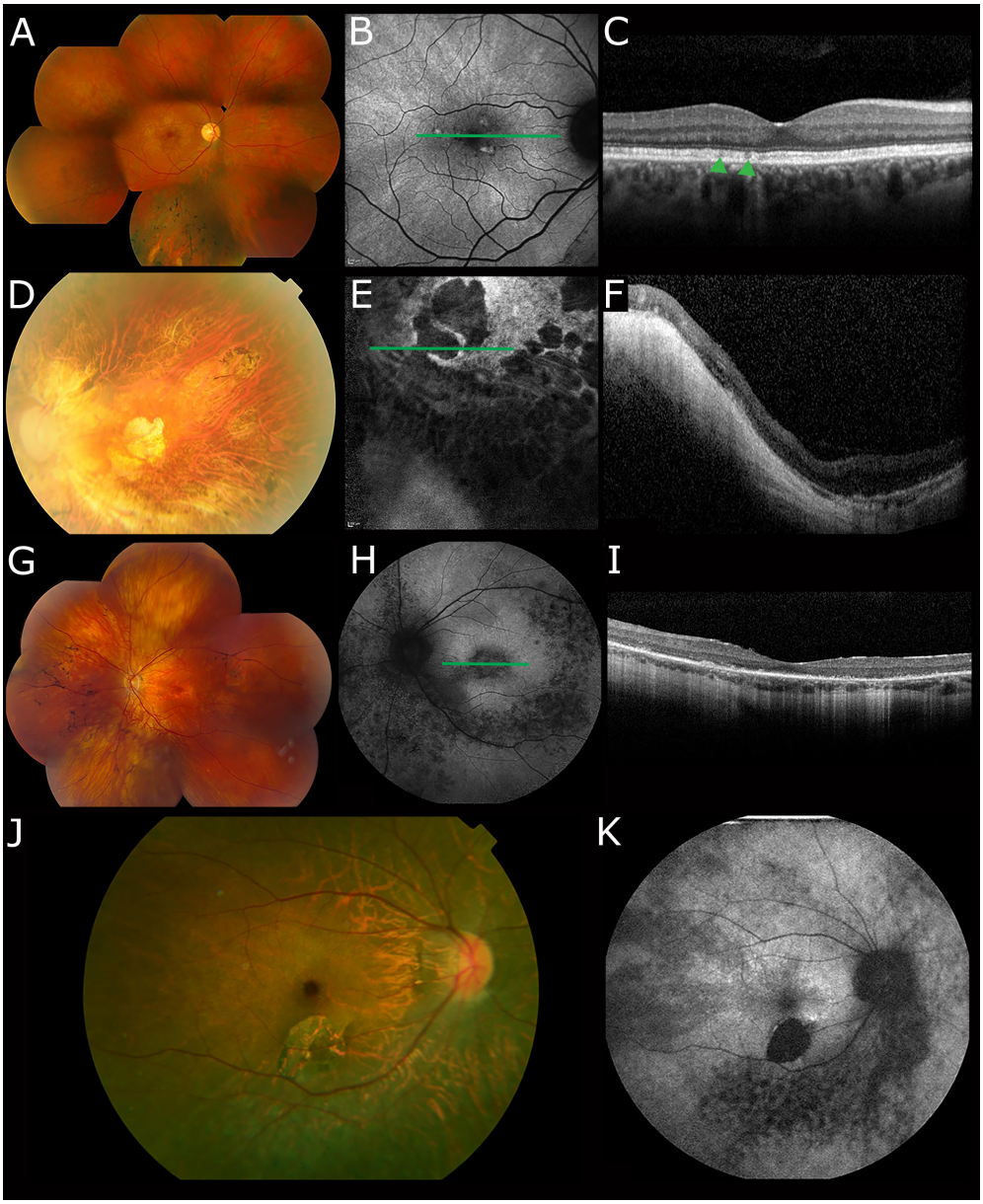

Figure 2. Multimodal imaging illustrating the phenotypical spectrum of *RPGR* heterozygotes from pedigrees of RP. A-C. The right eye of a 48-year-old heterozygote (ORF15: c.2200G>T) with optimal BCVA, sectorial pigmentary changes consistent with RP (**A**). On FAF with a 30° field of view (**B**), a radial pattern of different AF is clearly visible. FAF further shows small hyper-AF spots surrounded by a hypo-AF border, that colocalize with small hyporeflective ellipsoid zone irregularities on SD-OCT (**C**, *green arrowheads*). The appearance of a thick outer plexiform layer may indicate a non-well-aligned scan. **D-F.** The left eye of a 65-year-old highly myopic (-11 D) heterozygote (exon 3: c.248-28_248-10del) with light perception vision OU, showing a posterior staphyloma (**D**), an atrophic retina with

partially obliterated vessels, and bone-spicule pigmentations in the midperiphery (not shown). FAF with a 30° field of view (**E**) shows extensive patches of absent AF, but areas of normo-AF and hyper-AF are visible. SD-OCT (**F**) shows atrophy of all retinal layers, and the ellipsoid zone and external limiting membrane are not discernible. The markedly thinned, almost absent choroid points to an important myopic degenerative factor. **G-I.** The left eye of a 46-year-old moderately myopic heterozygote (ORF15: c.2536G>T) with RP and a decimal BCVA of 0.3/0.5. Her fundus shows vascular attenuation, bone-spicule pigmentation in the midperiphery, and alterations of the RPE in the macula (G). FAF imaging with a 55° field of view (**H**) shows an oval zone of mottled hypo-AF around the fovea, and more coarsely mottled hypo-AF in the perimacula and midperiphery, mainly nasal to the optic disc. The corresponding SD-OCT scan (**I**) shows generalized severe attenuation of the outer retinal layers, with only scattered granular remnants of the ellipsoid zone. The ONL is nearly absent outside of the fovea. **J-K.** The right eye of a 34-year-old highly myopic (-16 D) heterozygote (ORF15: c.2010del), whose fundus photograph (**J**) shows a paracentral patch of retinal atrophy, corresponding on FAF imaging with a 55° field of view (**K**) with a patch of absent AF. FAF further shows a ring of relative hyper-AF surrounding a normal fovea, and mottled areas of hypo-AF around the vascular arcade, more distinctly in the inferior retina.

Findings on retinal imaging

SD-OCT imaging of the macula in 47 heterozygotes showed a preservation of all retinal layers in 22 subjects (15 of 22 with peripheral retinal pigmentary changes; 4 of 22 with central RPE alterations), but showed outer retinal attenuation in 25 heterozygotes (53%), with relative foveal sparing in 23 of these subjects. There was no significant age difference between heterozygotes with outer retinal attenuation on SD-OCT (mean, 44.7 years; SD, 20.3; range, 11.7-80.0 years) and those with normal outer retinas on SD-OCTs (mean, 37.2; SD, 12.8; range, 14.3-59.8 years). Spearman's correlation testing showed no significant correlation between age and central retinal thickness (CRT; $p = 0.81$), foveal outer nuclear layer (ONL) thickness ($p = 0.67$), or thickness of the outer retinal layers ($p = 0.85$). The degree of attenuation varied from mild to moderate peripheral macular thinning of the ellipsoid zone, the external limiting membrane, and/or the outer nuclear layer (n = 12), to a nearly complete absence of these layers with only (para-)foveal remnants (n = 8 complete RP/CORD expression; Figures 2, 3), or a peripheral macular absence of these layers with only foveal and parafoveal granular remnants (n = 2; complete COD/CORD expression; Figure 3), whereas two remaining heterozygotes with RP had no foveal remnants of these layers. One additional subject had unilateral (para-)foveal attenuation of the ellipsoid zone after resolution of a Fuchs spot. No anatomical correlates were observed for the tapetal-like reflex on SD-OCT. Median CRT, ONL, and outer retinal layers + RPE complex thickness measured in the fovea were 220 µm (IQR, 28; range, 126 to 292), 95 µm (IQR, 23; range, 46 to 148), and 96 µm (IQR, 13; range, 42 to 115), respectively. Subjects with symptoms and pigmentary fundus changes had a significantly thinner foveal outer retina ($p = 0.006$), but no significantly thinner CRT ($p = 0.28$) or ONL ($p = 0.21$).

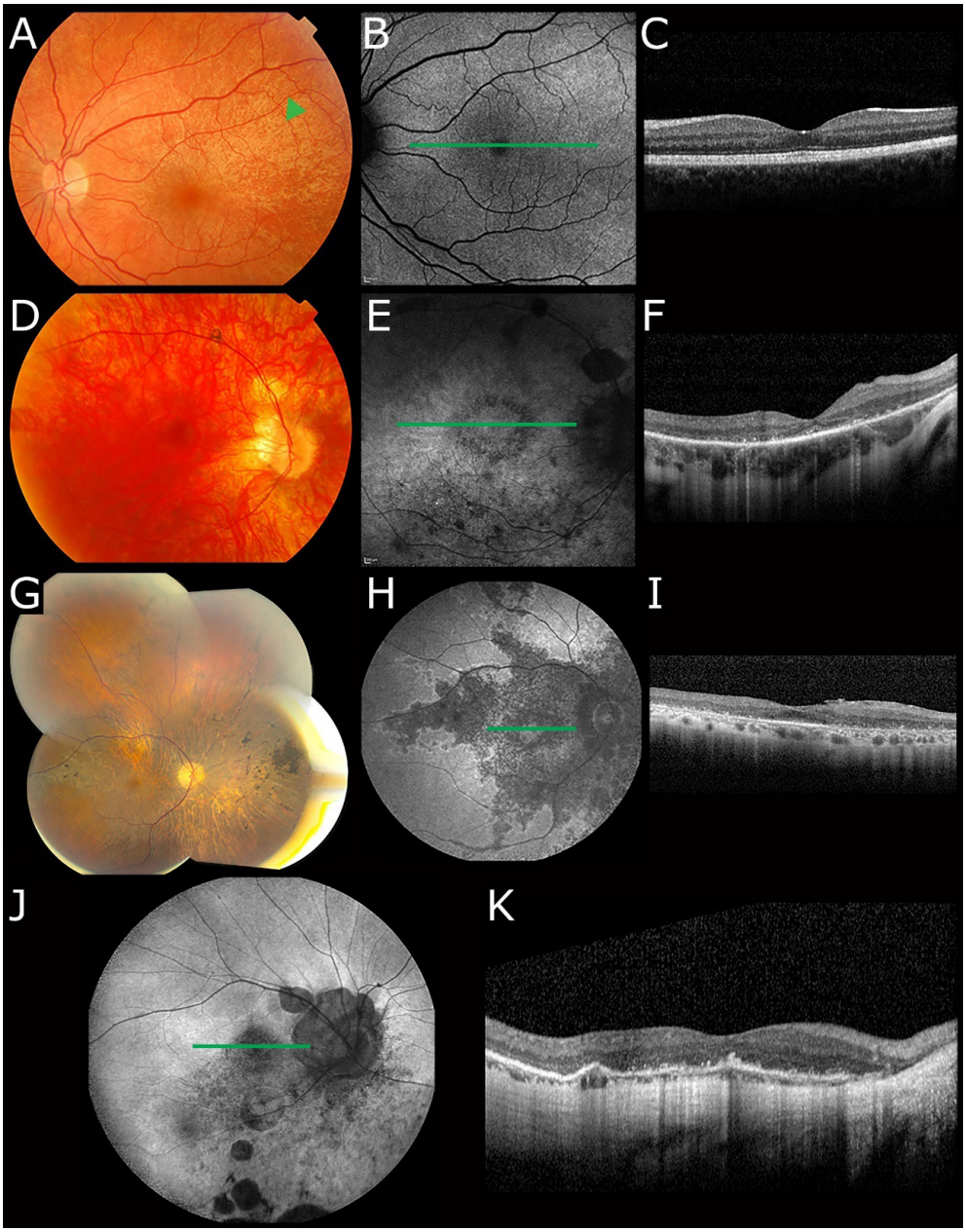

Figure 3. Multimodal imaging illustrating the phenotypical spectrum of *RPGR* heterozygotes from pedigrees of CORD. A-C. The left eye of a 32-year-old heterozygote (ORF15: c.2426_2627del) with optimal BCVA, a tapetal-like reflex on fundus photography (**A**) and FAF with a 30° field of view (**B**), and a normal appearance of the retina on SD-OCT (**C**). **D-F.** The right eye of a highly myopic (-13.5 D) 36-year-old heterozygote (ORF15: c.3092del) with a CORD phenotype and a BCVA of 0.5/0.1, showing peripapillary atrophy and a paravascular patch of chorioretinal atrophy. On FAF with a 30° field of view (**E**), mottled and granular hypo-AF changes are seen, predominantly along the

vascular arcade, with a granular hypo-AF ring around the central macula and a sharply demarcated patch of absent AF along the upper vascular arcade. A radial pattern can be discerned in the perimacular region around the hypo-AF ring. SD-OCT (**F**) shows severe extrafoveal and foveal attenuation of the outer retinal layers, ellipsoid zone, and external limiting membrane, with some granular and mottled remnants of the hyperreflective outer retinal bands. Outside of the fovea, the ONL is barely discernible. **G**-**I.** The right eye of a 63-year-old mildly myopic heterozygote (ORF15: c.2575G>T) with CORD. Fundus photography (**G**) shows extensive outer retinal atrophy in the posterior pole and (mid)periphery, with patches of relatively preserved retina, and bone-spicule pigmentations in the (mid) periphery, encroaching on the posterior pole. FAF with a 55° field of view (**H**) shows a large zone of hypo-AF in the macula, encompassing the peripapillary region and extending into the midperiphery, surrounded by a hyper-AF border. The corresponding SD-OCT scan (**I**) shows an overall attenuation of the outer retina, with granular remnants of the ellipsoid zone. The ONL is discernible in the fovea and direct parafovea but is nearly absent in the perimacula. **J**-**K.** The right eye of a 56-year-old highly myopic (-14.5 D) heterozygote (ORF15: c.3092del; maternal aunt of subject in (**D**-**F**) with CORD, with a BCVA of 0.1 OU. FAF with a 55° field of view of the right eye (**J**) shows peripapillary atrophy, sharply demarcated patches of absent AF along the upper and lower vascular arcade and below the vascular arcade, and a mottled decrease of AF in the posterior pole and below the vascular arcade. Some radial pattern can be detected outside of the vascular pole. SD-OCT (**K**) shows an atrophic ONL, a scarcely visible external limiting membrane, and a granular ellipsoid zone. As in Figure 2F, the thinned choroid points to an important myopic degenerative factor.

FAF imaging in 40 heterozygotes showed abnormalities in 32 subjects (Figures 2, 3), including a radial pattern in 26 of 40, mottled, granular, or patchy hypo-autofluorescent changes including in areas that appeared unaffected on fundoscopy or fundus photography in the posterior pole in 13 of 40, in the periphery in 17 of 40, and patchy areas of absent autofluorescence in seven highly myopic subjects (Figures 2, 3). Of the 26 carriers with a radial pattern on FAF, the tapetal-like reflex had not been detected on fundoscopy or fundus photography in 15 of 26 (58%). In the eight carriers without a radial pattern or other abnormalities on FAF, the fundus showed no RPE changes (n = 4), RPE atrophy in the periphery (n = 1), granular RPE alterations in the central macula (n = 1), or had not been documented (n = 2).

DISCUSSION

In this retrospective cohort study, we describe the phenotypic spectrum of 125 female carriers of pathogenic *RPGR* variants, from 49 pedigrees of RP and COD/CORD. This study is one of the largest studies on female *RPGR* carriers to date, and we identified a number of novel structural and functional characteristics, also in comparison to affected male relatives.

Signs and/or symptoms were common (70%) both in the RP and COD/CORD carrier groups, in carriers of mutations in exon 1-14 as well as in carriers of ORF15 mutations, with complete expression of RP or CORD in 29 heterozygotes (23%). Although the longitudinal results are

probably biased, as the follow-up was significantly longer and more frequent in heterozygotes with myopia or pigmentary changes, our results indicate that clinically severe phenotypes are not rare in heterozygous female *RPGR* mutation carriers.

Female carriers of X-linked retinal dystrophies have been reported to express RP characteristics,[21, 22] sometimes partial or sectorial, albeit in small cohorts.[7, 11, 17, 23] This variability has challenged the ability to identify the accurate disease inheritance mode in families with affected female patients.[24-26] In the early stages of genetic counselling of an RP pedigree, the presence of affected female subjects should raise suspicion of both an autosomal-dominant and an X-linked inheritance mode. In fact, typical RP fundus features, such as bone-spicular or nummular intraretinal pigmentation, optic disc pallor, and vascular attenuation, were common in this cohort, expectedly more so in heterozygotes from RP pedigrees (49%, 44%, and 56%; respectively; Table 1) than in those from COD/CORD pedigrees (18%, 18%, 18%, respectively). Previous reports have shown that female carriers of X-linked COD/CORD usually show either no or minimal fundus changes,[14, 27] but cases of heterozygotes displaying macular RPE alterations have been described,[15] and our cohort further expands this phenotypic spectrum, showing the frequent involvement of macular retina (32%; Table 1), including cases of full COD or CORD expression.

Myopia was associated with a lower BCVA, and high myopia (below -6 D) was found in a similar incidence as in the male cohort we previously investigated (35% in heterozygotes versus 38% in male hemizygotes), with 12% showing a tessellated fundus, four cases of posterior staphyloma, and eight cases of highly myopic patchy chorioretinal atrophy. Although the reasons for the association between *RPGR* mutations and high myopia remain unclear, a recent study analyzing refractive errors in inherited retinal dystrophies has postulated that the transport area between the inner and outer segment (i.e., the location of protein RPGR), is one of the critical sites for refractive error development.[28] Mutations in *RP1* and *RP2*, encoding an outer segment protein and another connecting cilium protein, respectively, have also been linked to high myopia,[29, 30] further corroborating this hypothesis. However, not all genes encoding connecting cilium proteins are associated with myopia, and some have been associated with hyperopia (e.g., *CEP290* and *RPGRIP1*), and biallelic mutations in these are generally associated with much more extreme visual loss due to Leber congenital amaurosis.[31, 32] The presence of (high) myopia in *RPGR* heterozygotes with no photoreceptor dysfunction on ERG supports the notion that photoreceptor degeneration and high myopia might be two parts of the same disease, although the association between high myopia and reduced rod/cone amplitudes would support the concept of scleral remodeling stimulation by signals from dysfunctional photoreceptors and/or more frequent near-focusing due to reduced BCVA. However, the interpretation of the latter is confounded by the association of high and degenerative myopia with reduced ERG amplitudes.[33]

The occurrence of a BCVA below 20/200 in at least one eye (13%; Figure 1) in this cohort was higher than in an earlier longitudinal report in a cohort of XLRP-carriers from a combination of genotyped and ungenotyped families, which reported this BCVA in 2%.[10] In keeping with earlier reports, abnormal GVF (46 of 53; 87%) and ERG (42 of 59; 71%) results were more common than pigmentary changes (73 of 117; 62%) or BCVA impairment (13%, 3%, and 9% low vision, severe visual impairment, or blind in one eye, respectively).[10, 11] However, GVF and ERG were consistently performed only in a subset of heterozygotes, as was the case in this retrospective cohort, and the availability of these test results may thus be subject to bias, as additional testing may have mostly been performed in heterozygotes with symptoms or signs of disease. However, even when assuming that all heterozygotes without additional testing would have no abnormalities, our study shows that a relatively large proportion of heterozygotes experience variable degrees of visual field constriction (46 of 125; 37%) or significant amplitude reduction on ERG (42 of 125; 34%).

Although there was noticeable intrafamilial variability in certain cases, heterozygotes with signs and/or symptoms of disease tended to originate from the same pedigrees. However, this aggregation may be overestimated, as possible (nonobligate) heterozygotes without signs or symptoms may never seek specialist advice from a geneticist or ophthalmologist. The intra- and interfamilial spectrum of severity in heterozygotes of X-linked retinal disorders has been at least partially attributed to the role of X-chromosome inactivation.[34, 35] Based on this X-chromosome inactivation, Dobyns et al.[36] proposed a penetrance and severity index for X-linked diseases, as opposed to using the terminology of X-linked dominant, semidominant, or recessive inheritance, as this concept is not based on X-inactivation in humans, but on the X-transcription speed and dosage compensation in the *Drosophila* model. Random X-inactivation is proposed to occur early in embryonic development, in each cell independently,[37] and would result in a mosaic pattern of cells expressing the normal and mutated gene. Our finding of a radial pattern on the available FAF images in 65% of the examined carriers, even in those who had no tapetal-like reflex on fundoscopy, indicates that FAF may be particularly helpful in detecting such retinal mosaicism. This radial pattern on FAF would support the earlier suggestion that X-inactivation might not occur in each cell independently, but in clusters of cells in a similar pattern,[38] followed by a centrifugal radial growth of the neuroretina during embryonic development.[8] However, random X-inactivation does not fully explain the clustering of nearly complete penetrance in several families in this cohort. There may be a role for skewed X-inactivation, in which the mutant allele is disproportionally (in)active. Extremely skewed X-inactivation has been shown in specific mutations in some non-retinal X-linked disease genes,[39, 40] and has been in favor of the nonmutated allele. Secondary X-inactivation skewing may manifest through a selective (dis)advantage for cells with the mutation-containing X-chromosome,[41] which may be hereditary.[42] The relative family-based, rather than mutation-based, aggregation of affected heterozygotes in this cohort, along with cases of intrafamilial variability, points to a highly likely role of genetic and/or environmental modifiers, as well as potentially skewed X-inactivation. Intraindividual asymmetry was a recurring finding in

this cohort. Left-right asymmetry in X-chromosome inactivation in several paired structures of the body, such as the retina, has been observed, but the biological basis remains unclear. Other than few reports on asymmetrical ERG responses in small numbers of heterozygotes from X-linked RP or COD/CORD pedigrees,[17, 43] this clinical asymmetry has remained largely unexplored. We found a high general correlation between the right and left eye in this cohort, but notable asymmetry in fundus phenotype (9%), in V4e or I4e size on GVF (20%), BCVA (26%), and refractive error (33%) was still observed.

As 23% of heterozygotes display a complete RP or COD/CORD phenotype, with a yearly BCVA decline rate of 1.9%, the question ensues if these heterozygotes may benefit from future therapeutic options. Recently, a submacular gene therapy trial for male patients with *RPGR*-associated RP has commenced,[16] and preclinical studies optimizing subretinal *RPGR* gene therapy have focused on the typical male severe phenotype, which includes an early onset.[44] Inclusion of heterozygotes in gene therapy trials may be challenging until safety and efficacy data are available in male subjects, since male subjects are consistently more severely affected. Nonetheless, in female cases with full disease expression, the macular RPE was frequently altered or atrophic (90% versus 32% of the total cohort), rendering the concept of gene therapy in affected heterozygotes a possibly appropriate treatment option in the future. Serious concerns in the inclusion of female subjects would include the limited comparability to male patients, and the definition of a window of therapeutic opportunity, further complicated by the variability in disease onset and progression. The mean age at which macular RPE involvement was first documented was 43 years, and blind heterozygotes were in their sixth or seventh decade of life, which would translate to a wider window of opportunity in female patients than in the male cohort.

Limitations of this study include its retrospective design, which means that not all subjects had undergone all clinical examinations, as not all clinical examinations were considered relevant or feasible in the clinical setting. While the gathered data are useful, even from subjects with single visits, potential bias should be taken into consideration. Furthermore, as a subgroup of subjects (37 of 125) originated from COD/CORD pedigrees, this compromises the generalizability of the reported findings.

In summary, the findings in this study provide useful insights for the genetic and clinical counselling of female carriers and may have implications for ongoing and future trials. This study displays the wide phenotypic spectrum for *RPGR* heterozygotes and shows that signs and/or symptoms of disease are common, although the visual prognosis is favorable compared with affected males. Myopia is a significant concern due to its effect on BCVA, as it is in affected male patients. A substantial proportion of heterozygotes displays a complete RP or COD/CORD phenotype, and further prospective natural history studies are necessary to determine if inclusion in future (gene) therapeutic trials would be feasible and useful in this subset of severely affected female *RPGR*

mutation carriers, and which outcome measures would provide the most sensitive detection of treatment effect.

Acknowledgements

The authors thank Nicki Hart-Holden, Simon C. Ramsden, and Graeme C. M. Black for the molecular analysis performed at the molecular laboratory of Genetic Medicine, Central Manchester University Hospitals NHS Foundation Trust, Manchester, United Kingdom.

Supported by Stichting Blindenhulp and Janivo Stichting.

REFERENCES

1. Michaelides M, Hardcastle AJ, Hunt DM, Moore AT. Progressive cone and cone-rod dystrophies: phenotypes and underlying molecular genetic basis. Surv Ophthalmol 2006;51:232-58.
2. Pelletier V, Jambou M, Delphin N, et al. Comprehensive survey of mutations in RP2 and RPGR in patients affected with distinct retinal dystrophies: genotype-phenotype correlations and impact on genetic counseling. Hum Mutat 2007;28:81-91.
3. Ayyagari R, Demirci FY, Liu J, et al. X-linked recessive atrophic macular degeneration from RPGR mutation. Genomics 2002;80:166-71.
4. Zito I, Downes SM, Patel RJ, et al. RPGR mutation associated with retinitis pigmentosa, impaired hearing, and sinorespiratory infections. J Med Genet 2003;40:609-15.
5. Fishman GA, Weinberg AB, McMahon TT. X-linked recessive retinitis pigmentosa. Clinical characteristics of carriers. Arch Ophthalmol 1986;104:1329-35.
6. Brouzas D. Psychophysical tests in X-linked retinitis pigmentosa carrier status. Surv Ophthalmol 1995;39 Suppl 1:S76-84.
7. Bird AC. X-linked retinitis pigmentosa. Br J Ophthalmol 1975;59:177-99.
8. Wegscheider E, Preising MN, Lorenz B. Fundus autofluorescence in carriers of X-linked recessive retinitis pigmentosa associated with mutations in RPGR, and correlation with electrophysiological and psychophysical data. Graefes Arch Clin Exp Ophthalmol 2004;242:501-11.
9. Acton JH, Greenberg JP, Greenstein VC, et al. Evaluation of Multimodal Imaging in Carriers of X-Linked Retinitis Pigmentosa. Exp Eye Res 2013;113:41-8.
10. Comander J, Weigel-DiFranco C, Sandberg MA, Berson EL. Visual Function in Carriers of X-Linked Retinitis Pigmentosa. Ophthalmology 2015;122:1899-906.
11. Grover S, Fishman GA, Anderson RJ, Lindeman M. A longitudinal study of visual function in carriers of X-linked recessive retinitis pigmentosa. Ophthalmology 2000;107:386-96.
12. Lorenz B, Andrassi M, Kretschmann U. Phenotype in two families with RP3 associated with RPGR mutations. Ophthalmic Genet 2003;24:89-101.
13. Fishman GA, Grover S, Jacobson SG, et al. X-linked retinitis pigmentosa in two families with a missense mutation in the RPGR gene and putative change of glycine to valine at codon 60. Ophthalmology 1998;105:2286-96.
14. Thiadens AA, Soerjoesing GG, Florijn RJ, et al. Clinical course of cone dystrophy caused by mutations in the RPGR gene. Graefes Arch Clin Exp Ophthalmol 2011;249:1527-35.
15. Ebenezer ND, Michaelides M, Jenkins SA, et al. Identification of novel RPGR ORF15 mutations in X-linked progressive cone-rod dystrophy (XLCORD) families. Invest Ophthalmol Vis Sci 2005;46:1891-8.
16. University of Oxford. New trial for blindness rewrites the genetic code. Available at: http://www.ox.ac.uk/news/2017-03-17-new-trial-blindness-rewrites-genetic-code. Accessed May 17, 2017.
17. Jacobson SG, Yagasaki K, Feuer WJ, Roman AJ. Interocular asymmetry of visual function in heterozygotes of X-linked retinitis pigmentosa. Exp Eye Res 1989;48:679-91.
18. van Huet RA, Oomen CJ, Plomp AS, et al. The RD5000 database: facilitating clinical, genetic, and therapeutic studies on inherited retinal diseases. Invest Ophthalmol Vis Sci 2014;55:7355-60.

19. McCulloch DL, Marmor MF, Brigell MG, et al. ISCEV Standard for full-field clinical electroretinography (2015 update). Doc Ophthalmol 2015;130:1-12.
20. Dagnelie G. Conversion of planimetric visual field data into solid angles and retinal areas. Clin Vis Sci 1990;5:95-100.
21. Al-Maskari A, O'Grady A, Pal B, McKibbin M. Phenotypic progression in X-linked retinitis pigmentosa secondary to a novel mutation in the RPGR gene. Eye (Lond) 2009;23:519-21.
22. Rozet JM, Perrault I, Gigarel N, et al. Dominant X linked retinitis pigmentosa is frequently accounted for by truncating mutations in exon ORF15 of the RPGR gene. J Med Genet 2002;39:284-5.
23. Wu DM, Khanna H, Atmaca-Sonmez P, et al. Long-term follow-up of a family with dominant X-linked retinitis pigmentosa. Eye (Lond) 2010;24:764-74.
24. Almoguera B, Li J, Fernandez-San Jose P, et al. Application of Whole Exome Sequencing in Six Families with an Initial Diagnosis of Autosomal Dominant Retinitis Pigmentosa: Lessons Learned. PLoS One 2015;10:e0133624.
25. Churchill JD, Bowne SJ, Sullivan LS, et al. Mutations in the X-linked retinitis pigmentosa genes RPGR and RP2 found in 8.5% of families with a provisional diagnosis of autosomal dominant retinitis pigmentosa. Invest Ophthalmol Vis Sci 2013;54:1411-6.
26. Sullivan LS, Bowne SJ, Reeves MJ, et al. Prevalence of mutations in eyeGENE probands with a diagnosis of autosomal dominant retinitis pigmentosa. Invest Ophthalmol Vis Sci 2013;54:6255-61.
27. van Everdingen JA, Went LN, Keunen JE, Oosterhuis JA. X linked progressive cone dystrophy with specific attention to carrier detection. J Med Genet 1992;29:291-4.
28. Hendriks M, Verhoeven VJM, Buitendijk GHS, et al. Development of Refractive Errors-What Can We Learn From Inherited Retinal Dystrophies? Am J Ophthalmol 2017;182:81-9.
29. Jayasundera T, Branham KE, Othman M, et al. RP2 phenotype and pathogenetic correlations in X-linked retinitis pigmentosa. Arch Ophthalmol 2010;128:915-23.
30. Chassine T, Bocquet B, Daien V, et al. Autosomal recessive retinitis pigmentosa with RP1 mutations is associated with myopia. Br J Ophthalmol 2015;99:1360-5.
31. Littink KW, Pott J-WR, Collin RWJ, et al. A Novel Nonsense Mutation in CEP290 Induces Exon Skipping and Leads to a Relatively Mild Retinal Phenotype. Invest Ophthalmol Vis Sci 2010;51:3646-52.
32. Walia S, Fishman GA, Jacobson SG, et al. Visual acuity in patients with Leber's congenital amaurosis and early childhood-onset retinitis pigmentosa. Ophthalmology 2010;117:1190-8.
33. Westall CA, Dhaliwal HS, Panton CM, et al. Values of electroretinogram responses according to axial length. Doc Ophthalmol 2001;102:115-30.
34. Koenekoop RK, Loyer M, Hand CK, et al. Novel RPGR mutations with distinct retinitis pigmentosa phenotypes in French-Canadian families. Am J Ophthalmol 2003;136:678-87.
35. Aguirre GD, Yashar BM, John SK, et al. Retinal histopathology of an XLRP carrier with a mutation in the RPGR exon ORF15. Exp Eye Res 2002;75:431-43.
36. Dobyns WB, Filauro A, Tomson BN, et al. Inheritance of most X-linked traits is not dominant or recessive, just X-linked. Am J Med Genet A 2004;129a:136-43.
37. Lyon MF. X-chromosome inactivation and human genetic disease. Acta Paediatr Suppl 2002;91:107-12.

38. Vajaranant TS, Seiple W, Szlyk JP, Fishman GA. Detection using the multifocal electroretinogram of mosaic retinal dysfunction in carriers of X-linked retinitis pigmentosa. Ophthalmology 2002;109:560-8.
39. Plenge RM, Hendrich BD, Schwartz C, et al. A promoter mutation in the XIST gene in two unrelated families with skewed X-chromosome inactivation. Nat Genet 1997;17:353-6.
40. Plenge RM, Tranebjaerg L, Jensen PK, et al. Evidence that mutations in the X-linked DDP gene cause incompletely penetrant and variable skewed X inactivation. Am J Hum Genet 1999;64:759-67.
41. Di Michele DM, Gibb C, Lefkowitz JM, et al. Severe and moderate haemophilia A and B in US females. Haemophilia 2014;20:e136-43.
42. Esquilin JM, Takemoto CM, Green NS. Female factor IX deficiency due to maternally inherited X-inactivation. Clin Genet 2012;82:583-6.
43. Brown J, Jr., Kimura AE, Gorin MB. Clinical and electroretinographic findings of female carriers and affected males in a progressive X-linked cone-rod dystrophy (COD-1) pedigree. Ophthalmology 2000;107:1104-10.
44. Beltran WA, Cideciyan AV, Boye SE, et al. Optimization of Retinal Gene Therapy for X-Linked Retinitis Pigmentosa Due to RPGR Mutations. Mol Ther 2017;25:1866-80.

SUPPLEMENTAL MATERIAL

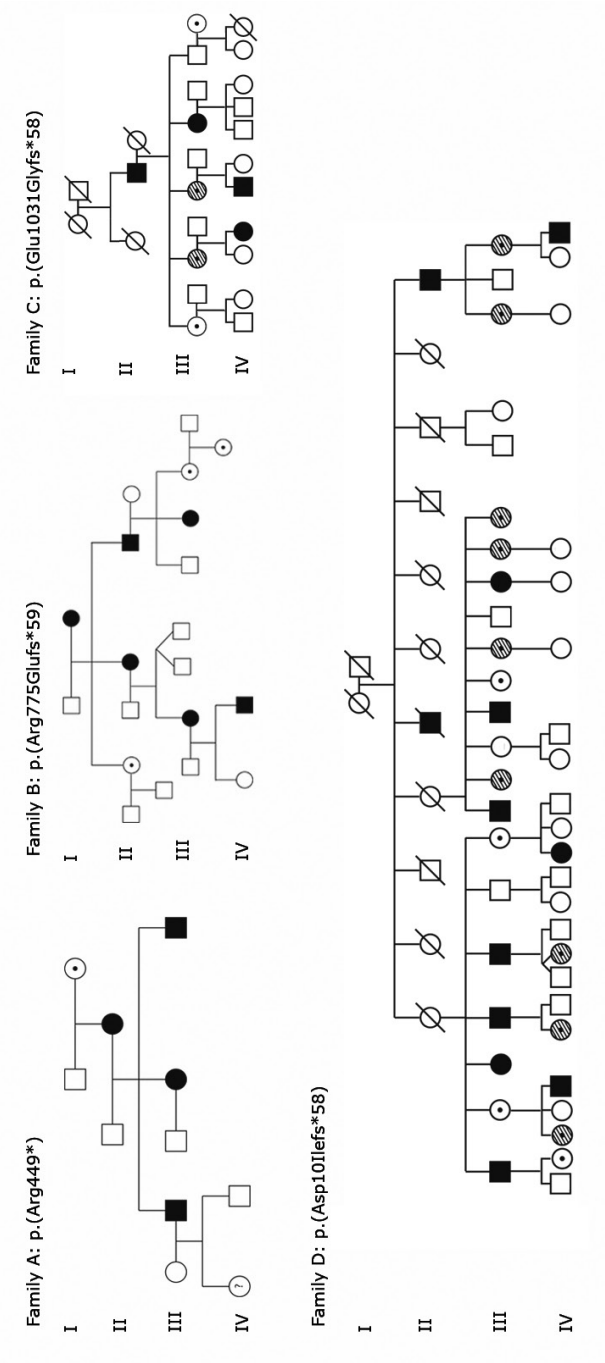

Supplementary Figure S1. Family trees of several female carriers of pathogenic *RPGR* variants. The mutations are depicted in the upper left corner of each family tree. The shaded background on female carriers signifies the presence of symptoms and/or pigmentary fundus changes, and a solid black fill signifies a phenotypical expression at the most severe end of the spectrum, i.e. the presence of visual symptoms beyond nyctalopia, along with intraretinal fundus changes and visual field constriction and/or significantly reduced scotopic and photopic amplitudes.

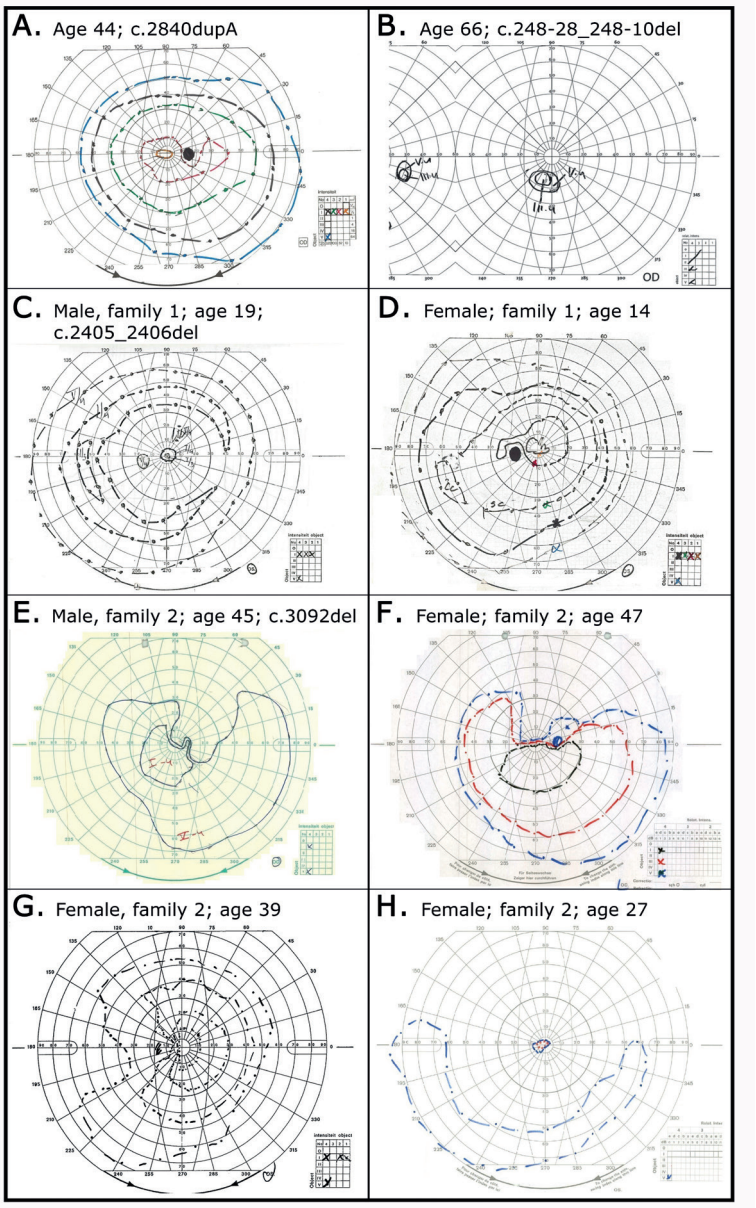

Supplementary Figure S2. Spectrum of visual field decline patterns in female carriers of pathogenic *RPGR* variants. A-B. Goldmann visual fields (GVFs) in individual heterozygotes. **C-D.** GVFs comparing the visual field in a male patient (**C**) with that of his heterozygote sister (**D**). **E-H.** GVFs comparing the visual field in a male patient (**E**) with that of his two carrier daughters (**F**, **G**) and granddaughter (**H**).

Supplementary Table S1. Mutations in the *RPGR* gene found in this cohort

Diagnosis in affected male relatives	Phenotype in female carriers	Exon	Nucleotide	Protein change	N female carriers (n families)
RP	Unaffected 3/15; F 7/15; S 2/15; SF 3/15	1	c.27del	p.(Asp10Ilefs*58)	15 (1)
RP	SF	Intron 1	c.28+2T>C	p.(?)	1
RP	Unaffected		c.112del	p.(Val38Tyrfs*30)	1
RP	SF	3	c.248-28_248-10del	p.(?)	1
Unknown	Unaffected	5	c.329C>A	p.(Ala110Glu)	1
Unknown†	SF	5	c.334_336del	p.(Glu778_799delinsGlu)	1
RP	F 3/3	5	c.425T>G	p.(Ile142Ser)	3 (1)
RP	F	7	c.706C>T	p.(Gln236*)	3 (2)
RP	F 1/3; SF 2/3	8	c.901del	p.(Ser301Leufs*9)	3 (1)
RP	SF 2/2	10‡	c.1060-2A>T	p.(?)	2 (1)
Unknown	NA	10	c.1207C>T	p.(Gln403*)	1
RP	F	10	1246-?_*1091-?	p.(?) deletion after exon 10	1
RP	SF	10	c.1336_1361dup	p.(Asn454Lysfs*31)	1
RP	SF 2/2	11	c.1345C>T	p.(Arg449*)	2 (1)
RP	NA	14	c.1573-?_1753+?del	p.(Lys525Argfs*17)	1
RP	SF	14-ORF15	c.1573-?_3459+?del	p.(?)	1
RP	SF 2/2	14	c.1600C>T	p.(Gln534*)	2 (1)
Unknown	SF	14	c.1685_1686del	p.(His562Argfs*20)	1
RP	Unaffected	ORF15	c.1773_1776del	p.(Gly592Glnfs*9)	1
Unknown	SF	ORF15	c.2010del	p.(Asp671fs)	1
No affected males*	SF	ORF15	c.2200G>T	p.(Glu734*)	1
RP	Unaffected 2/4; SF 1/4; NA ¼	ORF15	c.2237_2241del	p.(Glu746Glyfs*22)	4 (1)
RP	Unaffected ½; SF 1/2	ORF15	c.2257_2260del	p.(Gly753Lysfs*61)	2 (1)
RP		ORF15	c.2323_2324del	p.(Arg775Glufs*59)	5 (1)
RP	Unaffected 2/4; F 2/3	ORF15	c.2362_2366del	p.(Glu788Argfs*45)	4 (2)
RP	Unaffected 6/15; F 4/15; S 1/15; SF in 3/15; NA 1/15	ORF15	c.2405_2406del	p.(Glu802Glyfs*32)	15 (4)
CORD/RP	Unaffected 2/4; F 1/4; SF ¼ (RP)	ORF15	c.2426_2427del	p.(Glu809Glyfs*25)	4 (2)
CORD/RP	Unaffected 1/3; SF 2/3 (RP pedigrees)	ORF15	c.2536G>T	p.(Glu846*)	3 (3)

Supplementary Table S1. Continued

CORD	SF	ORF15	c.2575G>T	p.(Glu859*)	1
RP	Unaffected 2/3; SF 1/3	ORF15	c.2838_2839del	p.(Glu947Glyfs*131)	3 (1)
RP	SF	ORF15	c.2840dup	p.(Glu949Glyfs*130)	4 (1)
CORD	SF	ORF15	c.2872G>T	p.(Glu958*)	1
RP	Unaffected	ORF15	c.2917del	p.(Glu973Lysfs*116)	1
RP	F	ORF15	c.3058del	p.(Glu1020Lysfs*69)	1
CORD	S 1/4; SF 3/4	ORF15	c.3092del	p.(Glu1031Glyfs*58)	4 (1)
COD	S	ORF15	c.3263_3266del	p.(Val1088Alafs*3)	1
COD/CORD	Unaffected 6/21; F 11/21; SF 2/21	ORF15	c.3317dup	p.(Ser1107Valfs*4)	21 (1)
COD/CORD	Unaffected 4/6; SF 2/6 (same pedigree)	ORF15	c.3388_3389del	p.(Leu1130Lysfs*13)	6 (3)

* As reported by subject. S, symptoms only; F, fundus signs only; SF, symptoms and fundus signs; NA, not fully assessable.

† This subject of African descent was adopted and had no knowledge of ophthalmological family history.

‡ Intron 9/exon 10 splice site.

Supplementary Table S2. Clinical characteristics of *RPGR* heterozygotes stratified by genotype

Characteristics	All (n = 125)	Exon 1-14 (n = 42)	ORF15 (n = 83)	*P*-value
Origin RP pedigree, n (%)	83*	38 (46)	45 *(54)	**<0.00001**
Origin COD/CORD pedigree, n (%)	37	-	37 (100)	
Median refractive error (IQR; range), D†	-3.6 (8.6; -21.25D - +4.13D)	-6.1 (8.2; -18.0D - +4.13D)	-2.6 (6.6; -21.25D - +2.9D)	**0.04**
High myopia (< -6D), n (%)	36/101* (36)	17/32 (53)	19/68 (28)	**0.02**
Moderate myopia (-3D > SER ≥ -6D), n (%)	22 (22)	7/32 (22)	14/68 (21)	
Mild myopia (-0.75D > SER ≥ -3D), n (%)	16 (16)	3/32 (9)	13/68 (19)	
≥-0.75D	27 (27)	5/32 (16)	22/68 (32)	
Cataract, n (%)	32/107 (30)	8/34 (24)	24/73 (33)	0.45
SPC, n	9	2	7	
Other or unspecified, n	23	6	17	
Fundoscopic examination				
Optic disc pallor, n (%)	32/94 (34)	13/27 (48)	19/67 (28)	0.10
Peripapillary atrophy, n (%)	36/94 (38)	15/27 (55)	21/67 (31)	0.45
Vascular attenuation, n (%)	40/93 (43)	17/31 (55)	23/62 (37)	0.19
Fundus grade assessable	117	40	77	
Grade 0, n (%)	21 (17)	6	15	
Grade 1, n (%)	11 (9)	2	9	
Grade 0 or 1, n (%)‡	12 (10)	1	11	
Grade 2, n (%)	43 (34)	20	23	
Grade 3, n (%)	17 (14)	8	9	
Grade 2 or 3, n (%)‡	13 (10)	3	10	
Pigment changes, any type, n (%)	73/117 (62)	31/40 (78)	41/77 (53)	**0.02**
Bone spicule-like or round, n	46 (37)	24	22	
Salt-and-pepper, n	4 (4)	1	3	
Macular RPE alterations/atrophy, n	40 (32)	15	25	0.67
RPE alterations in periphery, n	37 (29)	13	24	
Tigroid/tessellated fundus, n	15 (12)	5	10	

Supplementary Table S2. Continued

ERG pattern§	59	23	36	
No abnormalities, *n* (%)	11 (19)	2/23 (9)	9/36 (25)	**0.04‖**
Subnormal/low-to-normal amplitudes, n (%)	6 (10)	2/23	4/36	
Electronegative, n (%)¶	2 (3)	2/23	-	
Rod-cone, n (%)	9 (15)	6/23	3/36	
Reduced rods and cones, no predominance specified, n (%)	19 (32)	10/23#	9/36	
Cone-rod, n (%)	8 (14)	1/23	7/36	
Isolated cone reduction, n (%)	2 (3)	-	2/36	
Nondetectable, n (%)	2 (3)	-	2/36	

Significant *p* values (<0.05) are indicated in bold. SER, spherical equivalent of the refractive error; SPC, subcapsularis posterior cataract.

* Five heterozygotes with mutations in exon 1-14 (n = 4) or ORF15 (n = 1) were not included in the columns distinguishing based on pedigree (RP or COD/CORD), as the diagnosis in the pedigrees could not be established or confirmed in four subjects, and one heterozygote with a mutation in exon 10 (deletion after exon 10) was from a mixed RP/CORD pedigree.

† Averaged between eyes.

‡ In 18 (20%) carriers, no distinction between fundus grades 0 and 1 (n = 9; 10%) or 2 and 3 (n = 9; 10%) could be made based on the notes in the medical record. In seven (8%) heterozygotes, no sufficient data on their fundus appearance were available to estimate the fundus grade.

§ One of the heterozygotes with nondetectable responses had previously documented rod-cone responses. One heterozygote with anisometropia had significantly reduced rod and cone amplitudes in her highly myopic eye, and normal amplitudes in her mildly myopic eye.

‖ Fisher's exact test.

¶ Markedly reduced b-wave with a response resembling an electronegative ERG.

One heterozygote had significantly reduced rod and cone amplitudes in one eye (OS), but normal amplitudes in OD. Other measures of visual function (GVF, BCVA) in this subject showed marked asymmetry in favor of OD.

Supplementary Table S3. Observations on Goldmann visual fields

Observation	N patients (n = 53)
Fully intact visual field for all targets tested	7 (13%)
Intact V4e-I4e; constriction for I3e or I2e and all smaller targets	7 (13%)
Intact V4e; constriction for I4e and all smaller targets	8 (15%)
Constriction for V4e and all smaller targets	31 (58%)
Intraindividual asymmetry*	11 (20%)
Spearman's correlation coefficient V4e isopter size	0.85 ($p < 0.00001$)
Spearman's correlation coefficient I4e isopter size	0.93 ($p < 0.00001$)

*Defined as unilateral constriction, or a difference of >100 mm^2 in the V4e isopter size.

5.
LRAT-associated retinal dystrophies

5.1

Long-term follow-up of retinal degenerations associated with *LRAT* mutations and their comparability to phenotypes associated with *RPE65* mutations

Mays Talib, MD[1], Mary J. van Schooneveld, MD, PhD[2], Roos J.G. van Duuren, MD[1], Caroline Van Cauwenbergh, PhD [3,4], Jacoline B. ten Brink, BAS[5], Elfride De Baere, MD, PhD[4], Ralph J. Florijn, PhD[5], Nicoline E. Schalij-Delfos, MD, PhD[1], Bart P. Leroy, MD, PhD[3,4,6], Arthur A. Bergen, PhD[5,7], Camiel J.F. Boon, MD, PhD[1,2]

Transl Vis Sci Technol 2019;8(4):24

1 Department of Ophthalmology, Leiden University Medical Center, Leiden, The Netherlands.
2 Department of Ophthalmology, Academic Medical Center, Amsterdam, The Netherlands.
3 Department of Ophthalmology, Ghent University and Ghent University Hospital, Ghent, Belgium.
4 Center for Medical Genetics, Ghent University and Ghent University Hospital, Ghent, Belgium.
5 Department of Clinical Genetics, Academic Medical Center, Amsterdam, The Netherlands.
6 Ophthalmic Genetics & Visual Electrophysiology, Division of Ophthalmology, The Children's Hospital of Philadelphia, Philadelphia, Pennsylvania, USA.
7 The Netherlands Institute for Neuroscience (NIN-KNAW), Amsterdam, The Netherlands.

ABSTRACT

Purpose: To investigate the natural history in patients with *LRAT*-associated retinal degenerations (RDs), in the advent of clinical trials testing treatment options.

Methods: A retrospective cohort of 13 patients with *LRAT*-RDs.

Results: Twelve patients from a genetic isolate carried a homozygous c.12del mutation. One unrelated patient carried a homozygous c.326G>T mutation. The mean follow-up time was 25.3 years (SD 15.2; range 4.8-53.5). The first symptom was nyctalopia (n = 11), central vision loss (n = 1), or light-gazing (n = 1), and was noticed in the first decade of life. Seven patients (54%) reached low vision (visual acuity < 20/67), four of whom reaching blindness (visual acuity < 20/400), respectively, at mean ages of 49.9 (SE 5.4) and 59.9 (SE 3.1) years. The fundus appearance was variable. Retinal white dots were seen in six patients (46%). Full-field electroretinograms (n = 11) were nondetectable (n = 2; ages 31-60), reduced in a nonspecified pattern (n = 2; ages 11-54), or showed rod-cone (n = 6; ages 38-48) or cone-rod (n = 1; age 29) dysfunction. Optical coherence tomography (n = 4) showed retinal thinning but relative preservation of the (para-)foveal outer retinal layers in the second (n = 1) and sixth decade of life (n = 2), and profound chorioretinal degeneration from the eighth decade of life (n = 1).

Conclusions: *LRAT*-associated phenotypes in this cohort were variable and unusual, but generally milder than those seen in *RPE65*-associated disease, and may be particularly amenable to treatment. The window of therapeutic opportunity can be extended in patients with a mild phenotype.

Translational relevance: Knowledge of the natural history of *LRAT*-RDs is essential in determining the window of opportunity in ongoing and future clinical trials for novel therapeutic options.

INTRODUCTION

Inherited retinal degenerations (IRD) comprise a collection of heterogeneous diseases characterized by variable progressive dysfunction of rods and/or cones. Leber congenital amaurosis (LCA) is the most severe IRD, characterized by severe visual impairment, nondetectable rod and cone function in the first year of life, and often nystagmus. Retinitis pigmentosa (RP) or rod-cone degeneration, the most common IRD, is characterized by progressive nyctalopia, (mid)peripheral visual field constriction, and finally, loss of central vision.[1] Pathogenic variants in several genes that are typically associated with LCA, can also cause RP.[2]

Genes that are mutated in IRDs encode proteins that function through multiple mechanisms and pathways involving structural and functional retinal integrity, such as the retinoid cycle.[3] This cycle regenerates the visual pigments that are used after light activation. Key enzymes in the retinoid cycle are retinal pigment epithelium (RPE)-specific protein 65 kDa (RPE65) and lecithin:retinol acetyltransferase (LRAT), which are encoded by the *RPE65* and *LRAT* gene, respectively. Photoactivation induces the configurational change of the visual chromophore 11-*cis*-retinal into all-*trans* retinal in the photoreceptor, and the subsequent reduction to all-*trans* retinol. The released all-*trans*-retinol is shuttled to the RPE cells, and esterified to all-*trans*-retinyl esters by the LRAT enzyme, providing the substrate for the RPE65 enzyme. Ultimately, 11-*cis* retinal is resupplied to the photoreceptors. LRAT and RPE65 are thus essential enzymes in the regeneration of functional visual pigment, and a deficiency of either enzyme leads to an impairment in the visual cycle.[4, 5] Mutations in *RPE65* have been associated with several severe IRDs in the autosomal recessive form, causing 6% to 8% of LCA cases, and 5% of cases of childhood-onset RP.[6-15] Rarely, cases of autosomal-dominant IRD have been described in association with mutations in *RPE65*.[16-18] Although reports on the phenotype associated with *LRAT* mutations are scarce, case reports and small case series have shown an association with LCA and childhood-onset RP.[19-23] *LRAT* mutations have been predicted to cause less than 1% of these cases.[6]

While no established and effective treatment is available for most IRDs, the advent of subretinal gene therapy in the treatment of LCA and RP associated with *RPE65* mutations and the favorable results have recently led to the first approval of subretinal gene therapy by the US Food and Drug Administration, and provide a promising perspective for related disorders.[24-26] A trial investigating the safety and efficacy of oral 9-*cis*-retinal supplementation has shown promising results in the treatment of IRDs associated with mutations in *RPE65* and *LRAT*, combining these two patient groups.[27,24] However, due to the rarity of IRDs associated with *LRAT* mutations, little is known about the associated phenotypic spectrum, and the degree of clinical resemblance to phenotypes associated with *RPE65* mutations.

The purpose of this study was to provide a description of the initial and longitudinal clinical characteristics of patients with IRDs associated with *LRAT* mutations, and to compare these findings with previously reported clinical characteristics of IRDs associated with *RPE65* mutations.

METHODS

Patient population and genetic analysis

Patients with bi-allelic molecularly confirmed pathogenic variants in *LRAT* were collected from the database for hereditary eye diseases (Delleman archive) at the Academic Medical Center (AMC) in Amsterdam, resulting in a cohort of 12 patients from a Dutch genetic isolate. One Turkish-Belgian patient (Turkish descent) was included from Ghent University Hospital, Belgium. Informed consent was obtained from Dutch patients in this study, and the study adhered to the tenets of the Declaration of Helsinki. For the Belgian patient, informed consent for this retrospective study was waivered by the Ethics Committee of Ghent University Hospital. Mutational analyses for Dutch patients were performed at the AMC, and at the Ghent University Hospital for the Belgian patient. In the Dutch patients, no pathogenic variants were found with the autosomal recessive RP chip (version 2011/2012; Asper Biotech,Tartu, Estonia), which included *RPE65*, but sequence analysis of *LRAT* revealed a previously described homozygous frameshift mutation,[28] which led to a premature stop codon (c.12del; p.[Met5Cysfs*53]; NM_004744.4), and segregated with the disease. Because the Dutch patients originated from the same genetic isolate as the previously described *CRB1*-RP cohorts,[29, 30] the presence of bi-allelic *CRB1* mutations was excluded in all patients. The Turkish-Belgian patient carried a homozygous missense mutation in *LRAT* (c.326G>T; p.[Arg109Leu]), found through identity by descent-guided Sanger sequencing,[31] and a heterozygous rare variant in *CRB1* (c.4060G>A; p.[Ala1354Thr]), found with LCA chip analysis. Sanger sequencing of the coding regions and intron-exon borders revealed no second *CRB1* mutation.

Clinical assessment and data collection

Through a standardized medical records review, data on initial symptoms, best-corrected visual acuity (BCVA), refractive error, slit-lamp biomicroscopy of the anterior segment, and dilated fundus examination were obtained for all patients. International Society for Clinical Electrophysiology of Vision standard full-field electroretinography (ERG) results and data on color vision testing were available for 11 patients (Ishihara in all patients; Farnsworth D-15 dichotomous color blindness test, Roth 28-hue desaturated test, and Hardy-Rand-Rittler plates in a subset).[32] Goldmann visual fields (GVFs) were performed in six patients. Fundus photographs were available for 11 patients, and spectral-domain optical coherence tomography (SD-OCT) with Heidelberg Spectrals (Heidelberg Engineering, Heidelberg, Germany) was available for four patients. Thirty-degree fundus autofluorescence images (FAF; Heidelberg Engineering) were available for three patients.

Statistical analysis

Data were analyzed using SPSS version 23.0 (IBM Corp, Armonk, NY). Kaplan Meier's methodology was used to analyze the time-to-event for low vision (BCVA < 20/67) and blindness (BCVA < 20/400), based on the World Health Organization criteria, using the better-seeing eye. GVF areas of the V4e target were digitized and converted to seeing retinal areas in millimeters squared using a method described by Dagnelie.[33] *P* values < 0.05 were considered statistically significant.

RESULTS

Of 13 subjects, seven were male. The mean age at first examination was 24.4 years (SD 15; range 1.6-53.6 years). The mean follow-up time was 25.3 years (SD 15.2; range 4.8-53.5 years), with a mean number of 9.5 visits per patient (SD 6.4; range 5-26). Symptoms started as early as the first decade of life in all patients (Table 1), but the 12 patients from the genetic isolate reported a slow progression. Nine patients (69%) first started using visual aids other than glasses between the ages of 29 and 43. A comparison of the phenotypes associated with mutations in *LRAT* and *RPE65* is provided in Table 2.

Ophthalmic and fundoscopic features

The mean spherical equivalent of the refractive error (SER) was +2.2 diopters (D; SD 2.1; range -2.4D to +4.7D), and all but two patients (85%) were mildly (+1D ≤ SER < +3D; n = 6) or moderately (+3D ≤ SER < +6D; n = 5) hyperopic. Hyperopic patients were aged 17 to 59 years, and nonhyperopic patients were aged 11 and 13 years at the time of initial examination of the SER. Nuclear (n = 2) or posterior subcapsular (n = 2) cataract was observed in four patients. Two patients underwent uncomplicated cataract surgery in their seventh decade of life.

Abnormalities in the vitreous were present in 10 of 13 patients (77%), all from the genetic isolate, and consisted of cells or dust-like particles (n = 6), veils (n = 6), or synchysis scintillans (n = 2).
All patients from the genetic isolate had optic disc pallor and vascular attenuation, and 11 of 13 patients (85%) had peripapillary chorioretinal atrophy, varying from a small to moderately sized (n = 2) or large (n = 1) but distinct atrophic border, to a large atrophic zone encompassing both the peripapillary region and parts of the posterior pole (n = 8). Bone-spicule-like pigment migration in the (mid)periphery was first seen at the mean age of 44.6 years (SD 8.8; range 31.5-55.2) in all but two patients aged 17.0 and 20.9 years at the last examination, but intraretinal pigmentation remained sparse in three patients (23%). Eight patients (62%) from the genetic isolate had sharply demarcated areas of atrophic depigmentation in the periphery (Table 1). White dots were seen in the (mid)periphery in six patients (46%) aged 17 to 64 years, including the Turkish-Belgian patient. Considerable intrafamilial variability was observed (Figure 2). Macular RPE involvement ranged from mild RPE alterations (n = 7), first described at a mean age of 39.8 years (SD 17.0;

range 11.7-59.4), to profound atrophy of the posterior pole and the central macula (n = 4), first described at a mean age of 42.6 (SD 20.5; range 22.1-68.3). The macular RPE had a normal aspect in two patients aged 17.0, and 55.2 years.

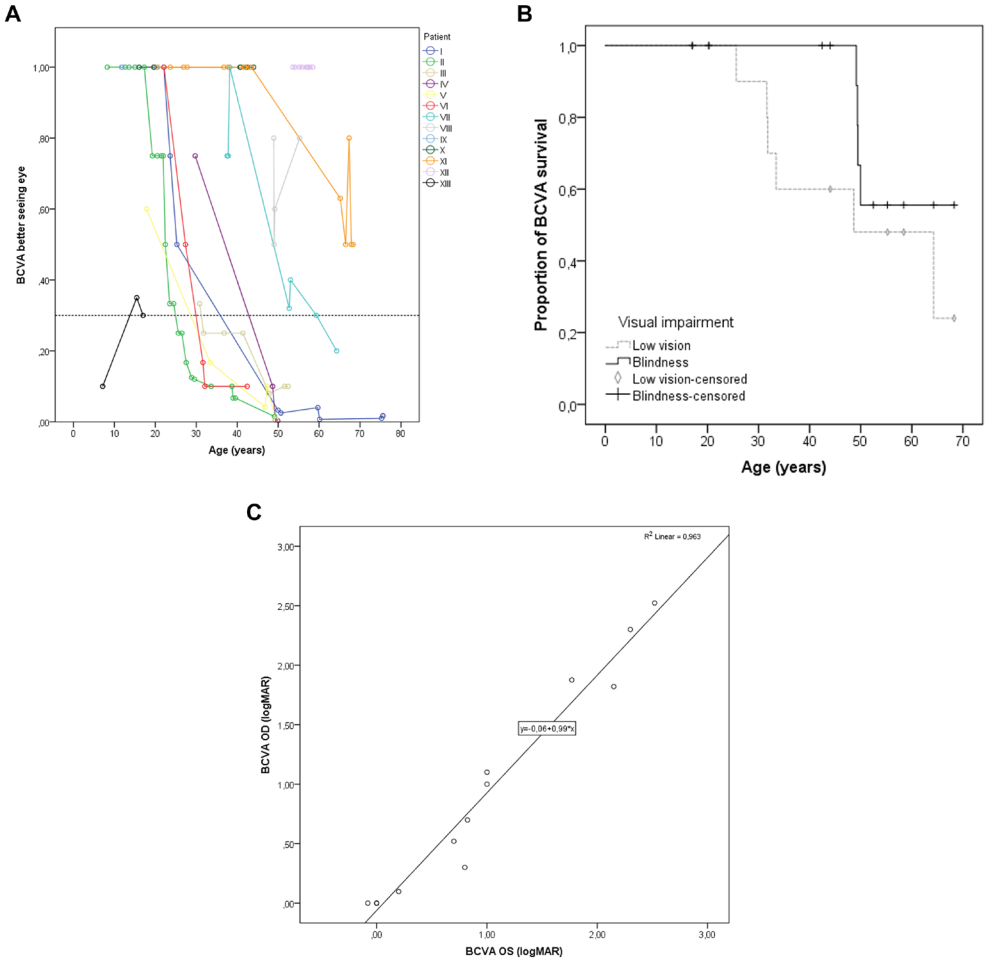

Figure 1. Visual acuities in patients with *LRAT*-associated retinal degeneration. A. The course of decline of the best-corrected visual acuity (BCVA) in individual patients. For illustrative purposes, a BCVA of 20/20 was considered the ceiling, also in patients with a BCVA > 20/20. The dashed line indicates the cutoff value for low vision (20/67), based on the World Health Organization criteria. The individual line for patient XII, the only patient not from the genetic isolate, is shown in black. **B.** Kaplan-Meier plots showing the proportion of patients with a BCVA above low vision (BCVA ≥ 20/67) and above blindness (BCVA ≥ 20/400). Censored observations (i.e. patients who had not reached low vision or blindness at the last follow-up moment) are depicted as vertical bars (blindness) or rhombi (low vision). The median age for reaching low vision was 48.6 years (standard error 14.1). The median age for reaching blindness could not be calculated, as fewer than 50% of subjects became blind during follow-up. **C.** The relation of the BCVA in logarithm of the minimum angle of resolution (logMAR) between the right and left eye at the last clinical visit, showing a linear relationship.

Table 1. Clinical characteristics of patients with *LRAT*-associated retinal degeneration

		Symptoms (DOL at onset)*				Fundus		
ID	Sex, Age (y)	Nyctalopia	VF loss	VA loss	BCVA	Macula	(Mid)periphery	ERG (Age)†
I	M, 75‡	+ (1st)	+ (3rd)	+ (2nd)	CF	Profound chorioretinal and RPE atrophy, sharply demarcated. Pigment clumping.	Bone spicule pigmentation, RPE mottling and depigmentation spots. No white-yellow dots.	ND (52)
II	M, 49‡	+ (infancy)	+ (1st)	+ (1st)	CF	Sheen, RPE alterations	Extensive bone spicule pigmentation, RPE atrophy. Extensive white-yellow dots.	CRD (28)
III	F, 52	+ (infancy)	+ (3rd)	+ (3rd)	20/200	Retinal and RPE atrophy.	Bone spicule pigmentations, extensive clumping in atrophic supra-temporal region, coarse salt and pepper. No white dots, but hypo-pigmented dots. Paving stone-like degeneration.	ND (30)
IV	M, 49	+ (infancy)	+ (3rd)	+ (2nd)	CF	RPE alterations, choroidal atrophy.	Bone spicule pigmentations, extensive pigment clumping. Salt and pepper. Paving stone-like degeneration in far periphery. RPE mottling. No white-yellow dots.	MR (31)
V	F, 49	+ (infancy)	+ (2nd)	+ (2nd /3rd)	CF	Sheen, RPE atrophic alterations	Extensive bone spicule and coarse pigmentation. Salt and pepper. RPE mottling. Paving stone-like atrophic depigmentation.	NA
VI	M, 42	+ (infancy)	+ (3rd)	+ (2nd)	20/200	Chorioretinal and RPE atrophy spanning posterior pole and beyond vascular arcade.	Bone spicule and coarse pigmentation. RPE mottling. Choroid atrophy. No white dots or paving stone degeneration.	NA
VII	F, 64	+ (infancy)	+ (3rd)	+ (<4th)	20/100	Difficult to assess due to synchysis scintillans. Small pigmentations.	Bone spicule pigmentation. RPE mottling. Paving stone-like degenerative depigmentation. White dots, which were no longer observed at the age of 59 onward, after they had been repeatedly observed between the ages of 34-52.	RCD (37)
VIII	M, 55	+ (1st)	+ (<5th)	+ (1st)	20/25	Sheen, RPE atrophy around spared fovea.	Few bone spicule pigmentations. RPE mottling, lobular atrophy. White-yellow dots in far periphery.	RCD (49)
IX	M, 20	+ (1st)	+ (1st)	-	20/20	Sheen, normal pigmentation, white dots.	Salt and pepper. RPE mottling. Drusen. White-yellow dots.	RCD (16)

Table 1. Continued

X	F, 44	+ (1st)	+ (2nd)	+ (2nd)	20/20	No sheen, subtle white dots on a pale retina, subtle granular RPE changes.	Bone spicule pigmentations. Patches of paving stone-like retinal and RPE atrophy, RPE mottling. White yellow dots. Retina generally hypo-pigmented.	RCD (40)
XI	F, 68	+ (infancy)	+ (5th)	-	20/40	Atrophic RPE alterations.	Choroideremia-like atrophic zones with relatively little bone spicule pigmentation. Paving stone-like degeneration.	RCD (42)
XII	F, 58	+ (infancy)	-	-	20/16	RPE alterations.	Few clustered bone-spicule and nummular pigmentations, mainly inferiorly. Midperipheral chorioretinal atrophy.	RR (53)
XIII	M, 17	+ (infancy)	+*	+ (1st)	20/66	Central macula with normal appearance, white dots in the superior posterior pole.	Outer retinal atrophy, no intra-retinal hyperpigmentation, white-greyish dots	RCD (1)

CRD, cone-rod degeneration pattern; DOL, decade of life; ERG, electroretinography; ND, nondetectable; MR, minimal response; NA, data not available; ND, no detectable amplitudes; RCD, rod-cone degeneration pattern; RR, reduced response, pattern not specified; VA, visual acuity; VF, visual field.

* The decade of life during which the patient started noticing the symptom is shown between parentheses. Mild adult-onset nystagmus was documented in patients I, II, and X, starting from the fifth decade of life. In patient XIII, light-gazing and nystagmus were noticed by the parents during the first months of life. Subjective visual field complaints were not documented, but there was concentric constriction on Goldmann kinetic perimetry in the second decade of life. Photopsias were reported in 7/13 patients (54%).

† Full-field ERGs were not performed at the last clinical visit, but the results of the initial ERG are shown, and the age at the time of ERG examination is shown in parentheses. In patients II and VIII, later ERGs showed nondetectable dark- and light-adapted, at the ages of 49 and 55 years, respectively. In the Turkish-Belgian patient, patient XIII, dark-adapted responses were nondetectable, with severely diminished light-adapted responses (<5 μV), leading to a diagnosis of early-onset panretinal degeneration.

‡ These patients are siblings.

Central visual function

The median initial BCVA was 20/20 (IQR in decimals 0.33; range 20/100-20/20), at a median age of 20.6 years (IQR 20.3; range 7.2-53.6 years). Figure 1 illustrates a better preservation of the BCVA in patients from the genetic isolate than in patient XIII, the youngest patient (aged 17 at the final visit), who was Turkish-Belgian. Survival analysis revealed no BCVA-based visual impairment until the third decade of life (Figures 1A, 1B). The mean ages for reaching low vision and blindness were 49.9 (SE 5.4; 95% CI 39.3-60.5) and 59.9 years (SE 3.1; 95% CI 53.8-66.0), respectively, with seven patients (54%) reaching low vision in the better seeing eye during the follow-up period, four of whom (31%) reaching blindness. Five patients (38%) maintained a BCVA of 20/40 or more into the third to seventh decades of life (BCVA > 20/25 in four patients), while patient XIII had a BCVA of 20/66 at the final visit. Spearman's rank correlation coefficients showed a high degree of intraindividual between-eye symmetry in BCVA at the first (0.78; $p = 0.002$) and last (0.98; $p < 0.00001$) visit.

Color vision testing in 11 patients (10 from the genetic isolate) showed a severe or near-complete deficiency in all axes in eight patients aged 15.5-59.4 (patients I, III, V-IX, XIII), or multiple errors in different axes in three patients aged 12.6-43.1 (patient II: protan; patient X and XI: tetartan and tritan; patient XI also deutan), despite a nonimpaired concurrent BCVA in seven of 11 cases.

Visual fields and electroretinography

Visual fields were recorded in 10 patients (Supplementary Table S1), using different modalities (GVF in six subjects). Visual fields predominantly showed peripheral constriction or midperipheral scotomas with relative preservation of central vision in seven of 10 patients (70%), and a central scotoma in three of 10 patients (30%) including two brothers (Supplementary Figure S1). Initial seeing retinal areas for the V4e target were large (>250 mm^2) in all patients, aged 15.5 to 48.9 years at the time of examination, with a median of 714.3 mm^2 (IQR 123.9; range 482.1-774.2). During follow-up, visual field-based low vision (central diameter <20°) or blindness (central diameter <10°) was observed in two patients from the genetic isolate at the ages of 23.6 (patient I) and 54.1 years (patient XII), despite a normal concurrent BCVA (Table 2). Patient I reached visual field-based blindness 26 years before reaching BCVA-based blindness. The degree of between-eye symmetry of seeing retinal areas was high (Spearman's rank correlation coefficient 0.89; $p = 0.019$).

Initial ERG examination showed a rod-cone pattern (n = 5; ages 37.6-49.0 in the genetic isolate; second year of life in patient XIII), cone-rod pattern (n = 1; age 28.9), severely reduced responses in a nonspecified pattern (n = 3; ages 11.9-53.6), or a nondetectable response (n = 2; ages 30.8-52.1 years). Later ERGs showed progression to nondetectable responses in two more patients in their fifth to sixth decades of life.

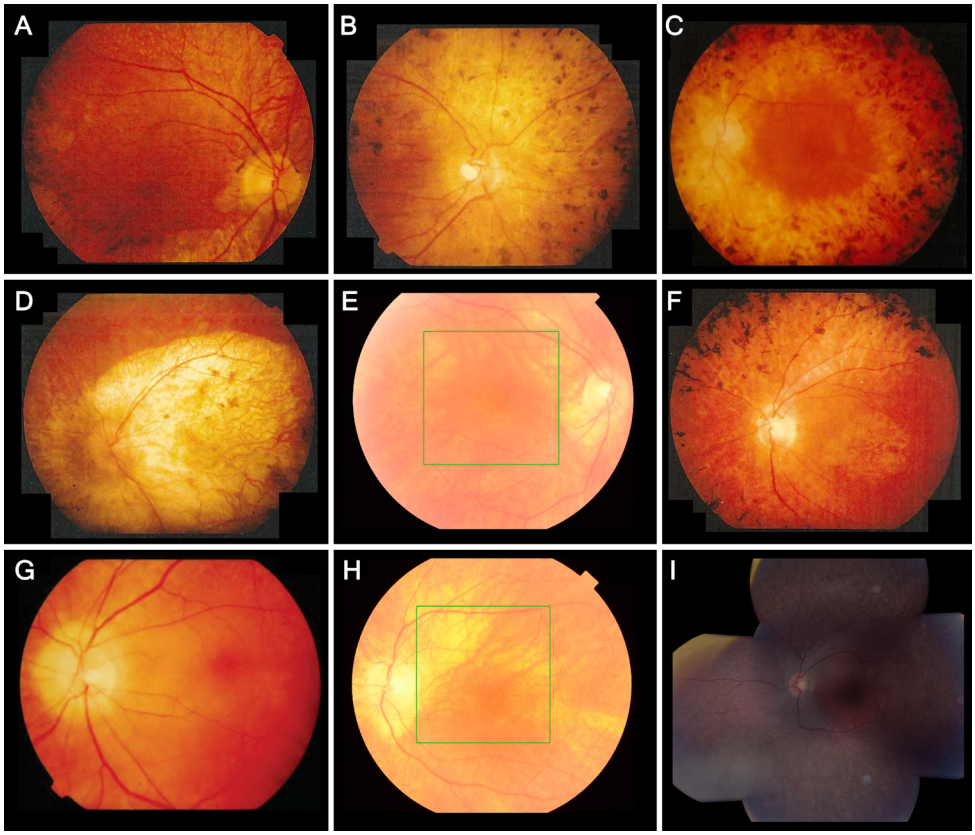

Figure 2. Fundus photographs showing retinal features and intrafamilial variability in patients with *LRAT*-associated retinal degeneration. Reported ages are at the time of fundus photography. **A.** Patient II, aged 39, showing pigmentary changes in the posterior pole, a macular sheen, and yellow-white dots, associated with retinitis punctata albescens, in the midperiphery. The periphery, not shown here, showed extensive bone spicule hyperpigmentation. **B.** Patient IV, aged 49, showing a pale optic disc, peripapillary atrophy, vascular attenuation, mottled retinal pigmentary epithelium (RPE) changes and clumping in the posterior pole, and atrophy in the nasal midperiphery. In the inferior midperiphery, not shown here, paving stone-like atrophic zones were seen with fundoscopy. **C.** Patient VI, aged 42, showing retinal atrophy, and widespread bone spicule-like and coarse hyperpigmentation extending into the posterior pole. The central macula is relatively spared, with mild RPE alterations. **D.** Patient I, aged 50, showed profound chorioretinal atrophy of the posterior pole and along the vascular arcade. The periphery, not shown here, showed mild RPE mottling, several paving stone-like degenerations, and little bone spicule-like hyperpigmentation. **E.** Patient XII, aged 56, showing peripapillary atrophy and areas of retinal thinning along the superior vascular arcade, with no RPE changes in the central retina. In the inferonasal mid-periphery, not shown here, a few round and bone spicule-like pigmentations were clustered. **F.** Patient V, aged 47, showed atrophic RPE alterations and a sheen in the central macula, atrophy around the optic disc and along the vascular arcade, and extensive bone spicule-like pigmentation in the midperipheral retina. **G-H.** Patient XI, showing the disease progression between the ages of 43 (**G**) and 67 (**H**). At the age of 43, this patient showed peripapillary atrophy, yellow-white dots below the superior vascular arcade, and no RPE changes of the central macula. At the age of 67, the white dots were no longer visible, and the posterior pole showed zones of atrophic RPE. **I.** Composite fundus photography of the left eye of patient XIII at the age of 15, showing peripapillary atrophy, a normal macula, limited intraretinal white dots in the superior macula

that appear less brightly yellow and less sharply circumscribed than the white-yellow dots seen in patients from the genetic isolate, and fleck-like outer retinal atrophy in the (mid-)periphery.

Findings on retinal imaging

SD-OCT scans of four patients (I, XI, XII, and XIII) showed outer retinal attenuation in the peripheral macula and a relatively well-preserved foveal and parafoveal outer retina in patient XIII during his second decade of life, and in patient XII until her sixth to seventh decades of life. Patient XI showed progressive thinning of the outer nuclear layer and hyperreflective outer retinal bands in her seventh decade of life (Figures 3D, 3F). In the mildly hyperopic patient I, an SD-OCT scan at the age of 76.5 showed a markedly thinned choroid, and generalized outer retinal atrophy (Figures 3G-I). FAF images in three patients showed granular or mottled hypo-autofluorescence and a hyperautofluorescent ring in two patients from the genetic isolate (Figures 3B, 3E).

Table 2. Overview of the current literature of *RPE65*- and *LRAT*-associated phenotypes

Phenotype	Additional features	*RPE65*	*LRAT*
IRD*		Biswas et al., 2017[34]	
LCA		Katagiri et al., 2016[10] Srilekha et al., 2015[11] Jakobsson et al., 2014[12] Chen et al., 2013[13] Roman et al., 2013[14] Xu et al., 2012[35] McKibbin et al., 2010[15] Pasadhika et al., 2010[36] Walia et al., 2010[37] Li et al., 2009[38] Simonelli et al., 2007[9] Jacobson et al., 2005;[39] 2008[40] Galvin et al., 2005[41] Booij et al., 2005[2] Silva et al., 2004[42] Hanein et al., 2004[7] Sitorus et al., 2003[43] Hamel et al., 2001[44] Dharmaraj et al., 2000[45]	Den Hollander et al., 2007[20] Sénéchal et al., 2006[22]
Autosomal recessive RP		Chebil et al., 2016 (French)[46] Walia et al 2010[37] Booij et al., 2005[2] Hamel et al., 2001[44] Morimura et al., 1998[47]	Preising et al., 2007 (German)[23] This study
Autosomal dominant IRD	Extensive chorioretinal atrophy	Hull et al., 2016*[16] Bowne et al., 2011[17] (RP)	-
	AVMD/foveal vitelliform lestions	Hull et al., 2016[16]	-

Table 2. Continued

EORD		Hull et al., 2016[16] Kabir et al., 2013[48] El Matri et al., 2006[49] Thompson et al., 2000[50]	Coppieters et al., 2014[31] Dev Borman et al., 2012[21]
EOSRD/ SECORD	Better visual functions than typically seen in LCA	Mo et al., 2014[51] Weleber et al., 2011[52] Lorenz et al., 2008[53] Preising et al., 2007 (German)[23] Paunescu et al., 2005[54] Lorenz et al., 2004[55] Yzer et al., 2003[56] Felius et al., 2002[57]	Thompson et al., 2001[19]
RPA	White-yellow dots		Littink et al., 2012[28] This study
FA	White-yellow dots	Katagiri et al., 2018[58] (flecks) Yang et al., 2017[59] Schatz et al., 2011[60]	
Early and prominent severe cone involvement		Jakobsson et al., 2014[12] (severe visual impairment in childhood)	
Cone-rod dystrophy			This study (good initial visual function; low vision in third decade of life)

AVMD, adult onset vitelliform macular dystrophy; EORD, early onset retinal dystrophy; EOSRD, early onset severe retinal dystrophy; FA, fundus albipunctatus; IRD, inherited retinal dystrophy; LCA, Leber's congenital amaurosis; RP, retinitis pigmentosa; RPA, retinitis punctata albescens; SECORD, severe early childhood onset retinal dystrophy.
* Retinal dystrophy, not otherwise specified.

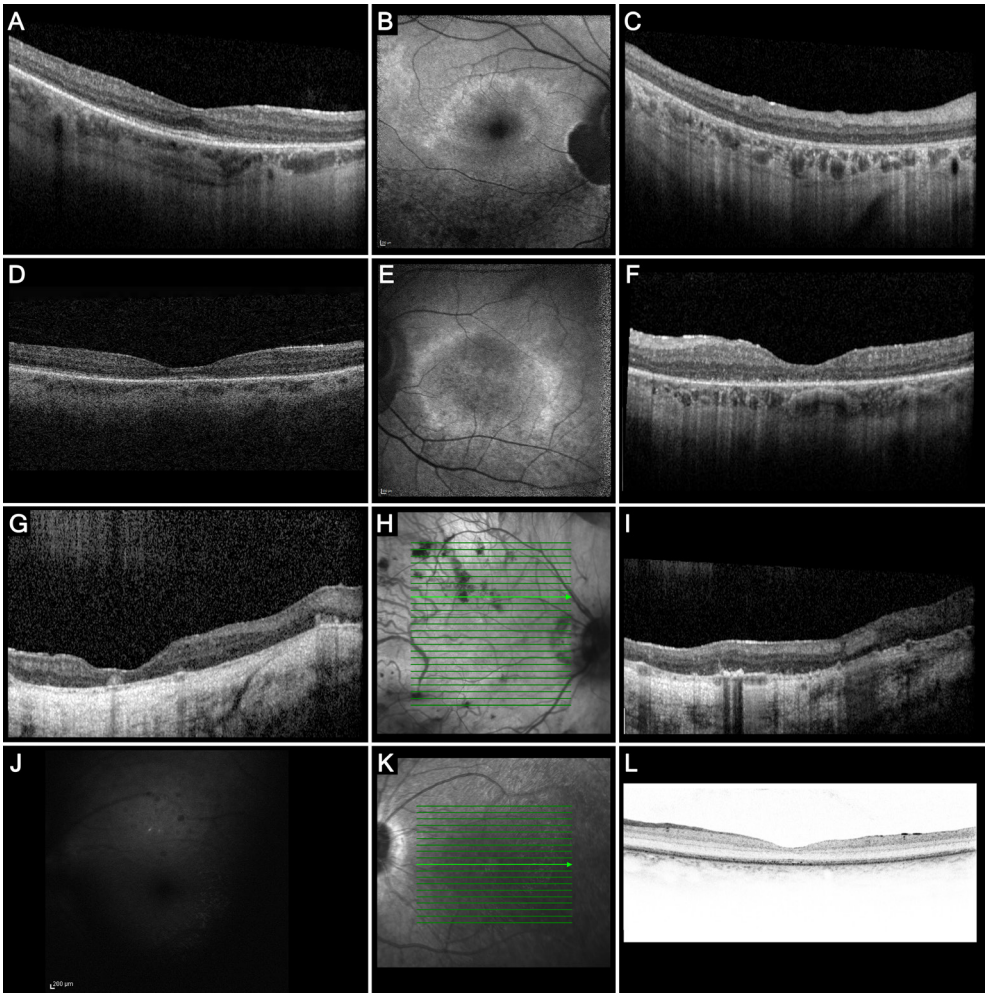

Figure 3. Imaging findings in patients with *LRAT*-associated retinal degeneration. A-C. Imaging in patient XII, aged 57 at the time of examination. Repeated SD-OCT scans between the ages of 54 and 58 showed relative foveal, parafoveal, and temporal perifoveal preservation of the outer nuclear layer and the external limiting membrane (ELM) and ellipsoid zone (EZ), although these hyperreflective outer retinal bands showed a few interruptions, with profound nasal thinning and near-complete disappearance of these layers in areas corresponding with atrophy on the fundus photograph. Follow-up SD-OCT scans over the course of 4 years showed mildly increased outer retinal thinning, mainly in the nasal peri- and parafoveal region. The transition zone between relatively spared outer retina and markedly thinned outer retina colocalized with the hyperautofluorescent ring on FAF (**B**), which also showed a juxtapapillary patch of absent AF, sharply demarcated by a hyper-AF border. Along the inferior vascular arcade, a zone of dense granular hypo-AF was visible. On SD-OCT of the peripheral macula (**C**), small hyperreflective foci with no shadowing were visible in the inner plexiform layer and the inner nuclear layer. To a milder degree, these hyperreflective foci are also visible in (**A**). **D-F.** SD-OCT scan of the right eye of Patient XI at the age of 65 years (**D**), showing a mild epiretinal membrane, and generalized outer retinal thinning and attenuation of the outer retinal hyperreflective bands that was more pronounced at the parafovea, with relative preservation more temporally and at the fovea. FAF imaging of the left eye at the age of 68 (**E**) showed peripapillary atrophy, and a perimacular hyper-AF

ring with mottled hypo-AF inside and outside this hyper-AF ring. The corresponding SD-OCT scan of the left eye (**F**) showed more pronounced outer retinal atrophy, and severe granulation of the EZ band. **G-I.** Patient I, aged 75, showing generalized severe atrophy of the outer nuclear layer, ELM, and EZ, a markedly thin choroid and a scleral tunnel. Large hyperreflective outer retinal accumulations above the RPE level were visible. No concurrent fundus photograph was made in order to attempt to colocalize these accumulations to a funduscopic structure, but earlier fundus photographs taken at the age of 52 (Figure 2D) showed profound atrophy of the retina inside and around the posterior pole. **J-L.** FAF imaging (**J**) of patient XIII at the age of 15 years, carrying a homozygous c.326G>T mutation, showing reduced image quality due to the nystagmus, and a generalized reduced AF with small hypo-AF spots in the posterior pole. No corresponding SD-OCT scan was available at that age, but an SD-OCT scan at the age of 17 years (**K-L**) showed no evident outer retinal thinning, but a granular appearance of the EZ and ELM, with relative preservation of the foveal structure.

DISCUSSION

In this retrospective cohort study of 13 patients with IRDs associated with *LRAT* mutations, we describe the long-term natural history of an unusually mild, albeit variable, phenotype, adding to the phenotypic spectrum of IRDs associated with *LRAT* mutations, and providing further insight regarding the window of opportunity for novel therapeutic strategies.[27, 61] We describe, to the best of our knowledge, the largest cohort to date of patients with IRDs associated with *LRAT* mutations.

While the presentation of the first symptom, usually nyctalopia, was within the first years of life, the retinal phenotypes and the natural disease course reflect a phenotypic variability in IRDs associated with *LRAT* mutations, even within the genetic isolate. Although little is known on the phenotype associated with *LRAT* mutations, due to its rarity, it has been associated with Leber congenital amaurosis and other types of severe early-onset retinal degeneration.[19, 20, 22] In contrast to earlier reports of visual impairment in childhood or adolescence,[20, 27] the mean ages for reaching low vision and blindness in the current cohort were 49.9 and 59.9 years, respectively, with five patients maintaining good BCVA until the final examination, in their third to seventh decade of life. In the Turkish-Belgian patient, symptomatology and visual function were evidently worse, with a BCVA less than 20/40 from the first decade of life, although he had not yet reached low vision at the final visit at the age of 17 years. An earlier study of retinitis punctata albescens included four Dutch patients with the same homozygous frameshift mutation in *LRAT* found in the genetic isolate in this cohort, who had relatively well-preserved BCVA and visual fields compared with patients with retinitis punctata albescens associated with other genes involved in the retinoid cycle, although the patients with *LRAT* mutations described in the previous study were younger (ages 7-19 years) than the patients in the current cohort.[28] In this study, color vision testing was markedly abnormal before BCVA started to decrease. Peripheral visual fields showed more variability, but were relatively well-preserved until the sixth decade of life, with most patients showing relative or absolute concentric constriction with a relatively large central residue, with or without (para)central scotomas. In contrast to these findings, previous reports on *LRAT*-RDs

have lacked quantitative visual field analysis, but where reported, visual field sizes were usually small (<25 mm^2) or intermediate (25-250 mm^2) in the second to third decades of life, with few exceptions,[27] or were reported as severely reduced,[19, 20] with variably sized peripheral crescents of vision.[21]

In gene- or cell-based therapeutic trials that are designed to compare the visual and retinal function between the treated and nontreated control eye, between-eye symmetry is an important assumption. Our findings in this cohort show a high degree of symmetry between affected eyes of the same individual in BCVA and seeing retinal area.

Marked intrafamilial variability was observed in the genetic isolate, with phenotypes varying from cone-rod to rod-cone patterns. This variability was most notable upon ophthalmoscopy, with some patients showing central and midperipheral profound chorioretinal atrophy and coarse hyperpigmentation (Figures 2C, 2D), while others showed midperipheral patchy paving stone-like degeneration, and some patients maintaining a relatively spared posterior pole with only mild RPE alterations (Figures 2E, 2G, 2H). This considerable phenotypic variability in patients originating from the same genetic isolate and carrying the same homozygous mutation points to the involvement of genetic and/or environmental modifiers. Certain *Rpe65* variants have been shown to modify the disease course in mouse models of RP and albinism,[62, 63] although no such variants were found in our study. Bone spicule-like pigmentation was absent in two patients (15%), and limited or sparsely scattered in three patients (23%; Fig. 2). Eight patients (62%) had distinct areas of depigmentation. This finding is in line with previous observations of no or minimal hyperpigmentation in phenotypes associated with *LRAT* and *RPE65* mutations,[21, 31, 49] and areas of hypo- or depigmentation.[20]

Retinal imaging, in line with visual function, showed relatively well-preserved outer retinas in two patients in their second and sixth decade of life, and marked retinal or chorioretinal degeneration in two patients in their seventh and eighth decades of life. Preservation of central retinal structure, including outer photoreceptor layers on SD-OCT has been reported before in a younger patient (27 years) with different *LRAT* mutations.[21] The long-term preservation of the outer retina in these patients, at least at the level of the fovea, is a favorable finding, as it has been demonstrated that a relatively preserved photoreceptor layer predicts a positive treatment response in patients with IRDs associated with mutations *RPE65* or *LRAT* receiving oral synthetic 9-cis-retinoid in a clinical trial.[61, 64]

As a systemic therapeutic trial targeting the retinoid cycle in human patients has grouped patients with *LRAT*- and *RPE65*-associated RP and LCA,[27] and the same systemic or novel cell-based therapeutic strategies have grouped *Lrat*(-/-) and *Rpe65*(-/-) mouse models together,[65, 66] understanding the comparability of these phenotypes is important. Comparable LCA phenotypes

have been found in *Rpe65*(-/-) and *Lrat*(-/-) mice.[67,68] Similarly in human patients, parallels between the phenotypes associated with *LRAT* and *RPE65* mutations have been suggested in previous case studies of *LRAT*-RDs.[21,22] *RPE65* mutations typically lead to severe retinal degeneration, presenting with severely reduced vision in the first year of life, nystagmus, and panretinal photoreceptor degeneration, leading to a diagnosis of LCA or early-onset severe retinal degeneration.[6, 9, 54, 69] However, cases of *RPE65*-RP and early-onset IRD with relatively preserved ambulatory vision into adolescence have also been described.[37, 47, 50, 52, 56] Distinctive fundus features include white dots, just like we observed in six (46%) of the *LRAT*-RD patients in the current cohort, sometimes fading with time as also observed in one patient in the current study.[35, 46, 52] In RPE65-associated IRD, these white-yellow dots have also been described in fundus albipunctatus.[59,60] SD-OCT scans in several patients with *RPE65*-LCA have shown preserved retinal thickness and foveal contour, and attenuated but detectable outer photoreceptor layers, even in cases of visual impairment.[9, 55, 70] However, lamellar disorganization and/or outer retinal and photoreceptor layer disintegration have also been found in *RPE65*-LCA, with differing reports on the relationship with age.[36, 40, 53] Our findings in this *LRAT*-RD population indicate similarities with the retinal phenotype of *RPE65*-RDs, although the exceptionally extended period of retinal structural and functional preservation in the genetic isolate is distinct. Moreover, the findings in our study are variable, complicating the ability to make a clear comparison between phenotypes associated with mutations in *LRAT* and those associated with mutations in *RPE65*.

The drawbacks of this study include its retrospective design, and the limited historical availability of imaging and all modalities of functional testing, as most tests were available only for a subset of patients. Although we have found a symptomatically and visually more severe phenotype in the patient with the homozygous c.326G>T mutation than in the patients from the genetic isolate with a homozygous c.12del mutation, a larger and more genetically heterogeneous cohort would have allowed for the exploration of genotype-phenotype correlations, subgroup analyses, and for a more comprehensive description of the phenotypic spectrum. As the current literature on phenotypes associated with bi-allelic mutations in *LRAT* is limited, the generalizability of our findings in this Dutch and Belgian cohort to the general population of patients with *LRAT*-RDs is uncertain.

In conclusion, our findings in patients with IRDs associated with *LRAT*-mutations due to the c.12del mutation or c.326G>T mutation indicate that *LRAT*-RDs may be particularly amenable to treatment. Not all pathogenic variants in *LRAT* lead to early severe visual dysfunction, and the window of therapeutic opportunity may be extended to later decades of life in some patients. While fundus phenotypes were heterogeneous within this genetic isolate, similarities can be found with the heterogeneous phenotypes associated with *RPE65*-mutations.

Acknowledgments

This study was performed as part of a collaboration within the European Reference Network for Rare Eye Diseases (ERN-EYE). ERN-EYE is co-funded by the Health Program of the European Union under the Framework Partnership Agreement #739543 – 'ERN-EYE' and co-funded by the Hôpitaux Universitaires de Strasbourg.

Supported by grants from Stichting Blindenhulp, Janivo Stichting (CJFB).

REFERENCES

1. Hartong DT, Berson EL, Dryja TP. Retinitis pigmentosa. Lancet 2006;368:1795-809.
2. Booij JC, Florijn RJ, ten Brink JB, et al. Identification of mutations in the AIPL1, CRB1, GUCY2D, RPE65, and RPGRIP1 genes in patients with juvenile retinitis pigmentosa. J Med Genet 2005;42:e67.
3. van Soest S, Westerveld A, de Jong PT, et al. Retinitis pigmentosa: defined from a molecular point of view. Surv Ophthalmol 1999;43:321-34.
4. Redmond TM, Yu S, Lee E, et al. Rpe65 is necessary for production of 11-cis-vitamin A in the retinal visual cycle. Nat Genet 1998;20:344-51.
5. Batten ML, Imanishi Y, Maeda T, et al. Lecithin-retinol acyltransferase is essential for accumulation of all-trans-retinyl esters in the eye and in the liver. J Biol Chem 2004;279:10422-32.
6. den Hollander AI, Roepman R, Koenekoop RK, Cremers FPM. Leber congenital amaurosis: Genes, proteins and disease mechanisms. Prog Ret Eye Res 2008;27:391-419.
7. Hanein S, Perrault I, Gerber S, et al. Leber congenital amaurosis: comprehensive survey of the genetic heterogeneity, refinement of the clinical definition, and genotype-phenotype correlations as a strategy for molecular diagnosis. Hum Mutat 2004;23:306-17.
8. Bramall AN, Wright AF, Jacobson SG, McInnes RR. The genomic, biochemical, and cellular responses of the retina in inherited photoreceptor degenerations and prospects for the treatment of these disorders. Annu Rev Neurosci 2010;33:441-72.
9. Simonelli F, Ziviello C, Testa F, et al. Clinical and molecular genetics of Leber's congenital amaurosis: a multicenter study of Italian patients. Invest Ophthalmol Vis Sci 2007;48:4284-90.
10. Katagiri S, Hayashi T, Kondo M, et al. RPE65 Mutations in Two Japanese Families with Leber Congenital Amaurosis. Ophthalmic Genet 2016;37:161-9.
11. Srilekha S, Arokiasamy T, Srikrupa NN, et al. Homozygosity Mapping in Leber Congenital Amaurosis and Autosomal Recessive Retinitis Pigmentosa in South Indian Families. PLoS One 2015;10:e0131679.
12. Jakobsson C, Othman IS, Munier FL, et al. Cone-rod dystrophy caused by a novel homozygous RPE65 mutation in Leber congenital amaurosis. Klin Monbl Augenheilkd 2014;231:405-10.
13. Chen Y, Zhang Q, Shen T, et al. Comprehensive mutation analysis by whole-exome sequencing in 41 Chinese families with Leber congenital amaurosis. Invest Ophthalmol Vis Sci 2013;54:4351-7.
14. Roman AJ, Cideciyan AV, Schwartz SB, et al. Intervisit variability of visual parameters in Leber congenital amaurosis caused by RPE65 mutations. Invest Ophthalmol Vis Sci 2013;54:1378-83.
15. McKibbin M, Ali M, Mohamed MD, et al. Genotype-phenotype correlation for leber congenital amaurosis in Northern Pakistan. Arch Ophthalmol 2010;128:107-13.
16. Hull S, Mukherjee R, Holder GE, et al. The clinical features of retinal disease due to a dominant mutation in RPE65. Mol Vis 2016;22:626-35.
17. Bowne SJ, Humphries MM, Sullivan LS, et al. A dominant mutation in RPE65 identified by whole-exome sequencing causes retinitis pigmentosa with choroidal involvement. Eur J Hum Genet 2011;19:1074-81.
18. Jauregui R, Park KS, Tsang SH. Two-year progression analysis of RPE65 autosomal dominant retinitis pigmentosa. Ophthalmic Genet 2018;39:544-9.

19. Thompson DA, Li Y, McHenry CL, et al. Mutations in the gene encoding lecithin retinol acyltransferase are associated with early-onset severe retinal dystrophy. Nat Genet 2001;28:123-4.
20. den Hollander AI, Lopez I, Yzer S, et al. Identification of novel mutations in patients with Leber congenital amaurosis and juvenile RP by genome-wide homozygosity mapping with SNP microarrays. Invest Ophthalmol Vis Sci 2007;48:5690-8.
21. Dev Borman A, Ocaka LA, Mackay DS, et al. Early onset retinal dystrophy due to mutations in LRAT: molecular analysis and detailed phenotypic study. Invest Ophthalmol Vis Sci 2012;53:3927-38.
22. Senechal A, Humbert G, Surget MO, et al. Screening genes of the retinoid metabolism: novel LRAT mutation in leber congenital amaurosis. Am J Ophthalmol 2006;142:702-4.
23. Preising MN, Paunescu K, Friedburg C, Lorenz B. Genetic and clinical heterogeneity in LCA patients. The end of uniformity [in German]. Ophthalmologe 2007;104:490-8.
24. Maguire AM, Simonelli F, Pierce EA, et al. Safety and Efficacy of Gene Transfer for Leber's Congenital Amaurosis. N Engl J Med 2008;358:2240-8.
25. Bennett J, Wellman J, Marshall KA, et al. Safety and durability of effect of contralateral-eye administration of AAV2 gene therapy in patients with childhood-onset blindness caused by RPE65 mutations: a follow-on phase 1 trial. Lancet 2016;388:661-72.
26. FDA approves novel gene therapy to treat patients with a rare form of inherited vision loss. U.S. Food and Drug Administration, 2017. Available at: https://www.fda.gov/newsevents/newsroom/pressannouncements/ucm589467.htm. Accessed April 2, 2019.
27. Koenekoop RK, Sui R, Sallum J, et al. Oral 9-cis retinoid for childhood blindness due to Leber congenital amaurosis caused by RPE65 or LRAT mutations: an open-label phase 1b trial. Lancet 2014;384:1513-20.
28. Littink KW, van Genderen MM, van Schooneveld MJ, et al. A homozygous frameshift mutation in LRAT causes retinitis punctata albescens. Ophthalmology 2012;119:1899-906.
29. Mathijssen IB, Florijn RJ, van den Born LI, et al. Long-term follow-up of patients with retinitis pigmentosa type 12 caused by CRB1 mutations: A Severe Phenotype With Considerable Interindividual Variability. Retina 2017;37:161-172.
30. Talib M, van Schooneveld MJ, van Genderen MM, et al. Genotypic and Phenotypic Characteristics of CRB1-Associated Retinal Dystrophies: A Long-Term Follow-up Study. Ophthalmology 2017;124:884-95.
31. Coppieters F, Van Schil K, Bauwens M, et al. Identity-by-descent-guided mutation analysis and exome sequencing in consanguineous families reveals unusual clinical and molecular findings in retinal dystrophy. Genet Med 2014;16:671-80.
32. McCulloch DL, Marmor MF, Brigell MG, et al. ISCEV Standard for full-field clinical electroretinography (2015 update). Doc Ophthalmol 2015;130:1-12.
33. Dagnelie G. Conversion of planimetric visual field data into solid angles and retinal areas. Clin Vis Sci 1990;5:95-100.
34. Biswas P, Duncan JL, Maranhao B, et al. Genetic analysis of 10 pedigrees with inherited retinal degeneration by exome sequencing and phenotype-genotype association. Physiol Genomics 2017;49:216-29.
35. Xu F, Dong Q, Liu L, et al. Novel RPE65 mutations associated with Leber congenital amaurosis in Chinese patients. Mol Vis 2012;18:744-50.

36. Pasadhika S, Fishman GA, Stone EM, et al. Differential macular morphology in patients with RPE65-, CEP290-, GUCY2D-, and AIPL1-related Leber congenital amaurosis. Invest Ophthalmol Vis Sci 2010;51:2608-14.
37. Walia S, Fishman GA, Jacobson SG, et al. Visual acuity in patients with Leber's congenital amaurosis and early childhood-onset retinitis pigmentosa. Ophthalmology 2010;117:1190-8.
38. Li Y, Wang H, Peng J, et al. Mutation survey of known LCA genes and loci in the Saudi Arabian population. Invest Ophthalmol Vis Sci 2009;50:1336-43.
39. Jacobson SG, Aleman TS, Cideciyan AV, et al. Identifying photoreceptors in blind eyes caused by RPE65 mutations: Prerequisite for human gene therapy success. Proc Natl Acad Sci U S A 2005;102:6177-82.
40. Jacobson SG, Cideciyan AV, Aleman TS, et al. Photoreceptor Layer Topography in Children with Leber Congenital Amaurosis Caused by RPE65 Mutations. Invest Ophthalmol Vis Sci 2008;49:4573-7.
41. Galvin JA, Fishman GA, Stone EM, Koenekoop RK. Evaluation of genotype-phenotype associations in leber congenital amaurosis. Retina 2005;25:919-29.
42. Silva E, Dharmaraj S, Li YY, et al. A missense mutation in GUCY2D acts as a genetic modifier in RPE65-related Leber Congenital Amaurosis. Ophthalmic Genet 2004;25:205-17.
43. Sitorus RS, Lorenz B, Preising MN. Analysis of three genes in Leber congenital amaurosis in Indonesian patients. Vision Res 2003;43:3087-93.
44. Hamel CP, Griffoin JM, Lasquellec L, et al. Retinal dystrophies caused by mutations in RPE65: assessment of visual functions. Br J Ophthalmol 2001;85:424-7.
45. Dharmaraj SR, Silva ER, Pina AL, et al. Mutational analysis and clinical correlation in Leber congenital amaurosis. Ophthalmic Genet 2000;21:135-50.
46. Chebil A, Falfoul Y, Habibi I, et al. [Genotype-phenotype correlation in ten Tunisian families with non-syndromic retinitis pigmentosa]. J Fr Ophtalmol 2016;39:277-86.
47. Morimura H, Fishman GA, Grover SA, et al. Mutations in the RPE65 gene in patients with autosomal recessive retinitis pigmentosa or leber congenital amaurosis. Proc Natl Acad Sci U S A 1998;95:3088-93.
48. Kabir F, Naz S, Riazuddin SA, et al. Novel mutations in RPE65 identified in consanguineous Pakistani families with retinal dystrophy. Mol Vis 2013;19:1554-64.
49. El Matri L, Ambresin A, Schorderet DF, et al. Phenotype of three consanguineous Tunisian families with early-onset retinal degeneration caused by an R91W homozygous mutation in the RPE65 gene. Graefes Arch Clin Exp Ophthalmol 2006;244:1104-12.
50. Thompson DA, Gyurus P, Fleischer LL, et al. Genetics and phenotypes of RPE65 mutations in inherited retinal degeneration. Invest Ophthalmol Vis Sci 2000;41:4293-9.
51. Mo G, Ding Q, Chen Z, et al. A novel mutation in the RPE65 gene causing Leber congenital amaurosis and its transcriptional expression in vitro. PLoS One 2014;9:e112400.
52. Weleber RG, Michaelides M, Trzupek KM, et al. The phenotype of Severe Early Childhood Onset Retinal Dystrophy (SECORD) from mutation of RPE65 and differentiation from Leber congenital amaurosis. Invest Ophthalmol Vis Sci 2011;52:292-302.
53. Lorenz B, Poliakov E, Schambeck M, et al. A comprehensive clinical and biochemical functional study of a novel RPE65 hypomorphic mutation. Invest Ophthalmol Vis Sci 2008;49:5235-42.

54. Paunescu K, Wabbels B, Preising MN, Lorenz B. Longitudinal and cross-sectional study of patients with early-onset severe retinal dystrophy associated with RPE65 mutations. Graefe's Archive for Clinical and Experimental Ophthalmology 2005;243:417-26.
55. Lorenz B, Wabbels B, Wegscheider E, et al. Lack of fundus autofluorescence to 488 nanometers from childhood on in patients with early-onset severe retinal dystrophy associated with mutations in RPE65. Ophthalmology 2004;111:1585-94.
56. Yzer S, van den Born LI, Schuil J, et al. A Tyr368His RPE65 founder mutation is associated with variable expression and progression of early onset retinal dystrophy in 10 families of a genetically isolated population. J Med Genet 2003;40:709-13.
57. Felius J, Thompson DA, Khan NW, et al. Clinical course and visual function in a family with mutations in the RPE65 gene. Arch Ophthalmol 2002;120:55-61.
58. Katagiri S, Hosono K, Hayashi T, et al. Early onset flecked retinal dystrophy associated with new compound heterozygous RPE65 variants. Mol Vis 2018;24:286-96.
59. Yang G, Liu Z, Xie S, et al. Genetic and phenotypic characteristics of four Chinese families with fundus albipunctatus. Sci Rep 2017;7:46285.
60. Schatz P, Preising M, Lorenz B, et al. Fundus albipunctatus associated with compound heterozygous mutations in RPE65. Ophthalmology 2011;118:888-94.
61. Scholl HP, Moore AT, Koenekoop RK, et al. Safety and Proof-of-Concept Study of Oral QLT091001 in Retinitis Pigmentosa Due to Inherited Deficiencies of Retinal Pigment Epithelial 65 Protein (RPE65) or Lecithin:Retinol Acyltransferase (LRAT). PLoS One 2015;10:e0143846.
62. Samardzija M, Wenzel A, Naash M, et al. Rpe65 as a modifier gene for inherited retinal degeneration. Eur J Neurosci 2006;23:1028-34.
63. Danciger M, Matthes MT, Yasamura D, et al. A QTL on distal chromosome 3 that influences the severity of light-induced damage to mouse photoreceptors. Mamm Genome 2000;11:422-7.
64. Wen Y, Birch DG. Outer Segment Thickness Predicts Visual Field Response to QLT091001 in Patients with RPE65 or LRAT Mutations. Transl Vis Sci Technol 2015;4:8.
65. Maeda T, Lee MJ, Palczewska G, et al. Retinal pigmented epithelial cells obtained from human induced pluripotent stem cells possess functional visual cycle enzymes in vitro and in vivo. J Biol Chem 2013;288:34484-93.
66. Maeda T, Dong Z, Jin H, et al. QLT091001, a 9-cis-retinal analog, is well-tolerated by retinas of mice with impaired visual cycles. Invest Ophthalmol Vis Sci 2013;54:455-66.
67. Fan J, Rohrer B, Frederick JM, et al. Rpe65-/- and Lrat-/- mice: comparable models of leber congenital amaurosis. Invest Ophthalmol Vis Sci 2008;49:2384-9.
68. Zhang H, Fan J, Li S, et al. Trafficking of membrane-associated proteins to cone photoreceptor outer segments requires the chromophore 11-cis-retinal. J Neurosci 2008;28:4008-14.
69. Gu SM, Thompson DA, Srikumari CR, et al. Mutations in RPE65 cause autosomal recessive childhood-onset severe retinal dystrophy. Nat Genet 1997;17:194-7.
70. Van Hooser JP, Aleman TS, He YG, et al. Rapid restoration of visual pigment and function with oral retinoid in a mouse model of childhood blindness. Proc Natl Acad Sci U S A 2000;97:8623-8.

SUPPLEMENTAL MATERIAL

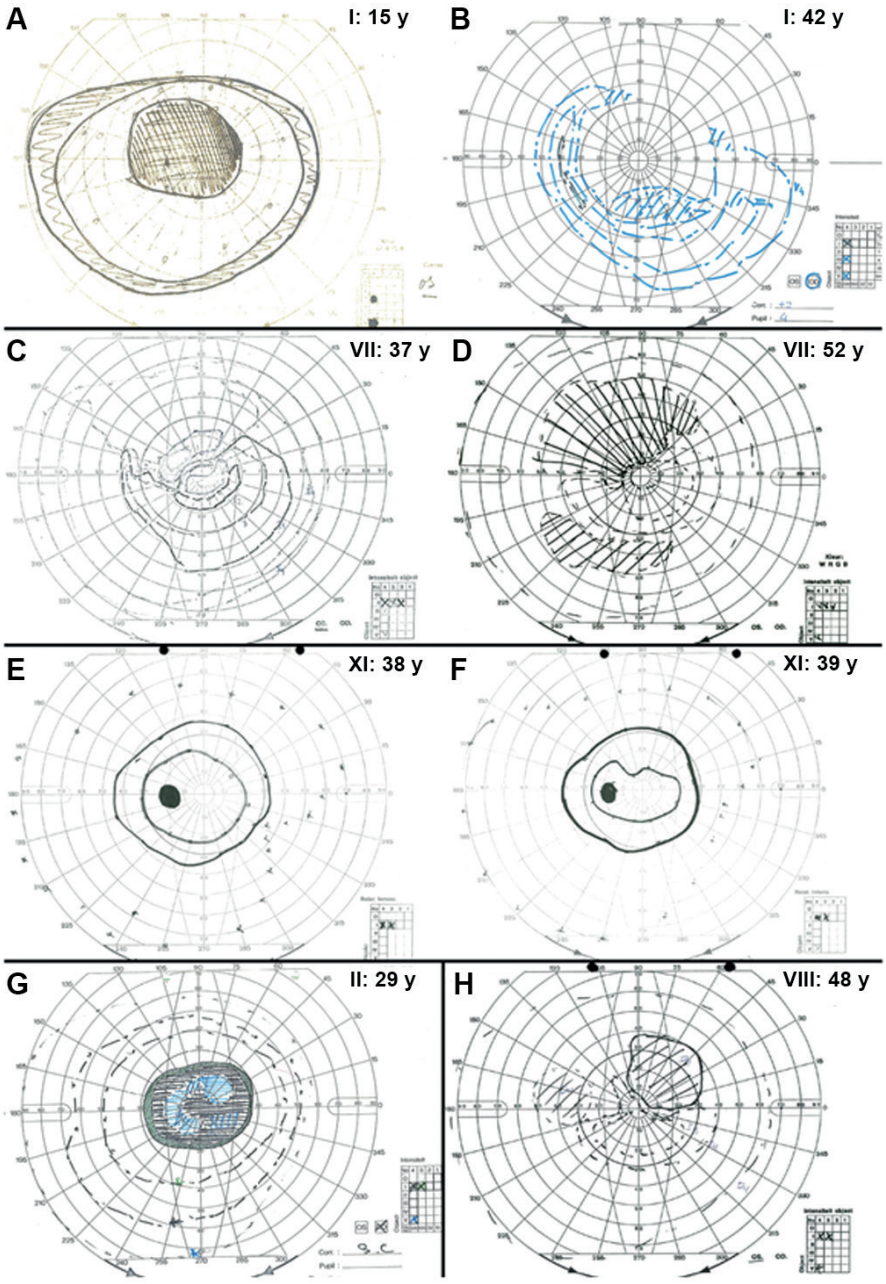

Supplementary Figure S1. Goldmann visual fields in patients retinal degeneration associated with mutations in *LRAT*. Shaded areas represent scotomas. **A-B.** Progression of the visual field defects in patient I between the ages

of 15 (**A**) and 42 (**B**) years. This patient had nondetectable rod or cone responses on electroretinography, but his sibling, patient II, was diagnosed with *LRAT*-associated cone-rod degeneration based on his electroretinogram. **C-D.** Progression of the visual field defects in patient VII, who was diagnosed with retinitis pigmentosa (RP), between the ages 37 (**C**) and 52 (**D**) years. **E-F.** Patient XI, who had RP, showing relative concentric constriction of the smaller (I4e) targets, with a relatively well-preserved V4e isopter size between the ages of 38 (**E**) and 39 (**F**) years. **G.** Patient II, a cone-rod degeneration patient, at the age of 29 years, showing an absolute central scotoma, with a sensitivity reduction in the fovea. **H.** Patient VIII, who had RP, at the age of 48, showing relative concentric constriction, and an absolute midperipheral scotoma encroaching on the fovea.

Supplementary Table S1. Visual fields in patients with retinal degeneration associated with mutations in *LRAT*

ID	Age[a] (y)	Central horizontal diameter V-4e (°)		Central horizontal diameter I-4e (°)		Min. seen[b]	Seeing retinal area V4e (mm^2)			Pattern
		OD	OS	OD	OS		OD	OS	Change (mm^2/year)	
I	50	0	0	0	0	I-4e	213.6	234.6	-16.8	Absolute central scotoma. Peripheral wedge of vision.
	23	1.5	2	0	0	III-4e	NA†	679.1		Large absolute central scotoma with small island of foveal sparing. Midperipheral remaining ring.
II	29	73	63	0	0	I-3e	768.3	725.7		Relative central scotoma (≤I4e). Absolute paracentral scotoma.
III	30	NA†		NA†		NA†	NA†			Supra-temporal absolute scotoma; relative central scotoma
VII	52	72	66	39-10	55	I-2e	543.9	543.5	-15.4	Midperipheral absolute scotomas, encroaching towards fovea. Relative concentric constriction.
	37	145	142	48-10	53	I-2e	782.8	765.7		Relative paracentral scotomas. Relative concentric constriction, mainly superior hemifield.
VIII	48	153	98	30-3	11	I-3e	707.1	691.9		Absolute midperipheral and paracentral scotomas.
IX	11	NA[c]		NA[c]		NA[c]	NA[c]			Multiple relative scotomas in periphery.
X	40	NA[c]		NA[c]		NA[c]	NA[c]			Absolute concentric constriction, 20° from fovea
XI	39	130	140	73	70	I-3e	700.6	716.2	-13.4	Absolute concentric constriction.
	38	140	150	75	77	I-3e	718.9	736.2		Absolute concentric constriction.
XII	54	NA[d]		NA[d]		NA[d]	NA[d]			Absolute scotoma encroaching upon 10° from fovea.

	17	134	123	0	3	II4e/ I4e	562.5	530.0	+41.9	Absolute concentric constriction.
XIII	16	116	128	0	2	II4e/ I4e	455.6	507.2		Increased concentric constriction.
	15	116	130	4	2	I4e	452.2	512.0		Absolute concentric constriction.

NA, not available.

The horizontal diameter, as measured from the vertical meridian, uninterrupted by scotomas, was used to determine the central visual field. When a paracentral scotoma interrupted the horizontal meridian, this was considered the border as measured from the center..

[a] Age at the moment of the examination with Goldmann kinetic perimetry.

[b] Minimal isopter size observed on Goldmann kinetic perimetry.

[c] No Goldmann visual field output available, only a description of the visual field in the medical record.

[d] No Goldmann visual field, but a different perimetry modality (Humphrey 30-2 perimetry).

6.
RHO-associated retinitis pigmentosa

6.1

Clinical characteristics and natural history of *RHO*-associated retinitis pigmentosa: A long-term follow-up study

Xuan-Thanh-An Nguyen, MD[1*], Mays Talib, MD[1*], Caroline van Cauwenbergh, PhD[2], Mary J. van Schooneveld, MD, PhD[3], Marta Fiocco, PhD[4,5], Jan Wijnholds, PhD[*], Jacoline B. ten Brink, BAS[††], Ralph J. Florijn, PhD[6], Nicoline E. Schalij-Delfos, MD, PhD[*], Gislin Dagnelie, PhD[7], Maria M. van Genderen, MD, PhD[8,9], Elfride de Baere, MD, PhD[†], Magda A. Meester-Smoor, PhD[10], Julie De Zaeytijd, MD[†], Irina Balikova, MD, PhD[†], Alberta A. Thiadens, MD, PhD[†††], Carel B. Hoyng, MD, PhD[11], Caroline C. Klaver, MD, PhD[†††,‡‡‡,12], L. Ingeborgh van den Born, MD, PhD[13], Arthur A. Bergen, PhD[††,14], Bart P. Leroy, MD, PhD[†,15], Camiel J.F. Boon, MD, PhD[*,‡]

Retina 2021;41(1):213-223

* Joint first authors.

1 Department of Ophthalmology, Leiden University Medical Center, Leiden, The Netherlands.

2 Department of Ophthalmology, Ghent University and Ghent University Hospital, Ghent, Belgium.

3 Department of Ophthalmology, Amsterdam UMC, Academic Medical Center, Amsterdam, The Netherlands.

4 Institute of Mathematic Leiden University, Leiden, The Netherlands.

5 Department of Biomedical Data Sciences, Leiden University Medical Center, Leiden, The Netherlands.

6 Department of Clinical Genetics, Amsterdam UMC, Academic Medical Center, Amsterdam, The Netherlands.

7 Wilmer Eye Institute, Johns Hopkins University, Baltimore, Maryland.

8 Bartiméus, Diagnostic Centre for complex visual disorders, Zeist, The Netherlands.

9 Department of Ophthalmology, University Medical Center Utrecht, Utrecht, The Netherlands.

10 Department of Ophthalmology, Erasmus Medical Center, Rotterdam, The Netherlands.

11 Department of Ophthalmology, Radboud University Medical Center, Nijmegen, The Netherlands.

12 Department of Epidemiology, Erasmus Medical Center, Rotterdam, The Netherlands.

13 The Rotterdam Eye Hospital, Rotterdam, The Netherlands.

14 The Netherlands Institute for Neuroscience (NIN-KNAW), Amsterdam, The Netherlands.

15 Ophthalmic Genetics & Visual Electrophysiology, Division of Ophthalmology, The Children's Hospital of Philadelphia, Philadelphia, Pennsylvania, USA.

ABSTRACT

Purpose: To investigate the natural history of *RHO*-associated retinitis pigmentosa (RP).

Methods: A multicenter, medical chart review of 100 patients with autosomal dominant *RHO*-associated RP.

Results: Based on visual fields, time-to-event analysis revealed median ages of 52 and 79 years to reach low vision (central visual field <20°) and blindness (central visual field <10°), respectively. For the best-corrected visual acuity (BCVA), the median age to reach mild impairment (20/67 ≤ BCVA < 20/40) was 72 years, whereas it could not be computed for lower acuities. Disease progression was significantly faster in patients with a generalized RP phenotype (n = 75; 75%) than in patients with a sector RP phenotype (n = 25; 25%), in terms of decline rates of BCVA (p < 0.001) and V4e retinal seeing areas (p < 0.005). The foveal thickness of the photoreceptor-retinal pigment epithelium (PR + RPE) complex correlated significantly with BCVA (Spearman's rho = 0.733; p < 0.001).

Conclusions: Based on central visual fields, the optimal window of intervention for *RHO*-associated RP is before the 5th decade of life. Significant differences in disease progression are present between generalized and sector RP phenotypes. Our findings suggest that the PR + RPE complex is a potential surrogate endpoint for the BCVA in future studies.

INTRODUCTION

Mutations in the *RHO* gene are associated with the autosomal dominant form of retinitis pigmentosa (RP).[1] Initial symptoms of RP include night blindness or peripheral visual field (VF) loss, which can be followed by loss of central vision in advanced stages of the disease. To date, more than 150 mutations in the *RHO* gene have been described, which are responsible for 25% to 30% of all autosomal dominant RP cases.[2] *RHO* mutations have also been described in congenital stationary night blindness,[3] and, even more rarely, in forms of autosomal recessive RP.[4] Another phenotype commonly described in *RHO* mutations is sector RP, which is characterized by regional photoreceptor degeneration, typically confined to the inferior quadrant of the retina.[5,6] Sector RP is considered a stationary to slowly progressive disease, but may eventually lead to a more severe, diffuse RP phenotype.[7]

The *RHO* gene encodes the protein rhodopsin, located in the outer segment of rod photoreceptor cells, containing extracellular, transmembrane, and cytoplasmic domains.[1] Previous studies have shown that the clinical expression of *RHO*-associated RP correlates with the protein domain affected by the mutation.[8] Mutations affecting the cytoplasmic domain of rhodopsin are more likely to cause a severe RP phenotype, with early loss of rod and cone function. By contrast, patients with mutations affecting the extracellular domain generally have a milder phenotype, with relatively preserved rod and cone function and slower disease progression.[9,10]

No curative treatment for *RHO*-associated RP is currently available, but promising results have been achieved by knockdown and replacement gene therapy in animal models.[11,12] To guide the design of upcoming clinical trials, more insights into the natural disease progression in *RHO*-associated RP are necessary. A more detailed clinical disease profile will aid in the selection of eligible candidates and in the establishment of appropriate clinical endpoints for future trials. The purpose of this longitudinal study was to provide a description of the clinical variability and the natural disease course in patients with *RHO*-associated RP in a large cohort.

MATERIALS AND METHODS

Study population

Data of patients with *RHO*-associated RP were collected from the patient database for hereditary eye diseases (Delleman Archive) at the Amsterdam University Medical Center (the Netherlands), from various other Dutch tertiary referral centers within the RD5000 consortium,[13] and from Ghent University Hospital in Belgium. Inclusion criteria were as follows: a molecular confirmation of a (likely) pathogenic variant in the *RHO* gene or a first-degree relative with similar clinical findings and molecular confirmation of a *RHO* mutation. In total, 100 patients with *RHO*-associated RP

were included for analysis in this study. Approval from the ethics committee was obtained before the study, as well as local institutional review board approval in all participating centers. Dutch participants provided informed consent for the use of their patient data for research purposes. For Belgian subjects, the local ethics committee waivered the need for informed consent on the condition of pseudonymization.

Data collection

A standardized review of medical records was performed for data on the initial symptoms, best-corrected visual acuity (BCVA), findings on slit-lamp examination and fundoscopy, Goldmann VFs, full-field electroretinogram (ERG), spectral-domain optical coherence tomography (SD-OCT), and fundus autofluorescence (FAF) imaging, where available. Goldmann VFs were digitized and converted to retinal seeing areas using methods previously described by Dagnelie.[14]

In patients with available OCT and FAF imaging in Heidelberg (Heidelberg Engineering, Heidelberg, Germany), automatic and manual measurements of retinal layers were performed using the inbuilt software of Heidelberg. The thickness of the photoreceptor-retinal pigment epithelium complex (PR + RPE), was defined as the foveal distance between the external limiting membrane and the basal border of the RPE, as described previously (see Figure, Supplemental Digital Content 1).[15] All measurements were performed by two authors (X.-T.-A.N. and M.T.) and reviewed by C.J.F. Boon in case of inconsistency between the aforementioned two authors.

Statistical analysis

Data were analyzed using SPSS version 23.0 (IBM Corp, Armonk, NY) and the R software environment.[16] Findings with a P value of < 0.05 were considered statistically significant. Normally and nonnormally distributed data were displayed as means with SDs and medians with interquartile ranges (IQR), respectively. To measure the time to visual impairment, a time-to-event analysis was performed using the nonparametric maximum likelihood estimator method to account for left-censored, interval-censored, and right-censored data. Visual impairment endpoints were based on the criteria of the World Health Organization: no visual impairment (BCVA $\geq$ 20/40), mild visual impairment (20/67 $\leq$ BCVA $<$ 20/40), low vision (20/200 $\leq$ BCVA $<$ 20/67), severe visual impairment (20/400 $\leq$ BCVA $<$ 20/200), or blindness (BCVA $<$ 20/400). For VFs, the following endpoints were used: mild impairment (20° $\leq$ central VF $<$ 70°), low vision (central VF $<$ 20°), and blindness (central VF $<$ 10°). Because of the presence of repeated measurements, a linear mixed model analysis was performed to measure disease progression. For hand movement vision, light perception vision, and no light perception, logarithm of the minimum angle of resolution (logMAR) values of 2.7, 2.8, and 2.9 were used, respectively.[17] Structure-function correlations were analyzed using Spearman correlation coefficients. To analyze genotype-phenotype associations, patients were stratified into the following three groups based the affected protein domain: cytoplasmic, transmembrane, or extracellular.

RESULTS

Clinical and genetic characteristics

One hundred patients from 47 families, with autosomal dominant *RHO* mutations, were included from the Dutch (n = 63; 63%) and Belgian (n = 37; 37%) population. No differences in baseline characteristics between these two populations were present (see Table, Supplemental Digital Content S2). Patients with available longitudinal data (n = 72; 72%) had a median follow-up time of 6.9 years (IQR 11.9; range: 0.2-41.0) and a median of 5.0 visits (IQR 6.0; range: 2.0-31.0). Seventy-five patients (75%) had a generalized form of RP on fundus examination (Figure 1), whereas 25 patients (25%) showed a sector RP phenotype, with pigmentary changes confined to the inferior hemisphere in all cases. The clinical characteristics of the entire cohort are summarized in Table 1.

In total, 23 different missense mutations, one in-frame deletion, and one novel splice-site mutation were found in the *RHO* gene (see Table, Supplemental Digital Content S3). Patients were stratified, based on the affected protein domain, as carrying extracellular (n = 64; 64%), transmembrane (n = 20; 20%), or cytoplasmic (n = 15; 16%) mutations, excluding the splice-site mutation. We found a high proportion of extracellular mutations (24/25; 96%) in the sector RP group. The most common pathogenic variant in this study, p.(Glu181Lys), was found in four families, comprising 23 of the 63 Dutch patients (37%). This mutation was not found in the Belgian cohort. Common mutations exclusively found in the Belgian cohort were p.(Ile255del) (n = 6) and p.(Tyr178Asp) (n = 6), each belonging to a single family, accounting for 12 of the 37 Belgian patients (32%).

Visual function

Best-corrected visual acuity data were available for 95 patients, with a high degree of symmetry between eyes (Spearman's rho = 0.888; $p < 0.001$). In 25 patients, a degree of BCVA-based visual impairment was present during the last examination (see Figure, Supplemental Digital Content 4). Time-to-event analysis of the entire cohort revealed a median age of 72 years to reach mild visual impairment, whereas the median ages for low vision, severe visual impairment, and blindness could not be computed (Figure 2). First occurrences of low vision were seen from the 3th decade of life onward, whereas severe visual impairment and blindness were seen from the 5th decade of life onward. In the sector RP cohort, the first occurrence of blindness was seen after the 8th decade of life in a patient with age-related macular degeneration. Linear mixed model analysis revealed an age effect on mean BCVA, which was 0.012 logMAR (-2.9%; $p < 0.001$) per year for the entire cohort. The BCVA decline was significantly faster in patients with a generalized RP phenotype than that in patients with a sector RP phenotype ($p = 0.002$), with BCVA progression rates of 0.012 logMAR (-3.8%; $p < 0.001$) and -0.002 logMAR (+0.4%; $p = 0.671$) per year, respectively. For patients with generalized RP, we found no differences in baseline BCVA values ($p = 0.360$) or in progression slopes ($p = 0.168$) between affected protein domains.

Initial ERG findings were documented in 52 patients (Table 1). Minimal and nondetectable ERG responses were only found in the generalized RP group. The mean age at which nondetectable ERG responses were first observed was 35.3 years (SD 16.1; range: 17.1-63.7). Longitudinal ERG data were available for 10 patients, with a mean follow-up time of 6.7 years (SD 4.0; range: 0.5-13.6). Eight patients showed no clear changes in ERG patterns during follow-up. Two patients, aged 29 and 26 years, displayed rod-cone patterns at the initial visit, which progressed to minimal and absent responses over a time span of 8.6 and 13.6 years, respectively.

Original Goldmann VF records were available for 59 patients, with high degree of symmetry between eyes for the V4e (Spearman's rho = 0.957; $p < 0.001$) and the I4e (Spearman's rho = 0.935; $p < 0.001$) retinal seeing areas. Various patterns of VF defects were observed, ranging from mild concentric constriction to central islands (Figure 3). Intrafamilial variability was present, as patients carrying the p.(Glu181Lys) mutation could demonstrate different VF defects (Figure 3, A and B). Time-to-event analysis of the VFs revealed median ages of 44, 52, and 79 years for mild visual impairment, low vision, and blindness, respectively (Figure 1B). For the V4e seeing areas, a faster decline of retinal seeing areas was observed in patients with generalized RP than in patients with sector RP ($p = 0.005$), with a significant decline rate of -5.6% per year ($p < 0.001$) for patients with generalized RP, but not in patients with sector RP (+1.7% per year; $p = 0.477$). No differences in V4e retinal seeing areas were seen between domains at baseline ($p = 0.240$) nor with increasing age ($p = 0.085$) in patients with generalized RP. For the I4e retinal seeing areas, we found the age effect to be -5.5% per year ($p < 0.001$) in patients with generalized RP and +0.2% per year ($p = 0.930$) in patients with sector RP. For patients with generalized RP, we found differences at baseline ($p = 0.013$), with larger I4e retinal seeing areas in patients with extracellular mutations than those in patients with transmembrane ($p = 0.005$) or cytoplasmic ($p = 0.026$) mutations. No differences in progression slopes of I4e retinal seeing areas were observed between affected domains ($p = 0.233$).

Table 1. Characteristics of patients with *RHO*-associated (sector) RP at the last examination

Characteristics	Total (n = 100)	Generalized RP (n = 75)	Sector RP (n = 25)	*P*
Male (%)	44 (44)	34 (46)	10 (39)	0.642
Age at last examination (n = 100)				
Mean ± SD	43.5 ± 18.5	42.5 ± 19.3	45.5 ± 22.6	0.204
Initial symptoms (n = 55)				
Nyctalopia, n (%)	41 (75)	28 (74)	2 (40)	
VF loss, n (%)	5 (9)	3 (8)	1 (20)	
Visual acuity loss, n (%)	3 (5)	2 (5)	1 (20)	
Multiple symptoms, n (%)	6 (11)	5 (13)	1 (20)	0.890*
Age at onset in years (n = 55)				
Early childhood, n (%)	21 (38)	16 (29)	5 (9)	
Median age (IQR)	13.5 (12.5)	11.0 (11.8)	15.7 (12.5)	0.829
Mean refractive error, in D (n = 66)				
Mean ± SD	0.8 ± 2.85	1.0 ± 3.27	0.2 ± 1.4	0.298
BCVA in the better-seeing eye (n = 95)				
Median BCVA, in Snellen (IQR)	20/25 (20/30)	20/30 (20/30)	20/20 (20/200)	**<0.001**
BCVA in the worst seeing eye (n=95)				
Median BCVA, in Snellen (IQR)	20/30 (20/25)	20/33 (20/30)	20/22 (20/60)	**0.002**
ERG patterns (n = 52)				
Normal responses, n (%)	2 (4)	-	2 (11)	
Reduced responses, n (%) †	5 (10)	1 (3)	4 (22)	
Rod-cone patterns, n (%)	28 (54)	16 (47)	12 (67)	
Minimal responses, n (%)	6 (11)	6 (18)	-	
Nondetectable, n (%)	11 (21)	11 (32)	-	**<0.001***
Retinal seeing areas, V4e (n = 57)*				
Median seeing areas, in mm^2 (IQR)	256.4 (545.6)	128.0 (552.4)	487.2 (248.3)	0.067
Retinal seeing areas, I4e (n = 55)‡				
Median seeing areas, in mm^2 (IQR)	17.4 (101.4)	14.5 (66.5)	130.6 (194.36)	**0.011**
VF patterns (n = 75)				
Normal, n (%)	1 (1)	1 (2)	-	
Peripheral constriction, n (%)	24 (32)	19 (32)	5 (31)	
Midperipheral scotoma, n(%)	6 (8)	5 (9)	1 (6)	
Central island with peripheral remnants, n (%)	18 (24)	15 (25)	3 (19)	
Central preservation, n (%)	19 (25)	18 (30)	1 (6)	
Superior hemisphere, n (%)	7 (10)	1 (2)	6 (38)	**0.002***
CME, n (%)	16/32 (50)	14/25 (56)	2/7 (29)	0.225*
Central retinal thickness (n = 32)‡				
Median thickness in µm (IQR)	253.0 (94.0)	254.0 (122.0)	248.5 (92.5)	0.858
Outer nuclear layer thickness (n = 32)‡				
Median thickness in µm (IQR)	97.5 (47.25)	89.5 (52.5)	110.5 (41.9)	0.121

Table 1. Continued

PR + RPE thickness (n = 32)‡				
Median thickness in µm (IQR)	90.5 (18.3)	89.5 (20.0)	95.3 (18.1)	0.147
EZ band width (n = 26)‡				
Mean width in µm ± SD	2704.5 ± 1881.9	2125.0 ± 1544.8	4277.5 ± 1909.6	**0.007**
Hyper-AF ring diameter (n = 15)‡				
Horizontal border in µm ± SD	3541.6 ± 1930.6	3484.9 ± 2058.5	3910.3 ± 1009.4	0.571
Vertical border in µm ± SD	2652.7 ± 1567.7	2594.9 ± 1628.0	3201.5 ± 883.2	0.286

Significant p values ($p < 0.05$) are indicated in bold. The last available examination was used for documentation.

* Fisher's exact test was performed.

† No clear rod or cone response was documented.

‡ Averaged between eyes.

D, diopters.

Figure 1. Color fundus photography in this cohort of *RHO*-associated RP. A-C. Illustrations of interfamilial and intrafamilial variability fundus in a family with p.(Tyr178Asn) mutations in the *RHO* gene. **A.** Patient-ID 65, aged 38 years, with mutation p.(Tyr178Asn). Peripapillary atrophy and moderate peripheral chorioretinal atrophy was present on fundus photography. No intraretinal hyperpigmentation was seen (BCVA: 20/20 in both eyes). **B.** Patient-ID 66, aged 45 years, with *RHO* mutation p.(Tyr178Asn). Fundus photography showed chorioretinal atrophy and

bone-spicule hyperpigmentation in the midperiphery (BCVA right eye: 20/25; BCVA left eye: 20/67). **C.** Patient-ID 63, aged 50 years, carrying a p.(Tyr178Asn) in *RHO*. Fundus photography revealed optic disc pallor, attenuated vessels, ring-shaped atrophy in the macula, and diffuse intraretinal bone-spicule hyperpigmentation (BCVA was 20/400 in both eyes). **D**. Patient-ID 52, aged 45 years, with *RHO* mutation p.(Glu28His). A sectorial RP phenotype is seen on color fundus photography of the right eye, with peripapillary atrophy, and atrophic areas and bone spicule hyperpigmentation around the inferior vascular arcade (BCVA: 20/20 in both eyes). **E**. Patient-ID 51, aged 87 years, with *RHO* mutation p.(Leu40Pro). Fundus photography showed mild optic disc pallor with retinal atrophy following the superior and inferior vascular arcade. Geographic atrophy is visible at the macula of the left eye, resulting in a BCVA of only light perception. **F**. Patient-ID 80, aged 74 years, carrying a p.(Asn15Ser) mutation in *RHO*. Fundus photography of the left eye revealed paravascular atrophy mainly in the inferior quadrant with pigment clumping around these atrophic areas. Drusen can be seen around the macula (BCVA right eye: 20/22; BCVA left eye: 20/67). **G**. Patient-ID 48, aged 74 years, with the p.(Asp190Gly) *RHO* mutation, showing advanced RP. A pale fundus with a waxy pale optic disc, severely attenuated vessels, CME, and bone-spicule hyperpigmentation in the midperipheral retina (BCVA right eye: 20/667; BCVA left eye: 20/1,000).

Multimodal imaging

Spectral-domain OCT imaging was performed in 32 patients, with thickness measurements of retinal layers specified in Table 1**.** We found cystoid macular edema (CME) in 16 of the 32 patients (50%), which was located in the fovea for 12 of the 16 (75%) patients. No significant age effect was found on central retinal thickness ($p = 0.371$) or outer nuclear layer thickness ($p = 0.502$), after exclusion of patients with foveal CME. For PR + RPE measurements, advancing age was associated with the loss of PR + RPE thickness (-0.6% per year; $p = 0.030$), which was not affected by a sector RP phenotype ($p = 0.611$). The PR + RPE thickness was the only parameter, after exclusion of patients with foveal CME and correction for multiple testing, that correlated with the BCVA (Table 2). The macular ellipsoid zone (EZ) bandwidth, measurable in 26 of the 32 (81%) patients, decreased with advancing age (-3.8%; $p < 0.001$), which was not significantly different in patients with sector RP ($p = 0.589$). However, a larger EZ bandwidth at baseline was seen in patients with a sector RP phenotype ($p = 0.018$). For patients with generalized RP, no differences in the EZ bandwidth at baseline ($p = 0.185$) or for the decline rates ($p = 0.886$) were observed between affected protein domains. In six of the 26 patients (23%), the EZ bandwidth went beyond the scanning range on SD-OCT (Figure 4A). A granular interrupted aspect of the EZ bandwidth was seen in nine of the 26 (35%) patients.

Fundus AF imaging, available for 38 patients, revealed hyperautofluorescent (hyper-AF) and hypo-autofluorescent (hypo-AF) patterns in variable degrees, including a hyper-AF macular ring in 26 of the 38 (68%) patients (Figure 4). In patients with sector RP, a common pattern seen on FAF was a hypo-AF distribution along the inferior vascular arcade, which corresponded with areas of degeneration seen on fundus photography (Figure 4D). A high degree of correlation was found between EZ bandwidth and the horizontal ($\rho = 0.923$; $p < 0.001$) and vertical borders ($\rho = 0.937$; $p< 0.001$) of the hyper-AF macular ring.

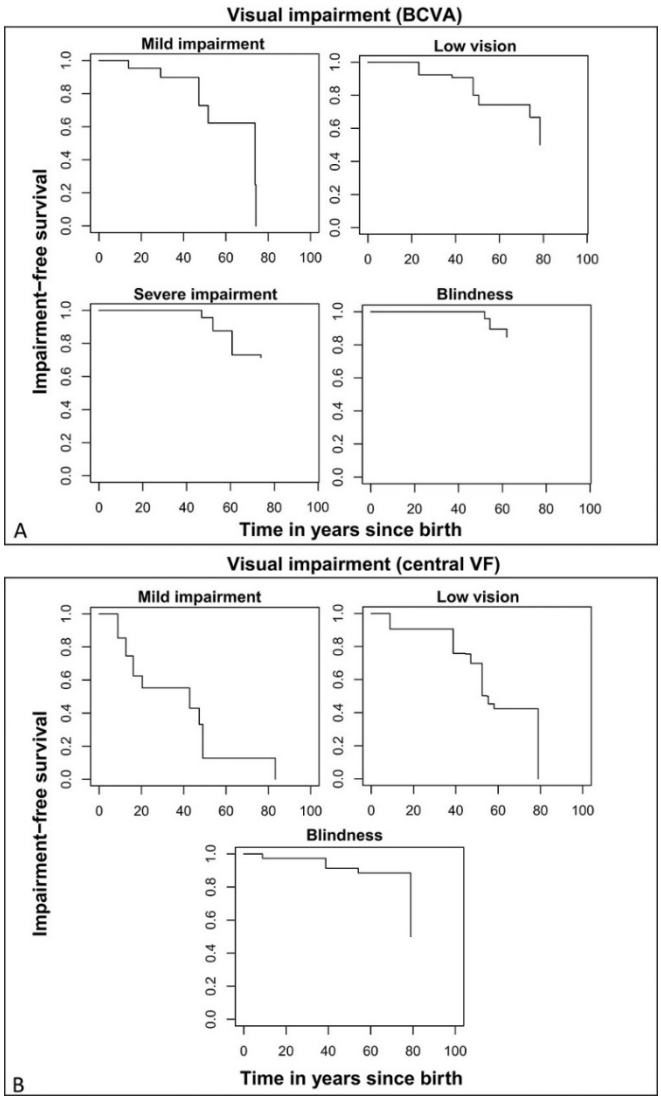

Figure 2. Time-to-event analysis illustrating the time to reaching visual impairment based on the definition set by the World Health Organization. Because of the presence of left-censored, interval-censored, and right censored data to estimate the time to low vision, severe impairment, and blindness, the nonparametric maximum likelihood estimator was employed**. A.** Time-to-event analysis of the BCVA in the better-seeing eye demonstrating the time to reaching mild visual impairment (20/67 ≤ BCVA < 20/40), low vision (20/200 ≤ BCVA < 20/67), severe visual impairment (20/400 ≤ BCVA < 20/200), or blindness (BCVA < 20/400). **B.** For central VFs, the following endpoints were used: mild impairment (20° ≤ central VF < 70°), low vision (central VF < 20°), and blindness (central VF < 10°).

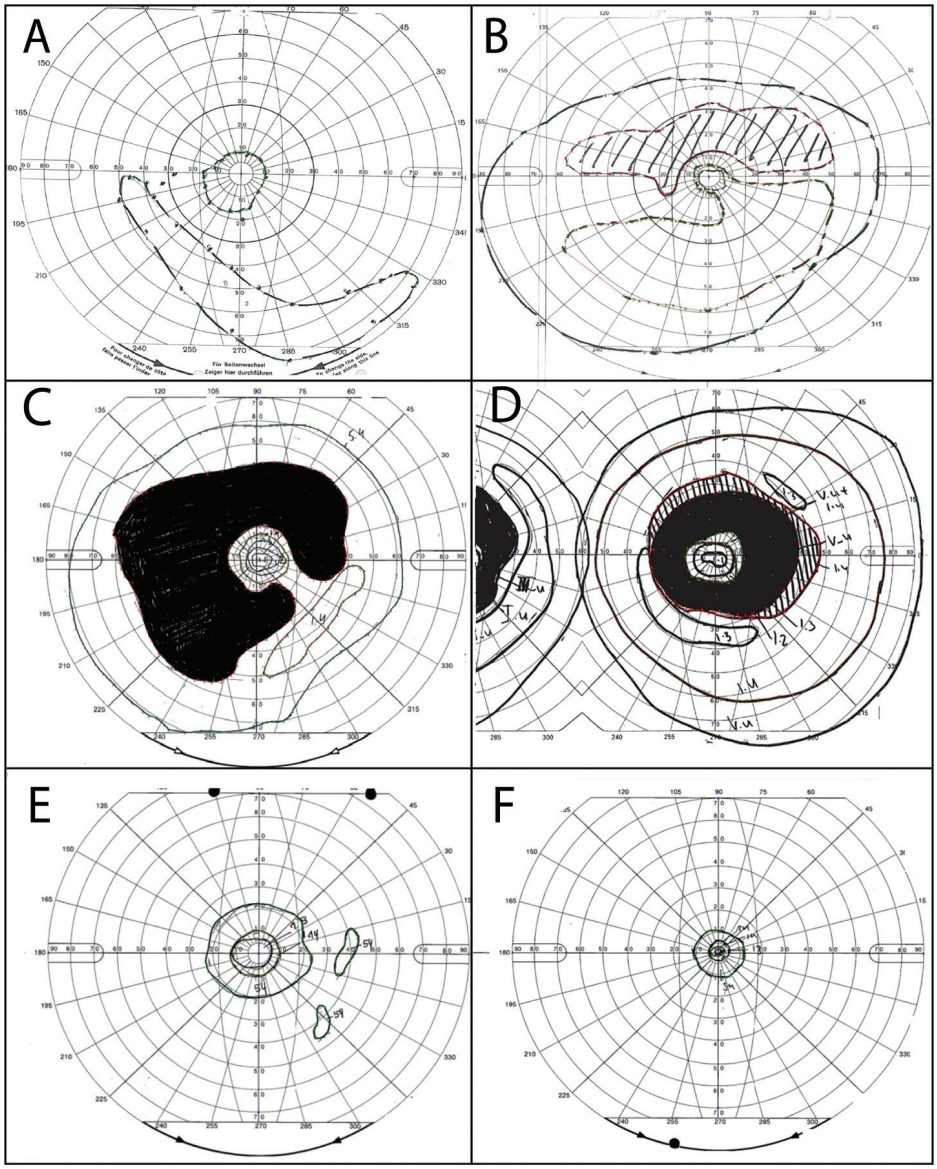

Figure 3. Representative patterns of VF loss in patients with *RHO*-associated RP. A-B. Intrafamilial variability in a family carrying the p.(Glu181Lys) mutation. **A.** Patient ID-30, aged 54 years, showed a central island with peripheral remnants (BCVA right eye: 20/100; BCVA left eye: 20/125) on kinetic perimetry, whereas the younger brother (**B**), aged 46 years, had an absolute scotoma in the superior hemifield (BCVA: 20/16 in both eyes). **C.** Patient-ID 52, aged 43 years, with the *RHO* missense mutation p.(Glu28His). An incomplete midperipheral annular scotoma was visible in the left eye (BCVA right eye: 20/25; BCVA left eye: 20/20). **D.** Patient-ID 39, aged 52 years, with a c.937-2A>C [p.(?)] splice site mutation in *RHO*, showing a complete ring scotoma in the right eye (BCVA right eye: 20/67; BCVA left eye: 20/400). **E.** Patient-ID 59, aged 22 years, with *RHO* mutation p.(Arg135Trp), showing severe constriction of the V4e and I4e isopters with central preservation of the VF and small midperipheral VF remnants (BCVA right eye:

20/67; BCVA left eye: 20/40). **F.** Patient-ID 44, aged 38 years, carrying the p.(Asp190Tyr) *RHO* mutation, had marked peripheral VF loss with only a residual central island remaining (BCVA right eye: 20/50; BCVA left eye: 20/32) .

Table 2. Structure and function correlations in *RHO*-associated RP

	BCVA (logMAR)		Seeing retinal area V4e		Seeing retinal area I4e	
Visual function parameter	**Spearman's rho**	***P***	**Spearman's rho**	***P***	**Spearman's rho**	***P***
SD-OCT imaging						
CRT*	-0.370	0.095	0.291	0.274	0.086	0.770
ONL thickness*	-0.234	0.366	-0.029	0.923	-0.162	0.596
PR + RPE thickness*	-0.733	**<0.001**	0.528	0.053	0.556	0.049
EZ bandwidth	-0.506	0.054	0.198	0.517	0.280	0.379
FAF imaging						
Horizontal ring diameter	-0.339	0.235	0.632	0.024	0.643	0.021
Vertical ring diameter	-0.245	0.419	0.615	0.037	0.566	0.059

The most recent mean values between right and left eyes were used for analysis. Imaging and measurements were performed using the Heidelberg inbuilt software (Spectralis SD-OCT + HRA, Heidelberg Engineering, Heidelberg, Germany). The significance level was set at 0.003 after Bonferroni correction. Significant values are in bold.
*Patients with CME located in the fovea were excluded from analysis.

CRT, central retinal thickness; ONL, outer nuclear layer.

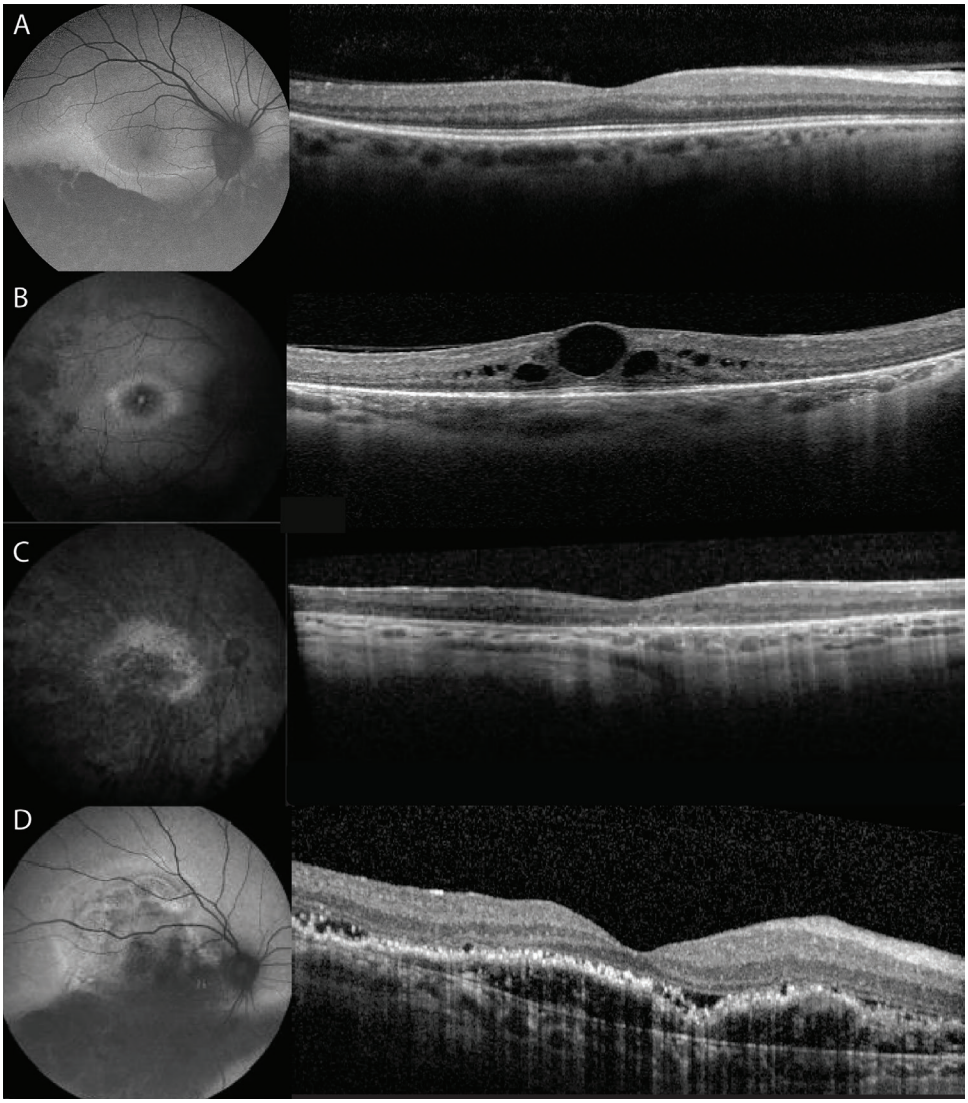

Figure 4. Fundus AF and corresponding SD-OCT imaging in patients with *RHO*-associated RP. A. Patient-ID 81, aged 47 years, carrying the missense mutation p.(Asn15Ser). Fundus AF imaging showed an inferior sectoral hypo-AF, and ERG responses were reduced in a rod-cone pattern. Spectral-domain OCT imaging in this patient revealed central preservation of outer retinal layers, but with thinning of these layers in the peripheral macula. The EZ bandwidth went beyond the scanning range nasally (BCVA right eye: 20/20; BCVA left eye: 20/22). **B.** Patient-ID 70, aged 26 years, with a p.(Glu181Lys) missense mutation. A well-demarcated hyper-AF ring was visible on FAF, with hypo-AF regions inside the hyper-AF ring. A small hyper-AF spot was seen at the foveal site, corresponding to the site of CME on SD-OCT. The midperipheral retina displayed normal AF regions surrounded by granular hypo-AF in variable intensities. Cystoid fluid collections were present in the inner and outer nuclear layer (BCVA right eye: 20/28; BCVA left eye, 20/33). **C.** Patient-ID 88, aged 60 years, carrying a p.(Pro347Leu) missense mutation in the *RHO* gene. Fundus AF imaging reveals the near absence of AF in the fovea and midperipheral retina, with residual

AF remaining in the posterior pole. No evident hyper-AF ring is seen. Profound atrophy of all retinal layers is present on SD-OCT, with increased visibility of the underlying choroidal vessels. Granular remnants of the EZ are seen at the central fovea, but the EZ is completely absent in the peripheral macula (BCVA was 20/400 in both eyes). **D.** Patient-ID 80, aged 74 years, carrying the *RHO* missense mutation p.(Asn15Ser). Fundus AF imaging showed sectoral hypo-AF along the inferior vascular arcade, corresponding with the RPE atrophy seen on fundus photography (Figure 1F). On SD-OCT, a pigment epithelial detachment was observed. The partly hyperreflective structures underlying the RPE detachment suggest the presence of a neovascular membrane. The different layers of the neuroretina were still discernible, with a BCVA of 20/33 and 20/22 in the right and left eye, respectively.

DISCUSSION

This multicenter study provides a detailed description of the natural history of *RHO*-associated autosomal dominant RP, using cross-sectional and longitudinal data. We found a high prevalence of the p.(Gly181Lys) mutation (n = 23) in four different families, accounting for 37% of the Dutch cohort. This mutations has rarely been described in other populations, which is suggestive of a founder effect of p.(Gly181Lys) in the Dutch *RHO*-associated autosomal dominant RP patients. Common mutations exclusively found in the Belgian patients of our cohort were p.(Ile255del) and p.(Tyr178Asp). The p.(Tyr178Asp) mutation has never been described outside the Belgian population,[18] whereas the p.(Ile255del) mutation has previously been found in a single Irish family.[19]

Several mutations, such as the p.(Glu181Lys), found in this cohort could present as either generalized or sector RP, which underlines the potential influence of genetic and/or other modifiers on the phenotype. As suggested previously, it is possible that sector RP will eventually transition into a generalized RP phenotype in later stages of the disease.[7] However, we were not able to observe this transition in any of our patients. In addition, we found patients that retained a sector RP phenotype up to the 8th decade of life.

Our reported progression rates of BCVA (-3.8% per year) and V4e seeing areas (-5.6% per year) in patients with generalized RP were faster than those reported by a previous natural history study on *RHO*-associated RP, which reported rates of -1.8% per year for BCVA and -2.6% per year for V4e retinal seeing areas.[9] One possible explanation for this discrepancy is the difference in statistical methods. In contrast to the study of Berson et al,[9] we analyzed patients with a sector RP separately, because these patients demonstrated minimal disease progression and may contribute to a ceiling effect. In addition, there are notable genetic differences between our population and the one in the American study by Berson et al. The p.(Pro23His) mutation, which is the most common *RHO* mutation in the United States (36% in their cohort), is known to express a particularly mild phenotype and is also described in patients with sector RP.[20] To the best of our knowledge, this founder mutation has never been reported in European studies, including the present one.[21,22]

Patients with a generalized form of RP were stratified based on the domains affected by *RHO* mutations. At baseline, we found larger EZ bandwidths on OCT and I4 retinal seeing areas on Goldmann VF in patients carrying extracellular mutations than in patients with transmembrane or cytoplasmic mutations. No differences in annual decline rates of EZ bandwidths and I4e retinal seeing areas were found between mutated protein domains. In addition, mutations causing sector RP, showing minimal disease progression, were predominantly found in the extracellular domains. These findings support previous research in suggesting that extracellular mutations causes milder phenotypes in *RHO*-associated RP.[23-25] The differences in disease expression between affected domains can be attributed to the biochemical defects caused by the mutations within these domains, although external modifiers such as increased light exposure, especially in the development of sector RP, may also play a role.[2,7]

A limitation of this study is its retrospective nature, which limited a complete ascertainment of clinical data. Electroretinogram data were not available for all patients and were mainly performed at baseline for diagnostic purposes. For this reason, a previously used classification system could not be applied to this cohort.[10,23,24] A prospective standardized natural history study on *RHO*-associated RP, which is currently unavailable to the best of our knowledge, should be able to address such limitations.

Preclinical studies on several gene knockdown and replacement strategies for *RHO*-associated RP have shown promising results, paving the way for human gene therapy trials.[11,12] Our current clinical findings can have significant implications for future clinical treatment trials. We found a high degree of between-eye symmetry for all visual parameters (BCVA, V4e, and I4e retinal seeing retinal areas), supporting the use of the fellow eye as a control in intervention studies. On SD-OCT imaging, we found a high prevalence of CME, which may be a concern for future gene therapy trials, because the presence of CME may alter the retinal morphology, challenging correct injection of viral vectors into the subretinal space and posing additional risks for peroperative and postoperative complications.[26] The borders of the hyper-AF ring on FAF imaging, which demarcates the transition zone between the affected and unaffected retina,[27] correlated strongly with the EZ bandwidth. Fundus AF imaging should be used in conjunction with SD-OCT to capture disease progression in less advanced stages of *RHO*-associated RP, in which the EZ bandwidth can go beyond the 30° scanning range of SD-OCT (occurring in 23% of our cases).

The optimal intervention window for *RHO*-associated RP is before the 5th decade of life, because time-to-event analysis of VFs revealed median ages of 52 and 79 years for low vision and blindness, respectively. The use of visual acuity as an endpoint may be impractical for *RHO*-associated RP, because of the relatively late onset of BCVA-based impairment. Therefore, the use of surrogate endpoints for the visual acuity could accelerate the measurement of disease progression and treatment response. We and others have previously found that the PR + RPE complex has been

suggested to be a good predictor of the visual acuity.[15,28-30] Similar results were found in this study, because the PR + RPE complex correlated strongly with BCVA, and it was the only parameter that remained significant after correction for multiple testing. The PR + RPE complex can potentially be used to identify early structural changes before the visual acuity loss may be noticeable, which can be particularly useful in diseases with relatively slow disease progression such as *RHO*-associated RP. In anticipation of future clinical trials for *RHO*, the establishment of potential clinical endpoints is a necessary step for an optimal study design. In this regard, this study highlights the potential use of the PR + RPE complex as a surrogate endpoint for the BCVA in future clinical trials.

Acknowledgements

This study was performed as part of a collaboration within the European Reference Network for Rare Eye Diseases (ERN-EYE). ERN-EYE is co-funded by the Health Program of the European Union under the Framework Partnership Agreement #739543 – 'ERN-EYE' and co-funded by the Hôpitaux Universitaires de Strasbourg.

REFERENCES

1. Dryja TP, Hahn LB, Cowley GS, et al. Mutation spectrum of the rhodopsin gene among patients with autosomal dominant retinitis pigmentosa. Proc Natl Acad Sci USA 1991;88:9370-9374.
2. Verbakel SK, van Huet RAC, Boon CJF, et al. Non-syndromic retinitis pigmentosa. Prog Ret Eye Res 2018;66:157-186.
3. Zeitz C, Gross AK, Leifert D, et al. Identification and functional characterization of a novel rhodopsin mutation associated with autosomal dominant CSNB. Invest Ophthalmol Vis Sci 2008;49:4105-4114.
4. Comitato A, Di Salvo MT, Turchiano G, et al. Dominant and recessive mutations in rhodopsin activate different cell death pathways. Hum Mol Genet 2016;25:2801-2812.
5. Kranich H, Bartkowski S, Denton MJ, et al. Autosomal dominant 'sector' retinitis pigmentosa due to a point mutation predicting an Asn-15-Ser substitution of rhodopsin. Hum Mol Geneti 1993;2:813-814.
6. Berson EL, Rosner B, Sandberg MA, et al. Ocular findings in patients with autosomal dominant retinitis pigmentosa and a rhodopsin gene defect (pro-23-his). Arch Ophthalmol 1991;109:92-101.
7. Ramon E, Cordomí A, Aguilà M, et al. Differential light-induced responses in sectorial inherited retinal degeneration. J Biol Chem 2014;289:35918-35928.
8. Iannaccone A, Man D, Waseem N, et al. Retinitis pigmentosa associated with rhodopsin mutations: Correlation between phenotypic variability and molecular effects. Vis Res 2006;46:4556-4567.
9. Berson EL, Rosner B, Weigel-DiFranco C, et al. Disease progression in patients with dominant retinitis pigmentosa and rhodopsin mutations. Invest Ophthalmol Vis Sci 2002;43:3027-3036.
10. Mendes HF, van der Spuy J, Chapple JP, et al. Mechanisms of cell death in rhodopsin retinitis pigmentosa: implications for therapy. Trends Mol Med 2005;11:177-185.
11. Tsai Y-T, Wu W-H, Lee T-T, et al. Clustered regularly interspaced short palindromic repeats-based genome surgery for the treatment of autosomal dominant retinitis pigmentosa. Ophthalmology 2018;125:1421-1430
12. Cideciyan AV, Sudharsan R, Dufour VL, et al. Mutation-independent rhodopsin gene therapy by knockdown and replacement with a single AAV vector. Proc Natl Acad Sci USA 2018;115:E8547.
13. van Huet RAC, Oomen CJ, Plomp AS, et al. The RD5000 Database: facilitating clinical, genetic, and therapeutic studies on inherited retinal diseases. Invest Ophthalmol Vis Sci 2014;55:7355-7360.
14. Dagnelie G. Technical note. Conversion of planimetric visual field data into solid angles and retinal areas. Clin Vis Sci 1990;5:95-100.
15. Spaide RF, Curcio CA. Anatomical correlates to the bands seen in the outer retina by optical coherence tomography: literature review and model. Retina 2011;31:1609-1619.
16. R: A language and environment for statistical computing [computer program]. Vienna, Austria: R Foundation for Statistical Computing; 2010.
17. Talib M, van Schooneveld MJ, Thiadens AA, et al. Clinical and genetic characteristics of male patients with RPGR-associated retinal dystrophies: A Long-Term Follow-up Study. Retina 2019;39:1186-1199.
18. Van Cauwenbergh C, Coppieters F, Roels D, et al. Mutations in splicing factor genes are a major cause of autosomal dominant retinitis pigmentosa in Belgian families. PLoS One 2017;12:e0170038.

19. Inglehearn CF, Bashir R, Lester DH, et al. A 3-bp deletion in the rhodopsin gene in a family with autosomal dominant retinitis pigmentosa. Am J Hum Genet 1991;48:26-30.
20. Oh KT, Weleber RG, Lotery A, et al. Description of a new mutation in rhodopsin, pro23ala, and comparison with electroretinographic and clinical characteristics of the pro23his mutation. Arch Ophthalmol 2000;118:1269-1276.
21. Blanco-Kelly F, García-Hoyos M, Cortón M, et al. Genotyping microarray: Mutation screening in Spanish families with autosomal dominant retinitis pigmentosa. Mol Vis 2012;18:1478-1483.
22. Audo I, Manes G, Mohand-Saïd S, et al. Spectrum of rhodopsin mutations in French autosomal dominant rod-cone dystrophy patients. Invest Ophthalmol Vis Sci 2010;51:3687-3700.
23. Cideciyan AV, Hood DC, Huang Y, et al. Disease sequence from mutant rhodopsin allele to rod and cone photoreceptor degeneration in man. Proc Natl Acad Sci USA 1998;95:7103-7108.
24. Jacobson SG, McGuigan DB, Sumaroka A, et al. Complexity of the class B phenotype in autosomal dominant retinitis pigmentosa due to rhodopsin mutations. Invest Ophthalmol Vis Sci 2016;57:4847-4858.
25. Schuster A, Weisschuh N, Jägle H, et al. Novel rhodopsin mutations and genotype-phenotype correlation in patients with autosomal dominant retinitis pigmentosa. Br J Ophthalmol 2005;89:1258.
26. Xue K, Groppe M, Salvetti AP, et al. Technique of retinal gene therapy: delivery of viral vector into the subretinal space. Eye. 2017;31:1308-1316.
27. Aizawa S, Mitamura Y, Hagiwara A, et al. Changes of fundus autofluorescence, photoreceptor inner and outer segment junction line, and visual function in patients with retinitis pigmentosa. Clin Exp Ophthalmol 2010;38:597-604.
28. Eliwa TF, Hussein MA, Zaki MA, et al. Outer retinal layer thickness as good visual predictor in patients with diabetic macular edema. Retina 2018;38:805-811.
29. Lim JI, Tan O, Fawzi AA, et al. A pilot study of Fourier-domain optical coherence tomography of retinal dystrophy patients. Am J Ophthalmol 2008;146:417-426.
30. Talib M, van Schooneveld MJ, Van Cauwenbergh C, et al. The Spectrum of Structural and Functional Abnormalities in Female Carriers of Pathogenic Variants in the RPGR Gene. Invest Ophthalmol Vis Sci 2018;59:4123-4133.

SUPPLEMENTAL MATERIAL

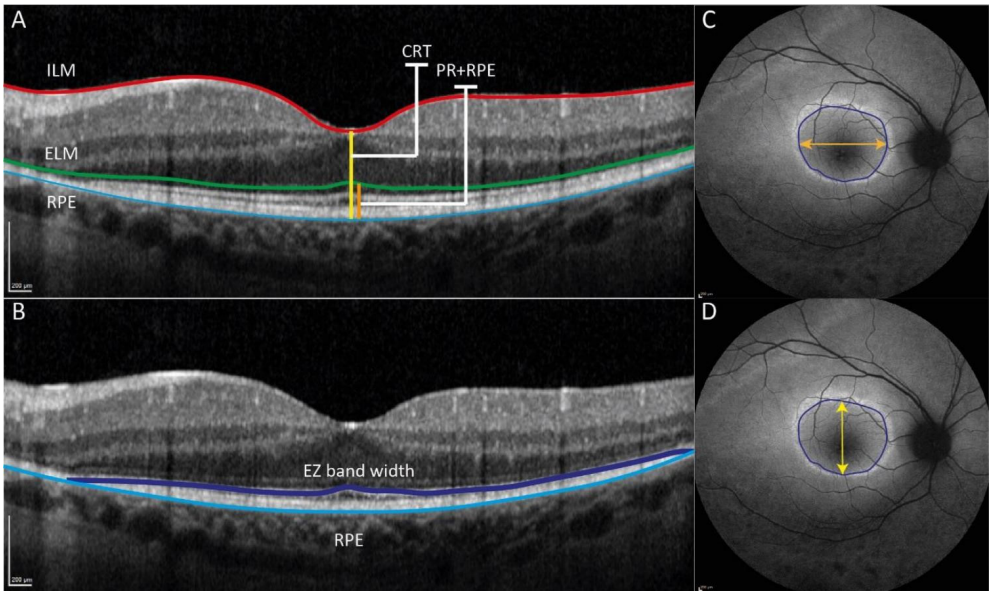

Supplemental Digital Content 1. Measurement of structures using the Heidelberg System (Spectralis SD-OCT + HRA, Heidelberg Engineering, Heidelberg, Germany). Errors in segmentation were corrected manually. A. Measurement of the central retinal thickness (CRT), which was defined as the foveal thickness between the internal limiting membrane (ILM) and the retinal pigment epithelium (RPE) layer. Measurement of the photoreceptor-retinal pigment epithelium complex (PR + RPE), was defined as the foveal thickness between the external limiting membrane (ELM) and the basal border of the RPE layer. **B.** The ellipsoid zone band width (dark blue) was followed nasally and temporally until it was indistinguishable from the retinal pigment epithelium (light blue). **C** and **D**. On fundus autofluorescence imaging, the inner borders of the hyperautofluorescent ring were measured in the horizontal (**C**) and vertical axis (**D**) as illustrated.

Supplemental Digital Content 2. Cohort characteristics of Dutch and Belgian patients with *RHO*-associated retinal dystrophies

Characteristics	Total	Dutch patients	Belgian patients	*P*-value
Age at last examination (years), n	100	63	37	
Mean ± SD	43.5±18.5	44.6±18.3	41.6±18.7	0.426
Range	10.0-87.7	14.3-87.7	10.0-82.4	
Follow-up time (years), no.	72	44	28	
Median FU time (IQR)	6.9 (11.9)	6.8 (13.3)	6.9 (7.5)	0.238
Range	0.2-41.0	0.2-36.4	0.2-41.0	
BCVA at the last visit (decimals), n	95	61	34	
Median BCVA, Snellen (IQR)	20/25 (20/30)	20/25 (20/30)	20/27 (20/36)	0.368
Range	LP-20/12	20/1000-20/12	LP-20/20	
Seeing areas at last visit (I4e, mm^2), n	55	25	30	
Median isopter size ((IQR)	17.4 (101.4)	29.1	15.0	0.106
Range	0.8-667.8	1.2-667.8	0.8-292.5	
Seeing areas at last visit (V4e, mm^2), n	57	24	33	
Median isopter size (IQR)	256.4 (545.6)	322.1 (547.5)	205.6 (545.6)	0.559
Range	4.0-764.9	14.5-763.9	3.7-764.9	

BCVA, best-corrected visual acuity; FU, follow-up; IQR, interquartile range; LP, light perception; SD, standard deviation.

Supplemental Digital Content 3. Overview of mutations included in this study of *RHO*-associated retinitis pigmentosa

Families affected	#	Nucleotide change	Amino acid change	Domain*	References
1	2	c.11C>A	p.(Thr4Lys)†	Extracellullar	Van den Born et al. 1994
3	4	c.44A>G	p.(Asn15Ser)†	Extracellullar	Yoshi et al. 1998
2	2	c.50C>T	p.(Thr17Met)†	Extracellullar	Dryja et al. 1991
2	2	c.68C>T	p.(Pro23Leu)†	Extracellullar	Dryja et al. 1991
3	8	c.84G>T	p.(Gln28His)†	Extracellullar	Fernandez al. 2014
1	1	c.119T>C	p.(Leu40Pro)	Transmembrane	De Sousa Dias et al. 2015
1	1	c.133T>C	p.(Phe45Leu)	Transmembrane	Dryja et al. 2000
1	3	c.265G>C	p.(Gly89Arg)	Transmembrane	Van Cauwenbergh et al. 2017
3	7	c.403C>T	p.(Arg135Trp)	Cytoplasmic	Jacobson et al 1991
1	4	c.512C>A	p.(Pro171Gln)	Transmembrane	Antiolo et al. 1994
1	6	c.532T>G	p.(Tyr178Asp)	Extracellullar	Van Cauwenbergh et al. 2017
1	1	c.538C>T	p.(Pro180Ser)	Extracellullar	Neveling et al. 2012
4	23	c.541G>A	p.(Glu181Lys)†	Extracellullar	Blanco-Kelly et al. 2012 Coussa et al. 2015
2	3	c.563G>A	p.(Gly188Glu)	Extracellullar	Macke et al. 1993
1	1	c.568G>A	p.(Asp190Asn)†	Extracellullar	Tsui et al. 2008
3	5	c.569A>G	p.(Asp190Gly)†	Extracellullar	Dryja et al. 1991
5	7	c.568G>T	p.(Asp190Tyr)	Extracellullar	Blanco-Kelly et al. 2012
1	1	c.641T>A	p.(Ile214Asn)†	Transmembrane	Neveling et al. 2012
1	1	c.759G>T	p.(Met253Ile)	Transmembrane	Van Huet et al. 2015
1	6	c.763_765del	p.(Ile256del)	Transmembrane	Inglehearn et al. 1991
1	3	c.911T>A	p.(Val304Asp)	Transmembrane	Van Cauwenbergh et al. 2017
1	1	c.937-2A>C	Splice site	-	Novel
2	3	c.1028G>A	p.(Ser343Asn)	Cytoplasmic	Van Cauwenbergh et al. 2017
2	2	c.1033G>A	p.(Val345Met)	Cytoplasmic	Grøndahl al. 2006
3	3	c.1040C>T	p.(Pro347Leu)	Cytoplasmic	Blanco-Kelly et al. 2012 Dryja et al. 1990

RP, generalized retinitis pigmentosa.

Frequency of affected individuals.

* Protein domain predicted to be affected by *RHO* mutations.

† Mutations associated with a sector RP phenotype.

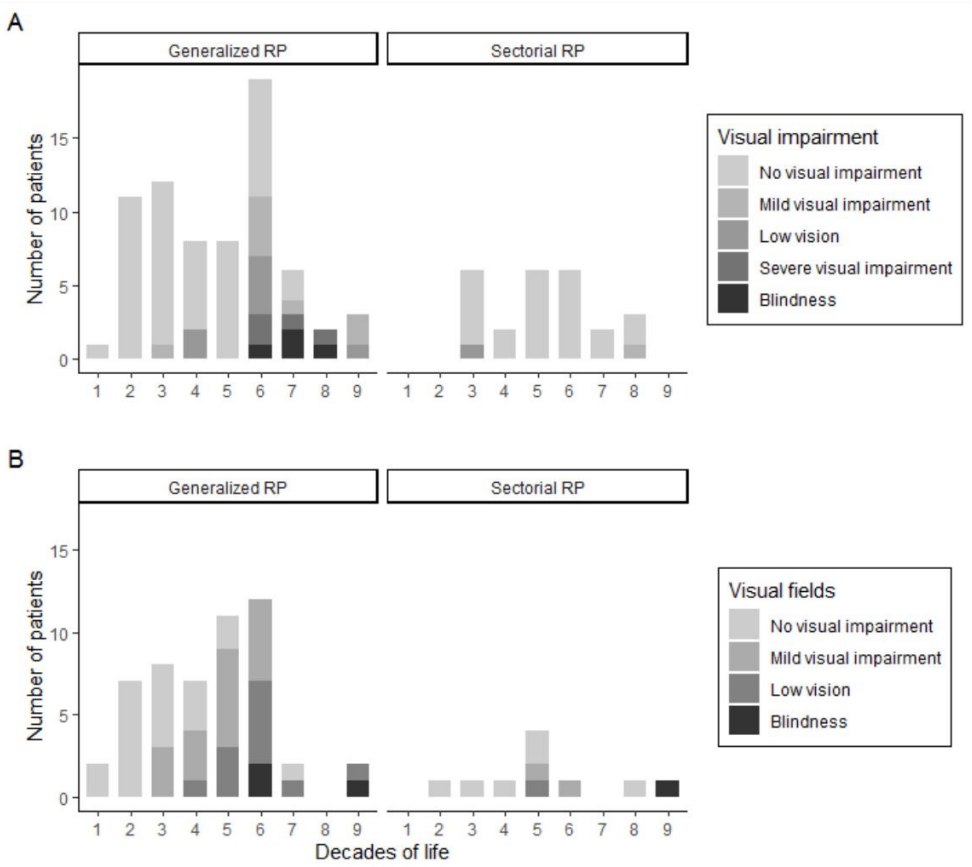

Supplemental Digital Content 4. Visual impairment in patients with *RHO*-associated retinitis pigmentosa (RP) by decades of life, classified as either generalized RP or sector RP. A. Visual impairment based on last available best-corrected visual acuity (BCVA), based on the criteria of the World Health Organization: No visual impairment (BCVA ≥ 20/40), mild visual impairment (20/67 ≤ BCVA < 20/40), low vision (20/200 ≤ BCVA < 20/200) or blindness (BCVA < 20/400). **B.** For visual impairment based on last available central visual fields (central VF; V4e), the following endpoints were used: mild visual impairment (20° ≤ central VF < 70°), low vision (central VF < 20°) and blindness (central VF < 10°).

7.

GENERAL DISCUSSION

Partly adapted from: Talib M[1], Boon CJF[1,2] . Retinal dystrophies and the road to treatment: clinical requirements and considerations.

Asia Pac J Ophthalmol 2020;9(3):159-179

1 Department of Ophthalmology, Leiden University Medical Center, Leiden, The Netherlands
2 Department of Ophthalmology, Amsterdam UMC, University of Amsterdam, Amsterdam, The Netherlands

The aim of this thesis was to clinically characterize several subsets of inherited retinal dystrophies (IRDs) for which gene therapy is under development, to study the disease progression, and to assess any genotype-phenotype correlations where possible. The relevance of these findings is pertinent to clinical practice, in order to inform patients on the specifics of their prognosis. Moreover, the emergence of gene-based therapeutic trials for these genes underscores the importance of these findings, and adds an urgency to their elucidation. This chapter elaborates on the primary findings of this thesis, placing them in a broader perspective, and discussing their clinical implications and future relevance.

IRDs comprise a collection of degenerative diseases characterized by the usually progressive and sometimes stationary dysfunction of rods and/or cones. With a prevalence of 1:3000 individuals,[1, 2] IRDs are not particularly rare. However, due to their genetic heterogeneity, with over 200 disease genes identified to date, each genetic subtype may be exceedingly rare. These diagnoses have a profoundly distressing impact on patient's lives, progressively affecting their mobility, professional functioning, and independence. Patients are often uncertain of their prognosis, questioning if and when they will go blind, and whether they will pass this disease onto their children. Children or adolescents diagnosed with IRD need to be informed on their prognosis, in order to make sound decisions on life planning such as future career paths. Special lighting, magnification requirements, and other requirements need to be tended to at their home, school, or professional environment, or they may need to visit a special needs school altogether.

The evolution of gene-based therapeutic trials

Due to the monogenic nature of most IRDs, as well as the relative immune privilege of the eye, its accessibility, and the ability to non-invasively monitor its function and structure, the eye is a particularly suitable target for investigational gene therapy. The blood-retinal barrier restricts the degree of vector dissemination outside the eye, and limits immune responses to the viral vector and gene product. Another advantage of the eye over other organs, is the lack of cell division in most retinal cells. Thus, the viral vector DNA does not have to integrate into the host cell genome in order to remain available in daughter cells after cell division, and the risk of malignancy is reduced.

Autosomal recessive disorders are characterized by loss of function or even (near) absence of the protein produced encoded by the gene. Therefore, for autosomal recessive disorders, gene therapy can be based "simply" on gene augmentation or replacement through the delivery of the normal gene. However, in autosomal dominant disease, such as *RHO*-associated RP, the phenotype is typically the result of gain-of-function mutations, where one gene copy expresses a normally functioning protein, and the other gene copy expresses a detrimental protein that needs to be suppressed. For autosomal dominant disease, therapeutic intervention generally focuses on the suppression or inactivation on the gain-of-function gene.

Important advances have been made with the turn of the millennium in the development of (gene) therapies that aim to slow or (temporarily) halt the disease progression in IRDs, or even to restore some visual function. The first successful gene therapy was applied in patients with *RPE65*-RD.[3] Several trials have found compelling results in other IRD subtypes, such as choroideremia,[4, 5] and *RPGR*-associated IRD,[6] and many other trials are ongoing (Table 1) or in the basic experimental or preclinical phase.[7, 8] However, an imbalance exists between the rapid advances in (gene) therapy development and the available literature on the clinical disease course and the phenotypic spectrum for each specific gene of interest. The dawn of therapeutic intervention, which accelerated at the turn of the millennium, has led to ongoing and planned gene therapy trials for a plethora of autosomal recessive and X-linked IRD subtypes (Table 1), and long-term results are available for several gene therapy forms.[3, 9-12] One such viral gene supplementation trial has already led to the market approval of voretigene neparvovec (Luxturna®) by the United States Food and Drug Administration.[13] For autosomal dominant IRD subtypes, preclinical gene therapy studies are focusing on gene suppression or gene silencing along with gene replacement or supplementation approaches.[14] Other therapeutic approaches, using e.g. antisense oligonucleotides or clustered regularly interspaced short palindromic repeats/Cas9 (CRISPR/Cas9), have also shown promising results.[15, 16] Conversely, until relatively recently, longitudinal studies on the detailed clinical characteristics and disease progression were scarce for several IRD subtypes that are potentially eligible for gene therapy. Prospective phenotyping studies have thus far been even rarer in these often relatively small patient populations. However, such information is crucial in determining the window of therapeutic opportunity, patient eligibility criteria, and clinical endpoints in ongoing and future trials to assess treatment efficacy.

In order to bridge the existing gaps in our knowledge on several IRD subtypes, retrospective data were obtained from medical records in the Delleman Archive on hereditary eye diseases at the Amsterdam UMC, Academic Medical Center in Amsterdam, and through a nationwide collaboration within the RD5000 Consortium,[17] and an international collaboration with the University of Ghent in Belgium, within the framework of the European Reference Network dedicated to Rare Eye Diseases (ERN-EYE).

1.1 Primary findings and clinical implications

1.1.1 Clinical perspectives in CRB1-associated retinal dystrophies

With the ongoing development of human *CRB1* gene therapy,[7, 8, 18] we described the phenotypic and genotypic characteristics of *CRB1*-associated retinal dystrophies (**Chapter 2**). Earlier studies from literature had mostly been case reports, case series, or genetic studies with only brief descriptions of the clinical phenotype, providing limited detail.[19-33]

The Dutch retrospective cohort is the largest described to date, which allowed for statistical analysis and robust results on clinical signs and course of visual decline, which were further validated in a

Belgian population, although the phenotypic and genotypic variability was higher in the Belgian population.[34] Furthermore, in the Belgian population, a larger proportion of patients had a more severe diagnosis of LCA or EOSRD, as compared to the Dutch population, where most patients had RP. While the classic RP features, such as optic disc pallor, vascular attenuation, and bone-spicule-like pigmentation, were commonly found in *CRB1*-RP, certain characteristics outline a specific and typical *CRB1*-associated phenotype, such as hyperopia, nanophthalmos, a shallow anterior chamber, peri-arteriolar preservation of the RPE, optic disc drusen, and Coats'-like exudative vasculopathy.[27, 28, 32, 34-45] Furthermore, our studies highlighted the need to monitor this patient group for the risk of developing acute angle-closure glaucoma. In the Dutch cohort, we found optic disc drusen in the genetic isolate only, which prompted the suggestion of a potential genotype-phenotype correlation. However, in the Belgian cohort, optic disc drusen and hamartomas were found in patients with several different genotypes. Coats'-like exudative vasculopathy had been described before in *CRB1*-assocatied disease,[38, 42, 45-48] and the large studies in Chapter 2 have shown cohort-wide prevalence of these vasculopathies in 10% of Dutch RP-patients, and 13% of Belgian patients.

It should be noted that, while these features together form a "typical" *CRB1*-associated phenotype, each feature may be found in other IRD subtypes as well. Optic disc drusen have been described e.g. in Usher syndrome,[49] albeit to a much rarer degree, and hyperopia has been a classic feature of *BEST1*-associated phenotypes,[50, 51] where it can also be associated with angle-closure glaucoma.[52] Mutations in *MFRP* are associated with RP along with nanophthalmos, optic disc drusen, and foveoschisis.[53-56] Aside from its association with *CRB1*,[19, 34, 57, 58] an initial or concurrent diagnosis of uveitis has also been described in association with *PRPF31*,[57] *RP1*,[57] Stargardt disease,[59] and Usher syndrome.[57, 60] While the exact mechanism of uveitis in RP remains unknown, several explanations have been suggested for the association between uveitis and RP. Circulating immune complexes have been detected in 43.5% of patients in a study, along with reduced levels of complement C3 and C4.[61] A B-lymphocyte-mediated auto-immune response against retinal S-antigen, which is present in rod photoreceptors, has been shown in some RP patients, showing a low-level auto-immune responsiveness in RP.[62] An as of yet unidentified genetic or auto-immune factor - or a combination thereof - may play a role.

An interesting recurrent finding is the Coats'-like exudative vasculopathy, which has a strong association with *CRB1*. In one case, it has been described in an RP patient from a pedigree where an *RPGR* ORF15 mutation segregated with disease, and where no other genes were tested.[63] It has also been reported in a single case of *RHO*-associated RP, where no *CRB1* mutations were found.[64] Otherwise, it has not been associated with another IRD gene, although it has regularly been described in genetically undifferentiated case reports or series,[65-67] particularly in older studies where genetic analysis had not been performed.[68] In some studies where the associated gene had not been identified, other features, such as perivascular retinal sparing,[65] or nanophthalmos,[69]

point towards an association with *CRB1*. Vasoproliferative retinal lesions have been reported in association with Usher syndrome type I or II, based on the presence of RP and congenital hearing impairment, but not on genetic analysis.[70, 71] Few other reports, again lacking genetic analysis, have found Coats'-like vasculopathy in RP thought to be X-linked or autosomal dominant, based on pedigree analysis.[72, 73] The underlying mechanism of Coats'-like exudative vasculopathy includes an abnormal vascular permeability, which may be an element of *CRB1*-RDs. The CRB1 protein is crucial in the regulation of the number and size of Müller glia cells.[74] Since Müller cells function as regulators of the tightness of the blood-retinal barrier,[75] this may in some way relate to the vascular abnormalities seen some patients with *CRB1*-RDs.

Another distinctive finding we that frequently observed in the Dutch and Belgian *CRB1*-RD patient cohorts, was thickening of the inner retina on SD-OCT, which was in line with earlier reports,[26, 27, 35, 37, 42, 46, 76-78] although some other studies have reported retinal thinning.[23, 40, 79, 80] Mouse studies have shown retinal thickening to be caused by proliferating retinal progenitor cells, resulting in an increase in the number of rod photoreceptors, Müller cells, and bipolar cells,[81] or by ectopic photoreceptors.[82] In both studies, loss of both Crb1 and Crb2 proteins has been postulated to play a role in the retinal thickening mechanism. Some other studies have suggested inner retinal thickening to be due to a remodeling process in association with loss of the outer nuclear layer,[83, 84] which could hinder efficacy of gene therapy. However, we found no correlation between outer retinal thinning and inner retinal thickening.

A crucial aspect of the *CRB1*-associated phenotype, is the (dis)organization of the normal retinal layers (lamination), and the degree of preservation of the external limiting membrane, which is assumed to include the Crumbs (CRB) complex and thus is at least in part *CRB1* gene therapy's target. The CRB complex plays a role in the adhesion between photoreceptors and Müller cells, between Müller cells,[85] and also between photoreceptors.[86, 87] Reports on the laminar structure have varied, with some describing loss of lamination,[22, 26] and others reporting normal lamination.[30, 88] Reasonably well-preserved lamination was a frequent observation in our cohorts, with 91% and 41% of the Dutch and Belgian patients with available SD-OCT scans, respectively.[34] This again confirmed a generally more severe phenotype in the Belgian *CRB1* cohort.

Findings of *CRB1*-associated disease do not only involve the retina, but also other ocular structures, pointing to a role of protein CRB1 in the ocular development, as has been suggested before in *BEST1*-associated disease.[51, 89] In the retina, Crumbs proteins have a crucial role in the retinal vascular development,[90] in the photoreceptor-to-photoreceptor adhesion, and photoreceptor-to-Müller cell adhesion.[82] Müller cells span throughout the entire neuroretina, from the Müller cell endfeet at the inner limiting membrane beyond the external limiting membrane into the Müller cell apical villi, and they are responsible for the structural stabilization of the retina.[91] They are essential for the survival of photoreceptors and neurons. Furthermore, they take up neurotransmitters, such as

glutamate and GABA, and thus are involved in regulating the synaptic activity in the inner retina. As for the role of Crumbs proteins outside of the retina, current knowledge remains limited. The findings in this thesis of cataracts, hyperopia, a shallow anterior chamber, and the associated risk of angle-closure glaucoma,[34] indicate that the CRB1 protein has a role greater than adhesion between photoreceptors and Müller cells, and that it also has at least a developmental role outside of the retina, in the ocular structure. In *Drosophila*, crumbs proteins are involved in the development and organization of epithelial cells.[92] Further research is necessary in mammalian eyes in order to elucidate the role of the Crumbs complex outside of the retina.

The only truly robust genotype-phenotype correlation that we were able to elucidate, is the link between the p.Ile167_Gly169del mutation in *CRB1*, either in homozygous or compound heterozygous form, and an isolated maculopathy. This association was observed in both Dutch and Belgian populations, and has been described in British patients as well.[93] In fact, this mutation has been present in at least one allele in all patients with *CRB1*-associated maculopathy described so far, and also in cases of *CRB1*-associated foveal retinoschisis.[80]

A striking degree of interfamilial variability was observed in both cohorts, even in the Dutch genetic isolate, where most patients had RP with variable visual results, as some patients became blind at a relatively early age, while others maintained ambulatory vision well into the later decades of life, and one patient had a cone-rod dystrophy, with macular atrophy and barely any (mid-) peripheral retinal changes. While interindividual variability in *CRB1*-associated IRDs has been described,[21] the particularity here is that this variability occurred despite the same homozygous mutation, and the same origin from a village with a comparatively high degree of consanguinity.[94, 95] This may indicate the involvement of genetic and possibly environmental modifiers, which have been implicated before in several IRD subtypes.[96, 97] Although IRDs are monogenic, the retina is a complex tissue involving numerous proteins in order to survive and function normally, that may influence the phenotypic outcome of monogenic diseases considerably.[98] Mouse studies may give direction on possible research on genetic modifiers in human *CRB1*-RDs.[99]

1.1.2 Clinical perspectives in RPGR-associated retinal dystrophies

As several human gene therapy trials for *RPGR*-associated RP emerge (NCT03116113; NCT03252847; NCT 03316560),[100, 101] and the initial results from the first human *RPGR* gene therapy trial show a promising safety and efficacy profile,[6] we have also focused on the clinical and genotypic characteristics of *RPGR*-associated IRDs. Some findings corroborated some earlier literature: we found an association between the ORF15 mutational hotspot and a cone- or cone-rod dystrophy (COD/CORD) phenotype, particularly if the mutation was at the 3' end of ORF15.[102-105] Symptom onset was in the first decade of life in RP. In COD/CORD, the median age at symptom onset was 23 years, approximately 10 years later than some earlier reports of COD/CORD,[106] although reports have varied, some describing a much later symptom onset.[107] Our study showed a

particularly high variability in the age at symptom onset in COD/CORD, followed by rapid decline of visual acuity, and a probability of being blind, defined by the World Health Organization as a best-corrected visual acuity of <20/400, at the age of 40 of 55%, as opposed to 20% in RP patients. Cystoid macular edema, an otherwise relatively common finding in RP, was not observed at any point during follow-up in our cohort of *RPGR*-RD patients, in line with other studies of *RPGR*-RD.[107, 108]

We described a particularly apparent intrafamilial variability in 2 families that comprised patients of RP and CORD phenotypes within the same family.[102] A pivotal factor here is time, as in later disease stages, both RP and CORD progressed to panretinal dysfunction and became indistinguishable from each other in some cases. Still, this variability in the early disease stage is striking. An earlier report has even shown variability in a pair of dizygotic twins, one with RP and the other with CORD,[109] as well as in other siblingships.[110]

A prominent finding in all subtypes of *RPGR*-associated IRD, was myopia, in line with previous literature.[111, 112] Mild, moderate, or high myopia was present in 84% of male patients with *RPGR* mutations and 73% of female carriers. Patients became more myopic with increasing age. Our study in male patients showed high myopia to be an evident risk factor for visual acuity loss in all IRD subtypes, and for visual field loss in RP. While *RPGR* mutations have been shown to coincide with the highest degree of myopia in IRDs,[50] to our knowledge, our study was the first to elucidate the quantitative effect of myopia on disease progression in *RPGR*-RDs. Other studies have followed, confirming the link between myopia and more severe retinal degeneration.[108] Refractive errors are not uncommon in IRDs,[50] and in some cases, the location and function of the protein product has been postulated to explain the refractive error. While mutations in some genes such as *RPGR* are associated with (high) myopia, other genes (e.g. *CRB1* and *BEST1*) are associated with hyperopia. The protein RPGR is located in the connecting cilium of the photoreceptor, the transport area between the inner and outer segment. Several genes that encode connecting cilium proteins have been linked to myopia, such as *RP1* and *RP2*, although this does not apply to all connecting cilium proteins.[113, 114] A study on induced refractive errors in a chick model has implicated a range of photoreceptor-related proteins involved in the development of myopia or hyperopia, and these implicated proteins were primarily linked to photoreceptor dystrophies, such as CNGB1, RS1, RPE65, and RLBP1.[115] The study unfortunately did not shed light on RPGR, and further studies are needed.

An important finding in this thesis was the phenotypic spectrum in female carriers of *RPGR* mutations.[116] Like in affected males, myopia had a deleterious effect on visual acuity. Visual symptoms were relatively common, being present in 40% of subjects, and complete expression of a disease, i.e. RP or CORD was found in 23% of subjects. Likewise, some earlier studies have identified *RPGR* mutations in disease-affected female patients,[112, 117-120] some of whom were

presumed to have sporadic or autosomal dominant RP.[121] This sheds light on multiple essential questions: Why do some female carriers develop disease and others don't, and can we predict either outcome? And what implications do these findings hold in the clinical and genetic counselling of female carriers? Regarding the first matter, random X-inactivation and variable mosaicism could account for the phenotypic variation observed among female individuals in our study,[122] or skewed X-inactivation,[123, 124] as the relatively family-based aggregation of affected female carriers makes random X-inactivation unlikely as a sole factor. In symptomatic female carriers of choroideremia, another X-linked IRD, severely skewed X-inactivation has indeed been demonstrated.[125] Genetic modifiers may also play a role. It is not yet possible to predict which female carrier will develop disease, although the phenotype in other heterozygotes from the same family may be predictive.[116] Presence of the tapetal-like reflex does not hold predictive value, and is not associated with symptoms or pigmentary retinal changes. Regarding the counselling of female carriers of *RPGR* mutations, it is vital that clinicians convey the risk of developing disease, while acknowledging that a complete disease expression does not occur in most heterozygotes.

When looking at genotype-phenotype correlations, we found a robust correlation between *RPGR*-ORF15 mutations and the COD/CORD phenotype. Mutations in the ORF15 region were associated with a higher degree of myopia, which, to our knowledge, has not been described before. In male RP patients, an *RPGR*-ORF15 mutation signified a higher hazard (twice as high) of reaching low vision or severe visual impairment than a mutation in exon 1-14.[102, 126] Also, *RPGR*-ORF15 mutations were associated with higher myopia, a significantly thinner central retina, and a significantly faster visual field decline. Previous literature, however, has shown the opposite finding of more severe disease in patients with mutation in exon 1-14 than those with mutations in *RPGR*-ORF15.[127, 128] This discrepancy may be explained by the higher degree of clinical variability in patients with mutations in *RPGR*-ORF15,[116] which may lead to skewed findings in one population compared to the next. Peculiarly enough, in female heterozygotes, mutations in *RPGR*-ORF15 were associated with a less severe phenotype, which is the opposite of our finding in men.[116] Previous literature on genotype-phenotype correlations in female subjects is limited, but has shown the opposite effect, with worse visual function in female subjects with *RPGR*-ORF15 than those with mutations in exon 1-14.[129] Genetic and/or environmental modifiers may again play a role in this clinical variability. Some proteins, such as RPGRIP1L and CEP290, have been shown to biochemically interact with RPGR,[97, 128] but additional research on such potential modifiers is needed.

1.1.3 Clinical perspectives in choroideremia

Choroideremia is a rare X-linked IRD caused by mutations in the *CHM* gene. It has been proposed that this dystrophy primarily affects the retinal pigment epithelium, and secondarily the photoreceptors and choroid.[130] Advances in gene therapy have resulted in multiple human gene therapy trials worldwide (Table 1), which have recently reached phase III.[4, 11, 12, 131-133] These advances prompted several studies on the associated phenotype and long-term clinical course. Symptoms of

choroideremia are usually noticed in the 1st or 2nd decade of life, and the degeneration usually starts in the midperiphery, after which it gradually extends centripetally towards the periphery and the fovea.[134-137] Prolonged relative sparing of foveal structure and function accounts for the long-term preservation of visual acuity, which usually remains until the 5th decade of life. This striking feature of foveal sparing, which is also typical for e.g. late-onset Stargardt disease and central areolar choroidal dystrophy,[138, 139] remains of unknown etiology. One study investigated the kinetics of the progression of macular atrophy in several macular diseases, and found nearly identical patterns across several IRD subtypes and age-related macula degeneration, suggesting a disease-independent mechanism.[139] One proposed mechanism has been the metabolic difference between different macular regions in susceptibility to atrophy of rods and cones, RPE, and choroid.[140] Our longitudinal clinical study in a cohort of choroideremia patients showed a stable plateau of good vision until the 5th decade of life, and generally a turning point in the visual acuity decline from the 4th decade of life onward.[134] Outer retinal tubulations, which have been associated with age-related macular degeneration and various other degenerative conditions,[141] were found in the majority of choroideremia patients (76%) in our study. This is in line with some previous studies where their incidence was reported between 69-94%[142-146], although smaller numbers have been reported as well.[147] They have also been demonstrated in symptomatic carriers, where they colocalized with areas of RPE atrophy and severe hypo-autofluorescence.[125] Outer retinal tubulations presumably result from the rearrangement of degenerating photoreceptors,[148] and areas containing them may be prone to surgical complications, such as macular hole formation as a result of subretinal injection of gene therapy vector solution. Moreover, areas containing outer retinal tubulations in choroideremia patients reportedly lack visual sensitivity despite the concomitant presence of viable cone inner segments in that same area.[147] This may guide in assessing which retinal areas of a particular patient are amenable to (gene) therapy. Choroideremia patients in general are at risk of developing a macular hole, the surgery of which seems to be effective in achieving anatomic closure.[149, 150] No clear genotype-phenotype correlations have been established in choroideremia.[151]

1.1.4 Clinical perspectives in LRAT-associated retinal dystrophies

In light of emerging therapeutic options, we also focused on an extremely rare IRD subtype: *LRAT*-associated IRDs. Having previously only been described in a small number of case reports or series,[33, 152-156] *LRAT*-associated IRDs are estimated to account for less than 1% of IRD cases, usually exhibiting Leber congenital amaurosis, early onset severe IRD, or retinitis punctata albescens. Therefore, our retrospective study in 13 patients - to our knowledge the largest series described in literature so far - is an important contribution to the limited literature available earlier.[157] Even more so, as we further broadened the phenotypic spectrum by describing a subset of patients with relatively preserved vision into mid- and late adulthood.[157] As our series consisted largely of patients from a genetic isolate, carrying the same homozygous c.12del *LRAT* mutation, we were able to elucidate the intrafamilial variability, with some patients carrying an RP phenotype and others a CORD phenotype. We also provided a comparison to the patient from outside the genetic

isolate, who had an overall more severe phenotype of panretinal dysfunction. The c.12del mutation in the genetic isolate is predicted to lead to severe protein truncation, and no residual protein function.[155] It is therefore unlikely that the specific protein change is the most prominent cause of the relatively slow disease course in these patients, as opposed to the early blindness described in literature.[33, 153] Genetic and/or environmental modifiers, that somehow affect the residual protein function, may be at play. However, it remains elusive why this mutation is associated with a relatively mild phenotype.[155, 157]

LRAT encodes lecithin retinol acyltransferase (LRAT), one of the retinoid cycle proteins. Protein LRAT forms a complex with RPE65 to act as the isomerol hydrolase in the regeneration of visual pigment in the retinoid cycle. Having this closely connected biological function, both *LRAT*-RD and *RPE65*-RD have been targeted in a single treatment phase I trial investigating the safety and efficacy of oral QLT091001, a synthetic chromophore 11-cis-retinal.[158, 159] This study enrolled patients with Leber congenital amaurosis due to mutations in *RPE65* or *LRAT*. While mouse studies have shown phenotypic similarities between *Rpe65*(-/-) and *Lrat*(-/-) mice, human studies comparing these phenotypes are lacking. In our study, we compared our clinical findings and earlier literature in *LRAT*-RD patients to the available literature on *RPE65*-RD, and this assessment demonstrated that there is a degree of phenotypic variability, with considerable overlap in this spectrum. To further substantiate any conclusion drawn from our study, a natural history study would ideally include extensive phenotyping of patients with *LRAT*-RDs and *RPE65*-RDs in the same study.

1.1.5 Clinical perspectives in RHO-associated retinal dystrophies

Autosomal dominant IRDs, which are caused by mutations in the *RHO* gene in up to 30-40% of cases,[160] present another challenge for gene therapy development. After all, the dominant disease is usually the result of a deleterious "gain-of-function" mechanism, e.g. where the altered gene product adversely affects the normal gene product from the wild-type allele. Mere gene supplementation would not suffice in slowing the disease process that is caused by a toxic gain-of-function mutant protein, and the gain-of-function effect leading to disease would have to be diminished. For *RHO*-associated RP, momentous advances have been made, with knockdown-and-replacement strategies,[161] CRISPR/Cas9 gene editing,[14, 162] and antisense oligonucleotides.[163] "Simple" gene augmentation could still provide some therapeutic benefit in *RHO*-associated RP, even when the disease is caused by a dominant-negative effect.[164]

Considering these advances, we aimed to establish a detailed clinical profile and natural history in a large cohort of patients with *RHO*-associated RP. We found an appreciable difference in disease progression between patients with sectorial RP (25% of our cohort) and those with generalized RP, as visual acuity decline was relatively stationary in the sectorial form, with the first case of blindness occurring after the 8th decade of life. In previous literature, an initial sectorial RP phenotype has

relatively rarely been reported to progress to the generalized form.[165] In our study, we did not find patients with sectorial RP whose phenotype progressed to generalized RP, although we were restricted by the limited availability of follow-up full-field fundus photographs in our retrospective study design.

In the general *RHO*-RP population (sectorial and generalized forms), best-corrected visual acuity generally remained well-preserved, with a median age of reaching mild visual impairment of 72 years. Based on visual fields, the median ages to reaching low vision and blindness were 52 and 79 years, respectively. This is in line with previous studies, that have shown that *RHO*-associated RP is a slowly progressive disease where patients generally maintain a good central visual function,[166-169] as opposed to e.g. *RPGR*-associated or *CRB1*-associated RP. This points to a particularly lengthy window of therapeutic opportunity for ongoing and future (gene) therapy trials. On the other hand, the slow disease progression may complicate ways to clearly show a potential effect in a treatment trial, as it may take several years for a change in the natural disease course to become apparent. Some studies have referred to the sectorial disease phenotype as a "class B" phenotype, defined by an altitudinal (hemifield) loss of photoreceptor function.[166, 170, 171] The degree of light exposure of the retina has been suggested to play a role in the retinal degeneration, and has been hypothesized due to the altitudinal degeneration mostly affecting the inferior retinal hemisphere.[165, 172, 173] In support of this theory, animals with *RHO*-RP, including the RHO^{P23H} mouse and rat,[174, 175] and the RHO^{T4R} dog,[176] that have been reared in complete darkness, have shown slower retinal degeneration. Mice that remain in red-tinted cages that filter short-wavelength light (<600 nm) have been shown to maintain a thicker photoreceptor layer and higher amplitudes of electroretinography responses than mice in non-tinted cages.[177] However, this effect has not been proven in humans, and would be challenging to prove in a clinical trial setting. Thus, it remains a controversial claim.

Over 150 mutations have been reported in *RHO*. Several studies have been performed in the $Rho^{P23H/+}$ mouse, as the p.(Pro23His) mutation is historically the first *RHO* mutation discovered, and one of the most common mutations in patients in the United States of America.[178] To our knowledge, this mutation has not been reported in European studies, including ours. In our Dutch cohort, 37% of patients had the p.Glu181Lys mutation. With regard to genotype-phenotype correlations, we found an association between the mild sectorial RP form, and mutations that correspond to the extracellular domain (i.e. the intradiscal domain). This is in line with previous literature, which has suggested milder phenotypes in association with mutations in the extracellular domain,[170, 171] particularly in comparison to mutations in the transmembrane domain.[179] However, we still found variation in the phenotype, e.g. sectorial versus generalized RP, in patients with identical genotypes, such as the p.Glu181Lys mutation. Conversely, mild and sectorial phenotypes have been reported in association with mutations in other domains.[180, 181] Extreme intrafamilial variability in the *RHO*-RP phenotype has been reported.[182] In fact, both RP and congenital stationary night blindness have

been reported in the same family carrying the c.337G>A (p.Glu113Lys) mutation,[183] which was not present in the Dutch and Belgian patients cohorts that we have described.

1.1.6 Clinical heterogeneity and potential modifiers in retinal dystrophies

A recurring finding in nearly all IRD subtypes, including the ones studied in this thesis, is clinical *heterogeneity*. The same gene or even the same mutation may cause different phenotypes, and a nearly identical phenotype may be caused by different genes. The presence of a genetic isolate in our cohort of *CRB1*-RDs, consisting of patients carrying the same homozygous p.Met1041Thr mutation, provided the opportunity to investigate not only genotype-phenotype correlations, but also the intrafamilial variability. While the phenotype was generally severe, and some hallmark features of *CRB1*-RDs were elucidated, one 41-year old patient had a mild CORD phenotype, while age-matched relatives had advanced RP. Even more variability was observed in our cohort of *LRAT*-RDs, again consisting largely of a genetic isolate. Similarly, in 2 families of *RPGR*-RD, some had RP while others had CORD. This last finding should be nuanced by the idea that different IRDs may not be entirely different entities, but members of a continuum. Advanced stages of CORD may be indistinguishable from RP, and it may prove difficult to retrieve early medical records in a retrospective setting. Nonetheless, variable degrees of intrafamilial variability were evident in several cohorts,[34, 35, 157] and patients at roughly similar ages may still have different phenotypes (CORD or RP).[102]

Environmental and genetic modifiers, such as heterozygous mutations in other IRD genes or single nucleotide polymorphisms,[47, 184, 185] may have a role, and may influence the degree of severity. In male patients with *RPGR*-RP, several single nucleotide polymorphisms (the minor allele (N) of I393N in *IQCB1* and the common allele (R) of R744Q in *RPGRIP1L*) have been significantly associated with more severe disease.[128] Another study has suggested an interaction between RPGRIP1L and RPGR proteins in photoreceptors, and indicated that *RPGRIP1L* could be a modifier in *RPGR*-associated IRD.[97] Some studies have described an "additive" effect of a heterozygous mutation in a potential modifier gene, in patients with homozygous or compound heterozygous mutations in the causative gene.[186] Such additional heterozygous mutations have been proposed to contribute to an increased disease severity. For example, additional heterozygous missense mutations in either *CRX* or *CRB1* have been shown in several patients with *AIPL1*-associated LCA, who had a much more severe disease phenotype than affected family members without these additional genetic factors at a comparable age.[185] A similar effect of a *GUCY2D* variant was found in patients with *RPE65*-LCA,[185] even in a siblingship.[187] In *PRPH2*-associated autosomal dominant macular dystrophy, the disease has been shown to be more severe in those with concurring heterozygous mutations in *ROM1*, than in affected family members without an additional *ROM1* mutation.[188] An earlier case report described a mother and daughter with *PROM1*-associated IRD, with a more severe phenotype in the daughter, who had profound macular chorioretinal atrophy and who also displayed pathognomonic features of Stargardt disease (flecks), while the mother had a

mild phenotype with some outer retinal thinning and relative macular sparing.[189] Further genetic analysis identified a heterozygous *ABCA4* variant in the daughter, but not in the mother, which was postulated to account for the more severe phenotype. In Usher syndrome, several genetic modifiers have been proposed: An additional heterozygous mutation in the *PDZD7* gene was found in a patient who had an earlier onset and more severe RP than her affected sister, who did not have a *PDZD7* mutation and who displayed a much milder retinal disease.[96] However, in another family, a heterozygous *PDZD7* mutation was found in an *USH2A* patient with a mild phenotype.[96] Altogether, evidence for genetic interaction between *PDZD7* and Usher syndrome genes have been found in at least 4 families.[96]

Besides mutations in other genes, minisatellite repeats (MSR) have been implicated as a cause for phenotypic variability, through the regulation of gene expression.[190] In *PRPF31*-associated RP, an autosomal dominant RP, some patients become blind, while others maintain good vision and remain asymptomatic.[191] One study identified a difference in the number of MSR1 copies (3 versus 4) between patients from the same family, who had considerable differences in disease severity.[190] The 4-copy-MSR1 allele, found in asymptomatic patients, was shown to have a protective effect. Another genetic modifier identified in *PRPF31*-RP is *CNOT3*,[192] a gene otherwise not associated as a monogenic cause of IRD. *CNOT3* was expressed at low levels in those with mild disease, but in high levels in those with severe disease.[192]

In mice with *Nr2e3*-associated IRD, disease expression has been shown to be modified by the *Nr1d1* gene, and the *in vivo* delivery of this modifier gene even led to a histological, functional and molecular restoration of the retina in these mice.[193] This study suggests that in some IRD subtypes, the modifier gene may even be a target for therapy.

In *CRB1*-RDs, no genetic modifiers have been found yet in human patients. In mouse studies, an interaction between CRB1 and CRB2 proteins has evidenced a disease-modifying role of CRB2,[82, 194, 195] where a loss of CRB2 protein aggravates the phenotype from RP to LCA.[85] This provides a compelling lead for future genotyping studies in human patients with *CRB1*-RDs. For choroideremia, *RHO*-RP, *LRAT*-RD, specific genetic modifiers remain to be identified.

In conclusion, while IRDs are typically monogenic diseases, rare cases of putative digenic inheritance have been reported,[196, 197] or suggested,[198] and the retina and RPE are complex tissues, whose survival and function depends on the proteins encoded by more than 18.000 genes for each tissue.[98] Further analysis of any concomitant heterozygous variants in other genes tested in patients with e.g. *CRB1*-associated IRD, may provide clues regarding differences in phenotypic expression and disease severity.

1.2 Current patient management

Before the advances made in gene therapy studies in this millennium, the management of IRD patients consisted of the regular follow-up and monitoring of disease progression, genetic and prenatal counselling, low vision aids where needed, and potential enrolment in a clinical trial. For patients who are blind due to outer retinal degeneration, but have maintained the inner retinal structure and an intact optic nerve, 2 retinal prostheses, the Argus II epiretinal prosthesis system and the Alpha IMS (first generation) and Alpha AMS (second generation) subretinal prostheses, may aid in gaining some mobility or performing specific daily tasks. However, they require careful pre-operative screening and expectation management, counselling, and a comprehensive post-operative rehabilitation program at a specialized center.[199, 200] The two most studied epiretinal implants, the Argus II and alpha-IMS/AMS, have shown performance results that can overall be considered similar, despite large differences in implant design.[201] While most patients with a retinal prosthesis show an improvement in mobility and orientation tasks, approximately one third experiences measurable visual acuity improvement.[202] Reading speed can be improved in a subset of patients, although single-letter recognition may still take up to several minutes.[203] Pre-operative counselling should comprise the advice that the output from the prosthesis is an entirely new type of functional vision rather than the recovery of previous vision.[204] Due to the guarded benefit, and the frequent visits and intensive rehabilitation required to achieve it, patient selection and expectation management are key.

The recent approval of voretigene neparvovec (Luxturna®), a prescription gene therapy for *RPE65*-RD, has marked the dawn of a new era: the availability of an IRD treatment in order to preserve and improve retinal function. However, for other IRD forms, therapeutic options, if applicable, are being investigated in a clinical trial setting, or are in an earlier preclinical investigative phase.

Associated ocular conditions, such as CME, should be monitored for development and treated. CME has been treated with different modalities. Topical and oral carbonic anhydrase inhibitors have shown morphological improvement with reduction of the CME,[205] although the effect on visual acuity has been inconsistent between studies and remains inconclusive.[206-210] One study has found that CME in the outer nuclear layer showed a better response to treatment with topical or oral carbonic anhydrase inhibitors than CME in the inner nuclear layer, where CME in IRD is commonly found.[211] An intravitreal dexamethasone implant (Ozurdex®) has shown improvement of visual acuity and edema resolution,[205, 212] while intravitreal triamcinolone acetonide showed anatomical improvement without improvement in visual acuity.[213, 214] When using steroids, the development of cataract, and perhaps more importantly, elevation of intraocular pressure should be closely monitored in these patients, who are at an increased risk of developing both.[34] Intravitreal injection of anti-vascular endothelial growth factor (VEGF) has shown inconsistent results with resolution of CME in some studies,[215, 216] and no effect in other studies.[217] No evident visual acuity improvement was established with the use of anti-VEGFs.[216] Intravenous immunoglobulin therapy

has been reported in the treatment of concomitant CME and uveitis in 1 patient, and has shown complete resolution of CME at 4 months and 1 year.[218] Octreotide has been postulated to have a role in the treatment of uveitis-associated CME,[219] and has been successful in reducing CME and stabilizing visual acuity in dominant cystoid macular dystrophy.[220] A study with a small sample has shown that octreotide leads to some improvement in visual acuity in those with post-surgical CME, but not to a change in retinal thickness or angiographic leakage.[221] Its effect on CME in retinitis pigmentosa has not been reported to date.

Treatment options for Coats'-like exudative vasculopathy have included laser photocoagulation or cryotherapy. This can lead to regression of the exudates and to improved or stabilized vision,[63, 67, 72, 222, 223] but it has also been complicated by a vitreous hemorrhage requiring vitrectomy.[67] In the case of an exudative retinal detachment, treatment with vitrectomy and endolaser has been described, with the aim of salvaging the eye and maintaining any remaining vision.[73, 224] More recently, the intravitreal injection of conbercept, a new anti-VEGF, has been described in RP patients with exudative retinal detachment due to Coats'-like exudative vasculopathy.[225] This led to complete resolution of the subfoveal serous detachment and improvement of the visual acuity. In a patient with *RHO*-associated RP and Coats'-like exudation, along with treatment-resistant CME, the intravitreal injection of a dexamethasone implant (Ozurdex®) led to resolution of the exudation, along with a reduction in the CME, and maintenance of a well-preserved visual acuity.[64] All these case reports appear too meagre to establish a clear guideline for the treatment of CME in the context of IRDs.

1.3 Implications of natural history studies for gene therapy trials

The findings in this thesis have several implications for ongoing and future gene therapy trials. Crucial factors in the design of a (gene) therapy trial, are the determination of:

a) a window of therapeutic opportunity;

b) patient eligibility criteria;

c) disease symmetry between eyes and the suitability of the contralateral eye as the untreated control; and

d) defining endpoints for the evaluation of clinical efficacy.

1.3.1 Window of opportunity

The window of therapeutic opportunity refers to the time span within which potential treatments may still prevent disease or positively modify the natural history. As gene therapy uses viral vectors that need to infect viable retinal cells, the window of opportunity closes when no viable photoreceptors remain, and no useful vision remains to be rescued. In a trial setting, the therapy is ideally applied in an early or intermediate disease stage, when enough vision remains to be rescued, and the natural disease progression is fast enough for a therapeutic effect to be detected, i.e. a change in the rate of disease progression. However, in treatment settings, intervening as

early as possible in the disease course may provide the best protective effect. In our cohort of patients with *CRB1*-RP, the median ages for reaching visual acuity-based low vision, severe visual impairment, and blindness were 18, 32, and 44 years, respectively. Thus, the window of therapeutic opportunity spans the first 3 decades of life, and could be expanded in some patients to the 4th decade of life. In *CRB1*-LCA or EOSRD, intervention would ideally be much earlier, within the 1st decade of life, as any remaining useful vision usually degenerates in this period. In contrast, the window of opportunity is considerably broader in patients with *RHO*-RP. In *RPGR*-RDs, the window of opportunity depends on the phenotype intended to treat in the trial: patients with COD/CORD have a 55% likelihood of being blind at the age of 40, as opposed to 20% in patients with RP. Patients with mutations in the ORF15 region had a higher risk of becoming blind at an earlier age, and would thus also require earlier therapeutic intervention, according to our study.

It should be noted that in our studies, we based our estimation of the window of opportunity primarily on the visual acuity decline and the degeneration of the central macula. Indeed, subretinal gene therapy trials have targeted the central macula.[6, 11, 13, 226] However, in our study of choroideremia, visual field constriction was reported by 70% of patients to be their most debilitating symptom. Therefore, addressing the preservation of the peripheral retina remains an important consideration for the near future. Therapeutic approaches that target the peripheral retina as well as the central retina, such as intravitreal antisense oligonucleotides,[15] may have to consider much earlier intervention in diseases where the peripheral retina degenerates first.

In *RPGR*- and *RHO*-associated IRDs, the presence of a hyperautofluorescent ring on fundus autofluorescence imaging may aid in determining which retinal area is most likely to benefit from a subretinal gene therapy injection, as this ring signifies the transitional zone between degenerated retina and relatively preserved – and thus rescuable – retina. In *RPGR*-RP, this ring was present in 47% of patients with *RPGR*-RP and 71% of patients with *RPGR*-COD/CORD. While the hyperautofluorscent ring provides useful information on the location of the transitional zone between atrophic and relatively preserved retina, it is unknown whether it has additional value in determining the likelihood of benefit from therapeutic intervention.

1.3.2 Patient eligibility criteria

Patient eligibility criteria for inclusion in a future trial are largely dependent on the window of therapeutic opportunity, and thus the patient age and remaining visual function. The presence of CME may render the macula more susceptible to the formation of a secondary macular hole, when subretinal injection of a viral vector in gene therapy increases the retinal stretching.[227] Even if such a complication would not occur, the natural fluctuation in the extent of CME and the visual acuity may confound any potential therapeutic effect. On the other hand, successful gene augmentation via gene therapy may also have a beneficial effect on the resolution of CME. Patients with *CRB1*-RDs should be assessed for the risk of developing acute angle-closure glaucoma, and a prophylactic

peripheral iridotomy or, if appropriate, cataract extraction may be warranted to reduce this risk prior to enrolment in a clinical trial that requires frequent mydriasis.

An extremely important point for consideration is the a priori amenability of the retina to (gene) therapy. A point of concern, particularly in some patients with *CRB1*-RD, would be the retinal disorganization, which would indicate a limited availability of viable cells for the viral vector to infect and/or the inability for the gene to function due to structural disintegration. Therefore, the degree of laminar disorganization was an area of focus in our retrospective and prospective studies. In the baseline report of our prospective study, the retinal laminar organization was preserved in 24% and showed only mild coarsening without disorganization in 38% of patients, indicating an amenability of the retina for gene therapy in 64% of patients. In the other 38% of patients, the retinal laminar organization was relatively disorganized, indicating a decreased amenability.

In choroideremia, the lengthy preservation of central visual function and initial (relative) sparing of the fovea afford a broad window of therapeutic opportunity for gene therapy.[4, 134, 137] Outer retinal tubulations, when present, may provide clues of areas retaining viable photoreceptors and remaining visual function, as they have been found to be present around areas of surviving retina.[134] Full-thickness macular holes have sporadically been described in choroideremia,[149, 150] and although successful closure may be achieved surgically, these patients may be at a higher risk of iatrogenic damage during subretinal injection in a gene therapeutic setting.

Gene therapy trials for male patients with *RPGR*-associated RP may take the additional detrimental effect of the associated high myopia into consideration when assessing patient eligibility and when interpreting safety and efficacy data, as we have found that high myopia is associated with worse visual function and a thinner retina.[102] This high myopia may thus be a complicating factor in the rescue of the remaining photoreceptors.

In our study in female heterozygous carriers of *RPGR* mutations we have shown that most of these individuals are mildly affected or asymptomatic, and treatment in these patients may not be necessary. However, in this study, we also found that 40% of female heterozygotes may experience variable degrees of visual symptoms, and 23% of cases express a full RP or CORD phenotype as in affected males, suggesting that *RPGR* gene therapy may also be a treatment option in significantly affected female heterozygotes in future clinical trial phases. Similarly, a study in a smaller series of female heterozygotes has found a subset of severely affected cases with a phenotype indistinguishable from the pattern found in male patients, and has found that these patients may be considered for *RPGR* gene therapy.[228]

Thus far, subretinal gene augmentation therapy trials have treated the posterior pole/macular region,[3, 4, 9, 10] while patients with RP or choroideremia may experience visual field constriction as a major problem. Indeed, our study has surveyed patient-reported visual complaints and their effects

on daily life, and has found that most choroideremia patients (70%) reported peripheral visual field constriction as the most disabling symptom.[134] In these patients, expectation management prior to enrollment in a clinical gene therapy trial is crucial, as the peripheral rods responsible for the visual field are not targeted through conventional subretinal gene therapy that mainly targets the posterior pole. Intravitreal gene therapy administration may theoretically provide a better outcome in the peripheral visual function these patients, although it currently holds a higher risk of inflammation and systemic biodistribution,[229-231] and a lower degree of efficacy than subretinal administration in the eyes of primates.[232] Should intravitreal gene therapy administration develop a better profile in the future, intervention would ideally happen at a much earlier stage, as rods degenerate already in the earlier disease stages, while central cone function and visual acuity may remain preserved for many years.

There appears to be no or minimal usefulness of gene therapy in cases of extensive atrophy of the photoreceptors, RPE, and choriocapillaris including the posterior pole of the eye. In these patients, stem cell-based therapeutic options may provide more benefit. Examples include the intravitreal or subretinal administration of induced pluripotent stem cells or retinal progenitor cells.[233] These studies are in the early stages: one phase I/II clinical trial on human embryonic stem cell-derived RPE cells has been completed in age-related macular degeneration and Stargardt disease,[234] and has shown an acceptable safety profile and some possible improvement in visual function. Clinical trials using induced patient-derived gene therapy corrected pluripotent stem cells may be expected,[226, 235] but are yet to be initiated. In patients with advanced chorioretinal atrophy, stem cells may need to differentiate into multiple cell types, not including not only the photoreceptors, but also the RPE and choriocapillaris. The injected cells then have to successfully convert into each mature and functional cell structure individually, and organize into a structurally and functionally intact unit. To facilitate proper insertion of cells in the subretinal space, scaffolds may be used.[236, 237] While these challenges complicate the treatment options for these patients, *in vitro* and *in vivo* studies have shown some promising results.[235, 238]

1.3.3 Interocular symmetry

As most retinal (gene) therapy studies have treated one eye, usually the worse-seeing eye, inter-eye symmetry within the same patient is an important aspect. Interocular symmetry enables the use of the contralateral eye as an ideal untreated control. A high degree of inter-eye symmetry has been confirmed in most IRD subtypes of interest for ongoing and future gene- and cell-based therapy trials.[34, 35, 102, 137, 157, 166, 169, 239-242] In cases of asymmetry in our studies, which we defined as a between-eye difference of >15 ETDRS letters, an underlying reason, such as more severe cataract or amblyopia, could usually be determined. Interocular symmetry, or lack thereof, should be determined prior to enrollment in an interventional trial, and investigators should aim to identify a potential cause of significant asymmetry.

1.3.4 Defining endpoints for evaluation of treatment efficacy

For many IRD subtypes, it has proven to be challenging to define clinical endpoints for the evaluation of treatment efficacy. A thorough understanding and quantification of important parameters in the natural disease course is crucial, as this may help define the most appropriate efficacy endpoints. Using the most appropriate endpoint may be pivotal in the process of market approval of gene therapy by regulatory bodies. In order to be an expeditious efficacy endpoint for a treatment aimed at slowing disease progression, a parameter would have to be expected to show significant decline within the clinical trial period, and a faster decline than any expected test-retest variability. Visual acuity, a measure of central cone function, usually shows significant decline over several decades of life, but may remain relatively stable over the course of a few years, while the duration of a clinical treatment trial is usually not much longer than two years. Visual acuity survival curves in *CRB1*-RP in the Dutch cohort have shown a relative plateau during the 2nd decade of life. Meanwhile, the visual acuity decline rate was 0.03 logMAR per year, corresponding to 7.2% per year. Similar rates were demonstrated in the decline of the visual field area. In order to calculate how long a trial should last in order for a true treatment effect to be detected, test-retest variability in the visual function values should be determined in the study population. The estimated time needed to detect a significant change may be longer than the trial period in most patients, but longitudinal prospective studies must further investigate this. In patients with *RPGR*-RP, visual acuity did not show any significant decline before the age of 20 years in our study,[102] indicating that in these young patients, visual acuity is not a sensitive marker for change. However, it would be a judicious safety marker, as any significant visual acuity decline may be for instance an indicator of iatrogenic damage to the retina.

Several studies have indicated that the ellipsoid zone width and ellipsoid zone area on SD-OCT may be sensitive biomarkers for disease progression,[240, 243] even within a time span of 2 years of follow-up.[244-246] In our study of *RHO*-RP, we found similar results for ellipsoid zone width. Several challenges accompany this particular biomarker: while this biomarker appears to be useful for instance in *RHO*-RP or *RPGR*-RDs, in *CRB1*-RDs, the ellipsoid zone disintegration will probably be at a too advanced stage to be able to sensitively detect a significant change in decline rate. Moreover, regulatory bodies such as the United States Food and Drug Administration and the European Medicines Agency, have not yet approved structural biomarkers as defining parameters for the approval of a therapy for retinal disease.[247] For such structural biomarkers to serve as surrogate endpoints, their reliability, as well as their strong correlation to direct measures of the patient's visual function (e.g. visual acuity) should be established. In our prospective study on *CRB1*-RD, the ellipsoid zone width did not maintain its significant correlation with visual acuity after correction for multiple testing. The thickness of the photoreceptor and RPE complex (i.e. as measured from the external limiting membrane to the RPE at the fovea), however, did correlate with visual acuity. Its rate of decline (-0.6%/year), however, was much slower than that of the EZ

band width (-3.8%/year), which means that the expected time needed to detect a treatment effect is much longer.

Looking back at the *RPE65* gene therapy trial that led to market approval of Luxturna®, useful endpoints have included the full-field stimulus testing,[13] which we have also employed in our prospective natural history study of *CRB1*-RD. Full-field stimulus testing is a psychophysical measure to determine the maximum retinal sensitivity in the full field, and chromatic stimuli can be added to determine whether this sensitivity is rod-mediated, cone-mediated, or mediated by a combination of the two.[248, 249] It may be employed in patients with non-detectable dark-adapted and light-adapted responses on the electroretinogram, and is therefore particularly helpful in patients who are (nearly) blind. Another useful endpoint in studies leading to marked approval of voretigene neparvovec (Luxturna®) was the multi-luminance mobility test (MLMT). This is a navigation course, where patients must maneuver past obstacles at different levels of environmental illumination, ranging from 1 lux (a moonless night) to 400 lux (a brightly lit office). It provides a reliable measure of functional vision, that is meaningful with regard to the patient's daily life. While this may be an impractical measure in natural history studies, it has proven useful in interventional trials, and its validity has been demonstrated in a non-trial setting.[250] Other mobility courses and artificial platforms for mobility and for the simulation of daily activities have been developed, such as The StreetLab and HomeLab platforms designed by the Institut de la Vision (Paris).[251]

In gene therapy trials, primary outcome measures should ideally focus not only on the objective improvement in visual acuity and other visual and structural parameters, but also on the efficacy of treatments to significantly improve parameters that are important of patients' daily lives, such as level of independence, quality of life, and other patient-reported outcomes (PRO). PRO tools, focusing on quality of life, monitor aspects such as physical and emotional well-being, and independence. PRO tools that focus on visual functioning questionnaires rate the difficulties patients have in performing vision-related tasks of daily living. Many PRO tools include a combination of these approaches, such as the "Impact of Vision Impairment" questionnaire.[252] Selecting a visual functioning questionnaire may be challenging, as no standardized questionnaires have been established thus far for such quality of life and social functioning aspects for this specific population with severe visual impairment due to IRDs.

Furthermore, a recent report of the National Eye Institute/Food and Drug Administration workshop on age-related macular degeneration and inherited retinal diseases has addressed the need to focus not only on *visual function*, but also on *functional vision*.[247] While visual function performance is tested using single parameters, e.g. visual acuity or visual field testing, in a controlled environment, functional vision tests aim to mimic real-world settings in a simulated environment. One such functional vision domain is mobility and orientation, and daily living at home environments and reading/occupational needs are the other main domains. The French

Institut de la Vision has developed the companies "Streetlab" and "Homelab" to simulate an urban environment and a living environment, respectively, designed to evaluate task performance in visually impaired patients in the context of consultancy and training. Functional vision testing has been performed in studies of retinal prostheses,[253, 254] and several gene therapy trials for IRDs assess patients' reading speed performance (Table 1).

1.4 Emerging therapies and future perspectives

Prior to the emergence of gene therapeutic trials, no evidence-based treatment options existed for IRDs that led to a clinically measurable improvement in visual function. The development of therapies for rare diseases has historically been challenging due to small patient populations for trials, and the challenges in post-approval marketing.

The great advances in gene therapy in the last two decades have led to market approval of voretigene neparvovec (Luxturna®) subretinal gene therapy for *RPE65*-associated early-onset IRD/LCA. This success, along with other advances in gene therapy development, have led to a spectacular expansion in the field of retinal gene therapy. Subretinal gene therapy is under development for *CRB1*-RDs,[7] and clinical trials are ongoing for *RPGR*-associated RP, choroideremia, achromatopsia (associated with *CNGB3* and *CNGA3*), Stargardt disease (associated with *ABCA4*), X-linked retinoschisis (associated with *RS1*) and several other entities (Table 1), are in the pipeline.[7, 255]

1.4.1 Gene replacement and gene silencing

Gene transfer to the target cells in the retina may happen through viral vectors, mostly adenoviruses, lentiviruses, or adeno-associated viruses (AAV), the latter representing the most efficient and stable gene transfer in most IRD forms.[18, 256] AAV vectors are currently the most used viral vectors in gene therapy, due to the extensive experience with AAV, and their excellent safety profile: in the retina, the risk for immunogenicity is low,[257] and they have low inflammatory and low retinal toxicity potential.[257, 258] Furthermore, they do not integrate their genome into the host-cell genome,[258] thus eliminating the risk of iatrogenic activation of oncogenes. Virtually all AAV serotypes are able to infect the RPE, and serotypes 2, 5, and 7-9 are able to infect photoreceptors.[259] Drawbacks of AAV vectors include their small size, which leads to a limited transgene capacity of up to 4.2 kb. In contrast, the larger lentivirus vectors have a transgene capacity of up to 10 kb.[260] However, they integrate their genome into the host-cell genome with great efficiency, although it has been shown that they do not preferentially integrate their genome in the vicinity of oncogenes.[261] Although the potential of viral vectors has been demonstrated repeatedly, nonviral gene delivery systems have been investigated as well. These transfer methods, using for instance nanoparticles, liposomes, or naked plasmid DNA, are cheaper and easier to produce, and have a lower risk of inducing an immune response. However, as of yet, they have not shown promising potential for safe gene delivery, due to e.g. lack of persistent transgene expression (naked DNA and nanoparticles), or the potential for retinal toxicity (liposomes).[262, 263]

While gene replacement or supplementation should be sufficient in autosomal recessive IRDs, in which a lack of gene expression leads to a deficit in the gene product, (additional) gene silencing is necessary in autosomal dominant IRDs. In autosomal dominant RPs, the gene mutations often lead to mutant gene expression resulting in altered protein products that impair normal function of the wild-type protein, leading to a toxic effect. In such cases, gene therapy is aimed at repairing or silencing the mutated gene, and gene supplementation in the case of additional haplo-insufficiency.

Such gene silencing has been proposed through the use of allele-specific inhibitors that induce the degeneration of the mutated messenger RNA (mRNA).[264] Another approach is the suppression of both the mutated and wild-type allele, and their replacement by a wildtype non-silenced allele.[265] Both strategies can be mediated for instance by small RNA inhibitors or ribozymes,[266-268] each with their own set of advantages and disadvantages,[269] such as a need for repeated injections.

1.4.2 Antisense oligonucleotides

Antisense oligonucleotides (AONs) consist of small DNA or RNA molecules that are able to modulate splicing after binding to pre-mRNA. Preclinical studies using e.g. fibroblasts from affected patients, and animal studies have shown promising results for *CEP290*-LCA,[270] and for *RHO*-RP.[163] AONs can be administered "naked" through intravitreal injections, or through subretinal injections with an adenoviral-associated viral vector, and have shown minimal toxic or immunological adverse effects.[271] As naked AONs are small-sized molecules, they may be able to reach their destination cells, the photoreceptors, more easily after intravitreal injections. This approach would require repeated injections throughout life, while a subretinal injection of an AAV-mediated AON may give a considerably more durable therapeutic benefit. However, intravitreal AONs target the entire retina, and the need for a vitrectomy and its associated complications is circumvented. A recent phase I/II trial investigating the effect of intravitreal AONs in the treatment of 10 patients with *CEP290*-associated LCA found no serious adverse events, and a clinically meaningful improvement in vision, defined in the study as 0.3 logMAR, in 5 patients.[15] These encouraging results are followed up in a phase II/III trial, the ILLUMINATE study (NCT03913143).

1.4.3 Gene editing: CRISPR/Cas9

An exciting potential alternative to gene replacement strategies is the therapeutic approach of gene editing. In gene editing, the genome can be altered by inducing double-stranded DNA breaks, single-stranded DNA breaks, or specific base changes in the DNA at target sites to correct the deleterious gene mutation. This can be achieved using several methods, such as zinc finger nucleases, meganucleases, and, more recently, clustered regularly interspaced short palindromic repeats (CRISPR) CRISPR-associated protein 9 (Cas9).[272] CRISPR/Cas9 gene editing is a fast, cheap and relatively efficient method to edit the genome and repair genetic mutations, typically by inducing double-stranded breaks. CRISPR is guided by RNA sequences, and multiple guide

RNA sequences may be packaged into one targeted delivery system (e.g. a viral vector). Thereby, CRISPR has the unique ability to target more than one genetic location.[273]

CRISPR/Cas9-based therapies have been used successfully in mouse models for instance *PDE6B*,[274] *CEP290*,[275] and *RHO*.[162, 276] In mouse models of *RHO*-RP, CRISPR/Cas9 has been used in a mutation-independent "ablate-and-replace" technique. Moreover, CRISPR/Cas9 has been used to generate accurate mouse models for RP and LCA.[277, 278]

Drawbacks of the CRISPR/Cas9 gene editing system include concerns on its accuracy and the potential of off-target effects.[279] Additionally, its efficiency may vary. In induced pluripotent stem cells of a patient with *RPGR*-RP, CRISPR-Cas9 was applied to correct the gene mutation and convert it to the wild-type allele.[280] This succeeded in 13% of *RPGR* gene copies, which still spectacularly exceeds previous gene correction rates of 1-3%, which used e.g. transcription activator-like effector nucleases (TALENs).[281] Furthermore, it is a large-sized system that cannot be packaged into a single viral vector, and typically a dual vector system is employed.[16]

The challenges associated with the CRISPR/Cas9 approach have driven the exploration of alternative precision gene editing approaches. One such approach is the recently published prime editing strategy,[282] which can alter DNA with single-nucleotide precision, potentially with greater safety, and with great versatility. It combines Cas9-mediated RNA-guided DNA breakage (or nicking) with reverse transcriptase-mediated DNA synthesis at the same target site. Different types of mutations, including insertions and deletions, can be corrected. It has been proposed that it can correct up to 89% of pathogenic human variants that have been described in the ClinVar archive of genetic variants in any part of the genome, which spectacularly broadens the range of mutations that can be corrected. The promising *in vitro* results of prime editing remain to be replicated *in vivo*.

1.4.4 Stem cell-based strategies

When retinal cells have already died, genetic therapies to correct mutated genes in the affected target cells appear useless as an isolated therapeutic approach. In these cases, replacement of these dead cells by new functional cells may prove to be a viable future treatment option.[226, 238] Human embryonic stem cells have been investigated as a treatment for several retinal disorders, and have shown some visual improvement in IRD rat models.[283, 284] In humans, a phase 1/2 trial transplanting human embryonic stem cells to the subretinal space in patients with Stargardt's disease or atrophic age-related macular degeneration has shown some modest visual improvement in more than half of the treated eyes.[234] However, the use of human embryonic stem cells as a therapy has raised ethical concerns, as well as concerns over immunological responses and/or the need for immunosuppression.

Fibroblast-derived induced pluripotent stem cells (iPSCs) are derived from the patient, and have been used in the treatment of several mouse and rat models of IRD, where they have led to potential preservation of the visual function.[285, 286] Concerns regarding the use of iPSCs as a treatment modality include immunogenicity,[287] and tumor formation due to incompletely differentiated iPSCs.[288] A safer and particularly exciting application of iPSCs, has been in the generation of retinal organoids,[289] where they aid in the examination of underlying disease mechanism and in the in-vitro study of treatment options, such as in *CRB1*-RDs.[18] In autologous IPSC-based cultured retinal cells of patients with IRDs, the genetic defect may be corrected *in vitro*, using for instance AAV-based gene replacement or gene editing techniques,[235] in preparation for subretinal administration. A key challenge may be not only to achieve a correct anatomical integration of such stem cells into the retina after surgical administration, but certainly also subsequent cellular function and interaction, leading to genuine functional improvement that matters to the patients.[226, 238, 290] Another important aspect when considering cell transplantation for advanced IRD is the fact that such cases do not only have photoreceptor atrophy, but also atrophy of the photoreceptor's 'nursing cells', the RPE and choriocapillaris. After all, the photoreceptor-RPE-Bruch's membrane-choriocapillaris interface normally forms a closely connected and inter-dependent functional unit. This means that administration of such a combination of cells, possibly using cell sheets and/or a cell-carrying scaffold, may be mandatory to achieve a (close to) normal cellular interaction for a durable and functionally relevant treatment effect.

Bone-marrow-derived mesenchymal stem cells have been used in intravitreal injections in phase I clinical trials for IRD patients, and in commercial "stem cell clinics" in the United States, where resulting vision-threatening complications, such as vitreous hemorrhage and rhegmatogenous retinal detachment, and blindness have been reported in patients with IRD and with age-related macular degeneration.[291, 292]

1.4.5 Optogenetics

In patients who are blind due to photoreceptor degeneration while still retaining a relatively intact inner retina, optogenetics may be a tool to re-introduce light perception. Optogenetics is a strategy whereby a gene encoding a photosensitive protein (an opsin) is introduced in inner retinal cells, i.e. retinal ganglion cells and bipolar cells, with the aim of sensitizing these inner retinal cells to light in the absence of photoreceptors.[293] It thus provides an alternative visual cycle to improve retinal activity. Opsins may have a microbial origin (type 1), such as channelrhodopsins or halorhodopsins, which function as light-gated ion channels, or an animal origin (type 2), such as melanopsin or rhodopsin. Preclinical data have suggested that blind patients with preservation of the photoreceptor nuclei, as visible on OCT, may be eligible for functional photoreceptor restoration through optogenetics.[294]

1.4.6 Nutritional approaches to the treatment of IRD

Several trials have investigated the safety and efficacy of oral supplementation of compounds thought to slow down the loss of visual function and photoreceptor degeneration. One such compound is QLT091001 (QLT), or synthetic 9-cis-retinyl acetate, a stable synthetic precursor which is converted to 9-cis retinal in the human body.[158] This replaces the missing 11-cis retinal in the retinas of patients with *RPE65*-RD or *LRAT*-RD, who lack 11-cis-retinal, and ultimately starts the phototransduction cascade upon photo-activation. A phase Ib trial of QLT091001 in patients with *LRAT*-RD and *RPE65*-RD has shown a meaningful improvement in visual acuity and visual field area in a large subset of patients, albeit temporarily in most patients, along with a favorable safety profile.[158, 159]

For Stargardt disease, orphan drug status was given to soraprazan,[295] a proton potassium-competitive acid-blocker which was developed for use in dyspepsia. Based on experimental data, this drug is expected to enter the retina, attach to the lipofuscin deposits, and partially eliminate the damaging lipofuscin.[296] As of yet, no clinical reports on its efficacy have been published, although a clinical trial is ongoing (EudraCT number: 2018-001496-20).

Likewise, deuterium-enriched vitamin A has been shown to slow down the biosynthesis of A2E, a lipofuscin component, in rodents.[297] It has therefore been suggested to have a potential protective effect in Stargardt disease and Best vitelliform macular dystrophy, although clinical data on this specific vitamin A type have not yet been reported. Otherwise, the supplementation of regular vitamin A is not recommended in Stargardt disease, as animal studies have found that high doses of vitamin A may accelerate the rate of lipofuscin deposition in the macula,[298] and may thus expedite vision loss. However, in RP, vitamin A palmitate supplementation has been associated with a potentially slower rate of cone amplitude loss on the electroretinogram in small patient samples,[299] but this is a subject of considerable controversy.

In a mouse model of RP, orally administered N-acetylcysteine led to long-term preservation of cone function.[300] A recently published phase I clinical trial investigating oral N-acetylcysteine has shown improvement in visual acuity and macular sensitivity in patients with moderately advanced RP.[301]

1.5 Expectation management in interventional clinical trials

While the advances of the last 2 decades have propelled research forward towards clinical application, with exciting new treatment possibilities for IRD patients, expectations should be managed and critically reconsidered. Gene supplementation therapy is notably costly to develop, to test, and to implement, and of the several gene replacement therapy trials that have been performed in the *RPE65*-RD population, only one has led to considerable long-term success and market approval to date: voretigene neparvovec (Luxturna®), priced at approximately US $850.000. While the bench-

to-bedside success of this first commercially available retinal gene therapy has further energized patient and research communities alike, the long term effects of the therapy on visual function in the other *RPE65*-gene therapy trials have been more guarded.[9, 10] For example, it has been found that retinal degeneration may continue, and the longevity of interventional therapy will be limited if the degree of photoreceptor degeneration has exceeded a certain limit prior to treatment.[302] Indeed, in most patients, retinal degeneration will have progressed to intermediate or advanced stages at the time of intervention. While any degree of visual restoration and/or preservation is a revolutionary move forward in an otherwise untreatable disease entity, FDA documents have revealed that approximately half of treated patients met the FDA criteria for minimally meaningful improvement.[303] The other half did not achieve the criteria for meaningful improvement, and 2 patients had permanent vision loss, due to injection-related macular thinning in one patient, and irreversible optic nerve atrophy due to increased intraocular pressure in the other patient, who received ocular steroids for the treatment of a *Staphylococcus* infection.[303] These results may be particularly disappointing to the patient, having undergone the surgical procedure and a period of recovery and frequent hospital visits.

In choroideremia, the first in-human gene therapy, which started in Oxford, UK in 2011, has led to a median gain in visual acuity of 4.5 letters in the treatment cohort, versus a visual acuity loss of 1.5 letters in the untreated eye at the 2-year post-treatment point, with 6/14 treated eyes gaining >5 letters of visual acuity improvement. In some patients, this vision improvement was sustained at up to 5 years of follow-up.[131] Most visual acuity gain was observed in patients with advanced disease and reduced baseline visual acuity, while in those with a good baseline visual acuity, this baseline visual acuity was maintained for 5 years in most patients. Nonetheless, complications arose in 2/14 patients (14%) – surgery-related retinal thinning and incomplete vector dosing in one patient, and postoperative inflammation in the other. In these patients, visual acuity loss was observed in the treated eye. This has led to the prolongation of the post-operative immune suppression regimen. Moreover, surgical techniques in these trials have since been refined, e.g. by incorporating the aid of intra-operative OCT.[304] Several other in-human choroideremia gene therapy trials used the same gene vector as the Oxford group.[12, 132, 305] Visual acuity results have been variable, with considerable visual acuity gain in some patients, visual acuity loss in others, usually due to intra-operative complications, and minor changes or maintenance of baseline visual acuity in most patients. As in the trial performed in Oxford, one other study found improvement in mean retinal sensitivity on microperimetry in most treated eyes,[305] while the other 2 studies found no significant post-treatment changes in mean retinal sensitivity.[12, 132]

The irreversibility of disease in cell populations that have already degenerated should be stressed to any potential participants in gene therapy trials. In the case of subretinal gene therapy that only targets the posterior pole, the treatment effect will be confined largely to the macula. Therefore, it should be explained to patients that peripheral visual field preservation is not expected when this is not the targeted area.

Issues regarding the cost of gene therapy remain a point of concern. As gene therapies for orphan indications, defined as diseases affecting fewer than 200.000 people in the United States, target specific genetic entities, and thus pertain to small patient populations, they remain among the most expensive drugs.

These considerations indicate that clinicians and researchers should exert caution not to oversell the capacities of investigative (gene) therapeutic strategies to patients, in whom hope for improvement and fear of further visual decline without treatment will be important factors in their decision whether or not to take part in a clinical trial. Therefore, in the context of informed consent, it is evident that eligible patients – who may already be small in number – are to be informed well on the risks of intervention, its investigative nature and thus uncertain outcome, and on the lengthy post-intervention trajectory.

1.6 Concluding remarks

New treatment opportunities emerge for IRDs at an exceedingly rapid pace, offering hopeful perspectives to many IRD patients worldwide. Given these developments, and the need to approve effective treatments for clinical use, prospective natural history studies are of eminent importance. However, this thesis has shown that retrospective studies, despite their inherent limitations, can provide robust and useful information on important disease characteristics, variability, and course of many years. National collaborations, such as the RD5000 consortium in the Netherlands, or international collaborations, as within the European context of ERN-EYE, are important to further strengthen the outcome of such studies in these relatively small patient populations. For example, access to large databases such as the Delleman archive for hereditary eye diseases at the Amsterdam University Medical Centers/Academic Medical Center in Amsterdam, have provided the unique opportunity to ascertain large sample sizes, and to assemble some of the largest retrospective cohorts described to date. Indeed, prospective studies will not be able to provide all the answers on disease progression and visual survival, and they will still have limitations, such as a limited capacity to include many patients, and a limited study duration. On the other hand, the limitations of retrospective research are well-described and include the lack of standardization of patient visits, interval censoring, and a limited availability of multimodal imaging. Improvement of phenotyping and genetic characterization remain of critical importance. Ongoing and future prospective studies should be geared at further assessing the rate of disease progression through different visual function parameters and biomarkers on multimodal retinal

imaging, and at investigating correlations between these measures. In the end, retrospective and prospective studies have the powerful capacity to augment each other. Such studies are pivotal for well-balanced decision making on patient eligibility for treatments, and endpoint selection to test treatment efficacy.

Table 1. An overview of ongoing or recently completed human gene therapy trials for inherited retinal degenerations

Route of administration/ vector	Target gene	Disease group	Study phase	Primary outcome measure*	Secondary outcome measure*	Clinicaltrials.gov number	Sponsor
Adeno-associated virus gene replacement therapy							
Subretinal AAV8-RPGR	*RPGR*	RP	2/3	Dose limiting toxicities; treatment emergent AE; MP	BCVA; MP; OCT (EZ); FAF; VF	NCT03116113	NightstaRx Ltd (now Biogen)
Subretinal rAAV2tYF-GRK1-RPGR	*RPGR*	RP	1/2	AE, abnormal clinically relevant hematology/ chemistry parameters	BCVA; perimetry; retinal structure by imaging; QoL questionnaire	NCT03316560	Applied Genetic Technologies Group
Subretinal AAV-RPGR	*RPGR*	RP	1/2	Adverse events	Visual function; retinal function; QoL questionnaire	NCT03252847	MeiraGTx UK II Ltd
Subretinal AAV2-REP1	*CHM*	CHM	2 (completed)	BCVA	Macular FAF; MP; AE	NCT02553135	Univ. of Miami, USA
Subretinal AAV2-REP1	*CHM*	CHM	1/2 (completed)	Ocular and systemic AE	Goldmann VF; MP; ERG; full-field scotopic threshold; SD-OCT; FAF; fundus photography	NCT02077361	Univ. of Alberta, Canada
Subretinal AAV2-REP1	*CHM*	CHM	1/2	Safety and tolerability	Not mentioned	NCT02341807	Spark Therapeutics; Children's Hospital of Philadelphia; Univ. of Pennsylvania, USA; Massachusetts Eye and Ear Infirmary
Subretinal AAV2-REP1	*CHM*	CHM	2	Treatment emergent AE	BCVA; FAF; OCT (EZ); MP	NCT03507686 (GEMINI TRIAL)	NightstaRx Ltd (now Biogen)
Subretinal AAV2-REP1	*CHM*	CHM	2	BCVA	MP; FAF	NCT02407678 (REGENERATE TRIAL)	Univ. of Oxford; Moorfields Eye Hospital, UK; University College London, UK

Subretinal AAV2-REP1	*CHM*	CHM	3	BCVA	FAF; OCT; MP; contrast sensitivity; color vision; reading performance; QoL questionnaire	NCT03496012 (STAR TRIAL)	NightstaRx Ltd (now Biogen)
Subretinal rAAV2.REP1	*CHM*	CHM	1/2 (completed)	BCVA	MP; OCT; FAF	NCT01461213	Univ. of Oxford, UK; multicenter***
Subretinal rAAV2.REP1	*CHM*	CHM	2 (completed)	BCVA	AE; FAF; MP; contrast sensitivity; color vision	NCT02671539 (THOR TRIAL)	Univ. of Tubingen, Germany
Subretinal rAAV2.REP1	*CHM*	CHM	Observational	AE	BCVA; FAF; EZ on OCT; MP	NCT03584165 (SOLSTICE TRIAL)	NightstaRx Ltd (now Biogen); multicenter
Subretinal rAAV2-CBSB-hRPE65	*RPE65*	LCA	1	Ocular examination; toxicity	Visual function	NCT00481546	Univ. of Pennsylvania; NEI
Subretinal AAV2-hRPE65v2, voretigene neparvovec-rzyl	*RPE65*	LCA	1/2	Safety and tolerability	Visual function	NCT00516477	Spark Therapeutics
Subretinal tgAAV76 (rAAV 2/2.hRPE65p.hRPE65)	*RPE65*	Severe early-onset IRD	1/2 (completed)	Intraocular inflammation	Visual function	NCT00643747	UCL, Moorfields Eye Hospital NHS Foundation Trust, Targeted Genetics Corporation
Subretinal rAAV2-CB-hRPE65	*RPE65*	LCA	1/2 (completed)	Ocular and non-ocular AE	VF in central 30°; BCVA	NCT00749957	Applied Genetic Technologies Corp; Oregon Health and Science Univ.; Univ. of Massachusetts, Worcester, USA
Subretinal rAAV2-hRPE65	*RPE65*	LCA	1 (completed)	Ocular and systemic safety	Visual function	NCT00821340	Hadassah Medical Organization

Table 1. Continued

Subretinal AAV2-hRPE65v2, voretigene neparvovec-rzyl	*RPE65*	LCA	3	MLMT	FST white light; MLMT; BCVA	NCT00999609	Spark Therapeutics, Children's Hospital of Philadelphia, University of Iowa, USA
Subretinal AAV2-hRPE65v2, voretigene neparvovec-rzyl	*RPE65*	LCA	1/2	Safety and tolerability	BCVA; VF; pupillary light response; mobility testing; FST; contrast sensitivity	NCT01208389	Spark Therapeutics
Subretinal rAAV2/4.hRPE65	*RPE65*	LCA or severe early-onset IRD	1/2 (completed)	Drug safety evaluation	Different efficacy parameters and immune parameters; global ERG; patient efficacy questionnaire, far and near BCVA; color vision, pupillometry, MP, DA	NCT01496040	Nantes University Hospital
Subretinal AAV RPE65	*RPE65*	RD	1/2 (completed)	AE	Visual function; retinal function; QoL questionnaire	NCT02781480	MeiraGTx UK II Ltd
Subretinal SAR422459	*ABCA4*	STGD	1/2 (study discontinued; not for safety reasons)	AE; ocular safety (BCVA; IOP; MP; static and kinetic VF; OCT; ERG)	BCVA; MP; static and kinetic VF; OCT; FAF	NCT01367444	Sanofi
Subretinal rAAV.hCNGA3	*CNGA3*	ACHM2	1/2	AE	Visual function; patient reported outcomes; retinal imaging	NCT02610582	STZ eyetrial; University Hospital Tuebingen; Ludwig-Maximillians – Univ of Munich
Subretinal AGTC-402	*CNGA3*	ACHM2	1/2	AE	BCVA; light discomfort testing; color vision	NCT02935517	Applied Genetic Technologies Corp

Subretinal AAV-CNGA3	*CNGA3*	ACHM2	1/2	AE	BCVA; MP; perimetry; QoL questionnaire	NCT03758404	MeiraGTx UK II Ltd
Subretinal AAV-CNGA3	*CNGB3*	ACHM3	1/2	AE	Visual function; retinal function; QoL questionnaire	NCT03001310	MeiraGTx UK II Ltd; EMAS Pharma; Syne Qua Non Limited
Subretinal rAAV2tYF-PR1.7-hCNGB3	*CNGB3*	ACHM3	1/2	AE	BCVA; light discomfort testing; color vision	NCT02599922	Applied Genetic Technologies Corp; NEI
Subretinal AAV2/8-hCARp.hCNGB3 and AAV2/8-hG1.7p.coCNGA3 (follow-up)	*CNGB3* and *CNGA3*	ACHM2 and ACHM3	1/2	AE	Visual function; retinal function; QoL questionnaire	NCT03278873	MeiraGTx UK II Ltd; Syne Qua Non Limited; EMAS Pharma
Subretinal AAV2/5-hPDE6B	*PDE6B*	RP	1/2	Ocular and non-ocular AE	Mobility test; VF; reading speed; NEI-VFQ-25	NCT03328130	Horama S.A.
Subretinal CPK850	*RLBP1*	RP	1/2	AE, SAE, deaths, DA	DA; static VF; contrast sensitivity; MP; multifocal and full-field ERG; reading speed; eye dominance; mobility test; NEI-VFQ-25; low-luminance questionnaire	NCT03374657	Novartis Pharmaceuticals
Subretinal rAAV2-VMD2-hMERTK	*MERTK*	RP	1	Ocular safety	ETDRS BCVA; FST	NCT01482195	Fowzan Alkuraya; King Khaled Eye Specialist Hospital; King Faisal Specialist Hospital & Research Center

Table 1. Continued

Subretinal SAR421869	*MYO7A*	USH1B	1/2	AE	Visual function	NCT01505062	Sanofi
Antisense oligonucleotides							
Intravitreal QR-1123	*RHO*	RP	1/2	Ocular and non-ocular AE	BCVA; low-luminance BCVA; DAC perimetry; static VF; MP, SD-OCT; FST; FAF; contrast sensitivity; color vision; serum levels of QR-1123	NCT04123626	ProQR Therapeutics
Intravitreal QR-110	*CEP290*	LCA	1/2 (completed), phase 2/3 started	Ocular AE	Non-ocular AE; ophthalmic examination findings; BCVA; infrared imaging; OCT; vital safety parameters; serum level parameters	NCT03140969; NCT03913130; NCT03913143	ProQR Therapeutics
Intravitreal QR-421a	*USH2A*	RP	1/2	Ocular and non-ocular AE	DAC perimetry; static VF; EZ area/width; BCVA; low luminance BCVA; MP; ERG; FAF; serum levels/ clearance/half-time	NCT03780257	ProQR Therapeutics

CRISPR-based genome editing medicine							
Subretinal AGN-151587	*CEP290*	LCA	1/2	AE; dose limiting toxicities	Maximum tolerated dose; mobility course score; BCVA; pupillary response; FST; macula thickness; contrast sensitivity; MP; color vision; QoL score; kinetic VF; gaze tracking	NCT03872479	Allergan; Editas Medicine, Inc.

Optogenetic treatment methods were not included in this table.

*As noted on clinicaltrials.gov. Accessed January 17th 2020.

AAV = adeno-associated viral vector. ACHM = achromatopsia. AE = adverse events. BCVA = best-corrected visual acuity. DA = dark adaptation. DAC = dark-adapted chromatic. ERG = electroretinogram. ETDRS = Early Treatment of Diabetic Retinopathy Study. EZ = ellipsoid zone. FAF = fundus autofluorescence. FST = full-field light sensitivity threshold testing. IOP = intra-ocular pressure. IRD = inherited retinal degeneration. MLMT = multi-luminance mobility testing. MP = microperimetry. NEI = National Eye Institute. NEI-VFQ-25 = National Eye Instittute – Visual function questionnaire 25 items. OCT = optical coherence tomography. rAAV = recombinant adeno-associated viral vector. SAE = serious adverse events. STGD = Stargardt disease. RP = retinitis pigmentosa. RPGR = retinitis pigmentosa GTPase Regulator. USH = Usher Syndrome. VF = visual fields. QoL = quality of life. UK = United Kingdom.

***Oxford University Hospitals NHS Trust; Moorfields Eye Hospital NHS Foundation Trust, University College, London; Manchester University NHS Foundation trust; Univ. of Manchester; Univ. Hospital Southampton NHS Foundation Trust, Univ. of Southampton, UK.

REFERENCES

1. Hamel C. Retinitis pigmentosa. Orphanet J Rare Dis 2006;1:40.
2. Hartong DT, Berson EL, Dryja TP. Retinitis pigmentosa. Lancet 2006;368:1795-809.
3. Maguire AM, Simonelli F, Pierce EA, et al. Safety and Efficacy of Gene Transfer for Leber's Congenital Amaurosis. N Engl J Med 2008;358:2240-8.
4. MacLaren RE, Groppe M, Barnard AR, et al. Retinal gene therapy in patients with choroideremia: initial findings from a phase 1/2 clinical trial. Lancet 2014;383:1129-37.
5. Cehajic Kapetanovic J, Barnard AR, MacLaren RE. Molecular Therapies for Choroideremia. Genes (Basel) 2019;10:738.
6. Cehajic-Kapetanovic J, Xue K, Martinez-Fernandez de la Camara C, et al. Initial results from a first-in-human gene therapy trial on X-linked retinitis pigmentosa caused by mutations in RPGR. Nat Med 2020;26:354-9.
7. Pellissier LP, Quinn PM, Alves CH, et al. Gene therapy into photoreceptors and Muller glial cells restores retinal structure and function in CRB1 retinitis pigmentosa mouse models. Hum Mol Genet 2015;24:3104-18.
8. Quinn PM, Pellissier LP, Wijnholds J. The CRB1 Complex: Following the Trail of Crumbs to a Feasible Gene Therapy Strategy. Front Neurosci 2017;11:175.
9. Bainbridge J, Mehat M, Sundaram V, et al. Long-Term Effect of Gene Therapy on Leber's Congenital Amaurosis. N Engl J Med 2015;372:1887-97.
10. Jacobson SG, Cideciyan AV, Roman AJ, et al. Improvement and Decline in Vision with Gene Therapy in Childhood Blindness. N Engl J Med 2015;372:1920-6.
11. Edwards TL, Jolly JK, Groppe M, et al. Visual Acuity after Retinal Gene Therapy for Choroideremia. N Engl J Med 2016;374:1996-8.
12. Lam BL, Davis JL, Gregori NZ, et al. Choroideremia Gene Therapy Phase 2 Clinical Trial: 24-Month Results. Am J Ophthalmol 2019;197:65-73.
13. Maguire AM, Russell S, Wellman JA, et al. Efficacy, Safety, and Durability of Voretigene Neparvovec-rzyl in RPE65 Mutation-Associated Inherited Retinal Dystrophy: Results of Phase 1 and 3 Trials. Ophthalmology 2019;126:1273-85.
14. Giannelli SG, Luoni M, Castoldi V, et al. Cas9/sgRNA selective targeting of the P23H Rhodopsin mutant allele for treating retinitis pigmentosa by intravitreal AAV9.PHP.B-based delivery. Hum Mol Genet 2018;27:761-79.
15. Cideciyan AV, Jacobson SG, Drack AV, et al. Effect of an intravitreal antisense oligonucleotide on vision in Leber congenital amaurosis due to a photoreceptor cilium defect. Nat Med 2019;25:225-8.
16. Yu W, Wu Z. In Vivo Applications of CRISPR-Based Genome Editing in the Retina. Front Cell Dev Biol 2018;6:53.
17. van Huet RA, Oomen CJ, Plomp AS, et al. The RD5000 database: facilitating clinical, genetic, and therapeutic studies on inherited retinal diseases. Invest Ophthalmol Vis Sci 2014;55:7355-60.
18. Quinn PM, Buck TM, Mulder AA, et al. Human iPSC-Derived Retinas Recapitulate the Fetal CRB1 CRB2 Complex Formation and Demonstrate that Photoreceptors and Muller Glia Are Targets of AAV5. Stem Cell Reports 2019;12:906-19.

19. Murro V, Mucciolo DP, Sodi A, et al. Retinal capillaritis in a CRB1-associated retinal dystrophy. Ophthalmic Genet 2017:1-4.
20. Morarji J, Lenassi E, Black GC, Ashworth JL. Atypical presentation of CRB1 retinopathy. Acta Ophthalmol 2016;94:e513-4.
21. Ghofrani M, Yahyaei M, Brunner HG, et al. Homozygosity Mapping and Targeted Sanger Sequencing Identifies Three Novel CRB1 (Crumbs homologue 1) Mutations in Iranian Retinal Degeneration Families. Iran Biomed J 2017;21:294-302.
22. Kousal B, Dudakova L, Gaillyova R, et al. Phenotypic features of CRB1-associated early-onset severe retinal dystrophy and the different molecular approaches to identifying the disease-causing variants. Graefes Arch Clin Exp Ophthalmol 2016;254:1833-9.
23. Hasan SM, Azmeh A, Mostafa O, Megarbane A. Coat's like vasculopathy in leber congenital amaurosis secondary to homozygous mutations in CRB1: a case report and discussion of the management options. BMC Res Notes 2016;9:91.
24. Vamos R, Kulm M, Szabo V, et al. Leber congenital amaurosis: first genotyped Hungarian patients and report of 2 novel mutations in the CRB1 and CEP290 genes. Eur J Ophthalmol 2016;26:78-84.
25. Wolfson Y, Applegate CD, Strauss RW, et al. CRB1-Related Maculopathy With Cystoid Macular Edema. JAMA Ophthalmol 2015;133:1357-60.
26. Kuniyoshi K, Ikeo K, Sakuramoto H, et al. Novel nonsense and splice site mutations in CRB1 gene in two Japanese patients with early-onset retinal dystrophy. Doc Ophthalmol 2015;130:49-55.
27. Cordovez JA, Traboulsi EI, Capasso JE, et al. Retinal Dystrophy with Intraretinal Cystoid Spaces Associated with Mutations in the Crumbs Homologue (CRB1) Gene. Ophthalmic Genet 2015;36:257-64.
28. Srilekha S, Arokiasamy T, Srikrupa NN, et al. Homozygosity Mapping in Leber Congenital Amaurosis and Autosomal Recessive Retinitis Pigmentosa in South Indian Families. PLoS One 2015;10:e0131679.
29. Jalkh N, Guissart C, Chouery E, et al. Report of a novel mutation in CRB1 in a Lebanese family presenting retinal dystrophy. Ophthalmic Genet 2014;35:57-62.
30. Tsang SH, Burke T, Oll M, et al. Whole exome sequencing identifies CRB1 defect in an unusual maculopathy phenotype. Ophthalmology 2014;121:1773-82.
31. Jonsson F, Burstedt MS, Sandgren O, et al. Novel mutations in CRB1 and ABCA4 genes cause Leber congenital amaurosis and Stargardt disease in a Swedish family. Eur J Hum Genet 2013;21:1266-71.
32. Yzer S, Leroy BP, De Baere E, et al. Microarray-based mutation detection and phenotypic characterization of patients with Leber congenital amaurosis. Invest Ophthalmol Vis Sci 2006;47:1167-76.
33. den Hollander AI, Lopez I, Yzer S, et al. Identification of novel mutations in patients with Leber congenital amaurosis and juvenile RP by genome-wide homozygosity mapping with SNP microarrays. Invest Ophthalmol Vis Sci 2007;48:5690-8.
34. Talib M, van Schooneveld MJ, van Genderen MM, et al. Genotypic and Phenotypic Characteristics of CRB1-Associated Retinal Dystrophies: A Long-Term Follow-up Study. Ophthalmology 2017;124:884-95.
35. Mathijssen IB, Florijn RJ, van den Born LI, et al. Long-term follow-up of patients with retinitis pigmentosa type 12 caused by CRB1 mutations: A Severe Phenotype With Considerable Interindividual Variability. Retina 2017;37:161-72.

36. Paun CC, Pijl BJ, Siemiatkowska AM, et al. A novel crumbs homolog 1 mutation in a family with retinitis pigmentosa, nanophthalmos, and optic disc drusen. Mol Vis 2012;18:2447-53.
37. Zenteno JC, Buentello-Volante B, Ayala-Ramirez R, Villanueva-Mendoza C. Homozygosity mapping identifies the Crumbs homologue 1 (Crb1) gene as responsible for a recessive syndrome of retinitis pigmentosa and nanophthalmos. Am J Med Genet A 2011;155a:1001-6.
38. Henderson RH, Mackay DS, Li Z, et al. Phenotypic variability in patients with retinal dystrophies due to mutations in CRB1. Br J Ophthalmol 2011;95:811-7.
39. Riveiro-Alvarez R, Vallespin E, Wilke R, et al. Molecular analysis of ABCA4 and CRB1 genes in a Spanish family segregating both Stargardt disease and autosomal recessive retinitis pigmentosa. Mol Vis 2008;14:262-7.
40. Simonelli F, Ziviello C, Testa F, et al. Clinical and molecular genetics of Leber's congenital amaurosis: a multicenter study of Italian patients. Invest Ophthalmol Vis Sci 2007;48:4284-90.
41. Bernal S, Calaf M, Garcia-Hoyos M, et al. Study of the involvement of the RGR, CRPB1, and CRB1 genes in the pathogenesis of autosomal recessive retinitis pigmentosa. J Med Genet 2003;40:e89.
42. Jacobson SG, Cideciyan AV, Aleman TS, et al. Crumbs homolog 1 (CRB1) mutations result in a thick human retina with abnormal lamination. Hum Mol Genet 2003;12:1073-8.
43. Lotery AJ, Malik A, Shami SA, et al. CRB1 mutations may result in retinitis pigmentosa without para-arteriolar RPE preservation. Ophthalmic Genet 2001;22:163-9.
44. Lotery AJ, Jacobson SG, Fishman GA, et al. Mutations in the CRB1 gene cause Leber congenital amaurosis. Arch Ophthalmol 2001;119:415-20.
45. den Hollander AI, Heckenlively JR, van den Born LI, et al. Leber congenital amaurosis and retinitis pigmentosa with Coats-like exudative vasculopathy are associated with mutations in the crumbs homologue 1 (CRB1) gene. Am J Hum Genet 2001;69:198-203.
46. Aleman TS, Cideciyan AV, Aguirre GK, et al. Human CRB1-associated retinal degeneration: comparison with the rd8 Crb1-mutant mouse model. Invest Ophthalmol Vis Sci 2011;52:6898-910.
47. Coppieters F, Casteels I, Meire F, et al. Genetic screening of LCA in Belgium: predominance of CEP290 and identification of potential modifier alleles in AHI1 of CEP290-related phenotypes. Hum Mutat 2010;31:E1709-66.
48. Galvin JA, Fishman GA, Stone EM, Koenekoop RK. Evaluation of genotype-phenotype associations in leber congenital amaurosis. Retina 2005;25:919-29.
49. Edwards A, Grover S, Fishman GA. Frequency of photographically apparent optic disc and parapapillary nerve fiber layer drusen in Usher syndrome. Retina 1996;16:388-92.
50. Hendriks M, Verhoeven VJM, Buitendijk GHS, et al. Development of Refractive Errors-What Can We Learn From Inherited Retinal Dystrophies? Am J Ophthalmol 2017;182:81-9.
51. Boon CJ, Klevering BJ, Leroy BP, et al. The spectrum of ocular phenotypes caused by mutations in the BEST1 gene. Prog Retin Eye Res 2009;28:187-205.
52. Othman MI, Sullivan SA, Skuta GL, et al. Autosomal dominant nanophthalmos (NNO1) with high hyperopia and angle-closure glaucoma maps to chromosome 11. Am J Hum Genet 1998;63:1411-8.
53. Weng CY, Barnett D. Nanophthalmos-Retinitis Pigmentosa-Foveoschisis-Optic Disc Drusen Syndrome (MFRP). Ophthalmol Retina 2018;2:1162.

54. Zenteno JC, Buentello-Volante B, Quiroz-Gonzalez MA, Quiroz-Reyes MA. Compound heterozygosity for a novel and a recurrent MFRP gene mutation in a family with the nanophthalmos-retinitis pigmentosa complex. Mol Vis 2009;15:1794-8.
55. Crespi J, Buil JA, Bassaganyas F, et al. A novel mutation confirms MFRP as the gene causing the syndrome of nanophthalmos-renititis pigmentosa-foveoschisis-optic disk drusen. Am J Ophthalmol 2008;146:323-8.
56. Ayala-Ramirez R, Graue-Wiechers F, Robredo V, et al. A new autosomal recessive syndrome consisting of posterior microphthalmos, retinitis pigmentosa, foveoschisis, and optic disc drusen is caused by a MFRP gene mutation. Mol Vis 2006;12:1483-9.
57. Hettinga YM, van Genderen MM, Wieringa W, et al. Retinal Dystrophy in 6 Young Patients Who Presented with Intermediate Uveitis. Ophthalmology 2016;123:2043-6.
58. Verhagen F, Kuiper J, Nierkens S, et al. Systemic inflammatory immune signatures in a patient with CRB1 linked retinal dystrophy. Expert Rev Clin Immunol 2016;12:1359-62.
59. Bax NM, Lambertus S, Cremers FPM, et al. The absence of fundus abnormalities in Stargardt disease. Graefes Arch Clin Exp Ophthalmol 2019;257:1147-57.
60. Benson MD, MacDonald IM. Bilateral uveitis and Usher syndrome: a case report. J Med Case Rep 2015;9:60.
61. Heredia CD, Huguet J, Cols N, et al. Immune complexes in retinitis pigmentosa. Br J Ophthalmol 1984;68:811-4.
62. Reid DM, Campbell AM, Forrester JV. EB-virus transformed human lymphocytes from uveitis and retinitis pigmentosa patients secrete antibodies to retinal antigens. J Clin Lab Immunol 1988;26:107-11.
63. Demirci FY, Rigatti BW, Mah TS, Gorin MB. A novel RPGR exon ORF15 mutation in a family with X-linked retinitis pigmentosa and Coats'-like exudative vasculopathy. Am J Ophthalmol 2006;141:208-10.
64. Patil L, Lotery AJ. Coat's-like exudation in rhodopsin retinitis pigmentosa: successful treatment with an intravitreal dexamethasone implant. Eye (Lond) 2014;28:449-51.
65. Jain S, Gupta S, Kumar V. Ultra-widefield imaging in Coats'-type retinitis pigmentosa. Indian J Ophthalmol 2018;66:997-8.
66. Jiang Y, Lim J, Janowicz M. Cholesterol Crystals Secondary to Coats-Like Response With Retinitis Pigmentosa. JAMA Ophthalmol 2017;135:e173132.
67. Ghassemi F, Akbari-Kamrani M. Retinitis Pigmentosa Associated with Vasoproliferative Tumors and Coats-like Fundus. J Ophthalmic Vis Res 2013;8:268-70.
68. Pruett RC. Retinitis pigmentosa: clinical observations and correlations. Trans Am Ophthalmol Soc 1983;81:693-735.
69. Urgancioglu B, Ozdek S, Hasanreisoglu B. Coats'-like retinitis pigmentosa variant and nanophthalmos. Can J Ophthalmol 2007;42:877-8.
70. Murthy R, Honavar SG. Secondary vasoproliferative retinal tumor associated with Usher syndrome type 1. J aapos 2009;13:97-8.
71. Kiratli H, Ozturkmen C. Coats-like lesions in Usher syndrome type II. Graefes Arch Clin Exp Ophthalmol 2004;242:265-7.
72. De Salvo G, Gemenetzi M, Luff AJ, Lotery AJ. Cystoid macular oedema successfully treated by cryotherapy in retinitis pigmentosa with Coats'-like retinal exudation. Eye (Lond) 2011;25:821-2.

73. Bansal S, Saha N, Woon WH. The management of "coats' response" in a patient with x-linked retinitis pigmentosa-a case report. ISRN Surg 2011;2011:970361.
74. van de Pavert SA, Sanz AS, Aartsen WM, et al. Crb1 is a determinant of retinal apical Muller glia cell features. Glia 2007;55:1486-97.
75. Tout S, Chan-Ling T, Hollander H, Stone J. The role of Muller cells in the formation of the blood-retinal barrier. Neuroscience 1993;55:291-301.
76. Al Sulaiman H, Schatz P, Nowilaty SR, et al. Diffuse retinal vascular leakage and cone-rod dystrophy in a family with the homozygous missense c.1429G>A (p.Gly477Arg) mutation in CRB1. Retin Cases Brief Rep 2020;14:203-10.
77. Shah N, Damani MR, Zhu XS, et al. Isolated maculopathy associated with biallelic CRB1 mutations. Ophthalmic Genet 2017;38:190-3.
78. Khan AO, Aldahmesh MA, Abu-Safieh L, Alkuraya FS. Childhood cone-rod dystrophy with macular cystic degeneration from recessive CRB1 mutation. Ophthalmic Genet 2014;35:130-7.
79. Bujakowska K, Audo I, Mohand-Said S, et al. CRB1 mutations in inherited retinal dystrophies. Hum Mutat 2012;33:306-15.
80. Vincent A, Ng J, Gerth-Kahlert C, et al. Biallelic Mutations in CRB1 Underlie Autosomal Recessive Familial Foveal Retinoschisis. Invest Ophthalmol Vis Sci 2016;57:2637-46.
81. Pellissier LP, Alves CH, Quinn PM, et al. Targeted ablation of CRB1 and CRB2 in retinal progenitor cells mimics Leber congenital amaurosis. PLoS Genet 2013;9:e1003976.
82. Quinn PM, Alves CH, Klooster J, Wijnholds J. CRB2 in immature photoreceptors determines the superior-inferior symmetry of the developing retina to maintain retinal structure and function. Hum Mol Genet 2018;27:3137-53.
83. Aleman TS, Cideciyan AV, Sumaroka A, et al. Inner retinal abnormalities in X-linked retinitis pigmentosa with RPGR mutations. Invest Ophthalmol Vis Sci 2007;48:4759-65.
84. Aleman TS, Cideciyan AV, Sumaroka A, et al. Retinal laminar architecture in human retinitis pigmentosa caused by Rhodopsin gene mutations. Invest Ophthalmol Vis Sci 2008;49:1580-90.
85. Quinn PM, Mulder AA, Henrique Alves C, et al. Loss of CRB2 in Müller glial cells modifies a CRB1-associated retinitis pigmentosa phenotype into a Leber congenital amaurosis phenotype. Hum Mol Genet 2019;28:105-23.
86. Alves CH, Pellissier LP, Wijnholds J. The CRB1 and adherens junction complex proteins in retinal development and maintenance. Prog Retin Eye Res 2014;40:35-52.
87. Spaide RF, Curcio CA. Anatomical correlates to the bands seen in the outer retina by optical coherence tomography: literature review and model. Retina 2011;31:1609-19.
88. McKay GJ, Clarke S, Davis JA, et al. Pigmented paravenous chorioretinal atrophy is associated with a mutation within the crumbs homolog 1 (CRB1) gene. Invest Ophthalmol Vis Sci 2005;46:322-8.
89. Toto L, Boon CJ, Di Antonio L, et al. Bestrophinopathy: A Spectrum of Ocular Abnormalities Caused by the c.614T>C Mutation in the BEST1 Gene. Retina 2016;36:1586-95.
90. Son S, Cho M, Lee J. Crumbs proteins regulate layered retinal vascular development required for vision. Biochem Biophys Res Commun 2020;521:939-46.
91. Reichenbach A, Bringmann A. Glia of the human retina. Glia 2020;68:768-96.

92. Tepass U, Theres C, Knust E. crumbs encodes an EGF-like protein expressed on apical membranes of Drosophila epithelial cells and required for organization of epithelia. Cell 1990;61:787-99.
93. Khan KN, Robson A, Mahroo OAR, et al. A clinical and molecular characterisation of CRB1-associated maculopathy. Eur J Hum Genet 2018;26:687-94.
94. Mathijssen IB, Henneman L, van Eeten-Nijman JM, et al. Targeted carrier screening for four recessive disorders: high detection rate within a founder population. Eur J Med Genet 2015;58:123-8.
95. van Soest S, van den Born LI, Gal A, et al. Assignment of a gene for autosomal recessive retinitis pigmentosa (RP12) to chromosome 1q31-q32.1 in an inbred and genetically heterogeneous disease population. Genomics 1994;22:499-504.
96. Ebermann I, Phillips JB, Liebau MC, et al. PDZD7 is a modifier of retinal disease and a contributor to digenic Usher syndrome. J Clin Invest 2010;120:1812-23.
97. Khanna H, Davis EE, Murga-Zamalloa CA, et al. A common allele in RPGRIP1L is a modifier of retinal degeneration in ciliopathies. Nat Genet 2009;41:739-45.
98. Li M, Jia C, Kazmierkiewicz KL, et al. Comprehensive analysis of gene expression in human retina and supporting tissues. Hum Mol Genet 2014;23:4001-14.
99. Markand S, Saul A, Tawfik A, et al. Mthfr as a modifier of the retinal phenotype of Crb1(rd8/rd8) mice. Exp Eye Res 2016;145:164-72.
100. Cehajic Kapetanovic J, McClements ME, Martinez-Fernandez de la Camara C, MacLaren RE. Molecular Strategies for RPGR Gene Therapy. Genes (Basel) 2019;10:674.
101. Giacalone JC, Andorf JL, Zhang Q, et al. Development of a Molecularly Stable Gene Therapy Vector for the Treatment of RPGR-Associated X-Linked Retinitis Pigmentosa. Hum Gene Ther 2019;30:967-74.
102. Talib M, van Schooneveld MJ, Thiadens AA, et al. Clinical and genetic characteristics of male patients with RPGR-associated retinal dystrophies: A Long-Term Follow-up Study. Retina 2019;39:1186-99.
103. Demirci FY, Rigatti BW, Wen G, et al. X-linked cone-rod dystrophy (locus COD1): identification of mutations in RPGR exon ORF15. Am J Hum Genet 2002;70:1049-53.
104. Ebenezer ND, Michaelides M, Jenkins SA, et al. Identification of novel RPGR ORF15 mutations in X-linked progressive cone-rod dystrophy (XLCORD) families. Invest Ophthalmol Vis Sci 2005;46:1891-8.
105. Zahid S, Khan N, Branham K, et al. Phenotypic conservation in patients with X-linked retinitis pigmentosa caused by RPGR mutations. JAMA Ophthalmol 2013;131:1016-25.
106. Thiadens AA, Phan TM, Zekveld-Vroon RC, et al. Clinical course, genetic etiology, and visual outcome in cone and cone-rod dystrophy. Ophthalmology 2012;119:819-26.
107. Thiadens AA, Soerjoesing GG, Florijn RJ, et al. Clinical course of cone dystrophy caused by mutations in the RPGR gene. Graefes Arch Clin Exp Ophthalmol 2011;249:1527-35.
108. Kurata K, Hosono K, Hayashi T, et al. X-linked Retinitis Pigmentosa in Japan: Clinical and Genetic Findings in Male Patients and Female Carriers. Int J Mol Sci 2019;20:1518.
109. Walia S, Fishman GA, Swaroop A, et al. Discordant phenotypes in fraternal twins having an identical mutation in exon ORF15 of the RPGR gene. Arch Ophthalmol 2008;126:379-84.
110. Ruddle JB, Ebenezer ND, Kearns LS, et al. RPGR ORF15 genotype and clinical variability of retinal degeneration in an Australian population. Br J Ophthalmol 2009;93:1151-4.

111. Parmeggiani F, Barbaro V, De Nadai K, et al. Identification of novel X-linked gain-of-function RPGR-ORF15 mutation in Italian family with retinitis pigmentosa and pathologic myopia. Sci Rep 2016;6:39179.
112. Koenekoop RK, Loyer M, Hand CK, et al. Novel RPGR mutations with distinct retinitis pigmentosa phenotypes in French-Canadian families. Am J Ophthalmol 2003;136:678-87.
113. Littink KW, Pott J-WR, Collin RWJ, et al. A Novel Nonsense Mutation in CEP290 Induces Exon Skipping and Leads to a Relatively Mild Retinal Phenotype. Invest Ophthalmol Vis Sci 2010;51:3646-52.
114. Walia S, Fishman GA, Jacobson SG, et al. Visual acuity in patients with Leber's congenital amaurosis and early childhood-onset retinitis pigmentosa. Ophthalmology 2010;117:1190-8.
115. Riddell N, Faou P, Murphy M, et al. The retina/RPE proteome in chick myopia and hyperopia models: Commonalities with inherited and age-related ocular pathologies. Mol Vis 2017;23:872-88.
116. Talib M, van Schooneveld MJ, Van Cauwenbergh C, et al. The Spectrum of Structural and Functional Abnormalities in Female Carriers of Pathogenic Variants in the RPGR Gene. Invest Ophthalmol Vis Sci 2018;59:4123-33.
117. Kousal B, Skalicka P, Valesova L, et al. Severe retinal degeneration in women with a c.2543del mutation in ORF15 of the RPGR gene. Mol Vis 2014;20:1307-17.
118. Rozet JM, Perrault I, Gigarel N, et al. Dominant X linked retinitis pigmentosa is frequently accounted for by truncating mutations in exon ORF15 of the RPGR gene. J Med Genet 2002;39:284-5.
119. Al-Maskari A, O'Grady A, Pal B, McKibbin M. Phenotypic progression in X-linked retinitis pigmentosa secondary to a novel mutation in the RPGR gene. Eye (Lond) 2009;23:519-21.
120. Jacobson SG, Buraczynska M, Milam AH, et al. Disease expression in X-linked retinitis pigmentosa caused by a putative null mutation in the RPGR gene. Invest Ophthalmol Vis Sci 1997;38:1983-97.
121. Birtel J, Gliem M, Mangold E, et al. Next-generation sequencing identifies unexpected genotype-phenotype correlations in patients with retinitis pigmentosa. PLoS One 2018;13:e0207958.
122. Lyon MF. X-chromosome inactivation and human genetic disease. Acta Paediatr Suppl 2002;91:107-12.
123. Plenge RM, Hendrich BD, Schwartz C, et al. A promoter mutation in the XIST gene in two unrelated families with skewed X-chromosome inactivation. Nat Genet 1997;17:353-6.
124. Plenge RM, Tranebjaerg L, Jensen PK, et al. Evidence that mutations in the X-linked DDP gene cause incompletely penetrant and variable skewed X inactivation. Am J Hum Genet 1999;64:759-67.
125. Syed R, Sundquist SM, Ratnam K, et al. High-resolution images of retinal structure in patients with choroideremia. Invest Ophthalmol Vis Sci 2013;54:950-61.
126. Andreasson S, Breuer DK, Eksandh L, et al. Clinical studies of X-linked retinitis pigmentosa in three Swedish families with newly identified mutations in the RP2 and RPGR-ORF15 genes. Ophthalmic Genet 2003;24:215-23.
127. Yang L, Yin X, Feng L, et al. Novel mutations of RPGR in Chinese retinitis pigmentosa patients and the genotype-phenotype correlation. PLoS One 2014;9:e85752.
128. Fahim AT, Bowne SJ, Sullivan LS, et al. Allelic heterogeneity and genetic modifier loci contribute to clinical variation in males with X-linked retinitis pigmentosa due to RPGR mutations. PLoS One 2011;6:e23021.
129. Comander J, Weigel-DiFranco C, Sandberg MA, Berson EL. Visual Function in Carriers of X-Linked Retinitis Pigmentosa. Ophthalmology 2015;122:1899-906.

130. Tolmachova T, Anders R, Abrink M, et al. Independent degeneration of photoreceptors and retinal pigment epithelium in conditional knockout mouse models of choroideremia. J Clin Invest 2006;116:386-94.
131. Xue K, Jolly JK, Barnard AR, et al. Beneficial effects on vision in patients undergoing retinal gene therapy for choroideremia. Nat Med 2018;24:1507-12.
132. Dimopoulos IS, Hoang SC, Radziwon A, et al. Two-Year Results After AAV2-Mediated Gene Therapy for Choroideremia: The Alberta Experience. Am J Ophthalmol 2018;193:130-42.
133. Fischer MD, Ochakovski GA, Beier B, et al. Changes in retinal sensitivity after gene therapy in choroideremia. Retina 2020;40:160-168.
134. van Schuppen SM, Talib M, Bergen AA, et al. Long-term follow-up of patients with choroideremia with scleral pits and tunnels as a novel observation. Retina 2018;38:1713-24.
135. Hariri AH, Velaga SB, Girach A, et al. Measurement and Reproducibility of Preserved Ellipsoid Zone Area and Preserved Retinal Pigment Epithelium Area in Eyes With Choroideremia. Am J Ophthalmol 2017;179:110-7.
136. Hariri AH, Ip MS, Girach A, et al. Macular spatial distribution of preserved autofluorescence in patients with choroideremia. Br J Ophthalmol 2019;103:933-7.
137. Jolly JK, Xue K, Edwards TL, et al. Characterizing the Natural History of Visual Function in Choroideremia Using Microperimetry and Multimodal Retinal Imaging. Invest Ophthalmol Vis Sci 2017;58:5575-83.
138. Westeneng-van Haaften SC, Boon CJ, Cremers FP, et al. Clinical and genetic characteristics of late-onset Stargardt's disease. Ophthalmology 2012;119:1199-210.
139. Bax NM, Valkenburg D, Lambertus S, et al. Foveal Sparing in Central Retinal Dystrophies. Invest Ophthalmol Vis Sci 2019;60:3456-67.
140. Bird AC, Bok D. Why the macula? Eye (Lond) 2018;32:858-62.
141. Goldberg NR, Greenberg JP, Laud K, et al. Outer retinal tubulation in degenerative retinal disorders. Retina 2013;33:1871-6.
142. Aleman TS, Han G, Serrano LW, et al. Natural History of the Central Structural Abnormalities in Choroideremia: A Prospective Cross-Sectional Study. Ophthalmology 2017;124:359-73.
143. Sun LW, Johnson RD, Williams V, et al. Multimodal Imaging of Photoreceptor Structure in Choroideremia. PLoS One 2016;11:e0167526.
144. Xue K, Oldani M, Jolly JK, et al. Correlation of Optical Coherence Tomography and Autofluorescence in the Outer Retina and Choroid of Patients With Choroideremia. Invest Ophthalmol Vis Sci 2016;57:3674-84.
145. Charng J, Cideciyan AV, Jacobson SG, et al. Variegated yet Non-Random Rod and Cone Photoreceptor Disease Patterns in RPGR-ORF15-associated Retinal Degeneration. Hum Mol Genet 2016;25:5444-59.
146. Jain N, Jia Y, Gao SS, et al. Optical Coherence Tomography Angiography in Choroideremia: Correlating Choriocapillaris Loss With Overlying Degeneration. JAMA Ophthalmol 2016;134:697-702.
147. Tuten WS, Vergilio GK, Young GJ, et al. Visual Function at the Atrophic Border in Choroideremia Assessed with Adaptive Optics Microperimetry. Ophthalmol Retina 2019;3:888-99.
148. Zweifel SA, Engelbert M, Laud K, et al. Outer retinal tubulation: a novel optical coherence tomography finding. Arch Ophthalmol 2009;127:1596-602.
149. Zinkernagel MS, Groppe M, MacLaren RE. Macular hole surgery in patients with end-stage choroideremia. Ophthalmology 2013;120:1592-6.

150. Talib M, Koetsier LS, MacLaren RE, Boon CJF. Outcome of Full-Thickness Macular Hole Surgery in Choroideremia. Genes (Basel) 2017;8:187.
151. Heon E, Alabduljalil T, Iii DB, et al. Visual Function and Central Retinal Structure in Choroideremia. Invest Ophthalmol Vis Sci 2016;57:377-87.
152. Thompson DA, Li Y, McHenry CL, et al. Mutations in the gene encoding lecithin retinol acyltransferase are associated with early-onset severe retinal dystrophy. Nat Genet 2001;28:123-4.
153. Senechal A, Humbert G, Surget MO, et al. Screening genes of the retinoid metabolism: novel LRAT mutation in leber congenital amaurosis. Am J Ophthalmol 2006;142:702-4.
154. Vallespin E, Cantalapiedra D, Riveiro-Alvarez R, et al. Mutation screening of 299 Spanish families with retinal dystrophies by Leber congenital amaurosis genotyping microarray. Invest Ophthalmol Vis Sci 2007;48:5653-61.
155. Littink KW, van Genderen MM, van Schooneveld MJ, et al. A homozygous frameshift mutation in LRAT causes retinitis punctata albescens. Ophthalmology 2012;119:1899-906.
156. Dev Borman A, Ocaka LA, Mackay DS, et al. Early onset retinal dystrophy due to mutations in LRAT: molecular analysis and detailed phenotypic study. Invest Ophthalmol Vis Sci 2012;53:3927-38.
157. Talib M, van Schooneveld MJ, van Duuren RJG, et al. Long-Term Follow-Up of Retinal Degenerations Associated With LRAT Mutations and Their Comparability to Phenotypes Associated With RPE65 Mutations. Transl Vis Sci Technol 2019;8:24.
158. Koenekoop RK, Sui R, Sallum J, et al. Oral 9-cis retinoid for childhood blindness due to Leber congenital amaurosis caused by RPE65 or LRAT mutations: an open-label phase 1b trial. Lancet 2014;384:1513-20.
159. Scholl HP, Moore AT, Koenekoop RK, et al. Safety and Proof-of-Concept Study of Oral QLT091001 in Retinitis Pigmentosa Due to Inherited Deficiencies of Retinal Pigment Epithelial 65 Protein (RPE65) or Lecithin:Retinol Acyltransferase (LRAT). PLoS One 2015;10:e0143846.
160. Ferrari S, Di Iorio E, Barbaro V, et al. Retinitis pigmentosa: genes and disease mechanisms. Curr Genomics 2011;12:238-49.
161. Cideciyan AV, Sudharsan R, Dufour VL, et al. Mutation-independent rhodopsin gene therapy by knockdown and replacement with a single AAV vector. Proc Natl Acad Sci U S A 2018;115:E8547-e56.
162. Tsai YT, Wu WH, Lee TT, et al. Clustered Regularly Interspaced Short Palindromic Repeats-Based Genome Surgery for the Treatment of Autosomal Dominant Retinitis Pigmentosa. Ophthalmology 2018;125:1421-30.
163. Murray SF, Jazayeri A, Matthes MT, et al. Allele-Specific Inhibition of Rhodopsin With an Antisense Oligonucleotide Slows Photoreceptor Cell Degeneration. Invest Ophthalmol Vis Sci 2015;56:6362-75.
164. Mao H, James T, Jr., Schwein A, et al. AAV delivery of wild-type rhodopsin preserves retinal function in a mouse model of autosomal dominant retinitis pigmentosa. Hum Gene Ther 2011;22:567-75.
165. Ramon E, Cordomi A, Aguila M, et al. Differential light-induced responses in sectorial inherited retinal degeneration. J Biol Chem 2014;289:35918-28.
166. Sumaroka A, Cideciyan AV, Charng J, et al. Autosomal Dominant Retinitis Pigmentosa Due to Class B Rhodopsin Mutations: An Objective Outcome for Future Treatment Trials. Int J Mol Sci 2019;20:5344.
167. Wang J, Xu D, Zhu T, et al. Identification of two novel RHO mutations in Chinese retinitis pigmentosa patients. Exp Eye Res 2019;188:107726.

168. Roshandel D, Rafati M, Khorami S, et al. Rhodopsin gene mutation analysis in Iranian patients with autosomal dominant retinitis pigmentosa. Int Ophthalmol 2019;39:2523-31.
169. Coussa RG, Basali D, Maeda A, et al. Sector retinitis pigmentosa: Report of ten cases and a review of the literature. Mol Vis 2019;25:869-89.
170. Jacobson SG, McGuigan DB, 3rd, Sumaroka A, et al. Complexity of the Class B Phenotype in Autosomal Dominant Retinitis Pigmentosa Due to Rhodopsin Mutations. Invest Ophthalmol Vis Sci 2016;57:4847-58.
171. Cideciyan AV, Hood DC, Huang Y, et al. Disease sequence from mutant rhodopsin allele to rod and cone photoreceptor degeneration in man. Proc Natl Acad Sci U S A 1998;95:7103-8.
172. Paskowitz DM, LaVail MM, Duncan JL. Light and inherited retinal degeneration. Br J Ophthalmol 2006;90:1060-6.
173. Athanasiou D, Aguila M, Bellingham J, et al. The molecular and cellular basis of rhodopsin retinitis pigmentosa reveals potential strategies for therapy. Prog Retin Eye Res 2018;62:1-23.
174. Naash ML, Peachey NS, Li ZY, et al. Light-induced acceleration of photoreceptor degeneration in transgenic mice expressing mutant rhodopsin. Invest Ophthalmol Vis Sci 1996;37:775-82.
175. Organisciak DT, Darrow RM, Barsalou L, et al. Susceptibility to retinal light damage in transgenic rats with rhodopsin mutations. Invest Ophthalmol Vis Sci 2003;44:486-92.
176. Iwabe S, Ying GS, Aguirre GD, Beltran WA. Assessment of visual function and retinal structure following acute light exposure in the light sensitive T4R rhodopsin mutant dog. Exp Eye Res 2016;146:341-53.
177. Orlans HO, Merrill J, Barnard AR, et al. Filtration of Short-Wavelength Light Provides Therapeutic Benefit in Retinitis Pigmentosa Caused by a Common Rhodopsin Mutation. Invest Ophthalmol Vis Sci 2019;60:2733-42.
178. Dryja TP, McGee TL, Reichel E, et al. A point mutation of the rhodopsin gene in one form of retinitis pigmentosa. Nature 1990;343:364-6.
179. Oh KT, Oh DM, Weleber RG, et al. Genotype-phenotype correlation in a family with Arg135Leu rhodopsin retinitis pigmentosa. Br J Ophthalmol 2004;88:1533-7.
180. Shah SP, Wong F, Sharp DM, Vincent AL. A novel rhodopsin point mutation, proline-170-histidine, associated with sectoral retinitis pigmentosa. Ophthalmic Genet 2014;35:241-7.
181. Napier ML, Durga D, Wolsley CJ, et al. Mutational Analysis of the Rhodopsin Gene in Sector Retinitis Pigmentosa. Ophthalmic Genet 2015;36:239-43.
182. Abdulridha-Aboud W, Kjellstrom U, Andreasson S, Ponjavic V. Characterization of macular structure and function in two Swedish families with genetically identified autosomal dominant retinitis pigmentosa. Mol Vis 2016;22:362-73.
183. Reiff C, Owczarek-Lipska M, Spital G, et al. The mutation p.E113K in the Schiff base counterion of rhodopsin is associated with two distinct retinal phenotypes within the same family. Sci Rep 2016;6:36208.
184. Miyadera K, Kato K, Boursnell M, et al. Genome-wide association study in RPGRIP1(-/-) dogs identifies a modifier locus that determines the onset of retinal degeneration. Mamm Genome 2012;23:212-23.
185. Zernant J, Külm M, Dharmaraj S, et al. Genotyping Microarray (Disease Chip) for Leber Congenital Amaurosis: Detection of Modifier Alleles. Invest Ophthalmol Vis Sci 2005;46:3052-9.

186. de Castro-Miro M, Tonda R, Escudero-Ferruz P, et al. Novel Candidate Genes and a Wide Spectrum of Structural and Point Mutations Responsible for Inherited Retinal Dystrophies Revealed by Exome Sequencing. PLoS One 2016;11:e0168966.
187. Silva E, Dharmaraj S, Li YY, et al. A missense mutation in GUCY2D acts as a genetic modifier in RPE65-related Leber Congenital Amaurosis. Ophthalmic Genet 2004;25:205-17.
188. Poloschek CM, Bach M, Lagreze WA, et al. ABCA4 and ROM1: implications for modification of the PRPH2-associated macular dystrophy phenotype. Invest Ophthalmol Vis Sci 2010;51:4253-65.
189. Lee W, Paavo M, Zernant J, et al. Modification of the PROM1 disease phenotype by a mutation in ABCA4. Ophthalmic Genet 2019;40:369-75.
190. Rose AM, Shah AZ, Venturini G, et al. Transcriptional regulation of PRPF31 gene expression by MSR1 repeat elements causes incomplete penetrance in retinitis pigmentosa. Sci Rep 2016;6:19450.
191. Audo I, Bujakowska K, Mohand-Said S, et al. Prevalence and novelty of PRPF31 mutations in French autosomal dominant rod-cone dystrophy patients and a review of published reports. BMC Med Genet 2010;11:145.
192. Venturini G, Rose AM, Shah AZ, et al. CNOT3 is a modifier of PRPF31 mutations in retinitis pigmentosa with incomplete penetrance. PLoS Genet 2012;8:e1003040.
193. Cruz NM, Yuan Y, Leehy BD, et al. Modifier genes as therapeutics: the nuclear hormone receptor Rev Erb alpha (Nr1d1) rescues Nr2e3 associated retinal disease. PLoS One 2014;9:e87942.
194. Alves CH, Boon N, Mulder AA, et al. CRB2 Loss in Rod Photoreceptors Is Associated with Progressive Loss of Retinal Contrast Sensitivity. Int J Mol Sci 2019;20:4069.
195. Pellissier LP, Lundvig DM, Tanimoto N, et al. CRB2 acts as a modifying factor of CRB1-related retinal dystrophies in mice. Hum Mol Genet 2014;23:3759-71.
196. Liu YP, Bosch DG, Siemiatkowska AM, et al. Putative digenic inheritance of heterozygous RP1L1 and C2orf71 null mutations in syndromic retinal dystrophy. Ophthalmic Genet 2017;38:127-32.
197. Dryja TP, Hahn LB, Kajiwara K, Berson EL. Dominant and digenic mutations in the peripherin/RDS and ROM1 genes in retinitis pigmentosa. Invest Ophthalmol Vis Sci 1997;38:1972-82.
198. Kariminejad A, Bozorgmehr B, Najafi A, et al. Retinitis pigmentosa, cutis laxa, and pseudoxanthoma elasticum-like skin manifestations associated with GGCX mutations. J Invest Dermatol 2014;134:2331-8.
199. Ho AC, Humayun MS, Dorn JD, et al. Long-Term Results from an Epiretinal Prosthesis to Restore Sight to the Blind. Ophthalmology 2015;122:1547-54.
200. Edwards TL, Cottriall CL, Xue K, et al. Assessment of the Electronic Retinal Implant Alpha AMS in Restoring Vision to Blind Patients with End-Stage Retinitis Pigmentosa. Ophthalmology 2018;125:432-43.
201. Stronks HC, Dagnelie G. The functional performance of the Argus II retinal prosthesis. Expert Rev Med Devices 2014;11:23-30.
202. Ahuja AK, Behrend MR. The Argus II retinal prosthesis: factors affecting patient selection for implantation. Prog Retin Eye Res 2013;36:1-23.
203. da Cruz L, Coley BF, Dorn J, et al. The Argus II epiretinal prosthesis system allows letter and word reading and long-term function in patients with profound vision loss. Br J Ophthalmol 2013;97:632-6.
204. Farvardin M, Afarid M, Attarzadeh A, et al. The Argus-II Retinal Prosthesis Implantation; From the Global to Local Successful Experience. Front Neurosci 2018;12:584.

205. Veritti D, Sarao V, De Nadai K, et al. Dexamethasone Implant Produces Better Outcomes than Oral Acetazolamide in Patients with Cystoid Macular Edema Secondary to Retinitis Pigmentosa. J Ocul Pharmacol Ther 2020;36:190-7.
206. Huang Q, Chen R, Lin X, Xiang Z. Efficacy of carbonic anhydrase inhibitors in management of cystoid macular edema in retinitis pigmentosa: A meta-analysis. PLoS One 2017;12:e0186180.
207. Cox SN, Hay E, Bird AC. Treatment of chronic macular edema with acetazolamide. Arch Ophthalmol 1988;106:1190-5.
208. Genead MA, Fishman GA. Efficacy of sustained topical dorzolamide therapy for cystic macular lesions in patients with retinitis pigmentosa and usher syndrome. Arch Ophthalmol 2010;128:1146-50.
209. Ikeda Y, Hisatomi T, Yoshida N, et al. The clinical efficacy of a topical dorzolamide in the management of cystoid macular edema in patients with retinitis pigmentosa. Graefes Arch Clin Exp Ophthalmol 2012;250:809-14.
210. Liew G, Moore AT, Webster AR, Michaelides M. Efficacy and prognostic factors of response to carbonic anhydrase inhibitors in management of cystoid macular edema in retinitis pigmentosa. Invest Ophthalmol Vis Sci 2015;56:1531-6.
211. Strong SA, Hirji N, Quartilho A, et al. Retrospective cohort study exploring whether an association exists between spatial distribution of cystoid spaces in cystoid macular oedema secondary to retinitis pigmentosa and response to treatment with carbonic anhydrase inhibitors. Br J Ophthalmol 2019;103:233-7.
212. Srour M, Querques G, Leveziel N, et al. Intravitreal dexamethasone implant (Ozurdex) for macular edema secondary to retinitis pigmentosa. Graefes Arch Clin Exp Ophthalmol 2013;251:1501-6.
213. Ozdemir H, Karacorlu M, Karacorlu S. Intravitreal triamcinolone acetonide for treatment of cystoid macular oedema in patients with retinitis pigmentosa. Acta Ophthalmol Scand 2005;83:248-51.
214. Scorolli L, Morara M, Meduri A, et al. Treatment of cystoid macular edema in retinitis pigmentosa with intravitreal triamcinolone. Arch Ophthalmol 2007;125:759-64.
215. Yuzbasioglu E, Artunay O, Rasier R, et al. Intravitreal bevacizumab (Avastin) injection in retinitis pigmentosa. Curr Eye Res 2009;34:231-7.
216. Artunay O, Yuzbasioglu E, Rasier R, et al. Intravitreal ranibizumab in the treatment of cystoid macular edema associated with retinitis pigmentosa. J Ocul Pharmacol Ther 2009;25:545-50.
217. Melo GB, Farah ME, Aggio FB. Intravitreal injection of bevacizumab for cystoid macular edema in retinitis pigmentosa. Acta Ophthalmol Scand 2007;85:461-3.
218. Ediriwickrema LS, Chhadva P, Rodger DC, et al. Intravenous immunoglobulin in the treatment of juvenile retinitis pigmentosa-associated cystoid macular edema and uveitis. Retin Cases Brief Rep 2018;12:242-6.
219. Missotten T, van Laar JA, van der Loos TL, et al. Octreotide long-acting repeatable for the treatment of chronic macular edema in uveitis. Am J Ophthalmol 2007;144:838-43.
220. Hogewind BF, Pieters G, Hoyng CB. Octreotide acetate in dominant cystoid macular dystrophy. Eur J Ophthalmol 2008;18:99-103.
221. Shah SM, Nguyen QD, Mir HS, et al. A randomized, double-masked controlled clinical trial of Sandostatin long-acting release depot in patients with postsurgical cystoid macular edema. Retina 2010;30:160-6.
222. Sarao V, Veritti D, Prosperi R, et al. A case of CRB1-negative Coats-like retinitis pigmentosa. J aapos 2013;17:414-6.

223. Kan E, Yilmaz T, Aydemir O, et al. Coats-like retinitis pigmentosa: Reports of three cases. Clin Ophthalmol 2007;1:193-8.
224. Lee SY, Yoon YH. Pars plana vitrectomy for exuduative retinal detachment in coats-type retinitis pigmentosa. Retina 2004;24:450-2.
225. Chu X, Du W, Xu M, et al. Intravitreal conbercept combined with laser photocoagulation for exudative retinal detachment in a patient with Coats-like retinitis pigmentosa. Ophthalmic Genet 2019;40:1-3.
226. MacLaren RE, Bennett J, Schwartz SD. Gene Therapy and Stem Cell Transplantation in Retinal Disease: The New Frontier. Ophthalmology 2016;123:S98-s106.
227. Xue K, Groppe M, Salvetti AP, MacLaren RE. Technique of retinal gene therapy: delivery of viral vector into the subretinal space. Eye (Lond) 2017;31:1308-16.
228. Nanda A, Salvetti AP, Clouston P, et al. Exploring the Variable Phenotypes of RPGR Carrier Females in Assessing their Potential for Retinal Gene Therapy. Genes (Basel) 2018;9:643.
229. Dalkara D, Byrne LC, Klimczak RR, et al. In vivo-directed evolution of a new adeno-associated virus for therapeutic outer retinal gene delivery from the vitreous. Sci Transl Med 2013;5:189ra76.
230. Reichel FF, Peters T, Wilhelm B, et al. Humoral Immune Response After Intravitreal But Not After Subretinal AAV8 in Primates and Patients. Invest Ophthalmol Vis Sci 2018;59:1910-5.
231. Seitz IP, Michalakis S, Wilhelm B, et al. Superior Retinal Gene Transfer and Biodistribution Profile of Subretinal Versus Intravitreal Delivery of AAV8 in Nonhuman Primates. Invest Ophthalmol Vis Sci 2017;58:5792-801.
232. Dias MS, Araujo VG, Vasconcelos T, et al. Retina transduction by rAAV2 after intravitreal injection: comparison between mouse and rat. Gene Ther 2019;26:479-90.
233. Tang Z, Zhang Y, Wang Y, et al. Progress of stem/progenitor cell-based therapy for retinal degeneration. J Transl Med 2017;15:99.
234. Schwartz SD, Regillo CD, Lam BL, et al. Human embryonic stem cell-derived retinal pigment epithelium in patients with age-related macular degeneration and Stargardt's macular dystrophy: follow-up of two open-label phase 1/2 studies. Lancet 2015;385:509-16.
235. Burnight ER, Gupta M, Wiley LA, et al. Using CRISPR-Cas9 to Generate Gene-Corrected Autologous iPSCs for the Treatment of Inherited Retinal Degeneration. Mol Ther 2017;25:1999-2013.
236. Kamao H, Mandai M, Ohashi W, et al. Evaluation of the Surgical Device and Procedure for Extracellular Matrix-Scaffold-Supported Human iPSC-Derived Retinal Pigment Epithelium Cell Sheet Transplantation. Invest Ophthalmol Vis Sci 2017;58:211-20.
237. Galloway CA, Dalvi S, Shadforth AMA, et al. Characterization of Human iPSC-RPE on a Prosthetic Bruch's Membrane Manufactured From Silk Fibroin. Invest Ophthalmol Vis Sci 2018;59:2792-800.
238. Singh MS, Park SS, Albini TA, et al. Retinal stem cell transplantation: Balancing safety and potential. Prog Retin Eye Res 2019;75:100779.
239. Bellingrath JS, Ochakovski GA, Seitz IP, et al. High Symmetry of Visual Acuity and Visual Fields in RPGR-Linked Retinitis Pigmentosa. Invest Ophthalmol Vis Sci 2017;58:4457-66.
240. Tee JJL, Yang Y, Kalitzeos A, et al. Natural History Study of Retinal Structure, Progression, and Symmetry Using Ellipzoid Zone Metrics in RPGR-Associated Retinopathy. Am J Ophthalmol 2019;198:111-23.

241. Tee JJL, Yang Y, Kalitzeos A, et al. Characterization of Visual Function, Interocular Variability and Progression Using Static Perimetry-Derived Metrics in RPGR-Associated Retinopathy. Invest Ophthalmol Vis Sci 2018;59:2422-36.
242. Seitz IP, Zhour A, Kohl S, et al. Multimodal assessment of choroideremia patients defines pre-treatment characteristics. Graefes Arch Clin Exp Ophthalmol 2015;253:2143-50.
243. Tee JJL, Carroll J, Webster AR, Michaelides M. Quantitative Analysis of Retinal Structure Using Spectral-Domain Optical Coherence Tomography in RPGR-Associated Retinopathy. Am J Ophthalmol 2017;178:18-26.
244. Birch DG, Locke KG, Wen Y, et al. Spectral-domain optical coherence tomography measures of outer segment layer progression in patients with X-linked retinitis pigmentosa. JAMA Ophthalmol 2013;131:1143-50.
245. Sujirakul T, Lin MK, Duong J, et al. Multimodal Imaging of Central Retinal Disease Progression in a 2-Year Mean Follow-up of Retinitis Pigmentosa. Am J Ophthalmol 2015;160:786-98.e4.
246. Takahashi VKL, Takiuti JT, Carvalho-Jr JRL, et al. Fundus autofluorescence and ellipsoid zone (EZ) line width can be an outcome measurement in RHO-associated autosomal dominant retinitis pigmentosa. Graefes Arch Clin Exp Ophthalmol 2019;257:725-31.
247. Csaky K, Ferris F, 3rd, Chew EY, et al. Report From the NEI/FDA Endpoints Workshop on Age-Related Macular Degeneration and Inherited Retinal Diseases. Invest Ophthalmol Vis Sci 2017;58:3456-63.
248. Roman AJ, Cideciyan AV, Aleman TS, Jacobson SG. Full-field stimulus testing (FST) to quantify visual perception in severely blind candidates for treatment trials. Physiol Meas 2007;28:N51-6.
249. Collison FT, Fishman GA, McAnany JJ, et al. Psychophysical measurement of rod and cone thresholds in stargardt disease with full-field stimuli. Retina 2014;34:1888-95.
250. Chung DC, McCague S, Yu ZF, et al. Novel mobility test to assess functional vision in patients with inherited retinal dystrophies. Clin Exp Ophthalmol 2018;46:247-59.
251. Lombardi M, Zenouda A, Azoulay-Sebban L, et al. Correlation Between Visual Function and Performance of Simulated Daily Living Activities in Glaucomatous Patients. J Glaucoma 2018;27:1017-24.
252. Lamoureux EL, Pallant JF, Pesudovs K, et al. The Impact of Vision Impairment Questionnaire: an evaluation of its measurement properties using Rasch analysis. Invest Ophthalmol Vis Sci 2006;47:4732-41.
253. Dagnelie G, Christopher P, Arditi A, et al. Performance of real-world functional vision tasks by blind subjects improves after implantation with the Argus(R) II retinal prosthesis system. Clin Exp Ophthalmol 2017;45:152-9.
254. Stingl K, Schippert R, Bartz-Schmidt KU, et al. Interim Results of a Multicenter Trial with the New Electronic Subretinal Implant Alpha AMS in 15 Patients Blind from Inherited Retinal Degenerations. Front Neurosci 2017;11:445.
255. Cideciyan AV, Sudharsan R, Dufour VL, et al. Mutation-independent rhodopsin gene therapy by knockdown and replacement with a single AAV vector. Proc Natl Acad Sci USA 2018;115:E8547-E56.
256. Ziccardi L, Cordeddu V, Gaddini L, et al. Gene Therapy in Retinal Dystrophies. Int J Mol Sci 2019;20:5722.
257. Hareendran S, Balakrishnan B, Sen D, et al. Adeno-associated virus (AAV) vectors in gene therapy: immune challenges and strategies to circumvent them. Rev Med Virol 2013;23:399-413.
258. Daya S, Berns KI. Gene therapy using adeno-associated virus vectors. Clin Microbiol Rev 2008;21:583-93.
259. Day TP, Byrne LC, Schaffer DV, Flannery JG. Advances in AAV vector development for gene therapy in the retina. Adv Exp Med Biol 2014;801:687-93.

260. Kumar M, Keller B, Makalou N, Sutton RE. Systematic Determination of the Packaging Limit of Lentiviral Vectors. Human Gene Therapy 2001;12:1893-905.
261. Sakuma T, Barry MA, Ikeda Y. Lentiviral vectors: basic to translational. Biochem J 2012;443:603-18.
262. Conley SM, Cai X, Naash MI. Nonviral ocular gene therapy: assessment and future directions. Curr Opin Mol Ther 2008;10:456-63.
263. Peeters L, Sanders NN, Braeckmans K, et al. Vitreous: a barrier to nonviral ocular gene therapy. Invest Ophthalmol Vis Sci 2005;46:3553-61.
264. Liang Y, Fotiadis D, Maeda T, et al. Rhodopsin signaling and organization in heterozygote rhodopsin knockout mice. J Biol Chem 2004;279:48189-96.
265. Farrar GJ, Kenna PF, Humphries P. On the genetics of retinitis pigmentosa and on mutation-independent approaches to therapeutic intervention. Embo j 2002;21:857-64.
266. O'Neill B, Millington-Ward S, O'Reilly M, et al. Ribozyme-based therapeutic approaches for autosomal dominant retinitis pigmentosa. Invest Ophthalmol Vis Sci 2000;41:2863-9.
267. Gorbatyuk M, Justilien V, Liu J, et al. Preservation of photoreceptor morphology and function in P23H rats using an allele independent ribozyme. Exp Eye Res 2007;84:44-52.
268. Kiang AS, Palfi A, Ader M, et al. Toward a gene therapy for dominant disease: validation of an RNA interference-based mutation-independent approach. Mol Ther 2005;12:555-61.
269. Kurz D, Ciulla TA. Novel approaches for retinal drug delivery. Ophthalmol Clin North Am 2002;15:405-10.
270. Garanto A, Chung DC, Duijkers L, et al. In vitro and in vivo rescue of aberrant splicing in CEP290-associated LCA by antisense oligonucleotide delivery. Hum Mol Genet 2016;25:2552-63.
271. Rowe-Rendleman CL, Durazo SA, Kompella UB, et al. Drug and gene delivery to the back of the eye: from bench to bedside. Invest Ophthalmol Vis Sci 2014;55:2714-30.
272. Suzuki K, Tsunekawa Y, Hernandez-Benitez R, et al. In vivo genome editing via CRISPR/Cas9 mediated homology-independent targeted integration. Nature 2016;540:144-9.
273. Cong L, Ran FA, Cox D, et al. Multiplex genome engineering using CRISPR/Cas systems. Science 2013;339:819-23.
274. Vagni P, Perlini LE, Chenais NAL, et al. Gene Editing Preserves Visual Functions in a Mouse Model of Retinal Degeneration. Front Neurosci 2019;13:945.
275. Maeder ML, Stefanidakis M, Wilson CJ, et al. Development of a gene-editing approach to restore vision loss in Leber congenital amaurosis type 10. Nat Med 2019;25:229-33.
276. Latella MC, Di Salvo MT, Cocchiarella F, et al. In vivo Editing of the Human Mutant Rhodopsin Gene by Electroporation of Plasmid-based CRISPR/Cas9 in the Mouse Retina. Mol Ther Nucleic Acids 2016;5:e389.
277. Zhong H, Chen Y, Li Y, et al. CRISPR-engineered mosaicism rapidly reveals that loss of Kcnj13 function in mice mimics human disease phenotypes. Sci Rep 2015;5:8366.
278. Arno G, Agrawal SA, Eblimit A, et al. Mutations in REEP6 Cause Autosomal-Recessive Retinitis Pigmentosa. Am J Hum Genet 2016;99:1305-15.
279. Fu Y, Foden JA, Khayter C, et al. High-frequency off-target mutagenesis induced by CRISPR-Cas nucleases in human cells. Nat Biotechnol 2013;31:822-6.
280. Bassuk AG, Zheng A, Li Y, et al. Precision Medicine: Genetic Repair of Retinitis Pigmentosa in Patient-Derived Stem Cells. Sci Rep 2016;6:19969.

281. Yang L, Guell M, Byrne S, et al. Optimization of scarless human stem cell genome editing. Nucleic Acids Res 2013;41:9049-61.
282. Anzalone AV, Randolph PB, Davis JR, et al. Search-and-replace genome editing without double-strand breaks or donor DNA. Nature 2019;576:149-57.
283. Lund RD, Wang S, Klimanskaya I, et al. Human embryonic stem cell-derived cells rescue visual function in dystrophic RCS rats. Cloning Stem Cells 2006;8:189-99.
284. Lu B, Malcuit C, Wang S, et al. Long-term safety and function of RPE from human embryonic stem cells in preclinical models of macular degeneration. Stem Cells 2009;27:2126-35.
285. Carr AJ, Vugler AA, Hikita ST, et al. Protective effects of human iPS-derived retinal pigment epithelium cell transplantation in the retinal dystrophic rat. PLoS One 2009;4:e8152.
286. Li Y, Tsai YT, Hsu CW, et al. Long-term safety and efficacy of human-induced pluripotent stem cell (iPS) grafts in a preclinical model of retinitis pigmentosa. Mol Med 2012;18:1312-9.
287. Zhao T, Zhang ZN, Rong Z, Xu Y. Immunogenicity of induced pluripotent stem cells. Nature 2011;474:212-5.
288. Pera MF. Stem cells: The dark side of induced pluripotency. Nature 2011;471:46-7.
289. Quinn PM, Buck TM, Ohonin C, et al. Production of iPS-Derived Human Retinal Organoids for Use in Transgene Expression Assays. Methods Mol Biol 2018;1715:261-73.
290. Scruggs BA, Jiao C, Cranston CM, et al. Optimizing Donor Cellular Dissociation and Subretinal Injection Parameters for Stem Cell-Based Treatments. Stem Cells Transl Med 2019;8:797-809.
291. Kuriyan AE, Albini TA, Townsend JH, et al. Vision Loss after Intravitreal Injection of Autologous "Stem Cells" for AMD. N Engl J Med 2017;376:1047-53.
292. Satarian L, Nourinia R, Safi S, et al. Intravitreal Injection of Bone Marrow Mesenchymal Stem Cells in Patients with Advanced Retinitis Pigmentosa; a Safety Study. J Ophthalmic Vis Res 2017;12:58-64.
293. Simunovic MP, Shen W, Lin JY, et al. Optogenetic approaches to vision restoration. Exp Eye Res 2019;178:15-26.
294. Busskamp V, Picaud S, Sahel JA, Roska B. Optogenetic therapy for retinitis pigmentosa. Gene Ther 2012;19:169-75.
295. Antoniu S. Fresh from the designation pipeline: orphan drugs recently designated in the European Union (September – November 2013). Expert Opinion on Orphan Drugs 2014;2:311-5.
296. Julien S, Schraermeyer U. Lipofuscin can be eliminated from the retinal pigment epithelium of monkeys. Neurobiol Aging 2012;33:2390-7.
297. Kaufman Y, Ma L, Washington I. Deuterium enrichment of vitamin A at the C20 position slows the formation of detrimental vitamin A dimers in wild-type rodents. J Biol Chem 2011;286:7958-65.
298. Radu RA, Yuan Q, Hu J, et al. Accelerated accumulation of lipofuscin pigments in the RPE of a mouse model for ABCA4-mediated retinal dystrophies following Vitamin A supplementation. Invest Ophthalmol Vis Sci 2008;49:3821-9.
299. Berson EL, Weigel-DiFranco C, Rosner B, et al. Association of Vitamin A Supplementation With Disease Course in Children With Retinitis Pigmentosa. JAMA Ophthalmol 2018;136:490-5.
300. Lee SY, Usui S, Zafar AB, et al. N-Acetylcysteine promotes long-term survival of cones in a model of retinitis pigmentosa. J Cell Physiol 2011;226:1843-9.
301. Campochiaro PA, Iftikhar M, Hafiz G, et al. Oral N-acetylcysteine improves cone function in retinitis pigmentosa patients in phase I trial. J Clin Invest 2020;130:1527-41.

302. Gardiner KL, Cideciyan AV, Swider M, et al. Long-Term Structural Outcomes of Late-Stage RPE65 Gene Therapy. Mol Ther 2020;28:266-78.
303. Darrow JJ. Luxturna: FDA documents reveal the value of a costly gene therapy. Drug Discov Today 2019;24:949-54.
304. Cehajic Kapetanovic J, Patricio MI, MacLaren RE. Progress in the development of novel therapies for choroideremia. Expert Rev Ophthalmol 2019;14:277-85.
305. Fischer MD, Ochakovski GA, Beier B, et al. Changes in retinal sensitivity after gene therapy in choroideremia. Retina 2020;40:160-8.

8.

8.1 English summary

8.2 Dutch summary

8.3 Acknowledgments

8.4 Curriculum vitae

8.5 List of publications

8.1

ENGLISH SUMMARY

Retinal dystrophies comprise relatively rare but devastating causes of progressive vision loss. They represent a spectrum of diseases with marked genetic and clinical heterogeneity. Mutations in the same gene may lead to different diagnoses, e.g. retinitis pigmentosa or cone dystrophy. Conversely, mutations in different genes may lead to the same phenotype. The age at symptom onset, as well as the rate and characteristics of vision decline, may vary widely per disease group and even within families. For most IRD cases, no effective treatment is currently available. However, preclinical studies and phase I/II/III gene therapy trials are ongoing for several IRD subtypes, and recently the first retinal gene therapy has been approved by the United States Food and Drug Administration for *RPE65*-associated IRDs: voretigene neparvovec-rzyl (Luxturna®).

Despite rapid advances in gene therapy studies, insight into the phenotypic spectrum and long-term disease course remains limited for several IRD types. The vast clinical heterogeneity presents another important challenge in the evaluation of potential efficacy in future treatment trials, and in establishing treatment candidacy criteria. This thesis responds to these challenges, aiming to provide detailed clinical descriptions of several forms of IRD that are caused by genes of interest for ongoing and future gene or cell-based therapy trials. Adequate insight into the clinical characteristics, variability, and long-term outcome of these IRDs is crucial in establishing an adequate diagnosis and in counselling the patient on the prognosis. Moreover, this knowledge is essential in the design of ongoing and future gene therapy trials.

Chapter 1 is a general introduction to the retinal anatomy and function, and the techniques commonly used to evaluate these features. It also features a description of several common subtypes of IRDs, their presentation and clinical signs, and a brief overview of several emerging experimental therapeutic options.

One of the genes of interest in the development of gene therapy is *CRB1*, which has been described in Leber congenital amaurosis (LCA), retinitis pigmentosa (RP), and macular dystrophy, and has been suggested to cause disorganization of the normal laminar structure of the retina, which may complicate gene therapy efficacy. **Chapter 2** discusses the clinical characteristics and phenotypic spectrum of *CRB1*-associated retinal dystrophies. **Chapter 2.1** presents the largest retrospective cohort of patients with *CRB1*-RD described published to date. Most patients (91%) were reported to have *CRB1*-RP, with a symptom onset at the median age of 4 years, and a subsequent mean yearly visual acuity decline rate and mean visual field decline rate of 0.03 logMAR and 5%, respectively. The median ages for reaching low vision and blindness were 18 and 44 years, respectively. Frequent characteristics were non-detectable rod and cone responses on full-field electroretinography (50%), cystoid fluid collections in the macula (50%), hyperopia (98%), vitreous abnormalities such as cells and/or veils (54%), and optic disc drusen (20%). Interestingly, the macula showed organization in identifiable retinal tissue layers on OCT in 91% of patients with available OCT scans. In patients with LCA, severe visual impairment or blindness occurred early in life, with

early degeneration of the macula. As in *CRB1*-RP, frequent characteristics were hyperopia (100%), and vitreous abnormalities such as cells and/or veils (40%). The available imaging was limited, and therefore the presence of cystoid fluid collections and the degree of retinal organization could not be evaluated in these LCA patients. Unlike in *CRB1*-RP, where 92% of patient had bone spicule-like pigmentation, in *CRB1*-LCA the pigmentary changes were limited to a granulated or "powdered" aspect of the retina. This could be due to the young *CRB1*-LCA population (age range 3-15 years at the last examination) versus the *CRB1*-RP population (age range 2-78 years at the last examination).

Chapter 2.2 reports the baseline cross-sectional results of an extensive prospective phenotyping study in Dutch patients with *CRB1*-RD. Patients had RP, cone-rod dystrophy, or an isolated macular dystrophy. SD-OCT scans were performed in nearly all patients, and showed fully discernible retinal layers in 62% of patients, with mild to moderate laminar disorganization of the retina in the remaining patients. Nanophthalmos was present in 36% of patients, and associated with a risk of acute angle-closure glaucoma. Full-field sensitivity testing provided a subjective outcome measure for retinal sensitivity in eyes with (nearly) extinguished amplitudes on the full-field electroretinogram. Using white, red, and blue light stimuli, we were able to determine the origin of the retinal response (rod, cone, or mixed response).

Chapter 2.3 describes a large Belgian cohort of patients with *CRB1*-associated IRDs, in which blindness was seen in the 1st decade of life in LCA and early-onset severe retinal dystrophy, and in the 5th decade of life in the group of RP patients. All patients with macular dystrophy carried the same mutation on at least 1 allele, confirming a genotype-phenotype correlation. Disorganization of the lamellar retinal structure was observed in 52% of patients, a higher proportion than in the Dutch cohort (described in Chapter 2.2).

The combined results from Chapter 2 indicate a window of therapeutic opportunity in the first 3 to 4 decades of life in *CRB1*-RP, but within the first years of life in *CRB1*-LCA.

Chapter 3 focuses on choroideremia, an X-linked form of rod-cone dystrophy, caused by mutations in the *CHM* gene. Choroideremia has been treated relatively successfully in phase I/II human gene therapy trials, with phase III clinical trials currently being conducted. Still, relatively few longitudinal studies have been conducted for this disease.

Chapter 3.1 evaluates the long-term clinical course and visual outcome of choroideremia patients, with a mean follow-up time of 25 years. Symptoms started at a mean age of 15 years. Visual acuity remained stable until the age of 35, after which a significantly faster deterioration occurred, albeit with a high variability between individual patients. A unique aspect of this study is its focus on the patient's experience of the disease. Patients reported discontinuing professional work at a mean age

of 48, which was vision-related in 60% of cases. Visual field constriction was reported as the most disabling symptom by 70% of patients. This study is the first to report scleral pits and tunnels as a novel finding on SD-OCT. **Chapter 3.2** describes the successful outcome of full-thickness macula hole surgery in choroideremia, followed by structural and functional improvement.

Chapter 4 focuses on *RPGR*-associated phenotypes. Several human gene therapy trials are ongoing for *RPGR*-associated RP, and the first reports from phase I and II/III trials have shown a promising safety and efficacy profile (https://clinicaltrials.gov/: NCT03116113). However, remarkably limited information was available on the phenotypic spectrum, long-term clinical course, prognostic factors, and genotype-phenotype correlations, while *RPGR* gene therapy development accelerated at a rapid pace.

Chapter 4.1 investigates the phenotype and clinical course in a large cohort of 74 male patients with *RPGR*-associated IRD, which consisted of RP in 70%, cone dystrophy (COD) in 7%, and cone-rod dystrophy (CORD) in 23%. This study found an earlier age at symptom onset in RP patients than in patients with COD/CORD (5 years vs. 23 years). However, the ensuing visual acuity decline was faster in COD/CORD than in RP, with the probability of being blind at the age of 40 being 20% in RP and 55% in COD/CORD. Mutations in the ORF15 hotspot region were associated with high myopia, and a faster visual acuity decline, both in RP and COD/CORD, and a faster visual field decline in RP.

Chapter 4.2 examines the phenotype in heterozygous (female) *RPGR* mutation carriers. While the X-linked inheritance mode of *RPGR*-RD places the focus on affected male patients, we also studied the spectrum of abnormalities in female mutation carriers. This chapter describes the clinical and genetic findings in 125 female *RPGR* mutation carriers, who were from RP pedigrees, COD/CORD pedigrees, or mixed pedigrees. Retinal pigmentary changes and visual symptoms were present in 58% and 40% of female subjects, respectively. Complete expression of the RP or CORD phenotype was observed in 23% of heterozygotes, although usually in milder forms than in their affected male relatives. Blindness was found in 9% of female subjects. Myopia was a frequent feature (73%), and was associated with a lower visual acuity. Ongoing and future *RPGR* gene therapy trials may consider including such severely affected female patients, as gene therapy may be a viable treatment option, as has been reported in affected male patients.

The results from Chapter 4 indicate a window of therapeutic opportunity ideally in the first 4 decades of life in men with *RPGR*-associated RP and the first 3 to 4 decades of life in men with *RPGR*-associated COD/CORD.

In **Chapter 5**, a retrospective cohort of 13 patients with *LRAT*-associated IRDs, the largest series to date, is described, over a mean follow-up time of 25 years. Symptoms occurred in the first decade

of life, and 54% of patients reached low vision, at the mean age of 49.9 years, illustrating a more favorable disease course than in earlier case reports in literature. In an earlier treatment trial of an oral supplement, patients with *LRAT*-RD and those with *RPE65*-RD were grouped together, due to the close-knit function of their respective protein products in the retinoid cycle. We therefore aimed to study the comparability of *LRAT*-associated phenotypes and *RPE65*-associated phenotypes, using our clinical data of *LRAT*-RDs, as well as earlier literature of phenotypes associated with each gene. There was considerable variability in the phenotypic findings as RP phenotypes and cone-rod phenotypes were present in the same genetic isolate. This variability complicated the ability to make a clear comparison between phenotypes associated with *LRAT* mutations and *RPE65* mutations.

Chapter 6 characterizes the natural history of *RHO*-associated RP in 100 patients from Dutch and Belgian cohorts. The phenotype was relatively favorable compared to the autosomal dominant IRDs and X-linked IRDs studied in our earlier chapters, with a sectorial RP in 25% of patients, and generalized RP in 75% of patients. Median ages to reaching low vision and blindness were 52 and 79 years, respectively. In sectorial RP, visual acuity and visual field decline was significantly slower than in those with generalized RP. The thickness of the photoreceptor-retinal pigment epithelium complex correlated with visual acuity, and may thus provide a surrogate endpoint to evaluate treatments in future clinical trials. The results from Chapter 6 indicate a wide window of therapeutic opportunity, ideally within the first 6 decades of life.

8.2

DUTCH SUMMARY

(NEDERLANDSE SAMENVATTING)

Retinale dystrofieën omvatten relatief zeldzame maar ernstige oorzaken van progressief verlies van het visuele functioneren door degeneratie van het netvlies. Er is sprake van aanzienlijke genetische en klinische variabiliteit. Mutaties in hetzelfde gen kunnen leiden tot verschillende ziektebeelden, bijvoorbeeld retinitis pigmentosa of kegeldystrofie. Omgekeerd kunnen mutaties in verschillende genen leiden tot hetzelfde ziektebeeld. De leeftijd waarop patiënten voor het eerst klachten ondervinden kan variëren per diagnosegroep en zelfs binnen dezelfde familie. Dit geldt ook voor de snelheid waarmee het zicht vervolgens verslechtert. Verder zal bij sommige patiënten vooral het centrale zicht aangetast zijn, terwijl bij andere het perifere gezichtsveld en het nachtzicht verminderd zullen zijn. Voor de meeste retinale dystrofieën is er nog geen effectieve behandeling beschikbaar. Wel worden er preklinische studies en fase I/II gentherapie trials uitgevoerd voor verschillende subtypes van retinale dystrofieën. Recent werd de eerste retinale gentherapie goedgekeurd door de Amerikaanse Food and Drug Administration voor *RPE65*-geassocieerde retinale dystrofieën, voretigene neparvovec-rzyl (Luxturna®).

Ondanks deze snelle ontwikkelingen op het gebied van gentherapiestudies, is het inzicht in het klinische ziektespectrum en het lange-termijn ziektebeloop nog opvallend beperkt. De eerder benoemde klinische variabiliteit vormt een uitdaging zowel in de evaluatie van een potentieel behandeleffect in toekomstige klinische trials, als in het samenstellen van inclusiecriteria voor dergelijke trials. Dit proefschrift heeft als doel op deze uitdagingen in te haken, door gedetailleerde klinische beschrijvingen te geven van enkele vormen van retinale dystrofieën. Een goed inzicht in de klinische kenmerken, variabiliteit en lange-termijn uitkomsten van retinale dystrofieën is van groot belang voor het stellen van een adequate diagnose en voor het informeren van de patiënt over de prognose en het te verwachten beloop. Daarnaast is zulke informatie van cruciaal belang voor de opzet van lopende en toekomstige gentherapietrials en voor de interpretatie van de resultaten die hieruit voortvloeien.

Hoofdstuk 1 is een algemene introductie in zowel de retinale anatomie en functie, als de technieken die gebruikt worden om deze te evalueren. Ook bevat het een beschrijving van de initiële ziektepresentatie en klinische bevindingen van verschillende vormen van retinale dystrofieën. Tevens bevat het een kort overzicht van de verschillende opkomende experimentele therapeutische opties.

Hoofdstuk 2 beschrijft de klinische eigenschappen en het fenotypische spectrum van retinale dystrofieën die geassocieerd zijn met mutaties in *CRB1*. Dit is een van de belangrijke genen die geassocieerd is met retinale dystrofieën zoals Leber congenitale amaurosis (LCA), retinitis pigmentosa (RP) en maculadystrofie en waar bovendien momenteel gentherapie voor wordt ontwikkeld. Dit gen is eerder ook geassocieerd met disorganisatie van de structuur van de netvlieslagen, wat de werkzaamheid van gentherapie zou kunnen belemmeren. **Hoofdstuk 2.1** biedt het grootst beschreven retrospectieve cohort uit de literatuur. De meeste patiënten (91%)

hadden *CRB1*-RP, waarbij de eerste symptomen op een mediane leeftijd van 4 jaar ontstonden, met een jaarlijkse achteruitgang van de visus en het gezichtsveld van respectievelijk 0.05 logMAR en 5%. De mediane leeftijden waarop slechtziendheid en blindheid werden bereikt, waren respectievelijk 18 en 44 jaar. Frequente bevindingen waren niet-detecteerbare staaf- en kegelresponsen op het electroretinogram (50%), cystoïde vochtcollecties in de macula (50%), hypermetropie (98%), glasvochtafwijkingen zoals cellen en/of sluiers (54%) en papildrusen (20%). Een opmerkelijke bevinding bij patiënten waarvan OCT scans beschikbaar waren, was de aanwezigheid van relatief goed identificeerbare retinale weefsellagen in de macula in 91% van de patiënten. Bij patiënten met Leber congenitale amaurosis (LCA) was er sprake van vroegtijdige visuele beperking of blindheid, met vroege degeneratie van de macula. Net als in *CRB1*-RP kwamen hypermetropie (100%) en glasvochtafwijkingen zoals cellen en/of sluiers (40%) veel voor. Er was een beperkte beschikbaarheid van retinale beeldvorming, waardoor de aanwezigheid van cystoïde vochtcollecties in de macula en de mate van retinale organisatie niet goed geëvalueerd konden worden in deze LCA-patiënten. In tegenstelling tot *CRB1*-RP, waar 92% van de patiënten beenbalk hyperpigmentatie van de retina had, waren de intraretinale pigmentveranderingen in *CRB1*-LCA beperkt tot een granulair of poederig hyperpigmentatie-aspect van de retina. Dit zou verklaard kunnen worden door de jonge leeftijd van de LCA patiënten in dit cohort (leeftijdsspreiding van 3-15 jaar bij het laatste oogheelkundige onderzoek) in vergelijking met de RP patiënten (leeftijdsspreiding van 2-78 jaar bij het laatste oogheelkundige onderzoek).

Hoofdstuk 2.2 rapporteert de baseline cross-sectionele resultaten van een uitgebreide prospectieve fenotyperingstudie in patiënten met *CRB1*-geassocieerde retinale dystrofieën. Patiënten hadden RP, kegel-staafdystrofie, of een geïsoleerde maculadystrofie. SD-OCT scans werden in bijna alle patiënten verricht en lieten volledig identificeerbare retinale weefsellagen zien in 62% van de patiënten, met milde tot matige disorganisatie in de andere patiënten. Nanopthalmos was aanwezig in 36% van de patiënten en was geassocieerd met een verhoogd risico op acute kamerhoek-afsluitingsglaucoom. “Full-field sensitivity testing” verschafte een subjectieve uitkomstmaat voor retinale sensitiviteit in ogen met (vrijwel) niet-detecteerbare amplitudes op het electroretinogram. Door middel van het gebruik van witte, rode en blauwe lichtstimuli kon de oorsprong van de retinale respons (staaf, kegel of gemengd) achterhaald worden.

Hoofdstuk 2.3 bekrachtigde verscheidene bevindingen uit de eerdere hoofdstukken. Dit hoofdstuk beschrijft een groot Belgisch cohort van patiënten met mutaties in het *CRB1* gen, waarin blindheid in het 1e levensdecennium optrad in patiënten met LCA en vroegtijdige ernstige retinale dystrofie, maar in het 5e levensdecennium in patiënten met RP. Alle patiënten met maculadystrofie hadden op tenminste 1 allel dezelfde mutatie als de Nederlandse patiënt met maculadystrofie, waardoor een genotype-fenotype correlatie werd bevestigd. Disorganisatie van de lamellaire retinale structuur werd in 52% van de patiënten gevonden, een hoger percentage dan in de Nederlandse onderzoeken.

Deze gecombineerde data uit hoofdstuk 2 wijzen erop dat therapeutische interventie middels gentherapie de meeste kans op succes zal hebben in de eerste 3 tot 4 levensdecennia in *CRB1*-RP en in de eerste paar levensjaren in *CRB1*-LCA.

Hoofdstuk 3 richt zich op choroideremie, een X-gebonden vorm van een staaf-kegeldystrofie, die veroorzaakt wordt door mutaties in het *CHM* gen. Choroideremie is reeds in fase I/II humane gentherapietrials relatief succesvol behandeld en op dit moment worden fase III gentherapie studies uitgevoerd. Niettemin zijn er relatief weinig longitudinale studies uitgevoerd. **Hoofdstuk 3.1** onderzoekt het lange-termijn klinisch beloop en de visuele uitkomst van choroideremie, met een gemiddelde follow-up duur van maar liefst 25 jaar. Symptomen begonnen gemiddeld op de leeftijd van 15 jaar. De visus bleef stabiel tot de leeftijd van 35 jaar, waarna er vaak sprake was van een snelle visusverslechtering, echter met een hoge variabiliteit tussen verschillende patiënten. Een uniek aspect van deze studie is de aandacht voor de individuele ziekte-ervaring van de patiënt. Zo rapporteerden patiënten uitval op het werk, op de gemiddelde leeftijd van 48 jaar – en deze uitval was gerelateerd aan het zicht in 60% van de gevallen. Gezichtsveldvernauwing werd gerapporteerd als het meest belemmerende symptoom door 70% van de patiënten. Tevens is dit de eerste studie die sclerale 'pits en tunnels' op de SD-OCT scan rapporteert bij deze ziekte. **Hoofdstuk 3.2** beschrijft het goede en ongecompliceerde resultaat van netvlieschirurgie aan een "full-thickness" maculagat in choroideremie, met een verbetering in de retinale structuur en visuele functie op microperimetrie.

Hoofdstuk 4 richt de aandacht op RPGR-geassocieerde fenotypes. Er lopen meerdere humane gentherapietrials voor *RPGR*-geassocieerde RP en de eerste klinische resultaten uit fase I en II/III trials laten een gunstig veiligheids- en werkzaamheidsprofiel zien (https://clinicaltrials.gov/: NCT03116113). Ondanks deze snelle ontwikkelingen is er beperkte kennis beschikbaar over het klinische spectrum en beloop op de lange termijn, prognostische factoren en genotype-fenotype correlaties in *RPGR*-geassocieerde retinale dystrofieën. **Hoofdstuk 4.1** onderzoekt het fenotype en het klinisch beloop in 74 mannen met *RPGR*-geassocieerde retinale dystrofieën, namelijk RP in 70%, kegeldystrofie in 7% en kegel-staafdystrofie in 23%. Deze studie vond een eerdere leeftijd waarop symptomen voor het eerst optraden in RP patiënten dan in patiënten met kegel(-staaf) dystrofie (5 jaar vs. 23 jaar). De hierop volgende visusdaling was echter sneller in patiënten met kegel(-staaf)dystrofie dan in RP, waarbij de kans om blind te zijn op 40-jarige leeftijd 20% bedroeg voor RP-patiënten en 55% voor kegel(-staaf)dystrofie-patiënten.
Mutaties in de ORF15 hotspot van het *RPGR* gen waren geassocieerd met hogere myopie en een snellere visusachteruitgang in vergelijking met *RPGR* mutaties buiten ORF15, zowel in RP als in kegel(-staaf)dystrofie. Daarnaast waren ORF15 mutaties geassocieerd met een snellere gezichtsveldachteruitgang in RP.

Ondanks de X-gebonden overerving van *RPGR*-geassocieerde retinale dystrofieën, zijn er aangedane vrouwelijke patiënten beschreven. Dit zou belangrijke gevolgen kunnen hebben voor de patiëntselectie voor gentherapietrials. **Hoofdstuk 4.2** beschrijft 125 (heterozygote) draagsters van *RPGR*-mutaties, afkomstig uit families met RP, kegel(-staaf)dystrofie, of beide. Pigmentatieveranderingen van het netvlies en visuele klachten waren aanwezig in respectievelijk 58% en 40% van de draagsters. Complete ziekte-expressie van het RP- of kegel(-staaf)dystrofie-fenotype werd gezien in 23% van de draagsters, hoewel het zich vaak in mildere vorm presenteerde dan in aangedane mannelijke familieleden. Van de draagsters werd 9% blind. Myopie was een veel voorkomende bevinding (73%) en was net als in mannelijke patiënten geassocieerd met een lagere visus. *RPGR* gentherapie trials kunnen de inclusie van dergelijke ernstig aangedane draagsters overwegen, aangezien gentherapie een gunstige uitkomst kan bieden voor deze patiënten, zoals dat ook bij aangedane mannelijke patiënten is beschreven.

De data uit hoofdstuk 4 wijzen erop dat therapeutische interventie middels gentherapie de meeste kans op succes zal hebben in de eerste 4 levensdecennia in *RPGR*-RP en in de eerste 3 tot 4 levensdecennia in *RPGR*-geassocieerde kegel(-staaf)dystrofie.

In **hoofdstuk 5** wordt een retrospectief cohort van 13 patiënten met *LRAT*-geassocieerde retinale dystrofieën gekarakteriseerd, de grootste patiëntenserie tot nu toe, over een lange periode van gemiddeld 25 jaar. Symptomen deden zich voor in het eerste levensdecennium en 54% van de patiënten werd uiteindelijk slechtziend, gemiddeld op 49-jarige leeftijd. Dit is een gunstiger ziektebeloop dan eerdere beschrijvingen uit case reports in de literatuur. In een eerdere klinische trial naar de veiligheid en werkzaamheid van een orale medicatie, werden patiënten met *LRAT*-geassocieerde retinale dystrofieën en patiënten met *RPE65*-geassocieerde retinale dystrofieën gezamenlijk behandeld, aangezien de functies van de eiwitproducten van deze genen nauw met elkaar verbonden zijn in de retinoïd cyclus. Een tweede doel van dit hoofdstuk was daarom om de vergelijkbaarheid tussen *LRAT*-geassocieerde fenotypes en *RPE65*-geassocieerde fenotypes te onderzoeken. Hiervoor gebruikten we onze klinische data over patiënten met *LRAT*-geassocieerde retinale dystrofieën en de beschikbare literatuur over de fenotypes die geassocieerd zijn met mutaties in *LRAT* of *RPE65*. Hoewel er gelijkenissen waren, was er aanzienlijke variabiliteit in de klinische bevindingen in zowel de *LRAT*-geassocieerde en *RPE65*-geassocieerde patiëntengroepen, waardoor een duidelijke vergelijking tussen *RPE65*-geassocieerde en *LRAT*-geassocieerde retinale dystrofieën bemoeilijkt werd.

Hoofdstuk 6 evalueert het klinisch beloop van *RHO*-geassocieerde RP in 100 patiënten uit Nederland en België. Het *RHO* gen is een relatief frequente oorzaak van RP in de autosomaal dominante overervingsvorm. Het fenotype dat wij vonden in deze grote patiëntengroep was relatief gunstig vergeleken met de autosomaal recessieve en X-gebonden retinale dystrofieën die in de eerdere hoofdstukken beschreven werden, met een milde, sectoriële RP in 25% van de patiënten,

en gegeneraliseerde RP in 75% van de patiënten. De mediane leeftijden waarop slechtziendheid en blindheid werden bereikt, waren ook significant later, namelijk respectievelijk 52 en 79 jaar. In sectoriële RP was de visus- en gezichtsveldachteruitgang significant langzamer dan in patiënten met een gegeneraliseerde RP. De dikte van het fotoreceptor-retinale pigmentepitheel-complex was gecorreleerd met de visus, waardoor het een mogelijk een goede surrogaat uitkomstmaat biedt voor toekomstige klinische trials. De resultaten uit dit hoofdstuk wijzen erop dat interventie middels gentherapie lange tijd plaats kan vinden, maar idealiter in de eerste 6 levensdecennia.

8.3

ACKNOWLEDGMENTS

Het is niet makkelijk om in maximaal 800 woorden mijn jarenlange dankbaarheid aan iedereen uit te drukken.

Graag bedank ik alle patiënten die aan dit onderzoek hebben deelgenomen.

Prof. Boon, beste Camiel, ik bewonder hoe jij wetenschap, klinische praktijk en onderwijs met zoveel enthousiasme en energie bij elkaar brengt en daarbij zo nuchter en gezellig blijft. Je ondersteunt waar nodig, je hebt een duidelijke visie, maar je hebt mij ook veel zelfstandigheid gegund. Dankzij jou kijk ik terug op een geweldige promotietijd.

Prof. Schalij-Delfos, beste Nicoline, bedankt voor je positieve en to-the-point instelling. Met jou aan boord, komt alles goed. Je zorgde ervoor dat de uitgebreide fenotyperingstudie een feit werd op een al drukke poli, waarvoor zeer veel dank.

Dr. Wijnholds, bedankt voor je deskundigheid en de mooie resultaten die je met het hele Crumbs team boekte.

Prof. Luyten, u wekte mijn interesse in de oogheelkunde en u stak me een hart onder de riem, vlak voor dit promotietraject. Bedankt dat u me vervolgens de prachtige kans gunde om tot oogarts te worden opgeleid. Prof. Jager, u heeft me tijdens mijn wetenschapsstage klaargestoomd voor onderzoek. Bedankt voor uw nuttige adviezen door de jaren heen.

Dr. van Schooneveld, lieve Mary, bedankt voor je gastvrijheid in het AMC, vaak nog tijdens de late uren, voor de in-promptu casusbesprekingen, je AMC-snoepwinkeltje en de bemoedigende kaartjes. Je hebt zoveel waardevolle kennis en deelt deze van harte. Veel geluk heb ik gehad, dat ik jou tijdens mijn promotieonderzoek heb leren kennen.

Prof. Bergen, Arthur, bedankt voor de geweldige samenwerking en je gortdroge ontnuchterende humor. Jaco, als Arthur's rechterhand heb je vele uren in dit onderzoek gestoken. Met je fotografische geheugen ben je onmisbaar geweest. Bedankt dat ik altijd bij je kon aankloppen. Ralph, bedankt voor je deskundigheid en de tijd die je voor me vrijmaakte.

Prof. Bart Leroy en dr. Caroline Van Cauwenbergh, bedankt voor de fijne samenwerking en het warme welkom in het prachtige Gent. Prof. Leroy, bedankt voor het delen van uw expertise en voor uw humor, waardoor het altijd een plezier is om even te kletsen/klappen. Caroline, bedankt dat je me bijstond in de late uren van dataverzameling en me onder je hoede nam. Heel fijn was het om samen stoom af te blazen na een lange dag ploeteren. Lieve Carine, bedankt voor je gastvrijheid en voor alle gezellige avonden en diners bij jou thuis.

Christien en Herman, bedankt voor jullie essentiële hulp in het onderzoek.

Alle mede-promovendi: bedankt voor de dagelijkse afleidingen en voor de avonturen op congres. Danial, jij staat altijd klaar om te helpen. Kasia en Cindy, wij hadden zoveel lol. Charlotte en Annemijn W., het was gezellig om samen op te trekken op congressen. Thanh, bedankt dat je dit onderzoek zo zorgvuldig hebt opgepakt.

Alle mede-(oud-)AIOS bedank ik voor de collegiale en mentale steun van de afgelopen jaren. Annemijn, Carlijn, Kasia, Melissa, het maakt werken zoveel leuker en gezelliger om jullie als collega's en vriendinnen te hebben. Bedankt aan alle oudere (oud-)AIOS die altijd bereid zijn/waren om hun jongere collega te helpen en de nodige lessen bij te brengen: Tessa, Valentijn, Elon en Ruben noem ik bij naam.

Iedereen uit mijn vriendenkring, waar ik in de afgelopen jaren altijd op terug kon vallen, bedank ik voor het aanhoren van mijn onderzoeks-beslommeringen en voor alle gezelligheid. Chinar, jarenlang heb ik te pas en te onpas bij jou terecht gekund. Bedankt voor je steun. Andrea, bijzonder vind ik het dat we al zo lang vriendinnen zijn. Sara, een lieve, enthousiaste vriendin, die altijd klaar staat met een luisterend oor. Julia, al vanaf dag één van de geneeskundestudie een superlieve vriendin waar ik altijd mee kan lachen en op kan steunen. Annemijn en Chiara, bedankt dat jullie me hebben bijgestaan als mijn paranimfen.

Ali en Jafer, het is altijd zo gezellig om als familie weer samen te komen. Ik bewonder jullie beiden en ik heb geluk gehad met zulke geweldige, lieve broertjes en zorgzame ooms voor mijn zoontje.

Lieve Papa en Mama, bedankt voor de onvoorwaardelijke steun en de warme, zorgeloze basis die ik veel te vaak voor lief neem. Bij jullie kan ik altijd terecht. Jullie hebben mij zoveel waardevolle levenslessen meegegeven. Bij jullie thuis komen blijft altijd aanvoelen als een warm bad. Dit proefschrift is voor jullie.

و لا انسى تقديم شكري الجزيل لمن لا انسى ذكريات طفولتي الجميلة معهم في بغداد:
جدتي شكرية
جدي عبد الرزاق
جدتي سميرة
جدي طالب

Ahmed, bedankt voor jouw liefdevolle steun tijdens dit promotietraject en de opleiding. Jouw vertrouwen in mijn capaciteiten en je gevoel voor humor beuren me op wanneer ik het nodig heb. Ik ben dankbaar dat wij het leven met elkaar delen. Lieve zoon, zo'n klein beertje ben je nog, maar zo groot is het geluk dat jij met je vrolijke snoet in ons leven brengt. Jullie zijn voor mij het allerbelangrijkste.

8.4

CURRICULUM VITAE

Mays Talib was born on the 29th of May in 1990, in Al-Karg, Iraq. She moved to The Netherlands at the age of 5 years. After graduating from the Gymnasium at the Stedelijk College Eindhoven and obtaining her International Baccalaureate at the International Secondary School of Eindhoven, she started her Medicine study at Leiden University in 2008. During her college years, she was active in several student committees, was selected for the Excellent Students' Program, and started working as a research student at the Department of Epidemiology of the Leiden University Medical Center (LUMC). In her last year of medical school, she started her research internship at the Schepens Eye Research Institute in Boston, Massachusetts, USA, under the supervision of Prof. Dr. D.F. Chen and Prof. Dr. M.J. Jager. She obtained her M.D. in 2015, and went on to pursue her Ph.D., researching hereditary retinal diseases under the auspices of Prof. Dr. Camiel Boon, Prof. Dr. Schalij-Delfos, and Dr. Wijnholds at the Department of Ophthalmology of the LUMC. The research results are presented in this thesis. During her Ph.D. trajectory, she presented her studies at several national and international conferences and meetings, won the First Prize at the Bayer Ophthalmology Research Award 2016 and the ARVO International Grant 2017, attended the Young Researcher Vision Camp 2017 at castle Wildenstein in Germany, gave a MedTalk at ARVO 2017 (Baltimore, USA) and ARVO 2018 (Honolulu, USA), and facilitated a patient-initiated fundraising effort for her research during the 2018 Scan Covery Trial to the North Cape, Norway. In 2018, she spent a month at the Department of Ophthalmology at the Ghent University Hospital in Belgium for her research activities. In that same year she started her residency training in Ophthalmology at the LUMC, under the auspices of Prof. Dr. G.P.M. Luyten and Prof. Dr. N.E. Schalij-Delfos.

8.5

LIST OF PUBLICATIONS

Genotypic and phenotypic characteristics of *CRB1*-associated retinal dystrophies: A long-term follow-up study.
Talib M, van Schooneveld MJ, van Genderen MM, Wijnholds J, Florijn RJ, ten Brink JB, Schalij-Delfos NE, Dagnelie G, Cremers FPM, Wolterbeek R, Fiocco M, Thiadens AA, Hoyng CB, Klaver CC, Bergen AA, Boon CJF.
Ophthalmology. 2017;124(6):884-895.

Outcome of full-thickness macular hole surgery in choroideremia.
Talib M, Koetsier LS, MacLaren RE, Boon CJF.
Genes. 2017;8(7): 187.

Long-term follow-up of patients with choroideremia with scleral pits and tunnels as a novel observation.
Van Schuppen SM*, Talib M*, Bergen AA, ten Brink JB, Florijn RJ, Boon CJF, van Schooneveld MJ.
Retina. 2018;38(9):1713-1724.
**Joint first authors*

Recording and analysis of Goldmann kinetic visual fields.
Talib M, Dagnelie G, Boon CJF.
Methods Mol Biol. 2018;1715:327-338.

Measuring central retinal sensitivity using microperimetry.
Talib M, Jolly JK, Boon CJF.
Methods Mol Biol. 2018;1715:339-349.

Clinical and genetic characteristics of male patients with *RPGR*-associated retinal dystrophies: a long-term follow-up study.
Talib M, van Schooneveld MJ, Thiadens AA, Fiocco M, Wijnholds J, Florijn RJ, Schalij-Delfos NE, van Genderen MM, Putter H, Cremers FPM, Dagnelie G, ten Brink JB, Klaver CCW, van den Born LI, Hoyng CB, Bergen AA, Boon CJF.
Retina. 2019;39(6):1186-1199.

The spectrum of structural and functional abnormalities in female carriers of pathogenic variants in the *RPGR* gene.
Talib M, van Schooneveld MJ, Van Cauwenbergh C, Wijnholds J, ten Brink JB, Florijn RJ, Schalij-Delfos NE, Dagnelie G, van Genderen MM, De Baere E, Meester-Smoor MA, De Zaeytijd J, Cremers FPM, van den Born LI, Thiadens AA, Hoyng CB, Klaver CC, Leroy BP, Bergen AA, Boon CJF.
Invest Ophthalmol Vis Sci. 2018;59(10):4123-4133.

Human iPSC-derived retinas recapitulate the fetal CRB1 CRB2 complex formation and demonstrate that photoreceptors and Muller Glia are targets of AAV5.
Quinn PM, Buck TM, Mulder AA, Ohonin C, Alves CH, Vos RM, Bialecka M, van Herwaarden T, van Dijk EHC, Talib M, Freund C, Mikkers HMM, Hoeben RC, Goumans MJ, Boon CJF, Koster AJ, Chuva de Sousa Lopes SM, Jost CR, Wijnholds J.
Stem Cell Reports. 2019;12(5):906-919.

Long-term follow-up of retinal degenerations associated with *LRAT* mutations and their comparability to phenotypes associated with RPE65 mutations.
Talib M, van Schooneveld MJ, van Duuren RJG, Van Cauwenbergh C, ten Brink JB, De Baere E, Florijn RJ, Schalij-Delfos NE, Leroy BP, Bergen AA, Boon CJF.
Transl Vis Sci Technol. 2019;8(4):24.

***RPGR*-associated dystrophies: clinical, genetic, and histopathological features.**
Nguyen XT, Talib M, van Schooneveld MJ, Brinks J, ten Brink J, Florijn RJ, Wijnholds J, Verdijk RM, Bergen AA, Boon CJF.
Int J Mol Sci. 2020;21(3):835.

Noninvasive electrical stimulation improves photoreceptor survival and retinal function in mice with inherited photoreceptor degeneration.
Yu H, Enayati S, Chang K, Cho K, Lee SW, Talib M, Zihlavnikova K, Xie J, Achour H, Fried SI, Utheim TP, Chen DF.
Invest Ophthalmol Vis Sci. 2020;61(4):5.

Clinical characteristics and natural history of *RHO*-associated retinitis pigmentosa: a long-term follow-up study.
Nguyen XT*, Talib M*, Van Cauwenbergh C, van Schooneveld MJ, Fiocco M, Wijnholds J, ten Brink JB, Florijn RJ, Schalij-Delfos NE, Dagnelie G, van Genderen MM, De Baere E, Meester-Smoor MA, De Zaeytijd J, Balikhova I, Thiadens AA, Hoyng CB, Klaver CC, van den Born LI, Bergen AA, Leroy BP, Boon CJF.
Retina. 2021;41(1):213-223.
**Joint first authors*

Retinal dystrophies and the road to treatment: clinical requirements and considerations.
Talib M, Boon CJF.
Asia Pac J Ophthalmol. 2020;9(3):159-179.

Defining inclusion criteria and endpoints for clinical trials: a prospective cross-sectional study in *CRB1*-associated retinal dystrophies.
Talib M, van Schooneveld MJ, Wijnholds J, van Genderen MM, Schalij-Delfos NE, Talsma HE, Florijn RJ, ten Brink JB, Cremers FPM, Thiadens AAHJ, van den Born LI, Hoyng CB, Meester-Smoor MA, Bergen AA, Boon CJF.
Acta Ophthalmol. 2021; Online ahead of print.

***CRB1*-associated retinal dystrophies in a Belgian cohort: genetic characteristics and long-term clinical follow-up.**
Talib M, Van Cauwenbergh C, De Zaeytijd J, Van Wynsberghe D, De Baere E, Boon CJF, Leroy BP.
Br J Ophtalmol. 2021; Online ahead of print.

The *Lrat*-/- Rat: CRISPR/Cas9 Construction and Phenotyping of a New Animal Model for Retinitis Pigmentosa.
Koster C, van den Hurk KT, Lewallen CF, Talib M, ten Brink JB, Boon CJF, Bergen AA.
Manuscript submitted.

Non-syndromic inherited retinal disease.
Talib M, Van Cauwenbergh C, Boon CJF.
In Practical Genomics for Clinical Ophthalmology. Elsevier. In preparation; expected release date June 1, 2021.